EMERGING INFECTIOUS DISEASES®

Zoonotic Infections

DECEMBER 2022

Rafael Barradas (1890–1929), *Paisaje urbano (Urban Landscape)*, 1919. Oil on cardboard, 23 1/2 in × 27 1/2 in / 59.7cm × 69.9 cm. The Museum of Fine Arts, Houston. Museum purchase funded by the 2017 Latin American Experience Gala and Auction, 2018.229.Photograph © The Museum of Fine Arts, Houston, Texas, USA; Will Michels.

EMERGING INFECTIOUS DISEASES®

EDITOR-IN-CHIEF
D. Peter Drotman

EMERGING INFECTIOUS DISEASES®

Zoonotic Infections

December 2022

On the Cover

Rafael Barradas (1890–1929), *Paisaje urbano*
(*Urban Landscape*)**, 1919.** Oil on cardboard, 23 1/2 in × 27
1/2 in / 59.7cm × 69.9 cm. The Museum of Fine Arts, Houston.
Museum purchase funded by the 2017 Latin American
Experience Gala and Auction, 2018.229.Photograph © The
Museum of Fine Arts, Houston, Texas, USA; Will Michels.

About the Cover p. 2588

2412

Orthopoxvirus Seroprevalence and Infection
Susceptibility in France, Bolivia, Laos, and Mali
L. Luciani et al.

Another Dimension

Research Letters

Dispatches

2517

2560

Thank You,
Emerging Infectious Diseases Reviewers

We only maintain high standards because of your support.

EID's 2021 Impact Factor of 16.126 ranked it 4th among open-access infectious disease journals and 9th out of 94 infectious disease journals.

The Google Scholar h-Index is 106; 2nd of top 20 publications in Epidemiology and 2nd among open-access journals; ranked 4th among top 20 publications in Communicable Diseases and 1st among open-access journals.

The electronic table of contents goes to 66,847 subscribers each month.

All articles published in the *Emerging Infectious Diseases* journal are peer-reviewed by volunteers from around the globe, enabling us to bring you high-quality content about new and emerging infectious diseases and trends world-wide.

A list of reviewers is posted at
http://wwwnc.cdc.gov/eid/page/reviewers

Emerging Infectious Diseases
Spotlight Topics
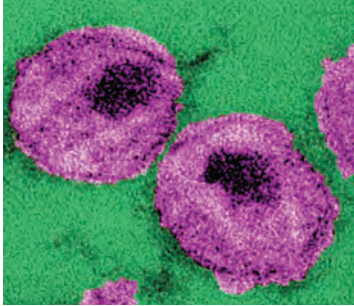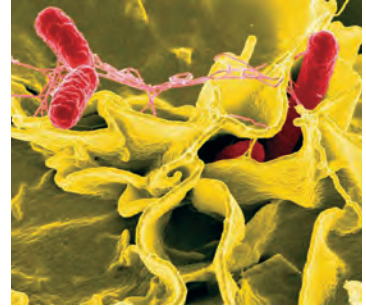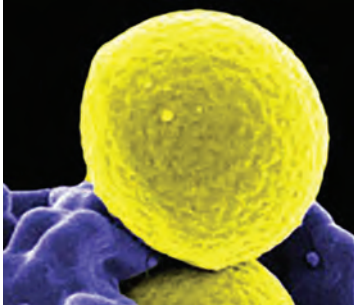
Antimicrobial resistance
Ebola • Etymologia
Food safety • HIV-AIDS
Influenza • Lyme disease
Malaria • MERS • Pneumonia
Rabies • Ticks • Tuberculosis
Coronavirus • Zika
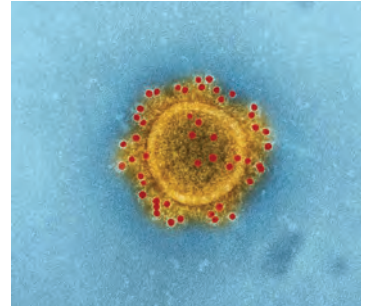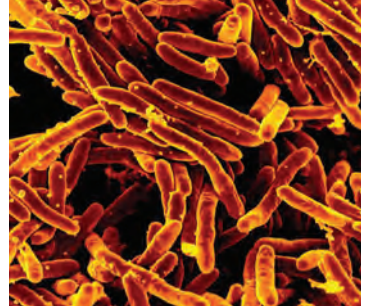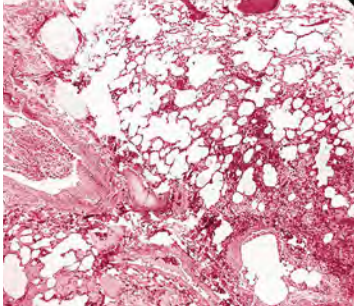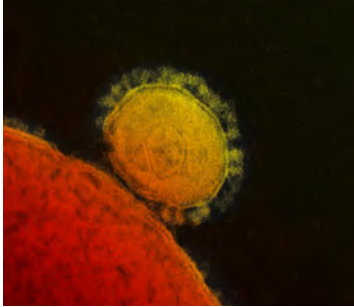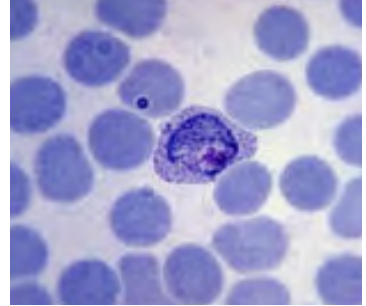
EID's spotlight topics highlight the latest articles and information on emerging infectious disease topics in our global community

https://wwwnc.cdc.gov/eid/page/spotlight-topics

Clinical and Epidemiologic Characteristics and Therapeutic Management of Patients with *Vibrio* Infections, Bay of Biscay, France, 2001–2019

Florence Hoefler,[1] Xavier Pouget-Abadie, Mariam Roncato-Saberan,
Romain Lemarié, Eve-Marie Takoudju, François Raffi, Stéphane Corvec, Morgane Le Bras,[2]
Charles Cazanave, Philippe Lehours, Thomas Guimard, Caroline Allix-Béguec

In support of improving patient care, this activity has been planned and implemented by Medscape, LLC and Emerging Infectious Diseases. Medscape, LLC is jointly accredited with commendation by the Accreditation Council for Continuing Medical Education (ACCME), the Accreditation Council for Pharmacy Education (ACPE), and the American Nurses Credentialing Center (ANCC), to provide continuing education for the healthcare team.

Medscape, LLC designates this Journal-based CME activity for a maximum of 1.00 **AMA PRA Category 1 Credit(s)™**. Physicians should claim only the credit commensurate with the extent of their participation in the activity.

Successful completion of this CME activity, which includes participation in the evaluation component, enables the participant to earn up to 1.0 MOC points in the American Board of Internal Medicine's (ABIM) Maintenance of Certification (MOC) program. Participants will earn MOC points equivalent to the amount of CME credits claimed for the activity. It is the CME activity provider's responsibility to submit participant completion information to ACCME for the purpose of granting ABIM MOC credit.

All other clinicians completing this activity will be issued a certificate of participation. To participate in this journal CME activity: (1) review the learning objectives and author disclosures; (2) study the education content; (3) take the post-test with a 75% minimum passing score and complete the evaluation at http://www.medscape.org/journal/eid; and (4) view/print certificate. For CME questions, see page 2597.

Release date: November 18, 2022; Expiration date: November 18, 2023

Learning Objectives

Upon completion of this activity, participants will be able to:

- Assess the epidemiology of infection with *Vibrio* spp. in the current study

- Evaluate common anatomic sites of infection with *Vibrio* spp.

- Distinguish the most common *Vibrio* spp. isolated in the current study

- Analyze the treatment and outcomes of *Vibrio* infections.

CME Editor

Jude Rutledge, BA, Technical Writer/Editor, Emerging Infectious Diseases. *Disclosure: Jude Rutledge has no relevant financial relationships.*

CME Author

Charles P. Vega, MD, Health Sciences Clinical Professor of Family Medicine, University of California, Irvine School of Medicine, Irvine, California. *Disclosure: Charles P. Vega, MD, has the following relevant financial relationships: served as an advisor or consultant for GlaxoSmithKline; Johnson & Johnson Pharmaceutical Research & Development, L.L.C.*

Authors

Florence Hoefler, MD; Xavier Pouget-Abadie, MD; Mariam Roncato-Saberan, MD; Romain Lemarié, MD; Eve-Marie Takoudju, MD; François Raffi, MD; Stéphane Corvec, MD; Morgane Le Bras, MS; Charles Cazanave, MD; Philippe Lehours, MD; Thomas Guimard, MD; Caroline Allix-Béguec, PhD.

Author affiliations: Centre Hospitalier La Rochelle, La Rochelle, France (F. Hoefler, X. Pouget-Abadie, M. Roncato-Saberan, R. Lemarié, C. Allix-Béguec); Centre Hospitalier Départemental Vendée, La Roche sur Yon, France (E.-M. Takoudju, T. Guimard); Centre Hospitalier Universitaire de Nantes, Nantes, France (F. Raffi, S. Corvec, M. Le Bras); Centre Hospitalier Universitaire de Bordeaux, Bordeaux, France (C. Cazanave, P. Lehours)

DOI: https://doi.org/10.3201/eid2812.220748

[1]Current affiliation: Centre Hospitalier Troyes, Troyes, France.

[2]Current affiliation: Centre Hospitalier d'Auxerre, Auxerre, France.

Noncholera vibriosis is a rare, opportunistic bacterial infection caused by *Vibrio* spp. other than *V. cholerae* O1/O139 and diagnosed mainly during the hot summer months in patients after seaside activities. Detailed knowledge of circulating pathogenic strains and heterogeneities in infection outcomes and disease dynamics may help in patient management. We conducted a multicenter case-series study documenting *Vibrio* infections in 67 patients from 8 hospitals in the Bay of Biscay, France, over a 19-year period. Infections were mainly caused by *V. alginolyticus* (34%), *V. parahaemolyticus* (30%), non-O1/O139 *V. cholerae* (15%), and *V. vulnificus* (10%). Drug-susceptibility testing revealed intermediate and resistant strains to penicillins and first-generation cephalosporins. The acute infections (e.g., those involving digestive disorder, cellulitis, osteitis, pneumonia, and endocarditis) led to a life-threatening event (septic shock), amputation, or death in 36% of patients. Physicians may need to add vibriosis to their list of infections to assess in patients with associated risk factors.

Some opportunistic pathogens associated with marine environments are already known but until now have caused rare infectious diseases. Among those pathogens are *Vibrio* spp. other than the well-known *V. cholerae* belonging to serogroups O1 and O139, which causes cholera. *Vibrio* spp. are gram negative, curved, rod-shaped bacteria that are natural inhabitants of the aquatic environment (*1*). *Vibrio* infections can be very severe or even fatal; they cause gastroenteritis, severe bacterial cellulitis, or necrotizing fasciitis and can lead to septic shock. Infections are more common in patients with multiple underlying conditions, including liver disease, heart failure, diabetes, liver cirrhosis, alcohol abuse, and immunocompromising conditions (*2–5*). *Vibrio* spp. can also cause mild diseases, such as chronic ear infections, which are more likely to affect younger patients (*6*). Humans acquire *Vibrio* infections after eating contaminated raw seafood, especially oysters, or after exposing an injury to the marine environment (*7*). Infections occur mainly during the hot summer months, which is probably attributable to higher water temperatures (*8,9*) and to increased seawater-related activities.

Because vibriosis is a relatively rare disease and is not reported in most national surveillance systems, the global incidence rate of *Vibrio* spp. infections other than *V. cholerae* O1/O139 is underestimated. In the United States, where those infections are notifiable, a marked seasonal distribution and an increasing incidence rate have been observed (*10–12*). Because of their rarity, *Vibrio* infections are very poorly known and therefore probably underdiagnosed. Delays in therapeutic management and, in particular, in the prescription of a targeted antibiotic regimen have been documented (*13*). Our study aimed to make an inventory of *Vibrio* infections diagnosed in hospitals in the Bay of Biscay on the west coast of France and to describe the clinical and epidemiologic characteristics of the patients and their therapeutic management.

Methods

Study Design and Participants

We conducted a multicenter case-series study based on data collected from 8 tertiary and secondary care hospitals in the Bay of Biscay, France. We included all cases of vibriosis other than those caused by *V. cholerae* O1/O139 diagnosed during January 2001–December 2019.

Diagnosis and Susceptibility Test

We defined a *Vibrio* infection as a positive biologic sample (e.g., blood, skin sample, surgical biopsy, stool sample, bronchoalveolar lavage, and ear sample) to a *Vibrio* species other than *V. cholerae* O1/O139. Conventional microbiologic methods were used to isolate bacteria from the different types of samples. BACTEC automated blood culture system (Becton, Dickinson and Company, https://www.bd.com) was used before conventional culture for the rapid detection of microorganisms in blood samples. Since 2018, automated diagnostic testing of stool samples for direct qualitative detection and differentiation of enteric bacterial pathogens has been performed with the BD MAX Enteric Bacterial Panel performed on the BD MAX system (Becton, Dickinson and Company). Before 2014, API 20 E biochemical tests (bioMérieux, https://www.biomerieux.com) were used for species identification. Since 2014, those tests have been replaced by the use of the Bruker Biotyper matrix-assisted laser desorption/ionization time-of-flight mass spectrometry (https://www.bruker.com). Antibiotic susceptibility was tested on the main class of antibiotics, including penicillins, cephalosporins, carbapenems, and fluoroquinolones. Antimicrobial susceptibility testing was performed using Mueller–Hinten agar disk diffusion tests (AST Disks; Bio-Rad, https://www.bio-rad.com) in accordance with the recommendations of the Committee on Antimicrobial Susceptibility of the French Society for Microbiology. Most isolates were sent to the national reference center for confirmation of species identification and susceptibility results.

Ethics and Regulation

This study received a favorable opinion from the Committee of Expertise for Health Research, Studies, and Evaluations (registration no. TPS 1170745). It was authorized by the Commission Nationale de l'Informatique et des Libertés (decision no. DR-2020–125). A letter explaining the study and the patients' rights regarding the use of their data was sent to the last known address of the patients. This study was registered on clinicaltrials.gov (identifier NCT04451707).

Variables and Statistical Methods

We retrieved sociodemographic data, sea-related activity, and clinical and therapeutic data from patient medical records. We used means ($\pm$SD) to describe continuous variables, and percentages and 95% CIs to describe categoric variables. We explored associated factors with sepsis. We used Mann–Whitney tests to compare continuous data of independent samples where appropriate. We used the Fisher test of homogeneity for categoric variables. We used an α level of 0.05 for statistical tests, for which we also calculated SDs and 95% CIs.

Results

Population and Temporality of Infections

Data from 67 patients diagnosed with *Vibrio* infection were available for the period 2001–2019 (Table 1). Most patients were men (81%), and the average age was 54 years (SD $\pm$24 years). In the subgroup of patients with acute infections (including cutaneous infections and gastroenteritis), the mean age was 60 (SD $\pm$20) years, and 71% of the patients had $\geq$1 underlying condition. Patients with chronic ear infections were younger (mean age 27 years [SD $\pm$24 years]), and all but 1 had no underlying conditions.

The description of environmental factors was available for 57% of patients. Among those patients, 55.3% of infections were contracted at the beach, 39.5% by handling or eating seafood, and 5.3% while abroad. Most infections (82%) occurred during June–September. The number of reported cases reached 2 peaks, in 2003 and 2018.

Clinical Features

The average duration between known exposure and onset of symptoms was 2.4 days (SD $\pm$3.8 days), and it varied from <1 day for patients with gastroenteritis, cellulitis, or pneumonia, to 20 days for patients with osteitis. Digestive disorders were reported in 23 (34.4%) of the patients, including 6% with severe intraabdominal infection. Cellulitis was reported in 23 (34.4%) of the patients, and 3 had soft tissue infection complicated by osteitis. Near drowning–associated pneumonia was reported in 8 (12%) of the patients. A case of endocarditis was described in a patient whose pacemaker had been exposed to seawater through a preexisting chronic wound while swimming in the Atlantic Ocean. Chronic ear

Table 1. Clinical characteristics of patients with *Vibrio* infection, by species, Bay of Biscay, France, 2001–2019*

Characteristic	V. alginolyticus	V. parahaemolyticus	V. cholerae non-O1/O139	V. vulnificus	Other species
Total patients	23 (100)	20 (100)	10 (100)	7 (100)	7 (100)
Demographics					
Age, y, median (SD)	50 ($\pm$26.7)	53 ($\pm$22.8)	69 ($\pm$19.7)	66 ($\pm$11.5)	40 ($\pm$24.8)
Sex					
M	19 (83)	15 (75)	7 (70)	7 (100)	6 (86)
F	4 (17)	5 (25)	3 (30)	0	1 (14)
Underlying condition					
Heart failure	8 (35)	6 (30)	5 (50)	4 (57)	1 (14)
Neoplasia	1 (4)	5 (25)	4 (40)	0 (0)	1 (14)
Diabetes	2 (9)	3 (15)	1 (10)	1 (14)	1 (14)
Kidney failure	2 (9)	1 (5)	1 (10)	0	3 (43)
Immune disease	2 (9)	2 (10)	1 (10)	0	2 (29)
Hemopathy	1 (4)	1 (5)	1 (10)	1 (14)	1 (14)
Liver disease	1 (4)	1 (5)	2 (20)	1 (14)	0
Alcohol use disorder	2 (9)	1 (5)	2 (20)	2 (29)	0
Preexisting wound	3 (13)	0	0	3 (43)	0
Digestive surgery	2 (9)	2 (10)	1 (10)	0	1 (14)
Time to symptom onset, d, median (SD)	2.4 ($\pm$2.0)	1.3 ($\pm$0.9)	3 ($\pm$4.4)	5.6 ($\pm$8.1)	1 ($\pm$0.0)
Infection type					
Acute	14 (61)	19 (95)	10 (100)	7 (100)	5 (71)
Chronic	9 (39)	1 (5)	0	0	2 (29)
Outcome					
Recovered	21 (91)	17 (85)	8 (80)	6 (86)	7 (100)
Died	2 (9)	3 (15)	2 (20)	1 (14)	0

*Values are no. (%) except as indicated.

Table 2. Available drug-susceptibility test results for the main antibiotics used to treat *Vibrio* infections, by species, Bay of Biscay, France, 2001–2019*

Antibiotic	*V. alginolyticus*			*V. parahaemolyticus*			*V. cholerae* non-O1/O139			*V. vulnificus*		
	S	I	R	S	I	R	S	I	R	S	I	R
Amoxicillin	1	0	15	1	6	7	2	2	3	5	0	0
Ticarcillin	5	0	10	2	2	9	5	0	1	5	0	0
First-generation cephalosporin	10	4	0	13	1	0	4	1	0	4	1	0
*Data are no. of cases. I, intermediate; R, resistant; S, susceptible.												

infection (chronic otitis or cholesteatoma) affected 12 (18%) of the patients.

Diagnostic Testing, *Vibrio* Species, and Drug-Susceptibility Testing

Vibrio infections were diagnosed from blood samples (26.9%), feces (20.9%), biopsies (20.9%), ear swab samples (17.9%), bronchoalveolar lavage samples (7.5%), and skin samples (6%). The most frequently identified species were *V. alginolyticus* (34%) and *V. parahaemolyticus* (30%). *V. cholerae* non-O1/O139 was found in 15% of patients, and *V. vulnificus* was found in 10%. The remaining patients were infected with other *Vibrio* species. Other bacteria were co-isolated in samples from 5 patients (methicillin-sensitive *Staphylococcus aureus* in 2 skin samples; *Streptococcus mitis* in a bronchoalveolar lavage; *Proteus vulgaris* and *Haemophilus influenza* in another bronchoalveolar lavage; and *Klebsiella pneumoniae*, *Enterococcus faecalis*, and *Enterobacter cloacae* in a bone biopsy).

Susceptibility testing revealed strains with resistance or intermediate resistance to amoxicillin in most *V. alginolyticus*, *V. parahaemolyticus*, and *V. cholerae* non-O1/O139 strains (Table 2). Strains with resistance or intermediate resistance to ticarcillin were also found in most *V. alginolyticus* and *V. parahaemolyticus* strains and to a lesser extent in *V. cholerae* non–O1/O139 strains. *V. vulnificus* strains were sensitive to all of these penicillins.

Diseases Caused by *Vibrio* infection

V. alginolyticus was responsible for various pathologies, but more particularly for otitis (39%) (Figure). *V. parahaemolyticus* was identified in patients with cellulitis (40%) and gastroenteritis (40%). *V. cholerae* non-O1/O139 was almost exclusively responsible for digestive disorders (90%). *V. vulnificus* was exclusively found in cellulitis and soft tissue infections complicated by osteitis.

Treatment

Most (84%) patients required hospitalization. The average time from symptom onset to treatment was 2.7 days (SD +4.9) days. Most of the patients received antibiotics (90%), of whom >50% received a multidrug regimen. The main prescribed antibiotics were penicillins (91%), quinolones (36%), cephalosporins (30%), metronidazole (15%), tetracycline (10%), and aminoglycosides (9%).

Twenty-two patients (33%) underwent surgery. Eleven patients with necrotizing cellulitis and 3 patients with osteitis required surgical debridement. For 6 of those 11 patients, amputation was necessary. Five patients with chronic ear infection required either surgical excision (n = 3), meatotomy (n = 1), or tympanoplasty (n = 1). Two patients had a cholecystectomy, and 1 patient with phlegmonous ileitis had partial colectomy.

Factors Associated with Severe Forms

All patients with chronic infection were cured. Among patients with acute infection, 13 (24%) went into septic shock (Table 3), 6 (11%) had amputations, and 8 (14%) died. Half of the amputations were associated with *V. vulnificus* infections. Older age and malignant hemopathy (e.g., acute leukemia and lymphoma under chemotherapy) were associated with death. Three patients suffered pneumonia after near
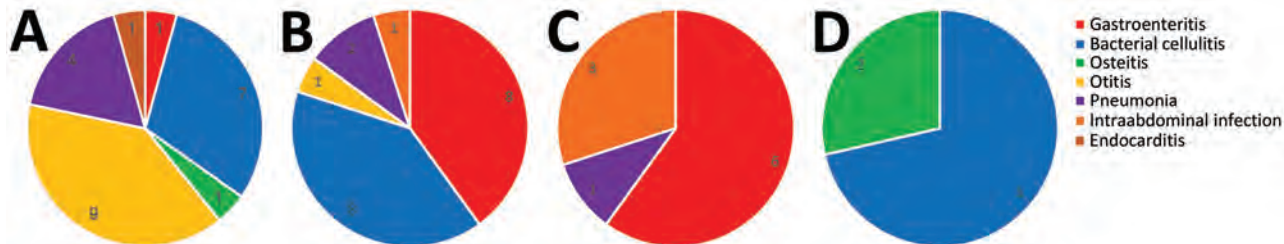
Figure. Diseases caused by *Vibrio* infection in 67 patients, by species, Bay of Biscay, France, 2001–2019. A) *V. alginolyticus.* B) *V. parahaemolyticus.* C) *V. cholerae* non-O1/O139. D) *V. vulnificus.* Numbers in chart sections indicate number of patients. Intraabdominal infection corresponds to pancreatitis, liver abscess, phlegmoneous ileitis, cholecystis, and peritonitis.

Table 3. Clinical characteristics and outcome of patients with and without septic shock after acute *Vibrio* infection, Bay of Biscay, France, 2001–2019*

Characteristic	No sepsis, n = 42		Septic shock, n = 13		p value
	No.	% (95% CI)	No.	% (95% CI)	
Patient sex					
M	35	83 (72–95)	10	77 (54–100)	0.685
F	7	17 (5–28)	3	23 (0.2–46)	
Underlying conditions					
Heart failure	18	43 (28–58)	6	46 (19–73)	Referent
Neoplasia	6	14 (4–25)	4	31 (6–56)	0.223
Diabetes	7	17 (5–28)	1	8 (0–22)	0.664
Kidney failure	5	12 (2–22)	2	15 (0–35)	0.664
Immune disease	5	12 (2–22)	2	15 (0–35)	0.664
Hemopathy	3	7 (0–15)	2	15 (0–35)	0.582
Liver disease	2	5 (0–11)	3	23 (0–46)	0.318
Alcohol use disorder	3	7 (0–15)	4	31 (6–56)	0.102
Preexisting wound	6	14 (4–25)	0	0 (0–0)	0.317
Digestive surgery	4	10 (1–18)	2	15 (0–35)	0.618
Species					
V. alginolyticus	10	24 (11–37)	4	31 (6–56)	
V. parahaemolyticus	14	33 (19–48)	5	38 (12–65)	
V. cholerae non-O1/O139	8	19 (7–31)	2	15 (0–35)	
V. vulnificus	6	14 (4–25)	1	8 (0–22)	
Other *Vibrio* species	4	10 (1–18)	1	8 (0–22)	
Outcome					
Recovered	40	95 (89–100)	7	54 (27–81)	0.001
Died	2	5 (0–11)	6	46 (19–73)	

*Median patient age (±SD) was 60 (±21.4) for no sepsis and 61 (±15.3) for septic shock.

drowning, and death may have been attributable to cardiorespiratory arrest and intensive care complications. A probable link between *Vibrio* infection and death could be established for 5 patients. The case-fatality rate was the highest for *V. vulnificus* infections (1 attributable death out of 7 infections), followed by *V. parahaemolyticus* (2 attributable deaths out of 19 infections) and *V. cholerae* non-O1/O139 (1 attributable death out of 10 infections). The case-fatality rate was the lowest for *V. alginolyticus* infections (1 attributable death out of 14 infections).

Discussion

The cases of *Vibrio* infections reported in this study are the most severe cases that ended up requiring hospitalization. Non–*V. cholerae* and *V. cholerae* non-O1/O139 bacteria can cause mild diarrhea and gastroenteritis, for which patients typically are not hospitalized (*7,14*), and the number of vibriosis incidents per year in the region is probably higher that those reported in our study. Comparing the demographics of our population with those described in a 1996–2010 review surveillance in the United States (*10*), we observed a higher proportion of men (81% vs. 68%), and the age group with the highest percentage of cases was 60–69 years in our population compared with 40–49 years in the United States. This difference is probably attributable to the fact that our population mainly consists of the most severe cases of infection that occur most often in older person (*15*). *Vibrio* infections

are usually initiated from exposure to contaminated water or consumption of raw or undercooked contaminated seafood. As reported in 2008 by Dechet et al. (*16*), seawater-related activities as simple as walking on the beach can lead to *Vibrio* infections (*16*), which was also reported for >50% of the patients with environmental factors identified in our study. *Vibrio* species are responsible for 20% of bacterial illnesses related to shellfish consumption (*17*). In our study, 39% of the cases were acquired after seafood handling or consumption. *Vibrio* bacteria caused more seafood-associated outbreaks during the warmer months (*11*), and all but 1 case occurred during June–September in our study population. Extreme heat waves led to unprecedented high sea surface temperatures, which appear to be responsible for the emergence of *Vibrio* bacteria in areas where they are usually not present (*18,19*). In 2003, France experienced the hottest summer in a century, which may have led to an increase in the concentration of *Vibrio* on the Bay of Biscay, given that the number of reported *Vibrio* infections also increased this year.

We compared the results of our study to a similar investigation conducted in the US state of Florida (*13*). The most common species reported in Florida over 10 years were *V. vulnificus* (33.1%), *V. parahaemolyticus* (29.4%), *V. alginolyticus* (15.7%), and *V. cholerae* non-O1/O139 (6.6%). In our study, we report a slightly different distribution: *V. alginolyticus* (34.3%), *V. parahaemolyticus* (29.9%), *V. cholerae* non-O1/O139 (14.9%),

and *V. vulnificus* (10.4%). The incubation period of *V. parahaemolyticus*, *V. vulnificus* (when exposed to a wound), and *V. cholerae* non-O1/O139 is <24 hours; for other clinical manifestations after infection with *V. vulnificus*, the incubation period ≈48 hours (*7,14*). In our study, the time between known exposure and onset of symptoms was <48 hours in 74% of cases.

Clinical manifestations are different depending on the type of *Vibrio* species. *V. alginolyticus* has been identified as a relevant cause of superficial wound and ear infections (*14*). In our study, *V. alginolyticus* was responsible for most cases of chronic otitis. However, contrary to what has been observed in Florida (*13*), this species also caused 1 death associated with wound infection. *V. parahaemolyticus* is the most prevalent foodborne bacterium associated with seafood consumption and typically causes acute gastroenteritis (*20*), but it has also been identified in wound-associated cases (*13*). In our study, most *V. parahaemolyticus* infections caused either gastroenteritis or bacterial cellulitis, but the species was also responsible for pneumonia, phlegmonous ileitis, and otitis. *V. cholerae* non-O1/O139 is the causative agent of gastrointestinal and extraintestinal infections and has been reported to be the cause of one third of deaths in infected patients (*21*). Of the 10 patients with *V. cholerae* non-O1/O139 infection reported in this study, 6 had ≥1 risk factor (e.g., cancer or malignant blood diseases, alcoholism, other liver diseases, and diabetes), and 1 died from the infection. *V. vulnificus* infections in Europe are rare and sporadic (*22*) but have the highest reported case-fatality rate of any foodborne pathogen (*12,23*). In our study, 7 total cases were reported in 2005, 2007, 2015, 2017, and 2018, and 4 resulted in either amputation, septic shock, or death.

Because *Vibrio* infections can cause severe reaction or disease, treatment with a combination of a third-generation cephalosporin and a tetracycline or a fluoroquinolone alone is recommended. Higher mortality rates were observed with a β-lactam alone, compared with fluoroquinolone alone or fluoroquinolone or tetracycline plus a β-lactam (*24*). In the United States, the most commonly used antibiotics for patients with *Vibrio* infections were quinolones (56.1%), followed by cephalosporins (24.1%), tetracyclines (23.5%), and penicillins (15.4%) (*24*). Less than one third of patients with *Vibrio* infections received appropriate antibiotic therapy (*13*). According to our study, in France, the main prescribed antibiotics for *Vibrio* infections were penicillins (91%), quinolones (36%), cephalosporins (30%), metronidazole (15%), and tetracycline (10%), and >50% of patients received a multidrug regimen.

The main limitations of our study are that vibriosis is not a notifiable disease in France, that not all hospitals in the Bay of Biscay participated, and that the reported cases probably underestimated the situation. Data were also not always complete on each case-patient, and details of food histories or other exposures were not always available.

In conclusion, the incidence of serious marine-related *Vibrio* infections has been low on the west coast of France. However, predicted rising ocean temperatures and demographic shifts (e.g., an aging population with increased risk factors) may lead to the emergence of opportunistic vibriosis in France and other coastal countries in temperate and tropical regions. Our retrospective case-series study provides a basis for identifying and treating new cases of *Vibrio* infections that might affect larger population sectors in the future.

About the Author

Dr. Hoefler is a clinician at the Infectious Diseases Department at Troyes Hospital, Troyes, France. Her primary research interests are zoonoses, tuberculosis, and bone and joint infections.

References

1. Vezzulli L, Colwell RR, Pruzzo C. Ocean warming and spread of pathogenic vibrios in the aquatic environment. Microb Ecol. 2013;65:817–25. https://doi.org/10.1007/s00248-012-0163-2
2. Engel MF, Muijsken MA, Mooi-Kokenberg E, Kuijper EJ, van Westerloo DJ. *Vibrio cholerae* non-O1 bacteraemia: description of three cases in the Netherlands and a literature review. Euro Surveill. 2016;21:21. https://doi.org/10.2807/1560-7917.ES.2016.21.15.30197
3. Jones MK, Oliver JD. Vibrio vulnificus: disease and pathogenesis. Infect Immun. 2009;77:1723–33. https://doi.org/10.1128/IAI.01046-08
4. Jacobs Slifka KM, Newton AE, Mahon BE. *Vibrio alginolyticus* infections in the USA, 1988–2012. Epidemiol Infect. 2017;145:1491–9. https://doi.org/10.1017/S0950268817000140
5. Liao Y, Li Y, Wu S, Mou J, Xu Z, Cui R, et al. Risk factors for *Vibrio parahaemolyticus* infection in a southern coastal region of China. Foodborne Pathog Dis. 2015;12:881–6. https://doi.org/10.1089/fpd.2015.1988
6. Dechet AM, Yu PA, Koram N, Painter J. Nonfoodborne *Vibrio* infections: an important cause of morbidity and mortality in the United States, 1997–2006. Clin Infect Dis. 2008;46:970–6. https://doi.org/10.1086/529148
7. Morris JG Jr, Acheson D. Cholera and other types of vibriosis: a story of human pandemics and oysters on the half shell. Clin Infect Dis. 2003;37:272–80. https://doi.org/10.1086/375600

8. Centers for Disease Control and Prevention. Foodborne Diseases Active Surveillance Network: FoodNet 2011 surveillance report. 2012 [cited 2019 Dec 10]. https://www.cdc.gov/foodnet/pdfs/2011_annual_report_508c.pdf

9. Centers for Disease Control and Prevention. Cholera and Other Vibrio Illness Surveillance (COVIS) annual summary, 2009. 2011 Nov [cited 2019 Dec 10]. https://www.cdc.gov/nationalsurveillance/pdfs/cstevibrio2009.pdf

10. Newton A, Kendall M, Vugia DJ, Henao OL, Mahon BE, Branch DE, et al. Increasing rates of vibriosis in the United States, 1996–2010: review of surveillance data from 2 systems. Clin Infect Dis. 2012;54(Suppl 5):S391–5. https://doi.org/10.1093/cid/cis243

11. Iwamoto M, Ayers T, Mahon BE, Swerdlow DL. Epidemiology of seafood-associated infections in the United States. Clin Microbiol Rev. 2010;23:399–411. https://doi.org/10.1128/CMR.00059-09

12. Scallan E, Hoekstra RM, Angulo FJ, Tauxe RV, Widdowson MA, Roy SL, et al. Foodborne illness acquired in the United States—major pathogens. Emerg Infect Dis. 2011;17:7–15. https://doi.org/10.3201/eid1701.P11101

13. Weis KE, Hammond RM, Hutchinson R, Blackmore CGM. *Vibrio* illness in Florida, 1998–2007. Epidemiol Infect. 2011;139:591–8. https://doi.org/10.1017/S0950268810001354

14. Baker-Austin C, Oliver JD, Alam M, Ali A, Waldor MK, Qadri F, et al. *Vibrio* spp. infections. Nat Rev Dis Primers. 2018;4:8. https://doi.org/10.1038/s41572-018-0005-8

15. Kendall PA, Hillers VV, Medeiros LC. Food safety guidance for older adults. Clin Infect Dis. 2006;42:1298–304. https://doi.org/10.1086/503262

16. Dechet AM, Yu PA, Koram N, Painter J. Nonfoodborne *Vibrio* infections: an important cause of morbidity and mortality in the United States, 1997–2006. Clin Infect Dis. 2008;46:970–6. https://doi.org/10.1086/529148

17. Butt AA, Aldridge KE, Sanders CV. Infections related to the ingestion of seafood. Part I: viral and bacterial infections. Lancet Infect Dis. 2004;4:201–12. https://doi.org/10.1016/S1473-3099(04)00969-7

18. Baker-Austin C, Trinanes JA, Salmenlinna S, Löfdahl M, Siitonen A, Taylor NGH, et al. Heat wave-associated vibriosis, Sweden and Finland, 2014. Emerg Infect Dis. 2016;22:1216–20. https://doi.org/10.3201/eid2207.151996

19. Vezzulli L, Grande C, Reid PC, Hélaouët P, Edwards M, Höfle MG, et al. Climate influence on *Vibrio* and associated human diseases during the past half-century in the coastal North Atlantic. Proc Natl Acad Sci U S A. 2016;113:E5062–71. https://doi.org/10.1073/pnas.1609157113

20. Baker-Austin C, Trinanes J, Gonzalez-Escalona N, Martinez-Urtaza J. Non-cholera vibrios: the microbial barometer of climate change. Trends Microbiol. 2017;25:76–84. https://doi.org/10.1016/j.tim.2016.09.008

21. Deshayes S, Daurel C, Cattoir V, Parienti JJ, Quilici ML, de La Blanchardière A. Non-O1, non-O139 *Vibrio cholerae* bacteraemia: case report and literature review. Springerplus. 2015;4:575. https://doi.org/10.1186/s40064-015-1346-3

22. Baker-Austin C, Stockley L, Rangdale R, Martinez-Urtaza J. Environmental occurrence and clinical impact of *Vibrio vulnificus* and *Vibrio parahaemolyticus*: a European perspective. Environ Microbiol Rep. 2010;2:7–18. https://doi.org/10.1111/j.1758-2229.2009.00096.x

23. Rippey SR. Infectious diseases associated with molluscan shellfish consumption. Clin Microbiol Rev. 1994;7:419–25. https://doi.org/10.1128/CMR.7.4.419

24. Wong KC, Brown AM, Luscombe GM, Wong SJ, Mendis K. Antibiotic use for *Vibrio* infections: important insights from surveillance data. BMC Infect Dis. 2015;15:226. https://doi.org/10.1186/s12879-015-0959-z

Address for correspondence: Florence Hoefler, Médecine Interne et Maladies Infectieuses, Centre Hospitalier de Troyes, 101 Av Anatole France, 10000 Troyes, France; email: florence.hoefler@hcs-sante.fr

Transmission of SARS-CoV-2 through Floors and Walls of Quarantine Hotel, Taiwan, 2021

Hsin-Yi Wei, Cheng-Ping Chang, Ming-Tsan Liu, Jung-Jung Mu, Yu-Ju Lin, Yu-Tung Dai, Chia-ping Su

We investigated a cluster of SARS-CoV-2 infections in a quarantine hotel in Taiwan in December 2021. The cluster involved 3 case patients who lived in nonadjacent rooms on different floors. They had no direct contact during their stay. By direct exploration of the space above the room ceilings, we found residual tunnels, wall defects, and truncated pipes between their rooms. We conducted a simplified tracer-gas experiment to assess the interconnection between rooms. Aerosol transmission through structural defects in floors and walls in this poorly ventilated hotel was the most likely route of virus transmission. This event demonstrates the high transmissibility of Omicron variants, even across rooms and floors, through structural defects. Our findings emphasize the importance of ventilation and integrity of building structure in quarantine facilities.

Transmission of SARS-CoV-2 through direct, person-to-person contact has been recognized since the early stages of the COVID-19 pandemic (*1*). However, mounting evidence suggests that the virus can be transmitted through the inhalation of virus-laden aerosols (*2,3*). Aerosols are small respiratory particles that can linger in the air and can disperse or travel over a distance of 2 meters under certain circumstances. Such transmission has been reported in restaurants, during a choir rehearsal, and at a bar (*4–6*). The World Health Organization and the US Centers for Disease Control and Prevention have officially acknowledged that aerosol transmission might occur in crowded indoor settings and poorly ventilated spaces (*7,8*).

Taiwan contains the COVID-19 pandemic mainly through tight quarantine measures for inbound travelers. In the weeks leading up to Lunar New Year of 2022 (February 1, 2022), there were strong demands for quarantine hotels because many overseas residents of Taiwan traveled back home. Consequently, many commercial hotels were adapted for use as quarantine hotels, although they were not designed for that purpose. Increased spread of the Omicron variant through aerosol transmission posed great risk for residents of these hotels, despite stringent quarantine measures.

The first outbreak of SARS-CoV-2 in a quarantine hotel in Taiwan was detected in December 2021. The outbreak affected 8 travelers and involved the Delta variant (*9*). Since then, 15 or more clusters of Omicron variant transmission have occurred within quarantine hotels; all clusters were confirmed by whole-genome sequencing (*10,11*). Previous reports in other countries likewise have revealed that aerosol transmission can happen across corridors (*12–14*) and floors (*15–18*) of quarantine hotels and apartments. Nonetheless, the relationship between disease transmission and building structure and ventilation remains largely unexplored.

On December 29, 2021, three cases of COVID-19 associated with a quarantine hotel in northern Taiwan were reported to the Taiwan Centers for Disease Control. The 3 patients stayed in nonadjacent rooms across floors and were diagnosed with COVID-19 during their quarantine period. The Taiwan Centers for Disease Control initiated an investigation to identify the infection source and possible transmission route and to recommend preventive measures.

Methods

Entry Screening and Quarantine Measures in Taiwan
Since December 2020, all travelers entering Taiwan must present a COVID-19 nucleic acid amplification testing report issued within 3 days before boarding a flight (*19*). Since July 2021, testing of a deep-throat saliva specimen for SARS-CoV-2 by reverse transcription PCR (RT-PCR) upon arrival at the airport also has been required (*20*). Because of the influx of inbound

travelers before the Lunar New Year holiday in 2022, all travelers were also required to undergo a 7-day, 10-day, or 14-day quarantine at a quarantine hotel (21). Arriving travelers took a quarantine vehicle to a quarantine hotel or a group quarantine facility. Before the end of the quarantine, travelers were required to undergo another RT-PCR test. Those who tested positive for SARS-CoV-2 were immediately transferred to a designated hospital for isolation.

Case Investigation and Contact Tracing
COVID-19 is a national notifiable disease in Taiwan. All RT-PCR–confirmed cases must be reported to public health sectors. We collected travel histories and laboratory findings for the 3 persons identified as COVID-19 case-patients in a quarantine hotel in northern Taiwan (case A, case B, case C). We defined close contacts as the guests who stayed on the same floor as the 3 case patients during December 22–29, 2021 (the period case B stayed in the hotel), because we believed those guests shared the same air with case B. For contact tracing, all staff workers and other guests in the building underwent a single RT-PCR test at the beginning of the investigation. The close contacts received an additional test at the end of quarantine, and the staff workers received tests every 3 days. We assumed case B to be the primary case because the patient travelled to Taiwan from New York, NY, USA, where active transmission of Omicron variants was occurring.

Investigation of Noncontact Practice
Two senior infection control nurses interviewed the hotel staff and the hotel owner about the compliance criteria that determined the facility's "noncontact" practice and inquired about specific preventative measures for preventing contact between the guests, such as food delivery, garbage collection, and respiratory sampling before the end of quarantine. The nurses also inspected personal protective equipment used at the hotel.

Laboratory Investigation
We conducted whole genome sequencing on all specimens from the 3 case patients using Illumina COVIDSeq Test protocol on the iSeq 100 system (Illumina Inc., https://www.illumina.com) (22). The ARTIC v3 primers produced 98 amplicons and were designed to amplify SARS-CoV-2 virus-specific sequences. We processed the obtained viral sequences using DRAGEN COVID Lineage application version 3.5.5 on Illumina's Basespace cloud analytical system and compared those with Nextclade software (https://clades.nextstrain.org). The median sequence read depth of the 3 samples was ≈4,000×, and ≥30×

coverage achieved >98% sequence coverage. The genomic sequences of the 3 cases in this study were deposited in the GISAID database (https://www.gisaid.org; accession nos. EPI_ISL_13535670, EPI_ISL_13535983, EPI_ISL_13536113). We constructed phylogenetic trees using IQ-TREE software by using the maximum-likelihood method (23). We performed the phylogenetic analysis with sequences from the United States (1,988 viruses), Japan (79 viruses), and China (1 virus) from the same time frame.

Environmental Investigation
We removed all quarantine guests from the building 2 days before the investigation. We checked the structural layout and ventilation system of the building by direct exploration. We observed the partition walls from the access opening. In the mezzanine above the ceiling—preserved for pipes, electrical wires, and air conditioners—we examined the integrity of the walls. We performed a simplified tracer-gas experiment to assess the interconnections between rooms. We detected total volatile organic compounds (TVOC) with an air quality monitor (INKBIRDPlus AK3, https://inkbird.aliexpress.com/) and used a CO_2 sensor (IAQ-CALC Model 7515; TSI Incorporated, https://tsi.com) for validation of CO_2 concentration.

Ethanol (75%) from a spray can of hand sanitizer was used as an indicator. Ethanol is a volatile organic compound and is detectable by the air quality monitor. The volume of a single press of the spray releases ≈0.9 mL of ethanol. To simulate the real situation during the cluster, we turned on the bathroom exhaust fan and the air conditioner of each test room during the experiment. We released ethanol with 10–15 presses in room 510 (case B, suspected index patient) and took measurements in room 610 and room 611 (case A).

Using methods recommended by the World Health Organization (24), we took environmental virus swab specimens for RT-PCR tests to provide supplementary aerosol transmission findings. We took samples in the rooms of the 3 case patients and samples from public areas on the involved floors. We conducted environmental swab sampling on January 1, 2022, eight days after the checkout of case A and 3 days after the checkouts of case B and case C.

Results

Case Investigation and Contact Tracing
The 3 case patients we studied all tested negative by RT-PCR for SARS-CoV-2 within 72 hours before arrival to Taiwan and by deep-throat saliva RT-PCR upon arrival at the airport (Figure 1). None had left
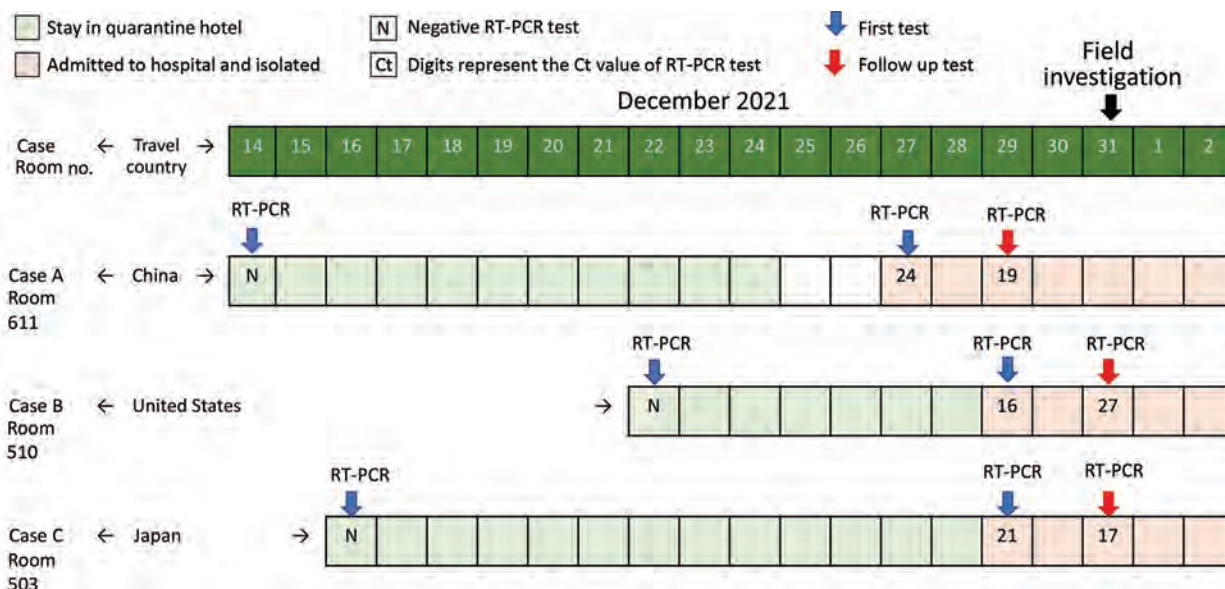
Figure 1. Timeline for Case A, Case B, and Case C in our investigation of aerosol transmission of the SARS-CoV-2 Omicron variant between separate, nonadjacent rooms in a quarantine hotel in Taipei City, Taiwan. Blue arrows indicate the results of the first RT-PCR testing, and red arrows indicate the results of the follow-up RT-PCR testing. The field investigation began on December 31, 2021.

their rooms at any point during the stay in the hotel. No other guest or staff member at the hotel had tested positive since the month prior to the start of the investigation.

Case A arrived in Taiwan from Shenzhen, China, on December 14, 2021, and was admitted to room 611 in the quarantine hotel. He had previously received 2 vaccine doses (Sinopharm, http://www.sinopharm.com); the second dose was given on August 11, 2021. He remained asymptomatic during the quarantine period.

Case B arrived in Taiwan from the United States on December 22, 2021, and was admitted to room 510 in the same quarantine hotel. He had previously received 2 vaccine doses (Pfizer-BioNTech, https://www.pfizer.com); the second dose was given on May 19, 2021. He claimed that he was asymptomatic until December 29, when he began to experience a sore throat.

Case C arrived from Japan on December 16, 2021, and was admitted to room 503. She had previously received 1 vaccine dose (Pfizer BioNTech), which was given on October 25, 2021. She remained asymptomatic during the quarantine period.

Because case A tested positive on December 28, the public health sector arranged RT-PCR tests the next day for hotel guests on the 5th and 6th floors to find the source. Cases B and C tested positive (Ct value for case B was 16; Ct value for case C was 21) on December 29. Both patients were transferred to the hospital for isolation.

All 8 members of the hotel staff had received 2 COVID-19 vaccinations and underwent enhanced surveillance RT-PCR testing every 3 days; each staff member had 5 negative test results after the transmission was recognized. The RT-PCR test results for the 70 other guests who stayed in the hotel during December 22–29, 2021, were all negative. The close contacts (14 guests on the 5th and 6th floors) were asked to quarantine for another 14 days, starting on December 29 (they were relocated to another quarantine hotel), and all tested negative before the end of the quarantine.

Investigation of Noncontact Practice

The quarantine hotel we studied requires staff members to wear personal protection equipment when entering the guest zone (on any floor, except the staff zone on the 1st floor), including gloves, gown, goggles, cap, shoe covers, and a medical mask. There is a trash bin and a chair for meal placement in front of every room. The food delivery and garbage collection are carried out by noncontact means and occur at specific times of the day. Hotel guests are strictly prohibited from having contact with other guests and could exit their rooms only for RT-PCR testing. Guests are instructed to open the door to their rooms only when wearing a mask. They receive advanced notification by phone to take meals into the room and to proceed downstairs for RT-PCR testing by turns to avoid brief encounters with others. A bus designed for respiratory sampling stops at the hotel, as arranged by the public health sector.

Laboratory investigation

We classified the virus sequences of specimens collected from the 3 case patients as the Omicron variant (BA.1.1 lineage). We conducted phylogenetic analysis with genomes from the United States, Japan, and China sampled from the same time frame, which revealed that the sequences of the 3 case patients fell into a subclade close to one from the United States (Figure 2). The sequences of the 3 case patients shared the same 3 unique single-nucleotide polymorphisms and differed by only 2 nucleotides from case A to case B (G17462A, C18877C) and case B to case C (C27874T).

Environmental Investigation

Room and Corridor Air Ventilation

The quarantine hotel we studied is located in downtown Taipei City. The building consists of 7 floors and 24-hour central air conditioning powered by an air-cooled chiller unit on the roof; each room has an independent ceiling-mounted fan coil unit. The air in each room is 100% recirculated; no fresh air is brought in from outside of the building. The bathroom of each room has an exhaust fan that cofunctions with the ceiling lamp. The bathroom exhaust fan outlet terminates to the space above the ceiling and is not ducted outside of the building (Appendix Figure 1, Figure 2, panels A, B, F). Hence, the air extracted by the fan returns to the room and recirculates. There is no high-efficiency particulate air filter and no ventilation system connecting separate rooms and floors. The corridor, room 611 (case A), and room 510 (case B) have no external windows, but room 503 (case C) has a small window that remained shut most of the time. The detected CO_2 concentration in room 510 (case B) was 562 ppm at the beginning of our investigation and 1,040 ppm in the presence of the investigation team (8 persons) after 10 minutes.

Investigation above the Ceiling

We found that partition walls above the ceiling, made of bricks and cement, had defects or gaps, mostly around pipes and electrical wires (Appendix Figure 2, panels B, C). Residual tunnels connected rooms 410 and 411, 510 and 511, 610 and 611, and 503 and 511; these tunnels might have been left when old pipes were removed (Appendix Figure 2, panels D, E, F). We also noted some abandoned and truncated pipes with protruding openings underneath the bottom of the bathtub in room 610 when we checked the ceiling of room 510 (Appendix Figure 2, panels G, H). We also noted some defects located in the partition wall between rooms 503 and 511 (Appendix Figure 2, panel I).

The Tracer-Gas Experiment

Before the tracer-gas experiment, the concentrations of TVOC in the air were extremely low. After the ethanol (75%) was released from room 510, a detectable concentration of TVOC was observed in rooms 610 and 611 (Table).

Environmental Sampling for RT-PCR

We collected a total of 20 specimens from the rooms of the 3 case patients and some public areas, including specimens from the exhaust fans, the air outlets of the fan coil units, the door handles on the corridor side, the spaces above the ceiling of each room, the stair handrail between the 5th and 6th floors, and the elevator buttons. Test results were all negative.

Discussion

We conclude that an episode of SARS-CoV-2 Omicron variant transmission occurred in the quarantine hotel we studied in Taipei City, Taiwan. It was the first domestic cluster of Omicron variant in Taiwan. The case-patients had stayed in different rooms and even on different floors. They had no direct contact with each other during their stay. The Omicron variant is highly transmissible (25–27), so aerosol transmission was the most plausible route in this investigation of what we determined to be a poorly ventilated quarantine hotel. The special setting of this and other quarantine hotels (that is, facilities used to place persons in closed and separated rooms) provided a unique opportunity to see that the highly transmissible Omicron variant can cause infections between floors and through wall defects.

We deduce the primary patient was case B, who was from New York, NY, which at that time had emerging cases related to Omicron. Case A traveled from China and case C traveled from Japan, areas where there was no active transmission of Omicron variants (28–30). The results of serial RT-PCR tests of case B showed decreasing viral loads (Ct 16 to Ct 27), whereas the results for the other 2 case patients showed increasing viral loads, indicating case B was infected earlier than case A and case C. Phylogenetic analysis further supports our assumption of case B as the primary case, revealing a viral genome sequence from case B to be similar to one from the United States (Figure 2).

Room 611 (case A) and room 503 (case C) are not directly adjacent to room 510 (case B). We found truncated pipes above the ceiling in the room 510 bathroom, which might have connected to room 610, and a residual tunnel above the ceiling that might connect room 610 to room 611 (case A). A residual tunnel in
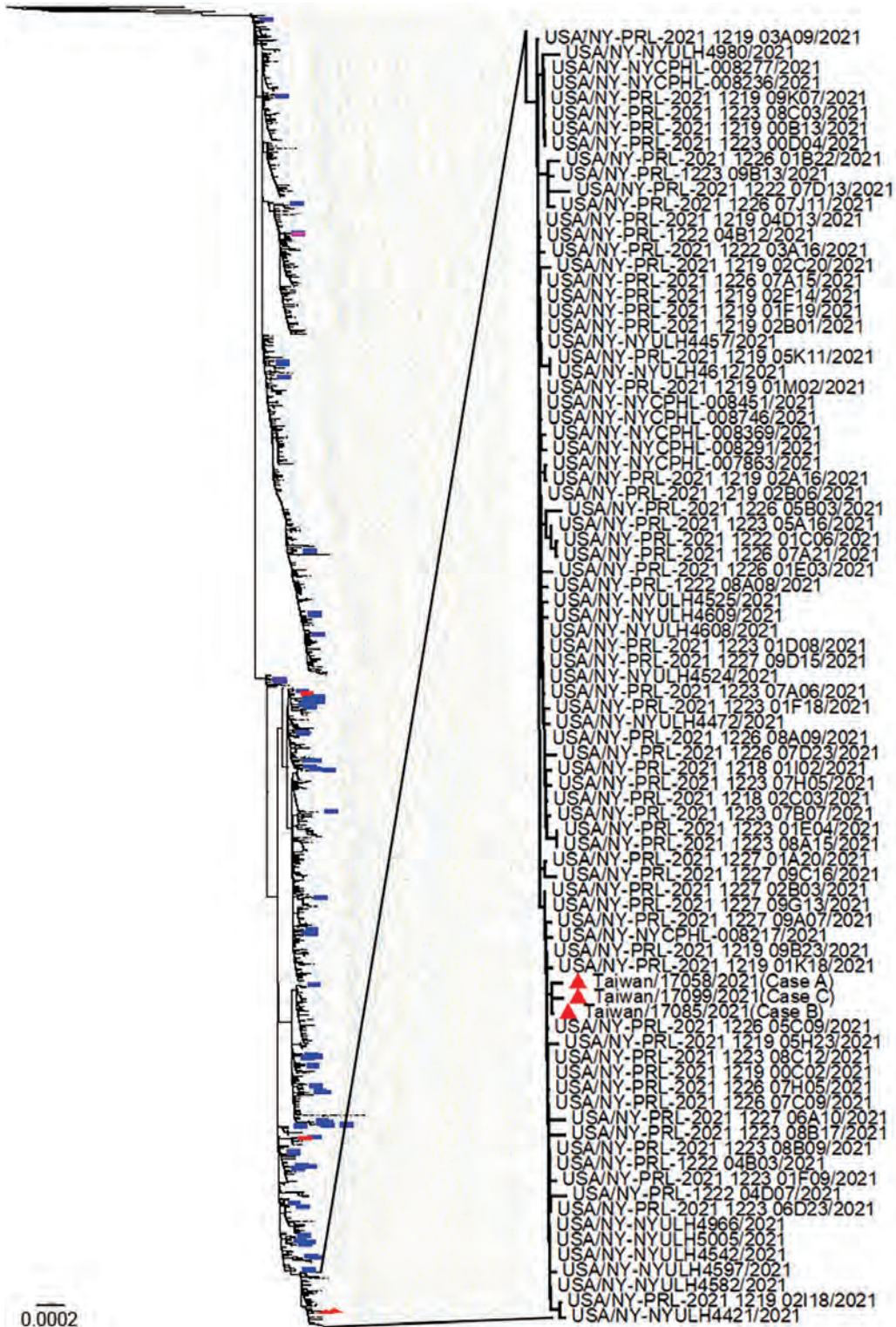
Figure 2. Whole-genome sequencing of SARS-CoV-2 from 3 case patients (indicated with red triangles) who contracted COVID-19 in a quarantine hotel in Taipei City, Taiwan, in December 2021 (GISAID with accession ID EPI_ISL_13535670, 13535983, 13536113). Phylogenetic trees were constructed using IQ-TREE software (http://www.iqtree.org/) by maximum likelihood. The phylogenetic analysis with sequences obtained from the United States (1988 viruses), Japan (79 viruses, blue lines), and China (1 virus, red line) sampled from the same timeframe revealed that sequences of the 3 case patients fell into a subclade close to one from the United States. Scale bar for enlarged tree section indicates substitutions per site.

Table. Concentrations of TVOC measured by detector in specific rooms of a quarantine hotel in Taiwan, December 2021*

Room no.	Baseline TVOC, mg/m^3	Read time from release in room 510, min	TVOC, mg/m^3)
611	0.013	6	0.163
610	0.011	13	0.134
*Ethanol (75%) was used as the indicator for detection of TVOC. TVOC, total volatile organic compounds.			

the same location was also found in the middle of room 510 (case B) and room 511, and another tunnel connected room 511 and room 503 (case C). Because the air conditioners in each room are constantly pushing the air, the airflow carries the virus-laden aerosol. This aerosol might penetrate wall defects or go through old tunnels to reach other rooms (Figure 3), even nonadjacent rooms that appear to be independently isolated. When exhaust fans are not running at the same time (persons usually turn them on only when using the bathroom), it can result in pressure differences between rooms.

In addition to the obvious structural defects we discovered, tiny cracks in walls and ceilings also might have enabled air flow between rooms. To confirm that the wall defects and pipes interconnected the air in each room, we conducted a simplified tracer-gas experiment using methods similar to those used widely by petrochemical and automotive industries. The tracer-gas is released in small quantities into the main body of air to determine if leakage exists in a ventilation system. Previous studies used similar methods to simulate the process of potential transmission through air in 2 communities in China (31,32). Although those researchers chose sulfur hexafluoride, chloroform, and carbon tetrachloride as tracers, we chose ethanol as an index tracer because it is a detectable TVOC that is not harmful to humans and is easily obtained. Our goal was to demonstrate that 2 seemingly independent, closed rooms had hidden interconnections. Because of the lack of background TVOC measurements in rooms 503 and 505, the results were insufficient for comparison. However, we were able to deduce that

the recirculated air transported through room 510 (case B) to room 503 (case C) based on observations in room 510 (case B) and room 611 (case A) during the experiment.

The hotel we studied had no fresh air supply to each room and no open window to the corridor on the guest floor, and the exhaust fan of each bathroom had no discharge tubes, indicating the air exhaled by the guest most likely stayed in the room. Because the concentration of CO_2 could be affected by the number of persons present and their dwelling time, the high CO_2 concentration we measured might reveal a poor ventilation rate but should be interpreted with caution. In the setting of underventilated indoor environments with recirculated air conditioning systems, the exhaled aerosol might remain suspended for a prolonged period and disperse across a long range (2,33,34). It is plausible, then, that a high concentration of virus-laden aerosol might have accumulated in a poorly ventilated room and might have been transported by the airflow across different rooms through the structural defects. Although the air flow might contain only small amounts of virus-laden particles, guests in quarantine stay in recirculated air for >1 week, making the risk of infection a logical possibility.

In Taiwan, at the time of the experiment, there were stringent requirements for hotels applying for quarantine status, such as daily environmental disinfection measures, no-contact service with adequate personal protection equipment, health surveillance, and infection control training programs for all staff members (35). However, there are not yet clear requirements relating to negative pressure capabilities, fresh air supply, full walls to the top, or air purifiers
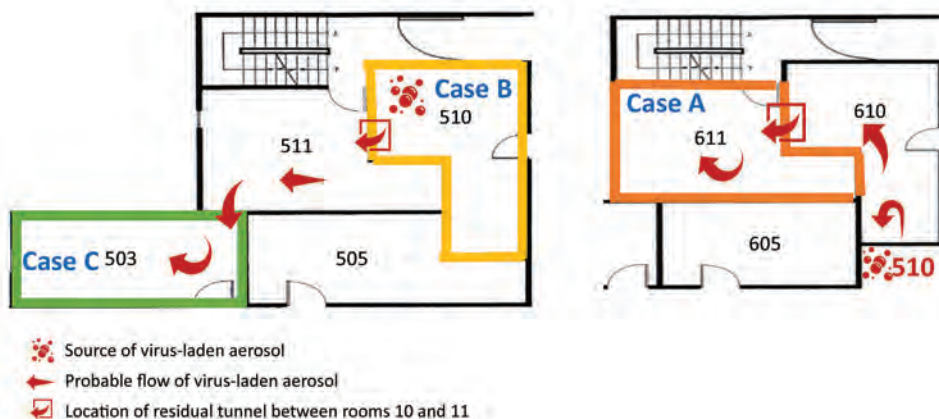
Figure 3. Simulation of probable air flow (arrows), implicating how virus-laden aerosol transported from the room of the primary case to the rooms of secondary cases in a quarantine hotel in Taipei City, Taiwan, December 2021. The bubbles symbol indicates the location of the source of transmission.

- Source of virus-laden aerosol
- Probable flow of virus-laden aerosol
- Location of residual tunnel between rooms 10 and 11

with high-efficiency particulate absorbing filters. As a reference, WHO has published a guide to improve indoor ventilation in the context of COVID-19 (*36*). Local governments in Taiwan have employed experts to carry out a comprehensive inspection of ventilation and air conditioning in all quarantine hotels (*37,38*). The inspection checklist noted some common structural problems: the partition wall of the guest room is not a solid wall to the ceiling, the gap of the pipe through the wall is not fully filled, the rooms have no dedicated supply of outdoor air, and the air from the bathroom leaks to other rooms or the corridor. Preliminary results of that inspection showed that around 25% of inspected hotels were ordered to address problems (*39*). We found almost all these problems in the single hotel we investigated; however, we note this as an extremely rare circumstance in which an unusual aerosol transmission occurred.

The first limitation of our investigation is that the simplified tracer-gas experiment used only 1 air quality monitor: a low-cost, non–research-grade instrument that was not calibrated before the experiment. In addition, TVOCs are ubiquitous in the indoor environment. Other sources of TVOCs in the rooms, including cleaning and beauty products, might interfere with readings. We should have compared the data of this tracer-gas experiment to the background instead of reading the absolute numbers. Second, ethanol is not an optimal surrogate for virus-laden aerosol, because an ethanol molecule is much smaller than a virus particle. The properties of vaporized organic solvent are different from exhaled droplets. The detection of a TVOC does not imply the possibility of virus transmission, but it did reveal structural defects. Third, instead of air sampling for the RT-PCR tests, we took only environmental swab samples to find evidence of virus-laden aerosols lingering in the rooms. Fourth, the capacity of the memory disc of the closed-circuit television video device in the public areas of the hotels was only 4 days, and we did not scrutinize it. Therefore, details such as frequency of door openings were not available.

Our findings support the possibility of SARS-CoV-2 aerosol transmission in a poorly ventilated quarantine hotel, which underscores the importance of ventilation and the integrity of building structure in selecting and approving quarantine facilities. To improve ventilation, a quarantine hotel should maintain a fresh air supply, and the exhaust gas from each quarantine unit must be properly collected and discharged. The building structure of a quarantine facility should be inspected to confirm that there is no gas exchange between units. The ethanol gas tracer test is a harmless, quick, and easy way to check for interconnections between rooms, a method that can be carried out by quarantine hotel personnel to confirm the integrity of rooms without requiring professional instruments or specialized techniques. To further reduce the risk for aerosol transmission in quarantine hotels, we recommend that the public health sector enhance surveillance during the quarantine period for inbound travelers, ensure good indoor ventilation, and promote public acknowledgment of aerosol transmission.

About the Author

Dr. Wei is a medical officer in the Centers for Disease Control, Ministry of Health and Welfare, Taiwan. Her primary interest is infectious disease epidemiology.

References

1. Meyerowitz EA, Richterman A, Gandhi RT, Sax PE. Transmission of SARS-CoV-2: a review of viral, host, and environmental factors. Ann Intern Med. 2021;174:69–79. https://doi.org/10.7326/M20-5008
2. Wang CC, Prather KA, Sznitman J, Jimenez JL, Lakdawala SS, Tufekci Z, et al. Airborne transmission of respiratory viruses. Science. 2021;373:373. https://doi.org/10.1126/science.abd9149
3. Greenhalgh T, Jimenez JL, Prather KA, Tufekci Z, Fisman D, Schooley R. Ten scientific reasons in support of airborne transmission of SARS-CoV-2. Lancet. 2021;397:1603–5. https://doi.org/10.1016/S0140-6736(21)00869-2
4. Li Y, Qian H, Hang J, Chen X, Cheng P, Ling H, et al. Probable airborne transmission of SARS-CoV-2 in a poorly ventilated restaurant. Build Environ. 2021;196:107788. https://doi.org/10.1016/j.buildenv.2021.107788
5. Katelaris AL, Wells J, Clark P, Norton S, Rockett R, Arnott A, et al. Epidemiologic evidence for airborne transmission of SARS-CoV-2 during church singing, Australia, 2020. Emerg Infect Dis. 2021;27:1677–80. https://doi.org/10.3201/eid2706.210465
6. Chau NVV, Hong NTT, Ngoc NM, Thanh TT, Khanh PNQ, Nguyet LA, et al.; OUCRU COVID-19 research group1. Superspreading event of SARS-CoV-2 infection at a bar, Ho Chi Minh City, Vietnam. Emerg Infect Dis. 2021;27:310–4. https://doi.org/10.3201/eid2701.203480
7. U.S. Centers for Disease Control and Prevention. Scientific brief: SARS-CoV-2 transmission. 2021 May 7 [cited 2022 Mar 30]. https://www.cdc.gov/coronavirus/2019-ncov/science/science-briefs/sars-cov-2-transmission.html
8. World Health Organization. Coronavirus disease (COVID-19): how is it transmitted? 2021 December 23 [cited 2022 Mar 30]. https://www.who.int/news-room/q-a-detail/coronavirus-disease-covid-19-how-is-it-transmitted

9. Chiang YC. Taiwan reports two new COVID-19 cases, two quarantine hotel clusters. Focus Taiwan; 2022 Feb 7 [cited 2022 Mar 30]. https://focustaiwan.tw/society/202202070023

10. Chen YT, Chiang YC. COVID-19 cluster confirmed at Taipei quarantine hotel. Focus Taiwan; 2022 Jan 5 [cited 2022 Mar 30]. https://focustaiwan.tw/society/202201050018

11. Taiwan Centers for Disease Control. In response to recent COVID-19 situation, CECC introduces four strengthened measures for quarantine hotels. 2021 Dec 16 [cited 2022 Mar 30]. https://www.cdc.gov.tw/En/Bulletin/Detail/_XgHQMInoUHearurdaaQ9w?typeid=158

12. The Government of the Hong Kong Special Administrative Region Press Release. CHP investigates six cases tested positive for SARS-CoV-2 virus involving Silka Seaview Hotel Hong Kong. 2022 Jan 16 [cited 2022 Mar 30]. https://www.info.gov.hk/gia/general/202201/16/P2022011600615.htm

13. The Government of the Hong Kong Special Administrative Region Press Release. CHP follows up on six cases tested positive and two cases tested preliminarily positive for SARS-CoV-2 virus at Tung Moon House of Tai Hang Tung Estate in Sham Shui Po. 2022 Jan 16 [cited 2022 Mar 30]. https://www.info.gov.hk/gia/general/202201/18/P2022011800692.htm

14. Fox-Lewis A, Williamson F, Harrower J, Ren X, Sonder GJB, McNeill A, et al. Airborne transmission of SARS-CoV-2 Delta variant within tightly monitored isolation facility, New Zealand (Aotearoa). Emerg Infect Dis. 2022;28:501–9. https://doi.org/10.3201/eid2803.212318

15. Gu H, Krishnan P, Ng DYM, Chang LDJ, Liu GYZ, Cheng SSM, et al. Probable Transmission of SARS-CoV-2 Omicron Variant in Quarantine Hotel, Hong Kong, China, November 2021. Emerg Infect Dis. 2022;28:460–2. https://doi.org/10.3201/eid2802.212422

16. Wong SC, Au AKW, Chen H, Yuen LLH, Li X, Lung DC, et al. Transmission of Omicron (B.1.1.529) - SARS-CoV-2 Variant of Concern in a designated quarantine hotel for travelers: a challenge of elimination strategy of COVID-19. Lancet Reg Health West Pac. 2022;18:100360. https://doi.org/10.1016/j.lanwpc.2021.100360

17. Han T, Park H, Jeong Y, Lee J, Shon E, Park M-S, et al. COVID-19 cluster linked to aerosol transmission of SARS-CoV-2 via floor drains. J Infect Dis. 2022;225:1554–60.

18. Hwang SE, Chang JH, Oh B, Heo J. Possible aerosol transmission of COVID-19 associated with an outbreak in an apartment in Seoul, South Korea, 2020. Int J Infect Dis. 2021;104:73–6. https://doi.org/10.1016/j.ijid.2020.12.035

19. Taiwan Centers for Disease Control. Travelers must present a COVID-19 RT-PCR test report issued within 3 days prior to boarding. 2021 Dec 2 [cited 2022 Mar 30]. https://www.cdc.gov.tw/File/Get/HCnZqyduepixUPeaSmUAtw

20. Taiwan Centers for Disease Control. In response to spread of Delta variant globally, Taiwan to tighten health monitoring measures for people entering Taiwan via airport/port starting 12:00 pm on July 2. 2021 Jul 1 [cited 2022 Mar 30]. https://www.cdc.gov.tw/En/Bulletin/Detail/FEq_1cKkRDoHZTPRTAGgDQ?typeid=158

21. Taiwan Centers for Disease Control. In response to influx of inbound travelers before Lunar New Year holiday, CECC explains three options to undergo quarantine during holiday for arrivals. 2021 November 11 [cited 2022 Mar 30]. https://www.cdc.gov.tw/En/Bulletin/Detail/OOwZHFMJKdRtZHrZH9CbgA?typeid=158

22. Goswami C, Sheldon M, Bixby C, Keddache M, Bogdanowicz A, Wang Y, et al. Identification of SARS-CoV-2 variants using viral sequencing for the Centers for Disease Control and Prevention genomic surveillance program. BMC Infect Dis. 2022;22:404. https://doi.org/10.1186/s12879-022-07374-7

23. Minh BQ, Schmidt HA, Chernomor O, Schrempf D, Woodhams MD, von Haeseler A, et al. IQ-TREE 2: New models and efficient methods for phylogenetic inference in the genomic era. Mol Biol Evol. 2020;37:1530–4. https://doi.org/10.1093/molbev/msaa015

24. World Health Organization. Surface sampling of Coronavirus disease (COVID-19): a practical "how to" protocol for health care and public health professionals. 2020 Feb 18 [cited 2022 Mar 30]. https://www.who.int/publications/i/item/surface-sampling-of-coronavirus-disease-(-covid-19)-a-practical-how-to-protocol-for-health-care-and-public-health-professionals

25. World Health Organization. Enhancing response to Omicron SARS-CoV-2 variant. 2022 Jan 21 [cited 2022 Mar 30]. https://www.who.int/publications/m/item/enhancing-readiness-for-omicron-(b.1.1.529)-technical-brief-and-priority-actions-for-member-states

26. UK Health Security Agency. Omicron daily overview: 2021 December 31 [cited 2022 Mar 30]. https://assets.publishing.service.gov.uk/government/uploads/system/uploads/attachment_data/file/1044522/20211231_OS_Daily_Omicron_Overview.pdf

27. Willett BJ, Grove J, MacLean OA, Wilkie C, Logan N, Lorenzo GD, et al. The hyper-transmissible SARS-CoV-2 Omicron variant exhibits significant antigenic change, vaccine escape and a switch in cell entry mechanism. Nat Microbiol 2022;7:1161–1179. https://doi.org/10.1038/s41564-022-01143-7

28. U.S. Centers for Disease Control and Prevention. Potential rapid increase of Omicron variant infections in the United States. 2021 Dec 20 [cited 2022 Mar 30]. https://www.cdc.gov/coronavirus/2019-ncov/science/forecasting/mathematical-modeling-outbreak.html

29. National Institute of Infectious Diseases. About the variant strain B.1.1.529 strain (Omicron strain) of SARS-CoV-2 (5th report). 2021 Dec 31 [cited 2022 Mar 30]. https://www.niid.go.jp/niid/ja/2019-ncov/2551-cepr/10876-sars-cov-2-b-1-1-529.html

30. The State Council, The People's Republic of China. The latest news on epidemic prevention and control on January 17. 2022 Jan 17 [cited 2022 Mar 30]. http://www.gov.cn/fuwu/2022-01/17/content_5668987.htm

31. Lin G, Zhang S, Zhong Y, Zhang L, Ai S, Li K, et al. Community evidence of severe acute respiratory syndrome coronavirus 2 (SARS-CoV-2) transmission through air. Atmos Environ (1994). 2021 Feb 1;246:118083. https://doi.org/10.1016/j.atmosenv.2020.118083 PMID: 33235537

32. Hong Kong Department of Health. Outbreak of severe acute respiratory syndrome (SARS) at Amoy Gardens, Kowloon Bay, Hong Kong main findings of the investigation. 2003 Apr 17 [cited 2022 Jul 13]. https://www.info.gov.hk/info/sars/pdf/amoy_e.pdf

33. Parienta D, Morawska L, Johnson GR, Ristovski ZD, Hargreaves M, Mengersen K, et al. Theoretical analysis of the motion and evaporation of exhaled respiratory droplets of mixed composition. J Aerosol Sci. 2011;42:1–10. https://doi.org/10.1016/j.jaerosci.2010.10.005

34. Hinds WC. Aerosol technology: properties, behavior, and measurement of airborne particles. New York: John Wiley & Sons; 1999.

35. Taiwan Centers for Disease Control. COVID-19 response guidelines: accommodation and management for quarantine hotel. 2021 December 27 [cited 2022 Mar 30].

https://www.cdc.gov.tw/File/Get/tUZdQJktoBVY
yMUUkM4GQQ

36. World Health Organization. Roadmap to improve and ensure good indoor ventilation in the context of COVID-19. 2021 March 1 [cited 2022 Mar 30]. https://www.who.int/publications/i/item/9789240021280

37. Taiwan Centers for Disease Control. In response to recent COVID-19 situation, CECC introduces four strengthened measures for quarantine hotels. 2021 December 16 [cited 2022 Sep 14]. https://www.cdc.gov.tw/En/Bulletin/Detail/_XgHQMInoUHearurdaaQ9w?typeid=158

38. Institute of Labor, Occupational Safety and Health, Ministry of Labor. Inspection manual of ventilation and air conditioning in epidemic prevention hotels [in Chinese]. 2022 January 3 [cited 2022 Sep 20]. https://laws.ilosh.gov.tw/ioshcustom/report/report-06?id=e37e3c08-92d1-4202-89a2-ed07e779efc9

39. Central News Agency. CECC reports 40 imported, three domestic cases. Taipei Times. 2022 Jan 7 [cited 2022 Sep 14]. https://news.ltn.com.tw/news/focus/breakingnews/3792815

Address for correspondence: Chia-ping Su, Taiwan Centers for Disease Control, No. 6, Linsen S Rd, Jhongjheng District, Taipei City 10050, Taiwan. email: cpsu@cdc.gov.tw

February 2022
Vectorborne Infections

- Viral Interference between Respiratory Viruses
- Novel Clinical Monitoring Approaches for Reemergence of Diphtheria Myocarditis, Vietnam
- Clinical and Laboratory Characteristics and Outcome of Illness Caused by Tick-Borne Encephalitis Virus without Central Nervous System Involvement
- Role of *Anopheles* Mosquitoes in Cache Valley Virus Lineage Displacement, New York, USA
- Burden of Tick-Borne Encephalitis, Sweden
- Invasive *Burkholderia cepacia* Complex Infections among Persons Who Inject Drugs, Hong Kong, China, 2016–2019
- Comparative Effectiveness of Coronavirus Vaccine in Preventing Breakthrough Infections among Vaccinated Persons Infected with Delta and Alpha Variants
- Effectiveness of mRNA BNT162b2 Vaccine 6 Months after Vaccination among Patients in Large Health Maintenance Organization, Israel
- Comparison of Complications after Coronavirus Disease and Seasonal Influenza, South Korea
- Rapid Spread of Severe Fever with Thrombocytopenia Syndrome Virus by Parthenogenetic Asian Longhorned Ticks
- Wild Boars as Reservoir of Highly Virulent Clone of Hybrid Shiga Toxigenic and Enterotoxigenic *Escherichia coli* Responsible for Edema Disease, France
- Public Acceptance of and Willingness to Pay for Mosquito Control, Texas, USA
- Epidemiology of Hospitalized Patients with Babesiosis, United States, 2010–2016
- West Nile Virus Transmission by Solid Organ Transplantation and Considerations for Organ Donor Screening Practices, United States
- Serial Interval and Transmission Dynamics during SARS-CoV-2 Delta Variant Predominance, South Korea
- Postvaccination Multisystem Inflammatory Syndrome in Adult with No Evidence of Prior SARS-CoV-2 Infection
- Tonate Virus and Fetal Abnormalities, French Guiana, 2019
- Widespread Detection of Multiple Strains of Crimean-Congo Hemorrhagic Fever Virus in Ticks, Spain
- SARS-CoV-2 Seroprevalence before Delta Variant Surge, Chattogram, Bangladesh, March–June 2021
- SARS-CoV-2 B.1.619 and B.1.620 Lineages, South Korea, 2021
- *Neisseria gonorrhoeae* FC428 Subclone, Vietnam, 2019–2020
- Zoonotic Infection with Oz Virus, a Novel Thogotovirus
- SARS-CoV-2 Cross-Reactivity in Prepandemic Serum from Rural Malaria-Infected Persons, Cambodia
- *Babesia crassa*–Like Human Infection Indicating Need for Adapted PCR Diagnosis of Babesiosis, France
- Clinical Features and Neurodevelopmental Outcomes for Infants with Perinatal Vertical Transmission of Zika Virus, Colombia
- SARS-CoV-2 Circulation, Guinea, March 2020–July 2021
- Probable Transmission of SARS-CoV-2 Omicron Variant in Quarantine Hotel, Hong Kong, China, November 2021
- Seroprevalence of SARS-Cov-2 Antibodies in Adults, Arkhangelsk, Russia
- Ulceroglandular Infection and Bacteremia Caused by *Francisella salimarina* in Immunocompromised Patient, France
- Surveillance of Rodent Pests for SARS-CoV-2 and Other Coronaviruses, Hong Kong

EMERGING INFECTIOUS DISEASES®

To revisit the February 2022 issue, go to:
https://wwwnc.cdc.gov/eid/articles/issue/28/2/table-of-contents

Iceland as Stepping Stone for Spread of Highly Pathogenic Avian Influenza Virus between Europe and North America

Anne Günther,[1] Oliver Krone,[1] Vilhjalmur Svansson,[1] Anne Pohlmann, Jacqueline King,
Gunnar Thor Hallgrimsson, Kristinn Haukur Skarphéðinsson, Heiða Sigurðardóttir,
Stefán Ragnar Jónsson, Martin Beer, Brigitte Brugger, Timm Harder

Highly pathogenic avian influenza viruses (HPAIVs) of hemagglutinin type H5 and clade 2.3.4.4b have widely spread within the northern hemisphere since 2020 and threaten wild bird populations, as well as poultry production. We present phylogeographic evidence that Iceland has been used as a stepping stone for HPAIV translocation from northern Europe to North America by infected but mobile wild birds. At least 2 independent incursions of HPAIV H5N1 clade 2.3.4.4b assigned to 2 hemagglutinin clusters, B1 and B2, are documented for summer–autumn 2021 and spring 2022. Spread of HPAIV H5N1 to and among colony-breeding pelagic avian species in Iceland is ongoing. Potentially devastating effects (i.e., local losses >25%) on these species caused by extended HPAIV circulation in space and time are being observed at several affected breeding sites throughout the North Atlantic.

Potentially zoonotic highly pathogenic avian influenza (HPAI) viruses (HPAIVs) of subtype hemagglutinin (HA) 5 (H5) emerged from a domestic geese flock in southern China in the mid-1990s. Since then, descendants of this so-called goose/Guangdong (gs/GD) lineage have continued to circulate, evolved into various clades, and formed a plethora of subgenotypes and genotypes that threaten poultry production worldwide (1,2). Because of repeated incursions from poultry into migratory aquatic wild bird populations in Asia, these viruses have spread, since 2005, in several waves westward and southward across Eurasia, into Africa and eastward, through the Bering strait, into North America. Infected but mobile migratory birds aided in linking geographically widely separated areas along overlapping flyways; palearctic breeding areas were serving as an additional link between Eurasia and America during 2014 (3,4).

Because Europe was facing the most severe HPAIV epizootics in the influenza winter seasons of 2020–21 and 2021–22 in terms of case numbers and genetic diversity of characterized viruses (5,6), concerns about spread to North America, this time by westward virus spread, were renewed. By December 2021, HPAI H5N1 detection in wild birds in Canada was reported, followed by numerous additional wild bird cases and incursions into poultry holdings along the eastern coastline of the United States (7,8). Phylogenetic analyses of the viruses in North America confirmed a close relationship to HPAIV H5N1 genotypes from Europe (7–9). Although the outcomes of the transatlantic HPAIV transfer are evident, the steps taken by the virus to cross the Atlantic are not. We present data supporting HPAIV transfer from Europe to North America by bird migration through Iceland.

Incursion of HPAIV H5N1 into Iceland

Although low pathogenicity avian influenza virus (AIV) strains have been detected in sea birds around Iceland (10,11), outbreaks of HPAIV were not reported from Iceland until spring 2022. However, retrospective screening of wild bird samples from

Author affiliations: Friedrich-Loeffler-Institute, Greifswald–Insel Riems, Germany (A. Günther, A. Pohlmann, J. King, M. Beer, T. Harder); Leibniz Institute for Zoo and Wildlife Research, Berlin, Germany (O. Krone); University of Iceland, Reykjavik, Iceland (V. Svansson, G.T. Hallgrimsson, H. Sigurðardóttir, S.R. Jónsson); Icelandic Institute of Natural History, Garðabær, Iceland (K.H. Skarphéðinsson); Icelandic Food and Veterinary Authority, Selfoss, Iceland (B. Brugger)

[1]These authors contributed equally to this article.

Iceland showed that an HPAI case was in a juvenile white-tailed sea eagle (*Haliaeetus albicilla*) found dead in the southern Westfjords, Iceland, during October 2021 (*12*). This bird had been equipped with a satellite transmitter (global positioning system/global system for mobile communications) as a nestling on July 24, 2021. After fledging on August 11, 2021, the eagle stayed in the nesting area of its parents and moved within a range of 1.6 km² (95% minimum complex polygon) for ≈2 months. The juvenile eagle died at the shore of the region in Iceland on October 8, 2021, and was kept frozen until necropsy in the spring of 2022.

Postmortem examination showed a female weighing 5,540 g that had extensive subcutaneous and body cavity fat tissue indicating a good nutritional condition. Gross pathologic alterations (fibrinous pericarditis, swollen hyperemic liver, spleen, and kidneys) were indicative of a severe infectious disease, which led to an acute death of the young eagle. We analyzed organ samples for AIV by using quantitative reverse transcription PCR as described (*13*). HPAIV of subtype H5N1 was found at high viral loads in all tissue samples examined, including the brain (cycle threshold 16.2).

Despite an appeal from the veterinary authorities in Iceland to the general public to report finding of sick or dead wild birds, only 17 birds came to be sampled and AIV was tested in the first 9 months of 2021, and all samples were AIV negative. In the beginning of 2022, the veterinary authorities in Iceland enhanced passive surveillance through reports from the public of sick or dead wild birds. In mid-April, a common raven (*Corvus corax*) and a pink-footed goose (*Anser brachyrhynchus*) tested HPAIV H5N1 positive. In addition, in the same period, a northern gannet (*Morus bassanus*) tested positive for H5N1, but HPAI could not be confirmed. The raven was found on a farm in southern Iceland where 6 days later a backyard chicken flock on the same farm showed abruptly increased mortality rate, and chicken carcasses tested HPAIV H5N1 positive. Consequently, public awareness and reporting of dead wild birds increased markedly after a press release on these first findings.

From April 2022 onward, including the already identified wild birds, HPAIV H5N1 was detected in 21 wild birds from 10 species: northern gannets (n = 7), European herring gull (*Larus argentatus*) (n = 2), great black-backed gull (*Larus marinus*) (n = 2), great skua (*Stercorarius skua*) (n = 2), greylag goose (*Anser anser*) (n = 2), pink-footed goose (n = 2), barnacle goose (*Branta leucopsis*) (n = 1), black-headed gull (*Chroicocephalus ridibundus*) (n = 1), common raven (n = 1), and lesser black-backed gull (*Larus fuscus*) (n =

1). Because in 1 sample from a northern gannet, neuraminidase 1 could not be confirmed, the bird was reported as positive for HPAIV H5Nx (last updated on June 21, 2022).

Phylogeographic Identification of ≥2 Virus Introduction Events

We performed direct MinION (Oxford Nanopore Technologies, https://nanoporetech.com) full-genome sequencing as described (*5*) for 3 samples from Iceland (2022AI02104: white-tailed eagle, brain tissues; 2022AI02564 and 2022AI02565: backyard chickens, oropharyngeal swab specimens) that were immediately available for analysis and showed high viral loads. Presence of HPAIV H5N1 of clade 2.3.4.4b was confirmed. Phylogenetic and phylogeographic analyses of the genomes (Appendix, https://wwwnc.cdc.gov/EID/article/28/12/22-1086-App1.pdf) and associated data (*14*) showed close relationships to HPAIV H5N1 viruses from Europe and North America, grouping in 2 different HA clusters (B1 and B2) recently defined in clade 2.3.4.4b viruses from Europe (Figure 1) (*6,15–18*).

Those findings point to ≥2 independent incursions into Iceland. The sequence from Iceland isolated during 2021 clusters in the B1 HA cluster between sequences from countries in northern Europe (the Netherlands, Ireland) and sequences from Canada and eastern coastal states of the United States (Figure 2). Analyses of concatenated genome sequences showed no evidence of reassortment with other AIV strains currently or recently circulating in Europe. Time-scaled phylogenetic analyses and inferred phylogeography (Figures 1, 2) demonstrate the circulation of similar viruses of the B1 HA cluster in northern Europe from the winter of 2020 to spring and summer of 2021 (*6*), and point toward viral spread from locations on the British Isles to Iceland and from there onwards to Canada and eastern coast of the United States.

White-tailed sea eagles are known to be a resident bird species in Iceland, and introduction of virus with this species is highly unlikely. Instead, the white-tailed sea eagle infection is likely caused by feeding of the eagle on infected, therefore weakened, prey or scavenging on carcasses, as described for raptor species (*19*). Some of the contemplable prey species of the taxonomic orders of *Anseriformes* or *Charadriiformes*, including geese, gulls and waders, are known to migrate from the British Isles and the North Sea region and are confirmed to have been infected in spring and early summer of 2021 in their overwintering areas (*20–22*). Iceland is situated along overlapping flyways that connect the Eastern and Western Hemispheres,

and it has been suggested that Iceland connects virus movements between mainland Europe and North America (*7–11,23*).

In addition, HPAIV H5N1 genomes from 2 chickens dying in a backyard farm on Iceland during April 2022 were sequenced and could be traced back to a second, independent incursion featuring viruses of HA cluster B2. Inferred phylogeographic analysis showed that viruses collected in northern Asia were a possible source of this second introduction into central Europe and further spread throughout the continent (*6*). The Iceland chicken sequences cluster between viruses of HA cluster B2 collected from the British Islands and Ireland during the winter of 2021/2022 (Figures 1, 2). Viruses of this HA cluster (B2) have not been detected in North America to date.

Epidemiologic, Conservational, and Public Health Concerns of Expanded HPAIV Circulation

Our data provide evidence for 2 translocation events of HPAIV H5N1 clade 2.3.4.4b viruses from central Europe through the British Isles into Iceland observed during October 2021 with a most recent ancestor in summer 2021 (most recent common ancestor 2021.5). Onward transmission to Newfoundland and possibly additional regions in the North Atlantic raises several concerns.

Large breeding colonies of pelagic bird species, such as puffins, northern gannets, and kittiwakes are located along the coasts of the North Atlantic. Confirmed HPAIV H5N1 infection in 9/12 gannet carcasses and daily public reporting of sick and dead gannets in the Reykjanes Peninsula, Iceland, since beginning of April 2022 underline that these colonies are now in danger of HPAIV H5 outbreaks of larger scale, which might affect the continuity of these local populations. Concerns extend to local populations of species with narrowly circumscribed breeding/resting ranges in the North Atlantic region such as great skua, long-tailed skua, red knots, pink-footed geese, and barnacle geese, as well as birds of prey exposed during opportunistic scavenging (e.g., white-tailed sea eagles and great skuas) and active hunting of weakened, infected prey (e.g., gyrfalcons [*Falco rusticolus*]). Therefore, enhanced passive surveillance should focus on such spots and scavenging and colony-breeding species.
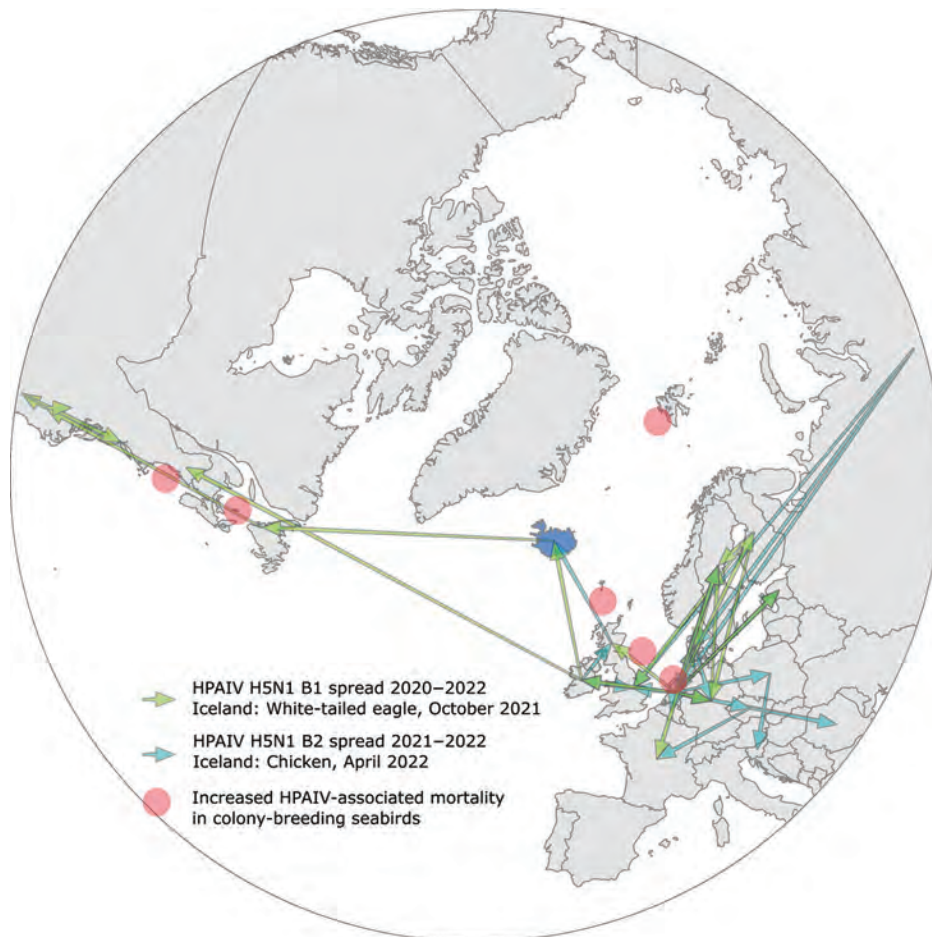
Figure 1. Polar map view of the palearctic and nearctic realm, and inferred spread of hemagglutinin clusters B1 and B2 of highly pathogenic avian influenza viruses (HPAIVs), subtype, clade 2.3.4.4b and their incursion routes to Iceland (blue) during 2021 (green arrows) and 2022 (turquoise arrows). Red dots indicate geographic locations where current (summer 2022) HPAIV-associated mass deaths in pelagic or colony-breeding seabirds have been reported. Data from were obtained from various sources (*15–18*).

HPAIV H5N1 B1 spread 2020–2022
Iceland: White-tailed eagle, October 2021

HPAIV H5N1 B2 spread 2021–2022
Iceland: Chicken, April 2022

Increased HPAIV-associated mortality in colony-breeding seabirds
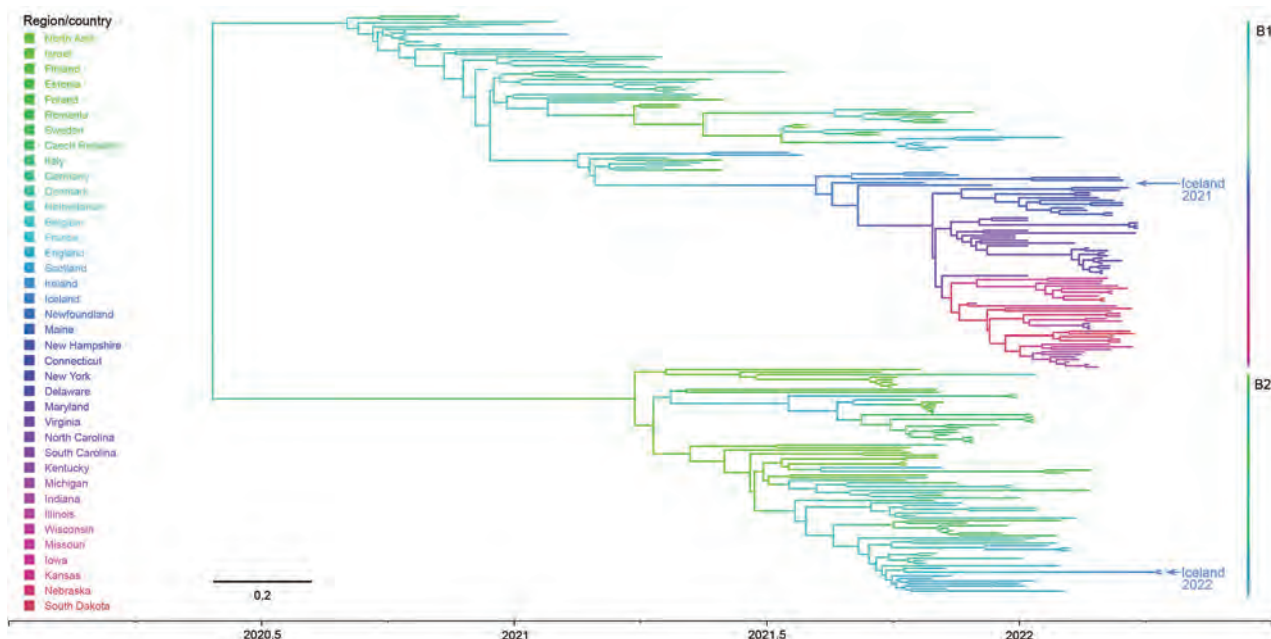
Figure 2. Phylogeographic tree of highly pathogenic avian influenza viruses. Taxa are colored according to their country of origin, and countries are arranged in geographic order from east to west. Arrows indicate viral genomes during 2021 and 2022 in Iceland and assigned to different hemagglutinin clusters B1 and B2. Method hints and basic data are presented in Hassan et al. (*13*). Scale bar indicates nucleotide substitutions per site.

The massively extended circulation in space and time of recent HPAIV H5N1 clade 2.3.4.4b viruses in migratory wild birds in the North Atlantic will further threaten endangered species. Grossly increased mortality rates for colonies of northern gannets and several tern species are being observed at several breeding sites throughout the North Atlantic (Figure 2). The most recent incursion of these viruses into wider palearctic areas of the Atlantic will inevitably lead to viral contamination of northern breeding habitats where ambient conditions prevail that are considered favorable for a prolonged retainment of viral infectivity outside avian hosts (*23,24*).

Increased alertness should now also extend to the Southern Hemisphere. In the 2 reported incursion events of gs/GD HPAI viruses into North America by migrating wild birds, during 2014 and 2021/2022, virus spread along the Pacific (2014) and the Atlantic coastline (2021) from north to south and further inland affecting wild birds and poultry in Canada, as well as in most of the United States (*7–9*). However, for unknown reasons, spread seems to be interrupted between North America and South America because no incursions had been reported during 2014/2015 or since 2021 from the Caribbean region and South America.

Similar observations have been made along the east side of the Pacific Ocean. Despite endemic presence of gs/GD HPAIV in several regions of Southeast Asia, and frequent incursions into migratory wild bird populations, cases have so far not been reported from Australia/Oceania (*4*). It is only at the most southern tip of Africa that gs/GD-like HPAIVs have reached and stayed within the Southern Hemisphere. However, this bridgehead of the virus might put geographically sequestrated subantarctic species, such as penguins and albatrosses, or the highly endangered avifauna of New Zealand at increased risk for exposure.

In conclusion, as shown by the rapid and devastating spread of HPAIV H5N1 through poultry holdings in North America after primary incursions from infected wild birds (*10*), the avian–human interface has expanded again. Infections in 1 human (*25*) and in several terrestrial scavenging carnivores, such as foxes, skunks, and raccoons (*12*), illustrate the increased risk for spillover transmissions.

About the Author

Dr. Guenther is a veterinarian and a doctoral candidate at the Friedrich-Loeffler-Institute, Greifswald–Insel Riems, Germany. Her primary research interests are avian viruses and other pathogens with potential influence on avian species conservation and public health.

References

1. Lee DH, Criado MF, Swayne DE. Pathobiological origins and evolutionary history of highly pathogenic avian influenza viruses. Cold Spring Harb Perspect Med. 2021;11:a038679. https://doi.org/10.1101/cshperspect.a038679
2. Dhingra MS, Artois J, Dellicour S, Lemey P, Dauphin G, Von Dobschuetz S, et al. Geographical and historical patterns in the emergences of novel highly pathogenic avian influenza (HPAI) H5 and H7 viruses in poultry. Front Vet Sci. 2018;5:84. https://doi.org/10.3389/fvets.2018.00084
3. Lee DH, Torchetti MK, Winker K, Ip HS, Song CS, Swayne DE. Intercontinental spread of Asian-origin H5N8 to North America through Beringia by migratory birds. J Virol. 2015;89:6521–4. https://doi.org/10.1128/JVI.00728-15
4. Global Consortium for H5N8 and Related Influenza Viruses. Role for migratory wild birds in the global spread of avian influenza H5N8. Science. 2016;354:213–7. https://doi.org/10.1126/science.aaf8852
5. King J, Harder T, Globig A, Stacker L, Günther A, Grund C, et al. Highly pathogenic avian influenza virus incursions of subtype H5N8, H5N5, H5N1, H5N4, and H5N3 in Germany during 2020–21. Virus Evol. 2022;8:veac025. doi: 10.1093/ve/veac035. eCollection 2022.
6. Pohlmann A, King J, Fusaro A, Zecchin B, Banyard AC, Brown IH, et al. Has epizootic become enzootic? Evidence for a fundamental change in the infection dynamics of highly pathogenic avian influenza in Europe, 2021. MBio. 2022;June 21:e0060922. https://doi.org/10.1128/mbio.00609-22
7. Caliendo V, Lewis NS, Pohlmann A, Baillie SR, Banyard AC, Beer M, et al. Transatlantic spread of highly pathogenic avian influenza H5N1 by wild birds from Europe to North America in 2021. Sci Rep. 2022;12:11729. https://doi.org/10.1038/s41598-022-13447-z
8. US Department of Agriculture, Animal and Plant Health Inspection Service. Detections of highly pathogenic avian influenza in wild birds. 2022 [cited 2022 Aug 4]. https://www.aphis.usda.gov/aphis/ourfocus/animal-health/animal-disease-information/avian/avian-influenza/hpai-2022/2022-hpai-wild-birds
9. Bevins SN, Shriner SA, Cumbee JC Jr, Dilione KE, Douglass KE, Ellis JW, et al. Intercontinental movement of highly pathogenic avian influenza A(H5N1) clade 2.3.4.4 virus to the United States, 2021. Emerg Infect Dis. 2022;28:1006–11. https://doi.org/10.3201/eid2805.220318
10. Gass JD Jr, Kellogg HK, Hill NJ, Puryear WB, Nutter FB, Runstadler JA. Epidemiology and ecology of influenza A viruses among wildlife in the Arctic. Viruses. 2022;14:1531. https://doi.org/10.3390/v14071531
11. Dusek RJ, Hallgrimsson GT, Ip HS, Jónsson JE, Sreevatsan S, Nashold SW, et al. North Atlantic migratory bird flyways provide routes for intercontinental movement of avian influenza viruses. PLoS One. 2014;9:e92075. https://doi.org/10.1371/journal.pone.0092075
12. Adlhoch C, Fusaro A, Gonzales JL, Kuiken T, Marangon S, Niqueux É, et al.; European Food Safety Authority. European Centre for Disease Prevention and Control; European Union Reference Laboratory for Avian Influenza. Avian influenza overview March–June 2022. EFSA J. 2022;20:e07415.
13. Hassan KE, Ahrens AK, Ali A, El-Kady MF, Hafez HM, Mettenleiter TC, et al. Improved subtyping of avian influenza viruses using an RT-qPCR-based low density array: 'Riems Influenza a Typing Array', Version 2 (RITA-2). Viruses. 2022;14:415. https://doi.org/10.3390/v14020415
14. Pohlmann A. Iceland as stepping stone for intercontinental spread of highly pathogenic avian influenza H5N1 virus between Europe and North America: data set on phylogeographic analysis, 2022 [cited 2022 Aug 17]. https://doi.org/10.5281/zenodo.6638282
15. The Guardian. The scale is hard to grasp: avian flu wrecks devastation on sea birds [cited 2022 Oct 18]. https://www.theguardian.com/environment/2022/jul/20/avian-flu-h5n1-wreaks-devastation-seabirds-aoe
16. Norwegian Veterinary Institute. Avian influenza detected on Svalbard [cited 2022 Oct 18]. https://www.vetinst.no/en/news/avian-influenza-detected-on-svalbard
17. Columbia Broadcasting System. Avian flu responsible for thousands of dead birds in Newfoundland, suggest preliminary tests [cited 2022 Oct 18]. https://www.cbc.ca/news/canada/newfoundland-labrador/avian-flu-newfoundland-1.6529433
18. Audubon. Avian flu threatens seabird nesting colonies on both sides of the Atlantic [cited 2022 Oct 18]. https://www.audubon.org/news/avian-flu-threatens-seabid-nesting-colonies-both-sides-atlantic
19. Krone O, Globig A, Ulrich R, Harder T, Schinköthe J, Herrmann C, et al. White-tailed sea eagle (Haliaeetus albicilla) die-off due to infection with highly pathogenic avian influenza virus, subtype H5N8, in Germany. Viruses. 2018;10:478. https://doi.org/10.3390/v10090478

20. Lean FZ, Vitores AG, Reid SM, Banyard AC, Brown IH, Núñez A, et al. Gross pathology of high pathogenicity avian influenza virus H5N1 2021–2022 epizootic in naturally infected birds in the United Kingdom. One Health. 2022;14:100392. https://doi.org/10.1016/j.onehlt.2022.100392

21. Loeb J. Scottish seabirds hit by avian influenza. Vet Rec. 2022;190:488. https://doi.org/10.1002/vetr.1915

22. Banyard AC, Lean FZ, Robinson C, Howie F, Tyler G, Nisbet C, et al. Detection of highly pathogenic avian influenza virus H5N1 clade 2.3.4.4b in Great Skuas: a species of conservation concern in Great Britain. Viruses. 2022;14:212. https://doi.org/10.3390/v14020212

23. Hill NJ, Bishop MA, Trovão NS, Ineson KM, Schaefer AL, Puryear WB, et al. Ecological divergence of wild birds drives avian influenza spillover and global spread. PLoS Pathog. 2022;18:e1010062. https://doi.org/10.1371/journal.ppat.1010062

24. Stallknecht DE, Goekjian VH, Wilcox BR, Poulson RL, Brown JD. Avian influenza virus in aquatic habitats: what do we need to learn? Avian Dis. 2010;54(Suppl):461–5. https://doi.org/10.1637/8760-033109-Reg.1

25. Centers for Disease Control and Prevention. U.S. case of human avian influenza A(H5) virus reported. 2022 [cited 2022 Jul 7]. https://www.cdc.gov/media/releases/2022/s0428-avian-flu.html

Address for correspondence: Timm Harder, Institute of Diagnostic Virology, Friedrich-Loeffler-Institut, Südufer 10, 17493 Greifswald–Insel Riems, Germany; e-mail: timm.harder@fli.de

---

March 2022

Mycobacterial Infections

EMERGING INFECTIOUS DISEASES

To revisit the March 2022 issue, go to:

Systematic Review and Meta-analysis of Lyme Disease Data and Seropositivity for *Borrelia burgdorferi*, China, 2005–2020

James H. Stark, Xiuyan Li, Ji Chun Zhang, Leah Burn, Srinivas R. Valluri, Jiaxin Liang, Kaijie Pan, Mark A. Fletcher, Raphael Simon, Luis Jodar, Bradford D. Gessner

Since its initial identification in 1986, Lyme disease has been clinically diagnosed in 29 provinces in China; however, national incidence data are lacking. To summarize Lyme disease seropositivity data among persons across China, we conducted a systematic literature review of Chinese- and English-language journal articles published during 2005–2020. According to 72 estimates that measured IgG by using a diagnostic enzyme-linked assay (EIA) alone, the seropositivity point prevalence with a fixed-effects model was 9.1%. A more conservative 2-tier testing approach of EIA plus a confirmatory Western immunoblot (16 estimates) yielded seropositivity of 1.8%. Seropositivity by EIA for high-risk exposure populations was 10.0% and for low-risk exposure populations was 4.5%; seropositivity was highest in the northeastern and western provinces. Our analysis confirms Lyme disease prevalence, measured by seropositivity, in many Chinese provinces and populations at risk. This information can be used to focus prevention measures in provinces where seropositivity is high.

Lyme disease is a tickborne zoonosis caused by genospecies of *Borrelia burgdorferi* sensu lato that occur primarily in the Northern Hemisphere, including North America, Europe, and some countries in Asia (*1*). In China, Lyme disease has been an emerging disease since the first human case was documented in Heilongjiang Province in 1986 (*2*). Multiple genospecies of *B. burgorferi* have been identified in China, although only *B. garinii*, *B. afzelii*, and *B. valaisiana*–related genospecies have been reported to cause disease in humans (*3,4*).

B. burgorferi is transmitted to humans by *Ixodes* ticks and in China specifically by *I. persulcatus*, *I. sinensis*, and *I. granulatus* ticks (*5–7*). Of those species, *I. persulcatus* ticks are regarded as the most competent vectors and are frequently identified in northeastern and select western, central, and eastern provinces (*6*). Lyme disease is widely distributed across China, and cases have been documented in 29 provinces across the country, several of which show endemicity in certain regions, specifically the northeastern provinces (*5*).

During the past several decades, Lyme disease has emerged as a public health issue for China; however, lack of information about disease burden makes it difficult for national and local governments to effectively develop and implement prevention strategies. No national Lyme disease surveillance exists in China, and no estimates of national disease incidence have been published. Thus, the only available approach for quantifying disease risk is human *B. burgorferi* seroprevalence, which reflects the proportion of persons in the population with positive serum test results for the pathogen. During 1987–1996, seroprevalence summarized from 22 provinces indicated an average seropositivity rate of 5.06% (*8*). Most of those early investigations focused on persons employed in forestry and were geographically limited to the northeastern provinces. Subsequently, human seropositivity data have been reported for provinces across all of China: in populations for which tick exposure varies, in populations in different

Author affiliations: Pfizer Inc., Collegeville, Pennsylvania, USA (J.H. Stark, K. Pan, L. Jodar, B.D. Gessner); Yale School of Public Health, New Haven, Connecticut, USA (X. Li); Pfizer China, Beijing, China (J.C. Zhang, J. Liang); P95 Pharmacovigilance & Epidemiology, Princeton, New Jersey, USA (L. Burn); Pfizer Inc., New York, New York, USA (S.R. Valluri); Pfizer Emerging Markets, Paris, France (M.A. Fletcher); Pfizer Vaccine Research & Development, Pearl River, New York, USA (R. Simon)

occupations and age groups, and by using different diagnostic testing approaches (*9*).

To summarize published human Lyme disease seropositivity data for 2005–2020, we reviewed data from the literature. We provide updated summary estimates of seropositivity for individual exposure risk, by distinct provinces and for China overall, based on diagnostic testing approaches to determine exposure to *B. burgorferi*.

Methods

Search Strategy and Selection Criteria

We conducted a global systematic literature review across 5 databases, following the Preferred Reporting Items for Systematic Reviews and Meta-Analyses (PRISMA) guidelines (*10*). We tailored the search to each database accessed: PubMed, EMBASE, CABI direct, China National Knowledge Infrastructure, and Wanfang Data (Appendix Table 1, https://wwwnc.cdc.gov/EID/article/28/12/21-2612-App1.pdf); we limited the search to articles published from January 1, 2005, through December 31, 2020. After performing the keyword search and reviewing the abstracts of retained articles, we assessed full-text articles to confirm their eligibility for inclusion. Articles were included only if they reported numerator (clearly indicating the number of seropositive persons) and denominator (the population tested) and had a diagnostic testing strategy that included an enzyme immunoassay (enzyme-linked assay [EIA] or ELISA), immunofluorescence assay (IFA), or Western immunoblot (WB). We excluded articles that did not describe the sample population for the study. We used a snowball technique to identify additional eligible articles in the reference lists of excluded literature review articles.

The protocol for the English-language literature review was published in the PROSPERO database (registration CRD42021236906, https://www.crd.york.ac.uk/prospero/display_record.php?ID=CRD42021236906). The search and extraction of the Chinese-language databases (China National Knowledge Infrastructure and Wanfang Data) occurred independently of the English-language literature review.

Variables

In China, human serum is analyzed for the presence of *Borrelia*-specific IgM or IgG with either an EIA (or ELISA) or an IFA (*11*). If the EIA or IFA result is positive or equivocal, a more specific WB (or line blot) is subsequently conducted; this method is referred to as a standard 2-tier testing approach. This approach emphasizes sensitivity initially with the first-tier test and then with the second-tier test (*12*). However, this approach is not consistently used in China (*13*). In general, diagnostic assays were not well characterized in many of the included articles because there was limited information on diagnostic performance data, standardization criteria for all genospecies, and consistency in assay specifications (e.g., antigens and reagents used).

The primary analytical strategy prioritized IgG measurements based on a single-tier EIA or IFA test. Although IgM-based tests are useful for clinical diagnosis of an early infection, they are also more likely than IgG-based tests to yield false-positive results; consequently, a sensitivity analysis was conducted for seropositivity estimates derived from an EIA or IFA that did not distinguish the results as either IgM or IgG positive. A second diagnostic sensitivity analysis was performed for estimates reporting 2-tier testing (EIA or IFA followed by WB), which may serve as a truer indicator of seropositivity. Neither sensitivity analysis included estimates used for the primary analytical strategy. We conducted subgroup analyses for estimates reported by exposure, sex, age group, and province based on an IgG measurement as determined by an EIA or IFA, similar to the primary analysis.

To adequately reflect potential variation in exposure to ticks and transmission of *Borrelia*, we characterized exposed populations. The study populations within reviewed articles were categorized into 2 broad categories: by clinical suspicion (sample identified from hospital or clinic settings, which is an unknown reflection of risk) or by exposure risk (risk for exposure to natural foci of Lyme disease, either by location or by occupation). Clinical suspicion cases are identified in hospital or clinic settings from persons with a history of suspected tick bites or with a clinical suspicion of Lyme disease (e.g., arthritis, nervous system disease, or early symptoms). To reduce biasing the risk assessment, we assessed exposure risk groups before performing statistical analyses. We categorized low exposure risk as persons who worked or lived in either nonforested plains areas or urban environments or who had minimal or no exposure to tick-infested habitats, medium exposure risk as persons whose work or location exposed them to tick-infested habitats but whose exposure was neither frequent nor prolonged, and high exposure risk as persons whose work or location frequently exposed them to forested areas or other areas where prolonged exposure to tick-infested habitat might have occurred.

Statistical Analyses

We descriptively summarized all articles for this meta-analysis and calculated fixed-effects summary estimates. Although the reviewed studies may be sufficient for drawing conclusions about the relationship between exposure and the outcome from the fixed-effects model, the studies themselves could be highly variable. Therefore, we conducted tests of homogeneity for the study samples for all studies. We assumed the variable "province" to be random and re-evaluated seropositivity to assess the robustness of the estimates by using the mixed-effects model. We considered a fixed-effects meta-analysis to be an appropriate method for summarizing seropositivity data for Lyme disease as the primary analytical strategy for the sensitivity analyses.

We used the number of available seropositivity estimates to calculate the overall least square mean summary estimate, SE, and lower and upper 95% CIs by using PROC Mixed in SAS (SAS Institute Inc., https://www.sas.com), in which the response term was the outcome (seropositivity) and the class term was province. We developed odds ratios to estimate the odds of an association between high-exposure risk group seropositivity and low-exposure risk group seropositivity, including corresponding 95% CIs. Given the paucity of data and variables available from each article, we made no adjustment for confounding in the fixed-effects models. We used forest plots to display the distribution of seropositivity and heterogeneity of the summarized seropositivity results. All analyses were conducted by using SAS version 9.4.

Results

Our literature review identified 3,657 articles that focused on China; 48 articles met the selection criteria (Figure 1), of which 42 articles met the criteria for the primary analytical strategy. In total, these 42 articles provided 72 estimates of seropositivity that we extracted for analysis. Some articles produced seropositivity estimates for multiple provinces or years (Appendix Table 2). Six articles did not meet the criteria for the primary analytical strategy; thus, they contributed data to only the 2 diagnostic sensitivity analyses. From the included studies, we compiled a description of estimates by subgroup (Table 1), by exposure group and province (Table 2), and by province (Figures 2, 3).

For the primary analytical strategy, the reported IgG seropositivity estimates based on a single-tier test (EIA or IFA) ranged from 0% to 37%; the fixed-effects modeled summary estimate was 9.1% (95% CI 7.5%–10.7%) (Table 1). When the random-effects model was used
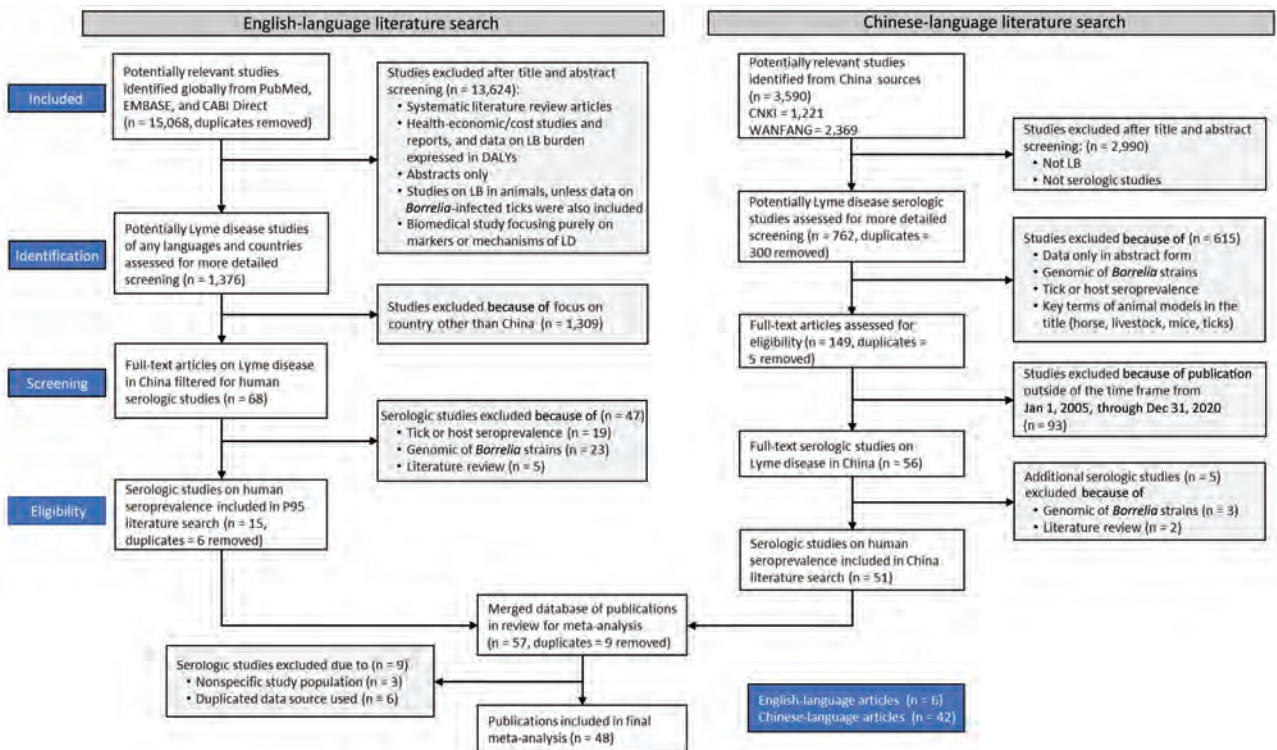
Figure 1. Preferred Reporting Items for Systematic Reviews and Meta-Analyses (PRISMA) (*10*) flow diagram of the 2 literature searches performed in review of seropositivity for *Borrelia burgdorferi* in China, 2005–2020. DALY, daily adjusted life years; LB, Lyme borreliosis; LD, Lyme disease.

Table 1. Modeled estimates of seropositivity for *Borrelia burgdorferi* sensu lato in China, 2005–2020*

Variable	Seropositivity estimates, no. (study denominator sample size)†	Modeled seropositivity, % (95% CI)
Primary analysis: IgG only	72 (34,719)	9.1 (7.5–10.7)
Sensitivity analysis		
IgM and IgG	35 (9,446)	14.5 (11.8–17.2)
EIA‡ + WB	16 (8,837)	1.8 (0.9–2.7)
Exposure group		
Clinical suspicion	10 (3,982)	7.1 (6.4–8.0)
Low risk	10 (5,245)	4.5 (3.9–5.1)
Moderate risk	12 (5,300)	6.1 (5.4–6.7)
High risk	40 (20,192)	10.0 (9.6–10.4)
Sex		
F	21 (7,542)	10.0 (6.6–13.2)
M	21 (8,223)	9.4 (6.2–12.6)
Age group, y		
<20	13 (1,420)	12.0 (4.4–19.6)
20–29	11 (1,416)	12.3 (6.3–18.4)
30–39	11 (1,734)	14.5 (5.9–23.1)
40–49	11 (1,757)	14.2 (8.5–20.0)
50–59	11 (1,434)	13.1 (8.5–17.7)
>60	12 (1,429)	12.6 (6.6–18.5)

*EIA, enzyme immunoassay; WB, Western blot.
†Positive test results: primary analysis = 2,859; sensitivity analysis IgM and IgG = 1,260; sensitivity analysis EIA + WB = 147.
‡First-tier test was either an ELISA or immunofluorescence assay.

for the primary analytical strategy, neither estimate nor variance differed. The total sample size producing this summary estimate was 34,719 (Table 1).

Fewer articles and estimates were available for the diagnostic sensitivity analyses. For the sensitivity analysis based on 35 estimates (sample size of 9,446 obtained from 5 articles) that did not distinguish between IgG and IgM results, seropositivity was 14.5% (95% CI 11.8–17.2%). For the sensitivity analysis that used a 2-tier testing system (16 estimates obtained from 6 articles with a sample size of 8,837), seropositivity was 1.8% (95% CI 0.9%–2.7%) (Table 1).

Seropositivity for the clinical suspicion sample was 7.1% (95% CI 6.4%–8.0%). Lyme disease seropositivity estimates by exposure risk populations were 4.5% (95% CI 3.9%–5.1%) for low risk, 6.1% (95% CI 5.4%–6.7%) for medium risk, and 10.0% (95% CI 9.6%–10.4%) for high risk (Table 1). The odds ratio of high exposure risk seropositivity compared with low exposure risk seropositivity was 2.4 (95% CI 2.1–2.7) and of moderate exposure risk seropositivity compared with low exposure risk seropositivity was 1.4 (95% CI 1.2–1.6).

Variation by province was substantial; the highest seropositivity estimates were 23.1% for Heilongjiang Province and 16.2% for Neimenggu (Inner Mongolia) Province (Figure 2). Moreover, variation across provinces was substantial (Figure 3). There was no discernable trend over time for seropositivity (data not shown).

Discussion

Our systematic literature review of *B. burgdorferi* seropositivity in China generated summary estimates

by diagnostic test, exposure risk, sex, age group, province, and year. Depending on the testing algorithm applied, the seropositivity ranged from 1.8% to 14.5%, reflecting Lyme disease endemicity in the population. Combined with the widespread distribution of *Ixodes* ticks, specifically *I. persulcatus* ticks in many provinces, this analysis reinforces that Lyme disease is a public health problem in China.

The summary estimates of 9.1% among EIA/IFA positive samples and 1.8% among samples confirmed with WB fell within the range identified in Europe. In Germany, the nationwide, population-based cross-sectional KiGGS study estimated seropositivity among children and adolescents of 4.8% by single-tier ELISA testing (4% when confirmed by line blot) (*14*). A similar nationwide, population-based, cross-sectional study among adults in Germany (DEGS) reported overall seropositivity of 9.4%, confirmed by line blot (*15*). A cross-sectional health survey among a representative sample of adults in Finland reported seropositivity of 3.9% according to 2-tier testing (*16*). A representative sample of healthy blood donors from the Tyrol region of Austria reported a seropositivity range of 1.5%–7.2% from samples confirmed by line blot (*17*). A regional study in Turkey among healthy volunteers revealed seropositivity of 4.1% by single-tier testing with ELISA and 2.2% confirmed by WB (*18*).

In China, results of the diagnostic sensitivity analyses were consistent with expectations based on Lyme diagnostic testing limitations. Several studies did not adequately delineate the results by IgM or IgG positivity, and this joint numerator resulted in a substantially higher estimate than IgG seropositivity

alone. IgM responses to *Borrelia* may persist over time, although IgM reactivity alone without isotype switching to IgG may reflect a false-positive result (*12,19*). False-positive results may provide an explanation for the higher seropositivity found when including results that did not distinguish between IgM and IgG. Testing results were further complicated in many studies by assays that used a whole-cell sonicate; such a lysate generates multiple antigens that can increase the likelihood that cross-reactive IgG or IgM creates a false-positive result compared with newer EIAs that focus on a reduced set of well-defined purified antigens specific to *B. burgdorferi* genospecies (*12*).

In many countries in Europe and in the United States, a 2-tier testing system for Lyme disease is used for clinical diagnosis and seroprevalence assessments. The sensitive first-tier test uses an ELISA, or less often an IFA, followed by a highly specific, second-tier WB

if the ELISA is positive or equivocal. Diagnostic sensitivity can vary widely, with estimates ranging from as low as 14% during the early stages of disease to 100% as symptoms and manifestations evolve (*12*). The value of this standard 2-tier testing approach is improved specificity compared with ELISA or IFA alone (*9,20*). Specificity in all clinical phases is robust at ≥99% after the second-tier test. Recently, a modified 2-tier testing system based on 2 EIAs, which substitutes an EIA for the second-tier WB, has been implemented. Third-generation EIAs focus on select antigens; as a result, pairing with different EIAs enables substantial orthogonality that improves sensitivity while maintaining specificity (*12*). Neither of those 2-tier testing approaches has been widely adopted in China (*13*), where studies reporting the seropositivity of antibodies to *B. burgdorferi* relied primarily on the first-tier EIA or IFA and less often on the confirmatory, specific WB.
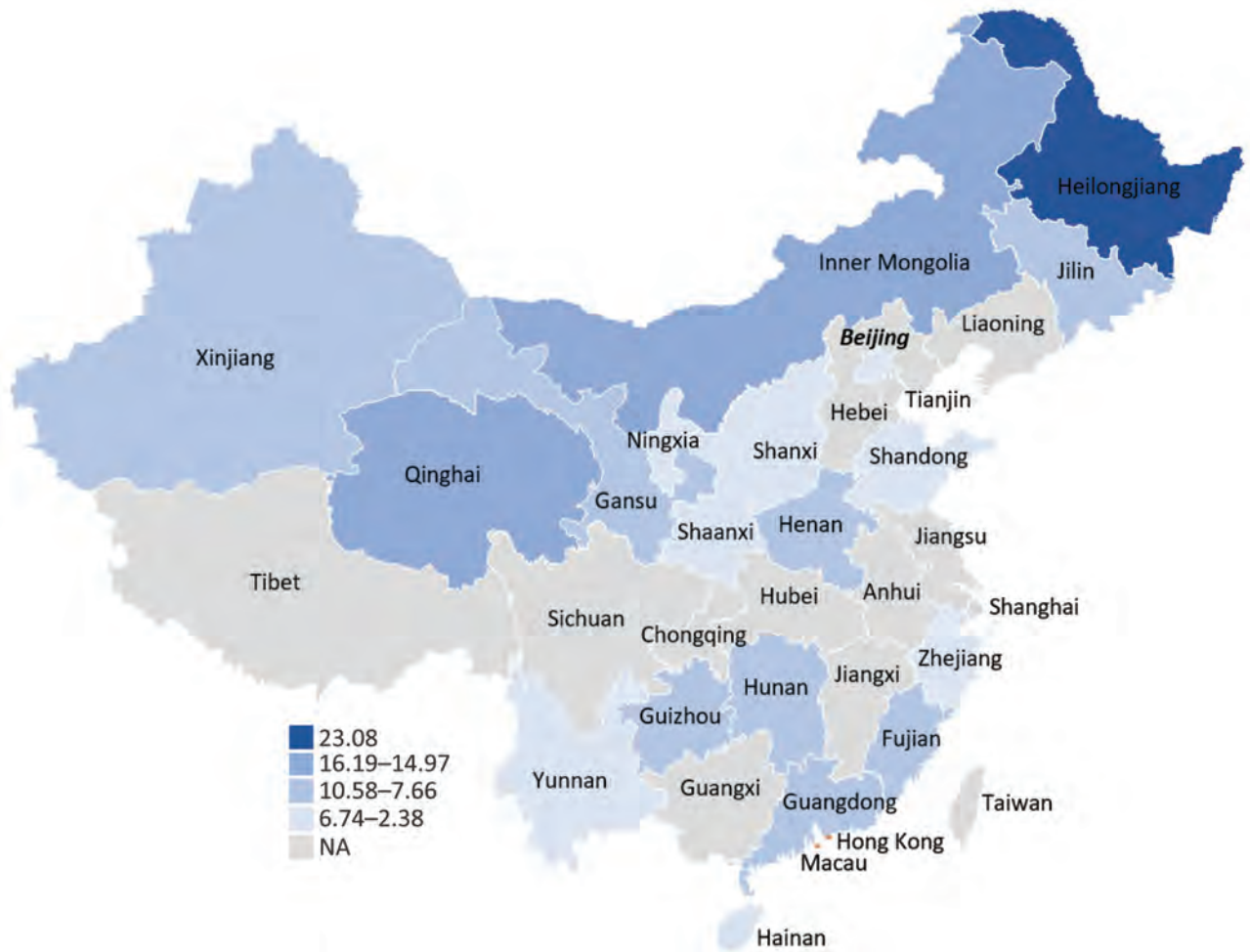
Figure 2. Estimated seropositivity for *Borrelia burgdorferi,* by province, China, 2005–2020. *Ixodes persulcatus* ticks, among the most frequently identified ticks in China, have been found across the northeastern and select western, central and eastern provinces. *I. sinensis* and *I. granulatus* ticks are the main identified vectors in the southern and eastern regions of the country. Variations in seropositivity reflect differences in tick competency, tick bite risk, and diagnostic tests. Numbers in key are percentages. NA, not applicable.

Furthermore, diagnostic performance data are not readily available from China, particularly across the range of testing procedures used. Some studies acknowledged use of reagents provided by the China Centers for Disease Control and Prevention, others used local commercial test kits, a few used nondomestic test kits, and several others did not describe the assays used. The China Centers for Disease Control and Prevention described criteria for standardization of a WB based on lysates of *B. garinii* bacteria; the assay used a single band for IgG or IgM, a criterion that differs from guidelines in Europe and the United States that require at least 2 of 3 bands by IgM or 5 of 10 bands by IgG to be classified as positive by WB (*12,13*). In addition, interpretation criteria were not consistent across associated articles. The few articles from our review that reported seropositivity with a confirmatory WB result led to a summary estimate substantially lower than the single-tier test (1.8% vs. 9.1%). The limited information on quality of assays, accreditation, and validation remains a major limitation of analytic interpretability. Nevertheless, the sampling for the 2-tier testing strategy occurred in 4 provinces across all types of exposure categories, providing some evidence of a representative seroprevalence estimate (Appendix Table 2).

Seropositivity was higher for populations that had been assessed as having a higher risk for exposure to a natural foci of Lyme disease, either by occupation or by location. These data were consistent with targeted samples of higher risk occupational groups from other countries. For instance, IgG seropositivity among farmers was 5.5%–9.7% in Belgium (*21*) and 10%–13.7% in Poland (*22,23*). Forestry workers are among the most

sampled high exposure risk occupational groups; reported seropositivity was 14% in Lithuania (*24*), 31% in Hungary (*25*), 7.8% in Italy (*26*), 11.8% in Serbia (*27*), 10.9% in Turkey (*28*), 21.6% in Belgium (*29*), and 14%–34% in Poland (*22,30*). Likewise, increased seropositivity seen in medium to high exposure risk populations in China and consistency with data from Europe provide initial confidence in the overall estimates provided in this report.

The summary estimate in the clinical suspicion sample, which reflected a mixture of studies focused on history of a suspected tick bite or clinical suspicion of Lyme disease, was 7.1%. The TBD STING study in Sweden and Finland reported seroconversion after a tick bite for 3.5% of participants (*31*). Nonetheless, seroconversion does not necessarily reflect clinical infection because Lyme disease manifestation during the 3-month follow-up period did not develop for 57.6% of the *Borrelia*-infected persons who seroconverted. Among the seroconversions that resulted in clinical manifestations, these included erythema migrans (85%), *Borrelia* lymphocytoma (3%), nervous system disease (6%), or nonspecific symptoms of Lyme disease (6%). A study conducted in China documenting clinical manifestations after tick bite reported a lower proportion of erythema migrans (69%) and a higher proportion of nervous system disease (21%) and arthralgia (21%), among other manifestations (*32*). In the United States, a randomized controlled trial of a vaccine candidate documented an asymptomatic proportion of <10%, potentially arising from the shorter duration of follow-up for symptoms compared with that in Europe (*33*). Notwithstanding, differences in asymptomatic proportions and clinical

Table 2. Distribution of estimates of seropositivity for *Borrelia burgdorferi* sensu lato, by exposure group and province, China, 2005–2020

| Province | Total no. estimates, n = 72 | Clinical suspicion estimates, n = 10 | Exposure group | | |
			Low risk, n = 10	Moderate risk, n = 12	High risk, n = 40
Beijing	6	2	1	1	2
Fujian	2	0	1	0	1
Gansu	4	0	0	0	4
Guangdong	2	0	0	1	1
Guizhou	3	0	1	1	1
Hainan	4	4	0	0	0
Heilongjiang	3	2	0	0	1
Henan	2	0	0	0	2
Hunan	2	0	0	0	2
Jilin	7	0	1	1	5
Neimenggu	4	1	1	0	2
Ningxia	1	0	0	0	1
Qinghai	2	0	0	0	2
Shaanxi	1	0	0	0	1
Shandong	1	0	0	0	1
Shanxi	2	0	0	0	2
Tianjin	2	0	1	0	1
Xinjiang	18	0	2	8	8
Yunnan	1	0	1	0	0
Zhejiang	5	1	1	0	3

Province, no. estimates
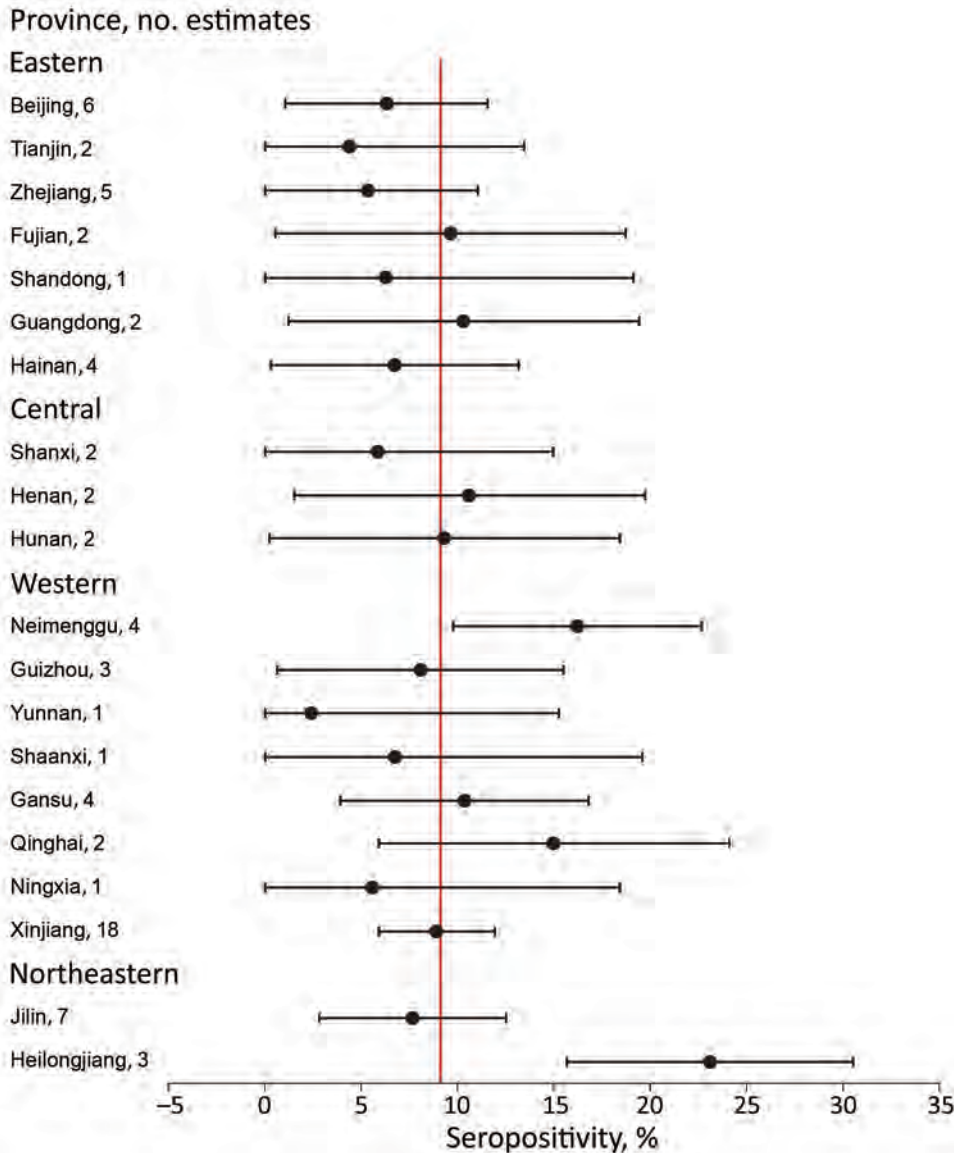
Figure 3. Forest plot illustrating seropositivity estimates for *Borrelia burgdorferi,* by province, China, 2005–2020. The red horizontal line indicates the summary estimate based on the primary analysis; error bars indicate 95% CIs. For 7 estimates, the lower bound of the 95% CI was <0 (a negative value); those values were fixed at 0% for interpretation.

manifestations between studies and countries may reflect differences in study design, duration of follow-up, diagnostic quality, timing of postinfection treatment, antibody waning, and circulating genospecies.

The highest summary seropositivity estimates were detected in 2 provinces in northeastern China (Heilongjiang Province, 23.1%) and western China (Neimenggu Province [Inner Mongolia], 16.2%). *I. persulcatus* ticks are among the most frequently identified ticks in China and have been found across the northeastern and select western, central, and eastern, provinces (*6*). Several other provinces that border Heilongjiang and Neimenggu Provinces have frequently reported the presence of *I. persulcatus* ticks, although the reported seropositivity has been lower (7%–10%). The lower calculated estimates within these

provinces could reflect differences in the sampled exposure groups because studies from Heilongjiang and Neimenggu Provinces largely focused on populations for which higher infection prevalence was expected (e.g., forest residents and forestry workers). In addition, no samples from Heilongjiang and Neimenggu Provinces were tested by using the more conservative 2-tier testing strategy, which probably would have resulted in lower seropositivity estimates. Alternatively, lower seropositivity in border regions could reflect true differences in exposure risk. Other regions of China, particularly those in the southern and eastern regions, reported somewhat lower seropositivity (2%–10%). The distribution of *I. persulcatus* ticks is limited in these regions, although *I. sinensis* and *I. granulatus* ticks have been reported and

are considered to be the main vectors in these provinces. However, demonstration of vector competency and efficiency of *I. sinensis* and *I. granulatus* ticks as vectors of *B. burgorferi* is unclear (*5*,*7*).

Other caveats to consider include the possibility that seropositivity may be driven by persons who become infected in higher incidence regions but reside in regions without efficient local transmission, because their limited awareness of Lyme disease precludes appropriate personal prevention measures. Another consideration is the local prevalence of Lyme disease for such persons. Despite good specificity of the test, a low a priori probability of disease will lead to a lower positive predictive value for true disease (*12*). Regardless of these caveats, increasing tick distributions across China has been attributed to planned reforestation and changing land use patterns leading to suitable environments to maintain the tick enzootic cycle and ultimately *Borrelia* transmission (*3*).

Among the study limitations, there were substantial variations in populations sampled (including persons seeking clinical care, or convenience samples), in risk exposure population targeting, and in varying study designs (none of the studies were designed to be nationally representative). More than half of the studies were conducted among a higher risk exposure population that probably elevated the summary estimate. With additional information on the percentage of the country's population at different levels of risk, a weighted average could be obtained, although this type of data is difficult to quantify. Second, the included studies used a range of testing methods that may not be comparable. For example, IFA was widely used to estimate seropositivity, but this traditional, manual method relies on the experience of the technician, leading to potentially lower specificity compared with enzyme immunoassay (EIA or ELISA) (*9*,*20*). In addition, 2-tier testing was not uniformly used, which could have resulted in potentially higher rates of false-positive results. Third, exposure risk may have been misclassified because an accurate description of specific testing populations may be missing from source manuscripts. Fourth, although *B. garinii* and *B. afzeli* have been reported as the predominant circulating genospecies, other circulating nonpathogenic genospecies may cause a false-positive result (*3*,*4*). Last, seropositivity estimates reflect exposure risk for infection regardless of clinically apparent disease; therefore, these summary estimates should not be interpreted as reflecting risk for clinical disease. Collectively, these limitations portend to overestimate seropositivity compared with other results as noted in Europe.

In conclusion, the results from this meta-analysis demonstrate seropositivity to *B. burgorferi* in China over the past several decades, particularly in certain provinces and in high exposure risk populations. By itself, however, the utility of this information for driving public health policy is limited because it gives no indication of clinical burden, either overall or by severity, and may not accurately represent geographic variations in risk. The expanding geographic range of infected ticks and increased likelihood of contact with humans will continue to present a public health challenge for China.

About the Author

Dr. Stark is an epidemiologist at Pfizer and the global medical and scientific lead for the Lyme disease vaccine candidate.

References

1. Steere AC, Strle F, Wormser GP, Hu LT, Branda JA, Hovius JW, et al. Lyme borreliosis. Nat Rev Dis Primers. 2016;2:16090. https://doi.org/10.1038/nrdp.2016.90
2. Ai CX, Wen YX, Zhang YG, Wang SS, Qiu QC, Shi ZX, et al. Clinical manifestations and epidemiological characteristics of Lyme disease in Hailin County, Heilongjiang Province, China. Ann N Y Acad Sci. 1988;539:302–13. https://doi.org/10.1111/j.1749-6632.1988.tb31864.x
3. Fang LQ, Liu K, Li XL, Liang S, Yang Y, Yao HW, et al. Emerging tick-borne infections in mainland China: an increasing public health threat. Lancet Infect Dis. 2015;15:1467–79. https://doi.org/10.1016/S1473-3099(15)00177-2
4. Wang Y, Li S, Wang Z, Zhang L, Cai Y, Liu Q. Prevalence and identification of *Borrelia burgdorferi* sensu lato genospecies in ticks from Northeastern China. Vector Borne Zoonotic Dis. 2019;19:309–15. https://doi.org/10.1089/vbz.2018.2316
5. Wu XB, Na RH, Wei SS, Zhu JS, Peng HJ. Distribution of tick-borne diseases in China. Parasit Vectors. 2013;6:119. https://doi.org/10.1186/1756-3305-6-119
6. Zhang G, Zheng D, Tian Y, Li S. A dataset of distribution and diversity of ticks in China. Sci Data. 2019;6:105. https://doi.org/10.1038/s41597-019-0115-5
7. Eisen L. Vector competence studies with hard ticks and *Borrelia burgdorferi* sensu lato spirochetes: a review. Ticks

Tick Borne Dis. 2020;11:101359. https://doi.org/10.1016/j.ttbdis.2019.101359

8. Zhang ZF, Wan KL, Zhang JS. Studies on epidemiology and etiology of Lyme disease in China [in Chinese]. Zhonghua Liu Xing Bing Xue Za Zhi. 1997;18:8–11.

9. Hao Q, Geng Z, Hou XX, Tian Z, Yang XJ, Jiang WJ, et al. Seroepidemiological investigation of Lyme disease and human granulocytic anaplasmosis among people living in forest areas of eight provinces in China. Biomed Environ Sci. 2013;26:185–9. https://doi.org/10.3967/0895-3988.2013.03.005

10. Moher D, Liberati A, Tetzlaff J, Altman DG; PRISMA Group. Preferred Reporting Items for Systematic Reviews and Meta-Analyses: the PRISMA statement. BMJ. 2009;339:b2535. https://doi.org/10.1136/bmj.b2535

11. National Health Commission of the People's Republic of China. GBZ 324-2019 Diagnosis of occupational Lyme disease [cited 2022 Oct 31]. http://www.nhc.gov.cn/wjw/pyl/201902/7bebbb45926347df843fab12490dc607/files/3a92b8f14083499d8347c328c28db944.pdf

12. Branda JA, Steere AC. Laboratory diagnosis of Lyme borreliosis. Clin Microbiol Rev. 2021;34:e00018-19. https://doi.org/10.1128/CMR.00018-19

13. Jiang Y, Hou XX, Geng Z, Hao Q, Wan KL. Interpretation criteria for standardized Western blot for the predominant species of *Borrelia burgdorferi* sensu lato in China. Biomed Environ Sci. 2010;23:341–9. https://doi.org/10.1016/S0895-3988(10)60074-8

14. Dehnert M, Fingerle V, Klier C, Talaska T, Schlaud M, Krause G, et al. Seropositivity of Lyme borreliosis and associated risk factors: a population-based study in children and adolescents in Germany (KiGGS). PLoS One. 2012;7:e41321. https://doi.org/10.1371/journal.pone.0041321

15. Wilking H, Fingerle V, Klier C, Thamm M, Stark K. Antibodies against *Borrelia burgdorferi* sensu lato among adults, Germany, 2008–2011. Emerg Infect Dis. 2015;21:107–10. https://doi.org/10.3201/eid2101.140009

16. van Beek J, Sajanti E, Helve O, Ollgren J, Virtanen MJ, Rissanen H, et al. Population-based *Borrelia burgdorferi* sensu lato seroprevalence and associated risk factors in Finland. Ticks Tick Borne Dis. 2018;9:275–80. https://doi.org/10.1016/j.ttbdis.2017.10.018

17. Sonnleitner ST, Margos G, Wex F, Simeoni J, Zelger R, Schmutzhard E, et al. Human seroprevalence against *Borrelia burgdorferi* sensu lato in two comparable regions of the eastern Alps is not correlated to vector infection rates. Ticks Tick Borne Dis. 2015;6:221–7. https://doi.org/10.1016/j.ttbdis.2014.12.006

18. Cikman A, Aydin M, Gulhan B, Karakecili F, Demirtas L, Kesik OA. Geographical features and seroprevalence of *Borrelia burgdorferi* in Erzincan, Turkey. J Arthropod Borne Dis. 2018;12:378–86.

19. Kalish RA, McHugh G, Granquist J, Shea B, Ruthazer R, Steere AC. Persistence of immunoglobulin M or immunoglobulin G antibody responses to *Borrelia burgdorferi* 10–20 years after active Lyme disease. Clin Infect Dis. 2001;33:780–5. https://doi.org/10.1086/322669

20. Auwaerter PG. Diagnostic testing for Lyme disease. In: Halperin JJ, editor. Lyme Disease: an Evidence-based Approach. 2nd ed. Wallingford (UK): CABI; 2018. p. 58–75.

21. De Keukeleire M, Robert A, Kabamba B, Dion E, Luyasu V, Vanwambeke SO. Individual and environmental factors associated with the seroprevalence of *Borrelia burgdorferi* in Belgian farmers and veterinarians. Infect Ecol Epidemiol. 2016;6:32793. https://doi.org/10.3402/iee.v6.32793

22. Tokarska-Rodak M, Plewik D, Kozioł-Montewka M, Szepeluk A, Paszkiewicz J. Risk of occupational infections caused by *Borrelia burgdorferi* among forestry workers and farmers [in Polish]. Med Pr. 2014;65:109–17. https://doi.org/10.13075/mp.5893.2014.017

23. Zając V, Pinkas J, Wójcik-Fatla A, Dutkiewicz J, Owoc A, Bojar I. Prevalence of serological response to *Borrelia burgdorferi* in farmers from eastern and central Poland. Eur J Clin Microbiol Infect Dis. 2017;36:437–46. https://doi.org/10.1007/s10096-016-2813-7

24. Motiejunas L, Bunikis J, Barbour AG, Sadziene A. Lyme borreliosis in Lithuania. Scand J Infect Dis. 1994;26:149–55. https://doi.org/10.3109/00365549409011778

25. Lakos A, Igari Z, Solymosi N. Recent lesson from a clinical and seroepidemiological survey: low positive predictive value of *Borrelia burgdorferi* antibody testing in a high risk population. Adv Med Sci. 2012;57:356–63. https://doi.org/10.2478/v10039-012-0060-4

26. Tomao P, Ciceroni L, D'Ovidio MC, De Rosa M, Vonesch N, Iavicoli S, et al. Prevalence and incidence of antibodies to *Borrelia burgdorferi* and to tick-borne encephalitis virus in agricultural and forestry workers from Tuscany, Italy. Eur J Clin Microbiol Infect Dis. 2005;24:457–63. https://doi.org/10.1007/s10096-005-1348-0

27. Jovanovic D, Atanasievska S, Protic-Djokic V, Rakic U, Lukac-Radoncic E, Ristanovic E. Seroprevalence of *Borrelia burgdorferi* in occupationally exposed persons in the Belgrade area, Serbia. Braz J Microbiol. 2015;46:807–14. https://doi.org/10.1590/S1517-838246320140698

28. Kaya AD, Parlak AH, Ozturk CE, Behcet M. Seroprevalence of *Borrelia burgdorferi* infection among forestry workers and farmers in Duzce, north-western Turkey. New Microbiol. 2008;31:203–9.

29. De Keukeleire M, Robert A, Luyasu V, Kabamba B, Vanwambeke SO. Seroprevalence of *Borrelia burgdorferi* in Belgian forestry workers and associated risk factors. Parasit Vectors. 2018;11:277. https://doi.org/10.1186/s13071-018-2860-2

30. Podsiadły E, Chmielewski T, Karbowiak G, Kędra E, Tylewska-Wierzbanowska S. The occurrence of spotted fever rickettsioses and other tick-borne infections in forest workers in Poland. Vector Borne Zoonotic Dis. 2011;11:985–9. https://doi.org/10.1089/vbz.2010.0080

31. Wilhelmsson P, Fryland L, Lindblom P, Sjöwall J, Ahlm C, Berglund J, et al. A prospective study on the incidence of *Borrelia burgdorferi* sensu lato infection after a tick bite in Sweden and on the Åland Islands, Finland (2008–2009). Ticks Tick Borne Dis. 2016;7:71–9. https://doi.org/10.1016/j.ttbdis.2015.08.009

32. Liu HB, Wei R, Ni XB, Zheng YC, Huo QB, Jiang BG, et al. The prevalence and clinical characteristics of tick-borne diseases at One Sentinel Hospital in Northeastern China. Parasitology. 2019;146:161–7. https://doi.org/10.1017/S0031182018001178

33. Steere AC, Sikand VK, Meurice F, Parenti DL, Fikrig E, Schoen RT, et al.; Lyme Disease Vaccine Study Group. Vaccination against Lyme disease with recombinant *Borrelia burgdorferi* outer-surface lipoprotein A with adjuvant. N Engl J Med. 1998;339:209–15. https://doi.org/10.1056/NEJM199807233390401

Address for correspondence: James H. Stark, Vaccines Medical Development, Scientific and Clinical Affairs, Pfizer Inc., 500 Arcola Rd, Collegeville, PA 19426, USA; email: james.h.stark@pfizer.com

Acinetobacter baumannii among Patients Receiving Glucocorticoid Aerosol Therapy during Invasive Mechanical Ventilation, China

Wenchao Zhang,[1] Mei Yin,[1] Wei Li, Nana Xu, Haining Lu, Weidong Qin, Hui Han, Chen Li, Dawei Wu, Hao Wang

In support of improving patient care, this activity has been planned and implemented by Medscape, LLC and Emerging Infectious Diseases. Medscape, LLC is jointly accredited with commendation by the Accreditation Council for Continuing Medical Education (ACCME), the Accreditation Council for Pharmacy Education (ACPE), and the American Nurses Credentialing Center (ANCC), to provide continuing education for the healthcare team.

Medscape, LLC designates this Journal-based CME activity for a maximum of 1.00 **AMA PRA Category 1 Credit(s)™**. Physicians should claim only the credit commensurate with the extent of their participation in the activity.

Successful completion of this CME activity, which includes participation in the evaluation component, enables the participant to earn up to 1.0 MOC points in the American Board of Internal Medicine's (ABIM) Maintenance of Certification (MOC) program. Participants will earn MOC points equivalent to the amount of CME credits claimed for the activity. It is the CME activity provider's responsibility to submit participant completion information to ACCME for the purpose of granting ABIM MOC credit.

All other clinicians completing this activity will be issued a certificate of participation. To participate in this journal CME activity: (1) review the learning objectives and author disclosures; (2) study the education content; (3) take the post-test with a 75% minimum passing score and complete the evaluation at http://www.medscape.org/journal/eid; and (4) view/print certificate. For CME questions, see page 2598.

Release date: November 17, 2022; Expiration date: November 17, 2023

Learning Objectives

Upon completion of this activity, participants will be able to:

- Distinguish the percentage of patients receiving invasive mechanical ventilation (IMV) who had a positive culture for *Acinetobacter baumannii* (AB)
- Assess the role of aerosol inhalation in the isolation of AB in the current study
- Analyze risk factors for the isolation of AB in the current study
- Evaluate the effects of aerosol inhalation and AB on the risk for mortality among patients receiving IMV

CME Editor

Amy J. Guinn, BA, MA, Technical Writer/Editor, Emerging Infectious Diseases. *Disclosure: Amy J. Guinn, BA, MA, has no relevant financial relationships.*

CME Author

Charles P. Vega, MD, Health Sciences Clinical Professor of Family Medicine, University of California, Irvine School of Medicine, Irvine, California. *Disclosure: Charles P. Vega, MD, has the following relevant financial relationships: served as an advisor or consultant for GlaxoSmithKline; Johnson & Johnson Pharmaceutical Research & Development, L.L.C.*

Authors

Wenchao Zhang, MD, PhD; Mei Yin, MD, PhD; Wei Li, MD, PhD; Nana Xu, MD; Haining Lu, MD; Weidong Qin, MD, PhD; Hui Han, MD; Chen Li, MD; Dawei Wu, MD; Hao Wang, MD, PhD.

Author affiliations: Qilu Hospital of Shandong University, Jinan, China (W. Zhang, M. Yin, W. Li, N. Xu, W. Qin, H. Han, C. Li, H. Wang); Qingdao Branch, Qilu Hospital of Shandong University, Qingdao, China (H. Lu, D. Wu)

[1]These authors contributed equally to this article.

Acinetobacter baumannii is a nosocomial pathogen associated with severe illness and death. Glucocorticoid aerosol is a common inhalation therapy in patients receiving invasive mechanical ventilation. We conducted a prospective cohort study to analyze the association between glucocorticoid aerosol therapy and *A. baumannii* isolation from ventilator patients in China. Of 497 enrolled patients, 262 (52.7%) received glucocorticoid aerosol, and *A. baumannii* was isolated from 159 (32.0%). Glucocorticoid aerosol therapy was an independent risk factor for *A. baumannii* isolation (hazard ratio 1.5, 95% CI 1.02–2.28; p = 0.038). Patients receiving glucocorticoid aerosol had a higher cumulative hazard for *A. baumannii* isolation and analysis showed that glucocorticoid aerosol therapy increased *A. baumannii* isolation in most subpopulations. Glucocorticoid aerosol was not a direct risk factor for 30-day mortality, but *A. baumannii* isolation was independently associated with 30-day mortality in ventilator patients. Physicians should consider potential *A. baumannii* infection when prescribing glucocorticoid aerosol therapy.

*A*cinetobacter baumannii, a gram-negative coccobacillus, is a major nosocomial pathogen worldwide. *A. baumannii* is particularly challenging in intensive care units (ICUs). According to the Extended Prevalence of Infection in Intensive Care study, aimed at providing information on the prevalence of infection in ICUs worldwide, *Acinetobacter* spp. constituted 8.8% of all culture-positive ICU infections in 2007 (1), which increased to 11.4% in 2017 (2). However, infection rates differed markedly, ranging from 1.0% in North America to 25.6% in Asia and the Middle East and 22.9% in eastern Europe (2). Patients on invasive mechanical ventilation are particularly vulnerable to *A. baumannii* infection and colonization due to airway barrier destruction and bacterial virulence factors such as motility, epithelial adherence, and biofilm formation that enable *A. baumannii* colonization in the airways (3,4). *A. baumannii* in patient airways is associated with longer hospitalization, higher medical expenses, and increased mortality rates (5–7). Identifying risk factors for *A. baumannii* infection is crucial for implementing preventive measures and decreasing overall illness and death.

Aerosol inhalation is widely used in patients requiring mechanical ventilation. Glucocorticoids are frequently administered during aerosol therapy, especially in China (8–10). Compared with systemic application, aerosol therapy has several advantages, including targeted delivery to the lungs, faster response, and fewer systemic side effects (11,12). However, the aerosols and droplets generated during aerosol inhalation can become sources of respiratory pathogens (13), and inhaled glucocorticoids might suppress pulmonary immunity (14), which could increase the opportunity for nosocomial acquisition. Inhaled corticosteroids are associated with an increased risk for pneumonia in patients with chronic obstructive pulmonary disease (COPD) (15). However, the effects of glucocorticoid aerosol inhalation on nosocomial infection risk has not been clearly elucidated.

Glucocorticoid aerosol therapy is mainly indicated for patients with asthma, COPD (16), acute respiratory distress syndrome (ARDS) (17), and some pathophysiological conditions, such as airway hyperresponsiveness (18), hyperinflammation, and mucosal edema (19). In the past decade, use of glucocorticoid aerosol therapy has increased in hospitals in China; on average, >40% of patients on mechanical ventilation receive this therapy (9). In addition, a market analysis determined that aerosolized glucocorticoid sales in China were almost 3-fold higher in 2018 than in 2012 (20).

Although epidemiology has demonstrated a slow increase in *A. baumannii* infection globally over the past decade (1,2), the increase in *A. baumannii* incidence in China appears to have outpaced increases in other regions worldwide (21–23). According to the China Antimicrobial Surveillance Network (CHINET), a national surveillance of the trends of bacterial strains isolated from the major hospitals in China, the number of *Acinetobacter* spp. strains increased by 2.7-fold in 2018 compared with 2012 (23,24). Previously, we reported a marked increase in the incidence of *A. baumannii*–related bloodstream infections and incidence of pneumonia-related *A. baumannii* infections in ICUs in China that were 3.2-fold higher during 2017–2018 than during 2011–2012 (25). *A. baumannii* was the most frequent bacterial isolate in ventilator-associated pneumonia in China, and rates were 35.7%–52.7% (26,27). Furthermore, the incidence of the drug-resistant phenotype of *A. baumannii* is high. According to CHINET reports, carbapenem-resistant *A. baumannii* strains increased from 31% in 2005 to 66.7% in 2014 (28), then to ≈80% in 2018 (29). We previously reported that carbapenem resistance rates in ICUs in China increased from 25% during 2011–2012 to 95.7% during 2017–2018 (25). A multicenter study of ICUs in China reported that multidrug-resistant (MDR) *A. baumannii* was detected in 40% of all cases (30).

We hypothesized that increased use of glucocorticoid aerosol therapy might contribute to increased *A. baumannii* incidence. Therefore, we performed a prospective cohort study of critically ill patients receiving invasive mechanical ventilation in China to determine whether use of aerosolized glucocorticoid increased the risk for *A. baumannii* isolation.

Methods

Study Design and Patients

During January 2018–August 2019, we conducted a prospective cohort study at 3 adult ICUs in 2 hospitals in Shandong Province, China: Qilu Hospital of Shandong University in Jinan and Qingdao Branch of Qilu Hospital in Qingdao. We enrolled patients on their first day of invasive mechanical ventilation in the ICU and obtained written informed consent for all patients. We divided the patients into 3 groups on the basis of their treatment: no aerosol inhalation therapy, glucocorticoid aerosol therapy, and aerosol inhalation without glucocorticoid. Within 48 hours of patient enrollment, we collected secretion samples from the lower respiratory tract by transtracheal aspiration for microbial culture; thereafter, we collected samples 3 times per week until we obtained an *A. baumannii*–positive culture. We followed patients for 30 days after enrollment. If the patient was hospitalized for >3 weeks, we reduced the culture frequency to once a week. We excluded patients who received invasive mechanical ventilation for <48 hours; received aerosol inhalation or glucocorticoid aerosol for <48 hours after enrollment and before *A. baumannii*–positive culture; were <18 years of age; were assumed to have *A. baumannii* infection or colonization at baseline because they were *A. baumannii*–positive before enrollment or within the first 48 hours of enrollment; or had been exposed to >1 of the following *A. baumannii* risk factors before enrollment: antimicrobial drugs for >7 days, invasive mechanical ventilation for >5 days, or vasopressor for >3 days. We also excluded patients who lacked follow-up data or had incomplete information. The Institutional Ethics Committee of Qilu Hospital of Shandong University approved our study.

Microbiology

We performed microbial cultures according to standard procedures. In brief, we incubated respiratory samples on MacConkey agar plates at 5% CO_2 and 35°C for 48 h. We identified *A. baumannii*, a gram-negative, nonfermentative, and oxidase-negative coccobacillus, by using the VITEK 2 compact system and GN ID card (bioMérieux, https://www.biomerieux.com). We used *Escherichia coli* (ATCC accession no. 25922) and *Pseudomonas aeruginosa* (ATCC accession no. 27853) as quality controls.

Definitions and Data Collection

We defined no aerosol inhalation as patients who did not receive aerosolized medications during the study. We defined glucocorticoid aerosol therapy as patients who received aerosolized glucocorticoids for >48 hours after enrollment and before *A. baumannii* isolation, with or without nonglucocorticoid aerosolized medications for any duration. We defined aerosol inhalation without glucocorticoid as patients who received only aerosolized nonglucocorticoid medications, such as bronchodilators and expectorants, for >48 hours after enrollment and before *A. baumannii* isolation. We excluded all other conditions.

The primary endpoint was *A. baumannii* isolation, which we defined as *A. baumannii*–positive culture from the lower respiratory tract samples collected during the ICU stay. Negative outcomes were no *A. baumannii* isolation before death, ICU discharge, or end of follow-up period. We recorded the time-to-event, which we defined as number of days from enrollment to *A. baumannii* isolation.

We collected baseline information at ICU admission, including age, sex, history of smoking and surgeries, underlying conditions, past inhaled steroids for chronic conditions, and Charlson comorbidity index. We used the Acute Physiology and Chronic Health Evaluation II (APACHE II) score to assess illness severity. We also recorded other possible *A. baumannii* risk factors, such as use of broad-spectrum antimicrobial drugs, invasive mechanical ventilation, urethral catheter placement, vasopressor treatment, renal dialysis, and length of ICU stay. In addition, we recorded indications for glucocorticoid aerosol therapy by reviewing patients' medical records. We reviewed patients' clinical data to determine *A. baumannii* isolation status as infection, colonization, or undefined.

Statistical Analyses

We expressed continuous variables as median and interquartile range (IQR) or mean and SD and categorical variables as number and percentage. We used univariate and multivariate Cox proportional hazards regression and hazard ratio (HR) and 95% CI to assess risk factors for *A. baumannii* isolation and 30-day mortality. We performed propensity score matching analysis to reduce the imbalance between the glucocorticoid aerosol therapy and nonglucocorticoid groups. We included all possible covariables (i.e., demographics, background history, underlying conditions, and disease severity) in the propensity score matching. We calculated propensity scores by using a logistic regression model. We applied a 1:1 nearest neighbor matching algorithm with a caliper of 0.02 and without replacement. We assessed balance of variables in both groups by standardized differences.

We analyzed *A. baumannii* isolation in complete cases and the propensity-matched cohort. We used Kaplan-Meier curves to visually compare cumulative hazards for *A. baumannii* isolation among the 3 groups, which we evaluated by using a log-rank test. To assess the consistency of glucocorticoid therapy in terms of its effect on *A. baumannii* isolation from prespecified subgroups with different characteristics, we applied Cox proportional hazards model with Efron's method for handling ties and used forest plots for HRs and 95% CIs. We assessed heterogeneity of efficacy of glucocorticoid therapy on *A. baumannii* isolation in subgroups by using an interaction test, expressed p values for interaction, and considered p<0.05 statistically significant. We performed all analyses by using SPSS Statistics 16.0 (IBM, https://www.ibm.com) and R version 3.0 (R Foundation for Statistical Computing, https://www.r-project.org).

Results

Participant Characteristics

We enrolled 671 patients from 3 ICUs and excluded 174 patients. The final cohort consisted of 497 patients: 137 (27.6%) received no aerosol inhalation, 262 (52.7%) received glucocorticoid aerosol, and 98 (19.7%) received aerosol inhalation without glucocorticoid (Figure 1). We isolated *A. baumannii* from 159 (32.0%) patients. The median patient age was 60.1 (IQR 49–73) years, and 67.8% were male. The median length of ICU stay was 15 (IQR 7–23) days. Besides *A. baumannii*, the 3 other bacteria commonly isolated were *Klebsiella pneumoniae* (n = 38, 7.6%), *P. aeruginosa* (n = 27, 5.4%), and *E. coli* (n = 15, 3.0%) (Appendix Table 1, https://wwwnc.cdc.gov/EID/article/28/12/22-0347-App1.pdf). Most (22.5%) study patients received glucocorticoid therapy for ARDS and for asthma or COPD (21.3%) (Appendix Table 2).

Risk Factors for *A. baumannii* Isolation

We performed univariate Cox regression analysis of risk factors for *A. baumannii* isolation (Table 1). Compared with no aerosol inhalation, glucocorticoid aerosol therapy had a statistically significant effect on *A. baumannii* isolation (HR 1.860, 95% CI 1.264–2.738; p = 0.002). Aerosol inhalation without glucocorticoid was not a risk factor for *A. baumannii* (p>0.05). Other candidate risk factors were cardiovascular diseases, chronic renal insufficiency, COPD or asthma, current or former smoking history, use of broad-spectrum antimicrobial drugs for ≥7 days, invasive mechanical ventilation for ≥5 days, vasopressor treatment, renal dialysis for ≥3 days, and APACHE II score.

To assess whether glucocorticoid aerosol therapy was an independent risk factor for *A. baumannii* isolation, we established 2 models using multivariate Cox regression analysis in complete cases. Model 1 included all variables, and model 2 only included variables with p<0.1 in the univariate analysis. Glucocorticoid aerosol was an independent risk factor for *A. baumannii*
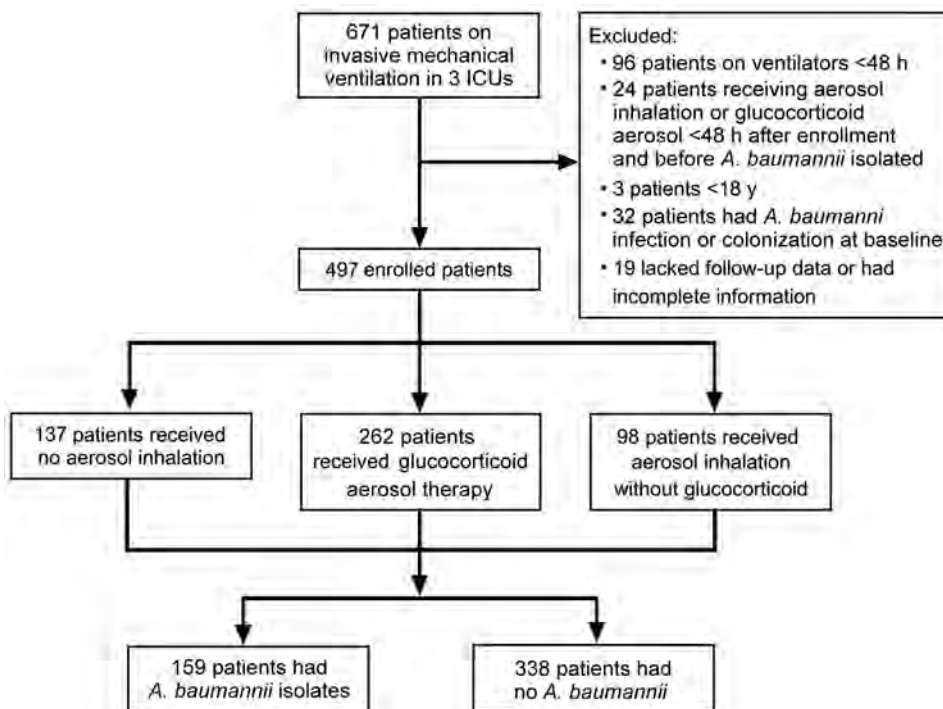
Figure 1. Flowchart for enrolling participants in a study of *Acinetobacter baumannii* among patients receiving glucocorticoid aerosol therapy during invasive mechanical ventilation, China. ICU, intensive care units.

Table 1. Univariate analysis of risk factors for *Acinetobacter baumannii* among patients during invasive mechanical ventilation, China*

Variables	Overall, n = 497	*Acinetobacter baumannii* isolated		p value	Hazard ratio (95% CI)
		Yes, n = 159	No, n = 338		
Median age, y (IQR)	60.1 (49–73)	61 (50–74)	59.6 (49–73)	0.444	1.004 (0.994–1.013)
Sex, no. (%)					
F	160 (32.2)	44 (27.7)	116 (34.3)	Referent	
M	337 (67.8)	115 (72.3)	222 (65.7)	0.139	0.769 (0.544–1.089)
Mean Charlson comorbidity index, (SD)	4.26 (2.12)	4.40 (2.14)	4.20 (2.11)	0.293	1.038 (0.968–1.113)
Underlying conditions, no. (%)					
Cardiovascular diseases	200 (40.2)	79 (49.7)	121 (358)	0.003	1.596 (1.169–2.178)
Chronic renal insufficiency	179 (36.0)	71 (44.7)	108 (32.0)	0.011	1.504 (1.200–2.056)
COPD and asthma	176 (35.4)	71 (44.7)	105 (31.1)	0.005	1.570 (1.148–2.146)
Type 2 diabetes mellitus	116 (23.3)	46 (28.9)	70 (20.7)	0.057	1.395 (0.990–1.965)
Solid tumor	100 (20.1)	36 (22.6)	64 (18.9)	0.363	1.188 (0.820–1.723)
Hematologic malignancy	31 (6.2)	8 (5.0)	23 (6.8)	0.497	0.781 (0.384–1.591)
Past inhaled steroids use for chronic conditions	47 (9.5)	17 (10.7)	30 (8.9)	0.450	1.214 (0.734–2.007)
Current or former smoker	187 (37.6)	74 (46.5)	113 (33.4)	0.005	1.565 (1.146–2.138)
Postoperative admission	142 (28.6)	38 (23.9)	104 (30.8)	0.134	0.757 (0.526–1.090)
Treatment, no. (%)					
No aerosol inhalation	137 (27.6)	33 (20.8)	104 (30.8)	Referent	
Glucocorticoid aerosol inhalation	262 (52.7)	107 (67.3)	155 (45.9)	0.002	1.860 (1.264–2.738)
Aerosol inhalation without glucocorticoid	98 (19.7)	19 (11.9)	79 (23.4)	0.337	0.760 (0.433–1.332)
Broad-spectrum antimicrobial drugs, >7 d	417 (83.9)	157 (98.7)	260 (76.9)	<0.001	9.539 (4.595–18.795)
Invasive mechanical ventilation, >5 d	221 (44.5)	112 (70.4)	109 (32.2)	<0.001	3.452 (2.453–4.858)
Urethral catheter placement, >3 d	493 (99.2)	158 (99.4)	335 (99.1)	0.875	1.171 (0.164–8.361)
Vasopressor treatment, >3 d	75 (15.1)	42 (26.4)	33 (9.8)	<0.001	2.634 (1.850–3.750)
Renal dialysis, >3 d	84 (16.9)	34 (21.4)	50 (14.8)	0.063	1.432 (0.980–2.093)
APACHE II score, mean (SD)	18.18 (6.03)	18.98 (6.44)	17.80 (5.80)	0.053	1.026 (1.000–1.053)
Median length of ICU stay, d (IQR)	15 (7–23)	20 (10–28)	13 (6–20)	0.057	1.005 (1.000–1.010)

*APACHE II, Acute Physiology and Chronic Health Evaluation II; COPD, chronic obstructive pulmonary disease; ICU, intensive care unit; IQR, interquartile range.

isolation in both model 1 (HR 1.499, 95% CI 1.001–2.246; p = 0.049) (Appendix Table 3) and model 2 (HR 1.528, 95% CI 1.024–2.278; p = 0.038) (Table 2). Cardiovascular diseases, prolonged use of broad-spectrum antimicrobial drugs, invasive mechanical ventilation, and vasopressor treatment were other independent risk factors for *A. baumannii* (Table 2; Appendix Table 3). As a whole variable, aerosol inhalation had no effect on *A. baumannii* isolation (Appendix Table 4).

In the propensity-matched cohort, the possible glucocorticoid-related covariables were balanced in both groups (Appendix Table 5). Univariate and multivariate Cox regression analyses also indicated that glucocorticoid aerosol therapy was an independent risk factor for *A. baumannii* isolation (Table 3; Appendix Table 6). In an independent model that included indications for glucocorticoid aerosol therapy, risk factors for *A. baumannii* isolation were glucocorticoid aerosol treatments for COPD or asthma and for ARDS (Appendix Table 7).

Log-rank analysis showed that the difference among the groups was statistically significant (p<0.001). The cumulative hazard for *A. baumannii*

Table 2. Multivariate analysis of risk factors for *Acinetobacter baumannii* among patients during invasive mechanical ventilation, China*

Variables	p value	Hazard ratio (95% CI)
Underlying conditions		
Cardiovascular diseases	0.054	1.394 (0.994–1.955)
Chronic renal insufficiency	0.730	0.937 (0.648–1.356)
COPD and asthma	0.132	1.299 (0.924–1.825)
Type 2 diabetes mellitus	0.325	1.197 (0.837–1.714)
Current or former smoker	0.098	1.307 (0.951–1.797)
Treatment		
No aerosol inhalation	Referent	
Glucocorticoid aerosol inhalation	0.038	1.528 (1.024–2.278)
Aerosol inhalation without glucocorticoid	0.524	0.829 (0.467–1.475)
Broad-spectrum antimicrobial drugs, >7 d	0.001	7.238 (2.758–15.788)
Invasive mechanical ventilation, >5 d	0.001	2.381 (1.664–3.405)
Vasopressor treatment, >3 d	<0.001	2.060 (1.402–3.028)
Renal dialysis, >3 d	0.841	1.046 (0.675–1.620)
APACHE II score	0.586	0.992 (0.965–1.020)

*Results are from model 2; only variables with p<0.1 in univariate analysis were included. APACHE II, Acute Physiology and Chronic Health Evaluation II; COPD, chronic obstructive pulmonary disease.

Table 3. Multivariate analysis of risk factors for *Acinetobacter baumannii* among propensity-matched patient cohort during invasive mechanical ventilation, China*

Variables	p value	Hazard ratio (95% CI)
Underlying conditions		
Cardiovascular diseases	0.117	1.361 (0.926–2.001)
Chronic renal insufficiency	0.800	1.052 (0.712–1.554)
Type 2 diabetes mellitus	0.243	1.271 (0.850–1.899)
Current or former smoker	0.051	1.442 (0.998–2.083)
Treatment		
Glucocorticoid aerosol inhalation	0.032	1.489 (1.036–2.141)
Broad-spectrum antimicrobial drugs, ≥7 d	0.004	6.315 (2.543–13.921)
Invasive mechanical ventilation, ≥5 d	<0.001	2.388 (1.614–3.534)
Vasopressor treatment, ≥3 d	0.501	1.188 (0.719–1.963)
APACHE II score	0.363	1.014 (0.984–1.045)

*Only variables with p<0.1 in univariate analysis of the propensity-matched cohort were included. APACHE II, Acute Physiology and Chronic Health Evaluation II; COPD, chronic obstructive pulmonary disease.

isolation was significantly higher in the glucocorticoid aerosol group compared with the no aerosol inhalation (HR 1.871; 95% CI 1.206–2.772; p<0.001) and aerosol inhalation without glucocorticoid (HR 2.316; 95% CI 1.482–3.620; p = 0.002) groups (Figure 2).

Effect of Glucocorticoid Aerosol Therapy on *A. baumannii* Isolation among Subgroups

We divided patients into subgroups to evaluate the contribution of glucocorticoid aerosol to *A. baumannii* isolation from different subpopulations. We found glucocorticoid aerosol was a promoting factor for *A. baumannii* isolation from most subpopulations, except patients with type 2 diabetes mellitus, hematologic malignancy, antimicrobial drug use for *A. baumannii*, and short ICU stays (p>0.05) (Figure 3). We noted no statistically significant interactions between most prespecified subgroups defined by demographics, medical history, underlying conditions, APACHE II score, treatment measures, and length of ICU stay (interaction p>0.05). The favorable effect of glucocorticoid aerosol on *A. baumannii* isolation was relatively greater in the subgroup of patients with longer vasopressor treatment (interaction p = 0.006) (Figure 3).

Association between Glucocorticoid Aerosol Therapy and Clinical Prognosis

We performed univariate and multivariate Cox regression analyses to evaluate the possible risk factors for 30-day mortality in critically ill patients on ventilators. We found glucocorticoid aerosol was not a risk factor for 30-day mortality in those patients, but *A. baumannii* isolation was independently associated with 30-day mortality (HR 1.824, 95% CI 1.317–2.104; p = 0.045) (Appendix Tables 8, 9). A further separate analysis of *A. baumannii* isolation status showed that *A. baumannii* infection was independently associated with 30-day mortality (HR 2.759, 95% CI 1.575–4.833; p = 0.012) (Appendix Tables 8, 10).

Discussion

In this study, we assessed the effect of the commonly used glucocorticoid aerosol therapy on the frequency of *A. baumannii*–positive cultures from lower respiratory tract samples in 3 ICUs in China. After controlling for other variables, our findings showed that glucocorticoid aerosol increased the risk for *A. baumannii* isolation from critically ill patients on invasive mechanical ventilation.

A. baumannii is ubiquitous in nature and is becoming more frequent in hospitals. In our study, 32% of patients acquired *A. baumannii* during the 30-day follow-up period. Over the past 2 decades,
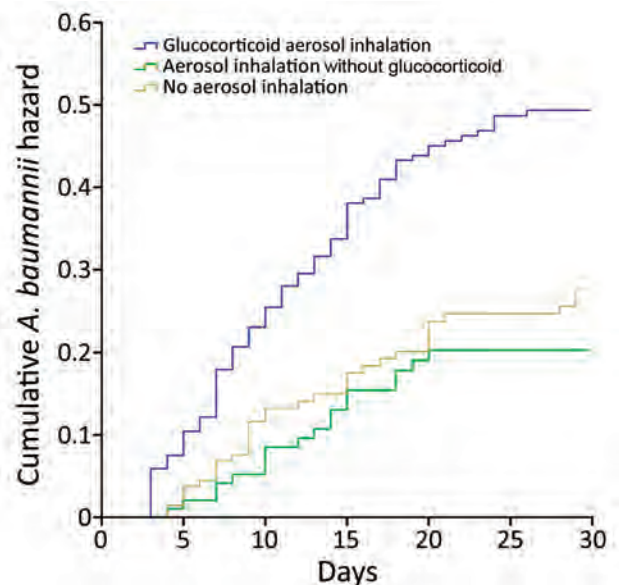
Figure 2. Kaplan-Meier curves of cumulative hazards of different aerosol inhalation treatments on *Acinetobacter baumannii* isolation among patients during invasive mechanical ventilation, China. We used log-rank analysis to compare hazard ratios over time among all groups (p<0.001), glucocorticoid aerosol therapy group with the no aerosol inhalation group (p<0.001), and the glucocorticoid aerosol therapy group with the aerosol inhalation without glucocorticoid group (p = 0.002).
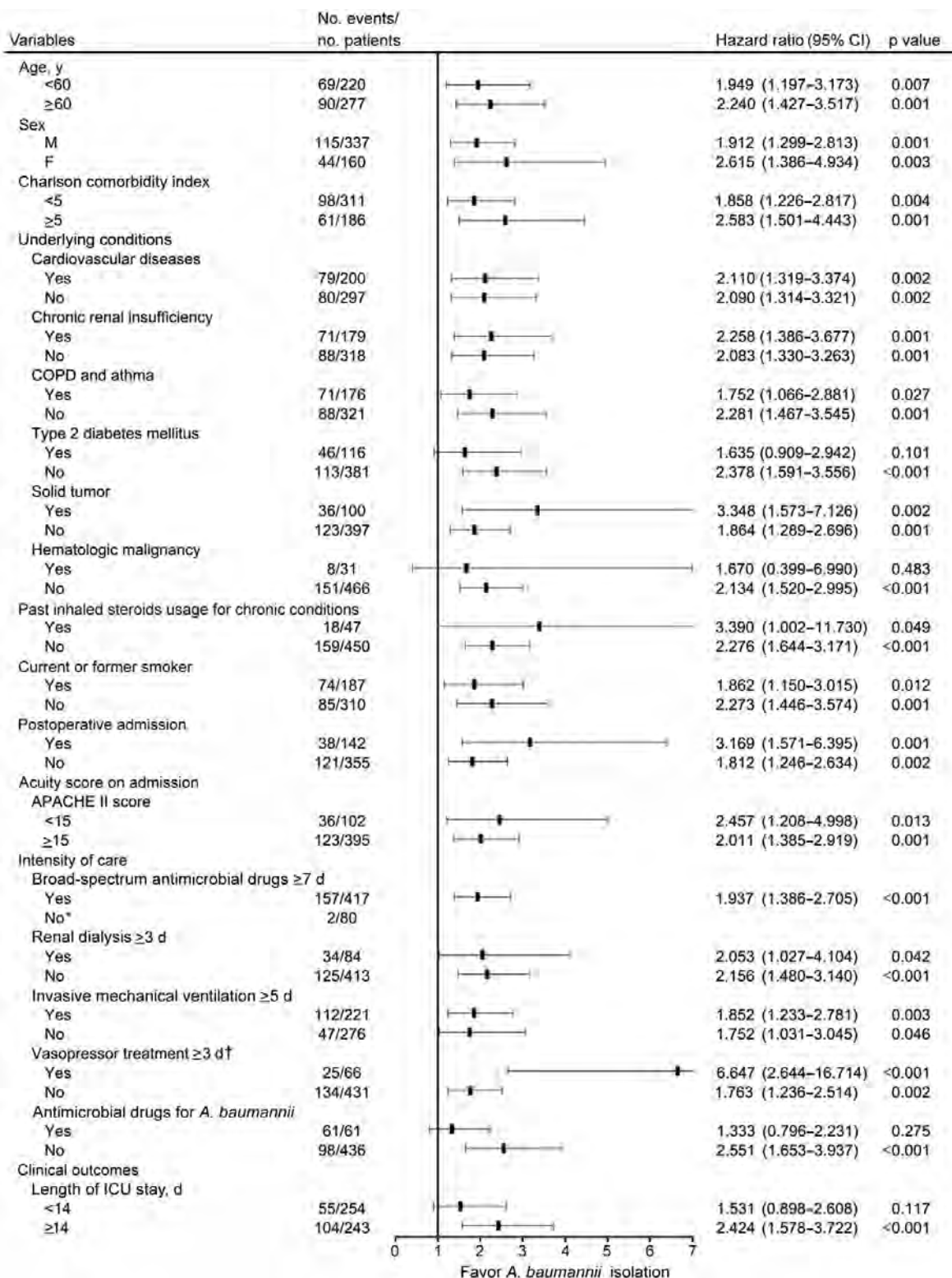
Figure 3. Effects of glucocorticoid aerosol therapy on *Acinetobacter baumannii* isolation during invasive mechanical ventilation among prespecified patient subgroups, China. We applied Cox proportional hazards model with Efron's method for handling ties between groups to assess favorable effects of glucocorticoid aerosol on *A. baumannii* isolation. Black horizontal marks indicate hazard ratios, and error bars indicate 95% CIs. APACHE II, Acute Physiology and Chronic Health Evaluation II; COPD, chronic obstructive pulmonary disease; ICU, intensive care unit. *Limited numbers for analysis. †For interaction, p = 0.006.

several studies have attempted to characterize and identify risk factors for *A. baumannii* colonization or infection. Invasive operations, such as endotracheal mechanical ventilation, inserted invasive devices, ICU stays, recent surgery, use of broad-spectrum antimicrobial drugs, ineffective antimicrobial therapy, and septic shock at diagnosis, are risk factors for MDR *A. baumannii* colonization or infection and for death (*5,31–33*).

We determined that prolonged use of broad-spectrum antimicrobial drugs, invasive mechanical ventilation, and vasopressor treatment were independent risk factors for *A. baumannii* isolation from ventilated patients, which is consistent with previous studies (*5,31–33*). A previous study reported that cardiovascular organ failure was an independent risk factor associated with *A. baumannii* bloodstream infection (*34*). Of note, model 1 of our study showed that cardiovascular disease also was an independent risk factor for *A. baumannii* isolation. Another population-based study reported that patients with chronic heart failure had a markedly increased risk for hospitalization with pneumonia (*35*), indicating a possible correlation between cardiovascular diseases and pneumonia. However, the specific underlying mechanisms by which cardiovascular disease promotes *A. baumannii* isolation remain unknown.

In critically ill patients undergoing mechanical ventilation, aerosol inhalation is a common intervention for treating various pulmonary diseases. An international survey demonstrated that 99% of 611 ICUs from 70 countries reported using aerosol therapy during mechanical ventilation, including noninvasive ventilation, and the most frequently delivered drugs were bronchodilators and steroids (*36*). A web-based survey involving 447 hospitals in mainland China recorded a high proportion of aerosol therapy in both invasive (90.8%) and noninvasive (91.3%) mechanical ventilation; bronchodilators (64.8%) and topical corticosteroids (43.4%) were the most commonly used drugs (*9*). Aerosol inhalation is aimed at reversing bronchoconstriction, decreasing the work of breathing, relieving dyspnea, modifying the inflammatory response (*19,37*), ameliorating lung injury (*38*), and reducing the rate of exacerbation in both asthma and COPD. However, in patients with COPD and asthma, inhaled corticosteroids are associated with an increased risk for upper respiratory tract infections (*39,40*), pneumonia, and lower respiratory tract infections (*15,41*).

Ventilated patients are already vulnerable to pneumonia. Therefore, evaluating whether commonly used aerosol therapy increases the risk for nosocomial pneumonia is crucial, especially when inhaled with glucocorticoids. Because *A. baumanni–*related pneumonia is associated with severe illness and death, we chose *A. baumannii* isolation as an outcome and explored its relationship with glucocorticoid aerosol therapy. Our study showed that glucocorticoid aerosol therapy was an independent risk factor for *A. baumannii* isolation from patients on ventilators. Compared with no aerosol inhalation, glucocorticoid aerosol inhalation increased the risk for *A. baumannii* by ≈1.5 times. Although further analysis revealed that glucocorticoid aerosol was not directly associated with 30-day mortality, it still might contribute to poor clinical prognosis due to its effect on *A. baumannii* isolation. As we described, *A. baumannii*, especially MDR *A. baumannii* pneumonia, is well recognized as a risk factor for death. In this study, we also found *A. baumannii* isolation was an independent risk factor for 30-day mortality in patients receiving invasive mechanical ventilation. Because glucocorticoid aerosol heightened the likelihood of acquiring *A. baumannii*, it might exert a secondary effect, death among *A. baumannii*–infected patients. Thus, further investigation in a much larger patient population could describe a downstream mortality effect of glucocorticoid aerosol therapy.

When we included glucocorticoid aerosol indications in multivariate analysis, we found COPD and asthma and possible ARDS were independent risk factors for *A. baumannii* isolation. Because these structural or underlying lung diseases and severe acute lung injury necessitate longer duration of mechanical ventilation, our results were compatible with previously described risk factors for *A. baumannii* infection. In contrast to glucocorticoid aerosol, we did not detect an association between aerosol inhalation without glucocorticoid and *A. baumannii*. Because both therapies generate aerosols, our previous concern that aerosols were a source of *A. baumannii* acquisition might not be reasonable.

Reasons why glucocorticoids increase the risk for *A. baumannii* isolation remain elusive. Previously considered sterile, healthy lungs harbor complex and dynamic microbiota communities (*42*). Pulmonary diseases, such as COPD (*43*), asthma (*44*), lung cancer (*45*), and ARDS (*46*), cause considerable alteration of lung microbiota. Pneumonia pathogenesis involves an abrupt and emergent disruption in the complex homeostasis of the lung microbial ecosystem (*47*). A recent study reported that inhaled corticosteroids altered the lung microbiota in both COPD patients and mouse models and impaired bacterial control in models with *Streptococcus pneumonia* infection (*14*).

Antimicrobial peptides, also known as host defense peptides, are short and generally positively charged peptides that participate in the regulation of the host's antibacterial actions and immune defense (*48*). Another study observed that cathelicidin, an antimicrobial peptide, was impaired by inhaled corticosteroids among COPD patients by increasing protease cathepsin D, thereby promoting the proliferation of *Streptococcus* (*14*). In a bacterial 16S rRNA gene sequencing and host transcriptomic analysis, another study reported that as COPD severity increased, the airway microbiome becomes associated with decreased abundance of *Prevotella* bacteria in concert with downregulation of genes promoting epithelial defense associated with inhaled corticosteroid use (*49*). Evidence also suggests that in asthma, inhaled corticosteroids can alter the relative abundance of genera in airway microbiome (*50*). Therefore, inhaled corticosteroids play a primary role in lung microbiota disruption and host-defense suppression, which could explain why glucocorticoid aerosol contributed to the increased risk for *A. baumannii* isolation from patients on ventilators.

Clinicians should individualize patient care and manage treatments on the basis of subgroup analysis results. Our results showed that, in most subpopulations, regardless of the presence or absence of the pre-specified characteristics, patients were at higher risk for *A. baumannii* isolation when receiving glucocorticoid aerosol. Based on our findings, we recommend that intensive care teams more carefully consider the risk of widespread usage of glucocorticoid aerosol in patients with invasive mechanical ventilation. Because glucocorticoid aerosol therapy had a much greater favorable effect on *A. baumannii* isolation in the subgroup of patients on vasopressors for >3 days, clinicians should be particularly cautious about giving glucocorticoid aerosol to patients on long vasopressor treatments. Because patients with diabetes, hematologic malignancy, and shorter ICU stays were at relatively lower risk for glucocorticoid aerosol–associated *A. baumannii* acquisition, glucocorticoid aerosol could be considered when appropriate for indications in these patients. Altogether, our study suggests ICU teams need to identify the specific patient subgroups that will truly benefit from glucocorticoid aerosol therapy rather than more generalized administration. Limiting glucocorticoid aerosol use might be considered as part of existing antimicrobial stewardship bundles. In addition, defining the duration of glucocorticoid aerosol therapy might help maximize benefit while reducing associated risk. Interventional studies exploring the effects of different glucocorticoid aerosol therapy durations on the occurrence of various types of nosocomial pneumonia are needed.

The first limitation of our study is that, because it was an observational study, confounders that might influence the effect of glucocorticoid aerosol on *A. baumannii* isolation remain, even after adjusting by subgroup analysis, propensity score matching analysis, and multivariable Cox regression. A similar situation exists for the analysis of risk factors for death. Second, a potential time bias remains, in which patients might have been exposed to risk factors before study enrollment. However, we have excluded patients with prolonged exposure to several well-known risk factors to minimize the possible effect of time bias. Third, exclusion of certain cases might pose a potential selection bias, including survivorship bias. Future randomized controlled interventional studies are expected to confirm our findings and minimize the effects of confounders and the above biases. Fourth, the study included only 3 ICUs in China and did not focus on pathogens other than *A. baumannii*. Research involving more centers and more cases could explore whether glucocorticoid aerosol is a common risk factor in the overall nosocomial pneumonia risk.

In conclusion, we found glucocorticoid aerosol therapy was an independent risk factor for *A. baumannii* isolation from patients receiving invasive mechanical ventilation. Because of high mortality rates associated with *A. baumannii*–related nosocomial pneumonia, clinicians should carefully consider both the beneficial and harmful effects of glucocorticoid aerosol before administering this therapy.

About the Author

Dr. Zhang is an attending physician and a research scientist at the Department of Critical Care Medicine, Qilu Hospital of Shandong University, Jinan, China. Her research interest is infection and multiorgan failure related to critical illnesses.

References

1. Vincent JL, Rello J, Marshall J, Silva E, Anzueto A, Martin CD, et al.; EPIC II Group of Investigators. International study of the prevalence and outcomes of infection in intensive care units. JAMA. 2009;302:2323–9. https://doi.org/10.1001/jama.2009.1754

2. Vincent JL, Sakr Y, Singer M, Martin-Loeches I, Machado FR, Marshall JC, et al.; EPIC III Investigators. Prevalence and outcomes of infection among patients in intensive care units in 2017. JAMA. 2020;323:1478–87. https://doi.org/10.1001/jama.2020.2717

3. Mea HJ, Yong PVC, Wong EH. An overview of *Acinetobacter baumannii* pathogenesis: motility, adherence and biofilm formation. Microbiol Res. 2021;247:126722. https://doi.org/10.1016/j.micres.2021.126722

4. Lynch JP III, Zhanel GG, Clark NM. Infections due to *Acinetobacter baumannii* in the ICU: treatment options. Semin Respir Crit Care Med. 2017;38:311–25. https://doi.org/10.1055/s-0037-1599225

5. Shi J, Sun T, Cui Y, Wang C, Wang F, Zhou Y, et al. Multidrug resistant and extensively drug resistant *Acinetobacter baumannii* hospital infection associated with high mortality: a retrospective study in the pediatric intensive care unit. BMC Infect Dis. 2020;20:597. https://doi.org/10.1186/s12879-020-05321-y

6. Sunenshine RH, Wright MO, Maragakis LL, Harris AD, Song X, Hebden J, et al. Multidrug-resistant *Acinetobacter* infection mortality rate and length of hospitalization. Emerg Infect Dis. 2007;13:97–103. https://doi.org/10.3201/eid1301.060716

7. Blanco N, Harris AD, Rock C, Johnson JK, Pineles L, Bonomo RA, et al.; CDC Epicenters Program. Risk factors and outcomes associated with multidrug-resistant *Acinetobacter baumannii* upon intensive care unit admission. Antimicrob Agents Chemother. 2017;62:e01631–17. https://doi.org/10.1128/AAC.01631-17

8. Zhang C, Mi J, Wang X, Lv S, Zhang Z, Nie Z, et al. Knowledge and current practices of ICU nurses regarding aerosol therapy for patients treated with invasive mechanical ventilation: a nationwide cross-sectional study. J Clin Nurs. 2021;30:3429–38. https://doi.org/10.1111/jocn.15639

9. Zhang Z, Xu P, Fang Q, Ma P, Lin H, Fink JB, et al.; China Union of Respiratory Care (CURC). Practice pattern of aerosol therapy among patients undergoing mechanical ventilation in mainland China: a web-based survey involving 447 hospitals. PLoS One. 2019;14:e0221577. https://doi.org/10.1371/journal.pone.0221577

10. Lyu S, Li J, Wu M, He D, Fu T, Ni F, et al.; Respiratory Care Committee in Chinese Thoracic Society. The use of aerosolized medications in adult intensive care unit patients: A prospective, multicenter, observational, cohort Study. J Aerosol Med Pulm Drug Deliv. 2021;34:383–91. https://doi.org/10.1089/jamp.2021.0004

11. Lyu S, Li J, Yang L, Du X, Liu X, Chuan L, et al. The utilization of aerosol therapy in mechanical ventilation patients: a prospective multicenter observational cohort study and a review of the current evidence. Ann Transl Med. 2020;8:1071. https://doi.org/10.21037/atm-20-1313

12. Dhand R. Inhaled drug therapy 2016: the year in review. Respir Care. 2017;62:978–96. https://doi.org/10.4187/respcare.05624

13. Ari A. Practical strategies for a safe and effective delivery of aerosolized medications to patients with COVID-19. Respir Med. 2020;167:105987. https://doi.org/10.1016/j.rmed.2020.105987

14. Singanayagam A, Glanville N, Cuthbertson L, Bartlett NW, Finney LJ, Turek E, et al. Inhaled corticosteroid suppression of cathelicidin drives dysbiosis and bacterial infection in chronic obstructive pulmonary disease. Sci Transl Med. 2019;11:eaav3879. https://doi.org/10.1126/scitranslmed.aav3879

15. Ernst P, Gonzalez AV, Brassard P, Suissa S. Inhaled corticosteroid use in chronic obstructive pulmonary disease and the risk of hospitalization for pneumonia. Am J Respir Crit Care Med. 2007;176:162–6. https://doi.org/10.1164/rccm.200611-1630OC

16. Sibila O, Soto-Gomez N, Restrepo MI. The risk and outcomes of pneumonia in patients on inhaled corticosteroids. Pulm Pharmacol Ther. 2015;32:130–6. https://doi.org/10.1016/j.pupt.2015.04.001

17. Artigas A, Camprubí-Rimblas M, Tantinyà N, Bringué J, Guillamat-Prats R, Matthay MA. Inhalation therapies in acute respiratory distress syndrome. Ann Transl Med. 2017;5:293. https://doi.org/10.21037/atm.2017.07.21

18. van Rensen EL, Straathof KC, Veselic-Charvat MA, Zwinderman AH, Bel EH, Sterk PJ. Effect of inhaled steroids on airway hyperresponsiveness, sputum eosinophils, and exhaled nitric oxide levels in patients with asthma. Thorax. 1999;54:403–8. https://doi.org/10.1136/thx.54.5.403

19. Horvath G, Wanner A. Inhaled corticosteroids: effects on the airway vasculature in bronchial asthma. Eur Respir J. 2006;27:172–87. https://doi.org/10.1183/09031936.06.00048605

20. Leading Industry Research Network. Analysis on market demand status and market development trend of budesonide inhalation preparations in China in 2020. 2020 Nov 23 [cited 2022 Jan 24]. http://www.leadingir.com/datacenter/view/5683.html

21. Gales AC, Seifert H, Gur D, Castanheira M, Jones RN, Sader HS. Antimicrobial susceptibility of *Acinetobacter calcoaceticus-Acinetobacter baumannii* complex and *Stenotrophomonas maltophilia* clinical isolates: results from the SENTRY antimicrobial surveillance program (1997–2016). Open Forum Infect Dis. 2019;6(Suppl 1):S34–46. https://doi.org/10.1093/ofid/ofy293

22. European Centre for Disease Prevention and Control. Surveillance of antimicrobial resistance in Europe 2018. Stockholm: The Centre; 2019.

23. Hu F, Guo Y, Zhu D, Wang F, Jiang X, Xu Y, et al. CHINET surveillance of bacterial resistance in China: 2018 report. Chin J Infect Chemother. 2020;20:1–10.

24. Wang F, Zhu D, Hu F, Jiang X, Hu Z, Li Q, et al. 2012 CHINET surveillance of bacterial resistance in China. Chin J Infect Chemother. 2013;13:321–30.

25. Meng X, Fu J, Zheng Y, Qin W, Yang H, Cao D, et al. Ten-year changes in bloodstream infection with *Acinetobacter baumannii* complex in intensive care units in eastern China: a retrospective cohort study. Front Med (Lausanne). 2021;8:715213. https://doi.org/10.3389/fmed.2021.715213

26. Chung DR, Song JH, Kim SH, Thamlikitkul V, Huang SG, Wang H, et al.; Asian Network for Surveillance of Resistant Pathogens Study Group. High prevalence of multidrug-resistant nonfermenters in hospital-acquired pneumonia in Asia. Am J Respir Crit Care Med. 2011;184:1409–17. https://doi.org/10.1164/rccm.201102-0349OC

27. Xie J, Yang Y, Huang Y, Kang Y, Xu Y, Ma X, et al. The current epidemiological landscape of ventilator-associated pneumonia in the intensive care unit: a multicenter prospective observational study in China. Clin Infect Dis. 2018;67(suppl_2):S153–61. https://doi.org/10.1093/cid/ciy692

28. Hu FP, Guo Y, Zhu DM, Wang F, Jiang XF, Xu YC, et al. Resistance trends among clinical isolates in China reported from CHINET surveillance of bacterial resistance,

2005–2014. Clin Microbiol Infect. 2016;22(Suppl 1):S9–14. https://doi.org/10.1016/j.cmi.2016.01.001

29. Hu F, Guo Y, Yang Y, Zheng Y, Wu S, Jiang X, et al.; China Antimicrobial Surveillance Network (CHINET) Study Group. Resistance reported from China antimicrobial surveillance network (CHINET) in 2018. Eur J Clin Microbiol Infect Dis. 2019;38:2275–81. https://doi.org/10.1007/s10096-019-03673-1

30. Huang H, Chen B, Liu G, Ran J, Lian X, Huang X, et al. A multi-center study on the risk factors of infection caused by multi-drug resistant *Acinetobacter baumannii*. BMC Infect Dis. 2018;18:11. https://doi.org/10.1186/s12879-017-2932-5

31. Bassetti M, Righi E, Vena A, Graziano E, Russo A, Peghin M. Risk stratification and treatment of ICU-acquired pneumonia caused by multidrug-resistant/extensively drug-resistant/pandrug-resistant bacteria. Curr Opin Crit Care. 2018;24:385–93. https://doi.org/10.1097/MCC.0000000000000534

32. Freire MP, de Oliveira Garcia D, Garcia CP, Campagnari Bueno MF, Camargo CH, Kono Magri ASG, et al. Bloodstream infection caused by extensively drug-resistant *Acinetobacter baumannii* in cancer patients: high mortality associated with delayed treatment rather than with the degree of neutropenia. Clin Microbiol Infect. 2016;22:352–8. https://doi.org/10.1016/j.cmi.2015.12.010

33. Yamada K, Yanagihara K, Araki N, Harada Y, Morinaga Y, Akamatsu N, et al. Clinical characteristics of tertiary hospital patients from whom *Acinetobacter calcoaceticus–Acinetobacter baumannii* complex strains were isolated. Intern Med. 2012;51:51–7. https://doi.org/10.2169/internalmedicine.51.6018

34. Jang TN, Lee SH, Huang CH, Lee CL, Chen WY. Risk factors and impact of nosocomial *Acinetobacter baumannii* bloodstream infections in the adult intensive care unit: a case-control study. J Hosp Infect. 2009;73:143–50. https://doi.org/10.1016/j.jhin.2009.06.007

35. Mor A, Thomsen RW, Ulrichsen SP, Sørensen HT. Chronic heart failure and risk of hospitalization with pneumonia: a population-based study. Eur J Intern Med. 2013;24:349–53. https://doi.org/10.1016/j.ejim.2013.02.013

36. Ehrmann S, Roche-Campo F, Sferrazza Papa GF, Isabey D, Brochard L, Apiou-Sbirlea G; REVA research network. Aerosol therapy during mechanical ventilation: an international survey. Intensive Care Med. 2013;39:1048–56. https://doi.org/10.1007/s00134-013-2872-5

37. Hashemian SM, Mortaz E, Jamaati H, Bagheri L, Mohajerani SA, Garssen J, et al. Budesonide facilitates weaning from mechanical ventilation in difficult-to-wean very severe COPD patients: association with inflammatory mediators and cells. J Crit Care. 2018;44:161–7. https://doi.org/10.1016/j.jcrc.2017.10.045

38. Ju YN, Yu KJ, Wang GN. Budesonide ameliorates lung injury induced by large volume ventilation. BMC Pulm Med. 2016;16:90. https://doi.org/10.1186/s12890-016-0251-z

39. Yang M, Zhang Y, Chen H, Lin J, Zeng J, Xu Z. Inhaled corticosteroids and risk of upper respiratory tract infection in patients with asthma: a meta-analysis. Infection. 2019;47:377–85. https://doi.org/10.1007/s15010-018-1229-y

40. Yang M, Chen H, Zhang Y, Du Y, Xu Y, Jiang P, et al. Long-term use of inhaled corticosteroids and risk of upper respiratory tract infection in chronic obstructive pulmonary disease: a meta-analysis. Inhal Toxicol. 2017;29:219–26. https://doi.org/10.1080/08958378.2017.1346006

41. McKeever T, Harrison TW, Hubbard R, Shaw D. Inhaled corticosteroids and the risk of pneumonia in people with asthma: a case-control study. Chest. 2013;144:1788–94. https://doi.org/10.1378/chest.13-0871

42. Wang J, Li F, Tian Z. Role of microbiota on lung homeostasis and diseases. Sci China Life Sci. 2017;60:1407–15. https://doi.org/10.1007/s11427-017-9151-1

43. Sze MA, Dimitriu PA, Hayashi S, Elliott WM, McDonough JE, Gosselink JV, et al. The lung tissue microbiome in chronic obstructive pulmonary disease. Am J Respir Crit Care Med. 2012;185:1073–80. https://doi.org/10.1164/rccm.201111-2075OC

44. Hilty M, Burke C, Pedro H, Cardenas P, Bush A, Bossley C, et al. Disordered microbial communities in asthmatic airways. PLoS One. 2010;5:e8578. https://doi.org/10.1371/journal.pone.0008578

45. Laroumagne S, Lepage B, Hermant C, Plat G, Phelippeau M, Bigay-Game L, et al. Bronchial colonisation in patients with lung cancer: a prospective study. Eur Respir J. 2013;42:220–9. https://doi.org/10.1183/09031936.00062212

46. Dickson RP, Singer BH, Newstead MW, Falkowski NR, Erb-Downward JR, Standiford TJ, et al. Enrichment of the lung microbiome with gut bacteria in sepsis and the acute respiratory distress syndrome. Nat Microbiol. 2016;1:16113. https://doi.org/10.1038/nmicrobiol.2016.113

47. Dickson RP, Erb-Downward JR, Huffnagle GB. Towards an ecology of the lung: new conceptual models of pulmonary microbiology and pneumonia pathogenesis. Lancet Respir Med. 2014;2:238–46. https://doi.org/10.1016/S2213-2600(14)70028-1

48. Lai Y, Gallo RL. AMPed up immunity: how antimicrobial peptides have multiple roles in immune defense. Trends Immunol. 2009;30:131–41. https://doi.org/10.1016/j.it.2008.12.003

49. Ramsheh MY, Haldar K, Esteve-Codina A, Purser LF, Richardson M, Müller-Quernheim J, et al. Lung microbiome composition and bronchial epithelial gene expression in patients with COPD versus healthy individuals: a bacterial 16S rRNA gene sequencing and host transcriptomic analysis. Lancet Microbe. 2021;2:e300–10. https://doi.org/10.1016/S2666-5247(21)00035-5

50. Huang C, Yu Y, Du W, Liu Y, Dai R, Tang W, et al. Fungal and bacterial microbiome dysbiosis and imbalance of trans-kingdom network in asthma. Clin Transl Allergy. 2020;10:42. https://doi.org/10.1186/s13601-020-00345-8

Address for correspondence: Hao Wang, Department of Critical Care Medicine, Qilu Hospital of Shandong University, 107 Wenhuaxi Rd, Jinan 250012, China; email: wanghao34@126.com

Observational Cohort Study of Evolving Epidemiologic, Clinical, and Virologic Features of Monkeypox in Southern France

Nadim Cassir, Florian Cardona, Hervé Tissot-Dupont, Christiane Bruel,
Barbara Doudier, Salima Lahouel, Karim Bendamardji, Céline Boschi, Sarah Aherfi,
Sophie Edouard, Jean-Christophe Lagier, Philippe Colson, Philippe Gautret,
Pierre-Edouard Fournier, Philippe Parola, Philippe Brouqui, Bernard La-Scola, Matthieu Million

We enrolled 136 patients with laboratory-confirmed monkeypox during June 4–August 31, 2022, at the University Hospital Institute Méditerranée Infection in Marseille, France. The median patient age was 36 years (interquartile range 31–42 years). Of 136 patients, 125 (92%) were men who have sex with men, 15 (11%) reported previous smallpox vaccinations, and 21 (15.5%) were HIV-positive. The most frequent lesion locations were the genitals (68 patients, 53%), perianal region (65 patients, 49%), and oral/perioral area (22 patients, 17%). Lesion locations largely corresponded with the route of contamination. Most (68%) patients had isolated anal, genital, or oral lesions when they were first seen, including 56 (61%) who had ≥1 positive site without a visible lesion. Concurrent sexually transmitted infections were diagnosed in 19 (15%) patients, and 7 patients (5%) were asymptomatic. We recommend vaccination campaigns, intensified testing for sexually transmitted infections, and increased contact tracing to control the ongoing monkeypox outbreak.

Monkeypox virus (MPXV), a zoonotic orthopoxvirus related to smallpox virus, was first described in humans in 1970 in the Democratic Republic of the Congo (1). Sporadic outbreaks of infection have been reported in Africa, typically occurring because of close contact with wild rodents, which represent the primary reservoir (2). Those outbreaks and travel-associated cases outside of Africa have been characterized by limited secondary spread (3). A new outbreak began in May 2022, when autochthonous cases of MPXV infection were initially reported in England and, subsequently, throughout Europe. The World Health Organization declared monkeypox a public health emergency on July 23, 2022 (4,5). As of September 6, 2022, a total of 54,911 laboratory-confirmed cases of monkeypox and 15 monkeypox-related deaths had been reported to the World Health Organization by 100 countries. Genomic analysis of viral strains causing the current outbreak revealed a distinct phylogenetic lineage of human MPXV. This lineage (B.1, belonging to clade IIb) is characterized by a heightened mutational signature compared with its ancestors and has been associated with milder disease than clade I (6).

Initial reports on the ongoing monkeypox outbreak suggest that cases have been atypical; patients have had rashes appearing on fewer regions of the body, frequent genital and perianal lesions, less frequent prodromal symptoms, and a generally benign course of disease (2,7–10). In contrast, in monkeypox-endemic countries in Africa, monkeypox predominantly affects young children and is characterized by rashes incorporating many simultaneous lesions in multiple regions of the body, including the face, that are associated with diffuse lymphadenopathy. The

Table 1. Demographic and epidemiologic characteristics of patients with monkeypox in Marseille during the 2022 outbreak in southern France*

Variable	No. patients†
Age, y, median (IQR)	36 (30–42)
Sex	
F	3 (2.2)
M	133 (97.8)
Sexual orientation	
Men who have sex with men	125 (91.9)
Using PrEP	30 (24)
Heterosexual men	2 (1.5)
Heterosexual women	3 (2.2)
History of smallpox vaccination	
Childhood vaccine	7 (5.1)
Postexposure vaccine	6 (4.4)
Preexposure vaccine	2 (1.5)
HIV-positive	
Total	21 (15.4)
<500 CD4/mm^3	5 (23.8)
<200 CD4/mm^3	0
Possible exposure to monkeypox	
Sexual partner with monkeypox	21 (15.4)
New sexual partners‡	115 (84.6)
Attendance at a Pride event	7 (5.2)
Recent travel to an endemic country	0
Recent travel to an epidemic country	17 (12.5)

*Values are no. (%) patients except as indicated. PrEP, preexposure prophylaxis; CD4, CD4 T lymphocyte.
†Total number of patients in the study was 136.
‡Single or multiple new sexual partners in the previous 21 d.

rash is preceded by systemic prodromal symptoms (*3*). Complications include pneumonitis, encephalitis, keratitis, and secondary bacterial infections. The case fatality rate ranges from 1%–10% depending on immune status and clade (*2*). However, these data come from relatively old studies in low resource settings where access to healthcare is limited; minor cases are almost certainly underreported, and ascertainment of cause of death is incomplete.

Detailed information regarding the changing epidemiology of monkeypox during the 2022 outbreak is needed. In this study, we aimed to comprehensively evaluate the epidemiologic, clinical, and virologic features of 136 patients who had a monkeypox diagnosis at the University Hospital Institute Méditerranée Infection in Marseille, France.

Materials and Methods

Study Design and Participants
In this retrospective, observational cohort study, we enrolled consecutive patients who had a monkeypox diagnosis during June 4–August 31, 2022, at the University Hospital Institute Méditerranée Infection in Marseille, France. We defined a confirmed monkeypox case as a positive real-time PCR result from skin, genital, rectal, or pharyngeal swab samples. We performed contact tracing and follow-up in collaboration with the regional health agency after mandatory declarations were made to the health agency. Asymptomatic patients were tested when they reported recent high-risk exposure. We only included adult patients in the analysis who had laboratory-confirmed monkeypox. Treatment was prescribed according to national standard of care procedures. Imvanex (Bavarian Nordic, https://www.bavarian-nordic.com) was the vaccine used in France for the preexposure and postexposure vaccination against MPXV.

Ethics Approval
The study was approved by the ethics committee at the University Hospital Institute Méditerranée Infection (no. 039-2022) and declared to the Règlement Général de la Protection des Données registry (no. 22-340). We extracted medical data from the hospital's electronic medical records system. We obtained oral informed consent from all patients in accordance with the Declaration of Helsinki (revised in 2013) and written informed consent for publication of clinical images when needed.

Laboratory Procedures
Laboratory confirmation of orthopoxvirus, including monkeypox virus, was performed at the University Hospital Institute Méditerranée Infection in Marseille, France. We tested skin, genital, rectal, and pharyngeal swabs for MPXV by using in-house real-time PCR (*11*). Genital or rectal swab refers to sampling of skin/mucosal lesions in the genital or rectal areas. No anoscopies were performed in this cohort. For 127 patients who were enrolled after being informed, we tested clinical samples for other sexually transmitted infections (STI) by using quantitative PCR to detect specific pathogens, including *Neisseria gonorrhoeae*, *Chlamydia trachomatis*, *Mycoplasma genitalium*, *Treponema pallidum*, herpesvirus, and *Trichomonas vaginalis* as previously described (*12,13*). Using serologic methods, we also tested for hepatitis B virus, hepatitis C virus, HIV, and syphilis in 9 of those 127 patients. All patients were examined in an isolation room where samples were collected for analysis. Sample collection to diagnose monkeypox and other STIs evolved during the time of the study, focusing first on the rash lesion and then associated systematically with pharyngeal, rectal, and genital swabbing together with blood samples for serologies contingent upon the patient's agreement. We handled all samples in a Biosafety Level 3 laboratory.

Data
We established case definitions before beginning data collection. For all patients attending our institute

for suspected monkeypox infection, we used a standardized medical questionnaire (in English or French) (Appendix Figures 1, 2, https://wwwnc.cdc.gov/EID/article/28/12/22-1440-App1.pdf) to obtain demographic information; patient's reported smallpox vaccination; HIV status; epidemiologic data, including exposure to someone with monkeypox, travel, attendance at large gatherings, and risk factors for sexually transmitted infections; sexual practices; symptoms; virologic results at multiple body sites, including analysis of PCR cycle threshold (Ct) values; and co-infection with other sexually transmitted pathogens.

We classified sexual orientation as heterosexual or men who have sex with men (MSM) according to the patient's declaration. We defined acute proctitis as perianal lesions with rectal pain because there were no cases of rectal pain without lesions. We defined tonsillitis as a sore throat and exanthem as a widespread maculopapular rash.

Statistical Analysis

We reported continuous variables as medians with interquartile ranges (IQRs), where appropriate, and categorical variables as absolute values and percentages. We compared continuous variables by using Mann-Whitney or Kruskal-Wallis nonparametric tests. All tests were 2-sided with a significance threshold of $p < 0.05$. We performed all analyses by using the statistical package R version 4.0.3 (The R Project for Statistical Computing, https://www.r-project.org). We generated graphs using Prism for Mac version 9.0 (GraphPad, https://www.graphpad.com).

Results

We enrolled a total of 136 patients who had a laboratory-confirmed monkeypox diagnosis; 133 were men, and 3 were women. We collected demographic (Table 1), clinical (Table 2), and microbiological (Table 3) information for the patients. We determined 125 (92%) patients were MSM and 5 (4%) patients were heterosexual. Information on sexual orientation was not available for the remaining 6 patients. The median age was 36.0 (IQR 30.0–42.0) years. Of the 136 enrolled patients, 15 (11%) reported previous smallpox vaccination, and 21 (16%) were HIV-positive, of whom 5 (24%) had a CD4 cell count of <500 cells/mm³. Among 3 heterosexual women, only 1 declared that her regular sexual partner had a monkeypox diagnosis, and the other 2 reported a new sexual partner within the previous 3 weeks. Travel to MPXV-endemic regions was not reported by any patient, whereas 17 (12.5%) reported recent travel to a country that is

part of the current outbreak, which includes Spain (n = 11 patients), United States (n = 2 patients), Germany (n = 1 patient), Belgium (n = 1 patient), Canada (n = 1 patient), and Italy (n = 1 patient). Seven (5.2%) patients had attended a Pride event in the previous 21 days in Spain (n = 2) and France (n = 5). The most frequent lesions were located in the genital (68 [53%] patients), perianal (65 [49%] patients), and oral/perioral (22 [17%] patients) areas (Figure 1). The number of skin lesions was ≤10 in 98 (73%) patients. An asynchronous rash was observed in 41 (30%) of 129 symptomatic patients. Localized lymphadenopathy in lesion areas was observed in 47 (36.4%) patients. Systemic manifestations before or when the patient was first seen included fever (72 [56%] patients), influenza-like illness (44 [35%] patients), and sore throat (11 [8.5%] patients), which preceded the rash in 90 (70%) patients.

Table 2. Clinical characteristics of symptomatic patients with monkeypox in Marseille during the 2022 outbreak in southern France*

Variable	No. (%) patients
Systemic features	
≥1 systemic feature	98 (73)
Systemic symptoms before rash onset	90 (69.8)
Fever	72 (55.8)
Influenza-like illness	44 (35.1)
Sore throat	11 (8.5)
Clinical features of rash	
Approximate number of lesions	
>50	0
11–50	17 (13.2)
1–10	98 (73)
Type of lesion	
Papular	26 (21)
Vesicular	60 (49)
Pustular	25 (20)
Scabbed	10 (7.8)
Asynchronous rash	41 (30.1)
Lesion location	
Genital	68 (52.7)
Perianal	63 (48.8)
Oral ulcer	3 (2.3)
Perioral	22 (17.1)
Hands and feet	13 (10.1)
Trunk	28 (21.7)
Lymphadenopathy	
Any lymphadenopathy	51 (39.5)
Regional at site of lesion	47 (36.4)
Cervical	26 (20.2)
Inguinal	28 (21.7)
Generalized	4 (3.1)
Complications	
Any complication	34 (26.4)
Complication by type	
Proctitis	30 (23.3)
Tonsillitis	5 (3.9)
Penile edema	5 (3.9)
Bacterial skin abscess	4 (3.1%)
Exanthem	3 (2.3%)

*Total number of patients evaluated was 129.

Table 3. PCR and microbiological results for patients with monkeypox in Marseille during the 2022 outbreak in southern France*

Variable	Positive samples/total (%)	Mean Ct (SD)
PCR results		
Skin swabs	69/84 (82)	28.3 (4.7)
Genital swabs	67/69 (97)	26.2 (4.0)
Throat swabs	50/116 (43)	32.2 (3.4)
Rectal swabs	68/105 (65)	26.1 (5.2)
Concurrent STIs		
HIV	2/9 (22.2)	NA
Chlamydia trachomatis	4/127 (3.1)	NA
Neisseria gonorrhoeae	13/127 (10.2)	NA
Mycoplasma genitalium	1/127 (0.8)	NA
Syphilis	4/127 (3.1)	NA
Trichomonas vaginalis	1/127 (0.8)	NA
Other STIs	19/127 (15)	NA

*Ct, cycle threshold; STI, sexually transmitted infection; NA, not applicable.

A concomitant diagnosis of another STI occurred for 19 (15%) patients, including 2 patients who had a new diagnosis of HIV-1 infection. Of 63 patients with perianal lesions, 55 (87.3%) reported practicing receptive anal sex, and 12 (19%) had concomitant *N. gonorrhoeae* (n = 9), *C. trachomatis* (n = 2), or *M. genitalium* (n = 1) infections diagnosed from a rectal swab sample. Of 23 patients with oral ulcers or peri-oral lesions, 6 (26%) had concomitant *N. gonorrhoeae* (n = 4), *C. tra-chomatis* (n = 1), or *T. vaginalis* (n = 1) infections, and 20 (87%) reported practicing oral-receptive sex. Concomitant syphilis was diagnosed in 1 patient from a genital swab sample, and 3 patients had serologic results indicating active syphilis infections.

We observed complications in 37 (27%) patients, which included proctitis (n = 30), tonsillitis (n = 5), penile edema (n = 5), skin abscesses (n = 5), and exanthem (n = 3). Hospital admission was required for 6 (4.5%) patients, some of whom had multiple issues; 5 required perianal pain relief, 3 required management of bacterial abscesses, 1 had dysphagia because of oral lesions, and 1 was admitted for social reasons. All 6 patients had favorable outcomes. None of the patients received antiviral treatment. Opioid prescription for perianal pain relief was required for 3 hospitalized patients and 2 outpatients.

We determined the PCR Ct values were lower for skin, genital, and rectal swabs (combined mean) than for pharyngeal specimens (mean Ct ± SD 27.4 ±4.9 vs. 32.2 ±3.4; $p < 0.0001$) (Figure 2). Of 129 symptomatic patients, 15 (12%) had samples taken from 4 sites (pharynx, rectum, skin lesion, genital lesion), 73 (57%) had samples taken from 3 sites, 43 (33%) had samples taken from 2 sites, and 5 (4%) had samples
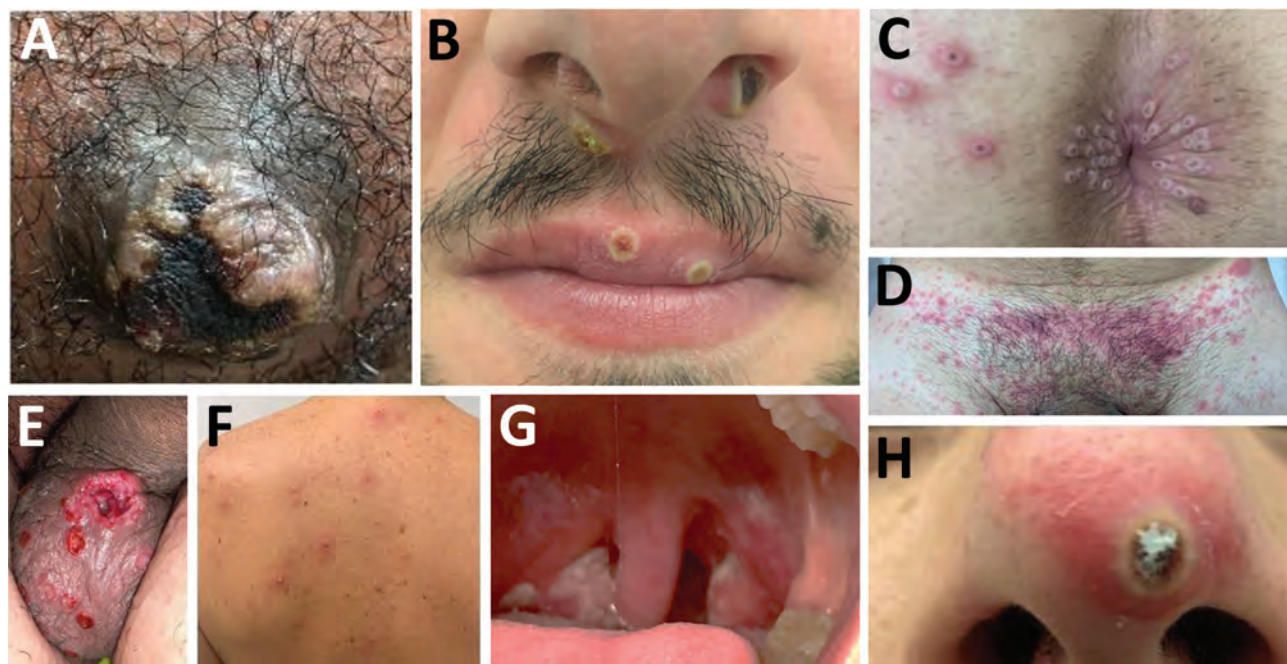
Figure 1. Sites of monkeypox lesions in observational cohort study of evolving epidemiologic, clinical, and virological features of monkeypox in southern France, 2022. A) Primary inoculation site showing an irregular pustule with necrotic crust of the right nipple. B) Pustular lesions with a crusted center on the mucosa of the upper lip, close to the left oral commissure and left nasal orifice. C) Pustules circumferentially distributed on the anal margin and perianal skin of varying sizes and stages of evolution; some with central necrotic crusts. D) Perineally extended purpuric lesions. E) Scrotal lesions of varying sizes and stages of evolution with edema surrounding the larger ulcero-hemorrhagic ulcers. F) Scattered papules, pustules, and umbilicated pustules surrounded by an erythematous halo on the back. G) Reddened and swollen right palatine tonsil with a fibrin-covered ulcer. H) Pustular lesion of the nose with a necrotic central crust, whitish deposit, and erythematous halo.

taken from only 1 site (4 skin swabs, 1 genital swab). We observed 92 (68%) patients with isolated anal, genital, skin, or oral lesions when they were first seen, including 56 (61%) patients who had ≥1 other PCR-positive site without visible lesions. Some PCR-positive samples did not come from visible lesions at the time of testing (40/50 oropharyngeal, 4/67 genital, and 5/68 rectal samples). PCR Ct values from the lesions were not significantly different from those for sites that had no visible lesions (data not shown). The combination of genital and rectal swab testing led to the diagnosis of 111 (86%) MPX cases.

We determined that 7 (5%) patients were asymptomatic; 1 had an MPXV-positive pharyngeal sample and 6 had MPXV-positive rectal samples. We showed that the PCR Ct values obtained from rectal swabs were not significantly different between asymptomatic patients (n = 6) and symptomatic patients (n = 62) (Appendix Figure 3). None of the asymptomatic patients had been previously vaccinated against smallpox virus. We did not find differences in clinical features and MPXV loads between clinical samples from patients who reported receiving smallpox vaccination and those who did not receive vaccination (data not shown) or between patients who reported being HIV-positive and those who did not (Appendix Figure 4).

Discussion

We report epidemiologic, clinical, and virologic data from 136 patients who had confirmed monkeypox at the outpatient unit of the University Hospital Institute Méditerranée Infection in Marseille, France, during June 4–August 31, 2022. We observed systemic manifestations in approximately two thirds of these patients. Lymphadenopathy often occurred in lesion areas, which differs from that reported for endemic monkeypox in countries of Africa. We observed that the evolution of rashes in our study was also atypical because rashes did not always occur with monomorphic and synchronous vesicular umbilicated lesions (3). Similar to recent studies, the cases in our study occurred almost exclusively within the MSM community (2,7–10). However, the percentage of MSM in this study (92%) was lower compared with a previous multicountry report (98%) (2). Of note, both male patients in our study who identified as heterosexual had perianal lesions, which raises the question of reporting bias. We also found that most patients had a low number of lesions (<10) located in the genital, anal, and oral regions. Most patients had previous sexual exposure to a person known to have monkeypox or had high risk for sexually transmitted diseases, such as having single or multiple new sexual partners with-
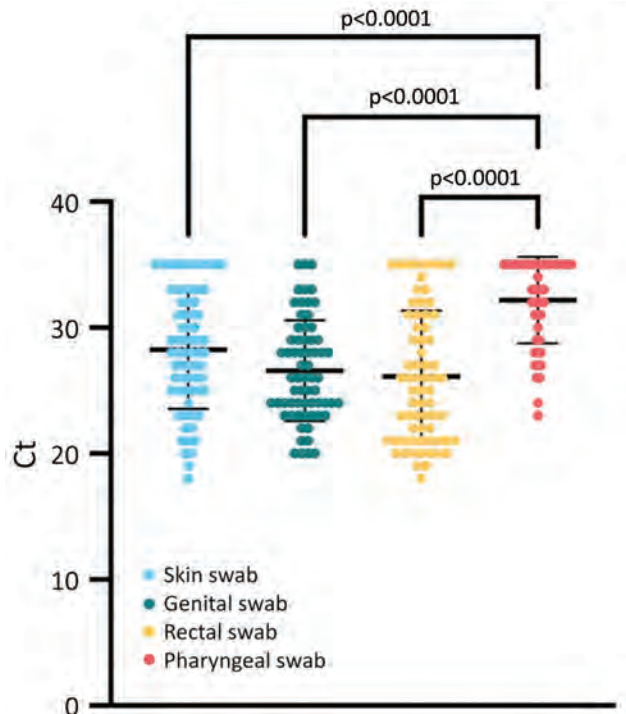
Figure 2. Comparison of monkeypox virus loads between different clinical sampling sites in an observational cohort study of evolving epidemiologic, clinical, and virological features of monkeypox in southern France, 2022. Each colored circle indicates a tested sample; thick horizontal lines indicate mean values; error bars indicate SD. We tested clinical samples for monkeypox virus by using quantitative PCR. We collected samples from skin (n = 69), genital (n = 67), rectal (n = 68), and pharyngeal (n = 50) swabs and calculated the mean Ct for each sample type. Viral loads were significantly lower in skin, genital, and rectal samples compared with pharyngeal samples. Ct, cycle threshold.

in 21 days before their monkeypox diagnosis or attendance at a Pride event. Similar to results from 3 other large cohorts of patients with monkeypox (2,8,9), we found a high rate (15%) of concurrent STI diagnoses, including 2 patients with a new diagnosis of HIV-1 infection. These findings suggest that the sexual route was the main transmission method for amplification of the monkeypox outbreak. For example, 3 large MSM gatherings have been implicated as monkeypox amplifying and superspreading events in Antwerp, Belgium, and in Madrid and the Canary Islands, Spain (14). Although we did not collect this specific information, some patients in our study likely participated in these events. Furthermore, we found that MPXV PCR Ct values in skin, genital, and rectal swab samples were substantially lower than in pharyngeal swab samples. In contrast to a previous report (15), we found that MPXV PCR Ct values in genital and rectal swab samples were not significantly lower than those in skin swab samples. These differences might

be explained in part by sampling bias; a single site swab might be insufficient for microbiological confirmation of monkeypox. Among clinical samples and independently of the lesion site, we found that genital swab specimens had the highest MPXV positivity rate (97%), followed by skin swab specimens (82%). Rectal swab specimens had a positivity rate of 65% and also contributed to a monkeypox diagnosis. In contrast, the MPXV positivity rate of pharyngeal swab samples was relatively low (43%). Genital and rectal swab specimens together had a remarkably high sensitivity (86%) in this patient cohort, which is noteworthy because these specimens are routinely collected in STI clinics. We also found that some positive samples did not come from areas with visible lesions at the time of testing. Testing specimens from multiple sites on persons with exposure history could, therefore, be relevant depending on the symptoms and potential risks the person had during close contact.

We observed that 15 patients had acquired monkeypox despite having been vaccinated against smallpox during childhood or having received a preexposure or postexposure vaccine. The median period between postexposure vaccination (first dose), and the onset of symptoms was 15 (IQR 8.6–22.4) days. Symptoms occurred at 33 and 35 days in 2 patients after first dose preexposure vaccination. These results warrant further investigation to determine the extent of protection provided by vaccination and highlight the insufficient protection provided by the first dose of vaccine. In addition, 15% of patients were HIV-positive, including 5 patients with CD4 cell counts of <500 cells/mm³. Clinical features and MPXV loads did not differ between persons who were HIV-positive and HIV-negative. None of the patients in our study had a CD4 cell count of <200 cells/mm³; therefore, we cannot extrapolate our results to immunocompromised patients. Although >25% of patients had complications that required supportive care and antimicrobial drugs for bacterial skin abscesses, we observed a benign course of disease that did not require antiviral therapy. Of note, hospitalized patients did not have conditions that were considered risk factors for a severe form of monkeypox, such as being immunocompromised, a child, or a pregnant or breastfeeding woman. However, to our knowledge, an evaluation of risk factors for severe outcomes during the current outbreak has not been performed. In a recent report on a cohort of 264 monkeypox cases (7), 6% of patients were hospitalized exclusively for the management of severe local complications at the site of the rash and for pain relief. All patients were men who were not immunosuppressed. Compassion-ate use of tecovirimat for the treatment of monkeypox infection has been proposed in some centers (16) but requires further evaluation and rational use considering the generally benign course of disease in the current outbreak.

In our study, 7 patients with laboratory-confirmed monkeypox were asymptomatic. In contrast, most large cohort studies during the outbreak have included only symptomatic patients who were positive for MPXV (2,7–9). We tested asymptomatic MSM attending our institute only when they reported recent high-risk exposure, and we likely underestimated the incidence of asymptomatic patients who had laboratory-confirmed monkeypox because this was not part of a systematic screening process. Positive MPXV quantitative PCR results have been identified from anal samples in 13/323 (4%) asymptomatic MSM by assessing the presence of MPXV in anorectal samples from asymptomatic MSM who were routinely tested for STIs (17). Moreover, MPXV was identified by PCR in anorectal samples from 3 asymptomatic men in another study; MPXV was cultured from 2 of these samples, indicating viral shedding that could lead to transmission (18). These findings suggest that testing and quarantine for only symptomatic persons might be insufficient to contain the current outbreak.

In conclusion, the ongoing human monkeypox outbreak features unusual characteristics, such as the predominant involvement of MSM who have isolated anal, genital, or oral lesions. The high proportion of concomitant STIs showed transmissibility of monkeypox occurred through local inoculations during sexual activity. Testing specimens from multiple sites in persons with relevant exposure history could be relevant, regardless of the presence of visible lesions. Furthermore, asymptomatic carriage of MPXV suggests that some monkeypox cases might remain undiagnosed, and testing and quarantine of only symptomatic patients might be insufficient to contain transmission. Undiagnosed infections might play a role in overall disease transmission during the outbreak among MSM who have a dense sexual network that includes anonymous contacts, which hampers efficient contact tracing. Physicians should be aware that monkeypox symptoms might overlap with those of other STIs, more specifically in MSM with at-risk sexual activity. Prevention, including vaccination campaigns targeting at-risk groups, are ongoing in multiple countries and should be expanded. Intensified testing for all STIs at different sites (pharynx, rectum, genital, and skin) and in urine and increased contact tracing might also be helpful to control the outbreak.

Acknowledgments

About the Author

Dr. Cassir is a physician specialist in infectious diseases and researcher in clinical microbiology at the IHU Méditerranée Infection in Marseille, France. His main interests focus on the epidemiology of infectious diseases, human microbiota, antibiotic stewardship, and infection control.

References

  1. Ladnyj ID, Ziegler P, Kima E. A human infection caused by monkeypox virus in Basankusu Territory, Democratic Republic of the Congo. Bull World Health Organ. 1972;46:593–7.
  2. Thornhill JP, Barkati S, Walmsley S, Rockstroh J, Antinori A, Harrison LB, et al.; SHARE-net Clinical Group. Monkeypox virus infection in humans across 16 countries—April–June 2022. N Engl J Med. 2022;387:679–91. https://doi.org/10.1056/NEJMoa2207323
  3. Yinka-Ogunleye A, Aruna O, Dalhat M, Ogoina D, McCollum A, Disu Y, et al.; CDC Monkeypox Outbreak Team. Outbreak of human monkeypox in Nigeria in 2017–18: a clinical and epidemiological report. Lancet Infect Dis. 2019;19:872–9. https://doi.org/10.1016/S1473-3099(19)30294-4
  4. World Health Organization. Multi-country outbreak of monkeypox, external situation report #5-7 September 2022 [cited 2022 Sep 28]. https://www.who.int/publications/m/item/multi-country-outbreak-of-monkeypox--external-situation-report--5---7-september-2022
  5. Vaughan AM, Cenciarelli O, Colombe S, Alves de Sousa L, Fischer N, Gossner CM, et al. A large multi-country outbreak of monkeypox across 41 countries in the WHO European Region, 7 March to 23 August 2022. Euro Surveill. 2022;27:2200620. https://doi.org/10.2807/1560-7917.ES.2022.27.36.2200620
  6. Luna N, Ramírez AL, Muñoz M, Ballesteros N, Patiño LH, Castañeda SA, et al. Phylogenomic analysis of the monkeypox virus (MPXV) 2022 outbreak: emergence of a novel viral lineage? Travel Med Infect Dis. 2022;49:102402. https://doi.org/10.1016/j.tmaid.2022.102402
  7. Mailhe M, Beaumont AL, Thy M, Le Pluart D, Perrineau S, Houhou-Fidouh N, et al. Clinical characteristics of ambulatory and hospitalised patients with monkeypox virus infection: an observational cohort study. Clin Microbiol Infect. 2022 Aug 23 [Epub ahead of print]. https://doi.org/10.1016/j.cmi.2022.08.012
  8. Tarín-Vicente EJ, Alemany A, Agud-Dios M, Ubals M, Suñer C, Antón A, et al. Clinical presentation and virological assessment of confirmed human monkeypox virus cases in Spain: a prospective observational cohort study. Lancet. 2022;400:661–9. https://doi.org/10.1016/S0140-6736(22)01436-2
  9. Girometti N, Byrne R, Bracchi M, Heskin J, McOwan A, Tittle V, et al. Demographic and clinical characteristics of confirmed human monkeypox virus cases in individuals attending a sexual health centre in London, UK: an observational analysis. Lancet Infect Dis. 2022;22:1321–8. https://doi.org/10.1016/S1473-3099(22)00411-X
  10. Patel A, Bilinska J, Tam JCH, Da Silva Fontoura D, Mason CY, Daunt A, et al. Clinical features and novel presentations of human monkeypox in a central London centre during the 2022 outbreak: descriptive case series. BMJ. 2022;378:e072410. https://doi.org/10.1136/bmj-2022-072410
  11. Scaramozzino N, Ferrier-Rembert A, Favier AL, Rothlisberger C, Richard S, Crance JM, et al. Real-time PCR to identify variola virus or other human pathogenic orthopox viruses. Clin Chem. 2007;53:606–13. https://doi.org/10.1373/clinchem.2006.068635
  12. Edouard S, Tamalet C, Tissot-Dupont H, Colson P, Ménard A, Ravaux I, et al. Evaluation of self-collected rectal swabs for the detection of bacteria responsible for sexually transmitted infections in a cohort of HIV-1-infected patients. J Med Microbiol. 2017;66:693–7. https://doi.org/10.1099/jmm.0.000481
  13. Schirm J, Bos PAJ, Roozeboom-Roelfsema IK, Luijt DS, Möller LV. *Trichomonas vaginalis* detection using real-time TaqMan PCR. J Microbiol Methods. 2007;68:243–7. https://doi.org/10.1016/j.mimet.2006.08.002
  14. European Centre for Disease Prevention and Control. Epidemiological update: monkeypox multi-country outbreak. 2022 May 31 [cited 2022 Sep 28]. https://www.ecdc.europa.eu/en/news-events/epidemiological-update-monkeypox-multi-country-outbreak-0
  15. Veintimilla C, Catalán P, Alonso R, de Viedma DG, Pérez-Lago L, Palomo M, et al. The relevance of multiple clinical specimens in the diagnosis of monkeypox virus, Spain, June 2022. Euro Surveill. 2022;27:2200598. https://doi.org/10.2807/1560-7917.ES.2022.27.33.2200598
  16. Desai AN, Thompson GR 3rd, Neumeister SM, Arutyunova AM, Trigg K, Cohen SH. Compassionate use of tecovirimat for the treatment of monkeypox infection. JAMA. 2022;328:1348–50. https://doi.org/10.1001/jama.2022.15336
  17. Ferré VM, Bachelard A, Zaidi M, Armand-Lefevre L, Descamps D, Charpentier C, et al. Detection of monkeypox virus in anorectal swabs from asymptomatic men who have sex with men in a sexually transmitted infection screening program in Paris, France. Ann Intern Med. 2022 Aug 16 [Epub ahead of print]. https://doi.org/10.7326/M22-2183
  18. De Baetselier I, Van Dijck C, Kenyon C, Coppens J, Michiels J, de Block T, et al.; ITM Monkeypox study group. Retrospective detection of asymptomatic monkeypox virus infections among male sexual health clinic attendees in Belgium. Nat Med. 2022 Aug 12 [Epub ahead of print]. https://doi.org/10.1038/s41591-022-02004-w

Address for correspondence: Nadim Cassir, Microbes, Evolution, Phylogeny and Infection, Aix-Marseille Université Institut de Recherche Pour le Développement IRD, Assistance Publique, Hôpitaux de Marseille, Institut Hospitalo-Universitaire Méditerranée Infection, 19-21 Boulevard Jean Moulin, 13385 Marseille CEDEX 05, France; email: nadimshams.cassir@ap-hm.fr

Continued Circulation of Tick-Borne Encephalitis Virus Variants and Detection of Novel Transmission Foci, the Netherlands

Helen J. Esser, Stephanie M. Lim, Ankje de Vries, Hein Sprong, Dinant J. Dekker, Emily L. Pascoe,
Julian W. Bakker, Vanessa Suin, Eelco Franz, Byron E.E. Martina, Constantianus J.M. Koenraadt

Tick-borne encephalitis virus (TBEV) is an emerging pathogen that was first detected in ticks and humans in the Netherlands in 2015 (ticks) and 2016 (humans). To learn more about its distribution and prevalence in the Netherlands, we conducted large-scale surveillance in ticks and rodents during August 2018–September 2020. We tested 320 wild rodents and >46,000 ticks from 48 locations considered to be at high risk for TBEV circulation. We found TBEV RNA in 3 rodents (0.9%) and 7 tick pools (minimum infection rate 0.02%) from 5 geographically distinct foci. Phylogenetic analyses indicated that 3 different variants of the TBEV-Eu subtype circulate in the Netherlands, suggesting multiple independent introductions. Combined with recent human cases outside known TBEV hotspots, our data demonstrate that the distribution of TBEV in the Netherlands is more widespread than previously thought.

Tick-borne encephalitis (TBE) is one of the most frequently occurring arboviral diseases in Europe and Asia; 10,000–15,000 human cases occur each year (1). TBE-endemic regions of Europe experienced a 400% increase in the number of cases during 1973–2003, but the notification rate has remained relatively stable over the past 2 decades (with the exception of some peak years, such as 2006 and 2018) (2,3). On the local scale, however, marked fluctuations in disease incidence have occurred over time (3). Ecologic, climatic, socioeconomic,

and cultural aspects might all play a role in explaining these dynamics, but their relative importance might vary across TBE-endemic regions (4–6). Transmission of TBE virus (TBEV) is dependent on complex ecologic interactions between TBEV, tick vectors (in Europe, principally *Ixodes ricinus*) and vertebrate reservoir hosts (small rodents of the genera *Apodemus*, *Myodes*, and *Microtus*) and appears to occur only under specific environmental conditions (7). As a result, the occurrence of TBEV is characterized by a scattered and strongly focal pattern, despite the widespread occurrence of both vector and reservoir hosts (7).

Of note, new endemic TBEV foci continue to emerge, both in countries where the virus has been present for a long time (e.g., Germany, Czech Republic, and Baltic states) and in countries where it was considered absent (e.g., the Netherlands and United Kingdom) (3,8,9). The recent detection of TBEV in previously unaffected countries indicates that the current distribution of the virus lies beyond what was predicted by past climate suitability models (10). The mechanisms underlying this unexpected emergence remain unclear and underline the need for systematic data collection on virus prevalence in emerging areas.

The Netherlands was long considered a nonendemic country for TBEV because human TBE cases were all associated with travel (11) and past surveillance studies did not find evidence of virus circulation in local wildlife or ticks (12). This situation changed in 2015, when TBEV was first detected in ticks collected in response to retrospective serologic screening of serum samples from roe deer (*Capreolus capreolus*), which indicated the virus might have been circulating in the Netherlands as far back as 2010 (13). A follow-up study also using roe deer as sentinel hosts suggested that the spatial distribution of the virus had increased by 2017 (14). Yet TBEV RNA–positive ticks and autochthonous

Author affiliations: Wageningen University and Research, Wageningen, the Netherlands (H.J. Esser, D.J. Dekker, E.L. Pascoe, J.W. Bakker, C.J.M. Koenraadt); Artemis One Health Research Institute, Delft, the Netherlands (S.M. Lim, B.E.E. Martina); National Institute for Public Health and the Environment, Bilthoven, the Netherlands (A. de Vries, H. Sprong, E. Franz); Sciensano, Brussels, Belgium (V. Suin)

human TBE cases had until then been reported from just 2 nature areas: National Park de Utrechtse Heuvelrug in the municipality of Zeist and National Park de Sallandse Heuvelrug in the municipalities of Hellendoorn and Rijssen-Holten (*9*). Thus, local circulation of TBEV in the potential foci identified by serologic screening of roe deer required confirmation. This need prompted us to undertake large-scale surveillance of ticks and wild rodents to investigate TBEV presence and prevalence in potential new foci in the Netherlands.

Materials and Methods

Sample Collection
We collected >46,000 questing ticks (3,321 adult females, 3,764 adult males, and 39,025 nymphs) by drag sampling in 46 locations in September 2018 and during March–June 2019 and April–September 2020 (Figure 1). In addition, we collected 320 rodents and 1,370 ticks feeding on those rodents (1,342 larvae and 28 nymphs) from 13 locations during August–October 2018 and March–June 2019 (Figure 1). All but 2 of the rodent sampling locations coincided with the 46 drag sampling locations. Thus, in total, we sampled 48 locations for questing ticks, rodents, or both. Sampling locations were all in forested nature areas throughout the Netherlands located as close as possible to places where seropositive roe deer were detected in Rijks et al. (*14*) or where the environmental suitability for TBEV circulation was highest according to Esser et al. (*15*). One location, however, involved the woodland garden of an autochthonous TBE patient, where TBEV RNA–positive ticks had been collected in 2017 and 2018 (*9*). That garden borders National Park de Sallandse Heuvelrug
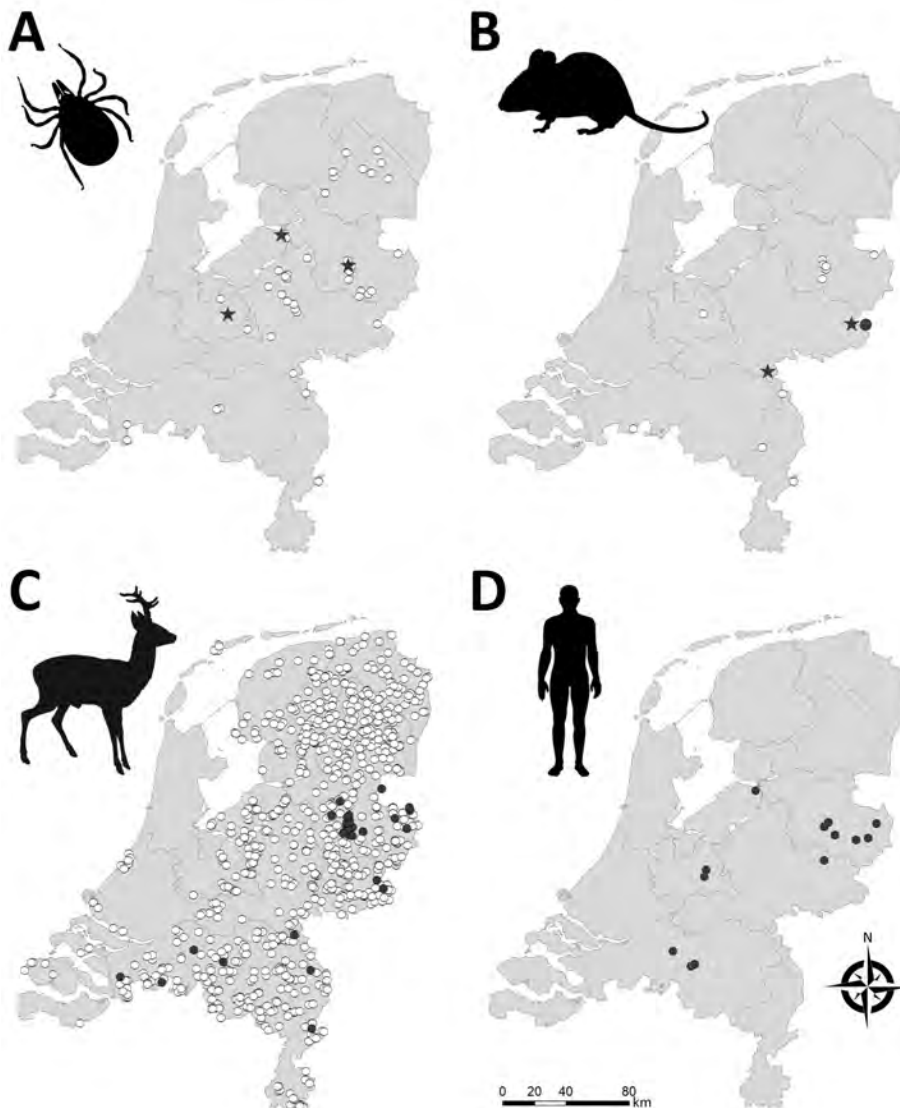
Figure 1. Geographic distribution of tick-borne encephalitis virus (TBEV) in the Netherlands based on sampling of ticks (A), rodents (B), roe deer (C), and reported human (D) tick-borne encephalitis cases. Stars indicate TBEV RNA–positive tick pools or rodent samples. Closed circles indicate serum samples that tested positive in TBEV serum neutralization tests. White circles indicate negative test results. Data for roe deer were reproduced from Rijks et al. (*14*) with permission. Maps were constructed with Arc-GIS software (ESRI, https://www.esri.com).

and lies within 2 km of the location where TBEV RNA–positive ticks and seropositive roe deer were found in 2016 (*13*). We refer to this garden as Nijverdal garden. We obtained research clearance from all terrain owners to collect ticks, rodents, or both.

At each location, we trapped rodents by using Heslinga live traps that were placed in a 7×7 grid with 10 meters' interspacing between traps. We filled traps with hay and baited them with a mixture of grains, carrots, and mealworms. We transported captured rodents to the laboratory facility, where we took blood samples from the submandibular vein under isoflurane anesthesia and subsequently euthanized the animals by cervical dislocation. We identified collected rodents to the species level by morphologic and molecular methods (*16*); the specimens consisted of *Apodemus flavicollis* mice (n = 29), *A. sylvaticus* mice (n = 199), *Microtus arvalis* voles (n = 2), and *Myodes glareolus* voles (n = 90). We collected brain and visceral organ tissues from each rodent and all feeding ticks, if present, and stored samples at −80°C until further analysis. All handling procedures were approved by the Animal Experiments Committee of Wageningen University (approval nos. 2017.W-0049.003 and 2017.W-0049.005) and by the Netherlands Ministry of Economic Affairs (approval no. FF/75A/2015/014).

TBEV RNA Detection and Tick Species Identification

We transported ticks collected from vegetation alive to the laboratory and pooled (4 females/pool, 8 males/pool, or 25 nymphs/pool) by sampling location. However, we tested ticks collected from the Nijverdal garden (37 females, 57 males, and 1,100 nymphs) individually, because we expected this location to have the highest probability of harboring TBEV-infected ticks. We homogenized ticks and extracted nucleic acid as previously described (*17*). To obtain sequences of real-time quantitative reverse transcription PCR (qRT-PCR)–positive tick samples, we performed conventional PCR targeting the polyprotein region of the virus by using primers and protocols as previously described (*18*), then performed sequencing.

In the laboratory, we removed ticks alive from rodents and pooled them per rodent ($\leq$3 nymphs/pool or $\leq$50 larvae/pool). However, we tested ticks collected from TBEV RNA–positive rodents (33 larvae in total) individually. We identified tick species by using a TaqMan qRT-PCR assay, which we also used to test the ticks for TBEV RNA (Appendix 1, https://wwwnc.cdc.gov/EID/article/28/12/22-0552-App1.pdf).

We placed small sections of spleens separately in Lysis Matrix D tubes (MPBio, https://www.mpbio.com) with added MagNa Pure 96 lysis buffer (Roche,

https://www.roche.com). We performed nucleic acid extraction as described for the questing ticks. We froze half-brains −80°C in 1 ml of Dulbecco's Modified Eagle Medium (ThermoFisher Scientific, https://www.thermofisher.com) before processing. We homogenized samples and extracted nucleic acid as described for the ticks collected from rodents and tested samples for TBEV by qRT-PCR.

Phylogenetic Analysis

We used MEGA version 10.0.5 (https://www.mega-software.net) to perform sequence alignments and distance matrix calculations and to construct a phylogenetic tree of polyprotein gene sequences from TBEV RNA–positive tick pools (*19*). We trimmed end-reading errors from each sequence and used BLAST (https://blast.ncbi.nlm.nih) to find and download the 10 most closely matching sequences published in GenBank (note that there was sequence repetition in BLAST results between some samples). We included sequences of the Neudoerfl strain (Genbank accession no. U27495) and Mandal strain (accession no. KF991107) for additional comparison and included Louping ill virus (accession no. NC001809) as an outgroup. We trimmed sequences to the same length (6,735 nt) and aligned by using the MUSCLE algorithm (*20*). We used the maximum-likelihood method and general time reversible model with a gamma distribution and invariant sites to construct the phylogenetic tree (*21*), as determined by jModeltest version 2.1.10 (*22*). We performed 1,000 bootstrap iterations and visualized the tree with the highest log likelihood (21093.04) (Figure 2).

Serologic Detection in Rodents

We tested 316 rodent serum samples for antibodies against TBEV by using a commercial ELISA kit (EIA TBEV Ig; TestLine Clinical Diagnostics, https://www.testlinecd.com) optimized and verified in-house for rodents (Appendix 1). We then conducted a rapid fluorescent focus inhibition seroneutralization test on the ELISA-positive or borderline samples using TBEV Neudoerfl NCPV#848 as reference strain, as previously described (*23*). The dilution of tested serum samples that neutralizes 50% of the virus (DIL_{50}) defines the seroneutralization titer. Serum samples were considered positive at $DIL_{50} > 1/15$ and negative at $DIL_{50} < 1/10$. We considered the DIL_{50} between both values doubtful.

Results

Of the 3,086 tick pools tested (representing 44,916 questing individual ticks), 7 from 3 locations were positive for TBEV RNA (minimum infection rate 0.02%)
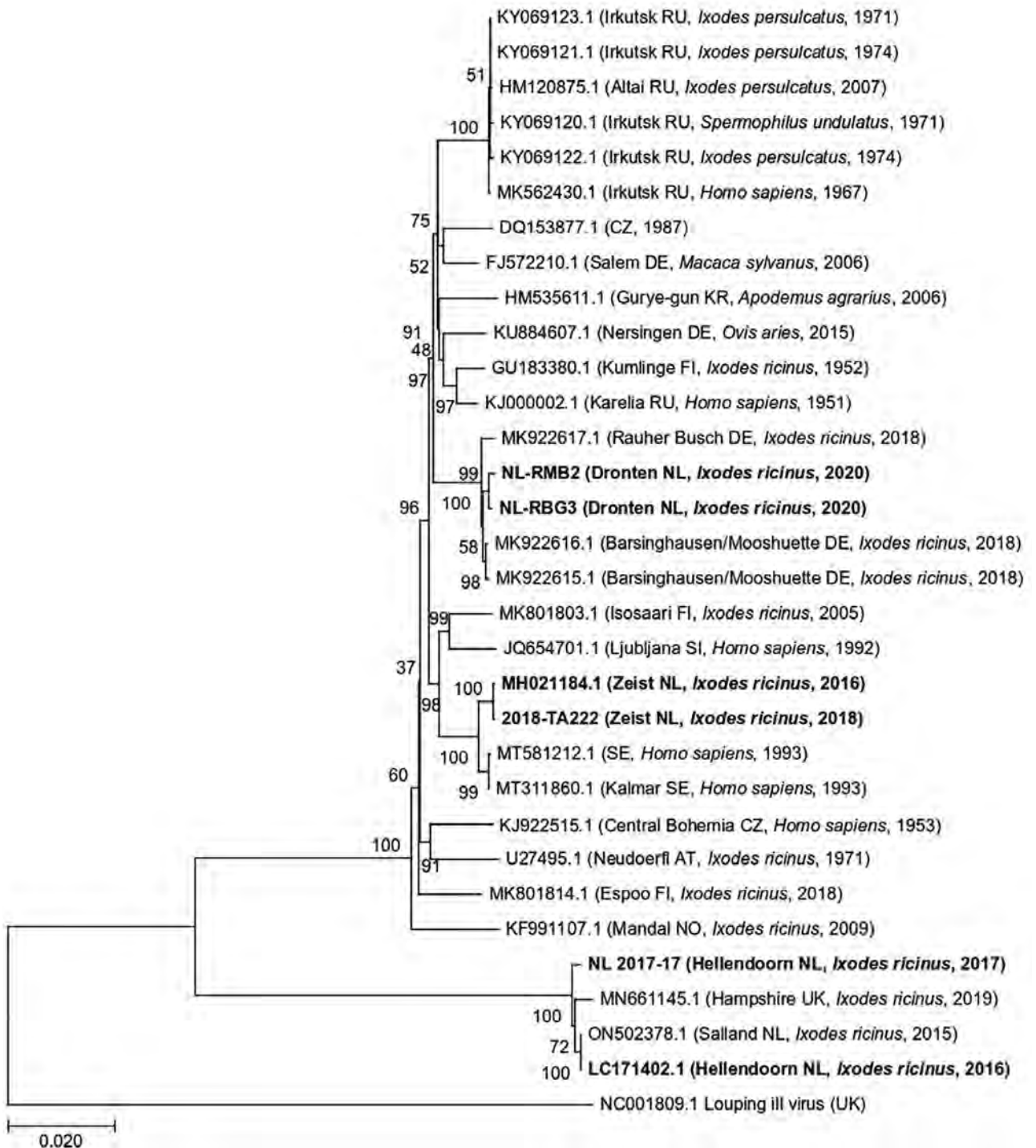
Figure 2. Maximum-likelihood phylogenetic tree of polyprotein sequences obtained from tick-borne encephalitis virus RNA–positive *Ixodes ricinus* ticks collected from 3 locations in the Netherlands during 2016–2020 (in bold). Additional published sequences obtained from GenBank are included for reference. Louping ill virus is used as the outgroup. Sample ID or GenBank accession numbers are indicated for each sequence, with location in brackets (if known) and country code, original isolation source, and collection year of each sample. Numbers next to each branch indicate the percentage of trees resulting from bootstrapping on the basis of 1,000 pseudoreplicate datasets for which the associated taxa clustered together. Scale bar represents the percentage of genetic variation along tree branches.

(Table 1; Figure 1). The 1,194 individually tested ticks collected from the Nijverdal garden (municipality of Hellendoorn) were all negative for TBEV RNA. Whole-genome sequences were obtained for 3 TBEV RNA–positive tick pools: 2018-TA222 from Zeist (GenBank accession no. MZ969636) and NL-RMB2 and NL-RBG3 from Dronten (accession nos. MZ969638 and MZ969639). The 2 sequences from Dronten were 99.82% similar to one another, and the sequence from Zeist was 99.96% similar to a sequence obtained from an *I. ricinus* tick in the same municipality 2 years before (*24*). Likewise, previously obtained sequences from *I. ricinus* ticks collected in Hellendoorn in 2015 and 2017 were 99.67% similar to each other (Appendix 2, https://wwwnc.cdc.gov/EID/article/28/12/22-0552-App2.xlsx). Sequence similarity between municipalities ranged from 89.45 to 97.76% and was significantly lower than similarity among ticks from the same municipality (*t* = 6.51, d.f. = 11.12; p<0.01).

Phylogenetic analyses revealed that all sequences clustered within the TBEV-Eu subtype (Figure 2). When we compared sequences with other strains circulating in Europe, we found that sequences from Dronten were most closely related to the Barsinghausen/Mooshuette (Germany) strain (accession no. MK922616) isolated from ticks in 2019, sharing 99.76% (NL-RBG3) and 99.70% (NL-RMB2) sequence similarity. Sequences from Zeist (Utrechtse Heuvelrug) were most closely related to a Sweden strain isolated from a human sample (accession no. MT311860), sharing 99.52% (2018-TA222) and 99.54% (MH021184) sequence similarity. The 2 sequences from Hellendoorn (Sallandse Heuvelrug) were strongly homologous to the TBEV-NL strain previously isolated from ticks from this area (99.67% for NL2017-17 and 100% for LC171402), as well as to TBEV-UK Hampshire from ticks (MN661145), sharing 99.46% (NL2017-17) and 99.55% (LC171402) sequence similarity.

We tested for the presence of TBEV RNA in brain and spleen tissue of 320 rodents and found evidence of TBEV infection in 3 rodents (0.9%) from 2 municipalities (Table 2; Figure 1). Sequencing a fragment of the envelope protein confirmed that these variants belonged to the TBEV-Eu subtype, but the sequences were too short to perform detailed phylogenetic cluster analyses. In addition, 5 rodents tested seropositive ($3 \times OD_{NC}$ [optical density of the negative control]) and 6 were borderline ($2 \times OD_{NC}$). However, only 1 of these samples (from a *Mi. arvalis* vole) was positive in the serum neutralization test (SNT), whereas 3 had insufficient serum volume left to be confirmed by SNT (Table 2). The rodent with TBEV-neutralizing antibodies was 1 of the rodents that also tested positive for TBEV RNA.

Tick infestation prevalence among rodents was high for each species: *A. flavicollis*, 96.3% (26/27); *A. sylvaticus*, 93.4% (142/152); *Mi. arvalis*, 100% (2/2); and *My. glareolus*, 66.7% (26/39). However, tick burdens varied considerably among species: *A. flavicollis*, range 0–14, median 4; *A. sylvaticus*, range 0–50, median 2; and *My. glareolus*, range 0–11, median 1. The 2 specimens of *Mi. arvalis* voles had 13 and 20 ticks. We found cofeeding between nymphs (n = 27) and larvae (n = 228) on 21 of 320 rodents (6.6%) and in 8 of 13 rodent trapping locations. In total, we tested 1,370 ticks that were removed from rodents for the presence of TBEV RNA and to determine the presence of tick species. Of the 214 tick pools tested, 192 pools contained *I. ricinus* ticks only (89.7%), 8 pools contained *I. trianguliceps* ticks only (3.7%), and 13 pools contained both species (6.1%). One tick pool was negative on both species tests, suggesting that these ticks belonged to other, unidentified tick species. Half of the tick pools that contained *I. trianguliceps* ticks were taken from *A. sylvaticus* mice (11/21) and the other half from *M. glareolus* voles (10/21). TBEV RNA was not detected in any of the tick pools collected from rodents or in the 33 individually tested larvae collected from TBEV RNA–positive rodents.

Discussion

We conducted an intensive national screening of ticks and rodents to obtain an ecoepidemiologic picture of TBEV circulation in the Netherlands. Our results build on earlier studies (*9,13,14,24*) and indicate that 3 different TBEV-Eu variants cocirculate in the country. We

Table 1. Pools of tick-borne encephalitis virus RNA–positive *Ixodes ricinus* ticks collected from vegetation in 3 locations in the Netherlands, 2018–2020*

Sample ID	Tick pool	Ct value	Nature area	Municipality	Year	GenBank
2018-TA222	25 nymphs	15.31	National Park Utrechtse Heuvelrug	Zeist	2018	NA
2018-TA226	25 nymphs	17.65	National Park Utrechtse Heuvelrug	Zeist	2018	MZ969636
A43	25 nymphs	19.84	National Park Utrechtse Heuvelrug	Zeist	2019	NA
4040	25 nymphs	19.42	National Park Sallandse Heuvelrug	Hellendoorn	2019	NA
NL-RGB1	4 females	29.1	Roggebotzand	Dronten	2020	NA
NL-RMB2	8 males	21.12	Roggebotzand	Dronten	2020	MZ969638
NL-RBG3	25 nymphs	17.64	Roggebotzand	Dronten	2020	MZ969639

*Ct, cycle threshold; NA, not applicable.

Table 2. Rodents that tested positive for the presence of tick-borne encephalitis virus antibodies by SNT or viral RNA in tissue samples by PCR, the Netherlands, 2018–2020*

Sample ID	Species	Sex	Serologic result†	SNT	PCR result, Ct value	Nature area	Municipality	Year
18–2752	*Apodemus sylvaticus*	M	Weak positive	Negative	Negative	National Park de Groote Peel	Peel en Maas	2018
18–2779	*A. sylvaticus*	F	Weak positive	Not tested‡	Negative	National Park Sallandse Heuvelrug	Rijssen-Holten	2018
18–2829	*A. sylvaticus*	M	Weak positive	Negative	Negative	National Park Sallandse Heuvelrug	Hellendoorn	2018
18–2830	*A. sylvaticus*	F	Positive	Negative	Negative	National Park Sallandse Heuvelrug	Hellendoorn	2018
19–2893	*A. sylvaticus*	F	Positive	Not tested‡	Negative	National Park Utrechtse Heuvelrug	Zeist	2019
19–2895	*A. sylvaticus*	F	Positive	Negative	Negative	National Park Utrechtse Heuvelrug	Zeist	2019
19–2896	*A. sylvaticus*	M	Positive	Negative	Negative	National Park Utrechtse Heuvelrug	Zeist	2019
19–2901	*A. sylvaticus*	M	Weak positive	Negative	Negative	Springendal	Tubbergen	2019
19–2916	*A. sylvaticus*	M	Positive	Not tested‡	Negative	Nijverdal Garden	Hellendoorn	2019
19–2997	*My. glareolus*	M	Weak positive	Negative	Negative	Natuurpark de Leemputten	Oost Gelre	2019
19–3001	*Microtus arvalis*	F	Negative	Not tested	Spleen 30.74, brain 30.09	Natuurpark de Leemputten	Oost Gelre	2019
19–3002	*Mi. arvalis*	F	Weak positive	Positive	Spleen 30.57; brain 28.33	Natuurpark de Leemputten	Oost Gelre	2019
19–3053	*Myodes glareolus*	F	Negative	Not tested	Spleen 35.68; brain negative	Rijk van Nijmegen	Berg en Dal	2019

*Ct, cycle threshold; SNT, serum neutralization test.
†Positive = 3 × OD$_{NC}$ (optical density of the negative control), borderline = 2 × OD$_{NC}$.
‡Not tested because of too little volume.

also present evidence of epizootic transmission in the nature areas of Roggebotzand (municipality of Dronten), Rijk van Nijmegen (Berg en Dal), and Natuurpark de Leemputten (Oost-Gelre), which are all located outside the known TBEV hotspots Utrechtse Heuvelrug (Zeist) and Sallandse Heuvelrug (Hellendoorn and Rijssen-Holten). Together with recent human cases in several municipalities where clinical TBE had thus far not been reported (Figure 1), these findings suggest that the distribution of TBEV in the Netherlands is more widespread than previously found.

We found a significantly lower phylogenetic similarity between TBEV sequences from questing ticks at different municipalities compared with sequences from the same municipality. In specific, whole-genome sequences from Dronten, Zeist, and Hellendoorn were more closely related to strains from Germany, Sweden, and England, respectively, than to each other. These findings are in line with other studies from elsewhere in Europe, which also found high genetic diversity among local TBEV strains in relatively small geographic areas (*25–28*). For example, TBEV isolates from southwestern Germany were closely related to strains from the Czech Republic, Austria, Switzerland, Slovakia, and Italy (*28*). In addition, the clustering of whole-genome sequences from Dronten with strains from Germany and of those from Hellendoorn with

a whole-genome sequence recently reported from England could be in line with the recent westward spread of TBEV in Europe (*29,30*).

The diversity of TBEV variants in both the Netherlands and England points toward multiple introduction events in both countries, possibly through migratory birds (*31*). Migratory birds have been implicated in the spread of TBEV before (*25,29,32*). However, additional whole-genome sequences are needed from other TBEV risk areas from Europe for a more complete phylogenetic and phylogeographic analysis to determine the mechanisms of spread of the virus. Also, it remains unclear which TBEV strain circulates in the province of Noord Brabant, where 3 human TBE cases have recently occurred, or the 2 nature areas, Rijk van Nijmegen and Natuurpark de Leemputten, where we detected TBEV RNA in rodents but could not perform detailed phylogenetic analyses because sequences were too short.

As found elsewhere in Europe, TBEV in the Netherlands appears to have a rather focal distribution. For example, we found TBEV RNA–positive ticks in the Utrechtse Heuvelrug in 2018 and 2019 at the exact same location but not elsewhere in this relatively large nature area. Moreover, it appears that the virus might locally disappear. For example, we did not find any TBEV RNA–positive ticks in the

Nijverdal garden, despite a remarkably high infection prevalence in 2017 (1/63 ticks) and 2018 (1/92 ticks) (*9*). Although absence of evidence is not evidence of absence, we thoroughly sampled the entire garden and collected 1,194 questing ticks during 3 sampling events in April, May, and June 2019. Although 1 of the rodents collected from this location in May 2019 was seropositive, this result could not be confirmed by an SNT because of insufficient serum volume. Experimental studies have shown that wild rodents mount a strong antibody response to TBEV that can still be detected at 168 dpi (*33*). Therefore, this animal could have been exposed to infected ticks in late 2018 rather than 2019. Local fade-out of TBEV in former transmission areas has also been reported elsewhere in Europe, including Germany (*34*), Denmark (*35*), and France (*36*), so this phenomenon appears common across a wide diversity of habitats. However, TBEV also reemerged in some of these areas, raising questions as to whether the virus was reintroduced (e.g., by migratory birds) or had actually persisted below levels at which it could be detected (*37*).

Our very large sampling effort of >46,000 questing ticks but low number of TBEV RNA–positive pools (n = 7, representing 137 individual specimens) underlines the challenges of using tick surveillance to identify TBEV risk areas (*38,39*). Instead, screening of humans and sentinel or reservoir hosts might provide a more effective indicator (*38,40–42*), although these methods also have their drawbacks (*39*). For example, a recent serologic survey of employees and volunteers of nature management organizations in the Netherlands found a seroprevalence of 0.5% (3/556; 95% CI 0.1%–1.6%) among participants (*43*). Although all seropositive participants had worked in provinces with confirmed cases, precise source attribution is difficult. Likewise, serologic surveillance of large sentinel hosts such as roe deer can only indicate past exposure to TBEV, and their relatively wide foraging range (≈51–136 ha) (*44*) hampers precise identification of TBEV foci (*39*). Moreover, cross-reactivity between different flaviviruses is well documented and might lead to false-positive results in both humans (e.g., in case of yellow fever vaccination) and sentinel hosts (e.g., when other flaviviruses circulate in the environment) (*45*), requiring SNT for confirmation. In contrast, wild rodents are natural reservoir hosts that develop levels of viremia high enough to demonstrate active TBEV circulation (*46,47*). Moreover, rodents have small home ranges (<0.5 ha in forest habitats) (*48,49*), which enables more accurate identification of foci (*39*). On the other hand, catching infected rodents during the small window of viremia is challenging, and cross-reactivity of flaviviruses remains an issue. Moreover, sampling a sufficiently large number of wild rodents to detect TBEV foci is a considerable endeavor that also poses ethical questions, such as potential impacts on local populations of *A. flavicollis* mice, still a relatively rare species in the Netherlands. Given that the spatial distribution of TBEV appears to be increasing in the Netherlands but that the minimum infection prevalence in ticks is extremely low (0.02% vs. 0.1%–2.7% elsewhere in Europe) (*39*), we suggest continued monitoring using an integrated approach that combines passive surveillance of humans and sentinel hosts such as game animals (e.g., deer) to detect potential TBEV risk areas, after which more targeted local screening of rodents and ticks may confirm actual virus circulation.

The mechanisms underlying the sustained circulation of TBEV in the Netherlands are unclear. Nonsystemic virus transmission from infected nymphs to uninfected larvae during simultaneous feeding on rodent hosts (cofeeding) is considered a prerequisite for endemic circulation of TBEV (*7,10*). Northwestern Europe was thought to lack the specific climatic conditions required for cofeeding transmission, and past modeling studies had therefore predicted that TBEV would not become established in this region (*10*). Nonetheless, we found cofeeding of larvae (n = 228) and nymphs (n = 27) on 21 (6.6%) of 320 rodents and in 8 of 13 locations. These findings suggest that cofeeding is a potential route of transmission in the Netherlands. Although none of the feeding ticks were TBEV RNA–positive, this finding might be explained by low sample size. Previous work showed that cofeeding also occurred on 3.6% of rodents in England (*50*). Past models might have accurately predicted TBEV foci in Central Europe based on climatic data (*10*), but the presumed underlying relationship cannot explain TBEV circulation in Northwestern Europe. Given the recent emergence of endemic foci in Northwestern Europe and the occurrence of cofeeding in this region, the distribution of TBEV will likely continue to change. Future studies should investigate how common cofeeding is in areas where TBEV does not circulate and identify the ecologic conditions that promote the synchronous activity of larvae and nymphs in emerging areas.

In summary, we found TBEV RNA in rodents and tick pools from 5 foci in the Netherlands and that 3 different variants of the TBEV-Eu subtype are currently circulating, suggesting multiple introductions. Our findings, along with other human cases outside known TBEV hotspots, show that the distribution of TBEV is more widespread than previously demonstrated in this country.

About the Author

Dr. Esser is an assistant professor at Wageningen University. Her primary research interest is disease ecology, specifically emerging zoonoses in changing landscapes.

References

1. Bogovic P, Strle F. Tick-borne encephalitis: a review of epidemiology, clinical characteristics, and management. World J Clin Cases. 2015;3:430–41. https://doi.org/10.12998/wjcc.v3.i5.430
2. Beauté J, Spiteri G, Warns-Petit E, Zeller H. Tick-borne encephalitis in Europe, 2012 to 2016. Euro Surveill. 2018;23:1800201. https://doi.org/10.2807/1560-7917.ES.2018.23.45.1800201
3. Süss J. Tick-borne encephalitis 2010: epidemiology, risk areas, and virus strains in Europe and Asia-an overview. Ticks Tick Borne Dis. 2011;2:2–15. https://doi.org/10.1016/j.ttbdis.2010.10.007
4. Rizzoli A, Hauffe HC, Tagliapietra V, Neteler M, Rosà R. Forest structure and roe deer abundance predict tick-borne encephalitis risk in Italy. PLoS One. 2009;4:e4336. https://doi.org/10.1371/journal.pone.0004336
5. Šumilo D, Bormane A, Asokliene L, Vasilenko V, Golovljova I, Avsic-Zupanc T, et al. Socio-economic factors in the differential upsurge of tick-borne encephalitis in Central and Eastern Europe. Rev Med Virol. 2008;18:81–95. https://doi.org/10.1002/rmv.566
6. Jaenson TGT, Petersson EH, Jaenson DGE, Kindberg J, Pettersson JHO, Hjertqvist M, et al. The importance of wildlife in the ecology and epidemiology of the TBE virus in Sweden: incidence of human TBE correlates with abundance of deer and hares. Parasit Vectors. 2018;11:477. https://doi.org/10.1186/s13071-018-3057-4
7. Randolph SE, Miklisová D, Lysy J, Rogers DJ, Labuda M. Incidence from coincidence: patterns of tick infestations on rodents facilitate transmission of tick-borne encephalitis virus. Parasitology. 1999;118:177–86. https://doi.org/10.1017/S0031182098003643
8. Holding M, Dowall SD, Medlock JM, Carter DP, Pullan ST, Lewis J, et al. Tick-borne encephalitis virus, United Kingdom. Emerg Infect Dis. 2020;26:90–6. https://doi.org/10.3201/eid2601.191085
9. Dekker M, Laverman GD, de Vries A, Reimerink J, Geeraedts F. Emergence of tick-borne encephalitis (TBE) in the Netherlands. Ticks Tick Borne Dis. 2019;10:176–9. https://doi.org/10.1016/j.ttbdis.2018.10.008
10. Randolph SE. The shifting landscape of tick-borne zoonoses: tick-borne encephalitis and Lyme borreliosis in Europe. Philos Trans R Soc Lond B Biol Sci. 2001;356:1045–56. https://doi.org/10.1098/rstb.2001.0893
11. Reusken C, Reimerink J, Verduin C, Sabbe L, Cleton N, Koopmans M. Case report: tick-borne encephalitis in two Dutch travellers returning from Austria, Netherlands, July and August 2011. Euro Surveill. 2011;16:20003. https://doi.org/10.2807/ese.16.44.20003-en
12. van der Poel WH, Van der Heide R, Bakker D, De Looff M, De Jong J, Van Manen N, et al. Attempt to detect evidence for tick-borne encephalitis virus in ticks and mammalian wildlife in The Netherlands. Vector Borne Zoonotic Dis. 2005;5:58–64. https://doi.org/10.1089/vbz.2005.5.58
13. Jahfari S, de Vries A, Rijks JM, Van Gucht S, Vennema H, Sprong H, et al. Tick-borne encephalitis virus in ticks and roe deer, the Netherlands. Emerg Infect Dis. 2017;23:1028–30. https://doi.org/10.3201/eid2306.161247
14. Rijks JM, Montizaan MGE, Bakker N, de Vries A, Van Gucht S, Swaan C, et al. Tick-borne encephalitis virus antibodies in roe deer, the Netherlands. Emerg Infect Dis. 2019;25:342–5. https://doi.org/10.3201/eid2502.181386
15. Esser HJ, Liefting Y, Ibáñez-Justicia A, van der Jeugd H, van Turnhout CAM, Stroo A, et al. Spatial risk analysis for the introduction and circulation of six arboviruses in the Netherlands. Parasit Vectors. 2020;13:464. https://doi.org/10.1186/s13071-020-04339-0
16. Schlegel M, Ali HS, Stieger N, Groschup MH, Wolf R, Ulrich RG. Molecular identification of small mammal species using novel cytochrome B gene-derived degenerated primers. Biochem Genet. 2012;50:440–7. https://doi.org/10.1007/s10528-011-9487-8
17. Schwaiger M, Cassinotti P. Development of a quantitative real-time RT-PCR assay with internal control for the laboratory detection of tick borne encephalitis virus (TBEV) RNA. J Clin Virol. 2003;27:136–45. https://doi.org/10.1016/S1386-6532(02)00168-3
18. Kupča AM, Essbauer S, Zoeller G, de Mendonça PG, Brey R, Rinder M, et al. Isolation and molecular characterization of a tick-borne encephalitis virus strain from a new tick-borne encephalitis focus with severe cases in Bavaria, Germany. Ticks Tick Borne Dis. 2010;1:44–51. https://doi.org/10.1016/j.ttbdis.2009.11.002
19. Kumar S, Stecher G, Li M, Knyaz C, Tamura K. MEGA X: molecular evolutionary genetics analysis across computing platforms. Mol Biol Evol. 2018;35:1547–9. https://doi.org/10.1093/molbev/msy096
20. Edgar RC. MUSCLE: multiple sequence alignment with high accuracy and high throughput. Nucleic Acids Res. 2004;32:1792–7. https://doi.org/10.1093/nar/gkh340
21. Nei M, Kumar S. Molecular evolution and phylogenetics. New York: Oxford University Press; 2000.
22. Darriba D, Taboada GL, Doallo R, Posada D. jModelTest 2: more models, new heuristics and parallel computing. Nat Methods. 2012;9:772–772. https://doi.org/10.1038/nmeth.2109
23. Roelandt S, Suin V, Riocreux F, Lamoral S, Van der Heyden S, Van der Stede Y, et al. Autochthonous tick-borne encephalitis virus-seropositive cattle in Belgium: a risk-based targeted serological survey. Vector Borne Zoonotic Dis. 2014;14:640–7. https://doi.org/10.1089/vbz.2014.1576
24. de Graaf JA, Reimerink JHJ, Voorn GP, Bij de Vaate EA, de Vries A, Rockx B, et al. First human case of tick-borne encephalitis virus infection acquired in the Netherlands, July 2016. Euro Surveill. 2016;21:30318. https://doi.org/10.2807/1560-7917.ES.2016.21.33.30318

25. Paulsen KM, Lamsal A, Bastakoti S, Pettersson JHO, Pedersen BN, Stiasny K, et al. High-throughput sequencing of two European strains of tick-borne encephalitis virus (TBEV), Hochosterwitz and 1993/783. Ticks Tick Borne Dis. 2021;12:101557. https://doi.org/10.1016/j.ttbdis.2020.101557

26. Bestehorn M, Weigold S, Kern WV, Chitimia-Dobler L, Mackenstedt U, Dobler G, et al. Phylogenetics of tick-borne encephalitis virus in endemic foci in the upper Rhine region in France and Germany. PLoS One. 2018;13:e0204790. https://doi.org/10.1371/journal.pone.0204790

27. Fajs L, Durmiši E, Knap N, Strle F, Avšič-Županc T. Phylogeographic characterization of tick-borne encephalitis virus from patients, rodents and ticks in Slovenia. PLoS One. 2012;7:e48420. https://doi.org/10.1371/journal.pone. 0048420

28. Ott D, Ulrich K, Ginsbach P, Öhme R, Bock-Hensley O, Falk U, et al. Tick-borne encephalitis virus (TBEV) prevalence in field-collected ticks (*Ixodes ricinus*) and phylogenetic, structural and virulence analysis in a TBE high-risk endemic area in southwestern Germany. Parasit Vectors. 2020;13:303. https://doi.org/10.1186/s13071-020-04146-7

29. Weidmann M, Frey S, Freire CCM, Essbauer S, Růžek D, Klempa B, et al. Molecular phylogeography of tick-borne encephalitis virus in central Europe. J Gen Virol. 2013;94:2129–39. https://doi.org/10.1099/vir.0.054478-0

30. Heinze DM, Gould EA, Forrester NL. Revisiting the clinal concept of evolution and dispersal for the tick-borne flaviviruses by using phylogenetic and biogeographic analyses. J Virol. 2012;86:8663–71. https://doi.org/10.1128/JVI.01013-12

31. Holding M, Dowall SD, Medlock JM, Carter DP, McGinley L, Curran-French M, et al. Detection of new endemic focus of tick-borne encephalitis virus (TBEV), Hampshire/Dorset border, England, September 2019. Euro Surveill. 2019;24:1900658. https://doi.org/10.2807/1560-7917. ES.2019.24.47.1900658

32. Waldenström J, Lundkvist A, Falk KI, Garpmo U, Bergström S, Lindegren G, et al. Migrating birds and tickborne encephalitis virus. Emerg Infect Dis. 2007;13:1215–8. https://doi.org/10.3201/eid1308.061416

33. Tonteri E, Kipar A, Voutilainen L, Vene S, Vaheri A, Vapalahti O, et al. The three subtypes of tick-borne encephalitis virus induce encephalitis in a natural host, the bank vole (*Myodes glareolus*). PLoS One. 2013;8:e81214. https://doi.org/10.1371/journal.pone.0081214

34. Klaus C, Hoffmann B, Hering U, Mielke B, Sachse K, Beer M, et al. Tick-borne encephalitis (TBE) virus prevalence and virus genome characterization in field-collected ticks (*Ixodes ricinus*) from risk, non-risk and former risk areas of TBE, and in ticks removed from humans in Germany. Clin Microbiol Infect. 2010;16:238–44. https://doi.org/10.1111/j.1469-0691.2009.02764.x

35. Petersen A, Rosenstierne MW, Rasmussen M, Fuursted K, Nielsen HV, O'Brien Andersen L, et al. Field samplings of *Ixodes ricinus* ticks from a tick-borne encephalitis virus micro-focus in Northern Zealand, Denmark. Ticks Tick Borne Dis. 2019;10:1028–32. https://doi.org/10.1016/j.ttbdis.2019.05.005

36. Bournez L, Umhang G, Moinet M, Boucher JM, Demerson JM, Caillot C, et al. Disappearance of TBEV circulation among rodents in a natural focus in Alsace, eastern France. Pathogens. 2020;9:930. https://doi.org/10.3390/pathogens9110930

37. Frimmel S, Krienke A, Riebold D, Loebermann M, Littmann M, Fiedler K, et al. Tick-borne encephalitis virus habitats in North East Germany: reemergence of TBEV in ticks after 15 years of inactivity. BioMed Res Int. 2014;2014:308371.

38. Klaus C, Beer M, Saier R, Schau U, Moog U, Hoffmann B, et al. Goats and sheep as sentinels for tick-borne encephalitis (TBE) virus—epidemiological studies in areas endemic and non-endemic for TBE virus in Germany. Ticks Tick Borne Dis. 2012;3:27–37. https://doi.org/10.1016/j.ttbdis.2011.09.011

39. Imhoff M, Hagedorn P, Schulze Y, Hellenbrand W, Pfeffer M, Niedrig M. Review: Sentinels of tick-borne encephalitis risk. Ticks Tick Borne Dis. 2015;6:592–600. https://doi.org/10.1016/j.ttbdis.2015.05.001

40. Gerth HJ, Grimshandl D, Stage B, Döller G, Kunz C. Roe deer as sentinels for endemicity of tick-borne encephalitis virus. Epidemiol Infect. 1995;115:355–65. https://doi.org/10.1017/S0950268800058477

41. Haut M, Girl P, Oswald B, Romig T, Obiegala A, Dobler G, et al. The red fox (*Vulpes vulpes*) as sentinel for tick-borne encephalitis virus in endemic and non-endemic areas. Microorganisms. 2020;8:1817. https://doi.org/10.3390/microorganisms8111817

42. Alfano N, Tagliapietra V, Rosso F, Ziegler U, Arnoldi D, Rizzoli A. Tick-borne encephalitis foci in northeast Italy revealed by combined virus detection in ticks, serosurvey on goats and human cases. Emerg Microbes Infect. 2020;9:474–84.

43. Hofhuis A, van den Berg OE, Meerstadt-Rombach FS, van den Wijngaard CC, Chung NH, Franz E, et al. Exposure to tick-borne encephalitis virus among nature management workers in the Netherlands. Ticks Tick Borne Dis. 2021;12:101762. https://doi.org/10.1016/j.ttbdis.2021.101762

44. Morellet N, Bonenfant C, Börger L, Ossi F, Cagnacci F, Heurich M, et al. Seasonality, weather and climate affect home range size in roe deer across a wide latitudinal gradient within Europe. J Anim Ecol. 2013;82:1326–39. https://doi.org/10.1111/1365-2656.12105

45. Dobler G, Treib J, Kiessig ST, Blohn WV, Frösner G, Haass A. Diagnosis of tick-borne encephalitis: evaluation of sera with borderline titers with the TBE-ELISA. Infection. 1996;24:405–6. https://doi.org/10.1007/BF01716097

46. Achazi K, Růžek D, Donoso-Mantke O, Schlegel M, Ali HS, Wenk M, et al. Rodents as sentinels for the prevalence of tick-borne encephalitis virus. Vector Borne Zoonotic Dis. 2011;11:641–7. https://doi.org/10.1089/vbz.2010.0236

47. Tonteri E, Jääskeläinen AE, Tikkakoski T, Voutilainen L, Niemimaa J, Henttonen H, et al. Tick-borne encephalitis virus in wild rodents in winter, Finland, 2008–2009. Emerg Infect Dis. 2011;17:72–5. https://doi.org/10.3201/eid1701.100051

48. Korn H. Changes in home range size during growth and maturation of the wood mouse (*Apodemus sylvaticus*) and the bank vole (*Clethrionomys glareolus*). Oecologia. 1986;68:623–8. https://doi.org/10.1007/BF00378782

49. Vukićević-Radić OD, Matić R, Kataranovski DS, Stamenković SZ. Spatial organization and home range of *Apodemus flavicollis* and *A. agrarius* on Mt. Avala, Serbia. Acta Zool Acad Sci Hung. 2006;52:81–96.

50. Cull B, Vaux AGC, Ottowell LJ, Gillingham EL, Medlock JM. Tick infestation of small mammals in an English woodland. J Vector Ecol. 2017;42:74–83. https://doi.org/10.1111/jvec.12241

Address for correspondence: Helen Esser, Wildlife Ecology & Conservation Group, Wageningen University & Research, Droevendaalsesteeg 3a, 6708 PB Wageningen, the Netherlands; email: helen.esser@wur.nl

Household Transmission of SARS-CoV-2 from Humans to Pets, Washington and Idaho, USA

Julianne Meisner, Timothy V. Baszler, Kathryn E. Kuehl, Vickie Ramirez, Anna Baines,
Lauren A. Frisbie, Eric T. Lofgren, David M. de Avila, Rebecca M. Wolking, Dan S. Bradway,
Hannah R. Wilson, Beth Lipton,[1] Vance Kawakami, Peter M. Rabinowitz

SARS-CoV-2 likely emerged from an animal reservoir. However, the frequency of and risk factors for interspecies transmission remain unclear. We conducted a community-based study in Idaho, USA, of pets in households that had ≥1 confirmed SARS-CoV-2 infections in humans. Among 119 dogs and 57 cats, clinical signs consistent with SARS-CoV-2 were reported for 20 dogs (21%) and 19 cats (39%). Of 81 dogs and 32 cats sampled, 40% of dogs and 43% of cats were seropositive, and 5% of dogs and 8% of cats were PCR positive. This discordance might be caused by delays in sampling. Respondents commonly reported close human–animal contact and willingness to take measures to prevent transmission to their pets. Reported preventive measures showed a slightly protective but nonsignificant trend for both illness and seropositivity in pets. Sharing of beds and bowls had slight harmful effects, reaching statistical significance for sharing bowls and seropositivity.

Coronaviruses infect multiple mammal species, and SARS-CoV-2, the etiologic agent of COVID-19, likely jumped to humans from a mammal source (*1*). Although the virus is currently spreading person-to-person, the angiotensin converting enzyme-2 receptor involved in SARS-CoV-2 transmission is present in multiple species, and there are numerous reports of infections in pets (*24*). As of October 17, 2022, a total of 110 domestic cats and 95 domestic dogs in the United States had been reported by the US Department of Agriculture Animal and Plant Health Inspection Service to have SARS-CoV-2 infection (*5*).

Workplace transmission of SARS-CoV-2 between humans and animals has also been documented, including in zoos (felids and nonhuman primates), on mink farms (*6,7*), and at pet warehouses/pet shops (*8,9*). These findings are consistent with previous reports of SARS-CoV-1 infecting cats and ferrets, and laboratory studies demonstrating experimental SARS-CoV-2 infection of nonhuman primates, ferrets, hamsters, and rabbits (*10*). However, less is known about the frequency of and risk factors for SARS-CoV-2 transmission between humans and companion animals in a household setting. Furthermore, the natural history of SARS-CoV-2 infection in pets is poorly understood.

Given the close contact many persons have with their pets and the intimate nature of their shared environment, exacerbated during periods of quarantine or isolation, it is useful to clarify the role of companion animals in community infection patterns, including contribution to virus evolution and emergence of novel strains. In light of evidence from mink farms that animal-origin variants might contain spike gene mutations and other changes that could affect clinical features of infection (*11,12*), evidence suggesting mouse origins of the Omicron SARS-CoV-2 variant (*13*), and the recent decision in Hong Kong to cull 2,000 hamsters after a pet shop worker was infected (*14*), ongoing monitoring of SARS-CoV-2 transmission between humans and animals remains critical.

We report findings from the COVID-19 and Pets Study, a cross-sectional community-based study of pets in households of persons that had documented COVID-19 infection in Washington and Idaho, USA. The goal of the study was to describe the frequency of transmission between humans and animals within

[1] Current affiliation: Washington State Department of Health, Shoreline, Washington, USA.

a household, and to determine human, animal, and environmental risk factors for that transmission, in a One Health framework.

Methods

Study Population and Design
The COHERE (15) and STROBE (16) statements were used to guide reporting of the findings and the preparation of this article. We defined a household as >1 persons >18 years of age living with >1 pet that does not live solely outdoors. Pets were defined as dogs, cats, ferrets, and hamsters, based on previous research documenting experimental COVID-19 infection in these species (17,18). We conducted this study in King, Snohomish, Yakima, Whitman, Pierce, Spokane, and Benton Counties in Washington and Latah County in Idaho during April 2020–September 2021. The COVID-19 and Pets Study is a cross-sectional study with individual-level and household-level data collection. Study participation involved 2 components: an online survey, followed by animal sampling.

Recruitment and Eligibility
Households were recruited through partnerships with other COVID-19 clinical trials and community studies, as well as by social media, word of mouth, community partners, and contact tracers from Public Health Seattle and King County during case investigation/contact tracing calls. We screened persons for eligibility by using the UW Research Electronic Data Capture (REDCap) system (19), a Health Insurance Portability and Accountability Act–compliant web tool for clinical research, which had criteria including county of residence, pet ownership, and >1 household member with confirmed SARS-CoV-2 infection by PCR or antigen testing by a provider or laboratory. Animals with known fearful or aggressive behavior were excluded. However, other animals in the corresponding household were eligible.

Ethics Statement
This study received ethics approval from the University of Washington Institutional Review Board (STUDY00010585) and the Office of Animal Welfare (PROTO201600308: 4355–01). We obtained informed consent by using REDCap or over the telephone with the study coordinator, after the nature and possible consequences of study involvement had been explained.

Survey
A household member completed a survey before the sampling visit was scheduled. Human survey items

included COVID-19 symptoms, onset, and severity; concurrent conditions; vaccination status, dates, and type; and reported COVID-19–like illness of any other household members, including those without confirmatory testing. Animal survey items included veterinary clinical variables, history of illness compatible with SARS-CoV-2 infection, and contact with specific members of the household. Environmental survey items included type and size of home, type of flooring (e.g., carpet, wood), and availability of outdoor space for pets to roam.

At the sampling visit, the field team inquired about updates for human and animal household members, including new hospitalizations, symptoms, or COVID-19 diagnoses. The study team also reviewed SARS-CoV-2 test results to confirm date and positive result; self-test results were not accepted.

Animal Sampling
A team of 2 study personnel, including at least 1 veterinarian, performed sampling in the home of a participant or at a veterinary hospital. No chemical restraint was used because of biosafety concerns, and no muzzles were used.

The team used species-appropriate restraint standard techniques for venipuncture and collection of 3 mL of blood into a labeled serum separator tube. Swab specimen samples collected from rostral nares and the caudal oropharynx were placed into 1 Primestore Molecular Transport Medium Tube (https://www.lhndv.com). A fecal swab specimen collected from the rectum was placed into a separate tube. All participants received educational information from the field team about measures to mitigate household COVID-19 transmission. Swab and serum samples were transported on ice within 24 hours to the Washington Animal Disease Diagnostic Laboratory (WADDL) for PCR and antibody testing.

Testing
We performed RNA extraction and SARS-CoV-2 real-time reverse transcription PCR (RT-PCR) for the SARS-CoV-2 RNA-dependent RNA polymerase gene (RdRp) as described for respiratory and fecal swab specimens (20). We also performed a second RT-PCR targeting the N1 region on the nucleocapsid gene as described for RdRp-detected samples (CDC 2019-Novel Coronavirus real-time RT-PCR [2019-nCoVEUA-01] (21). There was 100% concordance (agreement) between the RdRp PCR and N1 PCR. After initial viral detection by PCR, 3 dog samples and 1 cat sample were submitted to the University of Minnesota Genomics Center (Oakdale, MN, USA) for whole-

genome sequencing (WGS) (22). A second cat sample was submitted to the USDA National Veterinary Services Laboratory (NVSL; Ames, IA, USA) for WGS. Mutational analysis was performed by using the GISAID EpiFlu Database CoVsurver: Mutation Analysis of hCoV-19 (23,24). We deposited all 5 sequences into GISAID (accession nos. EPI_ISL_7845315–8, and EPI_ISL_8897004) and assigned SARS-CoV-2 lineages by using the PANGO lineage tool (25,26).

SARS-CoV-2 Spike Protein Receptor Binding Domain ELISA

WADDL developed canine and feline SARS-CoV-2 ELISAs by using recombinant SARS-CoV-2 spike receptor–binding domain (S-RBD) protein as antigen. The recombinant S-RBD protein was obtained from the University of Washington Center for Emerging and Reemerging Infectious Disease Laboratory of Wesley Van Voorhis through an institutional material transfer agreement. WADDL used an in-house standard operating procedure for indirect ELISA of SARS-CoV-2 in 96-well format based on a previous report for humans (27).

The major components of the assay were recombinant S-RBD coating of plates as target antigen (2 µg/mL in carbonate-bicarbonate buffer; Sigma-Aldrich, https://www.sigmaaldrich.com); a 1:100 dilution of test serum diluted in ChonBlock ELISA Buffer (Chondrex Inc., https://www.chondrex.com); anti-dog IgG–horseradish peroxidase conjugated as linker (goat anti-canine IgG; Southern BioTech, https://www.southernbiotech.com); and the 3,3',5,5'-tetramethylbenzidine liquid substrate system (Sigma-Aldrich) to develop the optical density (OD). Plates were blocked with ChonBlock ELISA buffer per the manufacturer's instructions, washing solution consisted of phosphate-buffered saline plus 0.1% Tween 20 (Sigma-Aldrich), and plates were read on a plate reader at 450 nM. Serum samples were tested in triplicate and used at the test OD.

For the dog RBD ELISA, negative controls consisted of serum samples collected from 6 dogs before COVID-19, archived at WADDL and tested for 5 canine viruses: adenovirus, distemper virus, coronavirus, parainfluenza, and parvovirus. All 6 samples had antibody on $\geq$1 of the tests performed. However, no serum sample reacted in the SARS-CoV-2 canine RBD ELISA.

For the cat RBD ELISA, negative controls consisted of serum samples collected from 3 cats before COVID-19 from WADDL archives and tested for feline coronavirus IgG and feline panleukopenia virus IgG. Two of the 3 samples had antibody on $\geq$1 of the

tests performed (including 2 for feline coronavirus). However, neither sample reacted in the SARS-CoV-2 feline RBD ELISA.

We tested negative controls in triplicate and used the mean as the negative control OD. We used a ratio of test OD:negative control OD to determine the results. The positive cutoff of 2.0 test OD:negative control OD ratio equated to the mean of negative controls +3 SDs of the mean. Use of +2 or +3 SDs from the mean OD of defined negative control serum samples is a commonly used method when no standard negative or positive control serum samples are available. Use of + 3 SDs from the mean of defined negative control serum samples was chosen as the most conservative SARS-CoV-2 RBD ELISA cutoff to reduce the risk for false-positive results.

We performed SARS-CoV-2 RBD ELISA in triplicate on 3 different occasions for all samples and tabulated the final results as a mean value obtained from the repeated testing. Initially, because no dog or cat in Washington or Idaho had previously been confirmed to be SARS-CoV-2 seropositive, the first antibody-positive case for each species and state was sent to the USDA NVSL for confirmation by virus neutralization (VN) assay in keeping with regulatory recommendations. Subsequently a subset of 30 SARS-CoV-2 RBD ELISA–positive serum samples that had a range of ELISA output (20 dogs and 10 cats) and 4 SARS-CoV-2 RBD ELISA–negative serum samples (2 dogs and 2 cats) were compared by inter-laboratory comparison to live SARS-CoV-2 VN testing performed at the USDA NVSL. Although a VN test is not a validation of an ELISA because they detect different biologic functions of antibody that could involve different epitopes, avidity or affinity, the SARS-CoV-2 RBD ELISA to VN comparison showed 91% overall agreement (31/34), and a Cohen κ of 0.68 (substantial agreement), a metric that takes into account agreement by chance.

Statistical Analyses

The primary aim was to estimate the burden of household SARS-CoV-2 transmission from humans to their pets. Secondary aims included describing the nature of human–animal contact within households and identifying risk factors for household transmission, including human–animal contact.

Outcome

We defined animal infection or illness with SARS-CoV-2 as an animal meeting $\geq$1 of the following criteria: SARS CoV-2 RBD ELISA–seropositive status, PCR-positive status, or illness consistent with

SARS-CoV-2 infection, hereafter referred to as illness, defined as participant answer of yes to the survey question "Since the time of COVID diagnosis/symptom onset in the household, has this animal had any new issues with difficulty breathing, coughing or decreased interest in playing, walking, or eating?" We parameterized serostatus as ELISA ratio, log-transformed for interpretability, and PCR-positive status and illness as binary variables.

Regression Models

We defined outcome as an animal case of SARS-CoV-2. Separate regression models were fit for each outcome definition.

Household-level exposures included residence in house versus apartment or condominium, home size in square feet, and the number of human confirmed SARS-CoV-2 cases. Animal-level exposures included sharing beds or bowls (separately) with human household members and SARS-CoV-2 positive household members taking precautions to prevent transmission to their pets. We also examined the association between canine seropositivity and illness compatible with SARS-CoV-2 infection in the animal and between seropositivity and time since the animal was first exposed, defined as 2 days before the first date any household member had symptoms of COVID-19 or a positive result.

We identified possible confounders a priori by using a directed acyclic graph (Figure 1). We defined the minimum sufficient adjustment set by using this graph and appropriate software (DAGitty, http://www.dagitty.net) separately for each exposure (28).

Figure 1. Directed acyclic graph for human–animal transmission of SARS-CoV-2, Washington and Idaho, USA. Squares indicate exposures of interest and circles indicate outcomes (approximated by serostatus, PCR result, and illness in separate models). Measured and unmeasured confounders are included. SARS-CoV-2–positive household member(s) took precautions to prevent transmission to pet. Indoor-only indicates the animal does not go outdoors; bedshare indicates the animal shares a bed with ≥1 household members. HAB, human–animal bond; SES, socioeconomic status.

Animal species was explored as an effect modifier by using a multiplicative interaction term, and stratified results presented for all cases in which this interaction term reached statistical significance ($p \leq 0.05$).

For each exposure of interest, we implemented a generalized estimating equation approach with an exchangeable working correlation structure, household as the clustering variable, and binomial models with a logit (binary outcomes) or Gaussian (continuous outcomes) link by using the geepack package in R (29). For regression of ELISA ratio on illness and time since first exposure, we performed linear regression by using the glm() function in R.

Results

Recruitment

A total of 107 eligible households enrolled and completed the survey; 83 households, corresponding to 100 dogs and 47 cats, had a sampling visit conducted (Figure 2). Of those animals, 6 dogs and 8 cats were not sampled because of temperament, leaving 94 dogs and 39 cats that had PCR results. An additional 13 dogs and 9 cats were safe to restrain for swab (PCR) samples but not for serum collection, leaving 81 dogs and 32 cats that had serologic results.

Descriptive Statistics

On average, at least 6 weeks (dogs) and 2 weeks (cats) elapsed between the last human COVID-19 diagnosis in the household and animal sampling (Table 1). Of the 119 dogs and 57 cats who had completed surveys, 20 dogs (20.4%, 95% CI 12.9%–29.7%) and 19 cats (38.8%, 95% CI 25.2%–53.8%) had reported illness. Of the 94 dogs and 39 cats who were PCR tested, 4 dogs (5.3%, 95% CI 1.8%–12%) and 3 cats (7.7%, 95% CI 1.6%–20.9%) were positive for any swab specimen; of the 81 dogs and 32 cats who had serum collected, 33 dogs (40.2%, 95% CI 29.6%–51.7%) and 13 cats (40.6%, 95% CI 23.7%–59.4%) were seropositive. SARS-CoV-2 RBD ELISA OD:negative control OD ratios in seropositive animals ranged from 2.03 to 21.22 for dogs (Figure 3) and from 3.01 to 30.35 for cats (Figure 4).

Of the 94 dogs and 39 cats who were PCR tested, 5 dogs (cycle threshold [Ct] 26.0–37.67 for RdRp PCR and Ct 26.07–37.67 for N1 PCR) and 3 cats (Ct 27.03–39.97 for RdRp PCR and 27.03–39.97 for N1 PCR) were PCR positive by nasal/oropharyngeal swab specimens; 1 of these dogs was also PCR positive by a fecal swab specimen (Ct 39.20). Five PCR positive samples (2 cats and 3 dogs) had Ct values sufficient for WGS (Ct<30): The earliest cat sample (April 2021) that underwent WGS was in the Pango

clade B.1.2. Another dog sample was identified as the Delta sublineage B.1.617.2.103 (AY.103), and the other 3 samples (1 cat and 2 dogs) were identified as

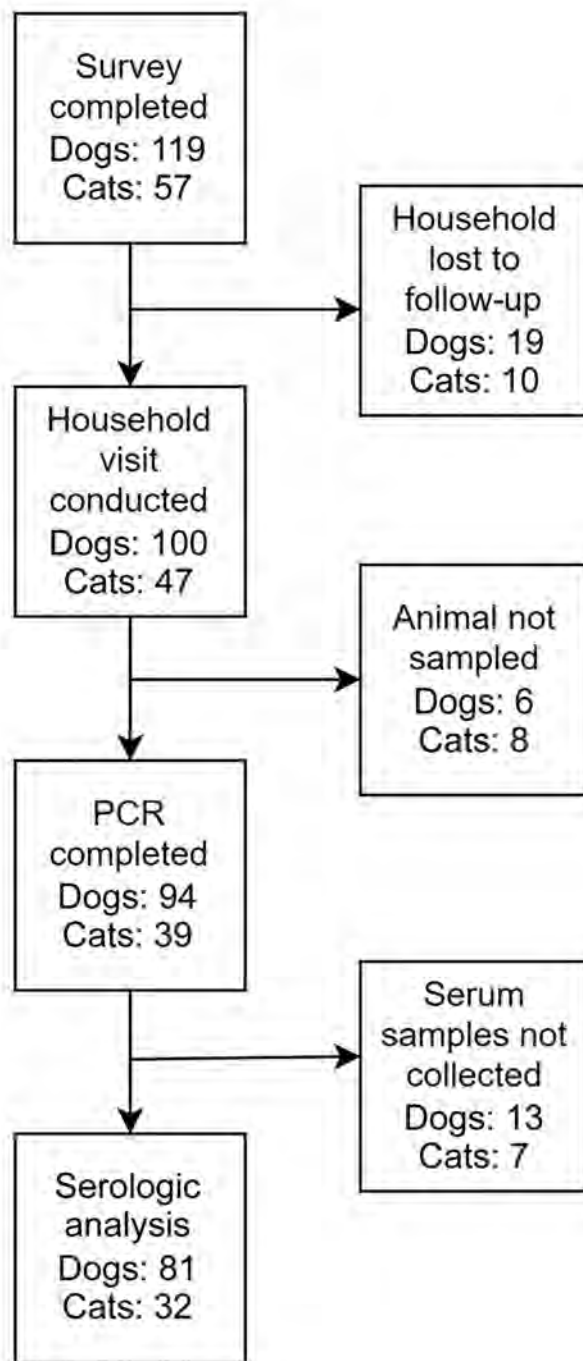**Figure 2.** Flowchart indicating serologic and PCR sampling for study of household transmission of SARS-CoV-2 from humans to pets, Washington and Idaho, USA. Of 119 dogs and 57 cats corresponding to 105 households that had completed surveys, PCR testing was complete for 94 dogs and 39 cats, and serologic testing was complete for 81 dogs and 32 cats. The remaining pets were not sampled because of safety concerns.

Table 1. Descriptive statistics for 119 dogs and 57 cats corresponding to 105 households for study of household transmission of SARS-CoV-2 from humans to pets, Washington and Idaho, USA*

Characteristic	Value	
	Dogs, n = 119	Cats, n = 57
Animal		
Illness consistent with SARS-CoV-2	20 (20)	19 (39)
Seropositive	33 (40)	13 (41)
PCR positive	5 (5)	3 (8)
ELISA ratio, mean (SD)	3.9 (4.93)	9.88 (12.51)
Activity during human quarantine†	33 (28)	7 (12)
Respondent took precautions‡	48 (41)	17 (30)
Age, y, mean (SD)	6.05 (3.86)	6.40 (4.50)
Male sex	66 (56)	28 (49)
Respondent aware of CDC guidelines§	62 (53)	29 (53)
Time from first diagnosis to sampling, d, mean (SD)¶	51.17 (60.64)	29.28 (19.17)
Time from last diagnosis to sampling, d, mean (SD)¶	43.06 (69.44)	15.16 (40.93)
Human		
Index case age, y, mean (SD)	41.78 (13.24)	47.91 (14.38)
Index case male sex	34 (29)	14 (25)
Index case underlying condition#	27 (23)	18 (32)
Index case was hospitalized	2 (2)	0
No. SARS-CoV-2–positive household members, mean (SD)	1.78 (1.28)	1.72 (1.13)
No. household members who had COVID-19-like symptoms, mean (SD)**	0.27 (0.63)	0.26 (0.55)
No. household residents, mean (SD)	3.43 (1.49)	3.07 (1.28)
Environment		
Reside in a house	91 (76)	51 (89)
Reside in an apartment or condominium	51 (24)	6 (11)
Square footage of housing, mean (SD)	1,856.32 (932.74)	1,980.88 (1,095.15)
No. bedrooms, mean (SD)	3.24 (1.4)	3.19 (1.22)
No. of floors, mean (SD)	1.87 (0.82)	1.84 (0.62)
Access to outdoor space where pets can roam	99 (83)	41 (72)
Human–animal contact		
Bowls used by animals cleaned in the kitchen	108 (91)	54 (95)
Humans and animals share bowls	15 (13)	8 (14)
Humans wash hands before handling animals	15 (13)	2 (4)
Humans wash hands after handling animals	50 (42)	12 (21)
Animal bedshares with humans	81 (69)	41 (73)
Animal shares a bedroom but not a bed with humans	54 (46)	19 (34)
Animal is indoor only	43 (37)	35 (61)
Animal sleeps outdoors	1 (1)	5 (9)
Humans pet the animal	117 (100)	56 (100)
Humans kiss the animal	88 (75)	38 (68)
Animal is allowed on furniture	101 (86)	56 (100)

*Values are no. (%) unless otherwise indicated. CDC, Centers for Disease Control and Prevention.
†Activity is defined as going to a veterinary clinic or groomer; being walked off-leash; or visiting an off-leash park, dog park, kennel, or daycare facility.
‡Precautions to prevent human–animal SARS-CoV-2 transmission following diagnosis: not petting or kissing the animal, staying in a different room, and having someone else feed and walk the animal.
§Guidelines to prevent human–animal SARS-CoV-2 transmission.
¶First diagnosis: earliest known, confirmed SARS-CoV-2 diagnosis in the household; final diagnosis: last known, confirmed SARS-CoV-2 diagnosis in he household.
#Prexisting conditions: diabetes, kidney disease, heart disease, hypertension, immunosuppression.
**Household members who had COVID-19-like symptoms but did not get tested.

Delta sublineage B.1.617.2.25 (AY.25). Of the 5 PCR-positive dogs, 3 were PCR positive before being seropositive and 2 were simultaneously PCR positive and seropositive.

There were 11 households that had >2 positive animals, and among multi-pet households that had >1 positive pet, mean prevalence (PCR or serology) was 91%. Of 8 PCR-positive cases, all were detected after April 2021, when the first case of the Delta variant was documented in Washington.

Nearly one third of dogs engaged in activities outside the household during periods of human isolation or quarantine. More than 50% of cats and dogs resided in households whose residents reported awareness of CDC guidelines to prevent human–animal transmission of SARS-CoV-2, and 48 (41%) dogs and 17 (30%) cats resided in households that reported taking precautions to prevent transmission to household pet(s). No cats and only 2 dogs resided in a household in which an infected person was hospitalized for COVID-19. Nearly all dogs (83%) and most cats (72%) had access to yards or gardens and were allowed on furniture (86% of dogs and 100% of cats), and most dogs and cats were kissed by (75% of dogs
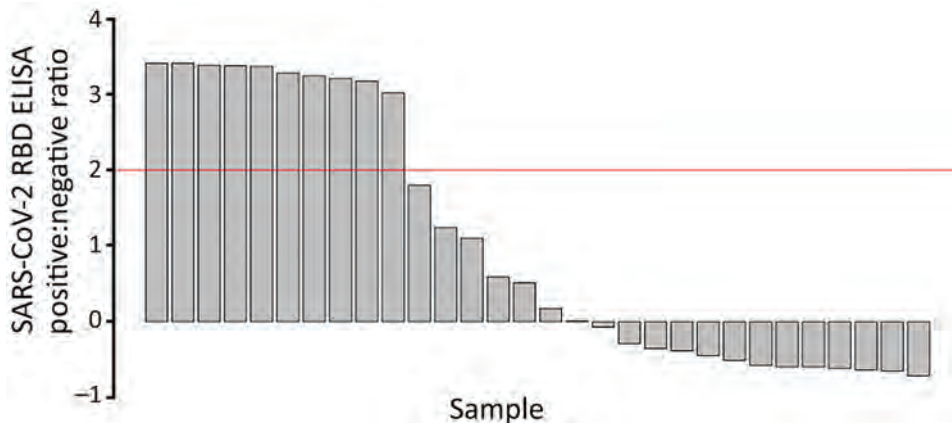
Figure 3. SARS-CoV-2 RBD ELISA serologic data for cats in study of household transmission of SARS-CoV-2 from humans to pets, Washington and Idaho, USA. PCR testing was complete for 39 cats, and serologic testing was complete for 32 cats. The remaining pets were not sampled because of safety concerns. Red line indicates cutoff value. RBD, receptor-binding domain.

and 68% of cats) and shared beds with (69% of dogs and 73% of cats) human household members. Almost all bowls for dogs (91%) and cats (95%) were washed in the kitchen.

Regression Models

We calculated results of regression models as prevalence odds ratios for the binary outcome of illness, reflecting the cross-sectional design of this study, and as exp^β for the outcome of ELISA ratio, which can be interpreted as the relative change (ratio scale) in ELISA ratio for a 1 unit change in the exposure (Table 2). Because so few animals were PCR positive, we did not run regression models for that outcome. With the exception of house size, which was adjusted for house type because the minimum sufficient adjustment set was small for that exposure, confounders were not adjusted for because of concerns regarding overfitting arising from the small sample size. Effect modification by species was found only for house type.

Dogs residing in houses on average had a 79% (95% CI 2%–211%) higher ELISA ratio than dogs residing in apartments or condos, and the inverse association was detected for cats (49% lower mean ELISA

ratio, 95% CI 75% lower to 3% higher) and for the outcome of illness in both cats and dogs (48% lower prevalence odds, 95% CI 80% lower to 34% higher). This association reached statistical significance for dogs only. No other effect estimates reached statistical significance. However, there were positive trends across both outcome definitions for bed sharing with humans, sharing bowls, and being indoor only and a negative effect for precautions taken to prevent SARS-CoV-2 transmission after diagnosis. We also found that the ELISA ratio was positively associated with illness. However, we did not find evidence of an effect of time since first exposure on ELISA ratio or of house square footage on either outcome.

Discussion

We present results of a cross-sectional, One Health study of SARS-CoV-2 transmission between persons and their pets. Results indicate that household transmission of SARS-CoV-2 from humans to animals occurs frequently, and infected animals commonly display signs of illness. We furthermore show that close human–animal contact is common among persons and their pets in this study population, that this contact ap-
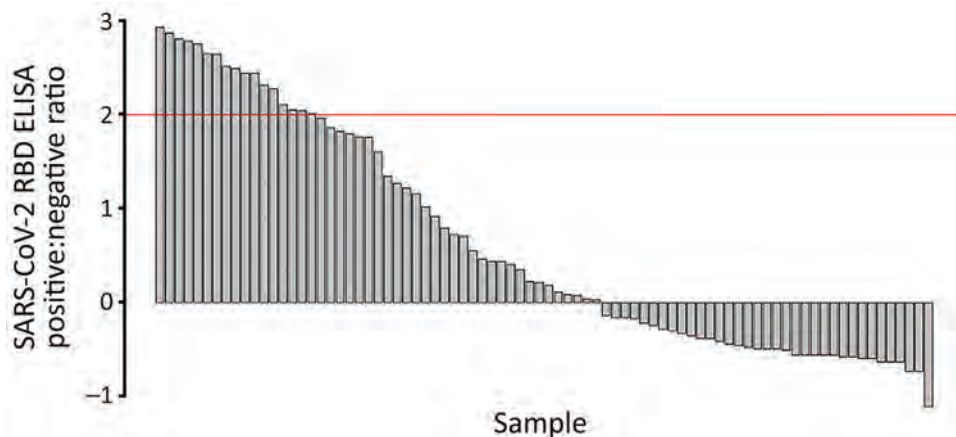

Figure 4. SARS-CoV-2 RBD ELISA serologic data for dogs in study of household transmission of SARS-CoV-2 from humans to pets, Washington and Idaho, USA. PCR testing was complete for 94 dogs, and serologic testing was complete for 81 dogs. The remaining pets were not sampled because of safety concerns. Red line indicates cutoff value. RBD, receptor-binding domain.

Table 2. Results of regression model analysis for study of household transmission of SARS-CoV-2 from humans to pets, Washington and Idaho, USA*

Characteristic	Illness consistent with SARS-CoV-2, POR (95% CI)†	ELISA ratio, exp$^\beta$ (95% CI)†
Exposure		
Indoor only	1.63 (0.77–3.45)	1.07 (0.61–1.88)
House type‡	0.52 (0.2–1.34)	1.79 (1.02–3.11) for dogs, 0.51 (0.25–1.03) for cats
House square footage	1 (1–1)	1 (1–1)
Share bowls§	1.29 (0.39–4.25)	1.78 (1.07–4.49)
Bedsharing	1.48 (0.66–3.33)	1.16 (0.68–1.95)
Took precautions¶	0.71 (0.29–1.75)	0.81 (0.48–1.37)
No. SARS-CoV-2 infected humans	0.78 (0.54–1.13)	1.18 (0.85–1.64)
Illness consistent with SARS-CoV-2	Not examined	1.09 (0.59–2.01)
Time since first exposure, days#	Not examined	1 (1–1)

*House size was adjusted for house type, but no other models were adjusted for confounders due to overfitting concerns. POR, prevalence odds ratio.
†Survey results were available for 119 dogs and 57 cats and serology results available for 81 dogs and 32 cats.
‡House versus apartment or condominium.
§Animals and humans use the same bowls.
¶Precautions taken to prevent human-to-animal SARS-CoV-2 transmission after diagnosis: not petting or kissing the animal, staying in a different room, and having someone else feed and walk the animal.
#First exposure was defined as 2 days before first positive diagnosis in the household or onset of symptoms, whichever was earlier.

pears to enable SARS-CoV-2 transmission, and that pet owners are familiar with and willing to adopt measures to protect their pets from COVID-19. Virus-positive animal prevalence was >90% in multi-pet households that had ≥1 positive pet. Our results largely align with results from Canada (30) (positive effect for bedsharing in cats; 41% of dogs and 52% of cats seropositive; however, few PCR-positive pets) and studies from Texas (31) and Arizona (32) indicating that household pet interspecies transmission of SARS-CoV-2 is common.

The first limitation of our study is that several weeks had elapsed from first reported exposure to household sample collection from animals in most households, possibly limiting our ability to detect viral shedding by PCR testing but strengthening our ability to detect seroconversion. Second, although we assume transmission is from humans to pets, the cross-sectional nature of this study precludes certainty regarding the direction of transmission. Nevertheless, because SARS-CoV-2 is transmitted predominantly human-to-human, few cases of SARS-CoV-2 have been documented in dogs and cats, and no cases have been documented to be transmitted from dogs or cats to humans, we believe transmission in this study was exclusively from humans to pets. Third, our study is subject to residual confounding caused by inability to adjust for confounders without risking over-fitting. We do not expect unmeasured or unadjusted confounders to exert strong effects other than latent (and therefore difficult to measure and model) constructs, such as socioeconomic status, strength of the human–animal bond, and level of concern about zoonotic disease transmission. Fourth, our definition of illness in pets is simple and vulnerable to misclassification if these clinical signs are caused by other etiologies.

We believe respondents misunderstood the question "Is this animal indoor only vs. indoor/outdoor?" because 37% of dogs were reported to be indoor only. However, we believe that this variable retains its connection to degree of animal contact. We do not expect strong measurement error in any of the other variables examined. Because there is no standard for canine anti–SARS-CoV-2 serology, validation of our ELISA was limited to analytic validation and we could not reliably estimate diagnostic sensitivity of our serologic test. Full diagnostic validation was not possible because of the absence of sufficient standard-positive and standard-negative samples, a limitation arising from emerging pathogen status of SARS-CoV-2. However, all pre–COVID-19 samples evaluated were negative, indicating that specificity approaches 100%; all samples sent to the USDA NVSL for confirmatory PCR had concordant results; and a subset of 30 SARS-CoV-2 RBD ELISA–positive serum samples that had a range of ELISA output; and 4 SARS-CoV-2 RBD ELISA–negative serum samples showed substantial agreement with a virus neutralization test in an interlaboratory comparison with the USDA NVSL.

Although our primary aim, to estimate the burden of human-animal SARS-CoV-2 transmission, was estimated with reasonable precision, because of small sample size, variance was high for effect estimates produced by our regression model. By nature of our recruitment methods and study population, generalizability of our findings is probably limited to highly-educated, higher-income persons in urban and suburban communities.

In conclusion, our study contributes useful and novel findings to the literature on cross-species transmission of SARS-CoV-2, with relevance to other

zoonoses transmitted in a household setting. In particular, our findings indicate households in this population are willing to adopt measures to protect their pets from SARS-CoV-2 infection and that these measures might be effective, indicating an opportunity to prevent household transmission of zoonoses through health education and policy.

About the Author

Dr. Meisner is an assistant professor in Global Health at the University of Washington, Seattle, WA. Her primary research interests are the intersection of human and animal health and the application of rigorous epidemiologic methods to research at this interface.

References

1. Konda M, Dodda B, Konala VM, Naramala S, Adapa S. Potential zoonotic origins of SARS-CoV-2 and insights for preventing future pandemics through One Health approach. Cureus. 2020;12:e8932. https://doi.org/10.7759/cureus.8932
2. Kiros M, Andualem H, Kiros T, Hailemichael W, Getu S, Geteneh A, et al. COVID-19 pandemic: current knowledge about the role of pets and other animals in disease transmission. Virol J. 2020;17:143. https://doi.org/10.1186/s12985-020-01416-9
3. Csiszar A, Jakab F, Valencak TG, Lanszki Z, Tóth GE, Kemenesi G, et al. Companion animals likely do not spread COVID-19 but may get infected themselves. Geroscience. 2020;42:1229–36. https://doi.org/10.1007/s11357-020-00248-3
4. Salajegheh Tazerji S, Magalhães Duarte P, Rahimi P, Shahabinejad F, Dhakal S, Singh Malik Y, et al. Transmission of severe acute respiratory syndrome coronavirus 2 (SARS-CoV-2) to animals: an updated review. J Transl Med. 2020;18:358. https://doi.org/10.1186/s12967-020-02534-2
5. US Department of Agriculture. Animal and Plant Health Inspection Service. Confirmed cases of SARS-CoV-2 in animals in the United States, 2022 [cited 2022 Oct 6]. https://www.Aphis.Usda.Gov/Aphis/Dashboards/Tableau/Sars-Dashboard
6. Molenaar RJ, Vreman S, Hakze-van der Honing RW, Zwart R, de Rond J, Weesendorp E, et al.; Clinical and pathological findings in SARS-CoV-2 disease outbreaks in farmed mink (). Vet Pathol. 2020;57:653–7. https://doi.org/10.1177/0300985820943535
7. Martina BE, Haagmans BL, Kuiken T, Fouchier RA, Rimmelzwaan GF, Van Amerongen G, et al. Virology: SARS virus infection of cats and ferrets. Nature. 2003;425:915. https://doi.org/10.1038/425915a
8. Yen H-L, Sit TH, Brackman CJ, Chuk SS, Gu H, Tam KW, et al.; HKU-SPH study team. Transmission of SARS-CoV-2 delta variant (AY.127) from pet hamsters to humans, leading to onward human-to-human transmission: a case study. Lancet. 2022;399:1070–8. https://doi.org/10.1016/S0140-6736(22)00326-9
9. Kok K-H, Wong S-C, Chan W-M, Wen L, Chu AW-H, Ip JD, et al. Co-circulation of two SARS-CoV-2 variant strains within imported pet hamsters in Hong Kong. Emerg Microbes Infect. 2022;11:689–98. https://doi.org/10.1080/22221751.2022.2040922
10. American Veterinary Medical Association. SARS-CoV-2 in animals [cited 2022 Oct 6]. https://www.avma.org/resources-tools/animal-health-and-welfare/covid-19/sars-cov-2-animals-including-pets
11. Pereira F. SARS-CoV-2 variants lacking ORF8 occurred in farmed mink and pangolin. Gene. 2021;784:145596. https://doi.org/10.1016/j.gene.2021.145596
12. Guo S, Liu K, Zheng J. The genetic variant of SARS-CoV-2: would it matter for controlling the devastating pandemic? Int J Biol Sci. 2021;17:1476–85.
13. Wei C, Shan KJ, Wang W, Zhang S, Huan Q, Qian W. Evidence for a mouse origin of the SARS-CoV-2 Omicron variant. J Genet Genomics. 2021;48:1111–21. https://doi.org/10.1016/j.jgg.2021.12.003
14. de Guzman C. Hong Kong says hamsters may have infected a pet shop worker with COVID-19. Now they all must die, 2022 [cited 2022 Jan 23]. https://time.com/6139876/hong-kong-hamsters-covid-19
15. Davis MF, Rankin SC, Schurer JM, Cole S, Conti L, Rabinowitz P, et al.; COHERE Expert Review Group. Checklist for One Health epidemiological reporting of evidence (COHERE). One Health. 2017;4:14–21. https://doi.org/10.1016/j.onehlt.2017.07.001
16. STROBE statement—checklist of items that should be included in reports of observational studies (STROBE initiative). Int J Public Health. 2008;53:3–4. https://doi.org/10.1007/s00038-007-0239-9
17. Imai M, Iwatsuki-Horimoto K, Hatta M, Loeber S, Halfmann PJ, Nakajima N, et al. Syrian hamsters as a small animal model for SARS-CoV-2 infection and countermeasure development. Proc Natl Acad Sci U S A. 2020;117:16587–95. https://doi.org/10.1073/pnas.2009799117
18. Shi J, Wen Z, Zhong G, Yang H, Wang C, Huang B, et al. Susceptibility of ferrets, cats, dogs, and other domesticated animals to SARS-coronavirus 2. Science. 2020;368:1016–20. https://doi.org/10.1126/science.abb7015
19. Harris PA, Taylor R, Minor BL, Elliott V, Fernandez M, O'Neal L, et al.; REDCap Consortium. The REDCap consortium: building an international community of software platform partners. J Biomed Inform. 2019;95:103208. https://doi.org/10.1016/j.jbi.2019.103208
20. Eckstrand CD, Baldwin TJ, Rood KA, Clayton MJ, Lott JK, Wolking RM, et al. An outbreak of SARS-CoV-2 with high mortality in mink () on multiple Utah farms. PLoS Pathog. 2021;17:e1009952. https://doi.org/10.1371/journal.ppat.1009952
21. Centers for Disease Control and Prevention. CDC 2019-novel coronavirus (2019-nCoV) real-time rRT-PCR panel: primers and probes, 2020 [cited 2022 Sep 27]. https://www.fda.gov/media/134922/download

22. Plitnick J, Griesemer S, Lasek-Nesselquist E, Singh N, Lamson DM St George K. Whole-genome sequencing of SARS-CoV-2: assessment of the ion torrent AmpliSeq panel and comparison with the Illumina MiSeq ARTIC protocol. J Clin Microbiol. 2021;59:e0064921. https://doi.org/10.1128/JCM.00649-21

23. GISAID. CoVsurver: mutation analysis of hCoV-19, 2022 [cited 2022 Oct 6]. https://www.gisaid.org/Epiflu-Applications/Covsurver-Mutations-App

24. Khare S, Gurry C, Freitas L, Schultz MB, Bach G, Diallo A, et al. GISAID's role in pandemic response. China CDC Wkly. 2021;3:1049–51. https://doi.org/10.46234/ccdcw2021.255

25. Rambaut A, Holmes EC, O'Toole Á, Hill V, McCrone JT, Ruis C, et al. A dynamic nomenclature proposal for SARS-CoV-2 lineages to assist genomic epidemiology. Nat Microbiol. 2020;5:1403–7. https://doi.org/10.1038/s41564-020-0770-5

26. O'Toole Á, Hill V, McCrone J, Scher E, Rambaut A. Pangolin COVID-19 lineage assigner, 2022 [cited 2022 Oct 6]. https://pangolin.cog-uk.io

27. Phan IQ, Subramanian S, Kim D, Murphy M, Pettie D, Carter L, et al. In silico detection of SARS-CoV-2 specific B-cell epitopes and validation in ELISA for serological diagnosis of COVID-19. Sci Rep. 2021;11:4290. https://doi.org/10.1038/s41598-021-83730-y

28. Textor J, van der Zander B, Gilthorpe MS, Liśkiewicz M, Ellison GT. Robust causal inference using directed acyclic graphs: the R package 'dagitty'. Int J Epidemiol. 2016;45:1887–94. https://doi.org/10.1093/ije/dyw341

29. Højsgaard S, Halekoh U, Yan J. The R package geepack for generalized estimating equations. J Stat Softw. 2005;15:1–11.

30. Bienzle D, Rousseau J, Marom D, MacNicol J, Jacobson L, Sparling S, et al. Risk factors for SARS-CoV-2 infection and illness in cats and dogs. Emerg Infect Dis. 2022;28:1154–62. https://doi.org/10.3201/eid2806.220423

31. Hamer SA, Pauvolid-Corrêa A, Zecca IB, Davila E, Auckland LD, Roundy CM, et al. SARS-CoV-2 infections and viral isolations among serially tested cats and dogs in households with infected owners in Texas, USA. Viruses. 2021;13:938. https://doi.org/10.3390/v13050938

32. Yaglom HD, Hecht G, Goedderz A, Jasso-Selles D, Ely JL, Ruberto I, et al. Genomic investigation of a household SARS-CoV-2 disease cluster in Arizona involving a cat, dog, and pet owner. One Health. 2021; 13:100333. https://doi.org/10.1016/j.onehlt.2021.100333

Address for correspondence: Julianne Meisner, Environmental and Occupational Health Sciences Hans Rosling Center for Population Health, University of Washington, 3980 15th Ave NE, 2nd Floor, Seattle, WA 98195-0005, USA; email: meisnerj@uw.edu

National Monkeypox Surveillance, Central African Republic, 2001–2021

Camille Besombes, Festus Mbrenga, Laura Schaeffer, Christian Malaka, Ella Gonofio,
Jordi Landier, Ulrich Vickos, Xavier Konamna, Benjamin Selekon, Joella Namsenei Dankpea,
Cassandre Von Platen, Franck Gislain Houndjahoue, Daniel Sylver Ouaïmon, Alexandre Hassanin,
Nicolas Berthet, Jean-Claude Manuguerra, Antoine Gessain, Arnaud Fontanet,[1] Emmanuel Nakouné-Yandoko[1]

We analyzed monkeypox disease surveillance in Central African Republic (CAR) during 2001–2021. Surveillance data show 95 suspected outbreaks, 40 of which were confirmed as monkeypox, comprising 99 confirmed and 61 suspected monkeypox cases. After 2018, CAR's annual rate of confirmed outbreaks increased, and 65% of outbreaks occurred in 2 forested regions bordering the Democratic Republic of the Congo. The median patient age for confirmed cases was 15.5 years. The overall case-fatality ratio was 7.5% (12/160) for confirmed and suspected cases, 9.6% (8/83) for children <16 years of age. Decreasing cross-protective immunity from smallpox vaccination and recent ecologic alterations likely contribute to increased monkeypox outbreaks in Central Africa. High fatality rates associated with monkeypox virus clade I also are a local and international concern. Ongoing investigations of zoonotic sources and environmental changes that increase human exposure could inform practices to prevent monkeypox expansion into local communities and beyond endemic areas.

Monkeypox, caused by monkeypox virus (MPXV), a member of the *Orthopoxvirus* genus, was considered a rare emerging disease before a multinational outbreak was identified in May 2022 (*1*).

Author affiliations: Sorbonne Université, Paris, France
(C. Besombes); Institut Pasteur, Paris (C. Besombes,
L. Schaeffer, C. Von Platen, N. Berthet, J.-C. Manuguerra,
A. Gessain, A. Fontanet); Institut Pasteur, Bangui, Central African
Republic (F. Mbrenga, C. Malaka, E. Gonofio, X. Konamna,
B. Selekon, J. Namsenei Dankpea, E. Nakouné Yandoko);
Aix Marseille Université, Marseille, France (J. Landier); Centre
Hospitalier Universitaire, Bangui (F.G. Houndjahoue,
D.S. Ouaïmon); Sorbonne Université, Paris (A. Hassanin);
Institut Pasteur of Shanghai, Shanghai, China (N. Berthet);
Conservatoire National des Arts et Métiers, Paris (A. Fontanet)

After global smallpox eradication in 1977, monkeypox became the most concerning human *Orthopoxvirus* infection. Clinical manifestations of monkeypox typically resemble those of smallpox, including a febrile prodrome and subsequent disseminated maculopapular rash, including vesicles and pustules, that occurs in successive stages (*2*). Lymphadenopathy is a prominent feature of monkeypox and usually does not occur for smallpox and chickenpox (*3*). Illness is less severe and death less likely among monkeypox cases than smallpox cases, but monkeypox mortality rates vary and are higher for clade I (formerly the Congo Basin clade) than for clade II (formerly the West African clade) viruses (*2*). Prior smallpox vaccination can confer cross-immunity for monkeypox, but smallpox vaccination programs worldwide ended in the early 1980s (*4*).

In 1970, a human monkeypox case was reported from Basankusu, Equateur Province, Democratic Republic of the Congo (DRC) (*5*). Subsequent sporadic monkeypox cases were reported among human and animal populations from remote areas of Central Africa during the 1970s and 1980s (*6,7*). Since 1990, increases in the frequency and scale of epidemics in Africa have been reported for clade I and, to a lesser extent, since 2000 for clade II. Since 2016, confirmed monkeypox cases have been reported in DRC, Central African Republic (CAR), Republic of Congo (hereafter Congo), Nigeria, Sierra Leone, Liberia, and Cameroon (*6*). The true burden, circulation rates, and geographic range of this emerging disease remain unknown because many countries lack systematic routine monkeypox surveillance and affected areas often are remote (*8,9*).

An outbreak of human monkeypox disease occurred outside Africa in 2003, after infected animals from Ghana were imported into the United States

---

[1]These senior authors contributed equally to this article.

(10). Since 2018, several self-limited monkeypox outbreaks have been reported among travelers from the United Kingdom, Singapore, Israel, and the United States after travel to Nigeria (11) (https://www.cdc.gov/poxvirus/monkeypox/outbreak/us-outbreaks.html). A large worldwide monkeypox outbreak was documented in May 2022 (https://www.who.int/emergencies/situations/monkeypox-oubreak-2022), including interhuman transmission in >85 countries outside Africa and 5 reported monkeypox-related deaths (12), highlighting the global public health threat posed by this disease. Primary zoonotic transmission presumably results from at-risk activities, such as hunting or butchering bushmeat or handling animal carcasses (13). Rodents, including arboreal rope squirrels (*Funisciurus* spp.) and terrestrial rodents (*Cricetomys* and *Graphiurus* spp.) (14), are believed to be the main sources for MPXV introduction into human populations, but the natural virus reservoir remains unknown and molecular sequencing of animal–human pairs has yet to identify the same MPXV strain in both organisms.

Human-to-human viral transmission seems to occur through direct contact with lesion exudates, bodily fluids, or respiratory droplets; or through indirect contact with environments contaminated by monkeypox patients (15). The 2022 outbreak primarily has occurred among men who have sex with men (MSM) and has highlighted the role of direct cutaneous and mucosal contact during sexual intercourse and the potential contribution of sexual transmission (2,16), but exact modes of transmission remain unclear.

Before the 2022 worldwide outbreak, CAR was fourth among monkeypox-affected countries, after DRC, Nigeria, and Congo (2), but epidemiologic data concerning monkeypox in CAR remains scarce (17–24). We provide a comprehensive analysis of national monkeypox surveillance in CAR during 2001–2021.

Methods

National Monkeypox Surveillance and Epidemiologic Outbreak Investigations

The population of CAR consists mainly subsistence farmers and hunter-gatherers who live in small villages or towns. The Institut Pasteur of Bangui (IPB), the CAR Ministry of Public Health and Population, and the World Health Organization (WHO) established the CAR national monkeypox surveillance system in 2001. Healthcare workers in the field receive regular training on the clinical manifestations of monkeypox and the importance of rapid case identification. These workers send blood, pus, and crust samples from suspected monkeypox cases to IPB, which serves as the national MPXV reference center. After virologic confirmation, IPB deploys an outbreak investigation team to the field to conduct a more thorough investigation of cases and their contacts. The IPB investigation team administers specific case-report questionnaires via paper surveys in the local language, Sango, to collect information about demographic characteristics, socioeconomic status, education, and contact with wildlife or other human cases. A trained practitioner on the IPB team uses sterile techniques to collect swab samples of pus, crusts, or lesions from each suspected case, and 3–5 mL whole-blood samples from contacts and suspected cases.

Monkeypox case definitions for the CAR national surveillance program follow international recommendations adapted from WHO, the US Centers for Disease Control and Prevention (CDC), and Nigeria Centre for Disease Control (NCDC; https://ncdc.gov.ng/diseases/info/M). Thus, we considered confirmed case-patients as persons with a history of fever and maculopapular rash on palms and soles and virologic confirmation of MPXV via PCR. We considered suspected cases as illness in persons with clinical manifestations but no virologic confirmation, and we considered contacts to be persons without skin lesions <3 weeks after exposure to a case-patient. We defined the index case as the first human case identified in a village, which might or might not be the primary human case (i.e., the initial case presumed to be from an animal source) (25,26). Because initial interhuman transmission between the primary and secondary cases might not have been recognized, the index case might not always be the primary case.

We assessed lesion severity by adding the total number of lesions and scars, then classified severity as mild (<25 lesions), moderate (26–100 lesions), severe (101–250 lesions), or serious (>250 lesions) (25). In the absence of easily identifiable scars to determine smallpox vaccination status, we considered persons born before 1980 to have been vaccinated. We defined outbreaks of monkeypox on the basis of >1 confirmed case of human monkeypox; we defined outbreaks of chickenpox on the basis of >1 biologically confirmed chickenpox case. All case-patients received symptomatic and supportive care in accordance with international guidelines for the management of monkeypox disease and were isolated in the hospital for >14 days after virologic diagnosis; isolation was longer when PCR results remained positive. Suspected case-patients were isolated in the nearest healthcare center until they received results of diagnostic procedures. Contacts

were quarantined at home for 21 days and received a daily visit from the epidemiologic surveillance point of contact. Smallpox vaccine is not available in CAR for postexposure prophylaxis.

Laboratory Procedures

WHO recommends PCR of swab samples from pus or crusts for laboratory confirmation of MPXV (https://www.who.int/news-room/fact-sheets/detail/monkeypox). Samples also are tested for MPXV via intracranial inoculation of suckling mice (23). National monkeypox surveillance in CAR uses a quantitative conventional PCR that targets the hemagglutinin gene and part of the A-type inclusion body gene by using generic and clade I primers (27), as described in previous outbreak investigations (18,21,22). Case-patients and contacts are also tested for IgG against monkeypox in blood by using an in-house ELISA and antigens from a local MPXV strain (GenBank access no. MN702450) obtained during a previous epidemic (18–22). This serologic assay has not been formally validated, and cross-reactivity between orthopoxviruses is likely, as reported for other similar assays (28).

Statistical Analysis

We compared groups by using Mann-Whitney or Kruskal-Wallis tests for continuous data or by using χ^2 test for discrete data. We investigated the monthly number of confirmed monkeypox outbreaks by assuming a Poisson distribution. We used univariable and multivariable logistic regression analyses to investigate factors associated with IgG against MPXV. We performed all statistical analyses in Stata version 15.0 (StataCorp LLC, https://www.stata.com).

Ethics Considerations

Outbreak investigations were conducted within the framework of the CAR national surveillance program. We obtained authorization to use these data for research purposes from the institutional review board of Institut Pasteur Paris (authorization no. IRB00006966) on January 10, 2020, and from the Comité Ethique et Scientifique of the Université de Bangui on February 21, 2021.

Results

During 2001–2021 the national surveillance system identified 95 suspected monkeypox outbreaks and investigated 468 persons. Of those persons, 99 were confirmed as monkeypox cases, 48 were confirmed as chickenpox cases, 109 were suspected co-infections, and 212 were contacts (Figure 1). From these findings, we identified 40 confirmed monkeypox outbreaks, including 2 persons with monkeypox–chickenpox co-infection, 32 exclusive confirmed chickenpox outbreaks, and 23 outbreaks of undetermined origin without confirmation of monkeypox or chickenpox (Figure 1).

The 40 confirmed monkeypox outbreaks encompassed 327 persons, including 99 confirmed monkeypox cases (including the 2 persons with chickenpox–monkeypox co-infection), 61 suspected monkeypox
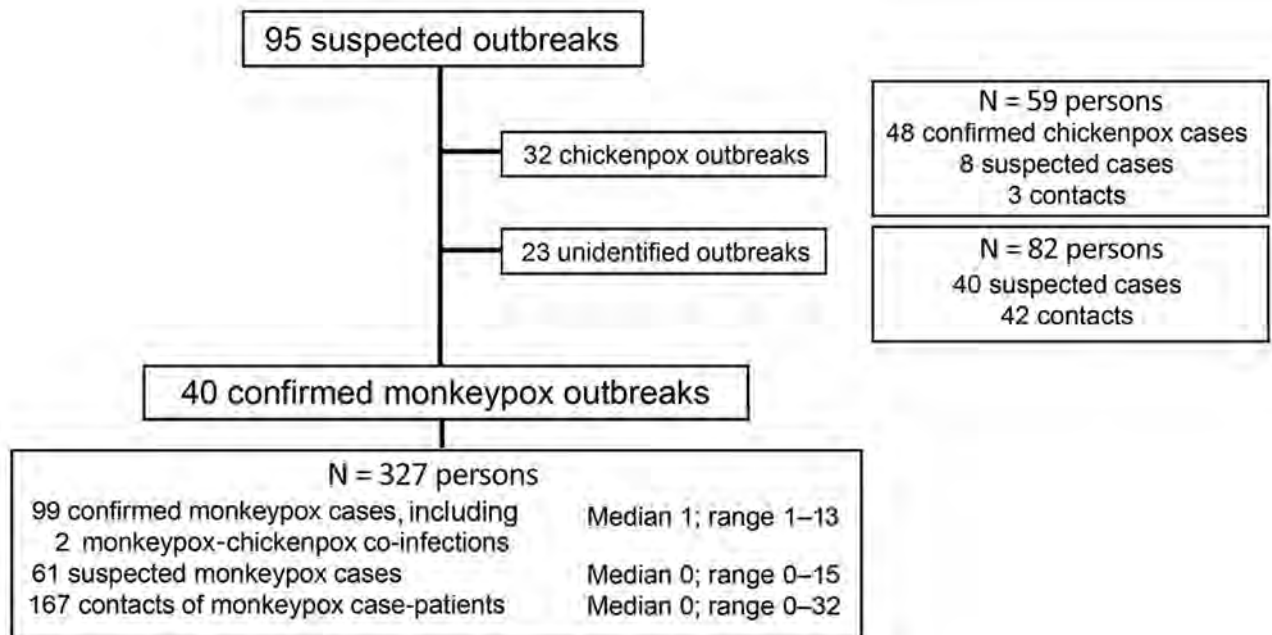

Figure 1. Cases detected and investigated during national monkeypox surveillance, Central African Republic, 2001–2021.

cases, and 167 contacts (Figure 1; Appendix Table 1, https://wwwnc.cdc.gov/EID/article/28/12/22-0897-App1.pdf). The size of the confirmed monkeypox outbreaks ranged from 1–13 confirmed cases, but no outbreak involved >25 confirmed and suspected cases. We detected 3 chickenpox outbreaks that were spatially and temporally concomitant with 3 confirmed monkeypox outbreaks. The maximum number of contacts investigated in a single confirmed monkeypox outbreak was 32 (Appendix Table 1).

During 2001–2017, very few (0–2 annually) monkeypox outbreaks were reported. Since 2018, the annual number of outbreaks reported climbed to 9, but a transient decrease occurred in 2020 during the COVID-19 pandemic (Figure 2; Appendix Table 1). Lobaye (40% of outbreaks) and Mbomou (25% of outbreaks), both part of the Congo Basin Forest (Figure 3), were the geographic areas principally affected. Outbreaks mostly occurred in remote rural areas, although a few recent outbreaks occurred in small towns, such as Ippy (population 17,000), Raffaï (population 13,000), and Bania (population 5,000), and in 2 affected artisanal gold-mining areas (Appendix Table 1). Monthly rates of confirmed monkeypox outbreaks were heterogeneous (p = 0.002), and most outbreaks occurred in September (Appendix Figure 1). For 16 outbreaks, index cases described exposure to wildlife, consistent with a zoonotic source (Appendix Table 1).

Among confirmed case-patients, 51 (53.1%) were female (Table; Appendix Figure 2); half were children <16 (interquartile range [IQR] 5.5–28) years of age, 54.4% of whom were male. The 40 outbreak index cases were evenly distributed between the sexes: 19 were male, 19 female, and 2 had missing data for sex; we observed no predominance of a particular age group. Only 3 confirmed case-patients were >42

years of age and we presumed they were vaccinated against smallpox (Table).

Information about the incubation period, the interval between exposure and symptom onset, was available for 29 persons. The median incubation period was 7 (range 0–17; IQR 1–13) days. The median time from rash onset to sample collection was 9.5 (range 0–31; IQR 5–17) days, and monkeypox was diagnosed via samples of blood in 45 cases, pus in 32 cases, and crusts in 14 cases. All (100%) confirmed case-patients had a rash, and most reported fever (93.2%), pruritus (81.5%), and lymphadenopathy (78.6%) (Figure 4). All case-patients reported a disseminated rash, but 91.3% (42/46) of those for whom information was available had recorded genital lesions. Rashes were graded as moderate (57.1%), severe (34.3%), or serious (5.7%) (Figure 5), and we noted no association between rash intensity and age or sex. Disease severity was not associated with presumed zoonotic or interhuman transmission. Among 18 confirmed case-patients for whom information was available, 11 experienced ≥1 disease complications, such as septicemia (n = 3), bronchopneumonia (n = 4), dehydration (n = 6), corneal ulceration (n = 2), cutaneous bacterial superinfection (n = 3), fistulation of axillary adenopathy (n = 1) (Figure 6), and keloid healing (n = 4). HIV testing is not systematically performed for monkeypox cases in CAR, and only 1 case of HIV co-infection was identified in a patient who recovered from monkeypox after experiencing a serious rash (>250 lesions). Eight case-patients experienced concomitant malaria.

Among confirmed and suspected monkeypox cases, 12 persons died, 8 children and 4 adults (Table; Appendix Table 2), corresponding to an overall case-fatality ratio (CFR) of 7.5% (12/160) and a CFR of
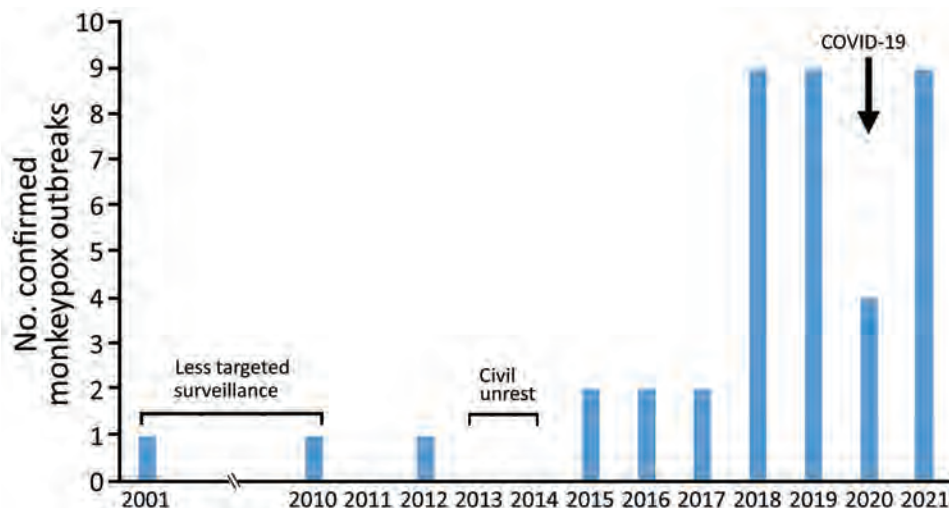

Figure 2. Confirmed outbreaks detected during national monkeypox surveillance, Central African Republic, 2001–2021.
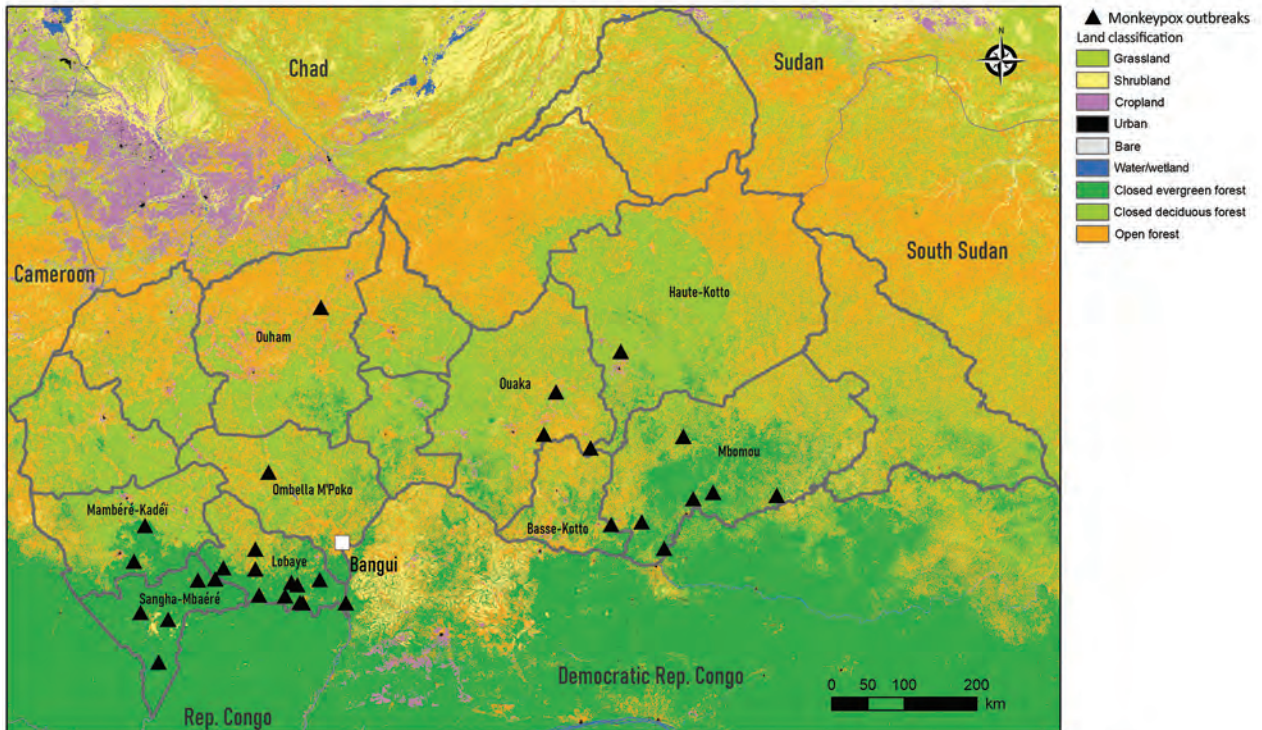
Figure 3. Confirmed outbreaks detected during national monkeypox surveillance, Central African Republic, 2001–2021. Source: Copernicus 2019 Global 100 m Landcover (https://doi.org/10.3390/rs12061044). Rep., Republic.

9.6% (8/83) in children <16 years of age. The CFR was 7.1% (7/99) for confirmed cases and 8.2% (5/61) for suspected cases. Information about the cause of death was available for only 3 (25%) deaths: 1 resulted from a severe cutaneous monkeypox form and septicemia, another from a pulmonary edema, and the third from probable neurologic impairment in a child (19) (Appendix Table 2).

Among 327 persons investigated during the 40 confirmed monkeypox outbreaks, serologic results were available for 288 (79 confirmed cases, 48 suspected cases, and 161 contacts); missing blood samples were the main reason serologic results were not available. Of 288 cases with serologic results, 159 (55.2%) tested positive for IgG against monkeypox virus. The median interval between outbreak onset and initial sampling was 15 (IQR 6–28.5) days for the confirmed cases and 39 (IQR 20–46.5) days for the suspected cases or contacts. In a multivariable model adjusted for age, sex, and time from outbreak onset to date of first blood sample collection, monkeypox virus IgG was more frequently detected for confirmed cases than for suspected cases and contacts (odds ratio [OR] 2.04, 95% CI 1.00–4.16) (Appendix Table 3). MPXV IgG positivity was bimodally distributed by age, with peaks at 15–19 years and >45 years of age (Appendix Table 3).

Discussion

CAR has conducted national monkeypox disease surveillance since 2001, although surveillance programs in CAR initially focused more on other eruptive fevers, such as measles and rubella (9). Monkeypox surveillance has been more systematic since 2010, albeit with interruptions during periods of civil unrest (2013–2014). The number of confirmed monkeypox outbreaks reported has increased since 2018, although we noted a transient decline in 2020, probably resulting from disruption of normal activities caused by the COVID-19 pandemic (29) and civil unrest surrounding CAR presidential elections in December 2020. Before 2018, no outbreaks had been reported between the outbreak in Sangha Mbaéré prefecture during 1983–1984 and the outbreak in Mbomou prefecture in 2001 (17,18). We observed a similar pattern in areas of sporadic endemicity, where recent outbreaks occurred in Cameroon in 2018 after 29 years of absence (30), in Sierra Leone in 2014 after 44 years (31), and in Nigeria in 2017 after 39 years (32). More generally, the recent increase in the number of outbreaks in CAR has been mirrored elsewhere, in West Africa and the Congo Basin region, and seems to reflect improvements in surveillance, as well as increased viral circulation in a region experiencing major ecologic disturbances (33). Indeed, considerable deforestation and

Table. Characteristics of 327 cases investigated during monkeypox national monkeypox surveillance, Central African Republic, 2001–2021*

Characteristics	Confirmed cases, n = 99	Suspected cases, n = 61	No. contacts, n = 167	p value
Sex				0.6
F	51 (53.1)	37 (60.7)	90 (53.9)	
M	45 (46.9)	24 (39.3)	77 (46.1)	
Data missing	3	0	0	
Median age, y (IQR)	15.5 (5.5–27)	8 (2–23)	27 (14–40)	<0.001
Age group, y				<0.001
0–9	33 (35.9)	30 (50.9)	23 (17)	
10–19	17 (18.5)	9 (15.2)	18 (13.3)	
20–29	22 (23.9)	11 (18.6)	30 (22.2)	
>30	20 (21.7)	9 (15.3)	64 (47.4)	
Missing data	7	2	32	
Born before 1980†				0.001
Y	3 (3.3)	4 (6.8)	28 (20.7)	
N	89 (96.7)	55 (93.2)	107 (79.3)	
Missing data	7	2	32	
Status/occupation				0.001
Child	37 (51.9)	26 (61.9)	5 (13.2)	
Farmer	16 (22.2)	11 (28.2)	15 (39.5)	
Hunter/fisherman	6 (8.3)	0	1 (2.6)	
Healthcare worker	0	1 (2.4)	4 (10.5)	
Mine worker	2 (2.8)	0	6 (15.8)	
Market trader	2 (2.8)	2 (4.8)	0	
Other	9 (12.5)	2 (4.7)	7 (18.4)	
Missing data	27	19	129	
Reported contact with a human case				0.004
Y	44 (65.7)	28 (75.7)	36 (94.7)	
N	23 (34.3)	9 (24.3)	2 (5.3)	
Missing data	32	24	129	
Contact setting				<0.001
Home	40 (95.2)	22 (81.5)	17 (56.7)	
Elsewhere	2 (4.8)	5 (18.5)	13 (43.3)	
Missing data	57	34	137	
Fever before rash				0.1
Y	51 (85)	29 (96.7)	NA	
N	9 (15)	1 (3.3)	NA	
Missing data	39	31	NA	
Diagnostic sample collected				<0.001
Blood	45 (49.5)	53 (86.9)	46 (97.9)	
Pus	32 (35.2)	5 (8.2)	0	
Crust	14 (15.4)	3 (4.9)	1 (2.1)	
Missing data	8	0	120	

*Values indicate no. (%) of available data except as indicated. Number of cases missing data are indicated for each characteristic. NA, not applicable
†Presumably persons born before 1980 were vaccinated against smallpox.

land-use changes have occurred in tropical rainforests in recent decades, causing habitat loss for wildlife and proliferation of several opportunistic species, such as rodents, thus increasing interactions between humans and animals and the risk for zoonotic disease emergence (*34,35*).

Since 2001, most confirmed monkeypox outbreaks in CAR have occurred in the Lobaye and Mbomou prefectures, forested regions located at the edge of the Congo Basin Forest, a favorable ecosystem for the suspected animal hosts. These 2 regions border DRC and Congo, and multiple commercial and social exchanges occur between these countries, potentially facilitating viral circulation, as demonstrated in previous phylogenetic studies (*18*). The occurrence of monkeypox predominantly in forested areas is characteristic of outbreaks in Central Africa (*2*) but differs from the distribution observed in Nigeria, where outbreaks have recently shifted to savanna and urban areas (*36*). The distribution shift in Nigeria reveals a change in the epidemiologic features of the disease (*32,35*) and an increase in the potential for international spread. In CAR, predominance of monkeypox outbreaks in September, at the end of the rainy season, might reflect the movement of local populations into forested areas for caterpillar picking. During that time of the year, entire families, including children on their school holidays, participate in these activities, which bring them into closer contact with wildlife and the deep forest environment, which could increase the risks for zoonotic and interhuman transmission.
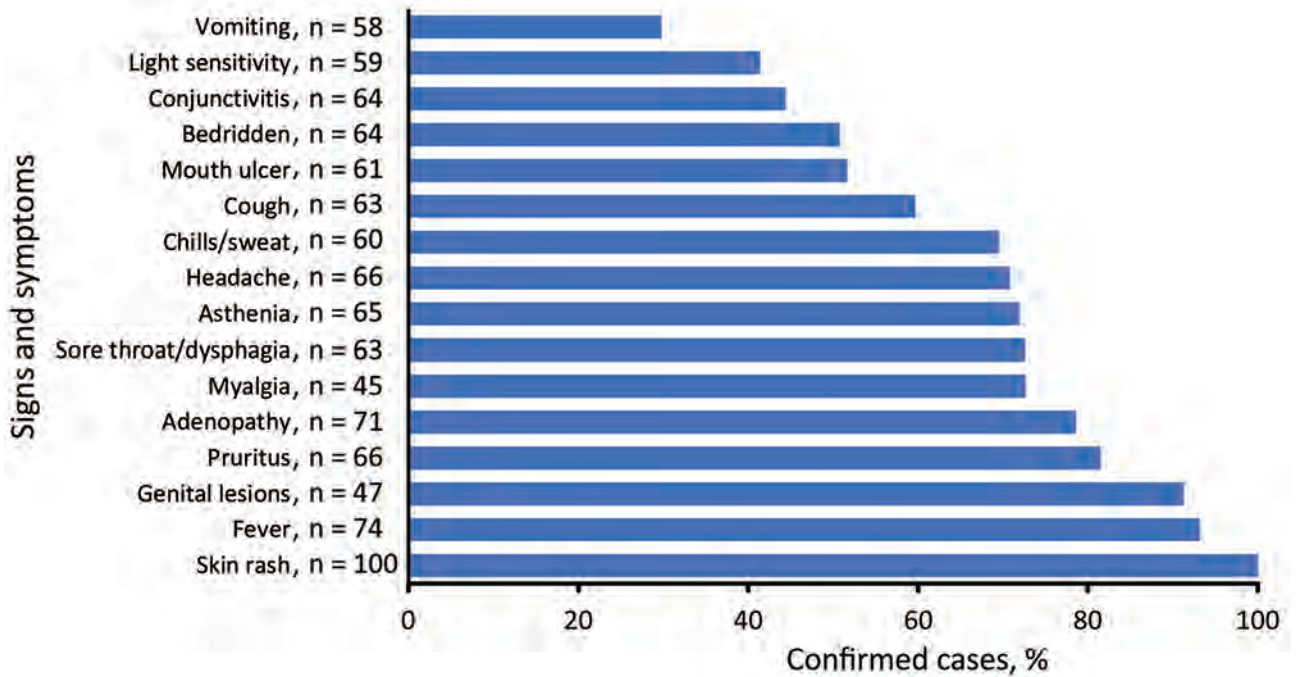
Figure 4. Frequency of signs and symptoms among 99 confirmed monkeypox cases detected during national surveillance, Central African Republic, 2001–2021.

As in DRC (*2*), identifying a zoonotic source for outbreaks in CAR has been difficult; only 16 of the 40 confirmed monkeypox outbreaks we identified included a suspected source. A study of 837 monkeypox cases in Tshuapa Province in DRC revealed a similar pattern: only 36.9% of case-patients reported prior contact with animals, and 33.3% reported contact with a symptomatic human case (*37*). The DRC national surveillance program has revealed multiple wildlife exposures in the populations of forested areas (*13,25*). Such exposures might be underreported in CAR, leading to an overestimation of the importance of secondary transmission within households (*38*). However, outbreaks in Central Africa seem to be related to iterative independent spillover events, whereas interhuman transmission seems more likely in the urban context of the disease in Nigeria (*36*). More precise identification of infection sources is essential for guiding specific prevention measures. The 2019 description of a case of monkeypox disease relapse in a UK patient also suggests alternative mechanisms underlying the repetition of outbreaks at the same location (*16*), such as interhuman transmission resuming after a virologic or clinical relapse in patients previously affected, as described for Ebola virus disease (*39*).

Figure 5. Examples of rash severity detected during national monkeypox surveillance, Central African Republic, 2001–2021. A) Serious rash on a patient's left hand. Serious rash was reported in 5.7% of cases. B) Moderate rash on a patient's back. Moderate rash was reported in 57.1% of cases.

Figure 6. Example of fistulation of axillary adenopathy detected during national monkeypox surveillance, Central African Republic, 2001–2021.

Among the 95 suspected monkeypox outbreaks we investigated (Figure 1), the preponderance of outbreaks of undetermined origin could partly be explained by the reliance on blood samples for diagnosis; monkeypox diagnosis on the basis of blood samples is known to be less sensitive than diagnosis through pus or crust samples (*6*). Indeed, for 68.2% (15/22) of monkeypox outbreaks of unknown origin, only blood samples were collected, and no pus or crust samples were tested. This lack of testing might be related to healthcare workers in remote areas who lack knowledge of the type of sampling needed for monkeypox diagnosis and their lack of training and medical materials for pus or crust sampling. Chickenpox and monkeypox outbreaks already were reported to simultaneously occur in villages (*40–42*), and co-infection was reported for 1 person, but whether these findings correspond to a true cocirculation of the 2 viruses or to false-positive results for chickenpox or monkeypox remains unclear. Concomitant malaria was also reported, and a similar case has been reported in DRC (P.R. Pittman et al., unpub. data, https://doi.org/10.1101/2022.05.26.22273379).

The age and sex distribution of confirmed case-patients might reflect the nature of exposure because young boys traditionally are more likely to have contact with infected animals through playing and hunting (*13,43*), whereas women more likely to be exposed through caring for ill persons (*44*). These 2 groups have been shown to be predominantly affected in Central Africa (*8,26,40*); however, outbreaks in West Africa have shown different patterns, in which the age distribution is older (median age 29 years [*1*]) and most (69%) cases occur among male persons (*32*).

The overall clinical description of cases in the CAR national surveillance program is consistent with reports for other endemic countries, except for the frequency of genital lesions, which were common among patients who were asked in CAR but were more rarely (5%–68%) reported elsewhere (*25,45*). Several authors have already suggested that skin-to-skin contact or contact with genital secretions during sexual intercourse might have played a role in transmission in the monkeypox outbreak in Nigeria (*46*). Thus, endemic settings might need improved documentation of genital lesions. The recent

monkeypox outbreak in countries outside sub-Saharan Africa, characterized by isolated genital lesions and a predominance of cases in MSM, supports the hypothesis of transmission through close and intimate contact during sexual intercourse (*1*).

The CFR (7.5%) detected in CAR was toward the upper end of the range, as expected for clade I (*3*), and was high (9.6%) for children, as reported elsewhere (*34,47*). This CFR is greater than that reported for epidemics in Nigeria (2.8% and 6% during 2017–2018) (*32,48*) and greater than CFRs reported since May 2022 from countries outside Africa (*12*); by September 17, 2022, CDC reported only 9 monkeypox deaths among >60,703 diagnosed cases in nonendemic countries (https://www.cdc.gov/poxvirus/monkeypox/response/2022/world-map.html). In endemic settings, CFR has been difficult to accurately estimate (*2*), and some deaths might have occurred before investigations began for those outbreaks, resulting in an underestimation of the number of cases. Also, stratifying CFR by HIV status would have been useful. Unfortunately, reluctance for testing among the local population in CAR limits available information about HIV status.

Smallpox vaccination appears likely to have a protective effect against monkeypox, particularly because we noted only 3 cases among persons born before 1980, the year in which vaccination campaigns with live-attenuated vaccinia virus ended in CAR. Thus, the population at risk for *Orthopoxvirus* infection would be expected to increase over time because fewer persons will be protected by vaccination. Over half the national surveillance population in our study tested positive for IgG against MPXV, as reported in other investigations of serologic response to orthopoxviruses in endemic countries from West or Central Africa (*49,50*), particularly in forested areas (*35*). However, in a context of serologic cross-reactions between *Orthopoxvirus* infections (*28*), the antibody peak we observed among persons 15–19 years of age might correspond to childhood exposure to monkeypox or other orthopoxviruses, and the peak among persons $\geq$45 years of age might correspond to smallpox vaccination.

In conclusion, characterization of the epidemiologic features of monkeypox in Africa and analysis of the ongoing outbreak outside sub-Saharan Africa is essential. Indeed, the recent increase in monkeypox virus circulation in CAR should be carefully considered in the context of decreasing cross-protective immunity from smallpox vaccination after 1980, the increased deforestation and land use changes in tropical forest, and the potential local and international effects associated with high lethality of clade I. Further investigation of zoonotic sources of infection and the environmental changes involved could enable design of appropriate preventive measures for avoiding expansion of this threatening clade into local communities and beyond endemic areas.

About the Author

Dr. Besombes is an infectious and tropical disease clinician who works as a medical epidemiologist in the Emerging Diseases Epidemiology Unit at Institut Pasteur, Paris, France. Her primary research interests include the understanding of emerging infectious diseases and zoonotic diseases, through One Health and EcoHealth approaches.

References

1. Thornhill JP, Barkati S, Walmsley S, Rockstroh J, Antinori A, Harrison L, et al. Monkeypox virus infection in humans across 16 countries—April–June 2022. N. Engl. J. Med. 2022;387:679–91. https://doi.org/10.1056/NEJMoa2207323
2. Bunge EM, Hoet B, Chen L, Lienert F, Weidenthaler H, Baer LR, et al. The changing epidemiology of human monkeypox—a potential threat? A systematic review. PLoS Negl Trop Dis. 2022;16:e0010141. https://doi.org/10.1371/journal.pntd.0010141
3. Damon IK. Status of human monkeypox: clinical disease, epidemiology and research. Vaccine. 2011;29:D54–9. https://doi.org/10.1016/j.vaccine.2011.04.014
4. Reynolds MG, Damon IK. Outbreaks of human monkeypox after cessation of smallpox vaccination. Trends Microbiol. 2012;20:80–7. https://doi.org/10.1016/j.tim.2011.12.001
5. Ladnyj ID, Ziegler P, Kima E. A human infection caused by monkeypox virus in Basankusu Territory, Democratic Republic of the Congo. Bull World Health Organ. 1972; 46:593–7.
6. Durski KN, McCollum AM, Nakazawa Y, Petersen BW, Reynolds MG, Briand S, et al. Emergence of monkeypox—West and Central Africa, 1970-2017. MMWR Morb Mortal Wkly Rep. 2018;67:306–10. https://doi.org/10.15585/mmwr.mm6710a5
7. Sklenovská N, Van Ranst M. Emergence of monkeypox as the most important orthopoxvirus infection in humans.

Front Public Health. 2018;6:241. https://doi.org/10.3389/fpubh.2018.00241

8. Rimoin AW, Mulembakani PM, Johnston SC, Lloyd Smith JO, Kisalu NK, Kinkela TL, et al. Major increase in human monkeypox incidence 30 years after smallpox vaccination campaigns cease in the Democratic Republic of Congo. Proc Natl Acad Sci U S A. 2010;107:16262–7. https://doi.org/10.1073/pnas.1005769107

9. Hoff NA, Doshi RH, Colwell B, Kebela-Illunga B, Mukadi P, Mossoko M, et al. Evolution of a disease surveillance system: an increase in reporting of human monkeypox disease in the Democratic Republic of the Congo, 2001–2013. Int J Trop Dis Health. 2017;25:1–10. https://doi.org/10.9734/IJTDH/2017/35885

10. Sejvar JJ, Chowdary Y, Schomogyi M, Stevens J, Patel J, Karem K, et al. Human monkeypox infection: a family cluster in the midwestern United States. J Infect Dis. 2004;190:1833–40. https://doi.org/10.1086/425039

11. Mauldin MR, McCollum AM, Nakazawa YJ, Mandra A, Whitehouse ER, Davidson W, et al. Exportation of monkeypox virus from the African continent. J Infect Dis. 2022;225:1367–76. https://doi.org/10.1093/infdis/jiaa559

12. Sah R, Mohanty A, Abdelaal A, Reda A, Rodriguez-Morales AJ, Henao-Martinez AF. First monkeypox deaths outside Africa: no room for complacency. Ther Adv Infect Dis. 2022;9:20499361221124027. https://doi.org/10.1177/20499361221124027

13. Quiner CA, Moses C, Monroe BP, Nakazawa Y, Doty JB, Hughes CM, et al. Presumptive risk factors for monkeypox in rural communities in the Democratic Republic of the Congo. PLoS One. 2017;12:e0168664. https://doi.org/10.1371/journal.pone.0168664

14. Khodakevich L, Szczeniowski M, Manbu-ma-Disu, Jezek Z, Marennikova S, Nakano J, et al. The role of squirrels in sustaining monkeypox virus transmission. Trop Geogr Med. 1987;39:115–22.

15. Alakunle E, Moens U, Nchinda G, Okeke MI. Monkeypox virus in Nigeria: infection biology, epidemiology, and evolution. Viruses. 2020;12:1257. https://doi.org/10.3390/v12111257

16. Adler H, Gould S, Hine P, Snell LB, Wong W, Houlihan CF, et al.; NHS England High Consequence Infectious Diseases (Airborne) Network. Clinical features and management of human monkeypox: a retrospective observational study in the UK. Lancet Infect Dis. 2022;22:1153–62. https://doi.org/10.1016/S1473-3099(22)00228-6

17. Khodakevich L, Widy-Wirsky R, Arita I, Marennikova SS, Nakano J, Meunier D. Monkeypox virus infection in humans in the Central African Republic [in French]. Bull Soc Pathol Exot. 1985;78:311–20.

18. Berthet N, Nakouné E, Whist E, Selekon B, Burguière AM, Manuguerra JC, et al. Maculopapular lesions in the Central African Republic. Lancet. 2011;378:1354. https://doi.org/10.1016/S0140-6736(11)61142-2

19. Kalthan E, Dondo-Fongbia JP, Yambele S, Dieu-Creer LR, Zepio R, Pamatika CM. Twelve cases of monkeypox virus outbreak in Bangassou District (Central African Republic) in December 2015 [in French]. Bull Soc Pathol Exot. 2016;109:358–63. https://doi.org/10.1007/s13149-016-0516-z

20. Kalthan E, Tenguere J, Ndjapou SG, Koyazengbe TA, Mbomba J, Marada RM, et al. Investigation of an outbreak of monkeypox in an area occupied by armed groups, Central African Republic. Med Mal Infect. 2018;48:263–8. https://doi.org/10.1016/j.medmal.2018.02.010

21. Besombes C, Gonofio E, Konamna X, Selekon B, Gessain A, Berthet N, et al. Intrafamily transmission of monkeypox virus, Central African Republic, 2018. Emerg Infect Dis. 2019;25:1602–4. https://doi.org/10.3201/eid2508.190112

22. Nakoune E, Lampaert E, Ndjapou SG, Janssens C, Zuniga I, Van Herp M, et al. A Nosocomial outbreak of human monkeypox in the Central African Republic. Open Forum Infect Dis. 2017;4:ofx168. https://doi.org/10.1093/ofid/ofx168

23. Berthet N, Descorps-Declère S, Besombes C, Curaudeau M, Nkili Meyong AA, Selekon B, et al. Genomic history of human monkey pox infections in the Central African Republic between 2001 and 2018. Sci Rep. 2021;11:13085. https://doi.org/10.1038/s41598-021-92315-8

24. Froeschl G, Kayembe PK. Pox-like lesions and haemorrhagic fever in two concurrent cases in the Central African Republic: case investigation and management in difficult circumstances. Pan Afr Med J. 2015;22:23. https://doi.org/10.11604/pamj.2015.22.23.6620

25. Doshi RH, Alfonso VH, Morier D, Hoff NA, Sinai C, Mulembakani P, et al. Monkeypox rash severity and animal exposures in the Democratic Republic of the Congo. EcoHealth. 2020;17:64–73. https://doi.org/10.1007/s10393-019-01459-7

26. Jezek Z, Grab B, Szczeniowski MV, Paluku KM, Mutombo M. Human monkeypox: secondary attack rates. Bull World Health Organ. 1988;66:465–70.

28. Li Y, Zhao H, Wilkins K, Hughes C, Damon IK. Real-time PCR assays for the specific detection of monkeypox virus West African and Congo Basin strain DNA. J Virol Methods. 2010;169:223–7. https://doi.org/10.1016/j.jviromet.2010.07.012

29. Dubois ME, Slifka MK. Retrospective analysis of monkeypox infection. Emerg Infect Dis. 2008;14:592–9. https://doi.org/10.3201/eid1404.071044

30. Amao, LK, Olatunji DI, Igbodo G, Okoli SC, Amaechi I, Goni MI, et al. Trend and enhanced surveillance of Monkeypox during COVID-19 pandemic in Nigeria. J Public Health Afr. 2022;13:2184. https://doi.org/10.4081/jphia.2022.2184

31. Sadeuh-Mba SA, Yonga MG, Els M, Batejat C, Eyangoh S, Caro V, et al. Monkeypox virus phylogenetic similarities between a human case detected in Cameroon in 2018 and the 2017–2018 outbreak in Nigeria. Infect Genet Evol. 2019;69:8–11. https://doi.org/10.1016/j.meegid.2019.01.006

32. Reynolds MG, Wauquier N, Li Y, Satheshkumar PS, Kanneh LD, Monroe B, et al. Human monkeypox in Sierra Leone after 44-year absence of reported cases. Emerg Infect Dis. 2019;25:1023–5. https://doi.org/10.3201/eid2505.180832

33. Yinka-Ogunleye A, Aruna O, Dalhat M, Ogoina D, McCollum A, Disu Y, et al.; CDC Monkeypox Outbreak Team. Outbreak of human monkeypox in Nigeria in 2017–18: a clinical and epidemiological report. Lancet Infect Dis. 2019;19:872–9. https://doi.org/10.1016/S1473-3099(19)30294-4

34. Nakazawa Y, Lash RR, Carroll DS, Damon IK, Karem KL, Reynolds MG, et al. Mapping monkeypox transmission risk through time and space in the Congo Basin. PLoS One. 2013;8:e74816. https://doi.org/10.1371/journal.pone.0074816

35. Haider N, Guitian J, Simons D, Asogun D, Ansumana R, Honeyborne I, et al. Increased outbreaks of monkeypox highlight gaps in actual disease burden in Sub-Saharan Africa and in animal reservoirs. Int J Infect Dis. 2022;122:107–11. https://doi.org/10.1016/j.ijid.2022.05.058

36. Nguyen P-Y, Ajisegiri WS, Costantino V, Chughtai AA, MacIntyre CR. Reemergence of human monkeypox and declining population immunity in the context of urbanization, Nigeria, 2017–2020. Emerg Infect Dis. 2021;27:1007–14. https://doi.org/10.3201/eid2704.203569

37. Ihekweazu C, Yinka-Ogunleye A, Lule S, Ibrahim A. Importance of epidemiological research of monkeypox: is incidence increasing? Expert Rev Anti Infect Ther. 2020; 18:389–92. https://doi.org/10.1080/14787210.2020.1735361

38. Whitehouse ER, Bonwitt J, Hughes CM, Lushima RS, Likafi T, Nguete B, et al. Clinical and epidemiological findings from enhanced monkeypox surveillance in Tshuapa Province, Democratic Republic of the Congo during 2011–2015. J Infect Dis. 2021;223:1870–8. https://doi.org/10.1093/infdis/jiab133

27. Nolen LD, Osadebe L, Katomba J, Likofata J, Mukadi D, Monroe B, et al. Extended human-to-human transmission during a monkeypox outbreak in the Democratic Republic of the Congo. Emerg Infect Dis. 2016;22:1014–21. https://doi.org/10.3201/eid2206.150579

39. Mbala-Kingebeni P, Pratt C, Mutafali-Ruffin M, Pauthner MG, Bile F, Nkuba-Ndaye A, et al. Ebola virus transmission initiated by relapse of systemic Ebola virus disease. N Engl J Med. 2021;384:1240–7. https://doi.org/10.1056/NEJMoa2024670

40. Rimoin AW, Kisalu N, Kebela-Ilunga B, Mukaba T, Wright LL, Formenty P, et al. Endemic human monkeypox, Democratic Republic of Congo, 2001–2004. Emerg Infect Dis. 2007;13:934–7. https://doi.org/10.3201/eid1306.061540

41. Hutin YJ, Williams RJ, Malfait P, Pebody R, Loparev VN, Ropp SL, et al. Outbreak of human monkeypox, Democratic Republic of Congo, 1996 to 1997. Emerg Infect Dis. 2001;7:434–8. https://doi.org/10.3201/eid0703.017311

42. Mande G, Akonda I, De Weggheleire A, Brosius I, Liesenborghs L, Bottieau E, et al. Enhanced surveillance of monkeypox in Bas-Uélé, Democratic Republic of Congo: the limitations of symptom-based case definitions. Int J Infect Dis. 2022;122:647–55. https://doi.org/10.1016/j.ijid.2022.06.060

43. Jezek Z, Grab B, Paluku KM, Szczeniowski MV. Human monkeypox: disease pattern, incidence and attack rates in a rural area of northern Zaire. Trop Geogr Med. 1988;40:73–83.

44. Jezek Z, Fenner F. Human monkeypox. In: Preiser W, editor. Monographs in virology, volume 17. Basel: Karger; 1988.

45. Ogoina D, Iroezindu M, James HI, Oladokun R, Yinka-Ogunleye A, Wakama P, et al. Clinical course and outcome of human monkeypox in Nigeria. Clin Infect Dis. 2020;71:e210–4. https://doi.org/10.1093/cid/ciaa143

46. Ogoina D, Izibewule JH, Ogunleye A, Ederiane E, Anebonam U, Neni A, et al. The 2017 human monkeypox outbreak in Nigeria—report of outbreak experience and response in the Niger Delta University Teaching Hospital, Bayelsa State, Nigeria. PLoS One. 2019;14:e0214229. https://doi.org/10.1371/journal.pone.0214229

47. Learned LA, Reynolds MG, Wassa DW, Li Y, Olson VA, Karem K, et al. Extended interhuman transmission of monkeypox in a hospital community in the Republic of the Congo, 2003. Am J Trop Med Hyg. 2005;73:428–34. https://doi.org/10.4269/ajtmh.2005.73.428

48. Beer EM, Rao VB. A systematic review of the epidemiology of human monkeypox outbreaks and implications for outbreak strategy. PLoS Negl Trop Dis. 2019;13:e0007791. https://doi.org/10.1371/journal.pntd.0007791

49. Leendertz SAJ, Stern D, Theophil D, Anoh E, Mossoun A, Schubert G, et al. A cross-sectional serosurvey of anti-Orthopoxvirus antibodies in Central and Western Africa. Viruses. 2017;9:278. https://doi.org/10.3390/v9100278

50. Lederman ER, Reynolds MG, Karem K, Braden Z, Learned-Orozco LA, Wassa-Wassa D, et al. Prevalence of antibodies against orthopoxviruses among residents of Likouala region, Republic of Congo: evidence for monkeypox virus exposure. Am J Trop Med Hyg. 2007; 77:1150–6. https://doi.org/10.4269/ajtmh.2007.77.1150

Address for correspondence: Arnaud Fontanet, Emerging Diseases Epidemiology Unit, Institut Pasteur, 25 rue du Docteur Roux, Paris 75015, France; email: arnaud.fontanet@pasteur.fr

Development of Differentiating Infected from Vaccinated Animals (DIVA) Real-Time PCR for African Horse Sickness Virus Serotype 1

Yifan Wang, Jasmine Ong, Oi Wing Ng, Tapanut Songkasupa, Eileen Y. Koh,
Jeslyn P.S. Wong, Kanokwan Puangjinda, Charlene Judith Fernandez,
Taoqi Huangfu, Lee Ching Ng, Siow Foong Chang, Him Hoo Yap

African horse sickness (AHS) is a highly infectious and often fatal disease caused by 9 serotypes of the orbivirus African horse sickness virus (AHSV). In March 2020, an AHS outbreak was reported in Thailand in which AHSV serotype 1 was identified as the causative agent. Trivalent live attenuated vaccines serotype 1, 3, and 4 were used in a targeted vaccination campaign within a 50-km radius surrounding the infected cases, which promptly controlled the spread of the disease. However, AHS-like symptoms in vaccinated horses required laboratory diagnostic methods to differentiate infected horses from vaccinated horses, especially for postvaccination surveillance. We describe a real-time reverse transcription PCR–based assay for rapid characterization of the affecting field strain. The development and validation of this assay should imbue confidence in differentiating AHS-vaccinated horses from nonvaccinated horses. This method should be applied to determining the epidemiology of AHSV in future outbreaks.

African horse sickness (AHS) is a fatal vectorborne disease affecting all species of equids. The disease has major economic consequences for the equine industry. The World Organisation for Animal Health (WOAH) lists AHS as a notifiable disease, which affects the movement of horses to and from affected areas (*1*). The disease is transmitted through biting midges of the *Culicoides* genus; the 2 species *C. imicola* and *C. bolitinos* are considered the most critical vectors of AHSV (*2,3*). AHS is known to be endemic to large areas of sub-Saharan Africa and to have spread to Morocco, the Middle East, India, and Pakistan (*4,5*). More recently, outbreaks were reported in the Iberian Peninsula, Thailand, and Malaysia (*6–10*).

AHS is caused by the AHS virus (AHSV), which belongs to the genus *Orbivirus* (family Reoviridae). The AHSV genome consists of 10 double-stranded RNA segments encoding 7 structural proteins (viral protein [VP] 1–7) and ≥3 nonstructural proteins (NS1–NS3) (*11,12*). To date, 9 known serotypes of AHSV (AHSV-1–9) have been determined by virus neutralization. Some evidence exists of serologic cross-reactions among serotypes 1 and 2, 3 and 7, 5 and 8, and 6 and 9 (*13–15*).

Currently no specific treatment for AHS exists aside from rest, supportive treatment, and care. Vaccination of at-risk equids remains the most effective way to prevent and control the disease (*16*). Live attenuated vaccines (LAV), which provide broad protection against all 9 AHSV serotypes, are produced by Onderstepoort Biologic Products (OBP; https://www.obpvaccines.co.za) and are commercially available. The vaccine is supplied as 2 polyvalent vials: trivalent, containing AHSV-1, AHSV-3, and AHSV-4; and tetravalent, containing AHSV-2, AHSV-6, AHSV-7, and AHSV-8 (*14,17,18*).

In March 2020, an AHS outbreak was reported in Nakhon Ratchasima Province in Thailand; 610 horses were affected, and the case-fatality rate was ≈93% (*7,19*). Samples were submitted to the National Institute of Animal Health, Thailand, and the Centre for Animal and Veterinary Sciences (CAVS) of the National Parks Board Singapore for laboratory investigation. At CAVS, full AHSV genome sequence

was obtained by using Oxford Nanopore Sequencing, and AHSV-1 virus was identified to be the strain responsible for this outbreak (9). Subsequently, a targeted vaccination campaign using the trivalent OBP vaccine was conducted in Thailand within a 50-km radius of the infected cases.

To distinguish infected equid from vaccinated equid, having a Differentiating Infected from Vaccinated Animals (DIVA) strategy in place becomes critical for detecting disease early, limiting the movement of at-risk equids, and enabling the authorities to better deal with the biosecurity threat posed by the virus in the outbreak. Sequence analysis of the full VP2 gene was performed for DIVA, and differences in the following amino acid positions could be identified between the outbreak strain (GenBank accession no. QM158105.1) and the OBP LAV strain (GenBank accession no. AKP20114). These 10 mutation occurrences—K357N, I383V, K522R, K580R, I587T, I588V, T660I, Y803N, T889M, and T910A—were observed in the wild-type AHS circulating in Thailand. These variants arose from mutations originating from wild-type and attenuated AHSV, which resulted in pathogenicity and severity of disease as demonstrated by reported symptoms or duration of disease in individual animals. However, sequencing of the full VP2 gene is time-consuming and hampered by the small amount of AHSV RNA in samples. We report the design and validation of a sensitive and rapid real-time reverse transcription PCR (rRT-PCR) that can differentiate the AHSV-1 outbreak strain in Thailand from the strain used in the vaccination campaign. This assay is designed to strengthen AHS surveillance programs and outbreak management by enabling confident and rapid detection of infected horses and better understanding of vaccine breakthrough, if it occurs.

Materials and Methods

Horse Samples and Vaccine Samples

Tissue homogenates (which include lung, spleen, and heart) and blood samples from horses exhibiting clinical signs of AHS were submitted to the National Institute of Animal Health, Thailand. Samples were collected from western (Prachuap Khiri Khan, Phetchaburi, and Ratchaburi), northeastern (Nakhon Ratchasima), and eastern (Chon Buri) provinces in Thailand. A total of 3 tissue homogenate samples and 4 blood samples from this initial batch of samples were received at CAVS for laboratory analysis (Table 1) (9). Separately, AHSV-1 OBP vaccine samples were obtained from the European Union Reference Laboratory for African horse sickness and Bluetongue, Central Veterinary Laboratory (Animal Health) in Madrid, Spain (Table 1). Samples from the initial batch cases were subsequently included for evaluation of the AHSV-1 DIVA assay. To further validate the DIVA assays designed in this study, whole blood preserved in EDTA and tissue homogenates were collected from clinically affected horses (n = 31) and vaccinated horses (n = 12) from the various provinces in Thailand (Table 1).

Detection and Serotyping of AHSV Using rRT-PCR

We performed RNA extraction by using the MagMax Pathogen RNA/DNA kit (ThermoFisher Scientific, https://www.thermofisher.com). In brief, 100 µL of the tissue homogenate, whole blood, and vaccine samples underwent nucleic acid extraction according to manufacturer recommendations. We eluted the extracted RNA in 90 µL elution buffer and performed an rRT-PCR targeting the AHSV VP7 gene to detect the presence of AHSV (20,21). Samples for which AHSV was detected were further characterized by a serotyping rRT-PCR targeting the AHSV VP2 gene (22). We used a volume of 2.5 µL of extracted RNA in both rRT-PCRs and subsequently used those confirmed to be AHSV-1 to validate the AHSV-1 DIVA assay.

AHSV-1 DIVA rRT-PCR Development

Primer and Probe

In a previous study (9), full-length genome segments of the AHSV-1 strain in Thailand were obtained by using the Single Primer Amplification approach (23,24), followed by Oxford Nanopore sequencing (GenBank accession nos. MT711958–67). Compared with the sequence of AHSV-1 strain (1/Labstr/ZAF/1998/OBP-116) used for production of the LAV-OBP vaccine (GenBank Accession nos. KT030330.1–9.1) (25), a region near the 3' end of the VP5 gene shared lower sequence similarity (Figure 1) and was thus exploited for primer and probe design. The VP5 protein is not involved in AHSV antibody–mediated neutralization tests, as compared to the widely used but more conserved VP7 protein (12). We then designed primers and probes by Primer3web version 4.1.0 (https://primer3.ut.ee) and further optimized them manually (Table 2).

We used 2 programs to assess the newly designed primers' and probes' annealing specificity: Primer-BLAST (https://www.ncbi.nlm.nih.gov/tools/primer-blast) and BLAST Global Alignment (https://blast.ncbi.nlm.nih.gov/Blast.cgi). Primer-

BLAST determined whether the primers were specific to the AHSV-1 strain and not the other 2 strains in the trivalent vaccine dose, whereas BLAST Global Alignment aligned the AHSV vaccines and wild-type nucleotide sequences with probes by Needleman-Wunsch algorithm to ensure differentiation between vaccine and outbreak strain (Appendix, https://wwwnc.cdc.gov/EID/article/28/12/22-0594-App1.pdf).

rRT-PCR

We designed 2 rRT-PCRs using different probes to target the same region of VP5 gene (1335–1513, numbering according to KT030334) of AHSV-1. Probe

Table 1. Horse samples and vaccine samples from Thailand used in characterization of affecting strain of AHSV by DIVA rRT-PCR*

No.	Sample ID	Sample type	Source
Initial batch of samples (n = 7) reported in (9)			
1	110983/63	Tissue homogenate	Pak Chong, Nakhon-Ratchasima
2	111495/63	Whole blood	Cha-am, Phetchaburi
3	111406/63	Tissue homogenate	Ko Chan, Chonburi
4	111146/63	Whole blood	Pak Chong, Nakhon-Ratchasima
5	112080/63	Whole blood	Hua Hin, Prachuap Khiri Khan
6	111789/63	Whole blood	Damnoen Saduak, Ratchaburi
7	111367/63	Tissue homogenate	Hua Hin, Prachuap Khiri Khan
8	AHSV-1 OBP VACCINE 10^{-3}	vaccine	EURL (Spain)
9	AHSV-1 OBP VACCINE 10^{-4}	vaccine	EURL (Spain)
10	AHSV-1 OBP VACCINE 10^{-5}	vaccine	EURL (Spain)
Samples collected from clinically affected horses (n = 31) in this study			
1	111146/63	Whole blood	Nakhon-Ratchasima
2	111147/63-5	Whole blood	Nakhon-Ratchasima
3	111147/63-19	Whole blood	Nakhon-Ratchasima
4	111147/63-20	Whole blood	Nakhon-Ratchasima
5	111147/63-21	Whole blood	Nakhon-Ratchasima
6	111147/63–22	Whole blood	Nakhon-Ratchasima
7	111162/63-A	Whole blood	Nakhon-Ratchasima
8	111162/63-B	Whole blood	Nakhon-Ratchasima
9	111164/63-1	Whole blood	Nakhon-Ratchasima
10	111164/63-4	Whole blood	Nakhon-Ratchasima
11	111367/63-B	Tissue homogenate	Prachuap Khiri Khan
12	111406/63-A	Tissue homogenate	Chonburi
13	111406/63-B	Tissue homogenate	Chonburi
14	111496/63	Whole blood	Prachuap Khiri Khan
15	111790/63	Whole blood	Phetchaburi
16	112080/63	Whole blood	Prachuap Khiri Khan
17	112590/63	Whole blood	Phetchaburi
18	112594/63	Whole blood	Phetchaburi
19	112680/63	Whole blood	Phetchaburi
20	113308/63	Whole blood	Srakaew
21	113480/63	Whole blood	Prachuap Khiri Khan
22	113481/63	Whole blood	Prachuap Khiri Khan
23	113489/63	Whole blood	Srakaew
24	113561/63-1	Whole blood	Phetchaburi
25	113561/63-3	Whole blood	Phetchaburi
26	113869/63	Whole blood	Prachuap Khiri Khan
27	113870/63-11	Whole blood	Prachuap Khiri Khan
28	113870/63-5	Whole blood	Phetchaburi
29	113871/63-N	Whole blood	Phetchaburi
30	113871/63-5140	Whole blood	Phetchaburi
31	113908/63	Whole blood	Phetchaburi
Samples collected from vaccinated horses (n = 12) in this study			
1	116187/63	Whole blood	Nakhon-Ratchasima
2	122045/63	Whole blood	Pathumthani
3	135560/63	Tissue homogenate	Lopburi
4	137720/63	Tissue homogenate	Rayong
5	118696/63	Whole blood	Srakaew
6	120865/63	Whole blood	Ratchaburi
7	136979/63	Whole blood	Suphanburi
8	121673/63-A	Whole blood	Prachuap Khiri Khan
9	121673/63-B	Whole blood	Prachuap Khiri Khan
10	121673/63-C	Whole blood	Prachuap Khiri Khan
11	124916/63-A	Whole blood	Prachuap Khiri Khan
12	124916/63-B	Whole blood	Prachuap Khiri Khan

*AHSV, African horse sickness virus; DIVA, Differentiating Infected from Vaccinated Animals; ID, identification; rRT-PCR, real-time reverse transcription PCR.
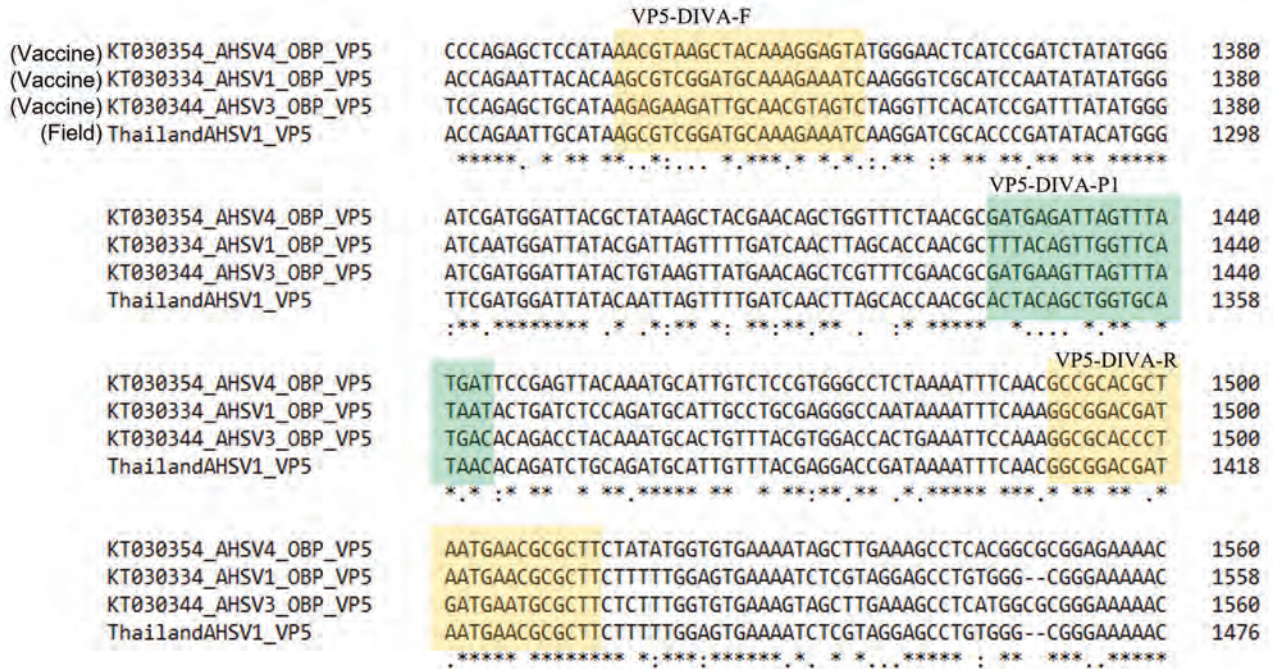
Figure 1. Nucleotide sequence alignment of the VP5 gene for the OBP AHSV vaccine strains and Thailand AHSV-1 field isolate at the 1321–1560 region (numbering according to the OBP AHSV-1 isolate, GenBank accession no. KT030334) by multiple sequence alignment tool in Clustal Omega (https://www.ebi.ac.uk/Tools/msa/clustalo). OBP strain GenBank accession nos.: AHSV-1, KT030334; AHSV-3, KT030344; AHSV-4, KT030354. Thailand AHSV-1 isolate GenBank accession no.: MT711962. Yellow indicates the primer-binding regions (VP5-DIVA-F/R) and green the probe-binding region (VP5-DIVA-P1). AHSV, African horse sickness virus; DIVA, Differentiating Infected from Vaccinated Animals; OBP, Onderstepoort Biologic Products (https://www.obpvaccines.co.za); VP, viral protein.

VP5-DIVA-P1 specifically targets the outbreak strain, whereas probe VP5-DIVA-P2-vac targets the LAV-OBP vaccine strain. We conducted the rRT-PCR in a 25-µL reaction mixture containing 12.5 µL of 2 × RT-PCR buffer (AgPath-ID One-Step RT-PCR; Thermo-Fisher Scientific), 1 µL of 25 × RT-PCR enzyme mix, 0.5 µL (0.2 µmol) each of forward (VP5-DIVA-F: 5′-AGC-GTCGGATGCAAAGAAATC-3′) and reverse (VP5-DIVA-R: 5′-AAGCGCGTTCATTATCGTCC-3′) primers (10 µmol/L), 0.5 µL (0.12 µmol) of probe (6 µmol/L) (AHSV-1 DIVA rRT-PCR1: VP5-DIVA-P1 5′-FAM-ACTACAGCTGGTGCATAAC-3′ MGB or AHSV-1 DIVA rRT-PCR2: VP5-DIVA-P2-vac 5′ FAM- TTTA-CAGTTGGTTCATAAT 3′ MGB), 7.5 µL of nuclease-free water, and 2.5 µL of extracted RNA. RNA was denatured at 95°C for 5 min and then cooled down in ice for 2 min before adding to the PCR plate. The thermal profile consisted of an initial reverse transcription step at 45°C for 10 min, denaturation at 95°C for 10 min, followed by 40 cycles of denaturation at 95°C for 15 s and annealing at 53°C for 45 s. A cycle threshold (Ct) value ≤40 indicated positive AHSV detections.

Calibration and Receiver Operating Curves
Ten-fold serial dilutions of viral DNA extracted from blood taken from a healthy horse determined the dynamic and linear ranges of the AHSV-1 DIVA assay. For the vaccine strain, we used 10-fold serial dilutions in each of the AHSV-1 DIVA assay for specificity tests and tested each dilution over 3 separate runs for all assays. We generated the standard calibration curves by plotting Ct values against the logarithm of starting DNA quantities and derived slope readings from the best-fit trendline.

Table 2. Sequence and position of the AHSV-1 DIVA primer and probes used in study of development of PCR to characterize affecting strain of AHSV, Thailand*

Primer/probe	Sequence, 5′ → 3′	Sense	Position
VP5-DIVA-F	5′ AGCGTCGGATGCAAAGAAATC 3′	+	1335–1355
VP5-DIVA-P1	5′ FAM- ACTACAGCTGGTGCATAAC 3′ MGB	+	1426–1444
VP5-DIVA-P2-vac	5′ FAM- TTTACAGTTGGTTCATAAT 3′ MGB	+	1426–1444
VP5-DIVA-R	5′ AAGCGCGTTCATTATCGTCC 3′	−	1494–1513

*Position numbering is with reference to AHSV-1 (GenBank accession no. KT030334). AHSV, African horse sickness virus; DIVA, Differentiating Infected from Vaccinated Animals.

We used the receiver operating curve (ROC) analysis as an estimation and visual evaluation of the sensitivity and specificity performances of quantitative PCR assays. The area under the ROC curve (AUC) can also be regarded as a cumulative quality indicator for a diagnostic assay (26). Here, we used the pROC package (27) in R software (The R Project for Statistical Computing, https://www.r-project.org) to plot the ROC curves and compute the AUC values.

Results

At the time of the outbreak in 2020, the causative strain was identified as AHSV-1 by both rRT-PCR targeting the VP7 and VP2 genes (9) and high-throughput sequencing (7,9), and contingency measures were implemented. The 2 rRT-PCRs we designed aimed to differentiate between clinically affected and vaccinated horses for outbreak identification and management. In silico analysis showed that the DIVA probes were specific to the AHSV-1 outbreak strain and vaccine strain and not to AHSV-3 or AHSV-4 in the trivalent vaccine (Appendix Figure 3). The VP5-DIVA-P1 probe designed for detecting the outbreak AHSV-1 strain was unable to align fully to the vaccine KT030334_AHSV1_OBP strain, whereas the same probe showed a high degree of specific alignment

to the Thailand AHSV-1 sequence (Appendix Figure 1). Conversely, the VP5-DIVA-P2 probe was aligned specifically to the AHSV-1 vaccine strain but not to the outbreak AHSV-1 strain (Appendix Figure 2). In addition, the DIVA primers and probes were aligned to selected AHSV-1 sequences retrieved from GenBank, whereas the DIVA-1 probe was specific to the Thailand outbreak strain for which it was designed in this study and the DIVA-2 probe was also distinctly specific for the VP5 gene identified from vaccinated horses reported elsewhere (18,28,29) (Figure 2).

Using the initial batch samples that were submitted for testing (9), we performed 2 separate AHSV-1 DIVA rRT-PCRs to demonstrate the specificities of the primers and probes in vitro. AHSV-1 RNA was detected in 7 horse samples when using the primers with VP5-DIVA-P1 probe but not with the primers with VP5-DIVA-P2-vac probe (Table 3). On the contrary, AHSV-1 RNA was detected in AHSV-1 OBP vaccine samples only when VP5-DIVA-P2-vac probe was used (Table 3). These data have demonstrated an accuracy (100%) for both AHSV DIVA rRT-PCR methods among the small number of samples.

To substantiate the observations that the designed primer pairs are indeed specific and sensitive enough to differentiate between the vaccine and wild

Figure 2. Nucleotide sequence alignment of the VP5 gene for the OBP vaccine AHSV-1 strain (GenBank accession no. KT030334), Thailand AHSV-1 field isolate (accession no. MT711962), and AHSV-1 field isolate sequences from earlier studies (accession nos. EU303175, KX987212, AM883169 and KT187161) at the 1321–1559 region (numbering according to the OBP AHSV-1 isolate), by multiple sequence alignment tool in Clustal Omega (https://www.ebi.ac.uk/Tools/msa/clustalo). Yellow indicates the the forward and reverse primer binding regions and green the probe-binding region (VP5-DIVA-P1 or P2). AHSV, African horse sickness virus; DIVA, Differentiating Infected from Vaccinated Animals; OBP, Onderstepoort Biologic Products (https://www.obpvaccines.co.za); VP, viral protein.

Table 3. Evaluation of AHSV-1 DIVA rRT-PCR using horse and vaccine samples from Thailand*

		Ct value by target gene (reference)			
				VP5 (this study)	
No.	Sample ID	VP7 AHSV rRT-PCR (20)	VP2 AHSV-1 serotyping rRT-PCR (22)	AHSV-1 DIVA rRT-PCR-1	AHSV-1 DIVA rRT-PCR 2
Testing of probes with initial batch samples reported in (9)					
1	110983/63	17.98	17.02	17.57	Undetermined
2	111495/63	22.61	20.72	22.06	Undetermined
3	111406/63	20.88	19.19	20.04	Undetermined
4	111146/63	27.49	22.70	24.69	Undetermined
5	112080/63	17.96	16.37	16.72	Undetermined
6	111789/63	19.86	18.31	18.24	Undetermined
7	111367/63	20.67	18.78	20.29	Undetermined
8	AHSV-1 OBP VACCINE 10^{-3}	24.52	24.17	Undetermined	27.65
9	AHSV-1 OBP VACCINE 10^{-4}	27.56	27.90	Undetermined	30.54
10	AHSV-1 OBP VACCINE 10^{-5}	31.81	32.15	Undetermined	34.78
11	AHSV-1 RSArah1/03	15.21	15.38	Undetermined	17.97
Validation testing of probes with samples from clinically affected horses in this study†					
1	111146/63	18.04	17.40	18.25	Undetermined
2	111147/63-5	17.12	16.89	17.32	Undetermined
3	111147/63-19	21.30	20.12	20.14	Undetermined
4	111147/63-20	26.56	27.30	28.57	Undetermined
5	111147/63-21	23.05	22.98	23.81	Undetermined
6	111147/63-22	30.15	29.80	31.47	Undetermined
7	111162/63-A	21.67	22.75	23.16	Undetermined
8	111162/63-B	22.40	22.06	22.23	Undetermined
9	111164/63-1	28.60	28.39	28.45	Undetermined
10	111164/63-4	26.85	27.36	27.72	Undetermined
11	111367/63-B	16.44	17.69	17.51	Undetermined
12	111406/63-A	24.12	23.97	23.82	Undetermined
13	111406/63-B	18.34	18.09	18.26	Undetermined
14	111496/63	20.84	22.19	22.36	Undetermined
15	111790/63	23.62	23.83	23.88	Undetermined
16	112080/63	21.04	21.12	21.23	Undetermined
17	112590/63	26.71	29.12	29.04	Undetermined
18	112594/63	25.59	22.34	22.28	Undetermined
19	112680/63	23.62	22.84	22.50	Undetermined
20	113308/63	25.20	18.98	19.15	Undetermined
21	113480/63	25.52	26.15	25.97	Undetermined
22	113481/63	27.01	20.59	20.45	Undetermined
23	113489/63	24.58	26.19	25.94	Undetermined
24	113561/63-1	20.79	19.12	18.93	Undetermined
25	113561/63-3	33.45	19.66	19.34	Undetermined
26	113869/63	27.49	22.18	21.99	Undetermined
27	113870/63-11	19.68	35.29	34.38	Undetermined
28	113870/63-5	27.43	28.98	28.70	Undetermined
29	113871/63-N	27.32	31.34	32.02	Undetermined
30	113871/63-5140	28.32	21.76	21.31	Undetermined
31	113908/63	26.16	23.53	23.45	Undetermined
Validation testing of probes with samples from vaccinated horses in this study					
1	116187/63	27.48	34.19	Undetermined	35.62
2	122045/63	31.60	33.12	Undetermined	35.37
3	135560/63	38.59	36.71	Undetermined	38.79
4	137720/63	34.29	33.36	Undetermined	35.32
5	118696/63	32.31	32.79	Undetermined	34.37
6	120865/63	32.23	34.03	Undetermined	35.16
7	136979/63	32.33	31.40	Undetermined	32.92
8	121673/63-A	33.24	31.16	Undetermined	33.22
9	121673/63-B	33.89	32.81	Undetermined	34.72
10	121673/63-C	34.37	32.39	Undetermined	33.85
11	124916/63-A	36.45	35.11	Undetermined	36.53
12	124916/63-B	36.45	33.69	Undetermined	35.51

*Samples that were initially submitted for testing (9) were used in the first round of designed assay optimization. Subsequently, EDTA blood and tissues samples were taken from clinically affected and vaccinated horses for assay validation. Ct values were used for classification of positive AHSV detections. AHSV, African horse sickness virus; Ct, cycle threshold; DIVA, Differentiating Infected from Vaccinated Animals; ID, identification; rRT-PCR, real-time reverse transcription PCR; VP, viral protein.
†AHSV-1 serotyping rRT-PCR was not carried out for the clinically affected and vaccinated horse samples used in the confirmatory rRT-PCR reactions to test the DIVA assays. Cycle threshold values not registered after 40 cycles were reported as undetermined.

Table 4. Comparison of assay sensitivity among different AHSV assays*

Sample	Method	Limit of detection	AUC	Slope
AHSV-1 Thailand 110983/63	AHSV VP7 rRT-PCR	[10^{-5}]	0.943	−3.89
	AHSV-1 VP2 Serotyping rRT-PCR	[10^{-4}]		
	AHSV-1 VP5 DIVA rRT-PCR 1	[10^{-4}]		
AHSV-1 OBP LAV	AHSV VP7 rRT-PCR	[10^{-6}]	0.900	−3.49
	AHSV-1 VP2 Serotyping rRT-PCR	[10^{-5}]		
	AHSV-1 VP5 DIVA rRT-PCR 2	[10^{-5}]		

*The limit of detection was reported from the lowest observed amount of DNA amplified below the Ct ≤40 threshold. The AUC and slope values derived from the calibration curve are also listed. AHSV, African horse sickness virus; AUC, area under the receiver operating curve; Ct, cycle threshold; DIVA, Differentiating Infected from Vaccinated Animals; OBP LAV, Onderstepoort Biologic Products (https://www.obpvaccines.co.za) live attenuated vaccine; rRT-PCR, real-time reverse transcription PCR; VP, viral protein.

strain of AHSV-1, we collected more blood and tissue samples from both the prevaccinated and postvaccinated animals from horses in the Thailand outbreak area. Using these samples, we again observed that AHSV-infected (i.e., clinically affected) and vaccinated horses could be differentiated by using the VP5-DIVA-P1 and VP5-DIVA-P2-vac assays designed in this study with an accuracy of 100% (Table 3). The Ct values obtained from 3 RT-PCR runs using the VP5-DIVA-P1 on clinically affected horses' samples were 17.32–34.38, whereas those obtained using the VP5-DIVA-P2-vac on the vaccinated horses' samples were 33.22–38.79. No cross-amplification of the samples with the alternate probe (i.e., clinically affected samples amplified with the VP5-DIVA-P2-vac probe and vice versa) resulted from the quantitative PCR run. These data suggest this VP5 gene–based DIVA assay can readily and accurately differentiate the vaccine strain from the outbreak strain with reproducibility. The samples were also confirmed by VP7- and VP2-targeted rRT-PCR for AHSV (Table 3). Two infected horses, 112080/63 and 110983/63, with high viral load (Ct values 17.96 and 17.98 by VP7 rRT-PCR) tested negative using DIVA rRT-PCR 2 (Table 3).

We also examined cross-reactivity between 2 DIVA PCRs. Because high-dose LAV was unavailable in our laboratory, we used a cell culture isolate AHSV-1 South Africa RSArah1/03 (supplied by the Pirbright Institute), which is highly similar to the OBP LAV vaccine strain (99.73% of genome similarity). The isolate produced signal only with DIVA rRT-PCR 2 (Ct 17.97) and not DIVA rRT-PCR 1 (Table 3).

We further tested the analytical sensitivity of the DIVA assay by testing 10-fold serial dilutions of 1 AHSV-1 outbreak sample (AUC = 0.943, slope = −3.89) (Table 4) as well as the vaccine sample (AUC = 0.900; slope = −3.49) (Table 4). The analytical sensitivity of the DIVA assays was comparable to the serotyping assay and 10-fold less than the AHSV VP7 rRT-PCR (Table 4). However, compared with the VP2 sequencing–based DIVA methodology, the DIVA rRT-PCR increases analytical sensitivity, reduces cost, and shortens turnaround time. The

detection rate of subclinical infections could also be substantially increased in the period leading up to a potential outbreak.

Discussion

Genetic recombination is a mechanism and strategy observed in most viruses for adaptation and survival. The introduction of polyvalent LAV could serve as a pool of readily available genetic segments for comultiplication and reassortment within the host (*18,28,29*). Immunized horses can still be infected by AHS, especially by the AHSV-1-LAV within the trivariant AHSV-LAV formulation (*30*). Manole et al. (*31*) also demonstrated by high-resolution imaging that the physical structure of certain serotypes of AHSV could undergo distortion in the event of host–virus interaction. However, the exact reversion-to-virulence mutants and reassortants in the presence of AHSV field strains are not well understood. Despite the considerations of using monovalent AHSV vaccines to confer immunity to horses (*32,33*), the protection coverage is not as good as the 2-dose polyvalent OBP LAV used in this outbreak (*34*).

After the Thailand outbreak in which AHSV-1 was the causative agent, efforts at disease outbreak management and animal protection were focused on this serotype. The AHSV-1 DIVA assay described in this study only applies to the OBP LAV currently used in the vaccination campaign in Thailand. The method should be modified if a different AHSV strain or a different vaccine is used. Recombinant vaccine with VP5 gene from AHSV strains other than the strain used by OBP might render this assay ineffective. Alternative candidate DIVA regions or vaccine candidates can also be examined and evaluated using the approach described here. Other molecular strategies deploying the DIVA strategy can be explored, such as high-resolution melting analysis to identify the variations between the vaccine and wild-type strains.

Early detection and differentiation of the AHSV causative agent is vital for identifying and managing at-risk horses. Complementing the earlier study by Toh et al. (*9*), our rapid development of a DIVA

assay relevant to the outbreak at hand was useful for surveillance and control of the outbreak to prevent wider onwards transmission of the disease. This DIVA strategy will be useful for a regional vaccination strategy in southeast Asia, where the wide distribution of the *Culicoides* spp. vector poses a biorisk of AHSV incursion. The DIVA assay also enables identification of vaccine breakthroughs. The next step is to validate the DIVA assay with field samples from horses worldwide, particularly for horses vaccinated using the OBP LAV. DIVA strategy could support the surveillance of AHSV at the genomic level to identify recombinants, reassortants, or mutants among vaccinated equids. This method to rapidly characterize the affecting field strain and develop a differentiating method should be applied in future outbreaks to determine the epidemiology of AHSV.

About the Author

Dr. Wang was a senior scientist at the Centre for Animal & Veterinary Sciences within the Animal & Veterinary Service of the National Parks Board, Singapore, from July 2010 until January 2022. Dr. Wang's research interests are focused on molecular biology of animal viruses and animal disease biosurveillance.

References

1. World Organisation for Animal Health. Infection with African horse sickness virus. In: Terrestrial animal health code. 2021 [cited 2021 Sep 30]. https://www.woah.org/en/what-we-do/standards/codes-and-manuals/terrestrial-code-online-access/?id=169&L=1&htmfile=chapitre_ahs.htm
2. Meiswinkel R, Paweska JT. Evidence for a new field *Culicoides* vector of African horse sickness in South Africa. Prev Vet Med. 2003;60:243–53. https://doi.org/10.1016/S0167-5877(02)00231-3
3. Mellor PS, Boorman J. The transmission and geographical spread of African horse sickness and bluetongue viruses. Ann Trop Med Parasitol. 1995;89:1–15. https://doi.org/10.1080/00034983.1995.11812923
4. Gohre DS, Khot JB, Paranjpe VL, Manjrekar SL. Observations on the outbreak of South African horse sickness in India during 1960–1961. Bombay Vet Coll Meg. 1965:5–15.
5. Hazrati A. Identification and typing of horse-sickness virus strains isolated in the recent epizootic of the disease in Morocco, Tunisia, and Algeria. Arch Razi Inst. 1967; 19:131–43.
6. Castillo-Olivares J. African horse sickness in Thailand: challenges of controlling an outbreak by vaccination. Equine Vet J. 2021;53:9–14. https://doi.org/10.1111/evj.13353
7. King S, Rajko-Nenow P, Ashby M, Frost L, Carpenter S, Batten C. Outbreak of African horse sickness in Thailand, 2020. Transbound Emerg Dis. 2020;67:1764–7. https://doi.org/10.1111/tbed.13701
8. Rodriguez M, Hooghuis H, Castaño M. African horse sickness in Spain. Vet Microbiol. 1992;33:129–42. https://doi.org/10.1016/0378-1135(92)90041-Q
9. Toh X, Wang Y, Rajapakse MP, Lee B, Songkasupa T, Suwankitwat N, et al. Use of nanopore sequencing to characterize African horse sickness virus (AHSV) from the African horse sickness outbreak in Thailand in 2020. Transbound Emerg Dis. 2021.
10. World Organisation for Animal Health. WOAH member's official African horse sickness status map (September 2020). 2020 [cited 2021 Sep 30]. https://www.woah.org/en/disease/african-horse-sickness
11. Roy P, Mertens PP, Casal I. African horse sickness virus structure. Comp Immunol Microbiol Infect Dis. 1994;17:243–73. https://doi.org/10.1016/0147-9571(94)90046-9
12. Zientara S, Weyer CT, Lecollinet S. African horse sickness. Rev Sci Tech. 2015;34:315–27. https://doi.org/10.20506/rst.34.2.2359
13. Erasmus BA. New approach to polyvalent immunization against African horsesickness. In: Proceedings of the 4th International Conference on Equine Infectious Diseases (1976: Lyons, France) Princeton, NJ: Veterinary Publications; 1978.
14. Mellor PS, Hamblin C. African horse sickness. Vet Res. 2004;35:445–66. https://doi.org/10.1051/vetres:2004021
15. World Organisation for Animal Health, African horse sickness (infection with African horse sickness virus). In: OIE Terrestrial Manual. 2019 [cited 2021 Sep 30]. https://www.woah.org/fileadmin/Home/eng/Health_standards/tahm/3.06.01_AHS.pdf
16. Dennis SJ, Meyers AE, Hitzeroth II, Rybicki EP. African horse sickness: a review of current understanding and vaccine development. Viruses. 2019;11:11. https://doi.org/10.3390/v11090844
17. Crafford JE, Lourens CW, Smit TK, Gardner IA, MacLachlan NJ, Guthrie AJ. Serological response of foals to polyvalent and monovalent live-attenuated African horse sickness virus vaccines. Vaccine. 2014;32:3611–6. https://doi.org/10.1016/j.vaccine.2014.04.087
18. Weyer CT, Grewar JD, Burger P, Rossouw E, Lourens C, Joone C, et al. African horse sickness caused by genome reassortment and reversion to virulence of live, attenuated vaccine viruses, South Africa, 2004–2014. Emerg Infect Dis. 2016;22:2087–96. https://doi.org/10.3201/eid2212.160718
19. Bunpapong N, Charoenkul K, Nasamran C, Chamsai E, Udom K, Boonyapisitsopa S, et al. African horse sickness virus serotype 1 on horse farm, Thailand, 2020. Emerg

Infect Dis. 2021;27:2208–11. https://doi.org/10.3201/eid2708.210004

20. Guthrie AJ, Maclachlan NJ, Joone C, Lourens CW, Weyer CT, Quan M, et al. Diagnostic accuracy of a duplex real-time reverse transcription quantitative PCR assay for detection of African horse sickness virus. J Virol Methods. 2013;189:30–5. https://doi.org/10.1016/j.jviromet. 2012.12.014

21. Quan M, Lourens CW, MacLachlan NJ, Gardner IA, Guthrie AJ. Development and optimisation of a duplex real-time reverse transcription quantitative PCR assay targeting the VP7 and NS2 genes of African horse sickness virus. J Virol Methods. 2010;167:45–52. https://doi.org/10.1016/j.jviromet.2010.03.009

22. Weyer CT, Joone C, Lourens CW, Monyai MS, Koekemoer O, Grewar JD, et al. Development of three triplex real-time reverse transcription PCR assays for the qualitative molecular typing of the nine serotypes of African horse sickness virus. J Virol Methods. 2015;223:69–74. https://doi.org/10.1016/j.jviromet.2015.07.015

23. Greninger AL, Chen EC, Sittler T, Scheinerman A, Roubinian N, Yu G, et al. A metagenomic analysis of pandemic influenza A (2009 H1N1) infection in patients from North America. PLoS One. 2010;5:e13381. https://doi.org/10.1371/journal.pone.0013381

24. Greninger AL, Naccache SN, Federman S, Yu G, Mbala P, Bres V, et al. Rapid metagenomic identification of viral pathogens in clinical samples by real-time nanopore sequencing analysis. Genome Med. 2015;7:99. https://doi.org/10.1186/s13073-015-0220-9

25. Guthrie AJ, Coetzee P, Martin DP, Lourens CW, Venter EH, Weyer CT, et al. Complete genome sequences of the three African horse sickness virus strains from a commercial trivalent live attenuated vaccine. Genome Announc. 2015;3:3. https://doi.org/10.1128/genomeA.00814-15

26. Nutz S, Döll K, Karlovsky P. Determination of the LOQ in real-time PCR by receiver operating characteristic curve analysis: application to qPCR assays for *Fusarium verticillioides* and *F. proliferatum.* Anal Bioanal Chem. 2011;401:717–26. https://doi.org/10.1007/s00216-011-5089-x

27. Robin X, Turck N, Hainard A, Tiberti N, Lisacek F, Sanchez J-C, et al. pROC: an open-source package for R and S+ to analyze and compare ROC curves. BMC Bioinformatics. 2011;12:77. https://doi.org/10.1186/1471-2105-12-77

28. Potgieter AC, Page NA, Liebenberg J, Wright IM, Landt O, van Dijk AA. Improved strategies for sequence-independent amplification and sequencing of viral double-stranded RNA genomes. J Gen Virol. 2009;90:1423–32. https://doi.org/10.1099/vir.0.009381-0

29. von Teichman BF, Smit TK. Evaluation of the pathogenicity of African horsesickness (AHS) isolates in vaccinated animals. Vaccine. 2008;26:5014–21. https://doi.org/10.1016/j.vaccine.2008.07.037

30. Molini U, Marucchella G, Maseke A, Ronchi GF, Di Ventura M, Salini R, et al. Immunization of horses with a polyvalent live-attenuated African horse sickness vaccine: serological response and disease occurrence under field conditions. Trials Vaccinol. 2015;4:24–8. https://doi.org/10.1016/j.trivac.2015.03.001

31. Manole V, Laurinmäki P, Van Wyngaardt W, Potgieter CA, Wright IM, Venter GJ, et al. Structural insight into African horsesickness virus infection. J Virol. 2012;86:7858–66. https://doi.org/10.1128/JVI.00517-12

32. House JA. Recommendations for African horse sickness vaccines for use in nonendemic areas. Rev Élev Méd Vét Pays Trop. 1993;46:77–81. https://doi.org/10.19182/remvt.9402

33. Aksular M, Calvo-Pinilla E, Marín-López A, Ortego J, Chambers AC, King LA, et al. A single dose of African horse sickness virus (AHSV) VP2 based vaccines provides complete clinical protection in a mouse model. Vaccine. 2018;36:7003–10. https://doi.org/10.1016/j.vaccine.2018.09.065

34. von Teichman BF, Dungu B, Smit TK. In vivo cross-protection to African horse sickness serotypes 5 and 9 after vaccination with serotypes 8 and 6. Vaccine. 2010;28:6505–17. https://doi.org/10.1016/j.vaccine.2010.06.105

Address for correspondence: Eileen Y. Koh, Animal and Veterinary Science, National Parks Board (NParks), 1 Cluny Rd, Singapore Botanic Gardens, 259569, Singapore; email: eileen_koh@nparks.gov.sg

Daily Rapid Antigen Exit Testing to Tailor University COVID-19 Isolation Policy

Rebecca Earnest, Christine Chen, Chrispin Chaguza, Anne M. Hahn, Nathan D. Grubaugh,[1]
Madeline S. Wilson,[1] for the Yale COVID-19 Resulting and Isolation Team[2]

We evaluated daily rapid antigen test (RAT) data from 323 COVID-19–positive university students in Connecticut, USA, during an Omicron-dominant period. Day 5 positivity was 47% for twice-weekly screeners and 26%–28% for less-frequent screeners, approximately halving each subsequent day. Testing negative $\geq$10 days before diagnosis (event time ratio (ETR) 0.85 [95% CI 0.75–0.96]) and prior infection >90 days (ETR 0.50 [95% CI 0.33–0.76]) were significantly associated with shorter RAT positivity duration. Symptoms before or at diagnosis (ETR 1.13 [95% CI 1.02–1.25]) and receipt of 3 vaccine doses (ETR 1.20 [95% CI 1.04–1.39]) were significantly associated with prolonged positivity. Exit RATs enabled 53%–74% of students to leave isolation early when they began isolation at the time of the first positive test, but 15%–22% remained positive beyond the recommended isolation period. Factors associated with RAT positivity duration should be further explored to determine relationships with infection duration.

In December 2021, the Centers for Disease Control and Prevention (CDC) reduced the recommended COVID-19 isolation period for the general population from 10 days to 5 days after symptom onset or a positive viral test (*1*). To end isolation, persons must have resolving symptoms and wear a mask for an additional 5 days; however, a negative exit test was not required. The rationale for the shortened isolation was based on practical and scientific considerations; namely, weighing the societal and economic burdens against the diminishing risk for transmission as a positive person proceeds through the infection. The CDC revised its guidelines as the SARS-CoV-2

Omicron variant rapidly grew to dominance in the United States, increasing from 1% to >50% of reported sequences over a 2-week period in December 2021 (*2*). Early analysis suggested different viral dynamics for Omicron versus Delta: lower peak viral RNA and shorter clearance periods for Omicron, but similar proliferation times and clearance rates (J.A. Hay et al., unpub. data, https://doi.org/10.1101/2022.01.13.22269257). Because the recommendations were based on estimates for earlier SARS-CoV-2 variants, more data were needed to understand their appropriateness for Omicron.

The updated guidance acknowledged the possibility of onward transmission after a 5-day isolation, citing an earlier UK modeling study estimating that 31% of persons remain infectious after day 5 (D. Bays et al., unpub. data, https://doi.org/10.1101/2021.12.23.21268326). Recent literature on exit testing from an Omicron-dominant period further indicates that high proportions of persons remain potentially infectious beyond day 5 (*3*; E. Landon et al., unpub. data,—https://doi.org/10.1101/2022.02.01.22269931; S.B. Nelson et al., unpub. data, https://doi.org/10.1101/2022.02.11.22270843). Studies of managed isolation programs through schools or employers found positivity of 31%–58% by rapid antigen test (RAT) on days 5–9, although daily testing among all persons was not conducted. Near-daily PCR testing found a day 5 positivity range of 39%–52% (J.A. Hay et al., unpub. data).

Although PCR tests are a preferred initial diagnostic option because of their high sensitivity, RATs are more suitable for exit testing when the goal is to determine when a person is likely no longer infectious. High PCR sensitivity may result in positive

[1]These authors contributed equally to this article.
[2]Members of the team are listed at the end of this article.

tests beyond the infectious period, leading to unnecessarily long isolations (*4,5*). RAT positivity is generally associated with culturable virus, which itself is often a proxy for infectiousness (*5–7*). In addition, to investigate concerns that RATs may have inferior performance for Omicron versus Delta infections, a study compared same-day positivity between the variants, finding similar sensitivity of RAT and PCR tests (*8*). Last, RATs have the advantage of relative affordability, fast turnaround time, and at-home self-administration compared with PCR tests, making them the only viable exit test option for much of the population (*9,10*).

In this study, we aimed to address the evidence gaps regarding changes in daily RAT positivity, factors influencing RAT positivity duration, and how exit RATs toward the end of isolation can be used to tailor isolation periods on the basis of risk. We evaluated daily RAT data from 323 persons who initially tested positive for SARS-CoV-2 during January 1–February 11, 2022, and were in a university-managed isolation program in Connecticut, USA. We designed our study to answer 2 questions: the percentage of SARS-CoV-2-positive persons that remained positive via RAT on day 5 of isolation and each subsequent day until testing negative; and the factors associated with RAT positivity duration. The Institutional Review Board (IRB) from Yale University Human Research Protection Program determined that the use of information, including information about biospecimens, is recorded by the investigator in such a manner that the identity of the human subjects cannot readily be ascertained directly or through identifiers linked to the subject and thus is exempt from IRB review of human subjects research (IRB protocol 2000032111).

Methods

The university required undergraduate students to screen at arrival on campus and then twice weekly on designated days. SARS-CoV-2–positive students isolated and participated in mandatory daily rapid antigen self-testing beginning on day 5 after diagnosis until they tested negative. We defined diagnosis (day 0) as the earliest positive or inconclusive test date. All inconclusive persons subsequently tested positive. Excluding 27 persons whose results were by external PCR or home RATs, all received diagnoses by Clinical Research Sequencing Platform SARS-CoV-2 real-time reverse transcription PCR diagnostic assay (*11*). Trained staff observed the exit testing process and confirmed the result. Upon testing negative, students ended isolation but continued mandatory masking until day 10. All rapid antigen testing was conducted using the Quidel QuickVue At-home COVID-19 test (https://www.quidel.com), a lateral flow immunoassay that qualitatively detects the SARS-CoV-2 nucleocapsid protein antigen (*12*). The test received a US Food and Drug Administration–granted emergency use authorization for prescribed home use with patient-collected anterior nares swab specimens; it has a sensitivity of 84.8% (95% CI 71.8–92.4) and specificity of 99.1% (95% CI 95.2–99.8).

We used R version 4.0.5 and RStudio version 1.4.1106 for our analyses (*13*). We calculated the percent still positive as the number of positive persons each day divided by the total number of positive persons. To assess prognostic factors associated with the time to event (i.e., testing negative), we coded an accelerated failure time (AFT) lognormal regression model using the R package survival version 3.2–13 (*14,15*). We selected the AFT model for its suitability for interval-censored data (*16*). Because students entered the study on day 0 but were not rapid tested until day 5, any persons testing negative on day 5 were interval censored; their true negative time was between day 1 and day 5. We compared model fits using various distributions and selected the fit resulting in the lowest Akaike information criterion value. We exponentiated the regression coefficients to calculate the event time ratio (ETR), which is associated with prolonged RAT positivity duration when >1 and decreased duration when <1. An ETR of 1 signifies that RAT positivity duration does not differ by covariate level. We checked the assumption that the ratio of survival times (i.e., the ETR) is constant for all fixed probabilities of S(t), the survival function, using the R package AFTtools version 0.2.1 to inspect QQ plots generated for each covariate level comparison (*17*).

Results

Our study population comprised primarily students 18–22 years of age living in university dormitory housing (N = 323) (Table 1). Among them, 63% self-reported symptoms before or at diagnosis. Symptomatic persons reported symptom onset a median of 0 days (IQR 0–1.25 days) before their initial test in the last negative test ≤4 days and last negative test 5–9 days groups and 1 day (IQR 0–4 days) before in the last negative test ≥10 days group. We did not track symptoms beyond diagnosis, although 18/205 symptomatic persons had a symptom onset date 1 day after diagnosis, potentially reflecting when they received their results and discussed symptoms. We found that 7% had a confirmed SARS-CoV-2 infection >90 days before their recent diagnosis: 62% of those with prior infections received 3 vaccine doses, 33% received 2

Table 1. Characteristics of population completing isolation in study of students in a university-managed isolation program, January 1–February 11, 2022*

Characteristic	No. (%) persons by days since last negative test				Total no. (%), N = 323
	≤4 d, n = 181	5–9 d, n = 48	≥10 d, n = 93	Unknown, n = 1	
Self-reported symptoms before or at diagnosis					
No	51 (28)	17 (35)	46 (49)	1 (100)	115 (36)
Yes	130 (72)	29 (60)	46 (49)	0 (0)	205 (63)
Unknown	0 (0)	2 (4)	1 (1)	0 (0)	3 (1)
Prior infection >90 d					
No	171 (94)	46 (96)	84 (90)	1 (100)	302 (93)
Yes	10 (6)	2 (4)	9 (10)	0 (0)	21 (7)
No. vaccine doses					
1	3 (2)	0 (0)	6 (6)	0 (0)	9 (3)
2	38 (21)	16 (33)	31 (33)	1 (100)	86 (27)
3	136 (75)	30 (62)	54 (58)	0 (0)	220 (68)
4	1 (1)	1 (2)	0 (0)	0 (0)	2 (1)
Unknown	3 (2)	1 (2)	2 (2)	0 (0)	6 (2)
*Category totals may not add to 100% because of rounding.					

doses, and 5% received an unknown number of doses. The university did not screen asymptomatic persons with an infection ≤90 days before because of the likelihood of false positives.

We categorized vaccinations into 1–4 doses. In general, a non-mRNA vaccine primary series counted as 1 dose, an mRNA vaccine primary series as 2 doses, and a booster as an additional dose. Two students reported receiving 2 boosters, giving each a total of 4 doses. Only doses administered ≥14 days before diagnosis were counted toward the total (*18*). The breakdown of doses was as follows: 3% of persons had 1 dose, 27% had 2 doses, 68% had 3 doses, and 1% had 4 doses; 2% had missing data (Appendix Table, https://wwwnc.cdc.gov/EID/article/28/12/22-0969-App1.pdf). RAT positivity duration, and thus isolation time if requiring a negative exit RAT to leave isolation, is dependent on where a person is in their infection course when COVID is diagnosed. To address this consideration, we used the time since the last negative test as an approximation of the time since infection; 56% of persons tested negative ≤4 days before diagnosis, 15% 5–9 days before, and 29% ≥10 days before. One person had missing data. The ≤4 days group represents students compliant with university twice-weekly screening policy, the 5–9 day group a mix of noncompliant routine screeners and arrival screeners, and the ≥10 day group arrival screeners.

To calculate the percent still positive on day 5 and beyond, we dropped 1 person with an unknown last negative test time and 7 persons who initially tested inconclusive but used the subsequent positive test date as the isolation start; the final dataset comprised 315 persons. Among twice-weekly screeners, 47% of all diagnosed (n = 177) remained positive on day 5, 22% on day 6, 8% on day 7, and 1%–2% on days 8–13

(Figure, panel A). Among students last testing negative 5–9 days before diagnosis, 28% of all diagnosed (n = 47) remained positive on day 5, 17% on day 6, 6% on day 7, and 2%–4% on days 8–9 (Figure, panel B). Students last testing negative ≥10 days before diagnosis (n = 91) had similar daily positivity rates to the 5–9 day group's (Figure, panel C).

To evaluate possible prognostic variables for RAT positivity duration, we conducted a survival analysis using an AFT lognormal regression model. We subset the final dataset to exclude those with 1 (n = 8), 4 (n = 2), or an unknown number (n = 6) of vaccine doses because of small category sizes, a missing PCR cycle threshold (Ct) value at diagnosis because of an external PCR test or home RAT (n = 27), a missing symptom status (n = 2), and receipt of an international vaccine (n = 8), resulting in a final sample of 263 persons. We included time since the last negative test category as a covariate to account for possible confounding, because persons in different infection stages would necessarily experience different RAT positivity durations. We also included symptom status, PCR Ct value, and prior infection >90 days before symptom onset as covariates. We created a new variable combining the number of vaccine doses (2 or 3) and the time since the last dose (<5 months or ≥5 months) (*19*). All students who had received 3 vaccine doses received their last dose <5 months except for 1 student. Finally, we included the primary series vaccine brand grouped into mRNA vaccines (Pfizer-BioNTech, https://www.pfizer.com, and Moderna, https://www.modernatx.com) and J&J/Janssen (https://www.jandj.com). We determined regression results (Table 2) and RAT positivity duration distribution for each covariate category (Appendix Figure 1) excluding time since last negative test (Figure 1). We found that having a last test ≥10 days
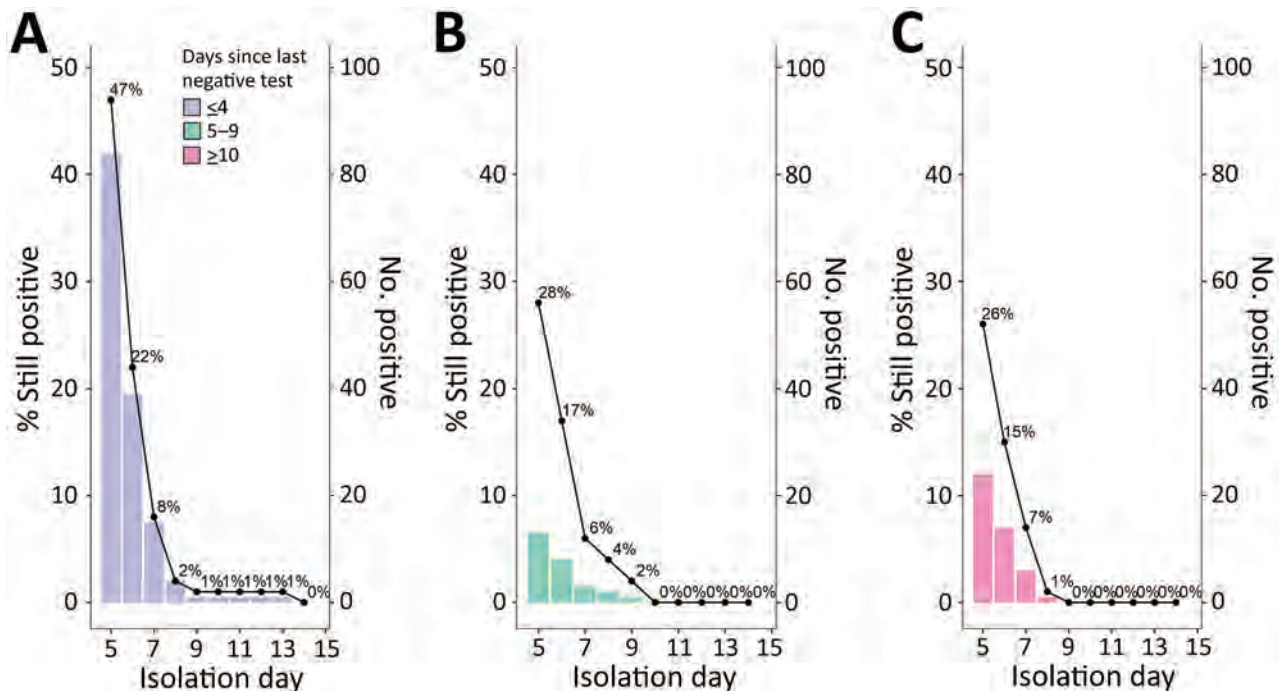
Figure. Rapid antigen testing results by isolation day and positivity duration by days since the last negative test category in study of students isolated for positive SARS-CoV-2 results. Left axis shows percent still positive of the original study population; right axis shows the number tested positive on each isolation day. A) Last negative test ≤4 days earlier (N = 177). B) Last negative test 5–9 days earlier (N = 47). C) Last negative test ≥10 days before the earliest test (inconclusive or positive) (N = 91). One person was removed due to missing last negative test data, and 10 persons were removed due to testing inconclusive initially but counted the first positive test as day 0.

prior was significantly associated with a 15% shorter RAT positivity duration (ETR 0.85, 95% CI 0.75–0.96) compared with having a last negative test ≤4 days prior. Being symptomatic was significantly associated with a 13% longer RAT positivity duration (ETR 1.13, 95% CI 1.02–1.25). Having a prior infection >90 days was significantly associated with a 50% shorter RAT positivity duration (ETR 0.50, 95% CI 0.33–0.76). Receipt of 3 vaccine doses was significantly associated with a 20% longer RAT positivity duration (ETR 1.20, 95% CI 1.04–1.39) compared to the 2 doses ≥5 months group. The results for other covariates were not significant.

Discussion

We analyzed data from a mandatory daily RAT program among university students in isolation to assess the percent still positive on day 5 and beyond and determine possible prognostic factors for RAT positivity duration. In addition, we approximately accounted for time since infection by stratifying our analysis by the time since last negative test. We found a day 5 positivity of 47% in the twice-weekly screening group and 26%–28% in the less frequently screened groups (Figure, panels A–C). For all groups, positivity approximately halved with each additional day. Those

results align with the expectation that more frequent screeners received their diagnosis earlier in their infection, thus experiencing a longer isolation. Our findings are similar to results reported in other analyses of managed isolation programs, although most did not conduct daily mandatory testing (*3*; J.A. Hay et al., unpub. data; E. Landon et al., unpub. data; S.B. Nelson et al., unpub. data). Those studies reported RAT positivity of 31%–58% on days 5–9 of isolation and PCR positivity of 39%–52% on day 5, 25%–33% on day 6, and 13%–22% on day 7 .

Two recent cohort studies comparing RAT and culture positivity found a 100% negative predictive value and 50% positive predictive value 4–6 days (n = 14) (*20*) and 6 days (n = 17) (L.A. Cosimi et al., unpub. data, https://doi.org/10.1101/2022.03.03.22271766) after diagnosis. Day 6 culture positivity was 11%–35% depending on the isolation start definition. A separate study found that 25% of persons still had culturable virus at day 8 (J. Boucau, unpub. data, https://doi.org/10.1101/2022.03.01.22271582) . The combined results suggest that a negative exit RAT toward the end of isolation is strongly indicative of culture negativity, whereas a positive exit RAT is only sometimes associated with culture positivity (and likely infectiousness). Thus, managed

isolation programs face the choice of whether and how to integrate RAT exit testing. In our study, negative RAT tests on day 5 enabled 78%–85% of students to confidently leave isolation 1 day early and negative RAT tests on day 6 to leave on time. For the 15%–22% who remained RAT positive on day 6, some unknown percentage likely remained infectious; the percentage remaining positive dropped to 6%–8% on day 7. We defined the isolation start as the initial test date; however, CDC guidelines define it as the initial test or the symptom onset. Persons using symptom onset as their isolation start may have longer RAT positivity durations than those we measured in our study, strengthening the argument for the use of exit tests, particularly given the innate subjectivity of self-reported symptoms. In addition, we note that the young age of our study population may have meant faster viral clearance than for the general population. An appropriate balance, particularly in the case of high-density settings such as university dormitories in which outbreaks can quickly spread, may be to use exit testing beginning on day 5 to end isolation and, for those still testing positive, remain in isolation until day 7 and continue masking until day 10.

A negative test ≥10 days before diagnosis, symptom status, prior infection >90 days before diagnosis, and receipt of 3 vaccine doses were significantly associated with RAT positivity duration in our survival analysis (Table 2). Results for the other covariates were not significant. For the last negative test covariate, we observed an association with shorter

duration time for the ≥10 days and 5–9 days groups compared with the ≤4 days group, although only the difference in ETR for the ≥10 days group was significant. The relationship between less frequent screening and shorter RAT positivity duration is intuitive; those persons are more likely to receive a diagnosis later in the infection. Reporting symptoms before or at diagnosis was significantly associated with longer RAT positivity duration. Symptomatic persons may receive diagnosis earlier in their infection, even when participating in routine screening, resulting in longer RAT positivity. Experiencing a prior infection >90 days earlier was significantly associated with decreased RAT positivity duration. In a highly vaccinated population, having a previous infection may confer greater immunity than not having one (21), reducing the RAT positivity duration.

Receipt of 3 vaccine doses was significantly associated with a longer RAT positivity duration compared with receipt of 2 doses ≥5 months before diagnosis, an unexpected finding. This finding was consistent under various formulations of the model during our exploratory phase and could be caused by immunologic or data factors. Another study found that vaccine-boosted persons were twice as likely to test positive on an initial RAT on days 5–10 than unboosted persons, although not all persons tested daily (E. Landon et al., unpub. data). That study suggested boosted persons might develop symptoms earlier due to a faster immune response, leading to speedier detection and longer RAT positivity durations. Accounting for the time since the

Table 2. Event time ratios of the association between covariates in study of students in a university-managed isolation program, January 1–February 11, 2022*

Covariate	Sample size	ETR (95% CI)	p value
Time since last negative test, d			
≤4†	155	NA	NA
5–9	40	0.88 (0.77NA1.01)	0.065
≥10	68	0.85 (0.75NA0.96)	0.008
Symptoms at diagnosis			
N	104	NA	Referent
Y	159	1.13 (1.02NA1.25)	0.016
Ct value at diagnosis	263	1 (0.99NA1)	0.378
Prior infection >90 d			
N†	244	NA	NA
Y	19	0.5 (0.33NA0.76)	0.001
No. dose/time since last dose			
2 doses / ≥5 mo†	44	NA	NA
2 doses / <5 mo	31	1.29 (0.97NA1.73)	0.083
3 doses	188	1.2 (1.04NA1.39)	0.012
Primary vaccine brand			
Janssen/Johnson & Johnson†	24	NA	NA
mRNA	239	1.21 (0.89NA1.65)	0.219

*N = 263 persons who were fully vaccinated with Pfizer-BioNTech (https://www.pfizer.com), Moderna (https://modernatx.com), or Janssen/Johnson & Johnson (https://jnj.com), did not additionally receive an international vaccine, and did not have a missing Ct value or symptom status. ETR >1 is associated with prolonged RAT positivity duration compared to the reference group. An ETR <1 is associated with a decreased RAT positivity duration. Ct, cycle threshold; Dx, diagnosis; ETR, event time ratio; mRNA, either of the mRNA vaccines from Pfizer or Moderna; NA, not applicable; RAT, rapid antigen test.

last negative test in our model would likely reduce some of the bias toward earlier detection of symptomatic persons; however, this explanation remains possible. In addition, the quantity and quality of anti-spike antibody levels substantially differ in 2-dose mRNA recipients shortly after they receive a booster dose, enhancing viral neutralization capacity (22). Timely onset of improved humoral and cellular immunity in boosted persons is expected to result in rapid control of the acute infection. After such containment, an apparent delay of viral clearance might result from remaining, potentially antibody-coated, viral particles or infected cells that are gradually cleared. In our study population, 68% of persons were boosted with a third dose ≥14 days before their positive test (Table 1), occurring on average 50 (IQR 35–61) days earlier. Conversely, it is also possible that selection bias exists among boosted persons in our dataset. Boosted persons who experience breakthrough infections may not mount as strong an immunologic response to the vaccine compared as boosted and exposed persons who do not experience breakthrough infections, leading to relatively longer infection durations. In addition, more persons in the 2-dose groups may have been infected with the Delta variant compared with the 3-dose group. We observed a higher proportion of persons belonging to the 2-dose groups earlier in our study, when Delta still circulated at low levels (Appendix Figure 2). If the incubation period or infection duration differ between Delta and Omicron infections, this could contribute to our findings. Although we did not have access to viral sequence data for our study population, Omicron reached 97% frequency among sequenced samples in New Haven County, Connecticut, by January 1, 2022; the remaining 3% were Delta (23). We observed a substantially larger sample size for the 3-dose group (n = 188) than the 2-dose ≥5 months (n = 44) and <5 months (n = 31) groups. The larger sample may have captured more RAT positivity duration outliers. Finally, our analysis assesses the relationship between these factors and the duration of RAT positivity, not infection. Other unaccounted factors may be associated with both the 3-dose group and RAT positivity duration.

Symptom status only captures self-reported symptoms before or at diagnosis and may not always be related to the subsequent SARS-CoV-2 diagnosis. Three persons reported a symptom onset >10 days before diagnosis. Some asymptomatic persons may have later become symptomatic. Prior infections >90 days earlier included confirmed infections reported in the medical records; prior infections that occurred during breaks or before routine screening began at the university in fall 2021 were likely missed. The PCR Ct value was measured only at diagnosis; some Ct values were missing because participants took external tests or home RATs. Our study population, primarily students 18–22 years of age, may not be representative of the general population because of their youth and likely lower rate of comorbidities. However, it is unlikely that older age groups or those with higher comorbidity rates would experience shorter RAT positivity durations. In addition, daily RAT positivity may change in this population as more time passes since their last vaccine dose. We do not have a full medical history for our study population, and it is possible that some persons may experience longer isolations because of their medical conditions. There could be changes in staff accuracy over time in reading RAT results, which are qualitative in nature, although their training procedures render this less likely. We do not have RAT data for days 1–4 and accounted for this interval-censoring in our analysis. RATs have a lower sensitivity than PCR, reducing the risk that a noninfectious person would remain in isolation but increasing the risk for a false negative (4,5). RAT positivity, although associated with culturable virus, does not mean that a person is necessarily infectious (5–7).

Incorporation of exit rapid antigen testing into its managed isolation program enabled the university to tailor isolation durations on the basis of onward transmission risk. When using the positive test collection date as the start of isolation, the university released 53%–74% of students testing negative via RAT 1 day early on isolation day 5, while identifying the 15%–22% of students who remained positive on isolation day 6. Using an earlier symptom onset date as an alternative isolation start would result in higher positivity. The recommended full 5-day isolation period may be too short, especially for persons using symptom onset as their isolation start or those with diagnoses early in their infections. Future research analyzing what, if any, onward transmission has resulted from the recommended 5-day isolation period would further refine our understanding of its suitability. In addition, the risk posed by a still-infectious person released from isolation after 5 days must also be considered in the broader context. In periods of high community incidence, the contribution of still-infectious released persons to onward transmission may be relatively small compared with that of other persons early in their infections. Conversely, in periods of low community incidence, their contribution may be relatively greater.

These considerations illustrate the complexity of recommending isolation periods for the general population, but our study adds to evidence that the recommended 5-day isolation period may be too short. Finally, our study highlights the utility of using exit RATs to tailor isolation periods on the basis of risk, especially in dense settings or ones with vulnerable populations.

This article was preprinted at https://www.medrxiv.org/content/10.1101/2022.03.11.22272264v1.

Yale COVID-19 Resulting and Isolation Team authors: Adam Cairns, Alyssa Cooksey, Arielle Pensiero, Asnath Mosha, Christina Pivirotto, Colleen Traub, Gabriel Velazquez, Heejun Lee, Jasper Larioza, Jelissa Neal, Jenna Bourgeois, Kathleen Donnelly, Karen Otterson, Kiley Carbone, Kristin Smith, Lauren Gillingham, Lauren Greenberg, Linda DiGangi Ehrenfels, Maen Adileh, Marie Toupou, Nathan Lubich, Nathan Yuen, Nick Davies, Nikkiyah Brown, Noor Khalid, Olivia Dumont, Onyi Umeugo, Oscar Monteagudo, Presley Hill, Quinn O'Leary, Rashea Banks, Richard Rousseau, Sam Duplantis, Sara Khalid, Saskia César, Sean Doran, Shannan Charney, Shinelle Wilkins, Sofia Martinez, Spencer Volpe, Victor Martinez Garcia, and Vittoria Cappuccia.

About the Author
Ms. Earnest is a PhD candidate at the department of epidemiology of microbial diseases, Yale University School of Public Health. Her primary research interests include the outbreak dynamics of emerging viruses in human and animal populations.

References

1. Centers for Disease Control and Prevention. Isolation and precautions for people with COVID-19. 2022 [cited 2022 Feb 16]. https://www.cdc.gov/coronavirus/2019-ncov/if-you-are-sick/quarantine-isolation-background.html

2. Lambrou AS, Shirk P, Steele MK, Paul P, Paden CR, Cadwell B, et al.; Strain Surveillance and Emerging Variants Bioinformatic Working Group; Strain Surveillance and Emerging Variants NS3 Working Group. Genomic surveillance for SARS-CoV-2 variants: predominance of the Delta (B.1.617.2) and Omicron (B.1.1.529) variants—United States, June 2021–January 2022. MMWR Morb Mortal Wkly Rep. 2022;71:206–11 https://doi.org/10.15585/mmwr.mm7106a4

3. Lefferts B, Blake I, Bruden D, Hagen MB, Hodges E, Kirking HL, et al. Antigen test positivity after COVID-19 isolation—Yukon-Kuskokwim Delta region, Alaska, January–February 2022. [cited 2022 Feb 25]. MMWR Morb Mortal Wkly Rep. 2022;71:293–8 https://www.cdc.gov/mmwr/volumes/71/wr/mm7108a3.htm. https://doi.org/10.15585/mmwr.mm7108a3

4. Centers for Disease Control and Prevention. Ending isolation and precautions for people with COVID-19: interim guidance. 2022 [cited 2022 Mar 2]. https://www.cdc.gov/coronavirus/2019-ncov/hcp/duration-isolation.html

5. Pekosz A, Parvu V, Li M, Andrews JC, Manabe YC, Kodsi S, et al. Antigen-based testing but not real-time polymerase chain reaction correlates with severe acute respiratory syndrome coronavirus 2 viral culture. Clin Infect Dis. 2021;73:e2861–6. https://doi.org/10.1093/cid/ciaa1706

6. Routsias JG, Mavrouli M, Tsoplou P, Dioikitopoulou K, Tsakris A. Diagnostic performance of rapid antigen tests (RATs) for SARS-CoV-2 and their efficacy in monitoring the infectiousness of COVID-19 patients. Sci Rep. 2021;11:22863. https://doi.org/10.1038/s41598-021-02197-z

7. Pickering S, Batra R, Merrick B, Snell LB, Nebbia G, Douthwaite S, et al. Comparative performance of SARS-CoV-2 lateral flow antigen tests and association with detection of infectious virus in clinical specimens: a single-centre laboratory evaluation study. Lancet Microbe. 2021;2:e461–71. https://doi.org/10.1016/S2666-5247(21)00143-9

8. Soni A, Herbert C, Filippaios A, Broach J, Colubri A, Fahey N, et al. Comparison of rapid antigen tests' performance between Delta and Omicron variants of SARS-CoV-2: a secondary analysis from a serial home self-testing study. Ann Intern Med. 2022 Oct 11 [Epub ahead of print]. https://doi.org/10.7326/M22-0760

9. Peeling RW, Heymann DL, Teo YY, Garcia PJ. Diagnostics for COVID-19: moving from pandemic response to control. Lancet. 2022;399:757–68. https://doi.org/10.1016/S0140-6736(21)02346-1

10. Rosella LC, Agrawal A, Gans J, Goldfarb A, Sennik S, Stein J. Large-scale implementation of rapid antigen testing system for COVID-19 in workplaces. Sci Adv. 2022;8:eabm3608. https://doi.org/10.1126/sciadv.abm3608

11. How does COVID-19 multiplex testing work? [cited 2022 Jun 15]. https://sites.broadinstitute.org/safe-for-school/how-does-covid-19-testing-work-0

12. Food and Drug Administration. In vitro diagnostics EUAs - antigen diagnostic tests for SARS-CoV-2 [cited 2022 Feb 25]. https://www.fda.gov/medical-devices/coronavirus-disease-2019-covid-19-emergency-use-authorizations-medical-devices/in-vitro-diagnostics-euas-antigen-diagnostic-tests-sars-cov-2

13. RStudio Team. RStudio: integrated development for R [cited 2022 Feb 25]. http://www.rstudio.com/

14. Therneau TM. Survival analysis [R package survival version 3.2–13]. Comprehensive R Archive Network (CRAN); 2021 [cited 2022 Feb 25]. https://CRAN.R-project.org/package=survival

15. Therneau TM, Grambsch PM. Modeling survival data: extending the Cox model. New York: Springer Science & Business Media; 2013.

16. Kleinbaum DG, Klein M. Survival analysis: a self-learning text, third edition. New York: Springer; 2011.

17. Zoche-Golob V. AFTtools: tools for the data preparation, fitting and diagnostics of accelerated failure times models. R package version 0.2.1. 2015 [cited 2022 Mar 6]. https://zenodo.org/record/46383

18. Centers for Disease Control and Prevention. COVID-19 vaccination. 2022 [cited 2022 Mar 10]. https://www.cdc.gov/coronavirus/2019-ncov/vaccines/second-shot.html

19. Centers for Disease Control and Prevention. Interim clinical considerations for use of COVID-19 vaccines. 2022 [cited 2022 Mar 1]. https://www.cdc.gov/vaccines/covid-19/clinical-considerations/covid-19-vaccines-us.html#table-02

20. Bouton TC, Atarere J, Turcinovic J, Seitz S, Sher-Jan C, Gilbert M, et al. Viral dynamics of Omicron and Delta SARS-CoV-2 variants with implications for timing of release from isolation: a longitudinal cohort study. Clin Infect Dis. 2022 June 23 [Epub ahead of print]. https://doi.org/10.1093/cid/ciac510

21. Hall V, Foulkes S, Insalata F, Kirwan P, Saei A, Atti A, et al.; SIREN Study Group. Protection against SARS-CoV-2 after Covid-19 vaccination and previous infection. N Engl J Med. 2022;386:1207–20. https://doi.org/10.1056/NEJMoa2118691

22. Muecksch F, Wang Z, Cho A, Gaebler C, Ben Tanfous T, DaSilva J, et al. Increased memory B cell potency and breadth after a SARS-CoV-2 mRNA boost. Nature. 2022;607:128–34. https://doi.org/10.1038/s41586-022-04778-y

23. Yale SARS-CoV-2 Genomic Surveillance Initiative. 2022 [cited 2022 Mar 7]. https://nextstrain.org/groups/grubaughlab-public/CT-SARS-CoV-2/connecticut

Address for correspondence: Rebecca Earnest, Yale School of Public Health, 60 College St, New Haven, CT 06510, USA; email: rebecca.earnest@yale.edu

Orthopoxvirus Seroprevalence and Infection Susceptibility in France, Bolivia, Laos, and Mali

Léa Luciani, Nathanaël Lapidus, Abdennour Amroun, Alessandra Falchi,
Chanthala Souksakhone, Mayfong Mayxay, Audrey Dubot-Pérès, Paola Mariela
Saba Villarroel, Issa Diarra, Ousmane Koita, Pierre Gallian, Xavier de Lamballerie

To determine a demographic overview of orthopoxvirus seroprevalence, we tested blood samples collected during 2003–2019 from France (n = 4,876), Bolivia (n = 601), Laos (n = 657), and Mali (n = 255) for neutralizing antibodies against vaccinia virus. In addition, we tested 4,448 of the 4,876 samples from France for neutralizing antibodies against cowpox virus. We confirmed extensive cross-immunity between the 2 viruses. Seroprevalence of antibodies was <1% in Bolivia, <5% in Laos, and 17.25% in Mali. In France, we found low prevalence of neutralizing antibodies in persons who were unvaccinated and vaccinated for smallpox, suggesting immunosenescence occurred in vaccinated persons, and smallpox vaccination compliance declined before the end of compulsory vaccination. Our results suggest that populations in Europe, Africa, Asia, and South America are susceptible to orthopoxvirus infections, which might have precipitated the emergence of orthopoxvirus infections such as the 2022 spread of monkeypox in Europe.

Immunity of human populations against viruses of the genus *Orthopoxvirus*, to which monkeypox virus (MPXV), variola virus, and vaccinia virus belong, has been questioned recently because of the emergence of MPXV infections. Broad cross-immunity exists between the viruses of this genus, which enabled the use of vaccinia virus as a vaccine to prevent smallpox. In addition, vaccinia virus–derived vaccines have been used to prevent or mitigate MPXV infections during the 2022 outbreak.

Since smallpox vaccination ended in 1980, immunity against orthopoxviruses has decreased worldwide. Decreased immunity has been associated with the emergence of zoonotic orthopoxviruses with extended host specificity. MPXV has been responsible for widespread epidemic episodes in Africa (*1–3*) and other continents (*4,5*). Similar episodes have been observed for buffalopox (*6–8*) and camelpox (*8–10*) viruses in Asia and for cowpox virus, which is ubiquitous (*11–13*). Orthopoxvirus infections will likely become more common because of increased travel and trade, ecosystem changes, and altered biodiversity and climates (*14–16*). Since smallpox eradication in 1980, medical research on orthopoxviruses has gradually declined. However, in 2001, several reports addressed the potential bioterrorism risk associated with smallpox (*17–19*). These reports led to attempts to assess the susceptibility of the general population to smallpox (*18*), which has generally been determined according to smallpox vaccination coverage. In 2001, the Santé Publique France (French Institute of Public Health) published a report using data from the country's National Institute of Statistics and Economic Studies and National Institute of Health and Medical Research that estimated smallpox vaccination coverage in France (*20*). Coverage was ≈0% for persons born after 1979, 50% for those born during 1972–1978, 65% for those born during 1966–1971, and 90% for those born before 1966.

The strategy to prevent smallpox in France and most developed countries was through systematic

Author affiliations: Aix-Marseille Université-IRD 190-Inserm 1207, Marseille, France (L. Luciani, A. Amroun, A. Dubot-Pérès, P.M. Saba Villarroel, I. Diarra, P. Gallian, X. de Lamballerie); Sorbonne Université, Inserm, Saint-Antoine Hospital, Paris, France (N. Lapidus); Université de Corse Pascal Paoli, Corte, France (A. Falchi); Lao Red Cross, Vientiane, Laos (C. Souksakhone); Ministry of Health, Vientiane (M. Mayxay); University of Health Sciences, Vientiane (M. Mayxay); Mahosot Hospital, Vientiane (M. Mayxay, A. Dubot Pérès); University of Oxford, Oxford, UK (M. Mayxay, A. Dubot Pérès); University of Sciences, Bamako, Mali (I. Diarra, O. Koita); Établissement Français du Sang, La Plaine Saint Denis, France (P. Gallian)

and mandatory vaccination of children. Vaccination consisted of 2 injections; the first injection was administered at 1 year of age and the second 10 years later. Smallpox vaccination in France was mandatory during 1902–1978 for the first injection and until 1984 for the booster. However, for many resource-limited countries, routine vaccination of the population was difficult to achieve, and the World Health Organization shifted to a containment strategy of case identification, isolation, and widespread vaccination of contacts in the 1960s. This strategy was successful in eradicating smallpox (*21*), but vaccination coverage of the general population in those countries (which conferred cross-immunity to other orthopoxviruses) was lower than in countries where routine vaccination had been organized.

We conducted a large-scale epidemiologic study of the prevalence of neutralizing antibodies against vaccinia and cowpox viruses. We tested ≈6,500 serum samples from persons in 4 countries on different continents: France, Bolivia, Laos, and Mali. We provide a demographic overview of orthopoxvirus seroprevalence that enables assessment of susceptibility of relevant populations to infection by this group of viruses.

Materials and Methods

Study Populations and Ethics Approval
We investigated human populations from France, Bolivia, Laos and Mali. We tested blood samples from all study participants for the presence of neutralizing antibodies against vaccinia virus. In addition, we tested a large cohort of the study participants in France for the presence of neutralizing antibodies against cowpox virus.

The population in France comprised 4,876 voluntary, unpaid blood donors whose serum samples were collected in 2012, 2013, and 2019 from 4 regions of metropolitan France: Auvergne-Loire (n = 837), Corsica (n = 596), Midi-Pyrénées (n = 1,738), and Provence-Alpes-Côte d'Azur (n = 1,705). Donors provided signed informed consent for the use of their blood samples for nontherapeutic research purposes. This study was approved by the local ethics committee in southern France, Comité de Protection des Personnes Sud Méditerranée I. Blood donors completed a questionnaire that included their year of birth, sex, and detailed information about their lifestyle, environment (home and workplace), and exposure to zoonotic diseases (*22*).

The population in Bolivia comprised 601 voluntary, unpaid, blood donors (*23*) whose serum samples were collected in 2017 in 5 departments: tropical climates of Santa Cruz de la Sierra (n = 165) and Beni (n = 102), Cochabamba (n = 151), and colder subtropical climates (highlands) of Tarija (n = 23) and La Paz (n = 160). This study was approved by the ethics committee of the Medical College of Santa Cruz, and donors provided signed informed consent for research use of their blood samples. The information collected included the year of birth, sex of participants, city of residence, and occupation.

In Laos, collection of blood samples from 657 blood donors was performed in the capital city of Vientiane in 2003, 2004, 2015, and 2018. Donors provided signed informed consent for research use of their blood samples, and the study was approved by the Lao National Health Research Ethics Committee and the Oxford Tropical Research Ethics Committee. Collected information was limited to year of birth and sex of participants.

In Mali, 257 blood samples were collected in 2019 in the villages of Leba, Tliemba, Soloba, Bougoudale, and Komana for a baseline study of health indicators in the villages of the Komana gold mine region (tropical forest area). Participants provided informed consent for research use of their blood samples, and the study was approved by the ethics committee of the National Institute for Public Health Research in Mali. Collected information was limited to the year of birth and sex of participants.

Seroneutralization Assay
We used the Western Reserve vaccinia virus strain, which is a reference laboratory strain, and the Compiègne strain of cowpox virus that is genetically distant from vaccinia virus. We isolated the Compiègne strain of cowpox virus in 2009 from a human infected by a domestic rat (*24*). We cultured both virus strains on Vero cells in Eagle's Minimum Essential Medium containing 1% penicillin/streptomycin, 1% glutamine, and 10% fetal calf serum (ThermoFisher Scientific, https://www.thermofisher.com) at 37°C in a 5% CO_2 incubator. We optimized virus production to obtain low and similar ratios of noninfectious to infectious particles for both strains. For both viruses, we infected Vero cells at 0.01 multiplicity of infection in a 12-well plate for 3 h at 37°C, then washed with Hanks' Balanced Salt solution. For vaccinia virus, we used clarified supernatant (centrifuged at 700 × *g* for 10 min) collected at 3 days postinfection that titrated at 1.04×10^9 genome copies/mL and 1.67×10^6 50% tissue culture infectious dose ($TCID_{50}$)/mL (*25*) (ratio of genome copies/$TCID_{50}$ = 624). For cowpox virus, we used clarified supernatant (centrifuged at 700 × *g* for 10 min) collected at 2 days postinfection. We

collected cowpox virus 1 day earlier than vaccinia virus because of the large number of noninfectious cowpox virions on day 3 postinfection. The clarified cowpox supernatant titrated at 6.82×10^7 genome copies/mL and 1.08×10^5 TCID$_{50}$/mL (25) (ratio = 613). We prepared aliquots in 15 mmol/L HEPES buffer and stored them at –80°C.

We used the same seroneutralization protocol for both viruses. Serum samples were stored at –80°C in specific low binding tubes and thawed before use. We prepared serial dilutions of serum samples in Eagle's Minimum Essential Medium with 1% penicillin/streptomycin in 96-well plates by using an epMotion 5075 workstation (Eppendorf, https://www.eppendorf.com). We added 50 µL of diluted serum to 50 µL of virus (50 TCID$_{50}$/well) to produce final serum dilutions of 1:20, 1:40, 1:80 and 1:160. We centrifuged the plates at $70 \times g$ for 30 s and incubated them for 1 h at 37°C. After neutralization, we added the serum/virus mixtures to 96-well cell culture plates containing confluent Vero cells and 100 µL of culture medium (described previously) and incubated the plates at 37°C in a 5% CO$_2$ incubator for 4 d. We included a positive control serum from a donor vaccinated multiple times with the Lister strain of vaccinia virus, which was supplied by the National Reference Centre, France (26).

A cytopathic effect appeared on day 3 postinfection for both viruses. We evaluated the plates on day 4 postinfection, and the cytopathic effect was extensive and assisted the analysis. We obtained live cell images by using Cytation (BioTek, https://www.biotek.com) or Incucyte (Sartorius, https://www.sartorius.com) readers. Each image was assigned a result that corresponded to the highest serum dilution that had no cytopathic effect: negative (default value, 1:10) or positive at 1:20, 1:40, 1:80, or 1:160. To assess intraassay reproducibility, we tested 10 replicates of a positive serum sample during the same experiment. To assess interassay reproducibility, we tested 10 replicates of the same serum sample in 5 different experiments (different day and operator). According to criteria classically used for serologic neutralization tests (27), we validated the assays by demonstrating that replicate titers were within 3-fold of each other for 80% of tested samples.

Statistics
We compared the distribution of serologic titers and the proportions of positive and negative serum samples between decades of birth by using Mann-Whitney tests. We compared regions or sex of participants by using Fisher exact test. We calculated geometric

means ±SD and created graphs by using GraphPad Prism software (https://www.graphpad.com). We calculated Cohen κ coefficients by using a free online tool (IDoStatistics, https://idostatistics.com/cohen-kappa-free-calculator) to determine correlations between antibodies against vaccinia and cowpox viruses. For samples tested for both viruses, we calculated an orthopoxvirus neutralization titer (ONT) from the geometric mean of vaccinia and cowpox neutralization titers. We performed Mann-Whitney tests for quantitative variables and Fisher exact tests for categorical variables. We compared seroprevalence between each pair of regions by using Fisher exact test without correction for test multiplicity. We identified factors associated with the serologic titer by using univariate analysis, then adjusted for the year of birth by using a parametric model according to the hypothesis of a lognormal distribution of titers and factoring in the interval censoring of serologic titers (28). For the study population in France, we analyzed covariates from the questionnaire, including sex, marital status, occupation, level of education, number of persons in the household, household income, general health status, travel outside Europe, housing type, time spent outdoors, air conditioning, mosquito net use, presence of garden/terrace/balcony and swimming pool, dwelling rurality, proximity to shops, presence of a pond or marsh nearby, contact with domestic or farm animals, exposure to mosquitoes or other biting insects and ticks, frequency of bites and protection used, type of water supply, contact with sewage, water consumption, hunting activity, type of meat consumed, and cooking. We used 2-tailed tests for all analyses and defined the significance level as $p < 0.05$.

Results

Neutralizing Antibodies against Vaccinia Virus
We determined the male:female ratio, birth decades, and titers for neutralizing antibodies against vaccinia virus for study participants from the different populations in France, Bolivia, Laos, and Mali (Table 1). Seroprevalence was calculated for samples using a threshold titer of ≥20 (ThT20) or ≥40 (ThT40).

Cross-Immunity between Vaccinia and Cowpox Viruses
A total of 4,448 serum samples from 4 regions of France had sufficient volumes to be tested for both vaccinia and cowpox viruses. We observed that 4,391 (98.8%) of the participants had similar antibody titers for both viruses within ±1 dilution. Among 320 participants who had a titer ≥20 for both viruses, 307

Table 1. Demographic characteristics of participants and results of vaccinia virus neutralization assay in study of orthopoxvirus seroprevalence and infection susceptibility in France, Bolivia, Laos, and Mali*

Characteristics	France	Bolivia	Laos	Mali
Total no. participants	4,876	601	657	255
M/F ratio	1.12	1.37	1.72	1.02
Mean year of birth ±SD	1967 ±14	1989 ±10	1985 ±9	1980 ±14
No. born before 1960	1,560 (32)	3 (0.5)	5 (0.8)	26 (10)
No. born before 1980	3,826 (78)	161 (27)	171 (26)	112 (43)
Antibody titers†				
<20	4,137 (84.84)	598 (99.50)	632 (96.19)	211 (82.74)
20	425 (8.72)	1 (0.17)	22 (3.35)	30 (11.76)
40	217 (4.45)	1 (0.17)	3 (0.46)	12 (4.71)
80	86 (1.76)	1 (0.17)	0 (0)	2 (0.78)
160	11 (0.23)	0 (0)	0 (0)	0 (0)
Titer $\geq$40, %	6.44	0.33	0.46	5.49
Titer $\geq$20, %	15.16	0.50	3.81	17.25

*Values are no. (%) unless otherwise noted. Percentages were calculated according to the total number of study participants in each population.
†No. (%) participants with different levels of neutralizing antibodies against vaccinia virus determined by seroneutralization assay.

(96%) had concordant titers for both viruses (within $\pm$1 dilution) (Table 2). Cohen κ coefficients were 0.43 for the 1:20 titer, 0.64 for the 1:40 titer, 0.48 for the 1:80 titer, and 0.29 for the 1:160 titer. We observed a substantial qualitative agreement between seroneutralization results for vaccinia and cowpox virus at the 1:40 threshold titer, and a concordant titer was found for most samples.

Epidemiologic Data and Prevalence of Neutralizing Antibodies against Orthopoxviruses in France

Among the 4,448 samples tested for both vaccinia and cowpox virus, the male:female ratio was 1.17 and mean year of birth ($\pm$)SD was 1966 ($\pm$13) (Table 3). Because of the differences observed between seroprevalence values calculated at ThT20 and ThT40 for vaccinia virus, we determined the ONT and considered samples with an ONT titer $\geq$20 to be positive.

The mean seroprevalence of orthopoxvirus neutralizing antibodies in France was 8.18%; seroprevalence was >10% in persons born before 1970 and dropped to 5% for those born during the 1970s and to <1% for those born after 1980. The geometric mean ONT for the entire sample population from France was 12.8. We observed limited differences in antibody titers according to age groups, but found a clear overall increase in the percentages of orthopoxvirus-positive persons in relation to age (Figure, panels A,

B; Appendix Table 1, https://wwwnc.cdc.gov/EID/article/28/12/22-1136-App1.pdf).

We observed different associations between the sex of study participants and presence of orthopoxvirus neutralizing antibodies in France depending on the decade of birth (Figure, panels C, D). Until the 1960s, orthopoxvirus seroprevalence was higher among men, but it became higher among women in the 1970s. Starting with the 1980s, we observed no difference between sexes.

The study population in France geographically covered 4 regions. We compared orthopoxvirus neutralizing antibody titers and percentages of seropositive participants in the different regions for each decade (Figure, panels E, F; Appendix Table 2). We observed some differences in antibody titers and percentages of seropositive persons between the regions. Seroprevalence was higher in Corsica and the Midi-Pyrénées regions than in the Provence-Alpes-Côte d'Azur and Auvergne-Loire regions.

During the collection of samples, participants in France filled in a detailed questionnaire concerning lifestyle, eating habits, rurality index, contact with livestock or wild animals, and other personal information. We estimated the association between each of these parameters and ONT. We evaluated 60 parameters and determined none of the parameters influenced seroprevalence after adjusting for age. The

Table 2. Cross-reactivity between antibodies against vaccinia and cowpox viruses in serum samples of study participants from France in study of orthopoxvirus seroprevalence and infection susceptibility in France, Bolivia, Laos, and Mali*

Antibody titers, vaccinia virus	Antibody titer, cowpox virus				
	10	20	40	80	160
10	3,443 (77.44)	407 (9.15)	4 (0.09)	2 (0.04)	1 (0.02)
20	234 (5.26)	85 (1.91)	12 (0.27)	5 (0.11)	0
40	7 (0.16)	77 (1.73)	62 (1.39)	12 (0.27)	3 (0.07)
80	0	4 (0.09)	31 (0.70)	21 (0.47)	3 (0.07)
160	0	1 (0.02)	0	2 (0.04)	2 (0.04)

*Values are no. (%). Percentages were calculated according to 4,448 participants in France who had serum samples tested for antibodies against both vaccinia and cowpox viruses by using the seroneutralization assay.

Table 3. Demographic characteristics of populations in 4 regions of France who had serum samples tested for antibodies against both vaccinia and cowpox viruses in study of orthopoxvirus seroprevalence and infection susceptibility in France, Bolivia, Laos, and Mali*

Characteristics	Corsica	Midi-Pyrénées	PACA	Auvergne-Loire	Total
M/F ratio	1.00	1.16	1.04	1.53	1.17
Mean year of birth ±SD	1966 ±12	1966 ±13	1967 ±13	1966 ±13	1966 ±13
Decade of birth					
1940s	14	185	162	77	438 (9.8)
1950s	38	443	371	213	1,065 (23.9)
1960s	59	457	491	228	1,235 (27.8)
1970s	33	308	359	166	866 (19.5)
1980s	21	244	252	106	623 (14.0)
1990s	3	101	70	47	221 (5.0)
Total	168	1,738	1,705	837	4,448

*Values are no. participants or no. (%) unless otherwise noted. Percentages were calculated according to a total of 4,448 participants in France who had serum samples tested by using the seroneutralization assay. PACA, Provence Alpes Côte-d'Azur.

only parameter directly associated with the titer of orthopoxvirus neutralizing antibodies was age.

Discussion

After the end of smallpox vaccinations in the 1980s, prevalence of antibodies against orthopoxviruses was expected to decline worldwide; seroprevalence would decrease in the youngest (and never vaccinated) age groups. Furthermore, circulation of orthopoxviruses other than smallpox was expected to contribute to immunity against smallpox by natural infection in some persons. Similarly, whereas smallpox vaccination can produce long-lasting immunity, immunosenescence in older vaccinated populations was expected to contribute to a decrease in seroprevalence in persons vaccinated in childhood. Consequently, prevalence of antibodies against orthopoxviruses is difficult to anticipate precisely in a given population because parameters that can modulate seroprevalence are numerous, including intensity of past vaccination campaigns, number of doses received, possible exposure to orthopoxvirus infections, and immunosenescence. Our study provides concrete information on seroprevalence of antibodies against orthopoxviruses and compares several populations on different continents.

Overall, our results are broadly consistent with the expectations described above. Seroprevalence of orthopoxvirus-specific antibodies was higher in countries that routinely vaccinated their population and in study participants born before the cessation of smallpox vaccinations. However, several points should be discussed.

Results from Bolivia and Laos are consistent with the previous World Health Organization containment strategy used when vaccination of the general population was not feasible. Orthopoxvirus seroprevalence was remarkably low in Bolivia (<0.5%, regardless of the threshold titer used) in those participants born before and after 1980. This result likely reflects both low vaccination coverage and lack of exposure to natural orthopoxvirus infections.

In Laos, overall seroprevalence using ThT40 was very low (<1%) but similar to ThT20 (4%). Prevalence values for persons born before 1980 were 1.8% (ThT40) and 7.0% (ThT20) compared with 0% (ThT40) and 2.7% (ThT20) for those born after 1980 (Appendix Table 3). Therefore, neutralizing antibodies against orthopoxviruses are found predominantly (but not exclusively) in persons born before 1980 and might be related to smallpox vaccination, although low-level exposure to other orthopoxviruses cannot be excluded.

In Mali, overall seroprevalence of orthopoxvirus antibodies using ThT40 was ≈5% and increased to ≈17% using ThT20. Seroprevalence values for persons born before 1980 were 10.7% (ThT40) and 27.7% (ThT20) compared with 1.4% (ThT40) and 9.0% (ThT20) for those born after 1980 (Appendix Table 3). Thus, seroprevalence was higher in older participants, but a substantial number of participants born after 1980 had neutralizing antibodies against vaccinia virus. Health authorities confirmed that no smallpox vaccination campaign existed in the study area after 1980. The distribution of seroprevalence in Mali for different age groups using ThT20 (Appendix Figure) suggests that exposure to natural orthopoxvirus infections accounts for part of the observed immunity. Samples were collected from persons in villages located in a forested area (southern Mali), and circulation of monkeypox virus in humans, monkeys, and rodents has been reported in central and western Africa for several decades, primarily at the edge of forests (3). However, vaccination might also explain the high prevalence of orthopoxvirus antibodies in the oldest age groups.

In France, we had the opportunity to perform testing for both vaccinia and cowpox viruses in a large portion of our study population to improve the
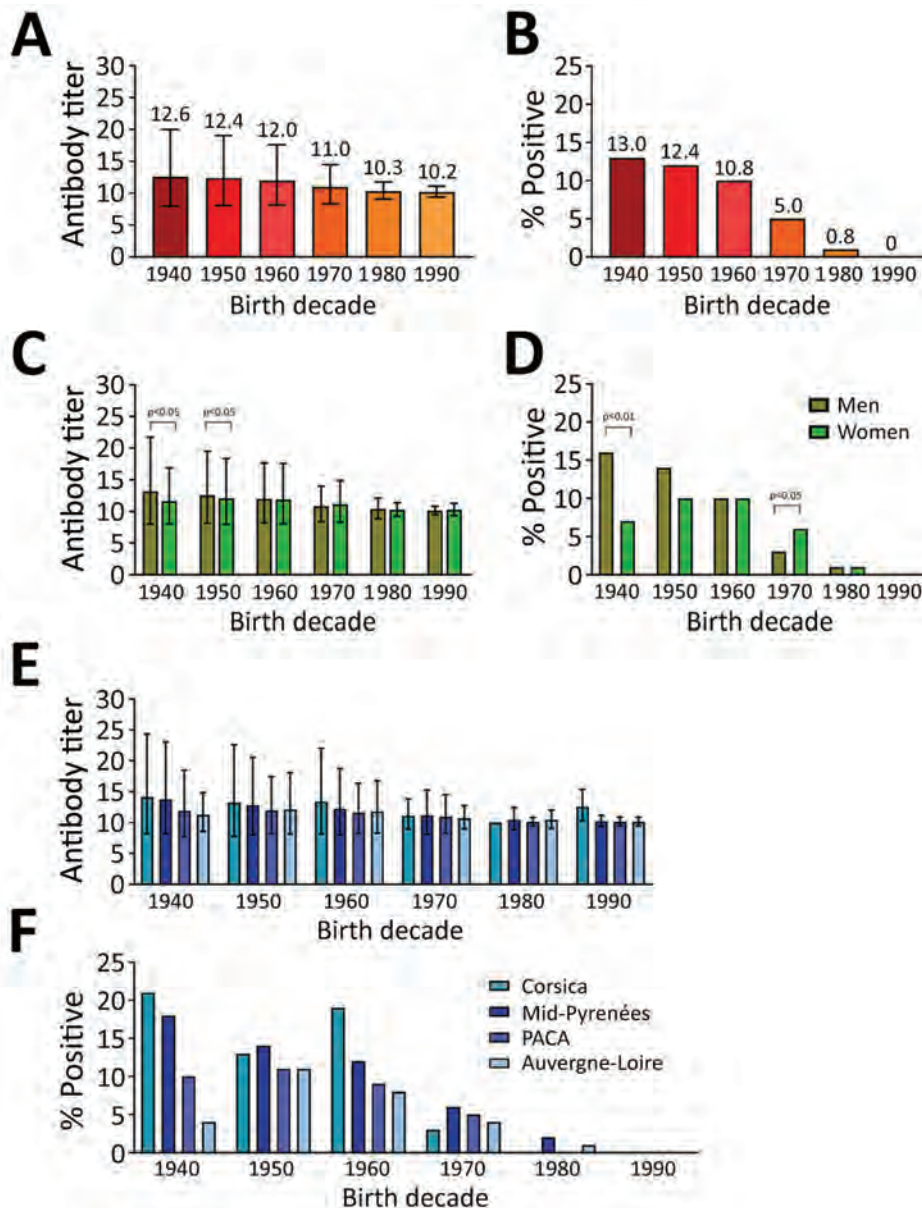
Figure. Antibody titers and percentage of population positive for antibodies against orthopoxviruses in France in study of seroprevalence and infection susceptibility in France, Bolivia, Laos, and Mali. Serum samples from 4,448 persons were tested for antibodies against both vaccinia and cowpox virus and an orthopoxvirus neutralization titer (ONT) was determined. A, B) Overall comparison of ONT geometric mean ±SD (A) and percentage of positive participants (ONT>20) (B) according to decade of birth (p values are described in Appendix Table 1, https://wwwnc.cdc.gov/EID/article/28/12/22-1136-App1.pdf). C, D) Comparisons of ONT geometric mean ±SD (C) and percentage of positive persons (ONT>20) (D) between male and female participants according to decade of birth. E, F) Comparisons of ONT geometric mean ±SD (E) and percentage of positive persons (ONT>20) (F) for populations in 4 different regions of France according to their decade of birth (p values are described in Appendix Table 2). Mann-Whitney tests were used to determine geometric means ±SD; Fisher exact tests were used to compare percentage of positive persons. A p value <0.05 was considered significant.

specificity of the neutralization assay. Our results for both viruses were similar and had a substantial qualitative agreement and concordant titers consistent with previously documented cross-immunity between orthopoxviruses (*29*). We found an orthopoxvirus antibody seroprevalence of 8.18%, which was mainly related to age and, thus, to smallpox vaccination coverage, and a sharp decline in prevalence beginning in the 1970s. We observed differences between sexes; antibodies were higher in men, especially those who were born before 1960. We suspect that the medical rigor resulting from military service for men in France might have contributed to higher seroprevalence in the older age groups.

In our study, we observed that some participants born in the early 1940s still had high neutralization titers for orthopoxviruses. This result is consistent with previous reports that smallpox vaccination generates long-term splenic memory lymphocytes that can lead to the production of antibodies against the vaccine >80 years after vaccination (*30–39*). However, we also show a low seroprevalence among participants born before 1960 (≈12.5%). Methodologically similar studies have also reported that age is the main factor affecting prevalence and antibody titer. The overall rate and decrease in prevalence is highly variable according to country (and likely vaccination policy) and serologic methods used for testing. In Japan (*40*), the

reported prevalence of neutralizing antibodies was high (>90%) for persons born before 1968 and then decreased sharply in the 1970s after the cessation of smallpox vaccination in 1976. A different pattern was observed in Australia (*41*); prevalence of antibodies was 48% among persons born before 1950 and progressively decreased by half each decade for persons born after 1950. The prevalence pattern in France is similar to that in Australia; initial vaccination coverage was estimated at 90% by Santé Publique France among persons born before 1966 (*20*), but the current seroprevalence was reported to be lower than expected (*36*). The remnants of humoral smallpox immunity appear to be conditioned by multiple factors, such as vaccine policy and population immunity. For previously vaccinated persons in whom no neutralizing antibodies have been found, the extent to which they retain functional immunity against orthopoxviruses remains unknown.

Our results also show that compliance with smallpox vaccination or booster shots in France declined well before the end of compulsory vaccination, and territorial disparities might exist. Smallpox disappeared from Europe after World War I, and the epidemics generated by imported cases in the 1950s (*42,43*) consistently suggest that vaccination coverage had already begun to decline, possibly driven by adverse effects of the vaccine.

Of note, the ThT20 prevalence values in persons born after 1980 were low (1.74% in Midi-Pyrénées, 0.65% in Auvergne-Loire, and 0% in Provence-Alpes-Côte d'Azur), suggesting the absence of natural orthopoxvirus infections. Further investigations with a larger number of study participants are needed to clarify the proportion of persons in Corsica born after 1980 with antibodies to vaccinia virus. No environmental factors were associated with antibody seroprevalence in the study population in France, despite a large database on living conditions.

The first limitation of our study is that the tested cohorts might not be representative of the general population. Differences existed in the recruitment of participants from the different international populations, and a limited number of older persons were tested. Second, individual vaccine data and collection of metadata were absent or weak. Finally, a strict internationally validated threshold value for neutralization tests was absent.

In conclusion, our study suggests that, overall, the different populations that we tested in Europe, Africa, Asia, and South America are markedly susceptible to orthopoxvirus infections. Even in Africa, where substantial evidence of natural circulation of orthopoxviruses exists, population immunity is modest. Levels of protection against orthopoxvirus infection are lowest in persons born after 1980 because smallpox vaccinations were discontinued. In practical terms, population immunity that might provide a barrier to the spread of orthopoxviruses does not appear to exist. Our study indicates that cessation of smallpox vaccinations might precipitate the emergence of orthopoxvirus infections, such as the currently observed spread of monkeypox in Europe.

About the Author

Dr. Luciani is a pharmacist/medical biologist working at the Assistance Publique Hôpitaux de Marseille and Unité des Virus Emergents, Aix Marseille Université, Marseille, France. Her primary research interests focus on poxviruses and diagnostics of emerging viral infections.

References

1. Beer EM, Rao VB. A systematic review of the epidemiology of human monkeypox outbreaks and implications for outbreak strategy. PLoS Negl Trop Dis. 2019;13:e0007791. https://doi.org/10.1371/journal.pntd.0007791
2. Doshi RH, Guagliardo SAJ, Doty JB, Babeaux AD, Matheny A, Burgado J, et al. Epidemiologic and ecologic investigations of monkeypox, Likouala Department, Republic of the Congo, 2017. Emerg Infect Dis. 2019;25:281–9. https://doi.org/10.3201/eid2502.181222
3. Durski KN, McCollum AM, Nakazawa Y, Petersen BW, Reynolds MG, Briand S, et al. Emergence of monkeypox—West and Central Africa, 1970–2017. MMWR Morb Mortal Wkly Rep. 2018;67:306–10. https://doi.org/10.15585/mmwr.mm6710a5
4. Centers for Disease Control and Prevention (CDC). Update: multistate outbreak of monkeypox—Illinois, Indiana, Kansas, Missouri, Ohio, and Wisconsin, 2003. MMWR Morb Mortal Wkly Rep. 2003;52:589–90.
5. Vaughan A, Aarons E, Astbury J, Balasegaram S, Beadsworth M, Beck CR, et al. Two cases of monkeypox imported to the United Kingdom, September 2018. Euro Surveill. 2018;23:1800509. https://doi.org/10.2807/1560-7917.ES.2018.23.38.1800509
6. Venkatesan G, Balamurugan V, Prabhu M, Yogisharadhya R, Bora DP, Gandhale PN, et al. Emerging and re-emerging zoonotic buffalopox infection: a severe outbreak in Kolhapur (Maharashtra), India. Vet Ital. 2010;46:439–48.
7. Kolhapure RM, Deolankar RP, Tupe CD, Raut CG, Basu A, Dama BM, et al. Investigation of buffalopox outbreaks in

Maharashtra State during 1992–1996. Indian J Med Res. 1997; 106:441–6.

8. Prabhu M, Yogisharadhya R, Pavulraj S, Suresh C, Sathish G, Singh RK. Camelpox and buffalopox: two emerging and re-emerging orthopox viral diseases of India. Adv Anim Vet Sci. 2015;3:527–41. https://doi.org/10.14737/journal.aavs/2015/3.10.527.541

9. Balamurugan V, Venkatesan G, Bhanuprakash V, Singh RK. Camelpox, an emerging orthopox viral disease. Indian J Virol. 2013;24:295–305. https://doi.org/10.1007/s13337-013-0145-0

10. Bera BC, Shanmugasundaram K, Barua S, Venkatesan G, Virmani N, Riyesh T, et al. Zoonotic cases of camelpox infection in India. Vet Microbiol. 2011;152:29–38. https://doi.org/10.1016/j.vetmic.2011.04.010

11. Duraffour S, Mertens B, Meyer H, van den Oord JJ, Mitera T, Matthys P, et al. Emergence of cowpox: study of the virulence of clinical strains and evaluation of antivirals. PLoS One. 2013;8:e55808. https://doi.org/10.1371/journal.pone.0055808

12. Kurth A, Wibbelt G, Gerber HP, Petschaelis A, Pauli G, Nitsche A. Rat-to-elephant-to-human transmission of cowpox virus. Emerg Infect Dis. 2008;14:670–1. https://doi.org/10.3201/eid1404.070817

13. Wolfs TFW, Wagenaar JA, Niesters HGM, Osterhaus ADME. Rat-to-human transmission of cowpox infection. Emerg Infect Dis. 2002;8:1495–6. https://doi.org/10.3201/eid0812.020089

14. Keesing F, Belden LK, Daszak P, Dobson A, Harvell CD, Holt RD, et al. Impacts of biodiversity on the emergence and transmission of infectious diseases. Nature. 2010;468:647–52. https://doi.org/10.1038/nature09575

15. Keesing F, Ostfeld RS. Impacts of biodiversity and biodiversity loss on zoonotic diseases. Proc Natl Acad Sci USA. 2021;118:e2023540118. https://doi.org/10.1073/pnas.2023540118

16. Schmeller DS, Courchamp F, Killeen G. Biodiversity loss, emerging pathogens and human health risks. Biodivers Conserv. 2020;29:3095–102. https://doi.org/10.1007/s10531-020-02021-6

17. Berche P. The threat of smallpox and bioterrorism. Trends Microbiol. 2001;9:15–8. https://doi.org/10.1016/S0966-842X(00)01855-2

18. Cohen J. Bioterrorism. Smallpox vaccinations: how much protection remains? Science. 2001;294:985. https://doi.org/10.1126/science.294.5544.985

19. Lane HC, Montagne JL, Fauci AS. Bioterrorism: a clear and present danger. Nat Med. 2001;7:1271–3. https://doi.org/10.1038/nm1201-1271

20. Lévy-Bruhl D, Guérin N, Members of the Eurosurveillance editorial board. The use of smallpox virus as a biological weapon: the vaccination situation in France. Euro Surveill. 2001;6:171–8. https://doi.org/10.2807/esm.06.11.00385-en

21. Fenner F, Henderson DA, Arita I, Jezek Z, Ladnyi ID. Smallpox and its eradication. Geneva: World Health Organization; 1988.

22. Poinsignon A, Boulanger D, Binetruy F, Elguero E, Darriet F, Gallian P, et al. Risk factors of exposure to *Aedes albopictus* bites in mainland France using an immunological biomarker. Epidemiol Infect. 2019;147:e238. https://doi.org/10.1017/S0950268819001286

23. Saba Villarroel PM, Nurtop E, Pastorino B, Roca Y, Drexler JF, Gallian P, et al. Zika virus epidemiology in Bolivia: a seroprevalence study in volunteer blood donors. PLoS Negl Trop Dis. 2018;12:e0006239. https://doi.org/10.1371/journal.pntd.0006239

24. Ninove L, Domart Y, Vervel C, Voinot C, Salez N, Raoult D, et al. Cowpox virus transmission from pet rats to humans, France. Emerg Infect Dis. 2009;15:781–4. https://doi.org/10.3201/eid1505.090235

25. Reed LJ, Muench H. A simple method of estimating fifty percent endpoints. Am J Epidemiol. 1938;27:493–7. https://doi.org/10.1093/oxfordjournals.aje.a118408

26. Leparc-Goffart I, Poirier B, Garin D, Tissier MH, Fuchs F, Crance JM. Standardization of a neutralizing anti-vaccinia antibodies titration method: an essential step for titration of vaccinia immunoglobulins and smallpox vaccines evaluation. J Clin Virol. 2005;32:47–52. https://doi.org/10.1016/j.jcv.2004.07.005

27. Timiryasova TM, Bonaparte MI, Luo P, Zedar R, Hu BT, Hildreth SW. Optimization and validation of a plaque reduction neutralization test for the detection of neutralizing antibodies to four serotypes of dengue virus used in support of dengue vaccine development. Am J Trop Med Hyg. 2013;88:962–70. https://doi.org/10.4269/ajtmh.12-0461

28. Lapidus N, de Lamballerie X, Salez N, Setbon M, Delabre RM, Ferrari P, et al. Factors associated with post-seasonal serological titer and risk factors for infection with the pandemic A/H1N1 virus in the French general population. PLoS One. 2013;8:e60127. https://doi.org/10.1371/journal.pone.0060127

29. Edghill-Smith Y, Golding H, Manischewitz J, King LR, Scott D, Bray M, et al. Smallpox vaccine-induced antibodies are necessary and sufficient for protection against monkeypox virus. Nat Med. 2005;11:740–7. https://doi.org/10.1038/nm1261

30. El-Ad B, Roth Y, Winder A, Tochner Z, Lublin-Tennenbaum T, Katz E, et al. The persistence of neutralizing antibodies after revaccination against smallpox. J Infect Dis. 1990;161:446–8. https://doi.org/10.1093/infdis/161.3.446

31. Demkowicz WE Jr, Littaua RA, Wang J, Ennis FA. Human cytotoxic T-cell memory: long-lived responses to vaccinia virus. J Virol. 1996;70:2627–31. https://doi.org/10.1128/jvi.70.4.2627-2631.1996

32. Crotty S, Felgner P, Davies H, Glidewell J, Villarreal L, Ahmed R. Cutting edge: long-term B cell memory in humans after smallpox vaccination. J Immunol. 2003;171:4969–73. https://doi.org/10.4049/jimmunol.171.10.4969

33. Pütz MM, Alberini I, Midgley CM, Manini I, Montomoli E, Smith GL. Prevalence of antibodies to vaccinia virus after smallpox vaccination in Italy. J Gen Virol. 2005;86:2955–60. https://doi.org/10.1099/vir.0.81265-0

34. Hammarlund E, Lewis MW, Hansen SG, Strelow LI, Nelson JA, Sexton GJ, et al. Duration of antiviral immunity after smallpox vaccination. Nat Med. 2003;9:1131–7. https://doi.org/10.1038/nm917

35. Combadiere B, Boissonnas A, Carcelain G, Lefranc E, Samri A, Bricaire F, et al. Distinct time effects of vaccination on long-term proliferative and IFN-γ-producing T cell memory to smallpox in humans. J Exp Med. 2004;199:1585–93. https://doi.org/10.1084/jem.20032083

36. Taub DD, Ershler WB, Janowski M, Artz A, Key ML, McKelvey J, et al. Immunity from smallpox vaccine persists for decades: a longitudinal study. Am J Med. 2008;121:1058–64. https://doi.org/10.1016/j.amjmed.2008.08.019

37. Sarkar JK, Mitra AC, Mukherjee MK. The minimum protective level of antibodies in smallpox. Bull World Health Organ. 1975;52:307–11.

38. Amanna IJ, Carlson NE, Slifka MK. Duration of humoral immunity to common viral and vaccine antigens. N Engl J Med. 2007;357:1903–15. https://doi.org/10.1056/NEJMoa066092
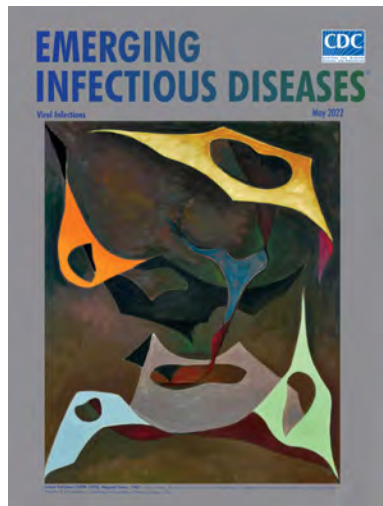
39. Mamani-Matsuda M, Cosma A, Weller S, Faili A, Staib C, Garçon L, et al. The human spleen is a major reservoir for long-lived vaccinia virus-specific memory B cells. Blood. 2008;111:4653–9. https://doi.org/10.1182/blood-2007-11-123844

40. Hatakeyama S, Moriya K, Saijo M, Morisawa Y, Kurane I, Koike K, et al. Persisting humoral antiviral immunity within the Japanese population after the discontinuation in 1976 of routine smallpox vaccinations. Clin Diagn Lab Immunol. 2005;12:520–4. https://doi.org/10.1128/CDLI.12.4.520-524.2005

41. Costantino V, Trent MJ, Sullivan JS, Kunasekaran MP, Gray R, MacIntyre R. Serological immunity to smallpox in New South Wales, Australia. Viruses. 2020;12:554. https://doi.org/10.3390/v12050554

42. Biraben JN. La diffusion de la vaccination en France au 19e siècle [in French]. Ann Bretagne Payes Ouest. 1979;86:265–76. https://doi.org/10.3406/abpo.1979.2981

43. Le Boukdelles B. The smallpox epidemic of 1955 in France [in French]. Bull Acad Natl Med. 1955;139:417–20.

Address for correspondence: Léa Luciani, Unité des Virus Émergents, UVE, Aix-Marseille Univ-IRD 190-Inserm 1207, Marseille, France; email: lea.luciani@univ-amu.fr

May 2022
Viral Infections

EMERGING INFECTIOUS DISEASES®

To revisit the May 2022 issue, go to:
https://wwwnc.cdc.gov/eid/articles/issue/28/5/table-of-contents

Association between Conflict and Cholera in Nigeria and the Democratic Republic of the Congo

Gina E.C. Charnley, Kévin Jean, Ilan Kelman, Katy A.M. Gaythorpe,[1] Kris A. Murray[1]

Cholera outbreaks contribute substantially to illness and death in low- and middle-income countries. Cholera outbreaks are associated with several social and environmental risk factors, and extreme conditions can act as catalysts. A social extreme known to be associated with infectious disease outbreaks is conflict, causing disruption to services, loss of income, and displacement. To determine the extent of this association, we used the self-controlled case-series method and found that conflict increased the risk for cholera in Nigeria by 3.6 times and in the Democratic Republic of the Congo by 2.6 times. We also found that 19.7% of cholera outbreaks in Nigeria and 12.3% of outbreaks in the Democratic Republic of the Congo were attributable to conflict. Our results highlight the value of providing rapid and sufficient assistance during conflict-associated cholera outbreaks and working toward conflict resolution and addressing preexisting vulnerabilities, such as poverty and access to healthcare.

Diarrheal diseases are the eighth leading cause of death worldwide; cholera contributes substantially, especially in low- and middle-income countries (*1*). Among cases reported by the World Health Organization (WHO), >94% are in Africa (*2*). Previous research has found several environmental and socioeconomic links with cholera, including temperature; precipitation; poverty; and water, sanitation, and hygiene (WASH) (*3,4*). Furthermore, extremes of these environmental and social conditions (e.g., droughts, floods, conflicts) can act as catalysts for outbreaks (*4–6*).

We focused on the effects of conflict on cholera outbreaks and compared the results for 2 countries in Africa, Nigeria and the Democratic Republic of the Congo (DRC), over the past 23 years. Several mechanisms through which conflict can lead to infectious disease outbreaks have been suggested (*7–9*). During conflicts, services can be disrupted, including access to WASH, disruption of disease control programs, and collapse of health systems (e.g., vaccination coverage). Persons displaced by conflict may also find it difficult to access healthcare (*10–12*). Populations may not seek medical treatment because they perceive healthcare facilities as unsafe. For example, during the 2018 Ebola outbreak in DRC, healthcare facilities were attacked, dampening efforts to control the virus (*12*). Conflict can worsen preexisting vulnerabilities, including poverty, because conflicts can cause loss of income, disruption to education, damage to livelihoods, and displacement (*13*).

Nigeria and DRC have social and environmental similarities as well as cholera outbreaks. Both countries experience active conflicts, such as the Boko Haram insurgency in northeastern Nigeria (*14*) and political unrest in eastern DRC (*15*). They also have the second (Nigeria) and third (DRC) highest numbers of estimated cholera cases per year in Africa (*16*); the most active cholera foci in the world are the DRC Kivu provinces (*17*). In addition, known cholera risk factors are present in Nigeria and DRC: tropical climate; poor access to WASH; and a large proportion of the population living in poverty (<$1.25/day), 87.7% for the DRC and 62% for Nigeria (*18*).

Few studies have investigated the effects of conflict on cholera outbreaks, especially quantitatively. Studies have commonly focused on cholera and conflict in Yemen (*8,19*), the effects of conflict on vaccination efforts (*20*), or the effects of conflict on other diseases such as Ebola (*12*) and COVID-19 (*21*).

Author affiliations: Imperial College London, London, UK (G.E.C. Charnley, K.A.M. Gaythorpe, K.A. Murray); Laboratoire MESuRS–Cnam Paris, Paris, France (K. Jean); Institut Pasteur, Paris, France (K. Jean); University College London, London (I. Kelman); University of Agder, Kristiansand, Norway (I. Kelman); MRC Unit The Gambia at London School of Hygiene and Tropical Medicine, Fajara, The Gambia (K.A. Murray)

[1]These senior authors contributed equally to this article..

Despite reporting a large proportion of global cases, Africa is a chronically understudied continent with regard to cholera (2).

To bridge this research gap, we used the self-controlled case series (SCCS) method, nationally and subnationally, and to provide insight into the effects of lag and cholera definition, we completed a sensitivity analysis. We used the SCCS method in a novel application and aim to explore and promote its use in other contexts (22). Previous uses include testing the effectiveness of drug and vaccine interventions at the individual (23,24) and population levels (25). Furthermore, to determine the proportion of cholera outbreaks attributable to conflict, we adapted the recently developed percentage attributable fraction (PAF) equations to this study (25). On the basis of these results, we suggest mechanisms for which conflict is driving cholera and potential risk factors, building on previous research in this area. We hope this information can be used to strengthen disease prevention in conflict settings and reduce additional illness and death during conflicts.

Methods

Datasets

We compiled cholera data from a range of publicly available sources: WHO disease outbreak news, ProMED, ReliefWeb, WHO Regional Office for Africa weekly outbreak and emergencies, UNICEF cholera platform (https://www.unicef.org), EM-DAT (https://emdat.be), the Nigerian Centre for Disease Control, and a literature search in English and French. The data are available in a GitHub repository (https://github.com/GinaCharnley/cholera_data_drc_nga), and additional information on data collation and validation are available in a complementary database paper (26). An outbreak was defined by the onset of the first cholera case, and the case definitions for the 2 countries are shown in the Appendix (https://wwwnc.cdc.gov/EID/article/28/12/21-2398-App1.pdf). Conflict data were provided by the United Nations Office for the Coordination of Humanitarian Affairs Humanitarian Data Exchange, which provides data from the Armed Conflict Location and Event Data Project (27). The data included subnational conflicts, categorized by type (e.g., battles, explosions, protests, riots, strategic developments, and violence against civilians).

The spatial granularity of the analysis was to administrative level 1 (states for Nigeria and provinces for DRC), and we aggregated all data points that were reported on a finer spatial scale to the upper level. The study period was January 1997–May 2020, the dates of the first and last reports in the conflict datasets. The temporal scale was set to weekly, with continuous weeks from epidemiological week 1 in 1997 through epidemiologic week 20 in 2020 (1–1,220 continuous weeks). We chose continuous weeks to be compatible with the model and to include periods of conflict that endured from one year into the next. We chose weeks, rather than days, to account for reporting lags because previous work has reported issues in the granularity of data and timeliness of reporting, especially during humanitarian crises, because of different sources of data and logistical difficulties (28,29) (Appendix).

Model Structure and Fitting

The SCCS method investigates the association between an exposure and an outcome event. The aim of SCCS is to estimate the effect, by comparing the relative incidence of the adverse events (outbreaks) within an exposure period of hypothesized excess risk (conflicts), compared with all other times (peace, according to the dataset used). The SCCS method is a case-only method and has the advantage of not needing separate controls by automatically controlling for fixed confounders that remain constant over the observation period (30,31).

Both the exposure and the event were set as binary outcomes, either being present (1) or not (0). The observation period was the full study period (1–1,220 continuous weeks). The exposure period was the first week after conflict onset and was reported as multiple onsets for each event, not 1 long exposure period incorporating all events in the specific week (or 2, 4, 6, 8, and 10 weeks). The event was defined by the week the cholera outbreaks were reported. Each event and exposure that occurred in the same state/province were assigned an identification number and a preexposure, exposure, and postexposure period (Appendix Table).

We fit the data to conditional logistic regression models by using the event (cholera outbreak onset) as the outcome variable [function clogit() in the R package survival] (32). As is standard for conditional logistic regression, the interval between the exposure to nonexposure period was offset (coefficient value of 1) in the model and the identification numbers were stratified. The model coefficient values were used to calculate incidence rate ratio (IRR), which quantifies the magnitude to which conflict increased the rate of cholera outbreaks.

To determine whether the significance of the effect of conflict on cholera outbreaks varied by subnational location and whether conflict was more influential in some states/provinces than others, we next split the datasets for each country by state/province and repeated the analysis for each. We conducted all statistical analyses by using R version 3.6.2 (The R Project for Statistical Computing, https://www.r-project.org), and the threshold for significance was p≤0.05.

Sensitivity Analysis

We used a sensitivity analysis to test different methods of defining the exposure end point, which was set to 1 week in the main analysis and 2, 4, 6, 8, and 10 weeks in the sensitivity analysis. Our aim was to further determine how long after conflict exposure the rate of cholera was heightened (Appendix Figures 1, 2).

To determine the effect of altering the cholera outbreak definition and to test for the temporal autocorrelation, we completed an additional sensitivity analysis that involved 2 scenarios. Scenario 1 removed all outbreaks within 2 weeks of each other (based on cholera biology: up to 10 days for bacterial shedding plus up to 5 days for incubation period) (33,34). Scenario 2 was an extreme scenario to fully test model robustness and removed all outbreaks within 6 months of each other.

PAF

We adapted the recently developed PAF equations (30) to the model output and data (Appendix). The PAF values estimate the percentage of outbreaks that could be attributed to conflict at a national level, and we used the full observation period of the datasets and the IRR values from the model results. We used bootstrap resampling (1,000 samples) to obtain 95% CIs. For each sample, we randomly sampled a value of IRR according to the parameters estimated in the SCCS analysis.

Results

Conflict and Cholera Occurrence

Temporal and spatial data showing the distribution of conflict and cholera in Nigeria and the DRC show an increase in reported conflict and cholera, especially after 2010 (Figure 1, panels A–D). A large proportion of the cholera cases have been reported in conflict-stricken areas (Figure 2).

The total number of conflicts and outbreaks for each state/province during the study period totaled 8,190 conflicts and 782 cholera outbreaks for Nigeria and 4,639 conflict and 396 cholera outbreaks for DRC (Figure 3). The outbreak distribution applied satisfactorily to the Poisson probability distribution (Appendix Figure 3).

To be included in the analysis, a state/province had to report outbreaks and conflicts during the study
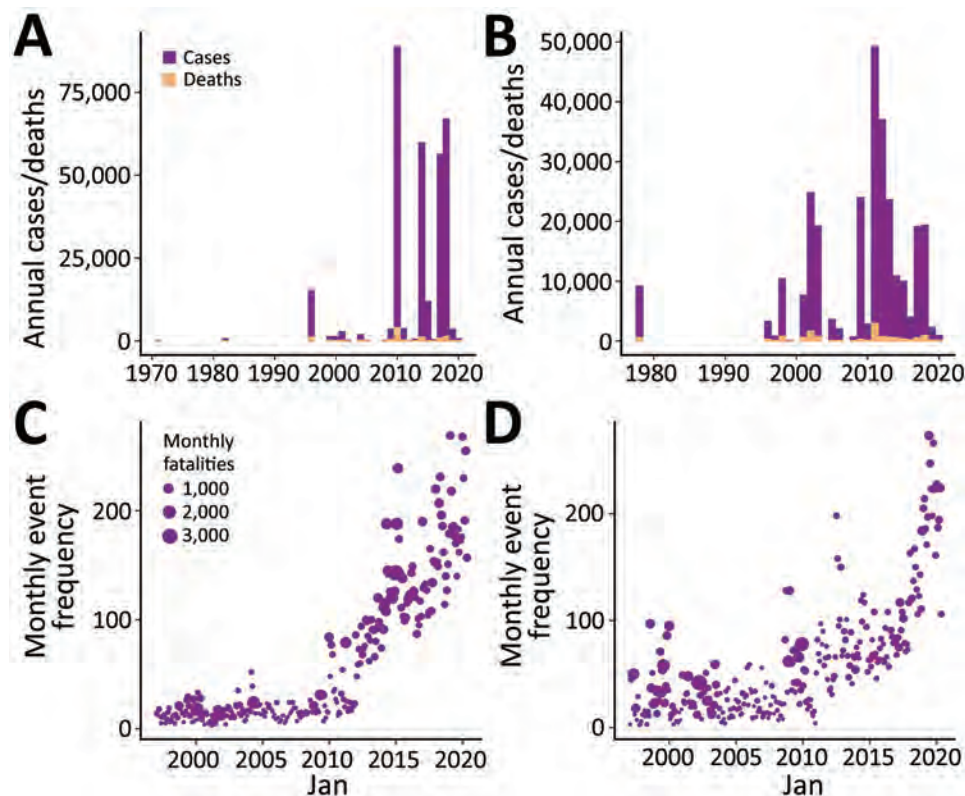

Figure 1. Changes in cholera and conflict for the full datasets used in study of the association between conflict and cholera in Nigeria and the Democratic Republic of the Congo (DRC). A, B) Monthly cholera cases and deaths for Nigeria (A) and DRC (B). C, D) Monthly frequency of conflict exposures and fatalities for Nigeria (C) and DRC (D).
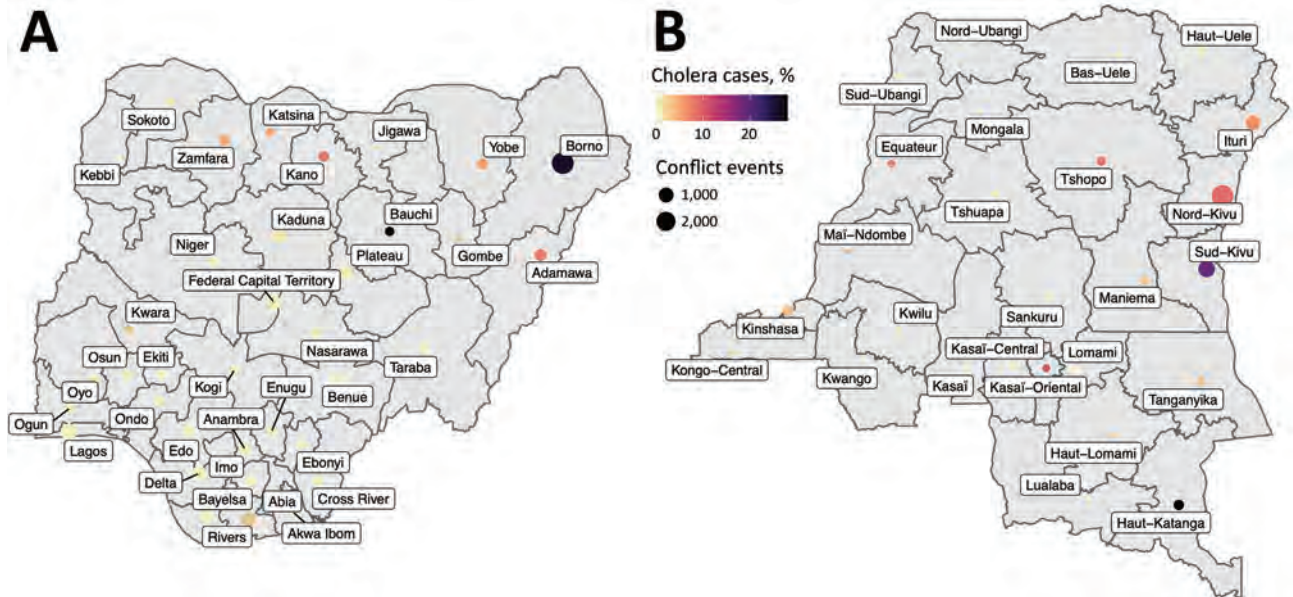
Figure 2. Number of conflicts and cholera cases as a percentage of the total number of national cases by administrative level 1 for Nigeria (A) and the Democratic Republic of the Congo (B).

period; because the SCCS method is a case-only approach, we excluded states/provinces that reported only conflicts (not any outbreaks). As such, 36 states were included for Nigeria and 22 provinces for DRC (Figure 4; Appendix).

Model Output

Conflict significantly increased the rate of cholera outbreaks (IRR) in the past 23 years in Nigeria and DRC (p≤0.05). The effect was of greater magnitude in Nigeria, increasing the risk for cholera outbreaks by up to 3.6 times (IRR 3.6 times, 95% CI 3.3–3.9 times), whereas, for DRC, the risk was increased by 2.6 times (IRR 2.6 times, 95% CI 2.3–2.9 times).

Of the 36 Nigeria states included in the analysis, we found statistically significant associations between conflict and cholera outbreaks for 24. The strongest effects were in Kebbi, Lagos, Osun, Borno, and Nasarawa; IRR values ranged from 6.2 to 6.8 times (Figure 5, panel A).

Of the 22 DRC provinces included in the analysis, we found a statistically significant relationship between conflict and cholera for 11. The strongest values were for Tanganyika, Kasaï-Oriental, Maniema, Nord-Kivu and Kasaï, and some were the highest values in the analysis. In Tanganyika, conflict increased cholera outbreak rate by 7.5 times and in Kasaï by 3.7 times (Figure 5, panel B).

Sensitivity Analyses

The effect of conflict on cholera outbreaks at the national and subnational level for Nigeria and DRC decreased with increasing exposure period. The

decrease in IRR from week 1 to week 10 was from 3.6 to 2.08 for Nigeria and 2.6 to 1.5 for DRC. By week 6, the change was minimal and plateaued or increased (Appendix Figures 4, 5).

Changing the outbreak onset definition yielded results similar to those of the original analysis. Removing events within 2 weeks and within 6 months of each other led to IRR values within the 95% CI of the initial definition. All results remained significant at p≤0.05 and provide evidence that temporal autocorrelation did not affect model robustness (Appendix Figure 6).

PAF

The IRR values from the model results indicating 3.6 for Nigeria and 2.6 for DRC were randomly resampled (1,000 samples). On the basis of these results, the onset of a conflict during the period from epidemiologic week 1 in 1997 to week 20 in 2020 was attributable to 19.7% (95% CI 18.2%–21.2%) of cholera outbreaks in Nigeria and 12.3% (95% CI 10.2%–14.4%) in DRC.

Discussion

Conflict was associated with an increased rate of cholera outbreaks by 3.6 times in Nigeria and 2.6 times in DRC. The percentages of cholera outbreaks attributable to conflicts during 1997–2020 (1,220 continuous weeks) were 19.7% for Nigeria and 12.3% for the DRC. The states/provinces where risk was highest were Kebbi, Nigeria, at 6.9 times, and Tanganyika,

DRC, at 7.3 times. This finding shows that the effect of conflict was much greater in some states/provinces than at the national level.

The sensitivity analysis evaluating the effect of lag showed decreasing effect as the weeks progressed; in some states/provinces, the effect plateaued or in-creased around 6 weeks after the exposure. The de-crease with the lag duration may be a diluting effect because the probability of an outbreak will increase across a longer period. The states/provinces that in-creased after week 6 were often those with the stron-gest initial effect, especially in the DRC. The larger
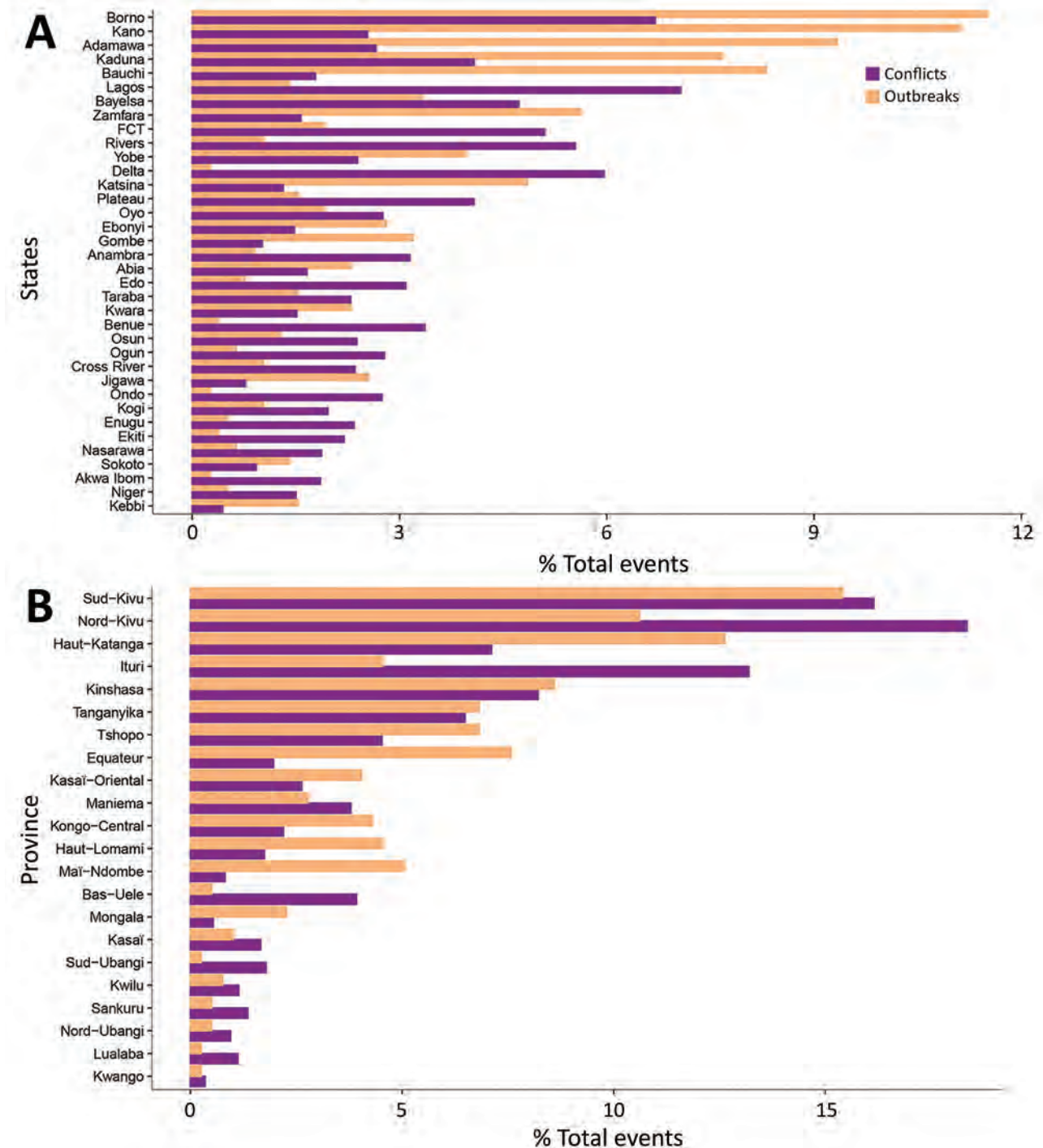

Figure 3. Percentage of events in each dataset used in study of the association between conflict and cholera for Nigeria (A) and the Democratic Republic of the Congo (B) by administrative level 1. FCT, Federal Capital Territory.
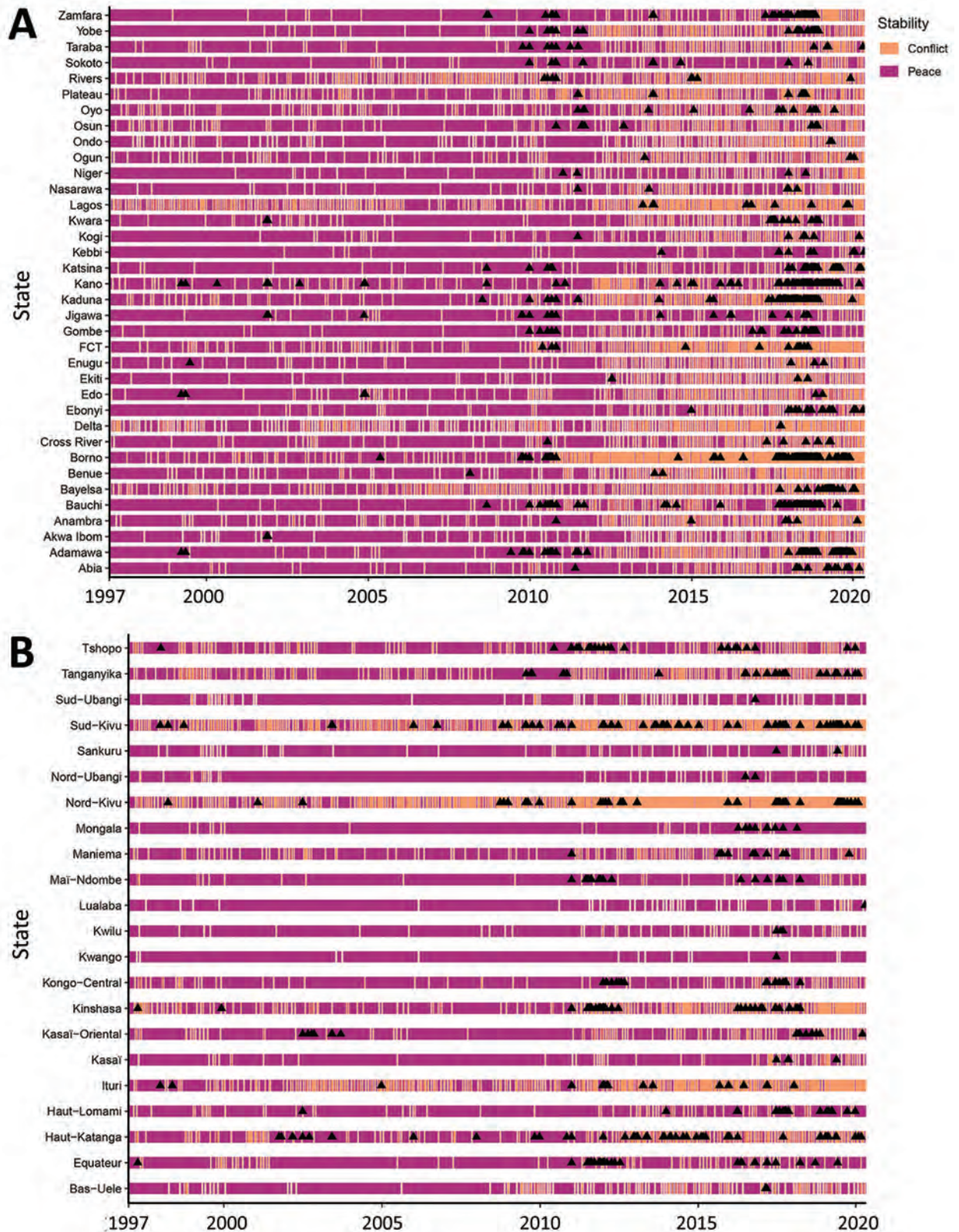
Figure 4. Swimmer plots showing the conflict exposure period in the self-controlled case series model (1 week after the onset) and the outbreaks (black triangles) for each state/province for Nigeria (A) and the Democratic Republic of the Congo (B). Data were compiled by epidemiologic week. FCT, Federal Capital Territory.
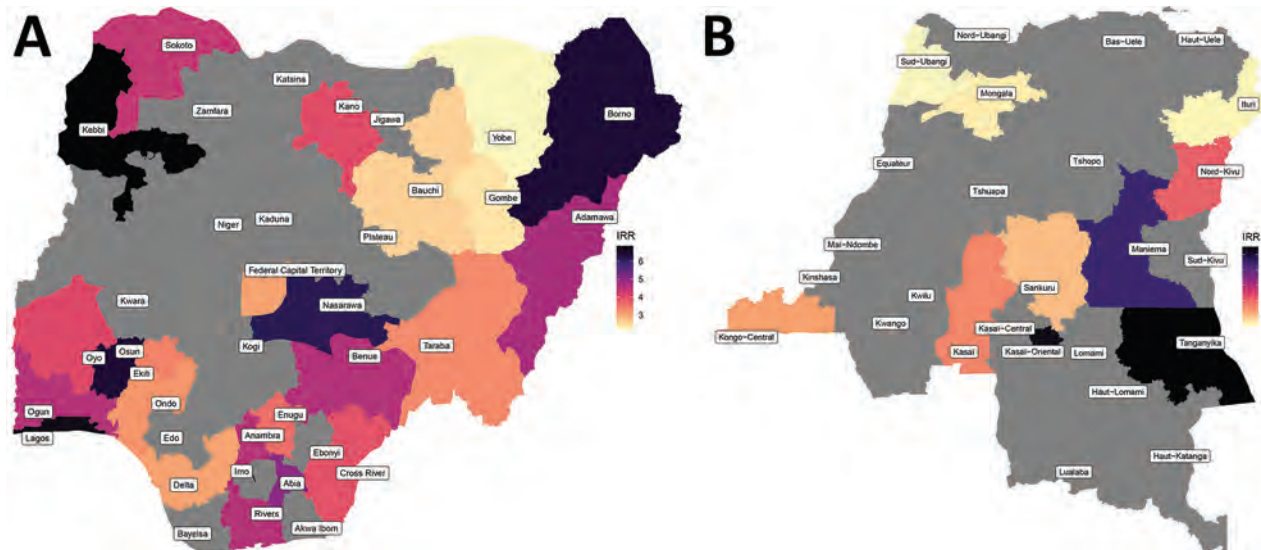
Figure 5. IRRs for the effect of exposure to conflict within 1 week of the event and cholera at a subnational level for Nigeria (A) and the Democratic Republic of the Congo (B). Only results that were significant at the threshold p≤0.05 are plotted. IRR, incidence rate ratio.

initial effect having a longer lasting effect may potentially result from conflict severity. The IRR values remained at >1 (2.08 Nigeria and 1.5 for DRC) at 10 weeks after the conflict, providing further evidence of a long-lasting effect of conflict.

States/provinces where rates of cholera increased most often coincided with areas of high conflict. This association further supports the hypothesis that conflict may be a driver of cholera in Nigeria and DRC. The effect of conflict exposure on cholera was also highly significant in states/provinces surrounding high-conflict areas (e.g., Abia, Ogun, Osun, Maniema, and Tanganyika), showing a potential spillover effect. The states/provinces were studied independently, but a possible explanation may be the fleeing of persons from areas of conflict or a cholera outbreak to neighboring states, because displacement is a known risk factor for disease outbreaks (9). This explanation is relevant for cholera because a large proportion of persons can be asymptomatic but still shed the pathogen into local reservoirs, which other persons use as drinking water because of a lack of alternatives (33).

Cholera outbreaks can be explosive and self-limiting because of the high number of asymptomatic persons, diluting the pool of susceptible persons (33), potentially explaining why the effects of conflict on cholera were seen just 1 week after the event. The incubation period of cholera is short (34), making the effect within the first week found here biologically possible for the pathogen and the time frame for elevated exposure realistic for resulting in cases. Other examples of cholera cases emerging within the first week after an adverse event include Cyclone Thane in the Bay of Bengal (35), water supply interruption in DRC (36), and Cyclone Aila in West Bengal, India (37). These examples provide further evidence of the need for quick and effective aid during humanitarian crises to avoid outbreaks and reduce deaths (38).

During periods of conflict, healthcare facilities can suffer and cholera outbreaks can overwhelm systems, potentially leading to the association between conflict and cholera. Care can be inaccessible because of direct infrastructure damage or difficulties getting to the facilities because of impromptu roadblocks (39). Supplies may be stolen or not deliverable, including oral rehydration solution, pathogen-sensitive antimicrobial drugs, and oral cholera vaccines, all of which are needed during cholera outbreaks (40). Last, safety is a serious concern for healthcare workers and patients; nongovernmental organizations can withdraw from these areas, citing an inability to ensure the safety of their staff (41). Steps need to be taken globally to reduce violence against healthcare workers, such as using active clinical management for all patients to enhance the acceptance of pathogen-specific treatment centers (42).

Conflict has the potential to worsen preexisting vulnerabilities, which can exacerbate poverty, another potential cause of the effect of conflict on cholera. The effects of poverty can be far-reaching and are a known risk for cholera (4,43) along with other diseases (44). For example, because of crowding and poor access to WASH, poor urban settlements have faced the brunt of outbreaks, including Zika infection, Ebola virus disease, typhoid, and cholera (45).

Conflict can result in loss of possessions, loss of habitual residence, and an inability to find employment, thereby reducing income generation, savings, and financial backstops (*13*). In times of worsening poverty, persons may not be able to afford healthcare and basic medical supplies, especially those in vulnerable groups. This disruption to daily life can cause many more deaths than direct battlefield fatalities and leads to stagnated development (*46*).

Although we did not directly evaluate WASH and poverty, a lack of WASH facilities is likely to have contributed to the positive association between cholera and conflict. Conflict can lead to disruption in sanitation and hygiene, and adverse events can act as catalysts in the interaction of contaminated water and the human populations (*3*). Displacement from conflict can cause difficulties accessing WASH (e.g., latrine access, soap availability), and rapid cholera outbreaks have occurred in several displacement camps, including in DRC after the Rwanda genocide in 1994 (*2*). Displacement of persons because of conflict may result in the use of water contaminated with toxigenic strains of *Vibrio cholerae* because alternative water sources are lacking, leading to outbreaks.

A potential limitation of our analysis is the plausible existence of multiple causal pathways, leading to misclassification because of time/variant confounders. Examples include a conflict in an adjacent geographic area being causally linked to the conflict in the current geographic area or the presence of bodies of water, which are considered fundamental in cholera transmission (*47,48*). Additional environmental factors (e.g., seasonal weather changes and preexisting vulnerabilities) are beyond the scope of the methods that we used, which investigate conflict in isolation.

The degree of effect that we found may be affected by underreporting, overreporting, and delayed reporting. Underreporting is a significant issue in global cholera and conflict estimates because of asymptomatic case-patients, disincentives to report, and logistics issues (*29,49*). Cholera surveillance is difficult during conflicts because of displaced populations and security concerns. In addition, our method may have resulted in a classification bias, underestimating the effect of conflict on cholera. If a cholera outbreak was imported from a neighboring state/province (spatial autocorrelation), it would be classified as a genuine, autochthonous event, which would probably be nondifferential (likely to happen during a period of exposure or nonexposure). Alternatively, during times of conflict, health surveillance can be enhanced by the government or nongovernmental organizations. Reporting delay is another potential

problem, and some national reporting delays have been found to range from 12 days for meningococcal disease to 40 days for pertussis (*28*).

The SCCS model is a case-only approach; analyzing cases only, instead of the corresponding complete cohort, results in loss of efficiency. However, previous work has shown that the loss is small, especially when the fraction of the sample experiencing the exposure is high (Appendix). Moreover, loss of efficiency must be weighed against better control of time-invariant confounders. Previous examples illustrated that the SCCS design is likely to produce more trustworthy results than the corresponding cohort analysis, especially when a strong residual confounding bias is likely (*30,31*).

We did not evaluate the severity or intensity of the conflict and cholera outbreaks; instead, we used a binary variable. Conflict severity is complex, far-reaching, and challenging to measure. Making assessments and assumptions of how conflict affects a health outcome is difficult and may involve oversimplification. Qualitative conflict severity research is needed but is beyond the scope of this article.

Despite the limitations of conflict and cholera data, the data that we used are of the highest standard available and have been used by several other studies, making the research comparable (*11,12*). In addition, we used several methods to validate the cholera data (*26*). Creating partnerships with those working on the ground and exploring more sensitive data options is an area of future research. Additional methods that we used to account for data limitations included setting both the event and the exposure to a binary outcome to reduce the effects of severity and using a weekly instead of daily temporal scale to account for delays.

In summary, our analysis shows a clear relationship between cholera and conflict in Nigeria and DRC; conflict was associated with an increased rate of cholera by up to 7.3 times in some states/provinces. The flexibility of SCCS and conditional logistic regression models makes future work evaluating different diseases, countries, and additional risk factors relatively simple. Cholera risks are probably multifactorial and complex; however, sufficient and rapid support, along with enhanced efforts to build community trust can reduce this excess risk. Finding conflict resolution and addressing preexisting vulnerabilities (poverty, healthcare, and WASH) should be the main priority. Reducing those vulnerabilities will give communities greater resources to adapt and reduce vulnerabilities in times of conflict as well as peace.

Acknowledgments

About the Author

Ms. Charnley is a postgraduate researcher in the School of Public Health at Imperial College London. She participates in the Science and Solutions for a Changing Planet doctoral training partnership through the Grantham Institute, and her PhD degree research focuses on infectious disease outbreaks during and after disasters such as natural hazards and conflict and how climate change may alter these outbreaks.

References

1. World Health Organization. The top 10 causes of death [cited 2018 Sep 9]. https://www.who.int/news-room/fact-sheets/detail/the-top-10-causes-of-death
2. Bompangue Nkoko D, Giraudoux P, Plisnier PD, Tinda AM, Piarroux M, Sudre B, et al. Dynamics of cholera outbreaks in Great Lakes region of Africa, 1978-2008. Emerg Infect Dis. 2011;17:2026–34.
3. D'Mello-Guyett L, Gallandat K, Van den Bergh R, Taylor D, Bulit G, Legros D, et al. Prevention and control of cholera with household and community water, sanitation and hygiene (WASH) interventions: a scoping review of current international guidelines. PLoS One. 2020;15:e0226549. https://doi.org/10.1371/journal.pone.0226549
4. Leckebusch GC, Abdussalam AF. Climate and socioeconomic influences on interannual variability of cholera in Nigeria. Health Place. 2015;34:107–17. https://doi.org/10.1016/j.healthplace.2015.04.006
5. Charnley GEC, Kelman I, Green N, Hinsley W, Gaythorpe KAM, Murray KA. Exploring relationships between drought and epidemic cholera in Africa using generalised linear models. BMC Infect Dis. 2021;21:1177. https://doi.org/10.1186/s12879-021-06856-4
6. Gormley M. Untangling the causes of the 2016-18 cholera epidemic in Yemen. Lancet Glob Health. 2018;6:e600–1. https://doi.org/10.1016/S2214-109X(18)30243-2
7. Al-Salem WS, Pigott DM, Subramaniam K, Haines LR, Kelly-Hope L, Molyneux DH, et al. Cutaneous leishmaniasis and conflict in Syria. Emerg Infect Dis. 2016;22:931–3. https://doi.org/10.3201/eid2205.160042
8. Dureab FA, Shibib K, Al-Yousufi R, Jahn A. Yemen: cholera outbreak and the ongoing armed conflict. J Infect Dev Ctries. 2018;12:397–403. https://doi.org/10.3855/jidc.10129
9. Watson JT, Gayer M, Connolly MA. Epidemics after natural disasters. Emerg Infect Dis. 2007;13:1–5. https://doi.org/10.3201/eid1301.060779
10. Charnley GEC, Kelman I, Gaythorpe KAM, Murray KA. Traits and risk factors of post-disaster infectious disease outbreaks: a systematic review. Sci Rep. 2021;11:5616. https://doi.org/10.1038/s41598-021-85146-0
11. Gayer M, Legros D, Formenty P, Connolly MA. Conflict and emerging infectious diseases. Emerg Infect Dis. 2007;13:1625–31. https://doi.org/10.3201/eid1311.061093
12. Wells CR, Pandey A, Ndeffo Mbah ML, Gaüzère BA, Malvy D, Singer BH, et al. The exacerbation of Ebola outbreaks by conflict in the Democratic Republic of the Congo. Proc Natl Acad Sci U S A. 2019;116:24366–72. https://doi.org/10.1073/pnas.1913980116
13. Okunlola OC, Okafor IG. Conflict–poverty relationship in Africa: a disaggregated approach. J Interdiscip Econ. 2020;34:1–26.
14. Agbiboa D. The ongoing campaign of terror in Nigeria: Boko Haram versus the state. Stability: International Journal of Security and Development. 2013;2:52.
15. Council on Foreign Relations. Violence in the Democratic Republic of Congo [cited 2018 Sep 9]. https://www.cfr.org/global-conflict-tracker/conflict/violence-democratic-republic-congo
16. Ali M, Nelson AR, Lopez AL, Sack DA. Updated global burden of cholera in endemic countries. PLoS Negl Trop Dis. 2015;9:e0003832. https://doi.org/10.1371/journal.pntd.0003832
17. Bompangue D, Giraudoux P, Piarroux M, Mutombo G, Shamavu R, Sudre B, et al. Cholera epidemics, war and disasters around Goma and Lake Kivu: an eight-year survey. PLoS Negl Trop Dis. 2009;3:e436. https://doi.org/10.1371/journal.pntd.0000436
18. United Nations Statistical Division. 2015. Millennium development goal indicators [cited 2018 Sep 9]. https://unstats.un.org/unsd/mdg/SeriesDetail.aspx?srid=580
19. Blackburn CC, Lenze PE Jr, Casey RP. Conflict and cholera: Yemen's man-made public health crisis and the global implications of weaponizing health. Health Secur. 2020;18:125–31. https://doi.org/10.1089/hs.2019.0113
20. Sato R. Effect of armed conflict on vaccination: evidence from the Boko Haram insurgency in northeastern Nigeria. Confl Health. 2019;13:49. https://doi.org/10.1186/s13031-019-0235-8
21. Tijjani SJ, Ma L. Is Nigeria prepared and ready to respond to the COVID-19 pandemic in its conflict-affected northeastern states? Int J Equity Health. 2020;19:77. https://doi.org/10.1186/s12939-020-01192-6
22. Farrington CP. Relative incidence estimation from case series for vaccine safety evaluation. Biometrics. 1995;51:228–35. https://doi.org/10.2307/2533328
23. Brauer R, Smeeth L, Anaya-Izquierdo K, Timmis A, Denaxas SC, Farrington CP, et al. Antipsychotic drugs and risks of myocardial infarction: a self-controlled case series study. Eur Heart J. 2015;36:984–92. https://doi.org/10.1093/eurheartj/ehu263
24. Douglas IJ, Evans SJ, Pocock S, Smeeth L. The risk of fractures associated with thiazolidinediones: a self-controlled case-series study. PLoS Med. 2009;6:e1000154. https://doi.org/10.1371/journal.pmed.1000154
25. Jean K, Raad H, Gaythorpe KAM, Hamlet A, Mueller JE, Hogan D, et al. Assessing the impact of preventive mass vaccination campaigns on yellow fever outbreaks in Africa: a population-level self-controlled case series study.

PLoS Med. 2021;18:e1003523. https://doi.org/10.1371/journal.pmed.1003523

26. Charnley GEC, Kelman I, Gaythorpe KAM, Murray KAM. Accessing sub-national cholera epidemiological data for Nigeria and the Democratic Republic of Congo during the seventh pandemic. BMC Infect Dis. 2022;22:288. https://doi.org/10.1186/s12879-022-07266-w

27. HDX. The Humanitarian Data Exchange [cited 2018 Sep 9]. https://data.humdata.org

28. Ri S, Blair AH, Kim CJ, Haar RJ. Attacks on healthcare facilities as an indicator of violence against civilians in Syria: an exploratory analysis of open-source data. PLoS One. 2019;14:e0217905. https://doi.org/10.1371/journal.pone.0217905

29. Weidmann NB. A closer look at reporting bias in conflict event data. Am J Pol Sci. 2016;60:206–18. https://doi.org/10.1111/ajps.12196

30. Petersen I, Douglas I, Whitaker H. Self controlled case series methods: an alternative to standard epidemiological study designs. BMJ. 2016;354:i4515. https://doi.org/10.1136/bmj.i4515

31. Whitaker HJ, Farrington CP, Spiessens B, Musonda P. Tutorial in biostatistics: the self-controlled case series method. Stat Med. 2006;25:1768–97. https://doi.org/10.1002/sim.2302

32. Therneau TM. A package for survival analysis in R [cited 2018 Oct 2]. https://CRAN.R-project.org/package=survival

33. King AA, Ionides EL, Pascual M, Bouma MJ. Inapparent infections and cholera dynamics. Nature. 2008;454:877–80. https://doi.org/10.1038/nature07084

34. Azman AS, Rudolph KE, Cummings DA, Lessler J. The incubation period of cholera: a systematic review. J Infect. 2013;66:432–8. https://doi.org/10.1016/j.jinf.2012.11.013

35. Fredrick T, Ponnaiah M, Murhekar MV, Jayaraman Y, David JK, Vadivoo S, et al. Cholera outbreak linked with lack of safe water supply following a tropical cyclone in Pondicherry, India, 2012. J Health Popul Nutr. 2015;33:31–8.

36. Jeandron A, Saidi JM, Kapama A, Burhole M, Birembano F, Vandevelde T, et al. Water supply interruptions and suspected cholera incidence: a time-series regression in the Democratic Republic of the Congo. PLoS Med. 2015;12:e1001893. https://doi.org/10.1371/journal.pmed.1001893

37. Bhunia R, Ghosh S. Waterborne cholera outbreak following Cyclone Aila in Sundarban area of West Bengal, India, 2009. Trans R Soc Trop Med Hyg. 2011;105:214–9. https://doi.org/10.1016/j.trstmh.2010.12.008

38. Tauxe RV, Holmberg SD, Dodin A, Wells JV, Blake PA. Epidemic cholera in Mali: high mortality and multiple routes of transmission in a famine area. Epidemiol Infect. 1988;100:279–89. https://doi.org/10.1017/S0950268800067418

39. Sousa C, Hagopian A. Conflict, health care and professional perseverance: a qualitative study in the West Bank. Glob Public Health. 2011;6:520–33. https://doi.org/10.1080/17441692.2011.574146

40. Cartwright EJ, Patel MK, Mbopi-Keou FX, Ayers T, Haenke B, Wagenaar BH, et al. Recurrent epidemic cholera with high mortality in Cameroon: persistent challenges 40 years into the seventh pandemic. Epidemiol Infect. 2013; 141:2083–93. https://doi.org/10.1017/S0950268812002932

41. Médecins Sans Frontières. DRC: violent attacks against staff force MSF to end projects in Fizi territory, South Kivu [cited 2018 Sep 9]. https://www.msf.org/msf-forced-pull-out-eastern-drc-territory-following-violent-attacks

42. Nguyen VK. An epidemic of suspicion—Ebola and violence in the DRC. N Engl J Med. 2019;380:1298–9. https://doi.org/10.1056/NEJMp1902682

43. Penrose K, de Castro MC, Werema J, Ryan ET. Informal urban settlements and cholera risk in Dar es Salaam, Tanzania. PLoS Negl Trop Dis. 2010;4:e631. https://doi.org/10.1371/journal.pntd.0000631

44. Fallah MP, Skrip LA, Gertler S, Yamin D, Galvani AP. Quantifying poverty as a driver of Ebola transmission. PLoS Negl Trop Dis. 2015;9:e0004260. https://doi.org/10.1371/journal.pntd.0004260

45. Eisenstein M. Disease: poverty and pathogens. Nature. 2016;531:S61–3. https://doi.org/10.1038/531S61a

46. Trani JF, Bakhshi P, Noor AA, Lopez D, Mashkoor A. Poverty, vulnerability, and provision of healthcare in Afghanistan. Soc Sci Med. 2010;70:1745–55. https://doi.org/10.1016/j.socscimed.2010.02.007

47. Birmingham ME, Lee LA, Ndayimirije N, Nkurikiye S, Hersh BS, Wells JG, et al. Epidemic cholera in Burundi: patterns of transmission in the Great Rift Valley Lake region. Lancet. 1997;349:981–5. https://doi.org/10.1016/S0140-6736(96)08478-4

48. Bompangue D, Giraudoux P, Handschumacher P, Piarroux M, Sudre B, Ekwanzala M, et al. Lakes as source of cholera outbreaks, Democratic Republic of Congo. Emerg Infect Dis. 2008;14:798–800. https://doi.org/10.3201/eid1405.071260

49. Elimian KO, Musah A, Mezue S, Oyebanji O, Yennan S, Jinadu A, et al. Descriptive epidemiology of cholera outbreak in Nigeria, January-November, 2018: implications for the global roadmap strategy. BMC Public Health. 2019;19:1264. https://doi.org/10.1186/s12889-019-7559-6

Address for correspondence: Gina E. C. Charnley, Imperial College London, School of Public Health, St. Mary's Campus, Norfolk Place, London, W2 1PG, UK; email: g.charnley19@imperial.ac.uk

Emergence and Evolutionary Response of *Vibrio cholerae* to Novel Bacteriophage, Democratic Republic of the Congo[1]

Meer T. Alam,[2] Carla Mavian,[2] Taylor K. Paisie, Massimiliano S. Tagliamonte, Melanie N. Cash, Angus Angermeyer, Kimberley D. Seed, Andrew Camilli, Felicien Masanga Maisha, R. Kabangwa Kakongo Senga, Marco Salemi, J. Glenn Morris, Jr., Afsar Ali

Cholera causes substantial illness and death in Africa. We analyzed 24 toxigenic *Vibrio cholerae* O1 strains isolated in 2015–2017 from patients in the Great Lakes region of the Democratic Republic of the Congo. Strains originating in southern Asia appeared to be part of the T10 introduction event in eastern Africa. We identified 2 main strain lineages, most recently a lineage corresponding to sequence type 515, a *V. cholerae* cluster previously reported in the Lake Kivu region. In 41% of fecal samples from cholera patients, we also identified a novel ICP1 (Bangladesh cholera phage 1) bacteriophage, genetically distinct from ICP1 isolates previously detected in Asia. Bacteriophage resistance occurred in distinct clades along both internal and external branches of the cholera phylogeny. This bacteriophage appears to have served as a major driver for cholera evolution and spread, and its appearance highlights the complex evolutionary dynamic that occurs between predatory phage and bacterial host.

Cholera remains an ongoing public health threat on the continent of Africa, especially in the Democratic Republic of the Congo (DRC), which in 2020 reported the largest number of cases (19,789) of any country in the world with the exception of Yemen (*1*). Biotype El Tor strains of the seventh cholera pandemic (P7ET) were first reported in Africa in the early 1970s (*2–6*). Major outbreaks occurred in DRC in 2008, 2009, 2011–2012, 2013, and 2015–2017; in 2017 alone, an estimated 53,000 cholera cases with 1,145 deaths were reported from 20 of 26 provinces in DRC (*2*). Outbreaks have been most persistent in the eastern part of DRC in the Great Lakes region, along the Albertine Rift (*2–4*).

As reported elsewhere (*3*), strains appear to have been initially introduced into this area as part of what has been characterized as the T5 introduction (1970–1972) under the first wave of P7ET. In 1992, as part of the third wave of P7ET, the disease was reintroduced by a strain from southern Asia, in what has been designated as the T10 introduction event (*3*). Subsequent studies have documented persistence of T10 strains in this region, and ongoing cholera outbreaks in the Great Lakes region and spread of strains from this area suggest establishment of a regional focus of endemic disease derived from the T10 introduction (*6*).

Bacteriophages (phages) and their host bacteria follow predator–prey dynamics that drive co-evolution, resulting in the long-term persistence of both within ecosystems (*7*). Phage predation has been linked with seasonal patterns of cholera emergence and with clinical response to infection in humans (*8–11*). Phages are generally highly specific to their host; thus, both phage and susceptible host must maintain a dynamic equilibrium to coexist. Recently, it has been shown that mobile genetic elements associated with sulfamethoxazole/trimethoprim (SXT) antimicrobial resistance, designated as SXT integrative conjugative

[1]Previously presented at Epidemics—8th International Conference on Infectious Diseases Dynamics [online], November 30–December 3, 2021.

[2]These authors contributed equally to this article.

elements (ICEs), can determine phage resistance in *V. cholerae* (*12*). Furthermore, another study has demonstrated that susceptibility to phage killing of marine *V. lentus* was mediated by as many as 6–12 mobile genetic elements (*13*). Taken together, these recent studies support the concept that phage/host in situ interplay has a major role in adaptation and evolution.

Using microbiologic, phylogenomic, and molecular clock analyses, we investigated endemic cholera in the DRC Great Lakes regional hotspot. We also explored the genetic resistance of these *V. cholerae* strains to a novel ICP1 (Bangladesh cholera phage 1) *V. cholerae* phage isolated in cholera patients in the region and genetically distinct from previous ICP1 phages detected in Asia (*14,15*).

Methodsphage/

Isolation and Characterization of Toxigenic
V. cholerae O1 and Virulent Phages
In an initial study involving the isolation and characterization of toxigenic *V. cholerae* O1 strains, we

collected fecal samples from suspected cholera patients admitted to cholera treatment centers around Goma, DRC, during 2015–2017 (Table). After collection, we brought the samples to the Laboratoire Provincial de Sante Publique du Nord-Kivu in Goma for microbiological and serologic analysis. We isolated bacteria and confirmed species using methods described elsewhere (*16*), then stored strains in soft Luria-Bertani (LB) Miller agar (0.7% agar) and sent them to the Emerging Pathogens Institute at the University of Florida (Gainesville, FL, USA) for sequencing.

In a second study, we tried to isolate phages preying on *V. cholerae* O1 strains from fecal samples obtained in 2016–2017 from 41 additional cholera patients. We centrifuged cholera rice-water fecal samples at 5,000 × *g* for 10 minutes and filtered resultant supernatant through a 0.22-µm syringe filter, stored them at 4°C in a sterile microfuge tube, and sent them to the Emerging Pathogens Institute for analysis. To identify virulent phages, we tested each filtered fecal sample using standard plaque assay against *V. cholerae* O1 AGC-15, a strain we randomly selected

Table. Characteristics of toxigenic *Vibrio cholerae* O1 strains isolated from the Democratic Republic of the Congo, 2015–2017*

Strain	Isolation date	Province/location	Serotype		Susceptibility of *V. cholerae* to ICP1_2017_A_DRC†	Mutation in O1 antigen and other genes‡	SRA ID
			Ogawa	Inaba			
AGC-1	2015 Apr 30	North Kivu/Kirotshe	–	+	S	–	SRR15192533
AGC-2	2015 May 18	Goma/Buhimba	–	+	S	–	SRR15192532
AGC-3	2015 May 20	Mutwanga	–	+	R	*rfbD*	SRR15192521
AGC-4	2015 Mar 07	Goma/Buhimba	–	+	R	*rfbN*	SRR15192516
AGC-5	2015 Mar 20	Goma/Buhimba	–	+	S	–	SRR15192515
AGC-6	2015 Jul 26	Goma/Buhimba	–	+	R	*rfbV*, VC0559 (hypothetical), *rplE*, *phrA*, *fliD*, VC0672 (hypothetical)	SRR15192514
AGC-7	2015 Jun 06	Goma/Buhimba	–	+	S	–	SRR15192513
AGC-8	2015 Aug 06	Goma/Buhimba	–	+	S	–	SRR15192512
AGC-9	2016 Jun 20	Maniema/Kabambare	+	–	S	–	SRR15192511
AGC-10	2016 Aug 09	Karisimbi/Hop Millitaire	–	+	R	*rfbD*	SRR15192510
AGC-11	2016 May 28	Alimbongo	–	+	R	*rfbD*	SRR15192531
AGC-12	2016 Jul 27	South Kivu/Fizi	+	–	S	–	SRR15192530
AGC-13	2016 Aug 08	Maniema/Kimbilulenge	+	–	S	–	SRR15192529
AGC-14	2017 May 18	Kirotshe/Rubaya	–	+	S	–	SRR15192528
AGC-15	2017 May 31	Rutshuru/Hgr	–	+	S	–	SRR15192527
AGC-16	2017 Jun 10	Rutshuru/Hgr	–	+	S	–	SRR15192526
AGC-17	2017 Jul 01	Nyiragongo/Turunga	–	+	S	–	SRR15192525
AGC-18	2017 Jul 03	Goma/Hop.Provincial	–	+	S§	*manA*	SRR15192524
AGC-19	2017 Jul 03	Goma/Hop.Provincial	–	+	S	–	SRR15192523
AGC-20	2019 Jul 03	Goma/Hop.Provincial	–	+	S	–	SRR15192522
AGC-21	2017 Jul 06	Karisimbi/Prison centrale	–	+	S	–	SRR15192520
AGC-22	2017 Jul 14	Karisimbi/Majengo	–	+	S§	*manA*	SRR15192519
AGC-23	2017 Jul 19	Karisimbi/Majengo	–	+	R	*rfbB*	SRR15192518
AGC-24	2017 Jul 15	Karisimbi/Majengo	–	+	S	*rfbU*	SRR15192517

*R, resistant; S, susceptible; +, positive; –, negative
†Susceptibility to a virulent ICP1 phage (ICP1_2017_A_DRC) determined by strains yielding either complete resistance or forming turbid plaques in response to phage infection in plaque assay. The penultimate column indicates which strains had mutations in the O1-antigen biosynthetic complex and in other genes in the chromosome, with the mutated gene designated. AGC-18, AGC-22, and AGC-24 sustained 1, 1, and 18 bp deletion mutations in the indicated gene(s), resulting in a frame shift mutation in that gene, but all other ICP1 phage-resistant isolates sustained $\geq$1 missense mutation in the O-antigen biosynthetic gene cluster.
‡As detected by analysis using single-nucleotide polymorphism, insertion/deletion, or both.
§Plaques were turbid as described elsewhere (*29*).

from the DRC isolates from the first part of the study (Table). AGC-15 has the wild-type *ompU* sequence, which encodes the receptor for ICP2; it also has the wild-type O1-antigen biosynthetic genetic region that serves as the receptor for ICP1 and ICP3 (*14*) and lacks any PLE elements mediating immunity to ICP1 (*17*). For phage purification, we picked a single clear plaque using a Pasteur pipette into 1 mL of LB broth and incubated it overnight at 4°C to enable the phage to diffuse out of the soft agar. We made high-titer stocks of purified phage by infecting AGC-15 with phage in LB broth culture.

Whole-Genome Mapping and High-Quality Single-Nucleotide Polymorphism Calling
We performed whole-genome sequencing on the 24 *V. cholerae* O1 isolates from the first part of the study with the Illumina MiSeq for 500 cycles (Qui); we further conducted high-quality single-nucleotide polymorphism (hqSNP) calling (Appendix, https://wwwnc.cdc.gov/EID/article/28/12/220572-App1.pdf). The final genomewide hqSNP alignment included 120 T10 sublineage *V. cholerae* genome sequences: 24 strains collected as part of our study (Table); 71 from publicly available genomes from outbreaks in eastern DRC during 2014–2016 (*6*); 6 archival and publicly available DRC genomes collected during 2001–2013; 17 genomes collected across Africa during 1998–2014; and 2 publicly available genomes from India, ancestors of T10 sublineage (*3*) (Appendix Table 1). We performed multilocus sequence typing analysis using the online tool PubMLST (K. Jolley, unpub data, https://doi.org/10.12688/wellcomeopenres.14826.1) (Appendix Table 2).

Phylogeography
All datasets used in this study passed phylogenetic quality checks (Appendix Figure 1). To explore the origins of strains in the eastern portion of DRC and neighboring countries we used the Bayesian phylogeographic coalescent-based method implemented in BEAST version 1.10.4 software (*18–20*). The reconstruction of *V. cholerae* O1 spatiotemporal spread from different locations through Bayesian phylogeography requires calibration of a molecular clock. We estimated evolutionary rates implementing a Hasegawa-Kishino-Yano nucleotide substitution model (*21*) with empirical base frequencies, gamma distribution of site-specific rate heterogeneity, and ascertainment bias correction (*22*), testing a constant demographic prior against nonparametric demographic models, Gaussian Markov random field Skyride (*23*) and Bayesian Skyline plot (*24*), to rule out spurious changes

in effective population size inferred by a nonparametric model, which would, in turn, effect timing of divergence events (*25*). We obtained the weighted average of synonymous (*dS*) and nonsynonymous substitution rates (*dN*) in the protein-coding regions of the *V. cholerae* O1 genome for all internal and external branches from a subset of 200 Bayesian maximum credibility clade (MCC) trees randomly obtained from the posterior distribution of trees, as described elsewhere (*26,27*).

Whole genome sequencing, genome assembly and annotation of DRC phages
We sequenced 8 plaque-purified phages isolated from 8 independent patient fecal samples with Illumina MiSeq for 50 cycles. We obtained >200-fold coverage that helped with de novo assembly of each phage genome into 1 complete contig using CLC Genomics Workbench (QIAGEN, https://www.qiagen.com). We manually confirmed and corrected low-coverage or problem areas as needed to ensure authentic genome assembly. We annotated phage genomes as described elsewhere (*15*) and deposited sequences into the National Center for Biotechnology Information Sequence Read Archive (BioProject identification no. PRJNA748018; Appendix Table 3).

Results
Of the 24 toxigenic *V. cholerae* O1 strains isolated from fecal samples from cholera patients attending cholera treatment centers during 2015–2017 in the Goma region, 21 (87.5%) were serotype Inaba and 3 (12.5%) serotype Ogawa (Table). All strains in wave 3 were *ctxB* genotype-I and within the T10 introductory clade (*3,6*). Consistent with findings published elsewhere (*3*), our MCC tree (Figure 1; Appendix Figure 2) indicated a mean time for the most recent common ancestor (tMRCA) of the T10 *V. cholerae* sublineage introduced to Africa of March 1994 (95% highest posterior density [HPD] September 1991–February 1996). In addition, our analysis showed that subsequent independent introductions (spillover events denoted by asterisks in Figure 1) in the DRC Great Lakes region likely occurred from Rwanda. The first spillover, in May 2001 (95% HPD September 1999–June 2001), is represented by a DRC isolate, ERR1878097_CD_2003, that branches out of a lineage circulating in Rwanda (Figure 1). The other event resulted in 2 major monophyletic clades that match multilocus sequence types reported elsewhere (*6*).

The tMRCA of the first major lineage (denoted as I in Figure 1), February 2009 (95% HPD November 2005–September 2011), corresponds to the sequence
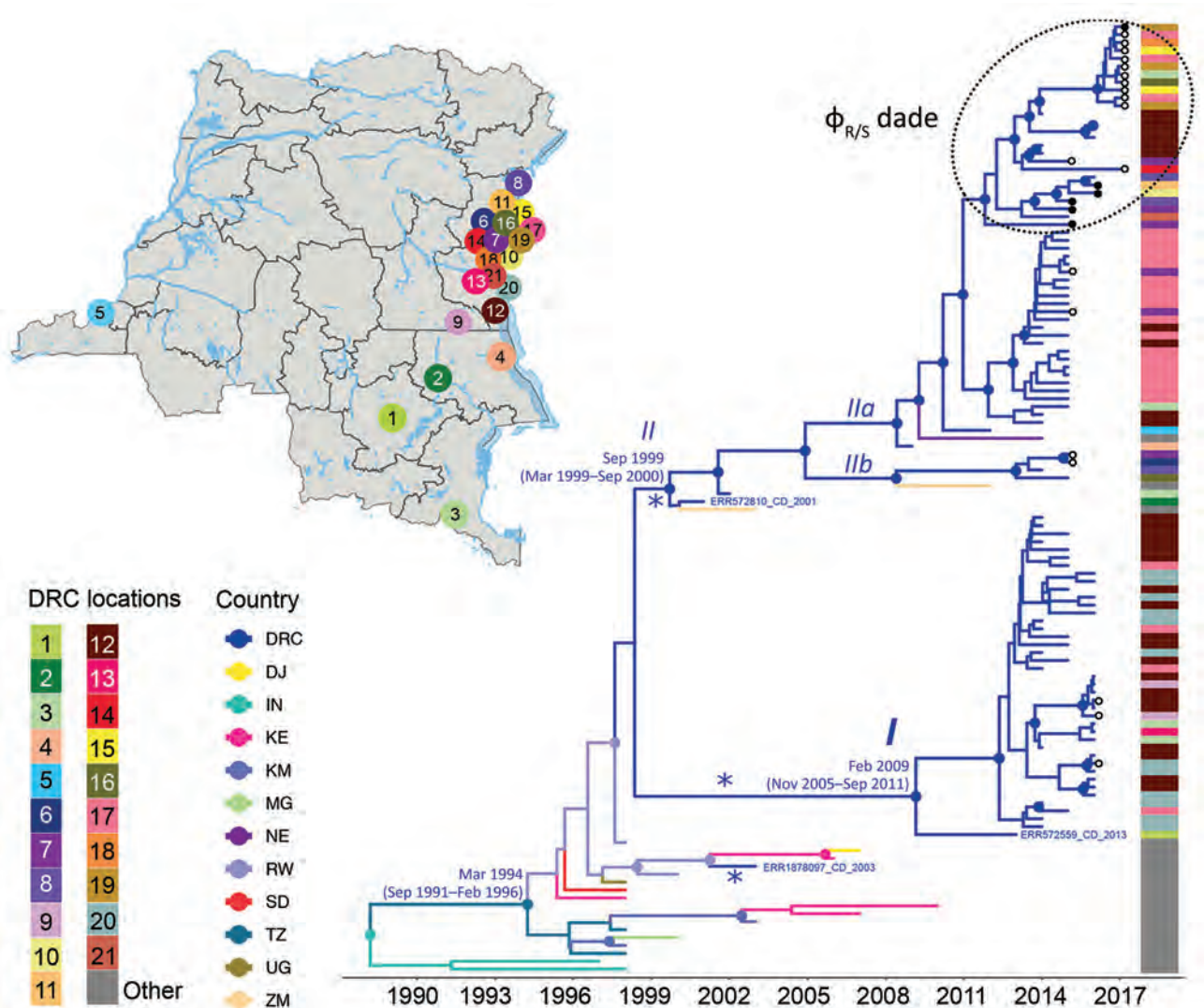
Figure 1. Spatiotemporal evolution and dissemination of *Vibrio cholerae* epidemic in the Democratic Republic of the Congo, 2015–2017. Sampling locations of *V. cholerae* strains sequenced in this study are indicated on the map. Each sampling location is coded by color and number, defined in the key; location colors are indicated for each tip in the maximum clade credibility tree as a heatmap (exact locations in Appendix Table 2, https://wwwnc.cdc.gov/EID/article/28/12/22-0572-App1.pdf). The tree was inferred from full genome *V. cholerae* isolates from DRC, neighboring countries, and Asia. Branches are scaled in time and colored by country of origin. Circles in internal nodes indicate posterior probability support >0.9, and the colors indicate ancestral countries inferred by Bayesian phylogeographic reconstruction. Circles at tips indicates the strains collected and sequenced in this study, with black circles designating phage-resistant strains. Notations *I*, *II*, *IIa*, and *IIb* indicate well-supported lineages and sublineages circulating in DRC during outbreaks. Asterisks (*) indicate potential spillover events within the Great Lakes region originated from neighboring countries. The tree with full tip labels is provided in Appendix Figure 2.

type 69 cluster (*6*) identified during the first reported outbreaks of cholera in DRC during 2008 and 2009. This cluster included the only Ogawa serotype isolates present in our collection. However, the long branch separating the isolate from the Tanganyika province (ERR572559_CD_2013) strain at the base of the monophyletic clade raises the possibility of unsampled *V. cholerae* strains (either from Rwanda or other neighboring countries) that could constitute

missing linkage between this DRC lineage and its actual ancestor. The second major lineage (denoted as II in Figure 1) contains all of the Inaba serotype strains collected. According to the molecular clock calibration, lineage II tMRCA dates to September 1999 (95% HPD March 1999–September 2000). The monophyletic clade also includes 3 strains identified in Zambia and Niger, which were likely the result of spillover events from DRC. This clade further divides into 2
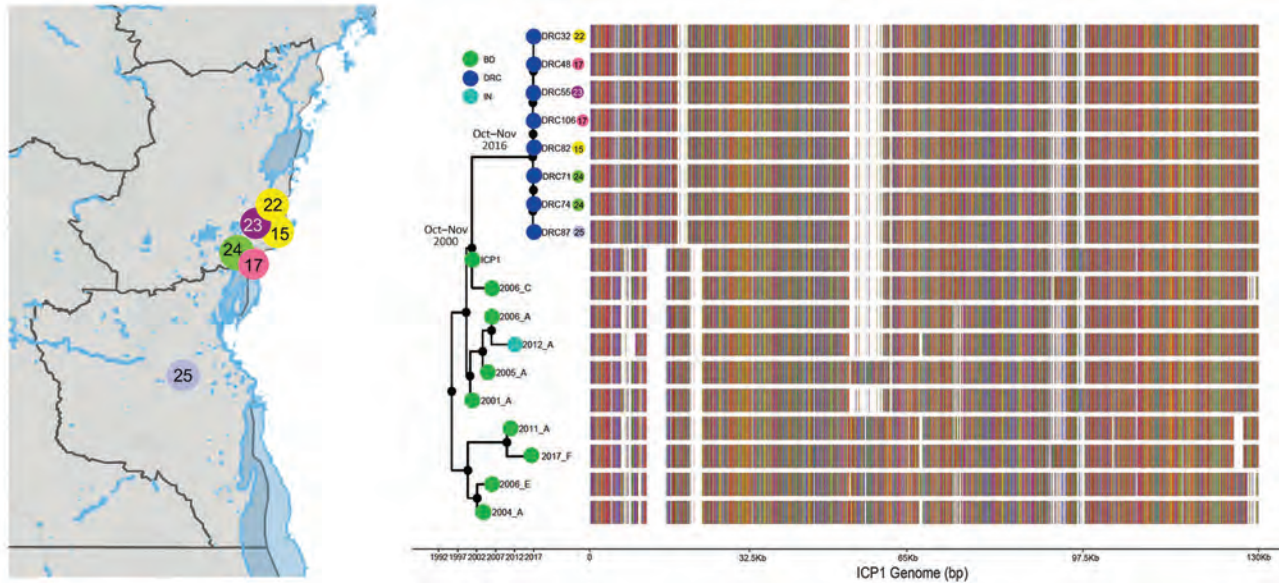
Figure 2. Bayesian inference of the phylogenetic relationship between phages and mutation patterns in the Democratic Republic of the Congo and ICP1 (Bangladesh cholera phage 1) patterns from Asia. Sampling locations of ICP1 strains from DRC are shown on the map. Each sampling location is coded by color and number, also indicated at the tip of the maximum clade credibility tree (exact locations in Appendix Table 2, https://wwwnc.cdc.gov/EID/article/28/12/22-0572-App1.pdf). The tree branches are scaled in time, and the circle tip points are colored by the location of origin, as indicated in the key. Circles in internal node indicate posterior probability support >0.9. To the right of the MCC tree, the genomic composition of each isolate is displayed: red, adenine; green, cytosine; yellow, guanine; and blue, thymine. White spaces indicate gaps at that location in the genome.

sublineages (IIa and IIb in Figure 1) that diverged in November 2004 (95% HPD September 2002–March 2007). Overall, molecular clock and phylogeographic reconstruction suggests circulation of cholera lineages in DRC years before the first reported cholera outbreaks in 2008–2009.

Phages were isolated from 17/41 (41.5%) fecal samples screened, on the basis of formation of plaques on strain AGC_15_CD_2017. Whole-genome sequencing of a subset (n = 8) of these phages showed that they shared high similarity in sequence (hqSNPs = 114) and diverged substantially (hqSNPs = 8,441) from the ICP1 phage isolated from Bangladesh and India (Figure 2). Previously, a total of 185 core open reading frames were identified as being conserved in ICP1 isolates collected over a 12-year period in Bangladesh and India (*15*). Uniquely, the DRC ICP1 lacks 15 of these core open reading frames and also has 10.6 kb of novel sequence in the first third of the genome. Of particular note, genomes do have the anti-*Vch*ind5 factor OrbA (*12*). However, like most ICP1-encoded gene products, most genes unique to DRC ICP1 are classified as hypothetical proteins because of a lack of an informative BLAST identification.

We screened our 24 DRC *V. cholerae* O1 strains for susceptibility to DRC ICP1 by plaque assays using ICP1_2017_A_DRC as a reference phage. Eighteen (75%) of the 24 *V. cholerae* strains were susceptible

to ICP1_2017_A_DRC (Table); we observed that 2 strains had turbid plaques on plaque assay, as described elsewhere (*28*). At the genome level, all resistant strains, and 3 of 6 sensitive strains, including the 2 strains that produced turbid plaques, carried >1 mutation in genes that belong to the O1-antigen biosynthetic gene cluster. ICP1 uses the O1 antigen as its receptor, and *V. cholerae* is known to undergo phase variation to decrease or produce modified forms of the O1 antigen to evade ICP1 infection (*7*). However, the fact that resistant strains gave a positive serologic response when tested for the O1 antigen suggests that there are mechanisms for resistance to ICP1 that lie elsewhere in the genome.

SXT-ICE has been reported to have 5 hotspots within the accessory region, including hotspot 5 (*Vch*Ind5), which confers resistance to ICP1 phage infection (*12*). When we evaluated the SXT-ICE sequence in all 24 DRC *V. cholerae* genomes, we found that all harbored genes identical to the wild-type SXT-ICE, which should make the strains phage-resistant. However, as already noted, the DRC ICP1 phage that we identified encodes the anti-BREX factor OrbA, which protects against the host *Vch*Ind5 (*12*). We did not detect other mechanisms usually associated with resistance of host cells to phage, such as acquisition and expression of a family of phage-inducible chromosomal island–like elements (*17*), and none of the DRC ICP1 isolates encoded a

previously described CRISPR-cas system specifically targeting phage-inducible chromosomal island–like elements for destruction, which might enable the phage to evade host immunity (*29*). At this point we cannot comment further on the mechanisms underlying resistance of our DRC *V. cholerae* strains to the regional DRC ICP1 phage other than to note the complexity of these regional phage/host interactions.

Comparison of genome-wide weighted averages of *dS* and *dN* along the internal branches of the cholera phylogeny showed a *dN/dS* ratio significantly >1 (p<0.001) (Appendix Figure 3, panel A). Moreover, the difference between *dN* and *dS* divergence accumulating over time along the internal branches of the phylogeny also appears to be increasing (Appendix Figure 3, panel B). In other words, the mixed presence of susceptible and resistant *V. cholerae* phenotypes, at least in the DRC Goma region where samples were collected, together with *dN/dS* patterns suggest that *V. cholerae* has been evolving under pressure of increasing diversifying selection, possibly driven by the co-circulation of predatory phages. Indeed, the map of sampling locations shows that phage-resistant or phage-susceptible *V. cholerae* strains, as well as independently sampled phages, have tended to co-circulate in the DRC Goma region and surrounding locales (Figure 3).

To examine in more detail the adaptive fitness landscape that might confer either resistance or sensitivity to phage predation, we optimized an MCC tree for the subset of *V. cholerae* sequences including all strains in the $\phi_{R/S}$ clade, as well as 2 outgroup strains,

AGC-2-CD-2015 and AGC-8-CD-2015, that clustered outside the clade (Figure 4). We used a Bayesian phylogeographic model with phage resistance or susceptibility as discrete phenotypic characters to infer the most likely phenotype of the ancestral (internal) nodes of the tree. The analysis clearly shows that the backbone path (trunk) of the $\phi_{R/S}$ clade, which represents the surviving lineage successfully propagating through time (*28*), is dominated by isolates with the phage-sensitive phenotype and connects phage-sensitive ancestral sequences that first generated a subcluster of strains circulating in 2015–2016 and then a subcluster including 2017 strains.

We cannot say which mutations are responsible for acquisition of phage resistance, but mutations in genes belonging to the O1-antigen biosynthetic gene cluster appear to have emerged, independently, along 3 distinct evolutionary lineages. The first lineage, leading to strain AGC-6-2015-DRC sampled in 2015, is characterized by amino acid substitutions in the *rfbV*, *rpIE*, *phrA*, and *fliD* genes. The second lineage resulted in a monophyletic clade of phage-resistant strains with mutations in either *rfbN* (strains sampled in 2015) or *rfbD* (sampled in 2016). The third lineage, leading to strain AGC-23-2017-DRC (sampled in 2017), was characterized again by an amino acid substitution in the *rfbB* gene.

Discussion

Cholera continues to be a major public health problem in the Great Lakes region of Africa (*1–4*). To optimize
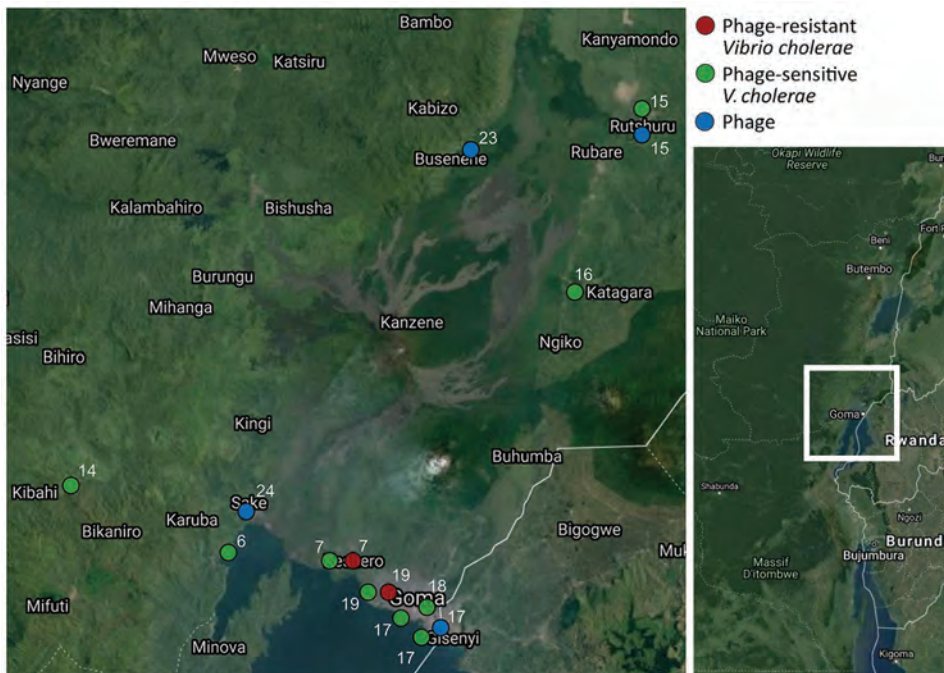

Figure 3. Sampling locations of phages and phage-resistant or sensitive *Vibrio cholerae* isolates in the Democratic Republic of the Congo. Each sampling location is coded by color (key) and number, which also appear at the tips of the maximum clade credibility tree in Figure 4 for comparison. Inset shows location of sampling area in the Democratic Republic of the Congo.
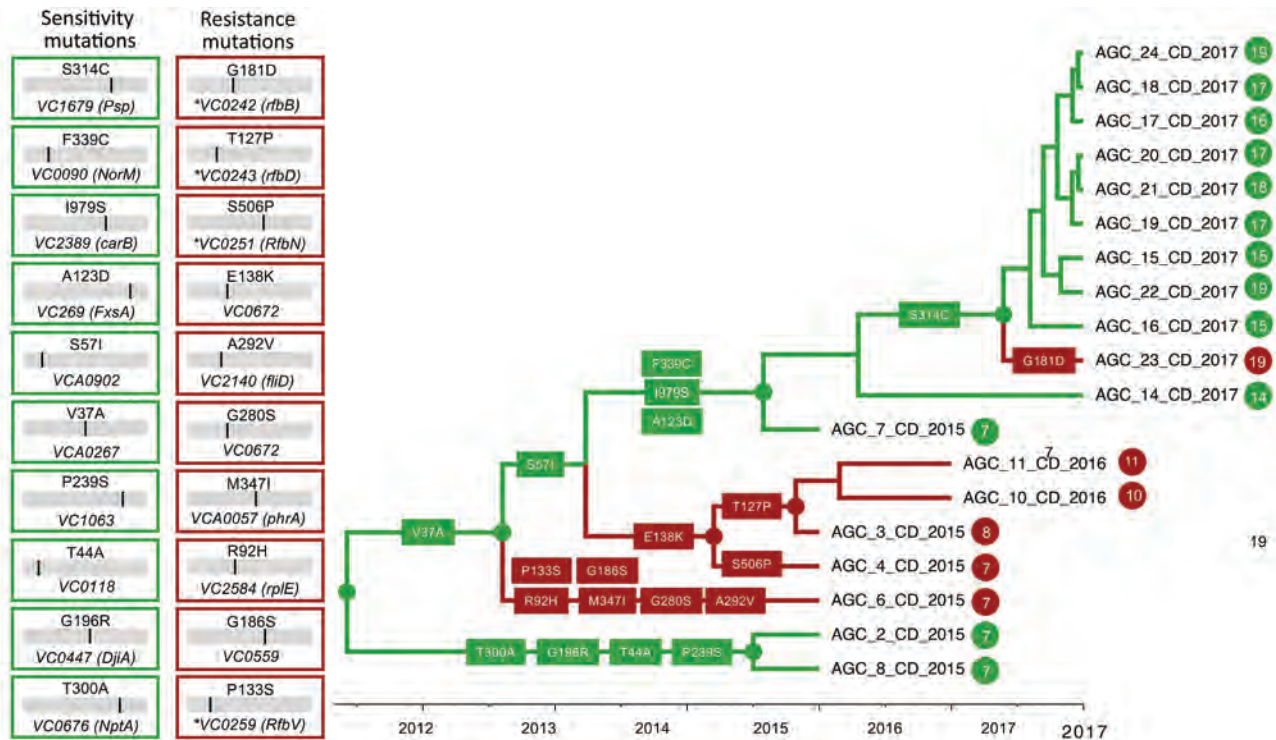
Figure 4. Phage-resistant or phase-sensitive dynamics and mutational patterns of *Vibrio cholerae* isolates in the Democratic Republic of the Congo. The boxes show the mutations that have been found along the backbone, internal, or external branches of the maximum clade credibility tree. Each number is the amino acid position of the protein where the mutation was mapped in the tree. The branches are scaled in time and colored on the basis of resistance (red) or sensitivity (green), matching colors in Figure 3. Circles and colors in internal node indicate posterior probability support >0.9 for an ancestor to be resistant or sensitive.

cholera control and appropriately target public health interventions, evolutionary drivers for *V. cholerae* in this area need to be determined, including reasons why certain *V. cholerae* strains emerge and persist while others fail to propagate. Our data provide further information on sources and subsequent development of endemic *V. cholerae* O1 in eastern DRC. Our work also highlights the effects a novel regional bacteriophage can have on cholera evolution. As reflected in the trunk of the phylogeny of the $\phi_{R/S}$ clade, *V. cholerae* isolates displaying the phage-sensitive phenotype appear to be successfully propagating, with every branch that leads to phage-resistant phenotypes in the phylogeny eventually dying out. Our findings are somewhat counterintuitive: phage resistance, rather than encouraging expansion of the epidemic clone, led to evolutionary dead ends; however, our data highlight the ability of *V. cholerae* to explore and quickly abandon different evolutionary pathways during epidemic spread. This finding is not surprising considering the potential fitness cost of phage resistance, particularly if resistance results in mutants highly attenuated for virulence (*30,31*). Further work will be needed to determine the exact mechanism by which the *V. cholerae* strains isolated in this study were either completely or partially resistant (turbid plaque) to ICP1_2017_A_DRC and whether the phage can mutate to regain virulence (*12*).

In summary, our study documents a complex coevolutionary dynamic involving *V. cholerae* and predatory phages (*30*) in the Great Lakes region of DRC. Phage-sensitive and highly infectious strains co-circulate with phage-resistant ones that occasionally emerge and eventually die out along different evolutionary pathways in response to the presence or absence of predatory phages in the environment, although the main phage-sensitive evolutionary lineage continued to propagate over time. The ability of *V. cholerae* to explore multiple mutational pathways in different genes and achieve phage resistance provides a substantial evolutionary advantage in terms of quick adaptive response to a changing environment, leading to emergence of new strains. Continuous monitoring of toxigenic *V. cholerae* and predator ICP1 phages in both patient fecal samples and aquatic environments in DRC and elsewhere could provide invaluable epidemiologic data for monitoring the spread of cholera, identifying environmental actors driving successful dissemination, and assessing the potential for new outbreaks.

About the Author

Dr. Alam is a biological scientist in the University of Florida College of Public Health and Health Professions and the Emerging Pathogens Institute. His research focuses on the factors and processes promoting persistence of *Vibrio cholerae* in aquatic reservoirs and evolution resulting from the lytic bacteriophage–*V. cholerae* in both clinical and environmental settings. Dr. Mavian is on the faculty at the University of Florida College of Medicine in the Department of Pathology, Immunology, and Laboratory Medicine. Her research focuses on intrahost evolution of HIV, population dynamics of cholera, and evolution and global spread of arboviruses and, since the beginning of the pandemic, the dynamics of SARS-CoV-2.

References

1. World Health Organization. Cholera annual report 2020. Wkly Epidemiol Rec. 2021;96:445–60.
2. Ingelbeen B, Hendrickx D, Miwanda B, van der Sande MAB, Mossoko M, Vochten H, et al. Recurrent cholera outbreaks, Democratic Republic of the Congo, 2008–2017. Emerg Infect Dis. 2019;25:856–64. https://doi.org/10.3201/eid2505.181141
3. Weill FX, Domman D, Njamkepo E, Tarr C, Rauzier J, Fawal N, et al. Genomic history of the seventh pandemic of cholera in Africa. Science. 2017;358:785–9. https://doi.org/10.1126/science.aad5901
4. Okeke IN. Africa in the time of cholera: a history of pandemics from 1817 to the present [book review]. Emerg Infect Dis. 2012;18:362. https://doi.org/10.3201/eid1802.111535
5. Moore S, Miwanda B, Sadji AY, Thefenne H, Jeddi F, Rebaudet S, et al. Relationship between distinct African cholera epidemics revealed via MLVA haplotyping of 337 *Vibrio cholerae* isolates. PLoS Negl Trop Dis. 2015;9:e0003817–0003817. https://doi.org/10.1371/journal.pntd.0003817
6. Irenge LM, Ambroise J, Mitangala PN, Bearzatto B, Kabangwa RKS, Durant JF, et al. Genomic analysis of pathogenic isolates of *Vibrio cholerae* from eastern Democratic Republic of the Congo (2014–2017). PLoS Negl Trop Dis. 2020;14:e0007642. https://doi.org/10.1371/journal.pntd.0007642
7. Seed KD. Battling phages: how bacteria defend against viral attack. PLoS Pathog. 2015;11:e1004847. https://doi.org/10.1371/journal.ppat.1004847
8. Faruque SM, Naser IB, Islam MJ, Faruque AS, Ghosh AN, Nair GB, et al. Seasonal epidemics of cholera inversely correlate with the prevalence of environmental cholera phages. Proc Natl Acad Sci U S A. 2005;102:1702–7. https://doi.org/10.1073/pnas.0408992102
9. Huq A, Sack RB, Nizam A, Longini IM, Nair GB, Ali A, et al. Critical factors influencing the occurrence of *Vibrio cholerae* in the environment of Bangladesh. Appl Environ Microbiol. 2005;71:4645–54. https://doi.org/10.1128/AEM.71.8.4645-4654.2005
10. Silva-Valenzuela CA, Camilli A. Niche adaptation limits bacteriophage predation of *Vibrio cholerae* in a nutrient-poor aquatic environment. Proc Natl Acad Sci U S A. 2019;116:1627–32. https://doi.org/10.1073/pnas.1810138116
11. Seed KD, Yen M, Shapiro BJ, Hilaire IJ, Charles RC, Teng JE, et al. Evolutionary consequences of intra-patient phage predation on microbial populations. eLife. 2014;3:e03497. https://doi.org/10.7554/eLife.03497
12. LeGault KN, Hays SG, Angermeyer A, McKitterick AC, Johura FT, Sultana M, et al. Temporal shifts in antibiotic resistance elements govern phage-pathogen conflicts. Science. 2021;373:eabg2166. https://doi.org/10.1126/science.abg2166
13. Hussain FA, Dubert J, Elsherbini J, Murphy M, VanInsberghe D, Arevalo P, et al. Rapid evolutionary turnover of mobile genetic elements drives bacterial resistance to phages. Science. 2021;374:488–92. 10.1126/science.abb1083 https://doi.org/10.1126/science.abb1083
14. Seed KD, Bodi KL, Kropinski AM, Ackermann HW, Calderwood SB, Qadri F, et al. Evidence of a dominant lineage of *Vibrio cholerae*–specific lytic bacteriophages shed by cholera patients over a 10-year period in Dhaka, Bangladesh. MBio. 2011;2:e00334–10. https://doi.org/10.1128/mBio.00334-10
15. Angermeyer A, Das MM, Singh DV, Seed KD. Analysis of 19 highly conserved *Vibrio cholerae* bacteriophages isolated from environmental and patient sources over a twelve-year period. Viruses. 2018;10:10. https://doi.org/10.3390/v10060299
16. Ali A, Chen Y, Johnson JA, Redden E, Mayette Y, Rashid MH, et al. Recent clonal origin of cholera in Haiti. Emerg Infect Dis. 2011;17:699–701. https://doi.org/10.3201/eid1704.101973
17. O'Hara BJ, Barth ZK, McKitterick AC, Seed KD. A highly specific phage defense system is a conserved feature of the *Vibrio cholerae* mobilome. PLoS Genet. 2017;13:e1006838. https://doi.org/10.1371/journal.pgen.1006838
18. Lemey P, Rambaut A, Drummond AJ, Suchard MA. Bayesian phylogeography finds its roots. PLOS Comput Biol. 2009;5:e1000520. https://doi.org/10.1371/journal.pcbi.1000520
19. Grenfell BT, Pybus OG, Gog JR, Wood JL, Daly JM, Mumford JA, et al. Unifying the epidemiological and evolutionary dynamics of pathogens. Science. 2004;303:327–32. https://doi.org/10.1126/science.1090727
20. Drummond AJ, Rambaut A. BEAST: Bayesian evolutionary analysis by sampling trees. BMC Evol Biol. 2007;7:214. https://doi.org/10.1186/1471-2148-7-214
21. Hasegawa M, Kishino H, Yano T. Dating of the human-ape splitting by a molecular clock of mitochondrial DNA. J Mol Evol. 1985;22:160–74. https://doi.org/10.1007/BF02101694
22. Leaché AD, Banbury BL, Felsenstein J, de Oca AN, Stamatakis A. Short tree, long tree, right tree, wrong tree:

new acquisition bias corrections for inferring SNP phylogenies. Syst Biol. 2015;64:1032–47. https://doi.org/10.1093/sysbio/syv053

23. Minin VN, Bloomquist EW, Suchard MA. Smooth skyride through a rough skyline: Bayesian coalescent-based inference of population dynamics. Mol Biol Evol. 2008;25:1459–71. https://doi.org/10.1093/molbev/msn090

24. Strimmer K, Pybus OG. Exploring the demographic history of DNA sequences using the generalized skyline plot. Mol Biol Evol. 2001;18:2298–305. https://doi.org/10.1093/oxfordjournals.molbev.a003776

25. Hall MD, Woolhouse ME, Rambaut A. The effects of sampling strategy on the quality of reconstruction of viral population dynamics using Bayesian skyline family coalescent methods: A simulation study. Virus Evol. 2016;2:vew003. https://doi.org/10.1093/ve/vew003

26. Lemey P, Kosakovsky Pond SL, Drummond AJ, Pybus OG, Shapiro B, Barroso H, et al. Synonymous substitution rates predict HIV disease progression as a result of underlying replication dynamics. PLOS Comput Biol. 2007;3:e29. https://doi.org/10.1371/journal.pcbi.0030029

27. Mavian C, Paisie TK, Alam MT, Browne C, Beau De Rochars VM, Nembrini S, et al. Toxigenic *Vibrio cholerae* evolution and establishment of reservoirs in aquatic ecosystems. Proc Natl Acad Sci U S A. 2020;117:7897–904. https://doi.org/10.1073/pnas.1918763117

28. Seed KD, Faruque SM, Mekalanos JJ, Calderwood SB, Qadri F, Camilli A. Phase variable O antigen biosynthetic genes control expression of the major protective antigen and bacteriophage receptor in *Vibrio cholerae* O1. PLoS Pathog. 2012;8:e1002917. https://doi.org/10.1371/journal.ppat.1002917

29. Seed KD, Lazinski DW, Calderwood SB, Camilli A. A bacteriophage encodes its own CRISPR/Cas adaptive response to evade host innate immunity. Nature. 2013;494:489–91. https://doi.org/10.1038/nature11927

30. Kamp HD, Patimalla-Dipali B, Lazinski DW, Wallace-Gadsden F, Camilli A. Gene fitness landscapes of *Vibrio cholerae* at important stages of its life cycle. PLoS Pathog. 2013;9:e1003800. https://doi.org/10.1371/journal.ppat.1003800

31. Oechslin F. Resistance development to bacteriophages occurring during bacteriophage therapy. Viruses. 2018;10:10. https://doi.org/10.3390/v10070351

Address for correspondence: Afsar Ali and Carla Mavian, Emerging Pathogens Institute, 2055 Mowry Rd, University of Florida, Gainesville, FL 32601, USA; email: afsarali@epi.ufl.edu and cmavian@ufl.edu

EID Podcast:

Asymptomatic Household Transmission of *Clostridioides difficile* Infection from Recently Hospitalized Family Members

While *C. difficile* infection (CDI) is predominantly associated with hospitals, reports of community-associated CDI cases, in which patients without a history of recent hospitalization are infected, have become more common. Although healthcare-associated CDI remains a considerable problem, more emphasis on community-associated CDI cases also is needed. Asymptomatic *C. difficile* carriers discharged from hospitals could be a major source of community-associated CDI cases.

In this EID podcast, Dr. Aaron Miller, a research assistant professor at the University of Iowa Roy J. and Lucille A. Carver College of Medicine discusses transmission of *C. difficile* to family members from recently hospitalized patients.

Visit our website to listen:
https://go.usa.gov/xJgxp

EMERGING INFECTIOUS DISEASES

Hedgehogs as Amplifying Hosts of Severe Fever with Thrombocytopenia Syndrome Virus, China

Chaoyue Zhao, Xing Zhang, Xiaoxi Si, Ling Ye, Kevin Lawrence, Yajun Lu, Chunhong Du, Haidong Xu, Qian Yang, Qianfeng Xia, Guoxiang Yu, Wei Xu, Fei Yuan, Junfeng Hao, Jia-Fu Jiang, Aihua Zheng

Severe fever with thrombocytopenia syndrome virus (SFTSV) is a tickborne bandavirus mainly transmitted by *Haemaphysalis longicornis* ticks in East Asia, mostly in rural areas. As of April 2022, the amplifying host involved in the natural transmission of SFTSV remained unidentified. Our epidemiologic field survey conducted in endemic areas in China showed that hedgehogs were widely distributed, had heavy tick infestations, and had high SFTSV seroprevalence and RNA prevalence. After experimental infection of *Erinaceus amurensis* and *Atelerix albiventris* hedgehogs with SFTSV, we detected robust but transitory viremias that lasted for 9–11 days. We completed the SFTSV transmission cycle between hedgehogs and nymph and adult *H. longicornis* ticks under laboratory conditions with 100% efficiency. Furthermore, naive *H. longicornis* ticks could be infected by SFTSV-positive ticks co-feeding on naive hedgehogs; we confirmed transstadial transmission of SFTSV. Our study suggests that the hedgehogs are a notable wildlife amplifying host of SFTSV in China.

Severe fever with thrombocytopenia syndrome (SFTS) is caused by SFTS virus (SFTSV), a new tickborne bandavirus identified in China in 2009 (*1*), and subsequently in South Korea in 2013 (*2*), Japan in 2014 (*3*), Vietnam in 2019 (*4*), and Myanmar and Pakistan in 2020 (*5,6*). The symptoms of SFTS include fever, thrombocytopenia, leukocytopenia, and gastrointestinal disorders; case-fatality rate is 2%–30% (*1,7,8*). The earliest cases in China were reported in the Dabie mountain range, which is located at the intersection of Henan, Hubei, and Anhui Provinces in central China. Shandong, Liaoning, and Zhejiang provinces are the other main hot spots for SFTS in China (*9*). Within Zhejiang Province, Daishan County, an archipelago of islands located in the East China Sea, is one of the most SFTS-endemic areas (*10*). The main industries in Daishan County are fishing and tourism. Agriculture is relatively unimportant; 4,000 sheep and 150 cattle were reported on the islands in 2019, as provided by the Department of Agriculture in Daishan County. As of 2020, SFTS cases have been reported in most other provinces of China (*9,11,12*).

The Asian long-horned tick, *Haemaphysalis longicornis*, is a primary vector for SFTSV and the dominant human-biting tick in SFTSV-endemic areas (*13,14*). *H. longicornis* ticks have both bisexual and parthenogenetic populations; parthenogenetic populations are widely distributed in China and strongly correlated with the distribution of SFTS cases (*15*).
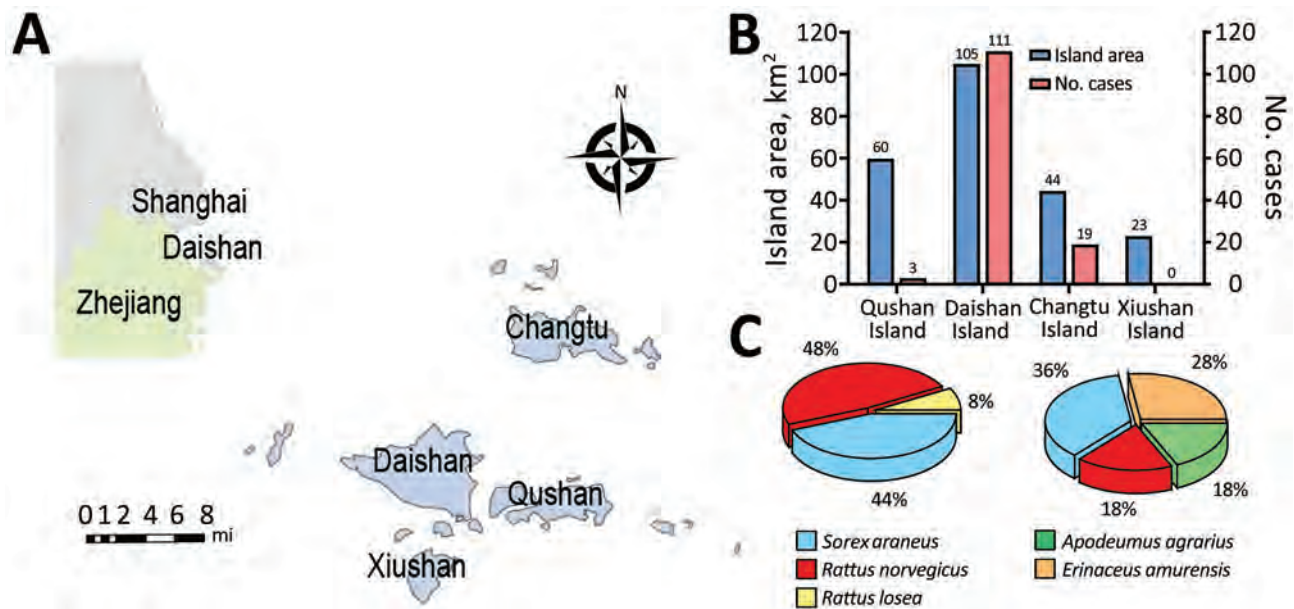
Figure 1. Association between hedgehogs and SFTSV endemicity of locations in China in study of hedgehogs as amplifying hosts of SFTSV. A) The main islands of Daishan County, Zhejiang Province, China. Inset shows location of Daishan County in China. B) Land area and SFTS case numbers for major islands in Daishan County. C) Species and relative rate of wild animals collected on Xiushan Island (left) and Daishan Island (right). SFTSV, severe fever with thrombocytopenia syndrome virus.

H. longicornis ticks go through a 3-stage life cycle: larva, nymph, and adult. Extensive reports suggest that *H. longicornis* ticks are the reservoir of SFTSV (*16–18*); however, transstadial transmission efficiencies of SFTSV varied under laboratory conditions. We compared results from Zhuang et al. (*16*) and Hu et al. (*19*): transmission rate from egg pools to larvae pools was 80% in Zhuang and 100% in Hu; from larval pools to nymph pools, 92% in Zhuang and 100% in Hu; and from nymph pools to adults, 40% in Zhuang and 50% in Hu. The corresponding SFTSV prevalence was extremely low, 0.2%–2.2%, in different developmental stages of host-seeking *H. longicornis* ticks collected from vegetation (*17,18,20*). These findings suggest that ticks alone are not sufficient to maintain a reservoir of SFTSV in the natural environment, and additional amplifying hosts are required.

Antibodies to SFTSV and viral RNA have been detected in a wide range of domestic animals, including goats, cattle, dogs, and pigs and wild animals such as shrews, rodents, weasels, and hedgehogs. The highest seroprevalence was found in sheep (69.5%), followed by cattle (60.4%), dogs (37.9%) and chickens (47.4%) (*21–23*). Given that most of the SFTS patients are farmers, who have frequent contacts with many of these susceptible domestic and wild animals, understanding the epidemiology of SFTSV is difficult and complex.

Hedgehogs belong to the family *Erinaceinae*, which are widely distributed in Europe, Asia, and Africa (*24*) and are invasive species in Japan and New Zealand (*25,26*). The Amur hedgehog, *Erinaceus amurensis*, is closely related to the European hedgehog, *E. europaeus*, and is common in northern and central China. The African pygmy hedgehog, *Atelerix albiventris*, native to central and eastern Africa, has been introduced into many countries as pets, including China (*25,26*). Both the Amur hedgehog and the Afri-

Table 1. Seroprevalence of severe fever with thrombocytopenia syndrome virus in wild animals captured in Xiushan Island and Daishan Island, China

Animal	No. sampled	No. (%) positive
Sorex araneus shrew	42	0
Erinaceus europaeus hedgehog	9	3 (33.33)
Rattus norvegicus brown rat	48	0
R. losea ricefield rat	6	0
Apodemus agrarius striped field mouse	3	0

Table 2. Population density of hedgehogs in rural and urban areas, China*

Site	Location	Density
Daao village†	Daishan County, Zhejiang Province	>80
Dongsha village†	Daishan County, Zhejiang Province	>90
Olympic Forest Park‡	Chaoyang District, Beijing	>60
Southeast Community‡	Haidian District, Beijing	>75

*Density was calculated by the number of trapped hedgehogs divided by the area (no. animals/km²).
†Rural.
‡Urban.

Table 3. Average number of ticks collected from wild mammals captured in Daishan County, China, in study of severe fever with thrombocytopenia syndrome virus

Animal	No. ticks
Sorex araneus shrew	1.5
Rattus norvegicus brown rat	1
Rattus losea ricefield rat	0
Apodemus agrarius striped field mouse	0
Erinaceus amurensis hedgehog	145

can pygmy hedgehog can become heavily infested by all kinds of ticks and are known to carry many zoonotic diseases, such as tick-borne encephalitis virus, Bhanja virus, and Tahyna virus (*27–29*). Hedgehogs are poikilothermal animals and hibernate during winter. During hibernation, their metabolism and immune system are suppressed (*30*), which has led to the suspicion that hibernating hedgehogs contribute to the long-term persistence of these viruses (*31*). A few previous studies have reported that SFTSV antibodies and RNA were detected in Amur hedgehogs in Shandong and Jiangsu Province. However, the prevalence of SFTV infection appeared low compared with that in other animals, such as goats, sheep, and cattle (*14,32*).

In China, the density of large wild animals is extremely low, especially in East China, where SFTS is endemic. Instead, the most abundant wildlife in these areas are rodents and insectivores (*33*). However, the potential role of rodents in the transmission of SFTSV was refuted when it was shown that immunocompetent rodents cannot develop SFTSV viremia after artificial inoculation (*34*). In contrast, hedgehogs are the only small wild animals that consistently show high SFTSV seroprevalence, high density, and high *H. longicornis* tick infestation in the SFTS-endemic areas (*32,35*), which has led us to speculate that hedgehogs might play an important role in the natural circulation of SFTSV in China. We conducted all animal studies in strict accordance with the recommendations in the Guide for the Care and Use of Laboratory Animals of the Ministry of Science and Technology of the People's Republic of China. The Committee on the Ethics of Animal Experiments of the Institute of Zoology, Chinese Academy of Sciences, approved the protocols for animal studies (approval no. IOZ20180058).

Methods

Field Survey of Hedgehogs in SFTS-Endemic Areas

To confirm the role of hedgehogs as potential wild amplifying hosts for SFTSV, we first performed an animal survey in Daishan County in 2019 (Figure 1, panel A). Daishan County is the worst-affected area for SFTS in Zhejiang Province (*10*); during 2011–2019, Daishan Center for Disease Control and Prevention reported 133 SFTS cases on 3 Daishan County islands—Daishan Island, Qushan Island, and Changtu Island—but none on Xiushan Island, even though Xiushan Island has a similar landscape, vegetation, and population density as the other major islands (Figure 1, panel B).

For the survey, we set small mammal traps and caught 33 animals on Daishan Island and 75 on Xiushan Island. On Daishan Island, 9/33 (28%) of the captured small mammals were *E. amurensis* Amur hedgehogs, 6/33 (18%) were *Rattus norvegicus* brown rats, 12/33 (36%) were *Sorex araneus* common shrews, and 6/33 (18%) were *Apodemus agrarius* striped field mice. On Xiushan Island, we caught no hedgehogs; 36/75 (48%) of the small mammals caught were *R. norvegicus* rats, 33/75 (44%) were *S. araneus* shrews, and 6/75 (8%) were *R. losea* lesser rice field rats (Figure 1, panel C). Antibody testing showed that 3/9 (33%) of *E. amurensis* hedgehogs from Daishan Island were positive for SFTSV (Table 1). Hedgehogs are abundant in the 2 villages in Daishan Island; we estimated population density as >80 animals per square kilometer based on the results of the trapping study (Table 2). In addition, the 9 trapped hedgehogs were all heavily infected by ticks, with an average of 145 ticks per hedgehog, including *H. longicornis* ticks (Table 3).

Additional *E. amurensis* hedgehog serum samples were collected from trapping studies conducted in other SFTS-endemic areas, including Weifang City of Shandong Province, Linfen City of Shanxi Province, and Xinyang City of Henan Province. SFTSV antibodies were detected in 9/35 (25.7%) of hedgehogs from Weifang City, of which 11.1% tested positive for SFTSV RNA; 2/6 (33.3%) from Linfen City, of which 50% tested positive; and 2/8 (25%) from Xinyang City, of which no hedgehogs tested positive. Of the hedgehogs from Weifang, 11.1% were infected by ticks positive for SFTSV RNA, as were 12.5% of those

Table 4. Epidemiological analysis of trapped animals in study of seroprevalence of SFTSV in hedgehogs, China

Location	Animal no.	SFTSV antibody positive rate, %	SFTSV RNA positive rate, %	Tick no.	SFTSV RNA–positive tick rate, %†
Linfen	6	33.3	16.7	104	50
Xinyang	8	25	0	160	12.5
Weifang	35	25.7	11.1	216	11.1

*Viral RNA was tested by PCR. SFTSV, severe fever with thrombocytopenia syndrome virus.
†Ratio of hedgehogs infested with SFTSV RNA–positive ticks.

Figure 2. Locations of Weifang in Shandong Province, Linfen in Shanxi Province, and Xinyang in Henan Province (red outlines)0, where hedgehogs were collected in study of hedgehogs as amplifying hosts of severe fever with thrombocytopenia syndrome virus in China.

from Linfen (Table 4; Figure 2). We believe these results strongly support our hypothesis that hedgehogs play an important role in the natural circulation of SFTSV. After collecting samples, we conducted several experiments to determine the role of the hedgehogs in SFTSV transmission (Appendix, https://wwwnc.cdc.gov/EID/article/28/12/22-0668-App1.pdf).

Results

Susceptibility of Hedgehogs to Experimental Infection with SFTSV

We inoculated 4 male and 4 female *E. amurensis* hedgehogs 6–12 months old with 4×10^6 FFU of SFTSV by intraperitoneal route. We observed viremia of ≈9 days in all animals and peak titers of 3.1 $\log_{10}$ RNA copies/µL at days 3–6, suggesting viral multiplication. Two *E. amurensis* hedgehogs showed a mild weight loss of <25% by day 9 (Figure 3, panels A, B).

We inoculated groups of 5 male and 5 female *A. albiventris* hedgehogs 6–12 months of age with 4×10^6 FFU of SFTSV by intraperitoneal (Figure 3, panels C, D) and subcutaneous (Figure 3, panels E, F) routes. We observed viremia of 9–11 days in all 10 animals; peak titers were 3.2 $\log_{10}$ RNA copies/µL at days 3–7 for the intraperitoneal route and 3.1 $\log_{10}$ RNA copies/µL at days 6–8 for the subcutaneous route (Figure 3, panels D, F). Most animals showed mild weight loss of <20%

(Figure 3, panels C, E). Those results suggest that *E. amurensis* and *A. albiventris* hedgehogs could develop similar viremias independent of inoculation routes, without substantially compromising their overall health. However, *E. amurensis* hedgehogs are shy and prone to dying during transport from their stress response. Thus, we performed most of the following experiments with *A. albiventris* hedgehogs, of which we had a stable supply through the local pet store.

SFTSV Viremia during Hibernation

We inoculated 4 *A. albiventris* hedgehogs with 4×10^6 FFU of SFTSV and kept them at 4°C to trigger hibernation. Two of the hedgehogs came out of hibernation at day 15 with viremias of 2.7 and 3.3 $\log_{10}$ RNA copies/µL; the other 2 hedgehogs continued in hibernation until day 30 and had viremias of 3.0 and 3.7 $\log_{10}$ RNA copies/µL. All the viremias measured in these hibernating hedgehogs were comparable to the peak virus titers previously measured in the nonhibernating hedgehogs (Figure 4). However, the duration of viremia in these 4 hibernating hedgehogs was much longer than that recorded in the nonhibernating hedgehogs, suggesting that hibernation could potentially extend the course of SFTSV viremia in hedgehogs and contribute to the overwintering of SFTSV in the field.

SFTSV-Induced Pathology

To assess the pathologic changes in hedgehogs resulting from SFTSV infection, we intraperitoneally inoculated 6 *A. albiventris* hedgehogs with 4×10^6 FFU of SFTSV. We euthanized 2 animals at 3 days, 6 days, and 2 months after infection and collected their organs for viral RNA evaluation and hematoxylin and eosin (H&E) staining. We detected a robust viremia on days 3 and 6 but none at 2 months after infection. We observed the highest level of viral RNA in the spleen, followed by the blood; the lowest level was in the heart (Figure 5). H&E-stained slides from the spleen showed hemorrhagic necrosis and lymphopenia at days 3 and 6. We assessed the severity of the lesions as +++ on day 3 and ++++ on day 6, but the lesions had largely recovered by 2 months, with a severity score of ++ (Appendix Figure 1). These results further confirmed that hedgehogs show a high tolerance to SFTSV without obvious long-term or permanent pathologic changes.

Transmission of SFTSV between *H. longicornis* Ticks and Hedgehogs

We used laboratory-adapted *H. longicornis* ticks and *A. albiventris* hedgehogs to model the natural transmission of SFTSV hypothesized to occur in the wild. We fed naive *H. longicornis* nymphs on hedgehogs

infected by intraperitoneal inoculation with 4×10^6 FFU of SFTSV at day 0. We detected viremia of 3.8 $\log_{10}$ RNA copies/μL in hedgehogs at day 5; fully engorged nymphs dropped off between days 4 and 8. The engorged nymphs molted after 2–3 weeks, and the adult ticks tested 100% positive for SFTSV at a level of 7.2 $\log_{10}$ RNA copies/mg tick.

Two to 3 weeks after they molted into adults, we fed the SFTSV-carrying ticks on 3 naive hedgehogs, 8 ticks per animal. We monitored weight and viremia for 12 days and observed a slow weight loss of <25% by day 12; the viremia peaked on days 8–10 at 4.1 $\log_{10}$ copies/μL. After peaking, the viremia decreased slowly until the 3 hedgehogs were euthanized on day 12 (Figure 6, panels A, B). We collected the fully engorged ticks on days 7–10 and then tested them. All 24 ticks were still positive for SFTSV RNA (Figure 6, panel C). We believe that these data strongly suggest that SFTSV can be efficiently transmitted between hedgehogs and *H. longicornis* ticks and that transstadial transmission occurs within *H. longicornis* ticks.

Hedgehogs as Amplifying Hosts for SFTSV

SFTSV can be transmitted both transovarially and transstadially in *H. longicornis* ticks; however, a decreased efficiency has been observed during passaging (*16*). Thus, an amplifying host will be necessary to improve the transmission efficiency. To determine if hedgehogs can serve as amplifying hosts, we prepared SFTSV-positive adult *H. longicornis* ticks as described above with 100% efficiency. Next, we fed 5 of the SFTSV-carrying adult *H. longicornis* ticks together with 14–16 naive nymphs and 3–4 naive adult ticks on each of 3 naive *A. albiventris* hedgehogs. We collected the fully engorged ticks at 7–10 days after bite and tested them for viral RNA levels. The viral load in the engorged nymphs was 2.5 $\log_{10}$ RNA copies/mg tick and in previously naive adults 2.7 $\log_{10}$ RNA copies/mg tick (Figure 7, panels A, B). After the nymphs molted, the adult ticks tested 100% positive for SFTSV, with a level of 6.9 $\log_{10}$ RNA copies/mg tick (Figure 7, panel C). Thus, these results suggest that hedgehogs could be acting as an amplifying host for SFTSV.
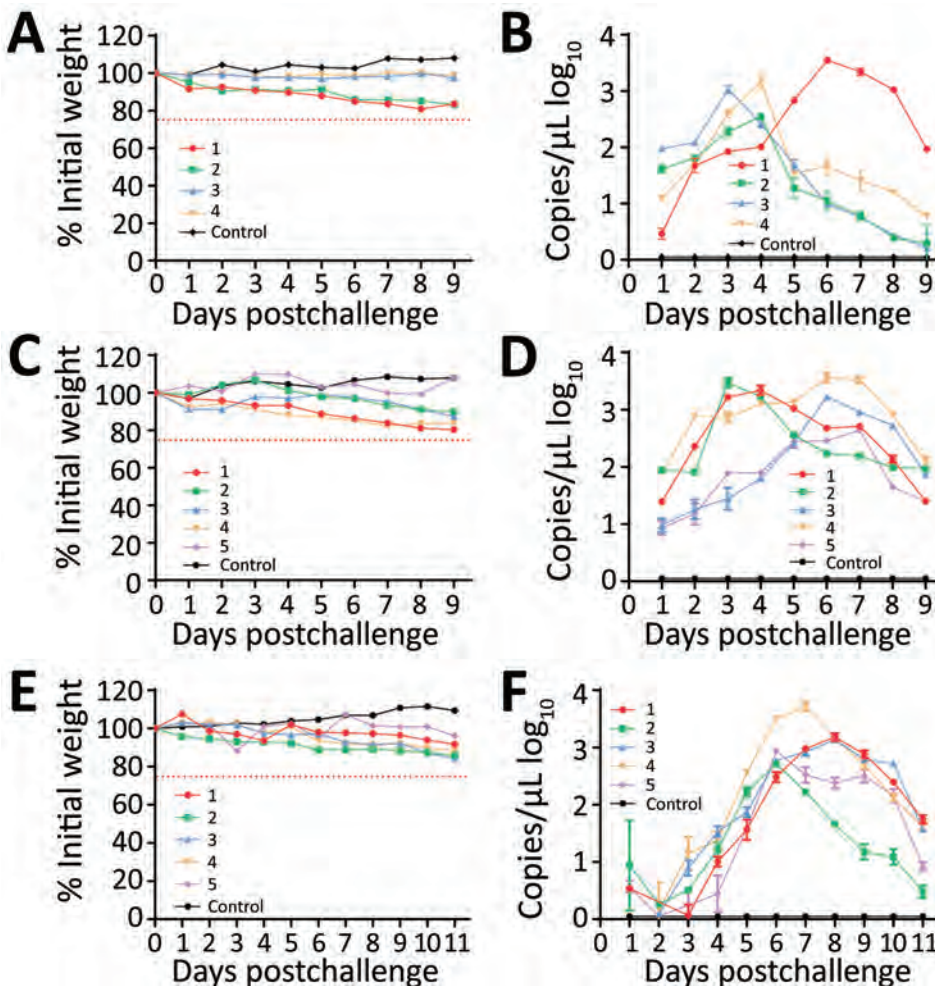

Figure 3. Severe fever with thrombocytopenia syndrome virus (SFTSV) viremia in experimentally infected *Erinaceus amurensis* and *Atelerix albiventris* hedgehogs in study of hedgehogs as amplifying hosts of SFTSV in China. A) Weight change in *E. amurensis* hedgehogs after intraperitoneal inoculation. B) Viremia in *E. amurensis* hedgehogs after intraperitoneal inoculation. C) Weight change in *A. albiventris* hedgehogs after intraperitoneal inoculation. D) Viremia in *A. albiventris* hedgehogs after intraperitoneal inoculation. E) Weight change in *A. albiventris* hedgehogs after subcutaneous inoculation. F) Viremia in *A. albiventris* hedgehogs after subcutaneous inoculation. Hedgehogs were challenged by intraperitoneal or subcutaneous inoculation with 4×10^6 FFU of SFTSV Wuhan strain and then monitored for weight change and viremia, tested by real-time PCR as RNA copies/μL of serum. Control was mock infected with phosphate buffered saline solution. Error bars indicate SDs.
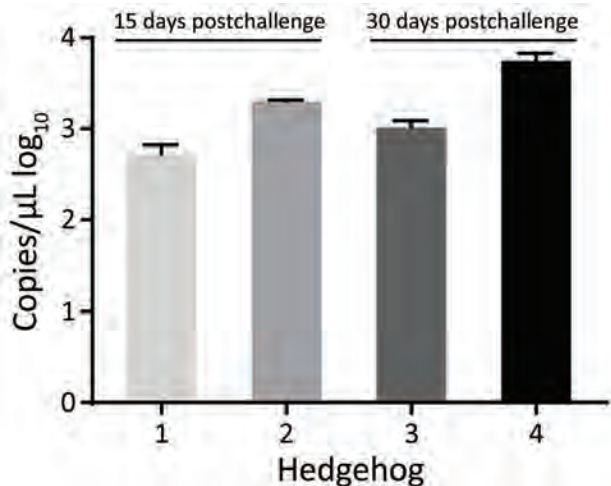
Figure 4. Severe fever with thrombocytopenia syndrome virus (SFTSV) viremia in 4 *Atelerix albiventris* hedgehogs in study of hedgehogs as amplifying hosts of SFTSV in China. Hedgehogs were challenged by intraperitoneal inoculation with 4×10^6 FFU of SFTSV Wuhan strain and then kept at 4°C to trigger hibernation. Viremia in hedgehogs 1 and 2 was monitored at 15 days postinoculation and in hedgehogs 3 and 4 at 30 days postinoculation. Error bars indicate SDs.

Discussion

Viremia in the vertebrate host is important for the arbovirus to transmit from host to vector. Previous epidemiologic surveys and experimental infections have revealed that many wild and domesticated animals are susceptible to SFTSV infection (*21*). However, these studies had similar findings that most vertebrate animals were subclinically infected with SFTSV, with
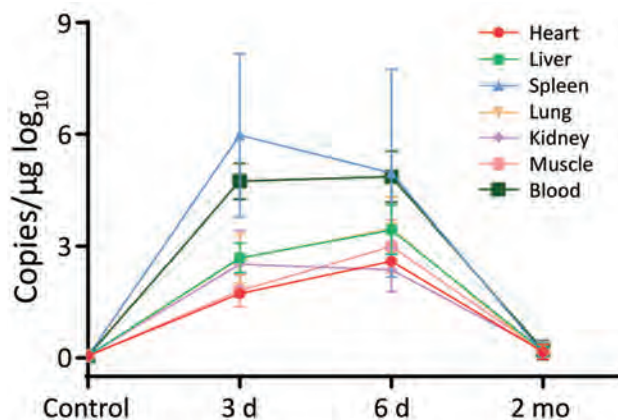

Figure 5. Pathology of severe fever with thrombocytopenia syndrome virus (SFTSV)–infected *Atelerix albiventris* hedgehogs in study of hedgehogs as amplifying hosts of SFTSV in China. Six hedgehogs were intraperitoneally inoculated with 4×10^6 FFU of SFTSV Wuhan strain, and 2 were mock infected with phosphate buffered saline solution as controls. Two hedgehogs were euthanized at 3 days, 6 days, and 2 months to test viral load in the organs. SFTSV viral load in organs was measured by real-time PCR.

limited viremia (*36*). For example, 80% of goats developed a viremia after subcutaneous inoculation with 10^7 PFU of SFTSV, which lasted for <24 hours (*37*). Similarly, beagle dogs intramuscularly inoculated with 2.51 $\times 10^7$ 50% tissue culture infectious dose of SFTSV did not have a detectable viremia until day 3 (*38*). Furthermore, the efficient transmission of SFTSV between tick vectors and these potential wild animal hosts has not been proven. In this study, we consistently detected robust viremias of ≈10^3 RNA copies/µL in both native *E. amurensis* and exotic *A. albiventris* hedgehogs after intraperitoneal or subcutaneous inoculation with 4 × 10^6 FFU of SFTSV at 100% efficiency; viremia lasted for 9–11 days and provided the basis for the effective transmission of SFTSV from host to tick. Moreover, hedgehogs were highly tolerant to SFTSV infection; they experienced slight weight loss and pathology that recovered after the clearance of virus.

H. longicornis ticks overwinter mostly as nymphs, but with an SFTSV-positive rate of 4% as measured by pool (*39*). Thus, we speculate that their role in overwintering of disease may be limited. Hedgehogs are involved in the overwintering of many pathogens during hibernation (*31*,*40*), which could include SFTSV. Our results suggest that the SFTSV viremia can be extended from 9 days when not hibernating to ≥1 month during hibernation, and with viremias no less than those seen in nonhibernating hedgehogs.

To meet the requirement for hedgehogs to be considered as maintenance hosts for SFTSV, the transmission cycle between vector and host needs to be established. Using laboratory-adapted *H. longicornis* ticks and *A. albiventris* hedgehogs, this study showed efficient infection transmission from nymph or adult ticks to hedgehogs, efficient infection transmission from hedgehogs to nymph or adult ticks, and transstadial infection transmission from nymph to adult tick. It is important to note that these results were observed in 100% of tested subjects. Naive nymph and adult *H. longicornis* ticks cofeeding with SFTSV-infected adult ticks on naive hedgehogs were also 100% infected. Our results show that hedgehogs fulfill the requirements to be considered competent amplifying hosts for SFTSV. Other animals or birds could also maintain the natural circulation of SFTSV; for example, experimentally inoculated spotted doves (*Streptopelia chinensis*) can develop SFTSV viremia (*41*). However, transmission between *H. longicornis* ticks and spotted doves is not proven.

To conclude that hedgehogs are major amplifying hosts of SFTSV in the real world, further studies should investigate abundance, tick association, geographic distribution in areas of transmission, and
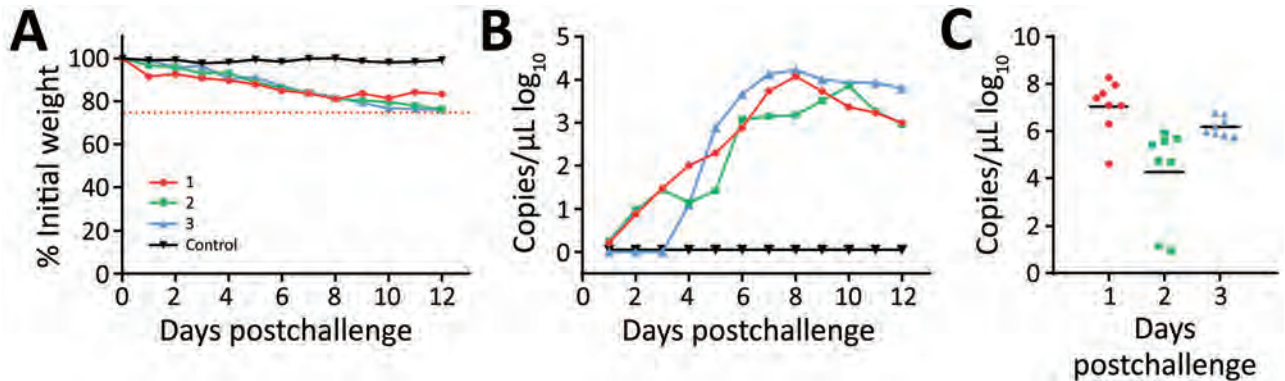
Figure 6. Transmission of severe fever with thrombocytopenia syndrome virus (SFTSV) between *Haemaphysalis longicornis* ticks and *Atelerix albiventris* hedgehogs in study of hedgehogs as amplifying hosts of SFTSV in China. A, B) Weight change (A) and SFTSV viremia (B) in naive hedgehogs bitten by SFTSV-carrying adult ticks that were monitored for 12 d. Adult ticks were inoculated with SFTSV by feeding on SFTSV-infected hedgehogs. Numbers represent individual hedgehogs; the control animal was not bitten. C) SFTSV RNA level in engorged adult ticks from 3 hedgehogs. Each dot indicates 1 tick; horizontal lines indicate medians.

field exposure. Our initial survey in SFTSV-endemic Daishan Island and nonendemic Xiushan Island reveals that the existence of hedgehogs was related to SFTSV transmission. The epidemiologic surveys we conducted in 4 SFTSV-endemic provinces consistently showed high SFTSV seroprevalence and that the population density of hedgehogs in SFTSV-endemic areas can be >60 animals/km². Hedgehogs are heavily infested by tick species including *H. longicornis*; we observed a density of 145 ticks per animal on Daishan Island. Hedgehogs are widely distributed across farms and rural communities, which contain the humans most likely to be bitten by *H. longicornis* ticks carrying SFTSV (*32,35*). Furthermore, hedgehogs share the same environment as domestic animals such

as dogs, goats, and cows, which are also natural hosts for *H. longicornis* ticks and show high seroprevalence for SFTS. Thus, it is possible that humans and domestic animals are similarly infected by ticks that had previously fed on SFTSV-positive hedgehogs at an earlier stage in their life cycle. As previously stated, SFTSV-endemic areas in China have few large wild animals; the most common animals are rodents and insectivores (*33*). Tests on rodents have shown that they are not capable of maintaining SFTSV infection (*34*). Our results show that of the mammals present in rural China, hedgehogs meet all the requirements to be major wildlife amplifying hosts for SFTSV.

SFTSV may also spread to other countries with competent hosts and vectors. *E. europaeus* hedgehogs
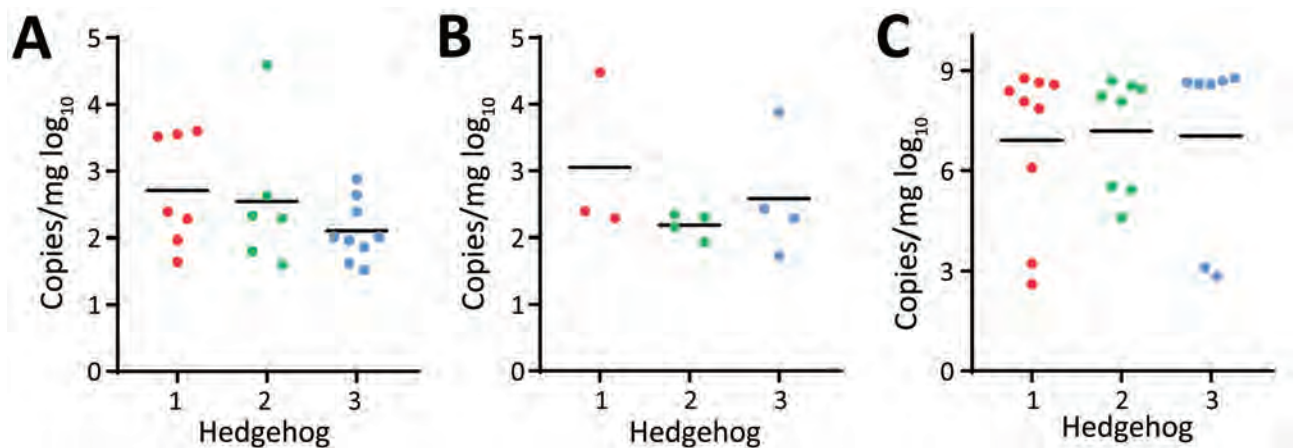

Figure 7. Naive *Haemaphysalis longicornis* ticks infected by SFTSV through cofeeding with severe fever with thrombocytopenia syndrome virus (SFTSV)–positive ticks on naive *Atelerix albiventris* hedgehogs in study of hedgehogs as amplifying hosts of SFTSV in China. A) Engorged nymph ticks. B) Engorged adult ticks. C) Adults molted from the engorged nymph ticks. Nymph ticks were inoculated with SFTSV by feeding on SFTSV-infected hedgehogs. After molting, the SFTSV-carrying adult ticks and naive nymph and adult *H. longicornis* ticks were fed on 3 naive *A. albiventris* hedgehogs. The fully engorged ticks were collected 7–10 days after biting. SFTSV RNA level was monitored in ticks as shown by RNA copies per mg of tick. Each dot indicates 1 tick; horizontal lines indicate medians. Numbers along baselines represent individual hedgehogs. .

were introduced to New Zealand by human intervention (*25,26*). The summer density of hedgehogs in 3 studies in New Zealand was estimated at 250–800 hedgehogs/km² (*42–44*). In addition, *H. longicornis* ticks are common in New Zealand and are all parthenogenetic (Appendix Figure 2) (*45*). New Zealand is also on the East Asian–Australian flyway, so it could be considered to have a high risk for SFTSV disease incursion through SFTSV–positive *H. longicornis* ticks infested in migratory birds (*46*).

In conclusion, our data strongly support our initial hypothesis that hedgehogs can maintain the natural circulation of SFTSV in rural areas. The high density and wide distribution, the high-level susceptibility and tolerance of hedgehogs to SFTSV, the heavy *H. longicornis* tick infestation rates, and the ability to amplify the infection level of feeding ticks are all compelling evidence that hedgehogs are a likely wildlife amplifying host of SFTSV.

About the Author

Dr. Zhao is a PhD student at Institute of Zoology, Chinese Academy of Sciences, China. Her primary research interest is interaction of vectors and vector-borne pathogens.

References
1. Yu XJ, Liang MF, Zhang SY, Liu Y, Li JD, Sun YL, et al. Fever with thrombocytopenia associated with a novel bunyavirus in China. N Engl J Med. 2011;364:1523–32. https://doi.org/10.1056/NEJMoa1010095
2. Yun SM, Lee WG, Ryou J, Yang SC, Park SW, Roh JY, et al. Severe fever with thrombocytopenia syndrome virus in ticks collected from humans, South Korea, 2013. Emerg Infect Dis. 2014;20:1358–61. https://doi.org/10.3201/eid2008.131857
3. Takahashi T, Maeda K, Suzuki T, Ishido A, Shigeoka T, Tominaga T, et al. The first identification and retrospective study of severe fever with thrombocytopenia syndrome in Japan. J Infect Dis. 2014;209:816–27. https://doi.org/10.1093/infdis/jit603
4. Tran XC, Yun Y, Van An L, Kim SH, Thao NTP, Man PKC, et al. Endemic severe fever with thrombocytopenia syndrome, Vietnam. Emerg Infect Dis. 2019;25:1029–31. https://doi.org/10.3201/eid2505.181463
5. Zohaib A, Zhang J, Saqib M, Athar MA, Hussain MH, Chen J, et al.; Sajjad-Ur-Rahman. Serologic evidence of severe fever with thrombocytopenia syndrome virus and related viruses in Pakistan. Emerg Infect Dis. 2020;26:1513–6. https://doi.org/10.3201/eid2607.190611
6. Win AM, Nguyen YTH, Kim Y, Ha NY, Kang JG, Kim H, et al. Genotypic heterogeneity of *Orientia tsutsugamushi* in scrub typhus patients and thrombocytopenia syndrome co-infection, Myanmar. Emerg Infect Dis. 2020;26:1878–81. https://doi.org/10.3201/eid2608.200135
7. Liu Q, He B, Huang SY, Wei F, Zhu XQ. Severe fever with thrombocytopenia syndrome, an emerging tick-borne zoonosis. Lancet Infect Dis. 2014;14:763–72. https://doi.org/10.1016/S1473-3099(14)70718-2
8. Liu S, Chai C, Wang C, Amer S, Lv H, He H, et al. Systematic review of severe fever with thrombocytopenia syndrome: virology, epidemiology, and clinical characteristics. Rev Med Virol. 2014;24:90–102. https://doi.org/10.1002/rmv.1776
9. Sun J, Lu L, Wu H, Yang J, Liu K, Liu Q. Spatiotemporal patterns of severe fever with thrombocytopenia syndrome in China, 2011–2016. Ticks Tick Borne Dis. 2018;9:927–33. https://doi.org/10.1016/j.ttbdis.2018.03.026
10. Fu Y, Li S, Zhang Z, Man S, Li X, Zhang W, et al. Phylogeographic analysis of severe fever with thrombocytopenia syndrome virus from Zhoushan Islands, China: implication for transmission across the ocean. Sci Rep. 2016;6:19563. https://doi.org/10.1038/srep19563
11. Lin TL, Ou SC, Maeda K, Shimoda H, Chan JP, Tu WC, et al. The first discovery of severe fever with thrombocytopenia syndrome virus in Taiwan. Emerg Microbes Infect. 2020;9:148–51. https://doi.org/10.1080/22221751.2019.1710436
12. Zhu L, Yin F, Moming A, Zhang J, Wang B, Gao L, et al. First case of laboratory-confirmed severe fever with thrombocytopenia syndrome disease revealed the risk of SFTSV infection in Xinjiang, China. Emerg Microbes Infect. 2019;8:1122–5. https://doi.org/10.1080/22221751.2019.1645573
13. Yun Y, Heo ST, Kim G, Hewson R, Kim H, Park D, et al. Phylogenetic analysis of severe fever with thrombocytopenia syndrome virus in South Korea and migratory bird routes between China, South Korea, and Japan. Am J Trop Med Hyg. 2015;93:468–74. https://doi.org/10.4269/ajtmh.15-0047
14. Li Z, Bao C, Hu J, Liu W, Wang X, Zhang L, et al. Ecology of the tick-borne phlebovirus causing severe fever with thrombocytopenia syndrome in an endemic area of China. PLoS Negl Trop Dis. 2016;10:e0004574. https://doi.org/10.1371/journal.pntd.0004574
15. Zhang X, Zhao C, Cheng C, Zhang G, Yu T, Lawrence K, et al. Rapid spread of severe fever with thrombocytopenia syndrome virus by parthenogenetic Asian longhorned ticks. Emerg Infect Dis. 2022;28:363–72. https://doi.org/10.3201/eid2802.211532
16. Zhuang L, Sun Y, Cui XM, Tang F, Hu JG, Wang LY, et al. Transmission of severe fever with thrombocytopenia syndrome virus by *Haemaphysalis longicornis* ticks, China. Emerg Infect Dis. 2018;24. https://doi.org/10.3201/eid2405.151435
17. Park SW, Song BG, Shin EH, Yun SM, Han MG, Park MY, et al. Prevalence of severe fever with thrombocytopenia syndrome virus in *Haemaphysalis longicornis* ticks in South Korea. Ticks Tick Borne Dis. 2014;5:975–7. https://doi.org/10.1016/j.ttbdis.2014.07.020

18. Luo LM, Zhao L, Wen HL, Zhang ZT, Liu JW, Fang LZ, et al. *Haemaphysalis longicornis* ticks as reservoir and vector of severe fever with thrombocytopenia syndrome virus in China. Emerg Infect Dis. 2015;21:1770–6. https://doi.org/10.3201/eid2110.150126

19. Hu YY, Zhuang L, Liu K, Sun Y, Dai K, Zhang XA, et al. Role of three tick species in the maintenance and transmission of severe fever with thrombocytopenia syndrome virus. PLoS Negl Trop Dis. 2020;14:e0008368. https://doi.org/10.1371/journal.pntd.0008368

20. Wang S, Li J, Niu G, Wang X, Ding S, Jiang X, et al. SFTS virus in ticks in an endemic area of China. Am J Trop Med Hyg. 2015;92:684–9. https://doi.org/10.4269/ajtmh.14-0008

21. Chen C, Li P, Li KF, Wang HL, Dai YX, Cheng X, et al. Animals as amplification hosts in the spread of severe fever with thrombocytopenia syndrome virus: a systematic review and meta-analysis. Int J Infect Dis. 2019;79:77-84.

22. Huang XY, Du YH, Wang HF, You AG, Li Y, Su J, et al. Prevalence of severe fever with thrombocytopenia syndrome virus in animals in Henan Province, China. Infect Dis Poverty. 2019;8:56. https://doi.org/10.1186/s40249-019-0569-x

23. Niu G, Li J, Liang M, Jiang X, Jiang M, Yin H, et al. Severe fever with thrombocytopenia syndrome virus among domesticated animals, China. Emerg Infect Dis. 2013;19:756–63. https://doi.org/10.3201/eid1905.120245

24. He K, Chen JH, Gould GC, Yamaguchi N, Ai HS, Wang YX, et al. An estimation of *Erinaceidae* phylogeny: a combined analysis approach. PLoS One. 2012;7:e39304. https://doi.org/10.1371/journal.pone.0039304

25. Brockie RE. Distribution and abundance of the hedgehog (*Erinaceus europaeus*) L. in New Zealand, 1869–1973. N Z J Zool. 1975;2:445–62. https://doi.org/10.1080/03014223.1975.9517886

26. Isaac JL. Introduced mammals of the world: their history, distribution and influence. Austral Ecol. 2005;30:237–8. https://doi.org/10.1111/j.1442-9993.2005.1414_1_1.x

27. Riley PY, Chomel BB. Hedgehog zoonoses. Emerg Infect Dis. 2005;11:1–5. https://doi.org/10.3201/eid1101.040752

28. Jahfari S, Ruyts SC, Frazer-Mendelewska E, Jaarsma R, Verheyen K, Sprong H. Melting pot of tick-borne zoonoses: the European hedgehog contributes to the maintenance of various tick-borne diseases in natural cycles urban and suburban areas. Parasit Vectors. 2017;10:134. https://doi.org/10.1186/s13071-017-2065-0

29. Dziemian S, Sikora B, Piłacińska B, Michalik J, Zwolak R. Ectoparasite loads in sympatric urban populations of the northern white-breasted and the European hedgehog. Parasitol Res. 2015;114:2317–23. https://doi.org/10.1007/s00436-015-4427-x

30. Bouma HR, Carey HV, Kroese FG. Hibernation: the immune system at rest? J Leukoc Biol. 2010;88:619–24. https://doi.org/10.1189/jlb.0310174

31. Simková A. Quantitative study of experimental Tahyna virus infection in hibernating hedgehogs. J Hyg Epidemiol Microbiol Immunol. 1966;10:499–509.

32. Sun Y, Liu MM, Luo LM, Zhao L, Wen HL, Zhang ZT, et al. Seroprevalence of severe fever with thrombocytopenia syndrome virus in hedgehog from China. Vector Borne Zoonotic Dis. 2017;17:347–50. https://doi.org/10.1089/vbz.2016.2019

33. Jiang Z, Liu S, Wu Y, Jiang X, Zhou K. China's mammal diversity (2nd edition). 2017;25(8):886–95.

34. Matsuno K, Orba Y, Maede-White K, Scott D, Feldmann F, Liang M, et al. Animal models of emerging tick-borne phleboviruses: determining target cells in a lethal model of SFTSV infection. Front Microbiol. 2017;8:104. https://doi.org/10.3389/fmicb.2017.00104

35. Li Z, Hu J, Bao C, Li P, Qi X, Qin Y, et al. Seroprevalence of antibodies against SFTS virus infection in farmers and animals, Jiangsu, China. J Clin Virol. 2014;60:185–9. https://doi.org/10.1016/j.jcv.2014.03.020

36. Casel MA, Park SJ, Choi YK. Severe fever with thrombocytopenia syndrome virus: emerging novel phlebovirus and their control strategy. Exp Mol Med. 2021;53:713–22. https://doi.org/10.1038/s12276-021-00610-1

37. Jiao Y, Qi X, Liu D, Zeng X, Han Y, Guo X, et al. Experimental and natural infections of goats with severe fever with thrombocytopenia syndrome virus: evidence for ticks as viral vector. PLoS Negl Trop Dis. 2015;9:e0004092. https://doi.org/10.1371/journal.pntd.0004092

38. Park SC, Park JY, Choi JY, Oh B, Yang MS, Lee SY, et al. Experimental infection of dogs with severe fever with thrombocytopenia syndrome virus: pathogenicity and potential for intraspecies transmission. Transbound Emerg Dis. 2022;69:3090–6. https://doi.org/10.1111/tbed.14372

39. Kim JY, Jung M, Kho JW, Song H, Moon K, Kim YH, et al. Characterization of overwintering sites of *Haemaphysalis longicornis* (Acari: Ixodidae) and tick infection rate with severe fever with thrombocytopenia syndrome virus from eight provinces in South Korea. Ticks Tick Borne Dis. 2020;11:101490. https://doi.org/10.1016/j.ttbdis.2020.101490

40. Nosek J, Grulich I. The relationship between the tick-borne encephalitis virus and the ticks and mammals of the Tribec mountain range. Bull World Health Organ. 1967;36(Suppl):31–47.

41. Li Z, Bao C, Hu J, Gao C, Zhang N, Xiang H, et al. Susceptibility of spotted doves (*Streptopelia chinensis*) to experimental infection with the severe fever with thrombocytopenia syndrome phlebovirus. PLoS Negl Trop Dis. 2019;13:e0006982. https://doi.org/10.1371/journal.pntd.0006982

42. Parkes J. Some aspects of the biology of the hedgehog (*Erinaceus europaeus* L.) in the Manawatu, New Zealand. N Z J Zool. 1975;2:463–72. https://doi.org/10.1080/03014223.1975.9517887

43. Brockie RE. The hedgehog population and invertebrate fauna of the west coast sand dunes. Proceedings of the New Zealand Ecological Society 1957;5:27–9.

44. Campbell PA. The feeding behaviour of the hedgehog (*Erinaceus europaeus* L.) in pasture land in New Zealand. Proceedings of the New Zealand Ecological Society. 1973;20:35–40.

45. Heath A. Biology, ecology and distribution of the tick, *Haemaphysalis longicornis* Neumann (Acari: Ixodidae) in New Zealand. N Z Vet J. 2016;64:10–20. https://doi.org/10.1080/00480169.2015.1035769

46. Zhang X, Zhao C, Cheng C, Zhang G, Yu T, Lawrence K, et al. Rapid spread of severe fever with thrombocytopenia syndrome virus by parthenogenetic Asian longhorned ticks. Emerg Infect Dis. 2022;28:363–72. https://doi.org/10.3201/eid2802.211532

Isolation of Bat Sarbecoviruses, Japan

Shin Murakami, Tomoya Kitamura, Hiromichi Matsugo, Haruhiko Kamiki, Ken Oyabu,
Wataru Sekine, Akiko Takenaka-Uema, Yuko Sakai-Tagawa, Yoshihiro Kawaoka, Taisuke Horimoto

Surveillance of bat betacoronaviruses is crucial for understanding their spillover potential. We isolated bat sarbecoviruses from *Rhinolophus cornutus* bats in multiple locations in Japan. These viruses grew efficiently in cells expressing *R. cornutus* angiotensin converting enzyme-2, but not in cells expressing human angiotensin converting enzyme-2, suggesting a narrow host range.

Human betacoronaviruses are divided into 2 pathotypes: endemic viruses, such as human coronavirus OC43 (HCoV-OC43) and HCoV-HKU1, which cause mild respiratory symptoms (*1*), and highly pathogenic viruses comprising severe acute respiratory syndrome coronavirus (SARS-CoV), Middle East respiratory syndrome coronavirus, and SARS-CoV-2, which have caused outbreaks in the past 2 decades (*1,2*). Because all these highly pathogenic human betacoronaviruses are considered to have originated from bat-derived viruses (*2–6*), surveillance of bat betacoronaviruses is crucial for understanding and assessing the spillover potential of betacoronaviruses in humans.

Bats belonging to the genus *Rhinolophus* are considered natural reservoirs of sarbecoviruses because most have been detected in *Rhinolophus* bats in countries in Asia (*3–8*), as well as in countries in Europe and Africa (*9,10*). We previously identified a bat sarbecovirus, Rc-o319, from *Rhinolophus cornutus* bats in the Iwate Prefecture of Japan, which was shown to phylogenetically belong to the SARS-CoV-2 lineage (*7*).

Vesicular stomatitis virus–based pseudotyped virus having the Rc-o319 spike (S) protein was able to infect cells expressing *R. cornutus* angiotensin-converting enzyme 2 (RcACE2), but not those expressing human angiotensin-converting enzyme 2 (hACE2), suggesting that the Rc-o319 virus uses RcACE2 as its receptor (*7*). Sarbecoviruses detected in China and other countries in Asia were shown to vary genetically; however, the distribution and genetic variation of bat sarbecoviruses in Japan have not yet been determined.

Despite surveillance-based genetic detection of numerous bat sarbecoviruses, cultivable viruses have been rarely isolated to date, leading to the application of a pseudovirus system as described above to analyze their entry mechanisms into cells. Receptor selectivity assessed in this system does not necessarily correspond to functional receptor specificity of intact bat sarbecovirus (*11*), emphasizing the need for cultivable virus for assessment of its spillover potential of bat sarbecoviruses. We report detection, isolation, and genetic and biologic characterization of cultivable bat sarbecoviruses from several locations in Japan.

The Study

We collected fecal samples from bats belonging to the *R. cornutus* and *R. ferrumequinum* species in Niigata, Chiba, and Shizuoka Prefectures (Appendix Figure 1, panel A, https://wwwnc.cdc.gov/EID/article/28/12/22-0801-App1.pdf). Using real-time reverse transcription PCR, we successfully detected the envelope gene sequence of sarbecovirus in 1 or 2 *R. cornutus* bat samples in each prefecture (Table 1). In contrast, all *R. ferremuquinum* bat samples were negative. These data suggested that bat sarbecoviruses are distributed among *R. cornutus* bats at various locations in Japan.

In our previous study, we showed that a vesicular stomatitis virus–based pseudotyped virus possessing the S protein of Rc-o319 sarbecovirus from *R. cornutus* only infected RcACE2-expressing cells, but not hACE2-expressing or other *Rhinolophus* ACE2–expressing cells (*7*). Therefore, to isolate bat sarbecoviruses, we established RcACE2-stably expressing

Author affiliations: The University of Tokyo, Tokyo, Japan
(S. Murakami, H. Matsugo, H. Kamiki, W. Sekine,
A. Takenaka-Uema, Y. Sakai-Tagawa, Y. Kawaoka, T. Horimoto);
National Agriculture and Food Research Organization, Tokyo
(T. Kitamura); Isumi County–City Nature Preservation Association,
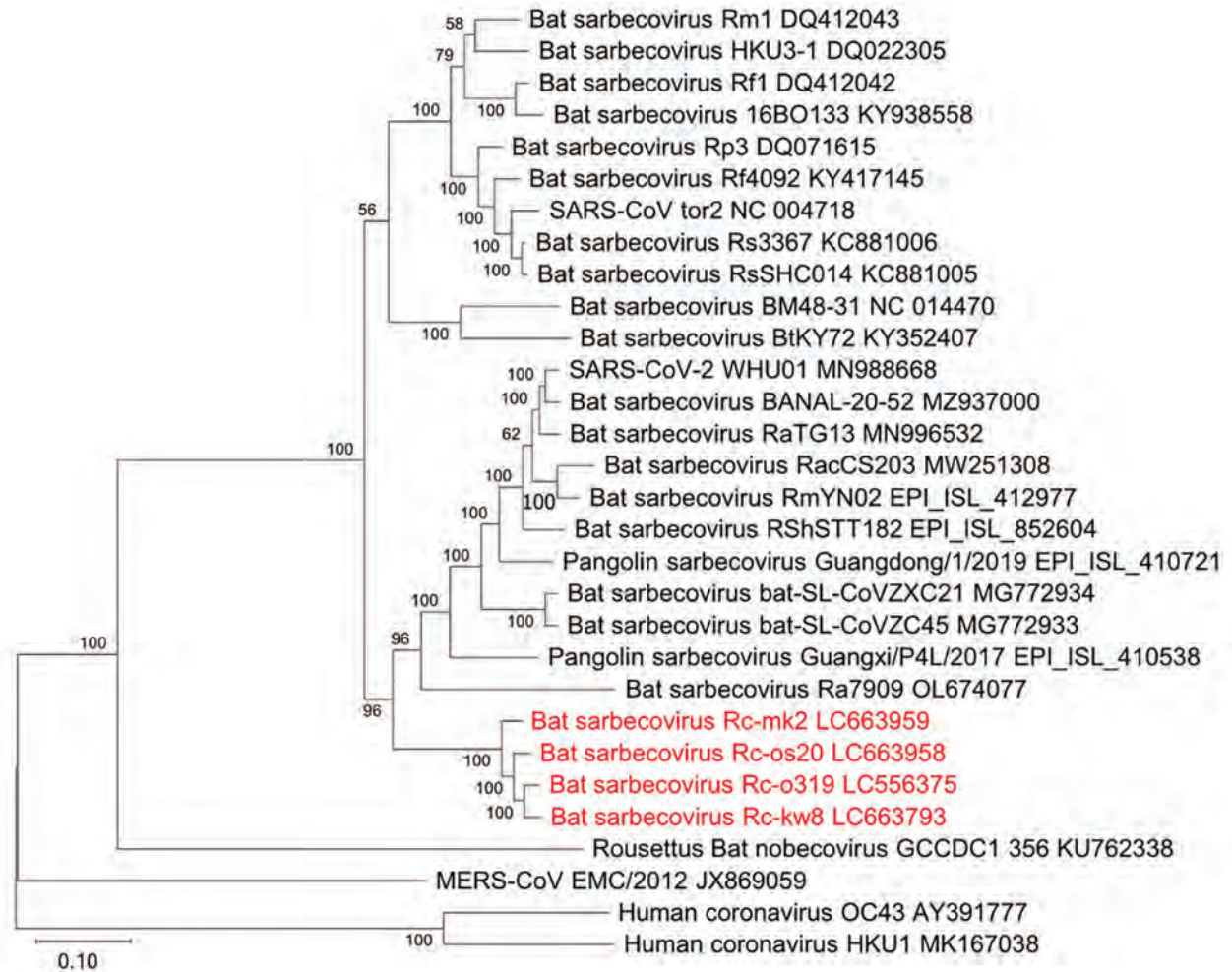Isumi-gun, Chiba, Japan (K. Oyabu)

Figure 1. Phylogenetic tree of sarbecoviruses from bats in Japan, generated by using the full-genome nucleotide sequences with the maximum-likelihood analysis combined with 500 bootstrap replicates. Red indicates strains isolated in this study. Bootstrap values are shown above and to the left of the major nodes. GenBank accession numbers are indicated. Scale bars indicate nucleotide substitutions per site.

cells (Vero-RcACE2) based on Vero/TMPRSS2 cells. Using Vero-RcACE2 cells, we successfully isolated bat sarbecoviruses, which exhibited extensive cytopathic effect with syncytium formation (Appendix Figure 1, panel B) from real-time reverse transcription PCR–positive fecal samples from each prefecture. We designated the Niigata isolate as Rc-os20, the Chiba isolate as Rc-mk2, and the Shizuoka isolate as Rc-kw8. We further isolated the cultivable Rc-o319 strain by using Vero-RcACE2 cells.

We determined the full-genome sequence of all isolates by using next-generation sequencing and deposited the sequences in GenBank (accession nos. LC663958, LC663959, and LC663793). We found that sequence homologies were high (range 94.8%–96.8%) among all isolates from Japan (Table 2), However, Rc-mk2 and Rc-os20 lacked the entire open reading frame 8 coding region.

We also performed similarity plot analysis of entire genome sequence by using each isolate as a query,

Table 1. Detection of sarbecoviruses in *Rhinolophus* bats by RT-PCR, Japan*

Location	Bat species	No. samples	No. positive RT-PCR samples
Niigata	*R. cornutus*	26	2
	R. ferrumequinum	1	0
Chiba	*R. cornutus*	11	1
	R. ferrumequinum	16	0
Shizuoka	*R. cornutus*	21	2
	R. ferrumequinum	13	0

*RT-PCR was performed by using sarbecovirus consensus primers targeting the envelope gene. RT-PCR, reverse transcription PCR.

which indicated that similarities among isolates were high throughout the entire genome sequence, except for coding regions of the N-terminal domain (NTD) and receptor-binding domain (RBD) of the S gene, although NTDs of Rc-o319 and Rc-kw8 were conserved (Appendix Figure 2). No clear recombination among the isolates were observed as analyzed by RDP5 software (*12*). Phylogenetic analysis showed that the isolates from Japan formed a single genetic cluster and positioned in a clade containing SARS-CoV-2–related sarbecoviruses, which might be designated the Japanese clade of bat sarbecoviruses (Figure 1).

We aligned the receptor-binding motif of the S protein of isolates from Japan with that of other sarbecoviruses (Appendix Figure 3, panel A). We observed that all isolates had a 9-aa deletion in this motif, as previously observed in Rc-o319, and had relatively conserved residues with Rc-o319. In addition, phylogenetic tree analysis of RBD showed that strains from Japan were included in the clade of viruses that use ACE2 orthologs as a strain receptor (Appendix Figure 3, panel B). Therefore, we assumed that these new strains from Japan use RcACE2 as a receptor.

To test this hypothesis, we compared the replication of isolates from Japan with that of a control SARS-CoV-2 (B.1.1.7, Alpha variant) in Vero-RcACE2, Vero-hACE2, Vero-ACE2KO, and Vero/TMPRSS2 cells. Whereas the 4 bat isolates replicated well in Vero-RcACE2 only, they did not replicate in Vero/TMPRSS2, Vero-hACE2, or Vero-ACE2KO cells, suggesting their RcACE2-dependent infectivity. In contrast, we observed that SARS-CoV-2 replicated efficiently in Vero/TMPRSS2, Vero-RcACE2, and Vero-hACE2 cells, but not in Vero-ACE2KO cells (Figure 2), suggesting multiple ACE2-dependent infectivity, includ-

Table 2. Full-genome nucleotide identity for sarbecovirus isolates from bats, Japan

Isolate	Rc-o319	Rc-os20	Rc-kw8	Rc-mk2
Rc-o319	–	95.6%	96.8%	94.8%
Rc-os20	–	–	95.4%	95.4%
Rc-kw8	–	–	–	95.1%
SARS-CoV-2	81.5%	80.7%	81.4%	80.7%

ing that of *R. cornutus* bats. These data suggested that at isolates from Japan use only bRcACE2 as a receptor, showing narrow host specificity.

Conclusions

We isolated bat sarbecoviruses from *R. cornutus* bats in several locations in Japan that were phylogenetically positioned in the same cluster of the SARS-CoV-2–related viruses. These isolates used only bat ACE2 as a receptor and did not replicate in hACE2-expressing cells, forming a unique type, and suggesting a low potential for human infection.

To our knowledge, this type of bat sarbecoviruses has not been previously isolated (*13*) because African green monkey Vero cells having highly similar ACE2 to hACE2 were used for viral isolation attempts in the previous studies (*4*,*5*). Cultivable bat sarbecoviruses provide a useful and powerful tool to determine their characteristics, such as receptor specificity and pathogenicity in animals, leading to elucidation of spillover potential.

Rhinolophus spp. bats are relatively short-distance migrants (*14*) and lack frequent cross-contact between bat groups, explaining why most genome sequences were highly conserved among strains from Japan. Exceptions were the RBD-coding and NTD-coding regions of the S gene, which show high variation caused by immune pressure (*15*), suggesting
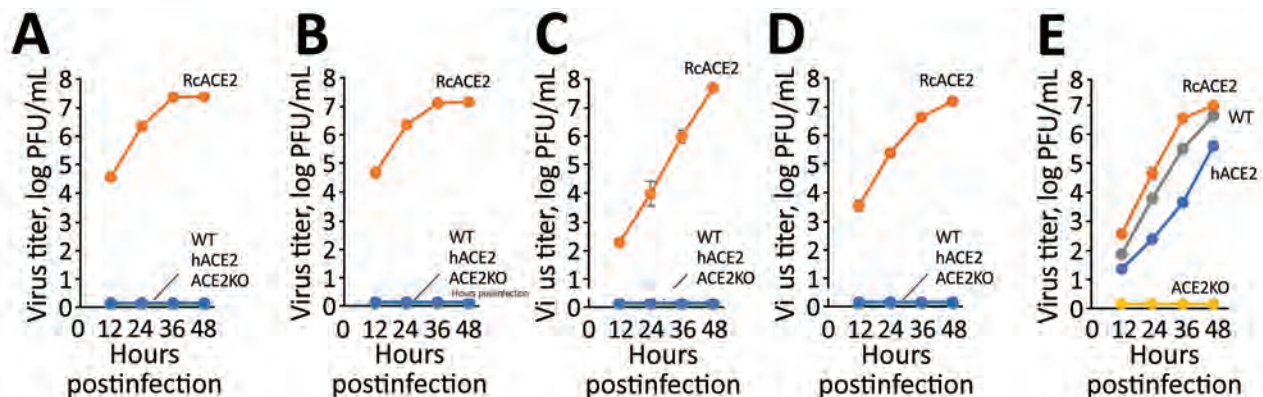

Figure 2. Growth kinetics of sarbecovirus isolates from bats in Japan. *Rhinolophus cornutus* bat isolates Rc-o319 (A), Rc-os20 (B), Rc-mk2 (C), and Rc-kw8 (D) or SARS-CoV-2 (B.1.1.7) (E) were inoculated into Vero/TMPRSS2 (WT), Vero-RcACE2 (RcACE2), Vero-hACE2 (hACE2), or Vero-ACE2KO (ACE2KO) cells at a multiplicity of infection of 0.01. The culture supernatants were collected at the indicated time points, and viral titers were determined by using a plaque assay. Data are reported as the mean titer with standard deviations from 3 independent experiments. ACE2, angiotensin converting enzyme 2; hACE2, human ACE2; RcACE2, *R. cornutus* ACE2; WT, wild-type

that they diverged relatively recently from the undefined ancestral virus. Because sarbecoviruses might mutate and infect humans by intermediate hosts in wildlife or livestock, epidemiologic studies of sarbecoviruses in wildlife, including bats, need to be conducted on a long-term basis for risk assessment of their zoonotic potential.

Acknowledgment

About the Author

Dr. Murakami is an associate professor at the Graduate School of Agricultural and Life Sciences, University of Tokyo, Tokyo, Japan. His primary research interests are epidemiologic and molecular biologic studies of animal viruses, including coronaviruses and influenza viruses.

References

1. Jo WK, de Oliveira-Filho EF, Rasche A, Greenwood AD, Osterrieder K, Drexler JF. Potential zoonotic sources of SARS-CoV-2 infections. Transbound Emerg Dis. 2021;68:1824–34. https://doi.org/10.1111/tbed.13872
2. Cui J, Li F, Shi ZL. Origin and evolution of pathogenic coronaviruses. Nat Rev Microbiol. 2019;17:181–92. https://doi.org/10.1038/s41579-018-0118-9
3. Li W, Shi Z, Yu M, Ren W, Smith C, Epstein JH, et al. Bats are natural reservoirs of SARS-like coronaviruses. Science. 2005;310:676–9. https://doi.org/10.1126/science.1118391
4. Ge XY, Li JL, Yang XL, Chmura AA, Zhu G, Epstein JH, et al. Isolation and characterization of a bat SARS-like coronavirus that uses the ACE2 receptor. Nature. 2013;503:535–8. https://doi.org/10.1038/nature12711
5. Temmam S, Vongphayloth K, Baquero E, Munier S, Bonomi M, Regnault B, et al. Bat coronaviruses related to SARS-CoV-2 and infectious for human cells. Nature. 2022;604:330–6. https://doi.org/10.1038/s41586-022-04532-4
6. Hu B, Zeng LP, Yang XL, Ge XY, Zhang W, Li B, et al. Discovery of a rich gene pool of bat SARS-related coronaviruses provides new insights into the origin of SARS coronavirus. PLoS Pathog. 2017;13:e1006698. https://doi.org/10.1371/journal.ppat.1006698
7. Murakami S, Kitamura T, Suzuki J, Sato R, Aoi T, Fujii M, et al. Detection and characterization of bat sarbecovirus phylogenetically related to SARS-CoV-2, Japan. Emerg Infect Dis. 2020;26:3025–9. https://doi.org/10.3201/eid2612.203386
8. Wacharapluesadee S, Tan CW, Maneeorn P, Duengkae P, Zhu F, Joyjinda Y, et al. Evidence for SARS-CoV-2 related coronaviruses circulating in bats and pangolins in Southeast Asia. Nat Commun. 2021;12:972. https://doi.org/10.1038/s41467-021-21240-1
9. Drexler JF, Gloza-Rausch F, Glende J, Corman VM, Muth D, Goettsche M, et al. Genomic characterization of severe acute respiratory syndrome-related coronavirus in European bats and classification of coronaviruses based on partial RNA-dependent RNA polymerase gene sequences. J Virol. 2010;84:11336–49. https://doi.org/10.1128/JVI.00650-10
10. Tao Y, Tong S. Complete genome sequence of a severe acute respiratory syndrome-related coronavirus from Kenyan bats. Microbiol Resour Announc. 2019;8:e00548–19. https://doi.org/10.1128/MRA.00548-19
11. Menachery VD, Yount BL Jr, Debbink K, Agnihothram S, Gralinski LE, Plante JA, et al. A SARS-like cluster of circulating bat coronaviruses shows potential for human emergence. Nat Med. 2015;21:1508–13. https://doi.org/10.1038/nm.3985
12. Martin DP, Varsani A, Roumagnac P, Botha G, Maslamoney S, Schwab T, et al. RDP5: a computer program for analyzing recombination in and removing signals of recombination from, nucleotide sequence datasets. Virus Evol. 2020;7:veaa087.
13. Starr TN, Zepeda SK, Walls AC, Greaney AJ, Alkhovsky S, Veesler D, et al. ACE2 binding is an ancestral and evolvable trait of sarbecoviruses. Nature. 2022;603:913–8. https://doi.org/10.1038/s41586-022-04464-z
14. Bontadina F, Schofield H, Naef-Daenzer B. Radio-tracking reveals that lesser horseshoe bats (Rhinolophus hipposideros) forage in woodland. J Zool (Lond). 2002;258:281–90. https://doi.org/10.1017/S0952836902001401
15. Liu L, Wang P, Nair MS, Yu J, Rapp M, Wang Q, et al. Potent neutralizing antibodies against multiple epitopes on SARS-CoV-2 spike. Nature. 2020;584:450–6. https://doi.org/10.1038/s41586-020-2571-7

Address for correspondence: Shin Murakami, Laboratory of Veterinary Microbiology, Graduate School of Agricultural and Life Sciences, The University of Tokyo, 1-1-1 Yayoi, Bunkyo-ku, Tokyo 113-8657, Japan; email: shin-murakami@g.ecc.u-tokyo.ac.jp

Severe and Rare Case of Human *Dirofilaria repens* Infection with Pleural and Subcutaneous Manifestations, Slovenia

Helena Biasizzo,[1] Barbara Šoba, Frosina Ilovski, Matevž Harlander,
Matej Lukin, Olga Blatnik, Matjaž Turel, Matevž Srpčič, Izidor Kern, Bojana Beović

We report a case of human *Dirofilaria repens* infection in a woman in Slovenia who had concomitant pleural and subcutaneous manifestations of the infection. This case report illustrates the clinical course of a severe symptomatic parasitic infection that had multisystemic manifestations.

*D*irofilaria repens is a filaria that causes infection primarily in dogs and other wild canids. The infection has been historically endemic in the Mediterranean countries. However, it has expanded to the rest of Europe in the past 2 decades, where it is considered an emerging infection (*1*).

Canids act as a reservoir for the parasite, where it can reach sexual maturity and produce microfilariae. Microfilariae are ingested by female mosquitoes, where they develop to infective larvae and are introduced to another definitive host during the blood meal of the vector (*2*). Humans can also acquire the infection, but are considered a dead-end host because microfilaremia in humans has only rarely been demonstrated (*3,4*).

Clinical symptoms of *D. repens* infection in humans are the consequence of the inflammatory reaction provoked by the migrating macrofilaria(e). The infection in humans is usually localized with only 1 parasite being found in most cases, and multiple parasites are rarely observed (*1,5–7*).

Depending on the anatomic location of the symptoms, *D. repens* infection has traditionally been divided into subcutaneous and ocular forms. The subcutaneous form is characterized by swelling and larva migrans–like symptoms, whereas the ocular form shows visual disturbances caused by the migrating parasite (*1,7,8*). In addition, cases of other organ involvement have been reported, including testicles and lungs (*1*). Another, quite rare form is a pleural form, which manifests as an incidentally detected pleural lesion mimicking malignancy (*9*).

The course of this infection in humans is usually indolent, except for the ocular form, which can lead to loss of vision and, on rare occasions, involvement of vital organs, such as the central nervous system. Excision of macrofilaria is usually curative because only 1 parasite is usually present. However, in some cases treatment with antiparasitic drugs is needed (*10*). We report an unusual case in a patient who had pleural and subcutaneous *D. repens* clinical manifestations.

The Study

A 40-year-old woman, a nonsmoker who had celiac disease but who was not receiving any regular medication and had no allergies, started having progressive dyspnea, dry cough, pain in the left hemithorax on inspiration, night sweats, and general malaise in September 2020. She reported no fever or weight loss. However, in addition, migratory, angioedematous skin changes measuring ≈15 cm × 15 cm started to appear on the upper trunk and axillary regions. Skin changes were present for 1–3 days and then disappeared (Figure 1, panel A). Her problems gradually intensified during the following months.

The patient sought medical attention in January 2021. Apart from decreased breath sounds on the left

Authors affiliations: University Medical Centre, Ljubljana, Slovenia (H. Biasizzo, F. Ilovski, M. Harlander, M. Lukin, M. Turel, M. Srpčič, B. Beović); University of Ljubljana, Ljubljana (B. Šoba); Institute of Oncology, Ljubljana (O. Blatnik); University Clinic Golnik, Golnik, Slovenia (I. Kern)

[1]Current affiliation: General Hospital, Novo Mesto, Slovenia.

side, the clinical examination was unremarkable. Results for complete blood count, leukocyte differential counts, and C-reactive protein level were within reference ranges. A chest radiograph showed left-sided pleural effusion (Figure 1, panel B). Diagnostic thoracocentesis showed exudative pleurisy with lymphocytic predominance. There were no malignant cells, and results of microbiological examinations were negative.

Thorax and abdomen computed tomography scan showed a lesion adjacent to the left posterobasal pleura, pleural thickening suspicious for pleural carcinomatosis, left-sided pleural effusion, and reactive mediastinal and mesenteric lymph nodes (Figure 1, panels C, D).

A video-assisted thoracoscopic surgical excision of the pleural lesion was then performed. A total of 2,000 mL of serohemorrhagic pleural fluid was evacuated during the procedure.

Histologic examination of the excised tissue showed necrotizing granulomas containing structures with a thick, laminated cuticle with external ridges, morphologically characteristic for the *Dirofilaria* spp. nematode (Figure 2). We extracted DNA from three 10 μm–thick sections of formalin-fixed, paraffin-em-

bedded tissue block by using a Deparaffinization Solution and a QIAamp DNA Mini Kit (all from QIAGEN, https://www.qiagen.com). *D. repens* infection was confirmed by using a species-specific, real-time PCR (qPCR), which amplified a 166-bp portion of the cytochrome c oxidase subunit 1 mitochondrial gene (*cox1*) (*11*). Sequencing and BLAST analysis (https://blast.ncbi.nlm.nih.gov/Blast.cgi) of a 689-bp fragment of *cox1* (*12*) showed 100% homology with several *D. repens* isolates from Europe (Appendix Figure, https://wwwnc.cdc.gov/EID/article/28/12/22-1366-App-F1.pdf). The sequence obtained has been deposited into GenBank (accession no. OP494268).

To detect microfilaremia, we extracted DNA from an EDTA–whole blood sample of the patient by using the QIAamp DNA Mini Kit and performed a filarial qPCR, amplifying a portion of the 28S rRNA gene (*11*). The filarial qPCR result was negative.

Once the diagnosis was established, the patient was asked about possible risk factors for acquisition of the infection. She reported visiting the Istria region in Croatia in March 2020, where she had contact with stray dogs and was bitten by mosquitoes.

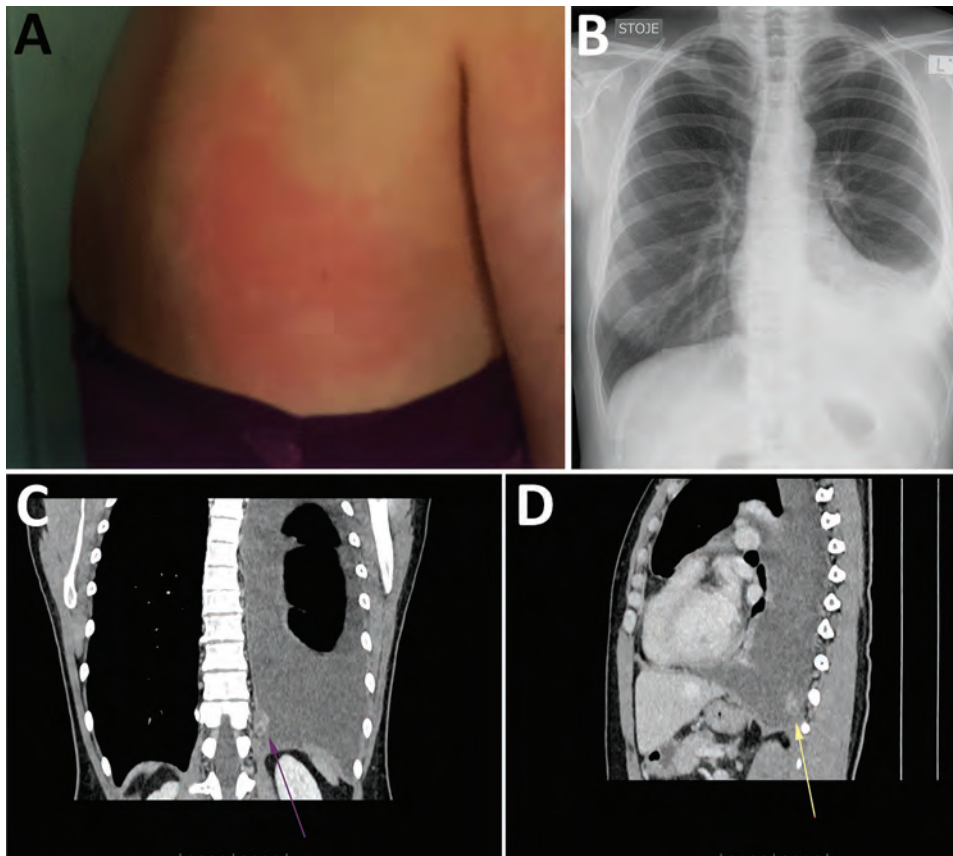After excision of the pleural lesion and evacuation of the pleural fluid, respiratory symptoms of the

Figure 1. *Dirofilaria repens* infection with subcutaneous and pleural manifestations in a woman in Slovenia. A) Erythematous itchy skin lesion on the patient's back measuring 15 cm x 15 cm (photograph taken by the patient). B) Frontal radiograph showing large left-sided pleural effusion. C, D) Contrast-enhanced computed tomography images showing large left-sided pleural effusion, uneven thickening of pleura, and a focal, heterogeneously enhancing soft tissue mass measuring 26 mm × 16 mm × 14 mm (arrows) in the posterior inferior part of the costal pleura in the coronal (C) and sagittal (D) plane.
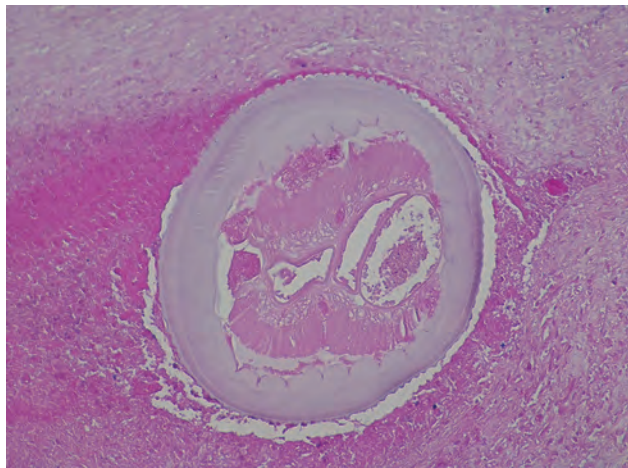
Figure 2. Photomicrograph of a cross-section of a *Dirofilaria repens* female in the background of necrosis in a sample from a woman in Slovenia. Image shows a multilayered cuticle with external ridges (feature that discriminates *D. repens* nematodes from other filariae infecting humans in the Mediterranean region); muscle cells, digestive tract and 2 uteri are well visible. The diameter at the widest point of the parasite is 0.6 mm. Hematoxylin and eosin stain; original magnification × 200.

patient slowly resolved. However, in March 2021, skin lesions persisted, and although not present initially, mild eosinophilia in peripheral blood (0.7 × 10^9 cells/L) was detected. An ophthalmic examination was performed to exclude the ocular form and showed no abnormality. Treatment with ivermectin (200 μg/kg/d for 4 days) and doxycycline (100 mg 2×/d for 7 days) was initiated.

After treatment, the skin lesions completely disappeared and have not reappeared. The last computed tomography scan of the chest was performed in September 2021 and showed no pleural lesions or pleural effusion and the disappearance or regression of mediastinal and mesenteric lymph nodes. The patient has since remained without any problems.

Conclusions

This case is noteworthy for several reasons. First, it illustrates human *D. repens* infection with pleural involvement, which is exceedingly rare. In our patient, the infection manifested not only with a pleural lesion but also with large pleural effusion, requiring evacuation of pleural fluid to relieve respiratory symptoms. In general, such clinical manifestations would be suspicious for malignancy, but this possibility was excluded by cytological and histological examinations.

Another filaria, *D. immitis*, which occurs sporadically in Slovenia and is endemic to neighboring Croatia, can also infect humans and cause predomi-

nantly pulmonary symptoms. Without detailed histological examination and molecular diagnosis, this clinical manifestation might be mistaken for *D. immitis* infection (*2*).

Second, unlike in most cases, it seems that our patient was infested with ≥2 macrofilariae, 1 located in the pleura and 1 located in the subcutaneous tissue of the upper body. Clinical manifestation with multiple parasites is rarely encountered in humans and might lead to microfilaremia in some exceptional cases (*3–6*). Because the filarial qPCR result of a whole blood sample with a detection limit of $1.5 × 10^{-4}$ microfilariae/mL of blood (*11*) was negative, microfilaremia was less probable for our patient.

Presentation with a subcutaneous nodule usually warrants surgical excision, which is diagnostic and curative. However, systemic treatment is needed if macrofilaria(e) cannot be surgically removed. Given the presence of numerous migratory erythematous lesions in our patient, antihelmintic therapy was prescribed.

The prevalence of *D. repens* infection among dogs in Slovenia is estimated to be 0.64%, whereas in some parts of Croatia it can be as high as 47.3% (*13,14*). Moreover, there have been case reports of human dirofilariasis in recent years in Slovenia (*13,15*). It can be assumed that the patient acquired the infection while visiting Croatia, although autochthonous infection cannot be ruled out.

This case illustrates an unusual manifestation of a *D. repens* nematode infection in a human. Clinicians should become familiar with possible clinical manifestations of this parasitosis, because we can expect an increased number of future cases.

About the Author

At the time of this study, Dr. Biasizzo was an infectious diseases research scientist at the University Medical Centre, Ljubljana, Slovenia. She is currently an infectious disease resident at the General Hospital, Novo Mesto, Slovenia. Her primary research interests are parasitic diseases, tropical diseases, and infections of the central nervous system.

References

1. Capelli G, Genchi C, Baneth G, Bourdeau P, Brianti E, Cardoso L, et al. Recent advances on *Dirofilaria repens* in dogs and humans in Europe. Parasit Vectors. 2018;11:663. https://doi.org/10.1186/s13071-018-3205-x
2. Simón F, Siles-Lucas M, Morchón R, González-Miguel J, Mellado I, Carretón E, et al. Human and animal dirofilariasis: the emergence of a zoonotic mosaic. Clin Microbiol Rev. 2012;25:507–44. https://doi.org/10.1128/CMR.00012-12
3. Huebl L, Tappe D, Giese M, Mempel S, Tannich E, Kreuels B, et al. Recurrent swelling and microfilaremia caused by *Dirofilaria repens* infection after travel to India. Emerg Infect Dis. 2021;27:1701–4. https://doi.org/10.3201/eid2706.210592
4. Lechner AM, Gastager H, Kern JM, Wagner B, Tappe D. Case report: successful treatment of a patient with microfilaremic dirofilariasis using doxycycline. Am J Trop Med Hyg. 2020;102:844–6. https://doi.org/10.4269/ajtmh.19-0744
5. Sałamatin RV, Pavlikovska TM, Sagach OS, Nikolayenko SM, Kornyushin VV, Kharchenko VO, et al. Human dirofilariasis due to *Dirofilaria repens* in Ukraine, an emergent zoonosis: epidemiological report of 1465 cases. Acta Parasitol. 2013;58:592–8. https://doi.org/10.2478/s11686-013-0187-x
6. Simón F, Diosdado A, Siles-Lucas M, Kartashev V, González-Miguel J. Human dirofilariosis in the 21st century: a scoping review of clinical cases reported in the literature. Transbound Emerg Dis. 2022;69:2424–39. https://doi.org/10.1111/tbed.14210
7. Ermakova LA, Nagorny SA, Krivorotova EY, Pshenichnaya NY, Matina ON. *Dirofilaria repens* in the Russian Federation: current epidemiology, diagnosis, and treatment from a federal reference center perspective. Int J Infect Dis. 2014;23:47–52. https://doi.org/10.1016/j.ijid.2014.02.008
8. Pupić-Bakrač A, Pupić-Bakrač J, Jurković D, Capar M, Lazarić Stefanović L, Antunović Ćelović I, et al. The trends of human dirofilariasis in Croatia: yesterday, today, tomorrow. One Health. 2020;10:100153. https://doi.org/10.1016/j.onehlt.2020.100153
9. Moskvina TV, Ermolenko AV. Dirofilariasis in Russian Federation: a big problem with large distribution. Russ Open Med J. 2018;7:1–12. https://doi.org/10.15275/rusomj.2018.0102
10. Poppert S, Hodapp M, Krueger A, Hegasy G, Niesen WD, Kern WV, et al. *Dirofilaria repens* infection and concomitant meningoencephalitis. Emerg Infect Dis. 2009;15:1844–6. https://doi.org/10.3201/eid1511.090936
11. Laidoudi Y, Davoust B, Varloud M, Niang EHA, Fenollar F, Mediannikov O. Development of a multiplex qPCR-based approach for the diagnosis of *Dirofilaria immitis, D. repens* and *Acanthocheilonema reconditum.* Parasit Vectors. 2020;13:319. https://doi.org/10.1186/s13071-020-04185-0
12. Casiraghi M, Anderson TJC, Bandi C, Bazzocchi C, Genchi C. A phylogenetic analysis of filarial nematodes: comparison with the phylogeny of *Wolbachia* endosymbionts. Parasitology. 2001;122:93–103. https://doi.org/10.1017/S0031182000007149
13. Kotnik T, Rataj AV, Šoba B. *Dirofilaria repens* in dogs and humans in Slovenia. J Vet Res (Pulawy). 2022;66:117–23. https://doi.org/10.2478/jvetres-2022-0008
14. Tasić-Otašević SA, Trenkić Božinović MS, Gabrielli SV, Genchi C. Canine and human *Dirofilaria* infections in the Balkan Peninsula. Vet Parasitol. 2015;209:151–6. https://doi.org/10.1016/j.vetpar.2015.02.016
15. Kramar U, Šoba B, Cvetko B, Cvetko A. First case of ocular dirofilariasis in patient from Slovenia: a case report. In: Klun I, Djurković-Djaković O, editors. Proceedings of the 13th European Multicolloquium of Parasitology; Belgrade, Serbia; October 16–21, 2021. Belgrade: Bulevar Oslobodjenja; 2021. p. 198.

Address for correspondence: Helena Biasizzo, General hospital Novo mesto, Šmihelska cesta 1, 8000 Novo mesto, Slovenia; email: helena.biasizzo@gmail.com

Myocarditis Attributable to Monkeypox Virus Infection in 2 Patients, United States, 2022

Guillermo Rodriguez-Nava, Peter Kadlecik, Thomas D. Filardo,
David L. Ain, Joseph D. Cooper, David W. McCormick, Bryant J. Webber,
Kevin O'Laughlin, Brett W. Petersen, Supriya Narasimhan, Harleen K. Sahni

We report 2 immunocompetent and otherwise healthy adults in the United States who had monkeypox and required hospitalization for viral myocarditis. Both patients were unvaccinated against orthopoxviruses. They had shortness of breath or chest pain and elevated cardiac biomarkers. No immediate complications were observed. They were discharged home after symptoms resolved.

Monkeypox is a zoonotic orthopoxvirus that is endemic to West and Central Africa and has caused sporadic outbreaks elsewhere (*1,2*). On July 23, 2022, the World Health Organization declared the 2022 monkeypox outbreak a Public Health Emergency of International Concern (*3*). Human monkeypox manifests as a viral syndrome, typically involving prominent lymphadenopathy and characteristic skin lesions (*2,4*). However, severe manifestations have been reported in children, pregnant women, and immunocompromised persons (*1,4,5*).

The Study

Both patients in this study provided informed consent for publication of deidentified medical information. Patient 1 was a healthy 32-year-old man who sought care at a hospital for his diagnosis of monkeypox. He reported having a sexual encounter with a new male partner 15 days earlier. Seven days after

that encounter, he had onset of a viral illness with cervical lymphadenopathy, followed by a disseminated rash and a painful penile lesion. Two days before his hospital visit, a nonvariola orthopoxvirus DNA PCR test on a skin lesion specimen was positive. In the hospital, the patient reported ongoing chest pain and dyspnea for 1 day (Figure 1). He reported prior treatment for syphilis. He did not report recent SARS-CoV-2 vaccination or infection and was unvaccinated for smallpox. Physical examination revealed multiple erythematous vesiculopapular and pustular lesions with erythematous borders, left inguinal lymphadenopathy, and ulceration at the base of the glans penis.

Laboratory results were notable for a nonreactive HIV by p24 antigen testing, negative HIV and hepatitis C PCR tests on serum samples, and a rapid plasma reagin titer of 1:2. Cardiac biomarkers revealed an elevated high-sensitivity troponin T (165 ng/L [reference <22 ng/L]) and elevated levels of N-terminal prohormone B-type natriuretic peptide (1,258 pg/mL [reference ≤450 pg/mL]). Electrocardiogram showed normal sinus rhythm, and chest radiograph results were unremarkable. A nasopharyngeal respiratory viral panel was unrevealing. C-reactive protein was 0.5 mg/dL (reference ≤0.5 mg/dL), and erythrocyte sedimentation rate was 11 mm/h (reference ≤15 mm/h). PCR on serum samples was negative for enterovirus and adenovirus. SARS-CoV-2 nucleocapsid antibody results were negative. Serologic test results for parvovirus, cytomegalovirus, Epstein–Barr virus, coccidioidomycosis, and human herpesvirus 6 were negative.

The patient was admitted for suspected myocarditis and started on oral tecovirimat for treatment of monkeypox and doxycycline (because of penicillin allergy) for syphilis of unknown latency. He received no specific treatment for myocarditis given the rapid resolution of symptoms and normalization of troponin levels.

Author affiliations: Stanford University School of Medicine, Stanford, California, USA (G. Rodriguez-Nava); Mid-Atlantic Permanente Medical Group, Rockville, Maryland, USA (P. Kadlecik); Centers for Disease Control and Prevention, Atlanta, Georgia, USA (T.D. Filardo, D.W. McCormick, B.J. Webber, K. O'Laughlin, B.W. Petersen); Mid-Atlantic Permanente Medical Group, Washington DC, USA (D.L. Ain); Santa Clara Valley Medical Center, San Jose, California, USA (J.D. Cooper, S. Narasimhan, H.K. Sahni)
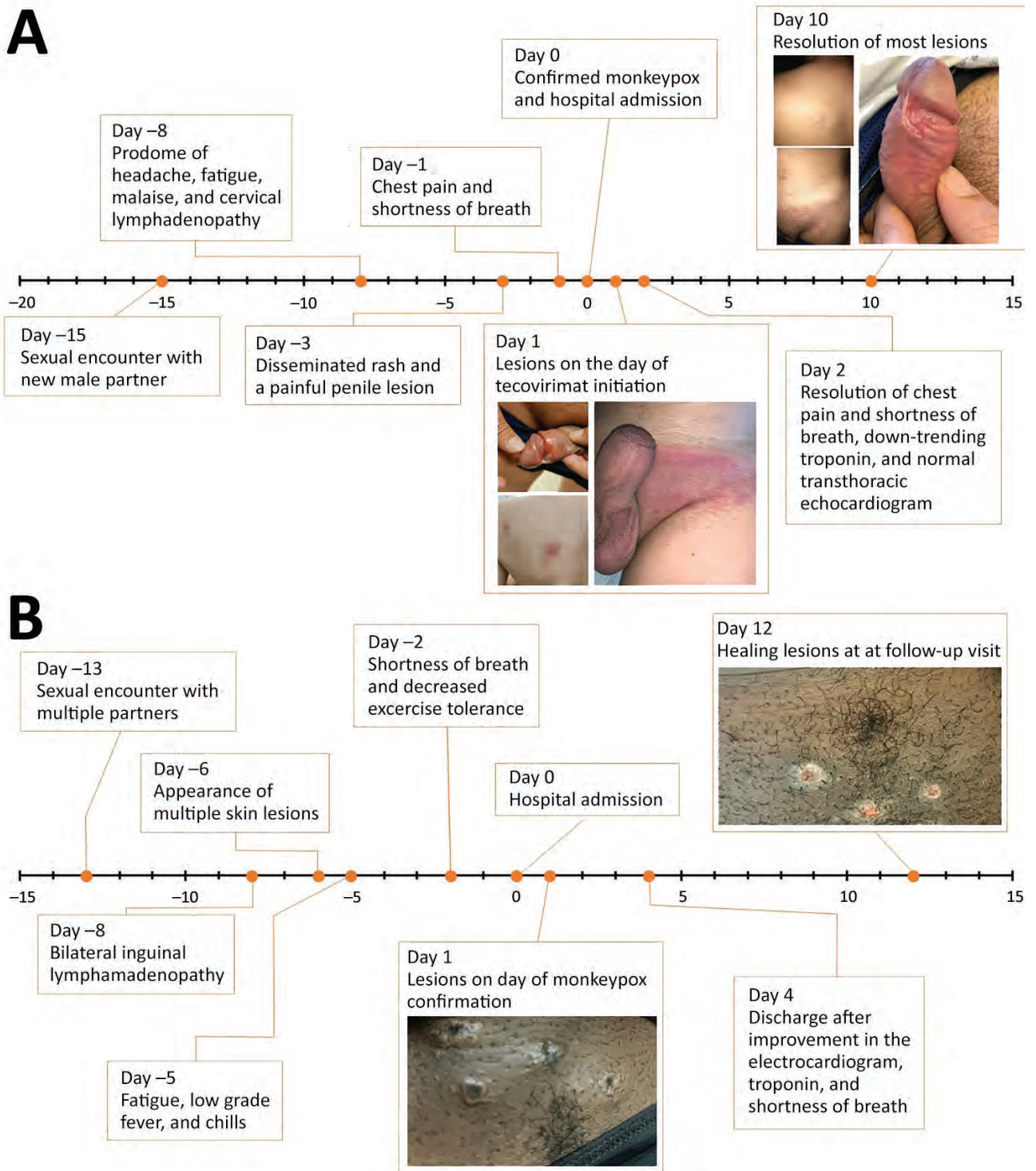
Figure 1. Timeline of events for 2 immunocompetent patients with monkeypox complicated by myocarditis, United States. A) A healthy 32-year-old man (patient 1) had chest pain and shortness of breath 7 days after a prodrome of headache, fatigue, malaise, and cervical lymphadenopathy and 2 days after the rash. Symptoms resolved after 10 days of illness onset and 1 day after initiation of tecovirimat. The patient received supportive care only for myocarditis. B) A healthy 37-year-old man (patient 2) had shortness of breath and decreased exercise tolerance 6 days after illness onset with bilateral inguinal lymphadenopathy and 4 days after the rash. Shortness of breath improved after 12 days of illness onset, and exercise tolerance normalized after 20 days. The patient received supportive care only for both monkeypox and myocarditis.

On hospital day 2, echocardiography showed an ejection fraction of 69% (reference 50%–75%) without wall motion abnormalities. By hospital day 6, the high-sensitivity troponin decreased to 11 ng/L from the initial peak of 165 ng/L. The skin and penile lesions had improved, with crusting and exfoliation of >80% of the lesions; however, the patient required prolonged hospitalization to maintain strict isolation. On hospital day 10, the only active lesion was a small penile ulcer in the process of epithelialization, and the patient was discharged to home with isolation precautions and instructions to complete a 14-day course of oral tecovirimat.

Patient 2 was a previously healthy 37-year-old man evaluated in the hospital for rash, fever, dyspnea, and decreased exercise tolerance 13 days after a sexual encounter with multiple partners. Five days after that encounter, he had onset of bilateral inguinal lymphadenopathy, followed by multiple skin lesions in both arms and a lesion at the base of the penis 2 days later. The next day, he had fatigue, low-grade fever, and chills. Two days before he sought care at the hospital, he had difficulty breathing and decreased exercise tolerance without chest pain. He reported dyspnea after climbing a single flight of stairs, a marked decrease from his baseline (Figure 1). He had a history of treated syphilis, was taking HIV preexposure prophylaxis, and reported that his mother died at age 40 from coronary artery disease. He did not report recent SARS-CoV-2 vaccination or infection and was unvaccinated for smallpox.

Physical examination showed multiple skin lesions with central umbilication in the lower pubic and inguinal areas with smaller vesicular lesions on upper extremities. Laboratory results were notable for an elevated serum troponin I (0.35 ng/mL [reference <0.07 ng/mL]); serial measurements at 4 and 8 hours were stable (0.34 and 0.39 ng/mL, respectively). B-type natriuretic peptide level was 49 pg/mL (reference <100 pg/mL). An electrocardiogram demonstrated normal sinus rhythm, with T wave inversions in the inferior and anterolateral leads (Figure 2). Subsequent tracings showed improvement in the repolarization abnormality. Echocardiography showed normal biventricular size and systolic function with normal regional wall motion, and diastolic indices were age-appropriate.

The diagnosis of monkeypox was confirmed by nonvariola orthopoxvirus PCR from skin lesion specimens. Additional testing showed negative HIV by p24 antigen testing, baseline rapid plasma reagin titer of 1:1 (consistent with treated syphilis), and a negative SARS-CoV-2 PCR result. Additional investigations for other causes of myocarditis were deferred.

The patient remained hospitalized for 4 days. Dyspnea improved on day 3 and resolved by day 4; cardiac enzymes normalized. The patient received supportive care without directed therapy for monkeypox or myocarditis. After improvement, he was discharged with isolation precautions.

Although clade testing results were unavailable, these patients were presumed to have clade IIb infection given the epidemiology of the ongoing global monkeypox outbreak and their lack of an epidemiologic link to clade I (i.e., no relevant travel history or animal exposures). Although monkeypox-associated
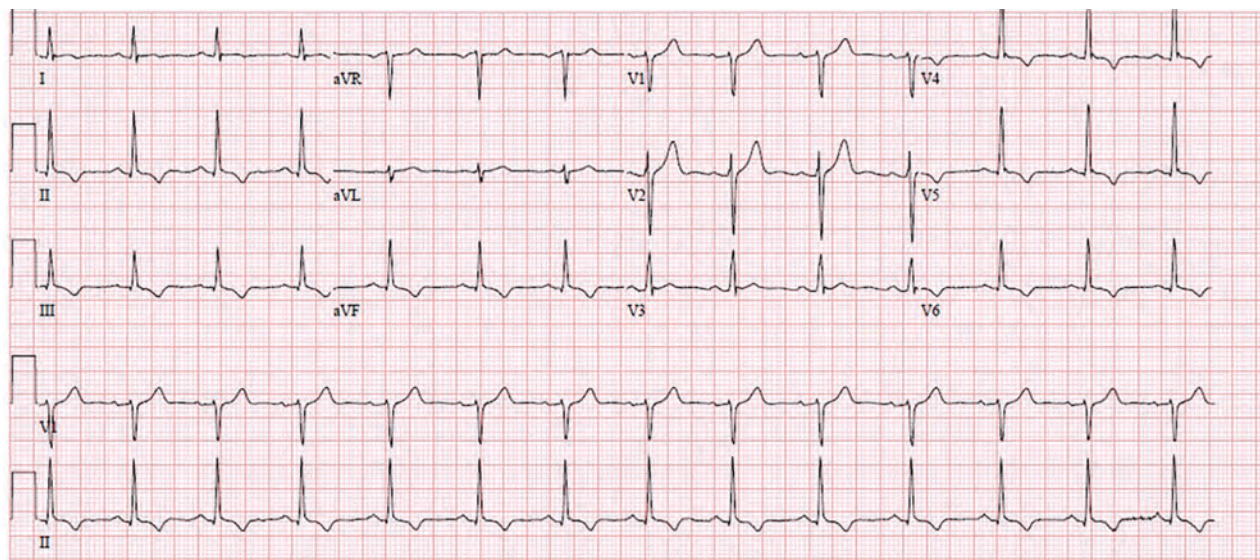

Figure 2. An electrocardiogram of a healthy 37-year-old man (patient 2) with monkeypox, shortness of breath, and decreased exercise tolerance shows normal sinus rhythm with T wave inversions in the inferior and anterolateral leads.

myocarditis was considered the most likely etiology for both patients, given the temporal relationship, we could not completely confirm the diagnosis with histopathologic tests or exclude other potential etiologies, including viral co-infections.

Conclusions

The clinical course of human monkeypox is milder than that of smallpox in immunocompetent hosts (*6*). However, severe complications have been identified, including pneumonitis, encephalitis, eyesight-threatening keratitis, secondary bacterial infections, acute kidney injury, and myocarditis (*1,2,4–6*). Thornhill et al. (*5*) recently reported 2 cases of self-limited myocarditis in patients with monkeypox that resolved within 7 days without major complications; 1 patient had a history of HIV with a normal CD4 cell count. Similarly, the patients in our report improved 10–12 days after illness onset; 1 patient received tecovirimat, an inhibitor of the orthopoxvirus VP37 envelope-wrapping protein that prevents the formation of egress-competent enveloped virions and has been shown to decrease circulating viral DNA in a nonhuman primate model (*7*).

Many viruses have been associated with myocarditis (*8,9*). The most common pathophysiology of viral myocarditis is lymphocytic myocarditis associated with myonecrosis that occurs 10–14 days postinfection; illness can be either self-limiting or result in fulminant myocarditis. In some cases, viral myocarditis can progress to a noninfectious chronic phase, characterized by myocardial fibrosis, cardiac dysfunction, and dilated cardiomyopathy (*9*).

Myocardial involvement of orthopox infections was initially reported when myocarditis was observed after smallpox vaccination with replicating vaccinia-based vaccines in young military recruits (*10*). The pathophysiology of orthopox-induced myocarditis remains unknown. However, an autoimmune-mediated phenomenon has been postulated because of the absence of direct viral infection of the myocytes observed on histopathologic examination of samples from vaccinees with myocarditis (*10*). Most cases are mild and self-limited; major sequelae, such as dilated cardiomyopathy, are rare (*11*).

Hemorrhagic smallpox, the most severe manifestation of variola major, is characterized by rapid onset fever, rash, and disseminated intravascular coagulation. Anatomopathologic studies in hemorrhagic smallpox patients showed myocardial and endocardial hemorrhages (*12*). In a macaque model of hemorrhagic smallpox, histopathologic tests at day 6 or 7 postexposure showed acute lymphohistiocytic myocarditis with myocardiocyte degeneration and hemorrhage, primarily driven by direct viral myocardial injury and mediated by CD14 monocytes, chemotactic cytokines, and interleukin 6 (*12*). Therefore, we hypothesize that direct myocardial infiltration associated with monkeypox viremia may also result in myocarditis and that antiviral agents could play a role in treatment.

About the Author

Dr. Rodriguez-Nava is an infectious disease fellow at Stanford University School of Medicine. His research interests include hospital epidemiology, infection prevention, and emerging infectious diseases.

References

1. Adler H, Gould S, Hine P, Snell LB, Wong W, Houlihan CF, et al.; NHS England High Consequence Infectious Diseases (Airborne) Network. Clinical features and management of human monkeypox: a retrospective observational study in the UK. Lancet Infect Dis. 2022 ;22:1153–62. https://doi.org/10.1016/S1473-3099(22)00228-6
2. Girometti N, Byrne R, Bracchi M, Heskin J, McOwan A, Tittle V, et al. Demographic and clinical characteristics of confirmed human monkeypox virus cases in individuals attending a sexual health centre in London, UK: an observational analysis. Lancet Infect Dis. 2022;22:1321–8.
3. World Health Organization. Second meeting of the International Health Regulations (2005) (IHR) Emergency Committee regarding the multi-country outbreak of monkeypox [cited 2022 Jul 23]. https://www.who.int/news/item/23-07-2022-second-meeting-of-the-international-health-regulations-(2005)-(ihr)-emergency-committee-regarding-the-multi-country-outbreak-of-monkeypox
4. Guarner J, Del Rio C, Malani PN. Monkeypox in 2022—what clinicians need to know. JAMA. 2022;328:139–40. https://doi.org/10.1001/jama.2022.10802
5. Thornhill JP, Barkati S, Walmsley S, Rockstroh J, Antinori A, Harrison LB, et al.; SHARE-net Clinical Group. Monkeypox virus infection in humans across 16 countries—April–June 2022. N Engl J Med. 2022;387:679–91. https://doi.org/10.1056/NEJMoa2207323
6. Huhn GD, Bauer AM, Yorita K, Graham MB, Sejvar J, Likos A, et al. Clinical characteristics of human monkeypox, and risk factors for severe disease. Clin Infect Dis. 2005;41:1742–51. https://doi.org/10.1086/498115
7. Mucker EM, Goff AJ, Shamblin JD, Grosenbach DW, Damon IK, Mehal JM, et al. Efficacy of tecovirimat (ST-246) in nonhuman primates infected with variola virus (smallpox). Antimicrob Agents Chemother. 2013;57:6246–53. https://doi.org/10.1128/AAC.00977-13
8. Patel T, Kelleman M, West Z, Peter A, Dove M, Butto A, et al. Comparison of multisystem inflammatory syndrome in children-related myocarditis, classic viral myocarditis, and COVID-19 vaccine-related myocarditis in children. J Am Heart Assoc. 2022;11:e024393. https://doi.org/10.1161/JAHA.121.024393
9. Lasrado N, Reddy J. An overview of the immune mechanisms of viral myocarditis. Rev Med Virol. 2020;30:1–14. https://doi.org/10.1002/rmv.2131
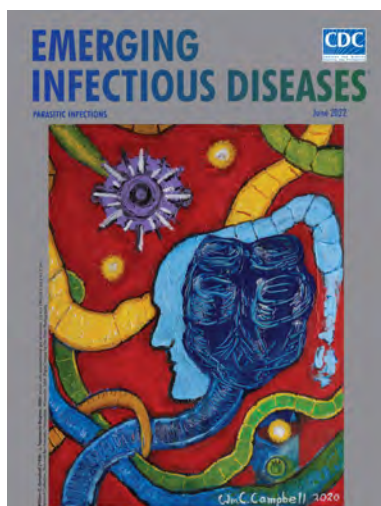
10. Mora LF, Khan AH, Sperling LS. Cardiac complications after smallpox vaccination. South Med J. 2009;102:615–9. https://doi.org/10.1097/SMJ.0b013e31819fe55b

11. Morgan J, Roper MH, Sperling L, Schieber RA, Heffelfinger JD, Casey CG, et al. Myocarditis, pericarditis, and dilated cardiomyopathy after smallpox vaccination among civilians in the United States, January–October 2003. Clin Infect Dis. 2008;46(Suppl 3):S242–50. https://doi.org/10.1086/524747

12. Johnson RF, Keith LA, Cooper TK, Yellayi S, Josleyn NM, Janosko KB, et al. Acute late-stage myocarditis in the crab-eating macaque model of hemorrhagic smallpox. Viruses. 2021;13:1571. https://doi.org/10.3390/v13081571

Address for correspondence: Guillermo Rodriguez Nava, Stanford University School of Medicine, 300 Pasteur Dr, Lane L-154, Stanford, CA 94305, USA; email: guiro@stanford.edu

June 2022
Parasitic Infections

EMERGING INFECTIOUS DISEASES®

To revisit the June 2022 issue, go to:
https://wwwnc.cdc.gov/eid/articles/issue/28/6/table-of-contents

Monkeypox Virus Detection in Different Clinical Specimen Types

Maan Hasso,[1] Stephen Perusini,[1] Alireza Eshaghi, Elaine Tang, Romy Olsha,
Hanyue Zhang, Evelyn Lau, Ashleigh Sullivan, Kirby Cronin, Seyeon Lee, Janet Obando,
Cedric DeLima, Sandeep Nagra, Tom Braukmann, Venkata R. Duvvuri, Melissa Richard-Greenblatt,
Antoine Corbeil, Julianne V. Kus, Anna Majury, Samir Patel, Jonathan B. Gubbay

A global monkeypox outbreak began in May 2022. Limited data exist on specimen type performance in associated molecular diagnostics. Consequently, a diverse range of specimen sources were collected in the initial weeks of the outbreak in Ontario, Canada. Our clinical evaluation identified skin lesions as the optimal diagnostic specimen source.

The rapid emergence of monkeypox in nonendemic regions of the world during 2022 has health systems on alert (1). Monkeypox is a zoonosis caused by monkeypox virus (MPXV) (genus *Orthopoxvirus* [OPXV]). MPXV forms 2 distinct clades: clade I (formerly the Congo Basin/Central African clade), associated with higher virulence and greater mortality rate, and clade II (formerly the West African clade), which is responsible for the current global outbreak (2,3).

The rapid increase in monkeypox cases in nonendemic areas has challenged clinical laboratories. MPXV shedding and transmission are poorly understood, and relevant data to support clinical management and public health response are lacking. Human-to-human transmission occurs by respiratory droplets, direct contact with skin lesions of infected persons, or contact with contaminated fomites (4). Skin lesions, when present, are presumed to be the primary source of viral shedding. Thus, testing of lesion swab specimens by real-time reverse transcription PCR (RT-PCR) is believed to be optimal for diagnosis (5,6). MPXV can also be detected in other sites, such as throat, nasopharynx, blood, urine, saliva, and semen (7).

We investigated detection of MPXV among different clinical specimen types. These specimens were submitted to the provincial reference laboratory for testing in the early weeks of the 2022 outbreak in Ontario, Canada.

The Study

The Public Health Ontario Ethics Review Board determined that this study did not require research ethics committee approval because it describes analyses that were completed at the Public Health Ontario laboratory as part of routine clinical testing and surveillance during the monkeypox outbreak in Ontario. Therefore, this study was considered to be public health practice and was exempt from this requirement.

This retrospective study was conducted on patient specimens submitted to Public Health Ontario's laboratory, the reference microbiology laboratory in Ontario and MPXV testing location, during the initial weeks of the provincial surge (May–June 2022). All specimens were collected from symptomatic patients with suspected monkeypox infection. Specimen types were categorized as blood, skin lesions, nasal or nasopharyngeal (NP) swab specimens, and oropharyngeal (throat) swab specimens. Urine, semen, and saliva were infrequently submitted. We extracted clinical data submitted on the laboratory requisition, including demographic variables, clinical information, and enterovirus laboratory test results if available.

We extracted DNA from clinical specimens using either the automated total nucleic acid method

[1]These authors contributed equally to this article.

(NucliSENS easyMAG; bioMérieux, https://www.biomerieux.com) or the manual method (QIAamp DNA Minikit; QIAGEN, https://www.qiagen.com). We conducted testing by using 1 of 2 assays developed by the US Centers for Disease Control and Prevention (CDC): the Laboratory Response Network pan-Orthopoxvirus (OPX) RT-PCR and an MPXV-specific RT-PCR endorsed by the World Health Organization (8–10). Both assays were validated in-house for clinical testing. The OPXV assay primer/probe set was supplied by CDC for restricted use through the Canadian Laboratory Response Network. The MPXV RT-PCR consists of a generic MPXV GR2-G target (MPX), an MPXV clade II–specific target, and an RNaseP extraction control.

Using the QuantStudio5 RT-PCR system and TaqPath ProAmp Multiplex master mix (Thermo Fisher Scientific, https://www.thermofisher.com), we amplified a 10-μL reaction containing 4 μL DNA, 0.5 μmol/L primers, and 0.2 μmol/L probe. Thermocycling conditions were 60°C for 30 s, 95°C for 5 min, and 45 cycles at 95°C for 5 s and 60°C for 30 s. Cycle threshold (Ct) values ≤38 was reported as detected, 38.01–39.99 as indeterminate, and ≥40 as not detected for MPXV DNA (11).

The testing algorithm shifted from the OPXV RT-PCR to the MPXV RT-PCR once the MPXV assay was validated. Some specimens were tested by both assays during validation. RT-PCR results, including Ct values, were evaluated by specimen type among patients who had multiple specimens collected during the same testing episode. Parallel testing for enterovirus by RT-PCR was conducted for pediatric (age <18 years) patients as the most likely differential diagnosis in this age group and for adults (age ≥18 years) upon request.

We tested 1,063 specimens from 372 patients (mean age 33.8 years, range >1–88 years); 71.2% were male. MPXV was detected in 81 (21.8%) patients, all adult males who had a mean age of 38 years (range 19–65 years). Specimen positivity rate was 23.4% (249/1,063); 2.8% (29/1,063) of all specimens tested had indeterminate results.

Among specimens submitted from the 81 MPXV-positive patients, skin lesions displayed the highest positivity rate (177/213, 83.1%), followed by oropharyngeal (31/46, 67.4%), nasal or NP (20/36, 55.6%), blood (29/67, 43.3%) and urine (6/21, 28.6%) (Table). MPXV was also detected in 2/5 semen specimens and 1/1 saliva specimen submitted from known MPXV-positive patients.

Across all positive specimens, the MPXV GR2-G target mean Ct (26.2) was 2.7 lower than that of the OPXV assay (29.9), and the clade II target mean Ct (26.3) was 2.6 times lower. The MPXV assay also had lower Ct values than the OPXV assay across all specimen types (Table), indicating higher analytical sensitivity. Skin lesion specimens were detected multiple cycles earlier, indicative of higher viral loads. Oropharyngeal samples had the second lowest Ct means.

Among 78 monkeypox confirmed case-patients with skin and NP or throat swab specimens submitted for testing, 72/78 (92.3%) had ≥1 positive skin specimen and 38/78 (48.7%) had ≥1 positive NP or throat swab specimens. MPXV was only detected in skin specimens in 34/78 (43.6%) patients. All patients with a positive blood specimen had ≥1 other positive

Table. Detection results for MPXV by real-time reverse transcription PCR in clinical specimen types submitted to the Public Health Ontario Laboratory, Toronto, Ontario, Canada*

Specimen types and number	Blood, n = 190	Nasal/NP, n = 137	Throat/OP, n = 106	Skin lesions, n = 559	Urine, n = 41
Positive	29 (15.3)	20 (14.6)	31 (29.2)	177 (31.7)	6/41 (14.6)
Specimens from positive patients	29/67 (43.3)	20/36 (55.6)	31/46 (67.4)	177/213 (83.1)	6/21 (28.6)
Target					
Orthopoxvirus					
No. positive	26	16	24	135	5
Mean Ct (SD), range	38.6 (4.1), 27.2–40.0	36.3 (6.3), 23.3–38.8	32.0 (6.5), 17.5–38.0	27.1 (7.3), 14.3–39.6	37.3 (5.1), 29.0–37.9
Monkeypox					
No. positive	15	11	13	74	4
Mean Ct (SD), range	35.9 (2.1), 32.2–37.9	32.4 (5.6), 18.2–37.7	27.8 (5.1), 19.2–36.0	23.1 (6.5), 12.0–37.9	32.2 (5.5), 27.2–37.7
Clade II					
No. positive	15	13	13	75	4
Mean Ct (SD), range	35.3 (2.3), 31.2–37.1	32.8 (5), 18.1–37.6	27.3 (4.5), 19.6–35.2	23.1 (6.6), 11.1–37.4	32.2 (5.1), 27.7–37.2

*Values are no. (%) except as indicated. Among 30 additional specimens not shown, MPXV was detected in 2/5 semen, 1/4 saliva, 0/1 cerebrospinal fluid, and none of 20 specimens with undocumented sources. Indeterminate results are not included; those are blood 6/190 (3.2%), nasal/NP 5/137 (3.6%), throat/OP 2/106 (1.9%), skin lesion 10/559 (1.8%), and urine 6/41 (14.6%). Ct, cycle threshold; MPXV, monkeypox virus; NP, nasopharyngeal; OP, oropharyngeal.

specimen type. Among 15 monkeypox confirmed case-patients who had both NP and throat swab specimens submitted, 8 had concordant (53.3%) positive and 2 (13.3%) had concordant negative results. One case-patient had a negative NP swab and positive throat swab specimens, and 4 discordant case-patients had 1 sample type indeterminate and the other negative.

Enterovirus was detected in 25 (71.4%) of the 35 children tested. It was also detected in 7 (46.7%) of the 15 adults tested.

Conclusions

In this study, MPXV was detected in specimens from multiple sites. Skin lesions most often tested positive, as observed in 92.3% of laboratory confirmed case-patients who had >1 skin specimens tested. This finding indicates that this is the most clinically relevant specimen when skin lesions are available. Positivity rates for other specimen types suggest their use as alternatives if skin lesions are not available. However, the high clinical sensitivity (83.1%) of single skin specimens for MPXV detection suggests that 2 (or 3) appropriately collected specimens from open skin lesions should be adequate for testing. Including additional specimen types probably provides limited value in patients who have lesions. The CDC recommendation of collecting 2 swab specimens from each skin lesion might not be required when >1 skin lesion can be swabbed, which will assist with use of laboratory resources should testing demands increase (*10*).

Because of our findings, Public Health Ontario advises that specimens other than skin lesions are not required if patients have multiple skin lesions that can be swabbed. However, blood should always be submitted along with NP or throat swab specimens for patients without open skin lesions (e.g., fever without rash or only macular/papular rash). Children are an exception to this strategy because collecting alternative specimens (such as NP swab specimens) enables investigation of other likely etiologies of rash and fever (e.g., respiratory viruses including adenovirus, enterovirus, and rhinovirus).

According to epidemiologic summaries for Ontario, the most common symptoms reported among monkeypox-confirmed case-patients (all tested at the Public Health Ontario laboratory) were rash, fever, lymphadenopathy, oral/genital lesions, and fatigue (*12*). Limitations of this study include lack of detailed clinical information (e.g., symptom onset date) for many patients when not described on the test requisition. Therefore, test performance could not be correlated with disease progression. Further evaluations of different specimen types with detailed temporal data is warranted.

About the Author

Dr. Hasso is a medical microbiologist at the Public Health Ontario Laboratory, Toronto, Canada. His primary research interests are emerging pathogens, antimicrobial drug resistance, and quality in laboratory medicine.

References

1. Centers for Disease Control and Prevention. Monkeypox signs and symptoms [cited 2022 Sep 30]. https://www.cdc.gov/poxvirus/monkeypox/index.html
2. Adler H, Gould S, Hine P, Snell LB, Wong W, Houlihan CF, et al.; NHS England High Consequence Infectious Diseases (Airborne) Network. Clinical features and management of human monkeypox: a retrospective observational study in the UK. Lancet Infect Dis. 2022; 22:1153–62. https://doi.org/10.1016/S1473-3099(22)00228-6
3. World Health Organization. Monkeypox: experts give virus variants new names [cited 2022 Sep 30]. https://www.who.int/news/item/12-08-2022-monkeypox--experts-give-virus-variants-new-names
4. McCollum AM, Damon IK. Human monkeypox. Clin Infect Dis. 2014;58:260–7. https://doi.org/10.1093/cid/cit703
5. Ahmed M, Naseer H, Arshad M, Ahmad A. Monkeypox in 2022: a new threat in developing. Ann Med Surg (Lond). 2022;78:103975. https://doi.org/10.116/j.amsu.2022.103975
6. Centers for Disease Control and Prevention. Guidelines for collecting and handling specimens for monkeypox testing [cited 2022 Sep 30]. https://www.cdc.gov/poxvirus/monkeypox/clinicians/prep-collection-specimens.html
7. Antinori A, Mazzotta V, Vita S, Carletti F, Tacconi D, Lapini LE, et al.; INMI Monkeypox Group. Epidemiological, clinical and virological characteristics of four cases of monkeypox support transmission through sexual contact, Italy, May 2022. Euro Surveill. 2022;27:2200421. https://doi.org/10.2807/1560-7917.ES.2022.27.22.2200421
8. World Health Organization. Laboratory testing for the monkeypox virus: Interim guidance [cited 2022 Sep 30]. https://www.who.int/publications/i/item/WHO-MPX-laboratory-2022.1
9. Li Y, Zhao H, Wilkins K, Hughes C, Damon IK. Real-time PCR assays for the specific detection of monkeypox virus West African and Congo Basin strain DNA. J Virol Methods. 2010;169:223–7. https://doi.org/10.1016/j.jviromet.2010.07.012
10. Centers for Disease Control and Prevention. Test procedure: non-variola orthopoxvirus generic real-time PCR test [cited 2022 Sep 30]. https://www.cdc.gov/poxvirus/monkeypox/pdf/Non-variola-Orthopoxvirus-Generic-Real-Time-PCR-Test.pdf
11. Public Health Ontario. Monkeypox testing indications [cited 2022 Sep 30]. https://www.publichealthontario.ca/en/laboratory-services/test-information-index/monkeypox-virus
12. Public Health Ontario. Monkeypox epidemiological summary [cited 2022 Sep 30]. https://www.publichealthontario.ca/-/media/Documents/M/2022/monkeypox-pisummary.pdf

Address for correspondence: Jonathan B. Gubbay, Public Health Ontario, Ontario Agency for Health Protection and Promotion, Public Health Laboratory, 81 Resources Rd, Toronto, ON M9P 3T1, Canada; email: jonathan.gubbay@oahpp.ca

Monkeypox after Occupational Needlestick Injury from Pustule

João P. Caldas, Sofia R. Valdoleiros, Sandra Rebelo, Margarida Tavares

We report a case of monkeypox in a physician after an occupational needlestick injury from a pustule. This case highlights risk for occupational transmission and manifestations of the disease after percutaneous transmission: a short incubation period, followed by a solitary lesion at the injured site and later by systemic symptoms.

The 2022 multicountry monkeypox outbreak has been linked primarily to intimate sexual contact. Although there are reported cases among healthcare workers (HCW), most are described to have been acquired in the community setting (1). We report a case of monkeypox after an occupational needlestick injury.

The Study

In late July 2022, a healthy 29-year-old male physician from the Infectious Diseases Department of a tertiary hospital in Portugal had a needlestick injury in the left index finger with a needle used to collect a fluid sample from a man who had a pustular rash, later confirmed to be monkeypox. The physician punctured a pustule with the needle because he was unable to obtain material by swabbing it. He was wearing the recommended personal protective equipment; the gloves appeared intact to him, and there was no wound or bleeding. Thus, he did not report the incident as an occupational exposure accident or considered it for postexposure vaccination. No other risk factors for monkeypox were present.

Four days later, a vesicle appeared on the pricked finger (Figure 1, panel A), and monkeypox virus (MPXV) was identified in its fluid by PCR, showing a cycle threshold (Ct) of 28. The HCW was sent on sick

Author affiliations: Centro Hospitalar Universitário de São João, Porto, Portugal (J.P. Caldas, S.R. Valdoleiros, S. Rebelo, M. Tavares); University of Porto, Porto (J.P. Caldas, S.R. Valdoleiros, S. Rebelo, M. Tavares); European Society for Clinical Microbiology and Infectious Diseases, Basel, Switzerland (S.R. Valdoleiros); Directorate-General of Health, Lisbon, Portugal (M. Tavares)

leave, with indication for the institution of contact and droplet isolation measures at home.

No other lesions or symptoms developed during the next 5 days. PCR results for MPXV in the samples collected from the oropharynx and blood were negative on the seventh day after exposure. The case-patient was considered not eligible for postexposure prophylaxis with the modified vaccinia virus Ankara Bavarian Nordic vaccine (https://www.bavarian-nordic.com) because the HCW already had a lesion that contained MPXV.

On the sixth day of illness, fever (temperature 38.4°C), chills, and malaise developed and lasted for ≈48 hours. The finger lesion became pustular and painful and showed surrounding erythema and swelling (Figure 1, panel B). A tender, indurated, erythematous and well-delimited linear streak from the left finger to the armpit appeared on the seventh day (Figure 2, panel A), without regional adenopathy. MPXV PCR was repeated in samples from the oropharynx and blood; again, results were negative.

On the eighth day and for the next 3 days, vesicles developed on the scalp, neck, forearm, first finger from both hands and fifth left finger, scrotum, and ankle. A painless right cervical adenopathy also appeared. Despite the absence of leukocytosis or elevation of C-reactive protein level, a bacterial superinfection was assumed because of worsening of the inflammatory signs of the left index finger and of the arm lymphangitis (Figure 2, panel B), and a course of 5 days of oral flucloxacillin was administered. The patient showed clinical improvement. Treatment with tecovirimat was discussed but considered unnecessary given the benign evolution (no mucosal involvement, <10 lesions) and the absence of concurrent conditions.

By the 18th day of illness, all skin lesions, except the one on the left index finger, had evolved through the pustular stage into crust. The index lesion became necrotic (Figure 1, panel C) and was debrided on the 24th day of illness, showing a necrotic scab that had a diameter of 0.5 cm underneath the devitalized tissue

(Figure 1, panel D). An MPXV PCR result was still positive in the crust and showed a Ct of 23, but viral culture was negative.

Conclusions

Several aspects of this case should be emphasized. First, it clearly exemplifies the risks of using sharp instruments for monkeypox testing, which is not recommended. Samples should be collected by vigorously swabbing the surface of lesions or by removing crusts with a forceps or other blunt-tipped sterile instruments (*2*). Unroofing, aspiration of lesions, or otherwise use of sharp instruments before swabbing is not necessary or recommended because of risk for injury from sharp instruments (*2*). The presence of material on the swab surface is indicative of an adequate collection, although it might not always be visible (*2*). For this case-patient, the physician was not certain of an adequate collection after swabbing the lesion, which led him to use a needle for sample collection. If sharp instruments are deemed fully essential for testing, their use, as an exception, should be performed with extreme care, and sharps should be discarded into an adequate container.

Second, this case should remind HCWs about the need to report needlestick injuries and other exposures promptly, regardless of a self-notion of absence of risk, to avoid missing opportunities for postexposure prophylaxis. Penetrating injury is considered a high-risk exposure and an indication for postexposure prophylaxis (*3*,*4*).

Third, the case alerts us to a possible different manifestation and evolution of monkeypox. This difference is especially true when the transmission route is percutaneous. In this case, a solitary lesion developed at the injured site after a short incubation period, followed a few days later by systemic symptoms and the characteristic rash.

Fourth, because of this different evolution, more evidence is needed for decision-making on the timing of postexposure vaccination and use of tecovirimat in similar cases. Despite its benign course, monkeypox might lead to prolonged work absenteeism because international guidelines recommend
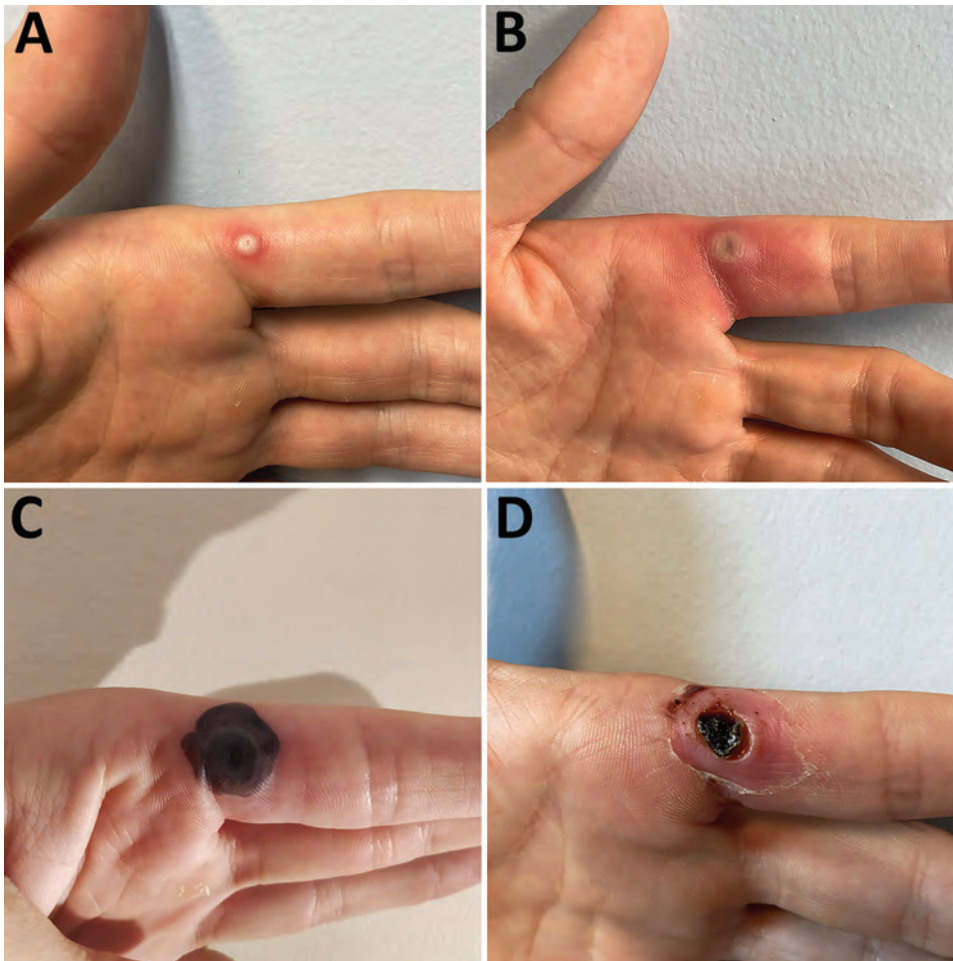

Figure 1. Progress of monkeypox lesion on the finger of a previously healthy male physician in Portugal after occupational needlestick injury from pustule. A) Index lesion on the fourth day of illness. B) Index lesion on the sixth day of illness. C) Index lesion on the 18th day of illness. D) Necrotic scab underneath the devitalized tissue of the index lesion on the 24th day of illness.
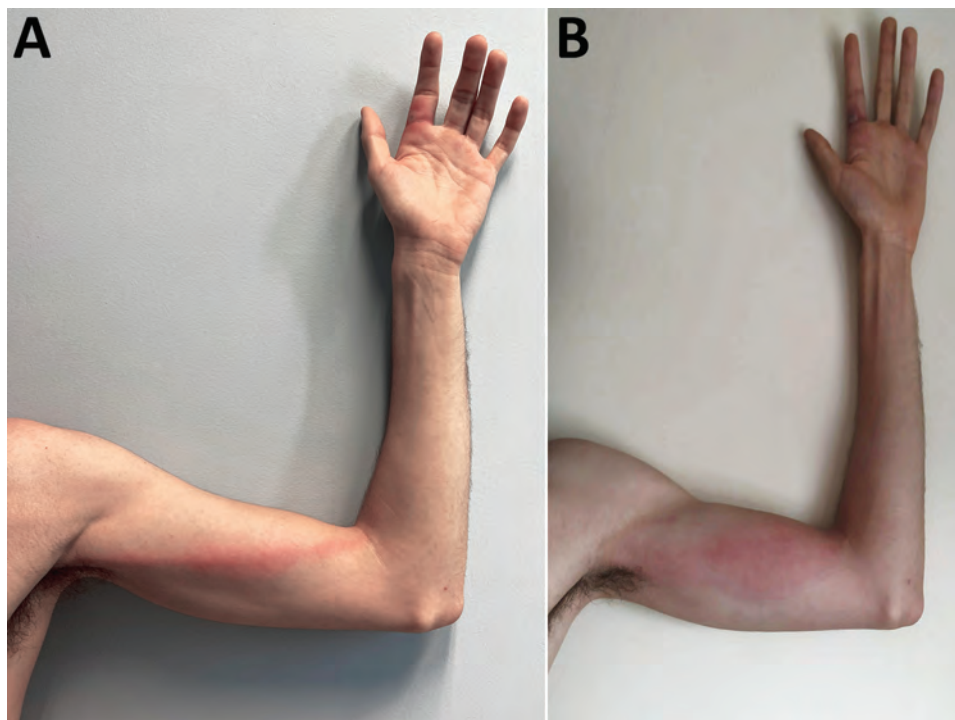
Figure 2. Monkeypox signs in a previously healthy male physician in Portugal after occupational needlestick injury from pustule. A) Tender, indurated, erythematous, and well-delimited linear streak from the left finger to the armpit, on the seventh day of illness. B) Aggravated lymphangitis on the ninth day of illness.

precautions remain in place until lesions have crusted, scabs have fallen off, and a fresh layer of skin has formed underneath (*5*), which might take several weeks. Thus, it might be reasonable to consider these therapeutic options to prevent or modify the disease course. In this case, when postexposure prophylaxis was discussed, the HCW was not considered eligible for postexposure vaccination because a lesion containing MPXV was already present, which is in accordance with the UK Health Security Agency and the Centers for Disease Control and Prevention recommendations (*3*,*6*). However, more evidence is needed in this field.

Fifth, it is useful to study the infectiousness of the scabs because their dropping off is considered a determinant for deisolation criteria. Pittman et al. verified that monkeypox scabs contained large quantities of viral DNA until and including when they fell off, but viral infectivity of specimens was not determined (*5*). In the case we describe, despite the positive PCR result, with an even lower Ct than the original lesion, the viral culture was negative. Therefore, persistence of positive PCR results might not be a reliable indicator of contagiousness and might lead to prolonged and unnecessary isolation.

Sixth, this case increases awareness of the need for accelerating production of vaccines and increasing their preexposure and postexposure availability. This activity is especially useful for HCWs who deal with monkeypox cases to provide adequate protection and security.

In summary, we report a case of monkeypox in an HCW after a needlestick injury. HCWs should be aware of the risk for transmission of MPXV while infected patients are being evaluated and tested, should report needlestick or other injuries promptly, and should take advantage of available preexposure and postexposure prophylaxis.

About the Author

Dr. Caldas is a medical resident of infectious diseases at Centro Hospitalar Universitário de São João, Porto, Portugal, and an invited assistant professor at Faculty of Medicine at the University of Porto. His primary research interests are HIV, AIDS, and sexually transmitted infections.

References

1. European Centre for Disease Prevention and Control. Monkey pox infection prevention and control guidance for primary and acute care settings. August 16, 2022. Stockholm: The Centre; 2022.
2. Centers for Disease Control and Prevention. Guidelines for collecting and handling specimens for monkeypox testing [cited 2022 Sep 20]. https://www.cdc.gov/poxvirus/monkeypox/clinicians/prep-collection-specimens.html
3. UK Health Security Agency. Recommendations for the use of pre and post exposure vaccination during a monkeypox incident: version 12, August 26, 2022 [cited 2022 Aug 26]. https://assets.publishing.service.gov.uk/government/
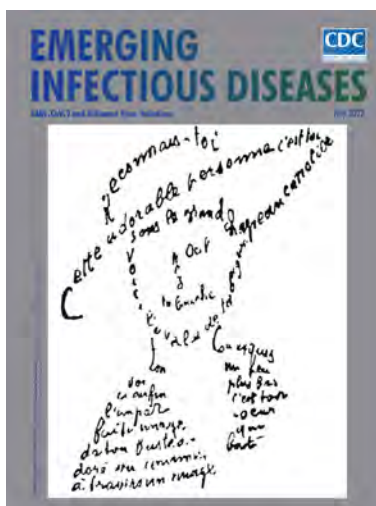
uploads/system/uploads/attachment_data/file/1100600/recommendations-for-pre-and-post-exposure-vaccination-during-a-monkeypox-incident-26-august-2022.pdf

4. UK Health Security Agency. Monkeypox contact tracing classification and vaccination matrix: version 13, September 27, 2022 [cited 2022 Oct 13]. https://assets.publishing.service.gov.uk/government/uploads/system/uploads/attachment_data/file/1106691/monkeypox-contact-tracing-classification-and-vaccination-matrix-version-13-27-sept-2022.pdf

5. World Health Organization. Clinical management and infection prevention and control for monkeypox: interim rapid response guidance, June 10, 2022. Geneva: The Organization; 2022.

6. O'Shea J, Filardo TD, Morris SB, Weiser J, Petersen B, Brooks JT. Interim guidance for prevention and treatment of monkeypox in persons with HIV infection—United States, August 2022. MMWR Morb Mortal Wkly Rep. 2022;71:1023–8. https://doi.org/10.15585/mmwr.mm7132e4

Address for correspondence: João P. Caldas, Department of Infectious Diseases, Centro Hospitalar Universitário de São João, Alameda Prof. Hernâni Monteiro, 4202-451 Porto, Portugal; email: jpcaldas92@gmail.com

July 2022

SARS-CoV-2 and Influenza Virus Infections

- Vaccine Effectiveness during Outbreak of COVID-19 Alpha (B.1.1.7) Variant in Men's Correctional Facility, United States
- Updated Estimates and Mapping for Prevalence of Chagas Disease among Adults, United States
- Enterovirus D68 in Hospitalized Children, Barcelona, Spain, 2014–2021
- Epidemiologic, Clinical, and Genetic Characteristics of Human Infections with Influenza A(H5N6) Viruses, China
- Measuring Basic Reproduction Number to Assess Effects of Nonpharmaceutical Interventions on Nosocomial SARS-CoV-2 Transmission
- Analyzing and Modeling the Spread of SARS-CoV-2 Omicron Lineages BA.1 and BA.2, France, September 2021–February 2022
- Effect of Returning University Students on COVID-19 Infections in England, 2020
- Nipah Virus Detection at Bat Roosts after Spillover Events, Bangladesh, 2012–2019
- Effect of Agroecosystems on Seroprevalence of St. Louis Encephalitis and West Nile Viruses in Birds, La Pampa, Argentina, 2017–2019
- Outbreak of IncX8 Plasmid–Mediated KPC-3–Producing Enterobacterales Infection, China
- Self-Reported and Physiologic Reactions to Third BNT162b2 mRNA COVID-19 (Booster) Vaccine Dose

- One Health Genomic Analysis of Extended-Spectrum β-Lactamase–Producing *Salmonella enterica*, Canada, 2012–2016
- Novel *Mycobacterium tuberculosis* Complex Genotype Related to *M. caprae*
- Targeted Screening for Chronic Q Fever, the Netherlands
- Chronic Pulmonary Disease Caused by *Tsukamurella toyonakaense*
- SARS-CoV-2 Delta–Omicron Recombinant Viruses, United States
- Highly Pathogenic Avian Influenza A(H5N8) Clade 2.3.4.4b Virus in Dust Samples from Poultry Farms, France, 2021

- Genetically Diverse Highly Pathogenic Avian Influenza A(H5N1/H5N8) Viruses among Wild Waterfowl and Domestic Poultry, Japan, 2021
- Multisystem Inflammatory Syndrome after Breakthrough SARS-CoV-2 Infection in 2 Immunized Adolescents, United States
- Natural History of and Dynamic Changes in Clinical Manifestation, Serology, and Treatment of Brucellosis, China
- *Anncaliia algerae* Microsporidiosis Diagnosed by Metagenomic Next-Generation Sequencing, China
- Use of Human Intestinal Enteroids to Evaluate Persistence of Infectious Human Norovirus in Seawater
- Isolation and Characterization of Novel Reassortant Influenza A(H10N7) Virus in a Harbor Seal, British Columbia, Canada
- Suspected Cat-to-Human Transmission of SARS-CoV-2, Thailand, July–September 2021
- Potential Threats to Human Health from Eurasian Avian-Like Swine Influenza A(H1N1) Virus and Its Reassortants
- Determining Infected Aortic Aneurysm Treatment Using Focused Detection of *Helicobacter cinaedi*
- Hodgkin Lymphoma after Disseminated *Mycobacterium genavense* Infection, Germany
- Natural Reassortment of Eurasian Avian-Like Swine H1N1 and Avian H9N2 Influenza Viruses in Pigs, China

EMERGING INFECTIOUS DISEASES®

To revisit the July 2022 issue, go to:
https://wwwnc.cdc.gov/eid/articles/issue/28/7/table-of-contents

Possible Occupational Infection of Healthcare Workers with Monkeypox Virus, Brazil

Richard Steiner Salvato, Maria Leticia Rodrigues Ikeda, Regina Bones Barcellos,
Fernanda Marques Godinho,Patrícia Sesterheim, Leticia Camiza Bulcão Bitencourt,
Tatiana Schäffer Gregianini, Ana Beatriz Gorini da Veiga, Fernando Rosado Spilki, Gabriel Luz Wallau

We evaluated epidemiologic and molecular characteristics of monkeypox virus (MPXV) infections sampled from 2 healthcare nurses. Five days after collecting samples from an infected patient, the nurses showed typical MPXV manifestations; quantitative PCR and whole-genome sequencing confirmed MPXV infection, most likely transmitted through contact with fomites.

In May 2022, the World Health Organization (WHO) confirmed a multicountry monkeypox virus (MPXV) outbreak caused by MPXV clade II. As of September 14, 2022, 59,147 infections had been described in 164 countries worldwide, 6,129 of those cases occurred in Brazil (*1*). Typical MPXV signs and symptoms include fever, intense headache, lymphadenopathy, back pain, myalgia, and intense asthenia. Skin eruptions usually begin within 1–3 days after fever onset and evolve from macules to pustules, then form crusts (*1,2*).

In this outbreak, most reported cases have been transmitted through sexual contact with multiple partners. However, MPXV can also be transmitted

Author affiliations: Secretaria Estadual da Saúde do Rio
Grande do Sul, Porto Alegre, Rio Grande do Sul, Brazil
(R. Steiner Salvato, M.L. Rodrigues Ikeda, R. Bones Barcellos,
F. Marques Godinho, P. Sesterheim, T. Schäffer Gregianini);
Universidade do Vale do Rio dos Sinos Programa de
Pós-Graduação em Saúde Coletiva, São Leopoldo, Rio Grande
do Sul (M.L. Rodrigues Ikeda, L.C. Bulcão Bitencourt);
Universidade Federal de Ciências da Saúde de Porto Alegre,
Porto Alegre, Rio Grande do Sull (A.B. Gorini da Veiga);
Universidade Feevale Laboratório de Microbiologia Molecular,
Novo Hamburgo, Rio Grande do Sul (F. Rosado Spilki); Instituto
Aggeu Magalhães (IAM), FIOCRUZ-PE, Recife, Brazil
(G.L. Wallau); National Reference Center for Tropical Infectious
Diseases, Hamburg, Germany (G.L. Wallau)

through direct contact with rash lesions, scabs, body fluids and respiratory secretions from an infected patient (*3,4*). Transmission through contact with fomites, infected objects, fabrics, or surfaces, has also been reported (*5*) and should be considered for disease control and prevention. By August 22, 2022, WHO had reported 256 MPXV cases among healthcare workers (HCW); only 3 of them were confirmed to be occupationally acquired. Of note, most infections among HCWs were acquired outside the workplace (*6*).

We describe MPXV infection that developed in 2 HCWs after they collected specimens from an infected patient in Brazil. Both healthcare workers signed a consent form for the use of their clinical data and publication of anonymized photographs in this article.

The Study

On July 22, 2022, a man in Brazil, 40 years of age, exhibited genital maculopapular lesions, adenomegaly, myalgia, fever, and chills. The patient had not traveled recently; he reported intimate contact with multiple partners. On July 29, two HCWs (HCW-1 and HCW-2) visited the patient's home to collect specimens and conduct an epidemiologic investigation interview. Upon entering the patient's home and during the entire visit, the HCWs wore personal protective equipment (PPE), including safety glasses, disposable isolation gowns, and N95 respiratory masks. The patient wore a cloth mask for the duration of the visit.

After entering the home, the patient and HCWs proceeded directly to the patient's bedroom, where the HCWs interviewed the patient and collected samples from him. During these procedures, the patient remained in bed; the HCWs placed their equipment on a nearby armchair. From the time they entered the patient's home to the end of the interview, the HCWs did not wear gloves; after the interview, both HCWs sanitized their hands with 70% ethanol and donned

latex gloves to collect samples. HCW-1 collected a lesion specimen using a dry sterile swab that the worker then placed in a screw-capped sterile plastic transport tube; HCW-2 collected a blood sample using a plastic evacuated tube. Both tubes were stored in a sample transport box. During the ≈1 hour visit, the HCWs had no skin-to-skin contact with the patient and reported no sharps injuries.

The HCWs removed their gloves only after leaving patient's home and placing the sample box in their car; they then discarded the gloves in a portable biohazard waste disposal container and sanitized their hands with 70% ethanol. They wore their remaining PPE (disposable gown, N95 respirators, glasses) until they arrived at the laboratory, where they immediately washed their hands with soap and water. However, they did not sanitize some work materials, such as a clipboard and the exterior surface of the sample transport box (Figure 1).

The HCWs did not have contact with other suspected or confirmed monkeypox case-patients before the day of or during the 4 days after collecting samples from the patient. Furthermore, on the day of the patient visit, they had no known skin injuries, skin breaks, or scrapes. A real-time quantitative PCR (qPCR) assay performed on August 2 following a protocol described elsewhere (7) confirmed that the patient was infected with clade II MPXV (cycle threshold [Ct] 20).

On August 3 (5 days after collecting the patient specimens), HCW-1 exhibited a single lesion on her left ring finger, a small macula with central umbilication. qPCR of a specimen collected from HCW-1 on August 4 confirmed MPXV infection (Ct 22). We observed no systemic symptoms or additional lesions until August 10, when HCW-1 experienced increased hyperemia and a small papule appeared lateral to the initial lesion. By August 12, HCW-1 exhibited lymphangitis in her left upper arm and worsened hyperemia; in addition, the lesion on her finger became a bleeding papule. On August 13, HCW-1 still had lymphangitis and a small papule had appeared on her forearm. By August 15, lesion fibrin had increased, and by August 23, fibrin reabsorption with crust formation had occurred (Figure 2).

By August 3, HCW-2 exhibited a papule on her forearm and fever and lymphadenopathy had developed. On August 4, we confirmed MPXV infection by qPCR (Ct 36). Lesions spread to her face and increased progressively until August 16 but did not evolve to crust. The lesions began to diminish on August 17 (Figure 2) and on August 24, HCW-2 was released from isolation because all lesions had healed.

Using the same qPCR protocol, we detected MPXV in 3 persons: the original patient, HCW-1, and HCW-2. We selected samples from the patient and HCW-1 for whole-genome sequencing because of their higher viremia. We performed whole-genome amplification as described elsewhere (8) and sequencing on an Illumina MiSeq sequencing platform (https://www.illumina.com), following best practices to avoid cross-contamination. We used ViralFlow (https://github.com/
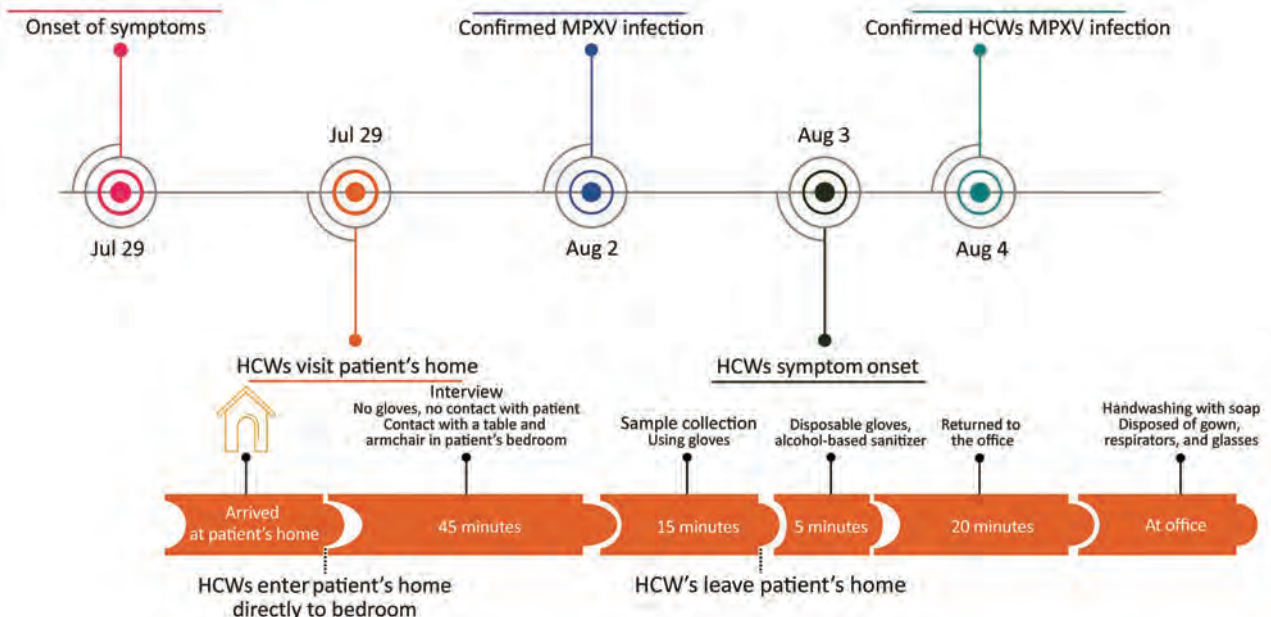

Figure 1. Timeline of monkeypox patient illness, HCW visit to the patient's home, and subsequent HCW illness, Brazil, 2022. HCW, healthcare worker; MPXV, monkeypox virus.

Figure 2. Timeline of skin lesions shown by HCW-1 and HCW-2, who had confirmed monkeypox virus infection after visit to home of monkeypox patient, Brazil, 2022. HCW, healthcare worker.

dezordi/ViralFlow) (*9*) for genome assembly and consensus generation, using an MPXV reference genome (GenBank accession no. MT903345.1). Analysis using the Nextclade tool (https://clades.nextstrain.org) showed that the sequenced genomes were 100% identical and belonged to MPXV clade IIb sublineage B.1.1 (Appendix Figures 1–3). We deposited consensus sequences in GISAID (accession nos. EPI_ISL_14465517 and EPI_ISL_14676265).

Conclusions

Our report provides evidence supporting the hypothesis that both HCW infections observed in this study were transmitted through fomite exposure with surfaces in the patient's home, their own PPE, or outer surfaces of the specimen transport box. These findings highlight that MPXV might be acquired through contact with fomites, such as patient belongings or surfaces contaminated with infectious viral particles. Close interaction between patients and HCWs are also risk factors for MPXV transmission (*4*). As notable routes of MPXV transmission, such interactions should be targeted along with diagnosis and

quarantine for MPXV containment measures (*4*). Recommendations for preexposure and postexposure prophylaxis include correct use of appropriate PPE (*10,11*). Infectious MPXV particles can remain on furniture and fabric surfaces (*12*), so caution is needed when in contact with general protection equipment and household objects that have been exposed to suspected case-patients.

We propose specific measures to prevent and curtail monkeypox infection acquired through fomites. HCWs must be properly trained to safely collect specimens, use PPE, implement control measures, and perform frequent hand hygiene. HCWs should wear gloves throughout entire visits and during contact with possibly infected persons and their belongings. Secondly, a disinfectant product effective against microbial pathogens such as nonenveloped viruses (e.g., norovirus, rotavirus, adenovirus, poliovirus) should be applied to object surfaces before and after interactions with suspected case-patients. Finally, vaccination campaigns should be conducted among high-risk groups, including certain HCWs. The possible transmission of MPXV by 2 HCWs from a patient environment

illustrates a potential source of transmission with broad implications for infection control and prevention and indicates the need for specific interventions in the context of the ongoing multicountry outbreak.

About the Author

Dr. Steiner Salvato is head of genomic surveillance at the Center for Health Surveillance of Rio Grande do Sul State Department of Health, Brazil. His research interests include the genomics of infectious diseases and genomic surveillance in the public health context.

References

1. World Health Organization. WHO health emergency dashboard [cited 2022 Aug 26]. https://extranet.who.int/publicemergency
2. World Health Organization. Monkeypox [cited 2022 Aug 26]. https://www.who.int/news-room/fact-sheets/detail/monkeypox
3. McCollum AM, Damon IK. Human monkeypox. Clin Infect Dis. 2014;58:260–7. https://doi.org/10.1093/cid/cit703
4. Vaughan A, Aarons E, Astbury J, Brooks T, Chand M, Flegg P, et al. Human-to-human transmission of monkeypox virus, United Kingdom, October 2018. https://www.doi.org/10.3201/eid2604.191164
5. Mauldin MR, McCollum AM, Nakazawa YJ, Mandra A, Whitehouse ER, Davidson W, et al. Exportation of monkeypox virus from the African continent. J Infect Dis. 2022;225:1367–76. https://doi.org/10.1093/infdis/jiaa559
6. World Health Organization. Multi-country outbreak of monkeypox, External situation report #4—24 August 2022 [cited 2022 Aug 26]. https://www.who.int/publications/m/item/multi-country-outbreak-of-monkeypox--external-situation-report--4---24-august-2022
7. Li Y, Zhao H, Wilkins K, Hughes C, Damon IK. Real-time PCR assays for the specific detection of monkeypox virus West African and Congo Basin strain DNA. J Virol Methods. 2010;169:223–7. https://doi.org/10.1016/j.jviromet.2010.07.012
8. Chen NFG, Gagne L, Doucette M, Smole S, Buzby E, Hall J, et al. Monkeypox virus multiplexed PCR amplicon sequencing (PrimalSeq) V.2. V.2 [cited 2022 Aug 26]. https://www.protocols.io/view/monkeypox-virus-multiplexed-pcr-amplicon-sequencin-cd8ds9s6
9. Dezordi FZ, Neto AMDS, Campos TL, Jeronimo PMC, Aksenen CF, Almeida SP, et al. on behalf of the Fiocruz Covid-Genomic Surveillance Network. ViralFlow: a versatile automated workflow for SARS-CoV-2 genome assembly, lineage assignment, mutations and intrahost variant detection. Viruses. 2022;14:217. https://doi.org/10.3390/v14020217
10. Rao AK, Petersen BW, Whitehill F, Razeq JH, Isaacs SN, Merchlinsky MJ, et al. Use of JYNNEOS (smallpox and monkeypox vaccine, live, nonreplicating) for preexposure vaccination of persons at risk for occupational exposure to orthopoxviruses: recommendations of the Advisory Committee on Immunization Practices—United States, 2022. MMWR Morb Mortal Wkly Rep. 2022;71:734–42. 10.15585/mmwr.mm7122e1 https://doi.org/10.15585/mmwr.mm7122e1
11. World Health Organization. Vaccines and immunization for monkeypox: interim guidance, 24 August 2022 [cited 2022 Aug 26]. https://www.who.int/publications/i/item/WHO-MPX-Immunization-2022.2-eng
12. Morgan CN, Whitehill F, Doty JB, Schulte J, Matheny A, Stringer J, et al. Environmental persistence of monkeypox virus on surfaces in household of person with travel-associated infection, Dallas, Texas, USA, 2021. Emerg Infect Dis. 2022;28:1982–9. https://doi.org/10.3201/eid2810.221047

Addresses for correspondence: Richard Steiner Salvato, Centro Estadual de Vigilância em Saúde, Secretaria Estadual da Saúde do Rio Grande do Sul, Av. Ipiranga 5400, CEP 90610-000, Porto Alegre, Rio Grande do Sul, Brazil; email: richard-salvato@saude.rs.gov.br; Gabriel Luz Wallau; Instituto Aggeu Magalhães (IAM)–FIOCRUZ-PE, Av. Prof. Moraes Rego s/n, CEP 50740-465, Recife, Pernambuco, Brazil; email: gabriel.wallau@fiocruz.br

Natural Mediterranean Spotted Fever Foci, Qingdao, China

Xiao-Lan Gu, Rui Wang, Chuan-Min Zhou, Jiang-Tao Cui, Ze-Min Li, Ze-Zheng Jiang,
Bang Li, Qiu-Ming Peng, Wen-Kang Zhang, Hui-Ju Han, Xue-Jie Yu

We sequenced DNA from spleens of rodents captured in rural areas of Qingdao, East China, during 2013–2015. We found 1 *Apodemus agrarius* mouse infected with *Rickettsia conorii*, indicating a natural Mediterranean spotted fever foci exists in East China and that the range of *R. conorii* could be expanding.

Mediterranean spotted fever (MSF) is an acute febrile, zoonotic disease caused by the bacterium *Rickettsia conorii* that is transmitted to humans by the brown dog tick, *Rhipicephalus sanguineus* (*1*). MSF was described from the Mediterranean region in 1910 (*2*); a similar disease, known as Indian tick typhus (ITT), was described in 1925 (*3*). The causative agent of ITT was later confirmed to be *R. conorii* (*4*). Since 1990, the natural foci of MSF has continued to expand into the Middle East, Africa, and central Europe (*5*). *R. conorii* ITT has been detected in ticks in Xinjiang Province in West China (*6*), and an MSF case recently was reported in Shandong Province in East China (*7*).

The city of Qingdao, located in the southeast part of Shandong Province, is on the pacific coast of East China (Figure 1). Qingdao has a temperate monsoonal climate that is ideal for rodent propagation, and many natural-focal diseases caused by *Rickettsia* spp., *Orientia tsutsugamushi*, and severe fever with thrombocytopenia syndrome virus (*8–10*). We used PCR amplification to investigate whether rodents in the region are infected with *Rickettsia* spp. and unexpectedly discovered *R. conorii*.

The Study

We performed a retrospective study by testing rodents captured from Huangdao District, Qingdao, China, during July–October every year from 2013–2015.

Author affiliations: Wuhan University, Wuhan, China (X.-L. Gu, R. Wang, C.-M. Zhou, Z.-M. Li, Z.-Z. Jiang, B. Li, Q.-M. Peng, W.-K. Zhang, H.-J. Han, X.-J. Yu); Laixi City for Disease Control and Prevention, Qingdao, China (J.-T. Cui)

The rodent collections were previously described (*11*). We aseptically collected rodent spleens and stored at −80°C. Animal use and sample collection were approved by the ethics committee of Medical School, Shandong University (approval no. 20150501), and performed in accordance with Shandong University Guidelines on the Care and Use of Laboratory Animals.

We extracted DNA from homogenized rodent spleen tissues by using the QIAamp DNA Mini Kit (QIAGEN, https://www.qiagen.com). We initially performed nested PCR on all rodents with 17-kDa antigen (*htrA*), then we further tested the PCR-positive samples by using primers of 16S ribosomal RNA (*rrs*) and outer membrane protein A and B (*ompA* and *ompB*) genes (*12,13*) (Table 1). We used nuclease-free water as a negative control in each experiment. We performed DNA extraction, PCR amplification, and PCR product analysis in separate rooms to avoid false-positive results. We visualized PCR products in 1.0%–1.5% agarose gels based on the length of amplified DNA segments. We excised and extracted expected DNA bands by using a gel extraction kit (Tsingke Biotech, https://tsingke.com). We cloned purified PCR products into T-Vector pMD19 (TaKaRa Bio, Inc., https://www.takara-bio.com). Both strands were sequenced by Sangon Biotech (https://www.sangon.com).

We edited DNA sequences by using DNAStar software (https://www.dnastar.com) to remove primers and analyzed sequences in BLAST (https://https://blast.ncbi.nlm.nih.gov/Blast.cgi) to compare with GenBank sequences. We constructed a phylogenetic tree by using the maximum-likelihood method with the Kimura 2-parameter model in MEGA version 7 (https://www.megasoftware.net), and we calculated bootstrap values with 1,000 replicates to determine the relative support for clades in the trees.

We used a total of 121 rodents in this study, including 60 striped field mice (*Apodemus agrarius*),

Figure 1. Location of rodent sampling sites in a study of natural Mediterranean spotted fever foci, Qingdao, Shandong Province, China. Inset map shows location of Shandong Province in China. Rodent species collected included striped field mice (*Apodemus agrarius*), Chinese hamsters (*Cricetulus barabensis*), house mice (*Mus musculus*), brown rats (*Rattus norvegicus*), greater long-tailed hamsters (*Cricetulus triton*), and Chinese white-bellied rats (*Niviventer confucianus*).

19 house mice (*Mus musculus*), 16 Chinese hamsters (*Cricetulus barabensis*), 10 brown rats (*Rattus norvegicus*), 8 greater long-tailed hamsters (*Cricetulus triton*), and 8 Chinese white-bellied rats (*Niviventer confucianus*) (Table 2). Among the rodents, 81.82% (99/121) were captured outdoors and 18.18% (22/121) indoors.

PCR amplification indicated that 1 *A. agrarius* mouse captured outdoors was positive for a *Rickettsia* species and the other 120 rodents were negative for *Rickettsia* by *htrA* primers. We further amplified the spleen tissue of the PCR-positive mouse by using *rrs*, *ompA*, and *ompB* primers. All 3 pairs of primers generated positive PCR products. Because the PCR fragment was too short and the sequence was conserved, we could not differentiate *Rickettsia* species by phylogenetic analysis of the *htrA* gene. However, the *rrs* gene sequence obtained in this study was 100% identical to *R. conorii* strains in GenBank (1,185/1,185 bp for accession no. KU364355, 1,267/1,267 bp for accession no. KY069267) that were obtained from *Rh. turanicus* ticks in Xinjiang, China. The obtained *rrs* sequence also matched 100% (1,331/1,331 bp) with

a GenBank *R. conorii* strain from India (accession no. L36107), and an *R. conorii* Malish 7 strain (accession no. NR_041934). The *ompA* sequence from the mouse was 100% identical to *R. conorii* strains from *Rh. turanicus* ticks (494/494 bp for GenBank accession nos. MF002512 and KY069258) and an *R. conorii* strain from a human blood sample (449/449 bp for accession no. MG190328) from Xinjiang, China. The obtained *ompA* sequence was also 100% (494/494 bp) identical to GenBank *R. conorii* strains from India (accession no. U43794) and Italy (accession no. JN944636). The *ompB* amplified from the mouse was 99.87% (798/799 bp) homologous to the corresponding sequences of *R. conorii* from *Rh. turanicus* ticks from Xinjiang, China (GenBank accession nos. MF002514 and KY069249) and an *R. conorii* strain from India (GenBank accession no. AF123726).

A phylogenetic tree of the concatenated sequences of the 4 genes, *rrs* (1,331 bp), *htrA* (169 bp), *ompA* (494 bp), and *ompB* (844 bp), showed that the rickettsial sequence from this study clustered with *R. conorii* ITT from ticks in India (GenBank accession no. AJHC01000000) and within the same clade as the *R. conorii* Malish 7 strain (GenBank

Table 1. Primers used for amplification of spotted fever group *Rickettsia* from natural Mediterranean spotted fever foci, Qingdao City, China*

Target gene	Primer	Nucleotide sequence, 5′ → 3′	Length, bp	Reference
17 kDa antigen	F1	CATTGTCCGTCAGGTTGGCG	371	(*12*)
	R1	GGAACACTTCTTGGCGGTG		
	F2	AACCGTAATTGCCGTTATCCGG	214	
	R2	GCATTACTTGGTTCTCAATTCGG		
16S rRNA	F1	TGATCCTGGCTCAGAACGAAC	1,486	(*12*)
	R1	TAAGGAGGTAATCCAGCCGC		
	F2	AACACATGCAAGTCGRACGG	1,371	
	R2	GGCTGCCTCTTGCGTTAGCT		
Outer membrane protein A	F	ATGGCGAATATTTCTCCAAAA	536	(*13*)
	R	AGTGCAGCATTCGCTCCCCCT		
Outer membrane protein B	F1	ATATGCAGGTATCGGTACT	1,355	(*12*)
	R1	CCATATACCGTAAGCTACAT		
	F2	GCAGGTATCGGTACTATAAAC	843	
	R2	AATTTACGAAACGATTACTTCCGG		

*Samples studied were from rodents collected in Huangdao District, Qingdao, China, during July–October every year in 2013–2015. The rodent collection was described in a previous study (*11*). F, forward; R, reverse.

Table 2. Number and location of rodents collected in a study of natural Mediterranean spotted fever foci, Qingdao, China*

Species, no.	Outdoors	Indoors	Total
Striped field mice (*Apodemus agrarius*)	59	1	60
Chinese hamsters (*Cricetulus barabensis*)	16	0	16
House mice (*Mus musculus*)	8	11	19
Brown rats (*Rattus norvegicus*)	0	10	10
Greater long-tailed hamsters (*Cricetulus triton*)	8	0	8
Chinese white-bellied rats (*Niviventer confucianus*)	8	0	8
Total	99	22	121

*Rodents were collected in Huangdao District, Qingdao, China, during July–October every year in 2013–2015. The rodent collection was described in a previous study (*11*).

accession no. AE006914), *R. conorii* Israel tick typhus strain (GenBank accession no. AJVP01000000), and *R. conorii* Astrakhan strain (GenBank accession no. AJUR01000000) (Figure 2). We deposited nucleotide sequence data from this study into GenBank (accession no. OM230141 for *rrs*, OM234678 for *htrA*, OM234679 for *ompA*, and OM234680 for *ompB* genes).

Conclusions

We identified *Rickettsia* spp. in a striped field mouse captured in Qingdao in East China. Phylogenetic analysis showed that the *Rickettsia* species we detected was identical in multiple gene sequences to *R. conorii* ITT, indicating the strain we identified is *R. conorii*. Our results could not be caused by PCR
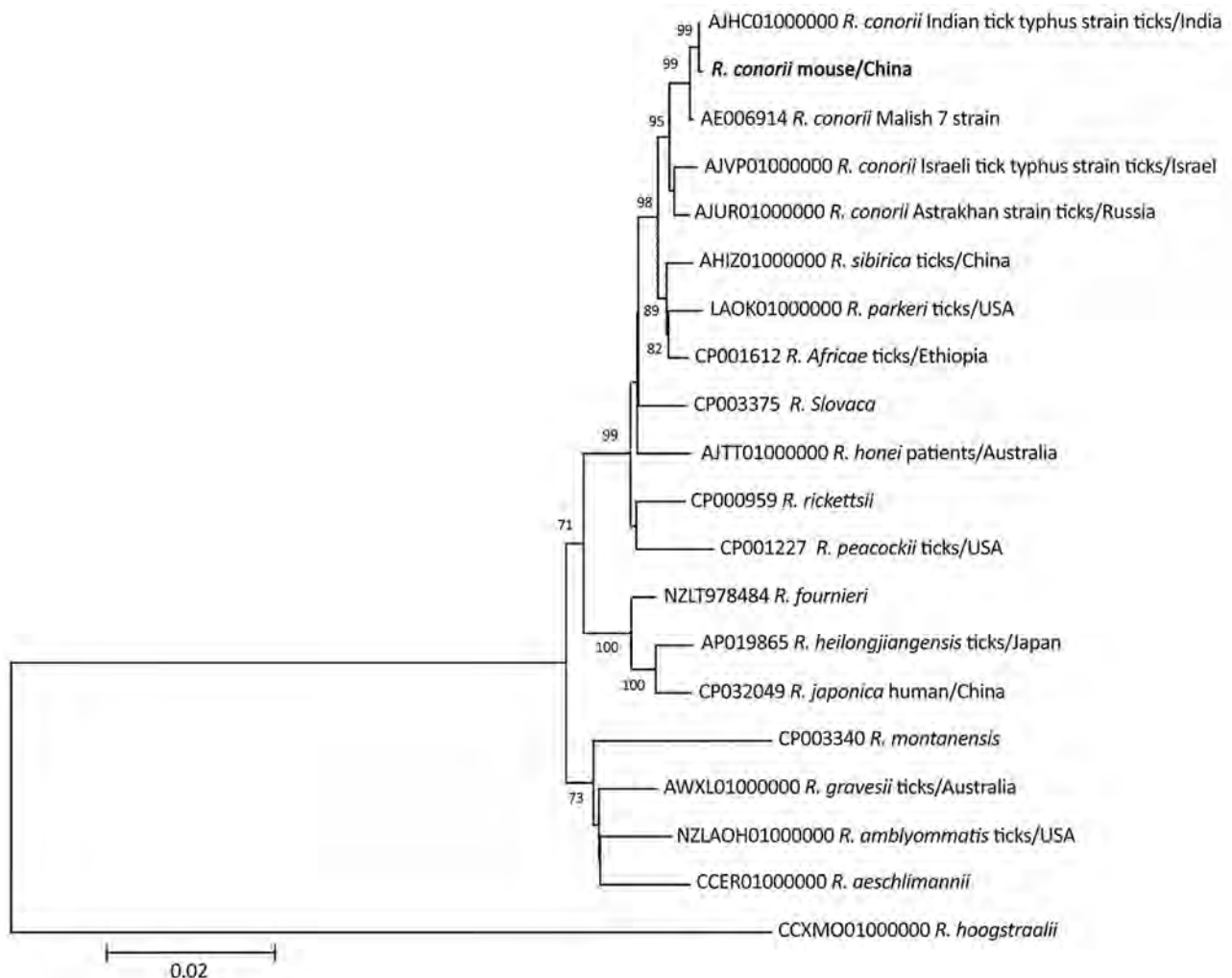
Figure 2. Phylogenetic tree of *Rickettsia conorii* identified from natural Mediterranean spotted fever foci, Qingdao, China. Bold text indicates *R. conorii* obtained from a striped field mouse (*Apodemus agrarius*) captured in 2015. The maximum-likelihood tree is based on the concatenated sequences of *rrs*, *htrA*, *ompA*, and *ompB* genes of *Rickettsia* species. Numbers at the nodes indicated the percentage of bootstrap proportions with 1,000 replicates; only bootstrap values >70% are shown. The reference sequences are indicated by the GenBank accession number, name of species, host, and country of isolation. Scale bar indicates nucleotide substitutions per site.

contamination because we do not have an *R. conorii* strain nor its DNA in our laboratory.

The prevailing vector of *R. conorii* is the brown dog tick, *Rh. sanguineus* (*2*). The widespread distribution of *R. conorii* might be related to the worldwide spread of its vector tick among dogs (*14*). *R. conorii* ITT sequences have been reported in *Rh. turanicus* ticks from Xinjiang Province in West China (*6*). We identified *R. conorii* in 1 rodent in Qingdao, located in the eastern part of Shandong Province. Another recent study reported *R. conorii* genomic sequences in a patient in the western part of Shandong Province (*7*). These results demonstrate that the endemic area of *R. conorii* either recently expanded into Shandong Province in East China or *R. conorii* has existed in East China but was not detected before.

We speculate that the expansion of MSF foci in China is caused by transportation of dogs from West China to East China (*15*), contributing to the spread of brown dog ticks and, thus, *R. conorii*. The tick vector of *R. conorii* in Shandong Province has not been identified.

In conclusion, we confirmed *R. conorii* infection in 1 rodent from Qingdao in East China. Further studies are needed to determine the epidemiology of *R. conorii* in East China. Our study increases our knowledge about the distribution of *R. conorii*. Identification of MSF foci in East China could indicate that the range of *R. conorii* and its tick vector are expanding.

Acknowledgments

X.-J.Y. and H.-J.H. organized and designed the study. J.-T.C., X.-L.G., C.-M.Z., R.W., Q.-M.P., Z.-Z.J., B.L., and W.-K.Z. performed the fieldwork. X.-L.G. and R.W. performed laboratory analysis of pathogens. X.-L.G. analyzed the data and drafted the manuscript. X.-J.Y. critically reviewed the manuscript. All authors read and approved the final manuscript.

About the Author

Ms. Gu is a PhD candidate at the School of Public Health, Wuhan University, Wuhan, Hubei, China. Her research interests include emerging infectious disease and vector-borne disease.

References

1. Colomba C, Saporito L, Polara VF, Rubino R, Titone L. Mediterranean spotted fever: clinical and laboratory characteristics of 415 Sicilian children. BMC Infect Dis. 2006;6:60. https://doi.org/10.1186/1471-2334-6-60
2. Rovery C, Brouqui P, Raoult D. Questions on Mediterranean spotted fever a century after its discovery. Emerg Infect Dis. 2008;14:1360–7. https://doi.org/10.3201/eid1409.071133
3. Megaw JWD. Indian tick-typhus. Ind Med Gaz. 1925; 60:58–61.
4. Sentausa E, El Karkouri K, Robert C, Raoult D, Fournier PE. Genome sequence of *Rickettsia conorii* subsp. indica, the agent of Indian tick typhus. J Bacteriol. 2012;194:3288–9. https://doi.org/10.1128/JB.00462-12
5. MacConnachie K, Tishkowski K. Boutonneuse fever. Treasure Island (FL): StatPearls Publishing; 2022 [cited 2022 Jul 5]. https://www.ncbi.nlm.nih.gov/books/NBK560914
6. Guo LP, Jiang SH, Liu D, Wang SW, Chen CF, Wang YZ. Emerging spotted fever group rickettsiae in ticks, northwestern China. Ticks Tick Borne Dis. 2016;7:1146–50. https://doi.org/10.1016/j.ttbdis.2016.08.006
7. Xu N, Gai W, Zhang Y, Wang W, Wang G, Dasch GA, et al. Confirmation of *Rickettsia conorii* subspecies indica infection by next-generation sequencing, Shandong, China. Emerg Infect Dis. 2021;27:2691–4. https://doi.org/10.3201/eid2710.204764
8. Qin XR, Han HJ, Han FJ, Zhao FM, Zhang ZT, Xue ZF, et al. *Rickettsia japonica* and novel *Rickettsia* species in ticks, China. Emerg Infect Dis. 2019;25:992–5. https://doi.org/10.3201/eid2505.171745
9. Li F, Zhang ZT, Fang LZ, Yu H, Qin XR, Yu XJ. Indoor and outdoor rodent hosts of *Orientia tsutsugamushi*, Shandong Province, China. Emerg Infect Dis. 2021;27:2731–4. https://doi.org/10.3201/eid2710.210393
10. Liu JW, Wen HL, Fang LZ, Zhang ZT, He ST, Xue ZF, et al. Prevalence of SFTSV among Asian house shrews and rodents, China, January-August 2013. Emerg Infect Dis. 2014;20:2126–8. https://doi.org/10.3201/eid2012.141013
11. Qin XR, Liu JW, Yu H, Yu XJ. *Bartonella* species detected in rodents from eastern China. Vector Borne Zoonotic Dis. 2019;19:810–4. https://doi.org/10.1089/vbz.2018.2410
12. Huang Y, Zhao L, Zhang Z, Liu M, Xue Z, Ma D, et al. Detection of a novel *Rickettsia* from *Leptotrombidium scutellare* mites (Acari: Trombiculidae) from Shandong of China. J Med Entomol. 2017;54:544–9. https://doi.org/10.1093/jme/tjw234
13. Yuan TT, Du CH, Xia LY, Que TC, von Fricken ME, Jiang BG, et al. Molecular evidence of *Candidatus Rickettsia longicornii* and a novel *Rickettsia* strain from ticks in Southern China. Ticks Tick Borne Dis. 2021;12:101679. https://doi.org/10.1016/j.ttbdis.2021.101679
14. Gray J, Dantas-Torres F, Estrada-Peña A, Levin M. Systematics and ecology of the brown dog tick, *Rhipicephalus sanguineus.* Ticks Tick Borne Dis. 2013;4:171–80. https://doi.org/10.1016/j.ttbdis.2012.12.003
15. Chen J, Zou L, Jin Z, Ruan S. Modeling the geographic spread of rabies in China. PLoS Negl Trop Dis. 2015;9:e0003772. https://doi.org/10.1371/journal.pntd.0003772

Address for correspondence: Hui-Ju Han or Xue-Jie Yu, Wuhan University, School of Public Health, Wuhan, 430071, Hubei Province, China; email: 00033074@whu.edu.cn or yuxuejie@whu.edu.cn

Highly Diverse Arenaviruses in Neotropical Bats, Brazil

Luiz Gustavo Bentim Góes, Carlo Fischer, Angélica Cristine Almeida Campos,
Cristiano de Carvalho, Andrés Moreira-Soto, Guilherme Ambar, Adriana Ruckert da Rosa,
Debora Cardoso de Oliveira, Wendy Karen Jo, Ariovaldo P. Cruz-Neto, Wagner André Pedro,
Luzia Helena Queiroz, Paola Minoprio, Edison L. Durigon, Jan Felix Drexler

We detected arenavirus RNA in 1.6% of 1,047 bats in Brazil that were sampled during 2007–2011. We identified Tacaribe virus in 2 *Artibeus* sp. bats and a new arenavirus species in *Carollia perspicillata* bats that we named *Tietê mammarenavirus*. Our results suggest that bats are an underrecognized arenavirus reservoir.

Bats are prominent hosts of zoonotic RNA viruses because of immunologic, physiologic, and ecologic factors (*1*). The Arenaviridae family comprises 4 genera: *Reptarenavirus* and *Hartmanivirus*, whose members infect reptiles; *Antennavirus*, whose members infect fish; and *Mammarenavirus*, whose members infect mammals. Mammarenaviruses can be separated into globally distributed lymphocytic choriomeningitis–Lassa virus serocomplex and New World arenaviruses (NWAs) (*2*). The NWAs Junin, Machupo, Sabia, Chapare, and Guanarito cause viral hemorrhagic fever and must be handled under Biosafety Level 4 conditions (*2*).

All highly pathogenic arenaviruses known thus far are hosted by and transmitted to humans from persistently infected rodents (*2*). Only Tacaribe virus (TCRV; *Tacaribe mammarenavirus*) has been identified in bats (*3,4*). Although TCRV is not considered a human pathogen, anecdotal evidence exists for potential laboratory acquired infection that causes influenza-like symptoms (*5,6*). In addition, TCRV is phylogenetically related to pathogenic arenaviruses that cause viral hemorrhagic fever; viral properties associated with severe disease, such as evasion of immune responses and cellular tropism, might be conserved in TCRV and genetically related animal arenaviruses (*7*).

Associations between TCRV and *Artibeus* spp. bats are supported only by limited epidemiologic data, including a single virus isolation and serologic evidence (*3,4*), considerable illness of bats during experimental infection (*5*), and isolation of TCRV from mosquitoes and ticks that primarily feed on rodents and rarely on bats (*3,6*). Limited genetic data exist for TCRV; a single genomic sequence was obtained from a bat-derived isolate generated in the 1950s from Trinidad that has been extensively passaged in mice and cell cultures and another from a recent tick-derived isolate (*3,4,8*).

The Study

We investigated diverse specimens from 1,047 adult bats belonging to 32 species collected from southeastern Brazil (Appendix, https://wwwnc.cdc.gov/EID/article/28/12/22-0980-App1.pdf). We analyzed a total of 3,670 different tissue specimens, including spleens (n = 893), lungs (n = 889), intestines (n = 973), and livers (n = 915), for arenavirus RNA by using reverse transcription PCR (RT-PCR) (*9*) modified to promote NWA amplification (Appendix Table 1, Figure 1).

We detected arenavirus RNA in 4 *Artibeus lituratus*, 1 *A. planirostris*, and 12 *Carollia perspicillata* bats; the overall detection rate was 1.62% (95% CI 0.95%–2.59%). Arenavirus-positive bats were collected during 2007–2011 from 3 sampling sites located in both forest and urban areas within a 60-km radius (Figure 1), suggesting arenavirus

Author affiliations: Charité-Universitätsmedizin Berlin, Freie Universität Berlin and Humboldt-Universität zu Berlin, Berlin, Germany (L.G.B. Góes, C. Fischer, A.C.A. Campos, A. Moreira-Soto; W.K. Jo, J.F. Drexler); Scientific Platform Pasteur-USP, São Paulo, Brazil (L.G.B. Góes, A.C.A. Campos, P. Minoprio); Universidade de São Paulo, São Paulo, Brazil (L.G.B. Góes, A.C.A. Campos, E.L. Durigon); Universidade Estadual Paulista, Araçatuba, Brazil (C. de Carvalho, W.A. Pedro, L.H. Queiroz); Universidade Estadual Paulista, Rio Claro, Brazil (G. Ambar, A.P. Cruz-Neto), Centro de Controle de Zoonooses, São Paulo (A. Ruckert da Rosa, D. Cardoso de Oliveira); German Centre for Infection Research (DZIF), Berlin (W.K. Jo, J.F. Drexler)
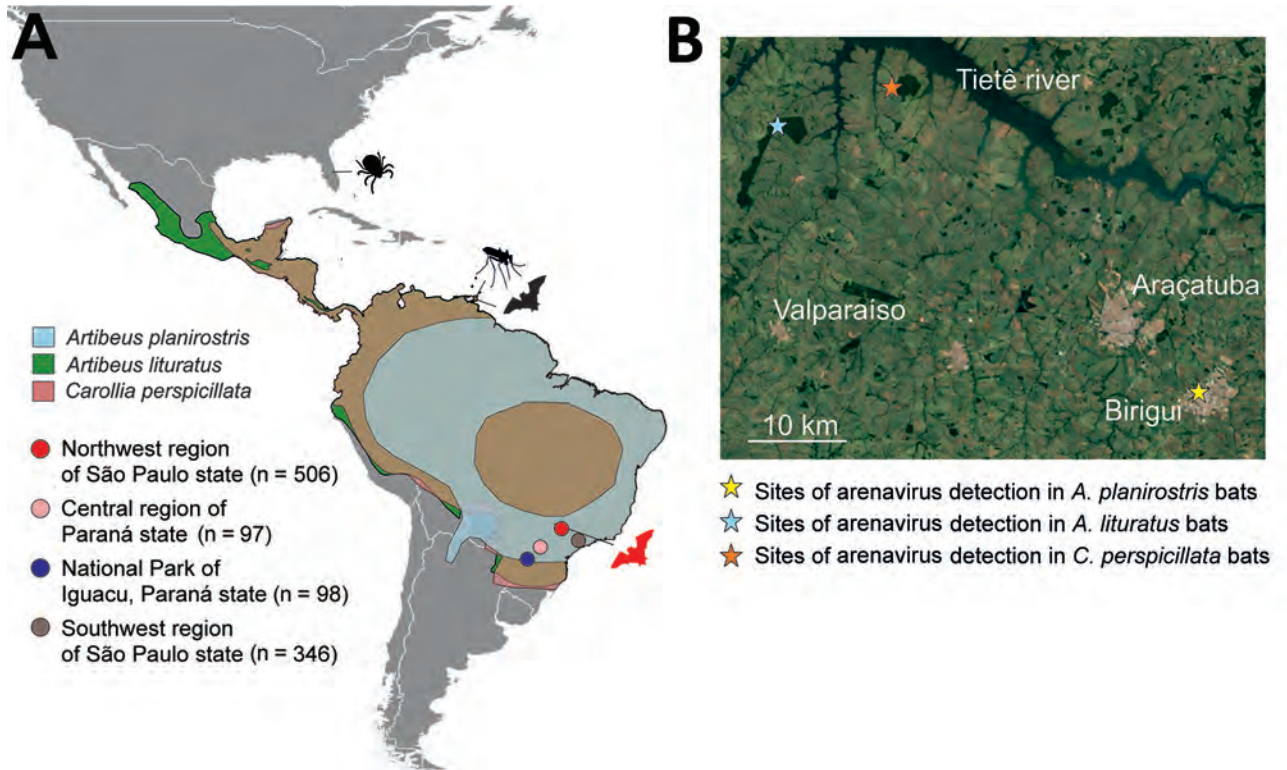
DOI: https://doi.org/10.3201/eid2812.220980

Figure 1. Bat mammarenavirus detection and host distribution in study of highly diverse arenaviruses in neotropical bats, Brazil. A) Geographic ranges of arenavirus-positive bat species indicated by blue (*Artibeus planirostris*), green (*A. lituratus*), and red (*Carollia perspicillata*) colors, according to the International Union for Conservation of Nature (https://www.iucnredlist.org). The brown areas in the map indicate the overlap of the distribution of *A. lituratus* and *C. perspicillata*. The absence of *A. planirostris* distribution in central Brazil likely represents lack of information regarding this species. Filled circles represent regions of sample collection: northwestern region of São Paulo state (red), central region of Paraná state (pink), National Park of Iguaçu, Paraná state (dark blue), and southwestern region of São Paulo state (gray). Number of bats obtained from each region is indicated. Red bat figure indicates where *Tacaribe mammarenavirus* and *Tietê mammarenavirus* were detected in the present study. Hosts from which Tacaribe virus was sequenced in other studies, including ticks (Florida, USA), mosquitoes, and bats (Port of Spain, Trinidad and Tobago) are indicated by black pictograms. Map prepared using QGIS desktop software version 3.24 (https://www.qgis.org). B) Areas of arenavirus detection in the northwestern region of São Paulo state, Brazil. Yellow star indicates the capture site of arenavirus-positive *A. planirostris*, blue star indicates the capture site of arenavirus-positive *A. lituratus*, and orange star marks the capture site of arenavirus-positive *C. perspicillata* bats. Tietê River and cities Araçatuba, Valparaíso, and Birigui are indicated. Dark green areas show forest fragments. Map obtained from Google Earth (https://earth.google.com)

maintenance in bat populations in this region. All 3 arenavirus-positive bat species are abundant in tropical environments and well-adapted to urban landscapes, indicating potential for dispersion and spillover to humans and other animals.

Most arenavirus-positive bats were collected in 2 forest fragments in 2007 (Tables 1, 2; Figure 1), where most bat species positive for arenavirus RNA were sampled. Whether high detection rates at those sites correspond to epizootics or sampling bias remains unknown.

All arenavirus-positive animals appeared healthy, suggesting limited negative effects of arenavirus infection on bat hosts. This observation was similar in rodent arenavirus hosts (*10*) and consistent with high TCRV seroprevalence in a serologic survey

(*4*) but different from experimental TCRV infections (*5*), likely because of different routes and high doses used for infecting bats in laboratory settings. High seroprevalence and low arenavirus detection rates suggest that arenaviruses do not infect bats persistently, which is distinct from results for rodent arenavirus infections (*11*). Lack of persistence is important for public health because it indicates potential limitations of arenavirus shedding by bat hosts whose lifespan is ≤8–12 years (*12*).

We detected arenavirus RNA in multiple organs at similar concentrations, including spleens (mean, 1.2×10^7 RNA copies/mg) and lungs (mean, 6.4×10^6 RNA copies/mg) ($p = 0.53$ by Mann-Whitney U test) (Table 2), suggesting systemic infection similar to that observed in experimentally infected bats (*5*). We

observed the highest arenavirus RNA concentration in the single arenavirus-positive intestine specimen, followed by the spleen, lung, liver, and kidney in that animal (Table 2). High arenavirus RNA concentrations in intestines are consistent with virus shedding through the enteric route, which has been observed during experimental infections with TCRV (5). Although rodents shed arenaviruses primarily through urine and saliva, shedding also occurs in feces (2). Determining differences in arenavirus transmission routes between bats and rodents will require further investigation. We were unsuccessful isolating bat arenaviruses from organ homogenates despite repeated attempts (Appendix), likely because of tissue degradation under tropical conditions.

We performed phylogenetic analysis of the partial sequence for the arenavirus RNA-dependent RNA polymerase gene obtained from RT-PCR screening. We found 2 NWA clades in bats from Brazil: 1 clade for both *Artibeus* spp. and 1 clade for *C. perspicillata* bats (GenBank accession nos. ON648806–16) (Figure 2, panel A). We obtained complete arenavirus coding sequences from 1 *A. planirostris* and 3 *C. perspicillata* bats (GenBank accession nos. ON648817–24) by using Illumina-based deep sequencing (Illumina, https://www.illumina.com); genome organization was identical to other mammarenaviruses. Both arenaviruses formed a well-supported monophyletic clade with TCRV in sister relationship to Junin and Machupo viruses (Figure 2, panel B) and

Table 1. Bat species screened for arenaviruses in study of highly diverse arenaviruses in neotropical bats, Brazil

Bat species	Family	No. bats	No. positive (%, 95% CI)*	Region†	Sampling year (no. bats)
Artibeus fimbriatus	Phyllostomidae	3	0	A	2012 (3)
A. lituratus	Phyllostomidae	155	4 (2.6, 0.7–6.5)	A–D	2007 (8), 2010 (26), 2011 (46), 2012 (45), 2013 (4), 2014 (12), 2015 (16)
A. obscurus	Phyllostomidae	2	0	C, D	2013, 2015
A. planirostris	Phyllostomidae	9	1 (11.1, 0.3–48.3)	A–C	2010 (3), 2011 (2), 2012 (2), 2013 (1), 2014 (1)
Carollia perspicillata	Phyllostomidae	63	12 (19.1, 10.3–30.9)	A–D	2007 (18), 2010 (13), 2011 (18), 2012 (12), 2015 (2)
Chrotopterus auritus	Phyllostomidae	1	0	A	2010
Cynomops planirostris	Molossidae	11	0	C, D	2013 (1), 2014 (7), 2015 (3)
Desmodus rotundus	Phyllostomidae	69	0	C, D	2007 (7), 2011 (44), 2012 (1), 2014 (15), 2015 (2)
Eptesicus furinalis	Vespertilionidae	17	0	C, D	2011 (2), 2013 (6), 2014 (3), 2015 (6)
Eumops auripendulus	Molossidae	2	0	D	2014, 2015
E. glaucinus	Molossidae	106	0	C, D	2009 (1), 2010 (1), 2011 (5), 2012 (5), 2013 (19), 2014 (34), 2015 (41)
E. perotis	Molossidae	12	0	C, D	2013 (1), 2014 (8), 2015 (3)
Glossophaga soricina	Phyllostomidae	70	0	C, D	2007 (3), 2011 (2), 2012 (1), 2013 (2), 2014 (30), 2015 (32)
Lasiurus blossevillii	Vespertilionidae	2	0	C, D	2011, 2012
L. cinereus	Vespertilionidae	1	0	C	2013
L. ega	Vespertilionidae	2	0	C, D	2013, 2014
Molossops neglectus	Molossidae	1	0	D	2014
M. temminckii	Molossidae	2	0	C	2011
Molossus molossus	Molossidae	242	0	C, D	2007 (1), 2010 (1), 2011 (25), 2012 (16), 2013 (60), 2014 (84), 2015 (55)
M. rufus	Molossidae	160	0	C, D	2009 (11), 2010 (1), 2011 (20), 2012 (28), 2013 (48), 2014 (27), 2015 (25)
Myotis nigricans	Vespertilionidae	35	0	C, D	2011 (1), 2012 (4), 2013 (9), 2014 (6), 2015 (15)
M. riparius	Vespertilionidae	1	0	C	2013
Noctilio albiventris	Noctilionidae	2	0	C	2007 (2)
Nyctinomops laticaudatus	Molossidae	4	0	C, D	2011 (1), 2014 (2), 2015 (1)
N. macrotis	Molossidae	1	0	D	2014 (1)
Phyllostomus discolor	Phyllostomidae	2	0	D	2014 (2)
Platyrrhinus lineatus	Phyllostomidae	6	0	C, D	2014 (5), 2015 (1)
Promops nasutus	Molossidae	1	0	D	2014 (1)
Pygoderma bilabiatum	Phyllostomidae	1	0	D	2015 (1)
Sturnira lilium	Phyllostomidae	29	0	A, B, D	2010 (5), 2011 (9), 2012 (14), 2015 (1)
Tadarida brasiliensis	Molossidae	30	0	C, D	2014 (15), 2015 (15)
Vampyressa pusila	Phyllostomidae	1	0	B	2012 (1)
Not identified		4	0	C, D	2011(1), 2013 (2), 2014 (1)
Total	4	1,047	17 (1.6, 0.9–2.6)	A–D	2007–2015

*Number of bats with arenavirus RNA detected by PCR.
†Bats were collected from 36 sites within 4 main geographic regions of Brazil: A, Iguaçu National Park; B, central region of Parana state; C, northwest São Paulo state; and D, southwest São Paulo state.

Table 2. Collection sites and arenavirus RNA concentrations in different organs from bats in study of highly diverse arenaviruses in neotropical bats, Brazil*

Sample no.	Bat species†	Sex	Collection site	No. RNA copies/mg tissue				
				Spleen	Lung	Intestine	Liver	Kidney
Br56	*Artibeus lituratus*	M	Valparaiso	5.54×10^2	7.24×10^2	NA	NA	NA
Br57	*A. lituratus*	M	Valparaiso	NA	3.14×10^2	NA	NA	NA
Br58	*A. lituratus*	M	Valparaiso	2.15×10^6	6.13×10^6	NA	NA	NA
Br59	*A. lituratus*	M	Valparais	NA	2.10×10^2	NA	NA	NA
A354	*A. planirostris*	M	Birigui	1.09×10^5	5.02×10^4	4.73×10^5	9.68×10^3	6.01×10^3
Br61	*Carollia perspicillata*	F	Araçatuba	4.73×10^4	1.17×10^3	NA	NA	NA
Br62	*C. perspicillata*	F	Araçatuba	1.99×10^7	6.96×10^7	NA	NA	NA
Br63	*C. perspicillata*	F	Araçatuba	2.71×10^2	8.61×10^0	NA	NA	NA
Br65	*C. perspicillata*	M	Araçatuba	2.23×10^1	2.88×10^2	NA	NA	NA
Br68	*C. perspicillata*	F	Araçatuba	2.35×10^1	Neg	NA	NA	NA
Br69	*C. perspicillata*	M	Araçatuba	5.95×10^7	1.99×10^6	NA	NA	NA
Br70	*C. perspicillata*	M	Araçatuba	8.20×10^7	1.85×10^5	NA	NA	NA
Br71	*C. perspicillata*	F	Araçatuba	5.37×10^3	5.38×10^2	NA	NA	NA
Br72	*C. perspicillata*	M	Araçatuba	4.70×10^2	6.11×10^1	NA	NA	NA
Br74	*C. perspicillata*	M	Araçatuba	3.54×10^5	8.84×10^6	NA	NA	NA
Br76	*C. perspicillata*	M	Araçatuba	1.18×10^6	1.52×10^7	NA	NA	NA
Br77	*C. perspicillata*	F	Araçatuba	Neg	1.81×10^2	NA	NA	NA

*Numbers in bold are samples used in arenavirus isolation attempts. NA, tissue not available; Neg, negative
†Samples were collected from *Artibeus lituratus* bats in forest areas of Valparaiso in 2007, *A. planirostris* bat in an urban area of Birigui in 2011, and *Carollia perspicillata* bats in forest areas of Araçatuba in 2007.

Ocozocoautla de Espinosa virus that was possibly responsible for a hemorrhagic fever outbreak in Mexico (Figure 2, panel C) (*13*). These results highlight the genetic relationship of those bat-associated arenaviruses with highly pathogenic NWAs (Appendix Table 2). Identical topology in phylogenetic reconstructions
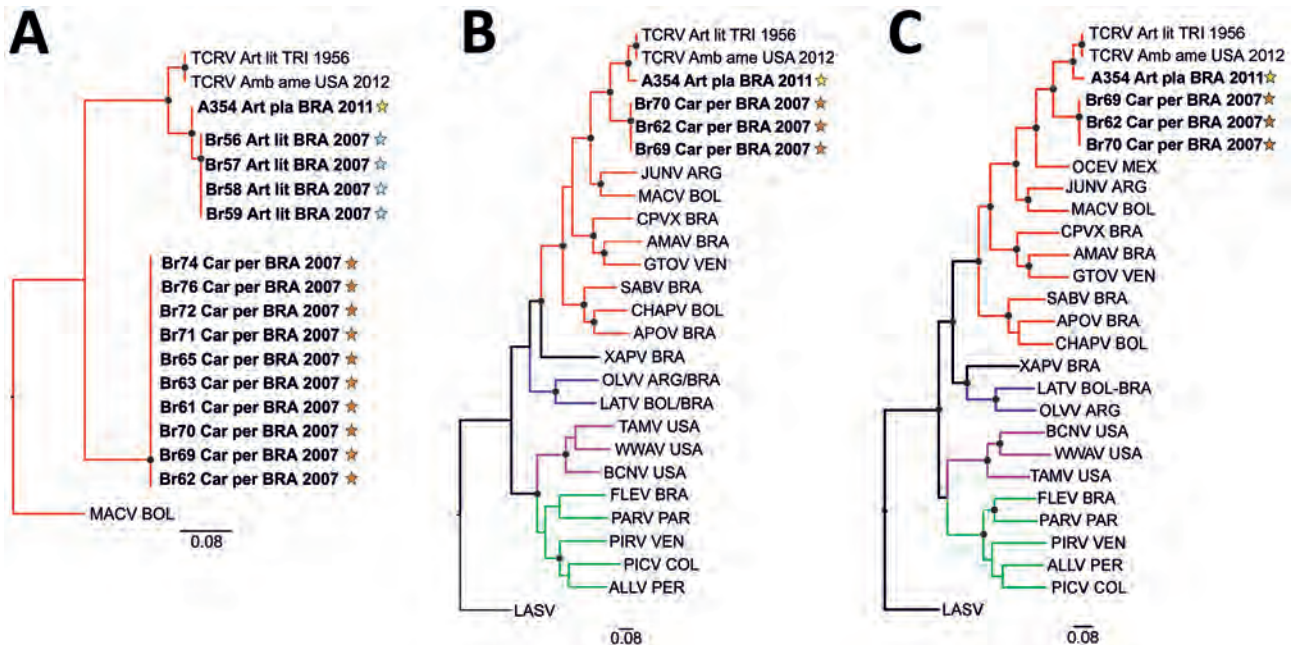

Figure 2. Phylogenetic analyses of highly diverse arenaviruses in neotropical bats, Brazil. Maximum-likelihood consensus trees compare partial RNA-dependent RNA polymerase genes (A), complete large (L) segment genes (B), and complete small (S) segment genes (C) from arenaviruses detected in *Artibeus* and *Carollia* spp. bats. Phylogenetic trees were generated using MEGA X software (https://www.megasoftware.net). Bold indicates sequences obtained from this study. Stars indicate regions where arenavirus-positive bat hosts were detected (Figure 1, panel B). Black dots at tree nodes represent bootstrap values ≥75% (1,000 replicates). Green lines indicate clade A new world arenaviruses, red lines indicate clade B new world arenaviruses, blue lines indicate clade C new world arenaviruses, and purple lines indicate recombinant new world arenaviruses (tentative clade D) (*14*). GenBank sequences used for comparisons and virus abbreviations are provided online (https://wwwnc.cdc.gov/EID/article/28/12/22-0980-F2.htm). Origins of arenaviruses are indicated for each sample: ARG, Argentina; BOL, Bolivia; BRA, Brazil; COL, Colombia; PER, Peru; TRI, Trinidad; USA, United States of America; VEN, Venezuela. Scale bars indicate nucleotide substitutions per site.

argued against potential reassortment (Figure 2, panels B, C), and homogeneous sequence distances and recombination analyses along the genome did not indicate recombination events (Appendix Figure 2).

The *A. planirostris* bat was infected with a previously unknown TCRV strain (Appendix Table 2) that had an amino acid identity of 93.8%–95.5% with other TCRV sequences, depending on the protein analyzed. The arenaviruses from *C. perspicillata* bats formed a separate species in clade B of the TCRV serogroup (Figure 2, panels B, C). Species assignment relied on taxonomic criteria (*14*) that included exclusive detection in a distinct host, nucleotide sequence identity of <80% in the small segment, and 88.6%–90% amino acid identity in the nucleocapsid protein compared with TCRV and pairwise sequence comparison (https://www.ncbi.nlm.nih.gov/sutils/pasc/viridty.cgi?textpage=overview) results for large and small segments (Appendix Figure 3). The 5′ and 3′ ends of large and small genomic segments obtained from the newly identified arenavirus from *C. perspicillata* bats were nearly identical to TCRV, consistent with a close genetic relationship between those NWAs (Appendix Table 3, Figure 4). We propose that the arenavirus sequenced from *C. perspicillata* bats should be named Tietê virus (species *Tiête mammarenavirus*) and abbreviated as TETV; the name comes from the main river located <4 km from the capture site (Figure 1).

Conclusions

Arenavirus genetic diversity is hypothesized to result from a complex macro-evolutionary pattern that includes both co-evolution and host switching in the Muridae family of rodents. In South America, arenaviruses might have co-evolved with rodents in the Sigmodontinae subfamily, with the exception of TCRV (*10*). Further investigation will be required to determine whether bat arenaviruses evolved from an ancestral host switch involving rodents, which would be consistent with the genetic relationship between TCRV or Tietê virus and rodent-derived Ocozocoautla de Espinosa virus, or whether bats and arenaviruses co-evolved. Of note, bats play an essential role in ecosystems, and stigmatization of bats as sources of zoonotic viruses is unwarranted.

In summary, the epidemiology, genealogy, and zoonotic potential of bat arenaviruses deserve further investigation. Our results suggest that bats are an underrecognized arenavirus reservoir.

About the Author

Dr. Góes is a postdoctoral researcher at the Institute of Virology at Charité-Universitätsmedizin, Berlin, Germany. His research focuses on pathogen discovery, virus epidemiology, and evolution of emerging viruses.

References

1. Guth S, Mollentze N, Renault K, Streicker DG, Visher E, Boots M, et al. Bats host the most virulent—but not the most dangerous—zoonotic viruses. Proc Natl Acad Sci USA. 2022;119:e2113628119. https://doi.org/10.1073/pnas.2113628119
2. Charrel RN, de Lamballerie X. Zoonotic aspects of arenavirus infections. Vet Microbiol. 2010;140:213–20. https://doi.org/10.1016/j.vetmic.2009.08.027
3. Downs WG, Anderson CR, Spence L, Aitken THG, Greenhall AH. Tacaribe virus, a new agent isolated from Artibeus bats and mosquitoes in Trinidad, West Indies. Am J Trop Med Hyg. 1963;12:640–6. https://doi.org/10.4269/ajtmh.1963.12.640
4. Malmlov A, Seetahal J, Carrington C, Ramkisson V, Foster J, Miazgowicz KL, et al. Serological evidence of arenavirus circulation among fruit bats in Trinidad. PLoS One. 2017;12:e0185308. https://doi.org/10.1371/journal.pone.0185308
5. Cogswell-Hawkinson A, Bowen R, James S, Gardiner D, Calisher CH, Adams R, et al. Tacaribe virus causes fatal infection of an ostensible reservoir host, the Jamaican fruit bat. J Virol. 2012;86:5791–9. https://doi.org/10.1128/JVI.00201-12
6. Sayler KA, Barbet AF, Chamberlain C, Clapp WL, Alleman R, Loeb JC, et al. Isolation of Tacaribe virus, a Caribbean arenavirus, from host-seeking *Amblyomma americanum* ticks in Florida. PLoS One. 2014;9:e115769. https://doi.org/10.1371/journal.pone.0115769
7. Moreno H, Möller R, Fedeli C, Gerold G, Kunz S. Comparison of the innate immune responses to pathogenic and nonpathogenic clade B New World arenaviruses. J Virol. 2019;93:e00148-19. https://doi.org/10.1128/JVI.00148-19
8. Holzerland J, Leske A, Fénéant L, Garcin D, Kolakofsky D, Groseth A. Complete genome sequence of Tacaribe virus. Arch Virol. 2020;165:1899–903. https://doi.org/10.1007/s00705-020-04681-9
9. Vieth S, Drosten C, Lenz O, Vincent M, Omilabu S, Hass M, et al. RT-PCR assay for detection of Lassa virus and related Old World arenaviruses targeting the L gene. Trans R Soc

Trop Med Hyg. 2007;101:1253–64. https://doi.org/10.1016/j.trstmh.2005.03.018

10. Grande-Pérez A, Martin V, Moreno H, de la Torre JC. Arenavirus quasispecies and their biological implications. Curr Top Microbiol Immunol. 2016;392:231–76. https://doi.org/10.1007/82_2015_468

11. Hoffmann C, Wurr S, Pallasch E, Bockholt S, Rieger T, Günther S, et al. Experimental Morogoro virus infection in its natural host, *Mastomys natalensis*. Viruses. 2021;13:851. https://doi.org/10.3390/v13050851

12. Jones ML. Longevity of captive mammals. Zool Garten N. F. Jena. 1982;52:113–28 [cited 2022 Nov 10]. http://www.rhinoresourcecenter.com/pdf_files/125/1256468598.pdf

13. Cajimat MNB, Milazzo ML, Bradley RD, Fulhorst CF. Ocozocoautla de espinosa virus and hemorrhagic fever, Mexico. Emerg Infect Dis. 2012;18:401–5. https://doi.org/10.3201/eid1803.111602

14. Radoshitzky SR, Bào Y, Buchmeier MJ, Charrel RN, Clawson AN, Clegg CS, et al. Past, present, and future of arenavirus taxonomy. Arch Virol. 2015;160:1851–74. https://doi.org/10.1007/s00705-015-2418-y

Address for correspondence: Jan Felix Drexler, Helmut-Ruska-Haus, Institute of Virology, Campus Charité Mitte, Charitéplatz 1, 10098 Berlin, Germany; email: felix.drexler@charite.de

August 2022
Zoonotic Infections

- Incidence of Nontuberculous Mycobacterial Pulmonary Infection, by Ethnic Group, Hawaii, USA, 2005–2019

- Investigation of COVID-19 Outbreak among Wildland Firefighters during Wildfire Response, Colorado, USA, 2020

- Lack of Evidence for Ribavirin Treatment of Lassa Fever in Systematic Review of Published and Unpublished Studies

- Dominant Carbapenemase-Encoding Plasmids in Clinical Enterobacterales Isolates and Hypervirulent *Klebsiella pneumoniae*, Singapore

- Increasing and More Commonly Refractory *Mycobacterium avium* Pulmonary Disease, Toronto, Ontario, Canada

- Characterization of Emerging Serotype 19A Pneumococcal Strains in Invasive Disease and Carriage, Belgium

- COVID-19 Symptoms and Deaths among Healthcare Workers, United States

- Association of Environmental Factors with Seasonal Intensity of *Erysipelothrix rhusiopathiae* Seropositivity among Arctic Caribou
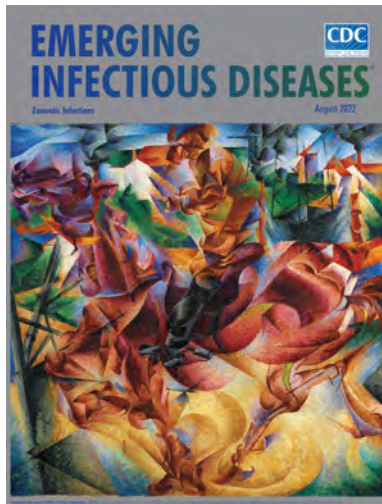
- Factors Associated with Delayed or Missed Second-Dose mRNA COVID-19 Vaccination among Persons >12 Years of Age, United States

- COVID-19 Vaccination Intent and Belief that Vaccination Will End the Pandemic

- Invasive Pneumococcal Disease and Long-Term Mortality Rates in Adults, Alberta, Canada

- Dog Ownership and Risk for Alveolar Echinococcosis, Germany

- Novel Chronic Anaplasmosis in Splenectomized Patient, Amazon Rainforest

- Transmissibility of SARS-CoV-2 B.1.1.214 and Alpha Variants during 4 COVID-19 Waves, Kyoto, Japan, January 2020–June 2021

- Culling of Urban Norway Rats and Carriage of *Bartonella* spp. Bacteria, Vancouver, British Columbia, Canada

- Zoonotic Threat of G4 Genotype Eurasian Avian-Like Swine Influenza A(H1N1) Viruses, China, 2020

- Increased Incidence of Invasive Pneumococcal Disease among Children after COVID-19 Pandemic, England

- Anthelmintic Baiting of Foxes against *Echinococcus multilocularis* in Small Public Area, Japan

- *Spiroplasma ixodetis* Infections in Immunocompetent and Immunosuppressed Patients after Tick Exposure, Sweden

- Child Melioidosis Deaths Caused by *Burkholderia pseudomallei*–Contaminated Borehole Water, Vietnam, 2019

- Association of Phylogenomic Relatedness among *Neisseria gonorrhoeae* Strains with Antimicrobial Resistance, Austria, 2016–2020

EMERGING INFECTIOUS DISEASES®

To revisit the August 2022 issue, go to:
https://wwwnc.cdc.gov/eid/articles/issue/28/8/table-of-contents

Highly Pathogenic Avian Influenza A(H5N1) Clade 2.3.4.4b Virus in Poultry, Benin, 2021

Idrissa Nonmon Sanogo, Fidelia Djegui, Yao Akpo, Corneille Gnanvi, Gabriel Dupré,
Adam Rubrum, Trushar Jeevan, Pamela McKenzie, Richard J. Webby, Mariette F. Ducatez

In August 2021, we detected highly pathogenic avian influenza A(H5N1) clade 2.3.4.4b viruses in poultry in southern Benin. The isolates were genetically similar to H5N1 viruses of clade 2.3.4.4b isolated during the same period in Africa and Europe. We also found evidence for 2 separate introductions of these viruses into Benin.

Highly pathogenic avian influenza (HPAI) viruses represent a major threat to animal and public health. HPAI A/Goose/Guangdong/1/96-lineage subtype H5N1 viruses first emerged in southern China in 1996, and their descendants have since evolved into different phylogenetic clades causing large outbreaks in poultry and wild birds worldwide (*1*). Since first being detected in Nigeria in 2006, HPAI H5N1 viruses have been responsible for numerous outbreaks in many countries in Africa, causing high mortality in domestic and wild birds over the past 15 years (*2*,*3*).

Beginning in January 2021, outbreaks caused by HPAI H5N1 clade 2.3.4.4b virus have been reported in many countries in West Africa, including Mali, Nigeria, Niger, and Senegal (*3*). Clade 2.3.4.4 H5 viruses are of particular concern because of their potential for reassortment and ability to cross the species barrier and infect new hosts, including humans, seals, and foxes (*4*,*5*). In addition, increasing infectivity of these HPAI H5 viruses in humans could accelerate their adaptation to human-to-human

transmission, which might increase the possibility for emergence of a novel influenza strain with pandemic potential (*6*). In August 2021, HPAI H5N1 viruses were detected in poultry in the southern region of Benin. In this study, we carried out genetic and antigenic analyses to investigate the origin of the virus and its relationship with viruses detected in neighboring countries.

The Study

During August–September 2021, high mortality was reported in chickens from poultry farms in Seme-Podji and Ouidah Provinces in southern Benin. Clinical signs in the affected birds included prostration, respiratory distress, severe diarrhea, depression, and lack of coordination. Based on the epidemiologic status of avian influenza in the region, which involved outbreaks in neighboring countries Nigeria and Niger, and the possibility of infected birds being moved across country borders through legal or illegal trade of poultry, HPAI was suspected.

We collected 468 samples (organ tissues and oropharyngeal swabs) from among poultry at 6 infected farms and poultry markets. We performed one-step real-time reverse transcription PCR (rRT-PCR) targeting the influenza A virus H5 and N1 genes and detected avian influenza H5N1 virus RNA in 11 samples. We isolated viruses from positive samples in embryonated eggs, then performed molecular characterization by whole-genome sequencing using an Illumina MiSeq system (https://www.illumina.com) as described elsewhere (*7*). We obtained 5 H5N1 virus isolates from which we generated full-genome sequences and designated them A/poultry/Benin/21-A-08-009-O/2021, A/poultry/Benin/21-A-09-031-O/2021, A/poultry/Benin/21-A-09-033-O/2021, A/poultry/Benin/21-A-09-034-O/2021, and A/poultry/Benin/21-A-09-035-O/2021; we deposited all sequences into GenBank (accession nos.

Author affiliations: Université de Ségou, Ségou, Mali
(I.N. Sanogo); Institut national de recherche pour l'agriculture,
l'alimentation et l'environnement, Ecole Nationale Vétérinaire
de Toulouse, Toulouse, France (I.N. Sanogo, G. Dupré,
M.F. Ducatez); Laboratoire de Diagnostic vétérinaire et de
Sérosurveillance, Parakou, Benin (F. Djegui); Direction de
l'Elevage, Cotonou, Benin (Y. Akpo, C. Gnanvi); St. Jude
Children's Research Hospital, Memphis, Tennessee, USA
(A. Rubrum, T. Jeevan, P. McKenzie, R.J. Webby)

ON870413–47). The isolates shared a high nucleotide sequence identity of 98.62%–99.91% and amino acid similarity among one another.

To determine the origin of the Benin H5N1 viruses, we performed phylogenetic analysis for all 8 genomic segments from the 5 isolates using the maximum-likelihood method and inferred phylogenetic trees using IQ-TREE version 2.1.2 software (http://www.iqtree.org) with automatic model selection and 1,000 nonparametric bootstrap replicates (8). Our analysis revealed that the Benin HPAI H5N1 viruses were closely related to H5N1 viruses isolated in Nigeria in 2021 and, to a lesser extent, to viruses detected in Lesotho in 2021 and Europe in 2020–2021, suggesting a possible transmission route from Nigeria to Benin. The topology of the hemagglutinin (HA) gene tree (Appendix Figure 1, https://wwwnc.cdc.gov/EID/article/28/12/22-1020-App1.pdf) indicated that the H5N1 viruses from Benin belonged to clade 2.3.4.4b (9). Phylogenetic trees based on the other gene segments (Appendix Figures 2–8) indicated that no reassortment event had occurred within the Benin H5N1 isolates. However, A/poultry/Benin/21-A-09-031-O/2021 did not cluster with the other HPAI H5N1 from Benin, suggesting 2 independent introductions of the virus into the country.

To estimate the time to the most recent common ancestor (tMRCA), we conducted Bayesian Markov Chain Monte Carlo sampling in BEAST version 1.10.4 (https://beast.community) (10) under the general time-reversible plus invariant sites plus Γ4 nucleotide substitution model, using an uncorrelated log-normal relaxed clock and Bayesian Skygrid coalescent prior as described elsewhere (11).

The H5N1 isolates from Benin originated from the same common ancestor as the H5N1 viruses isolated in Nigeria in 2021 (Figure 1); based on the HA maximum clade credibility tree, the average tMRCA of these viruses was estimated as February 2020 (95% highest posterior density interval December 2019–April 2020). The likelihood of 2 independent introductions of the H5N1 viruses into Benin was supported by the tMRCAs estimated for each gene segment (Appendix Table 1), the first involving A/poultry/Benin/21-A-09-031-O/2021, during March–April 2020, and the second involving the other 4 Benin isolates, during July–August 2020.

To study the antigenic profiles of the HPAI H5N1 isolated in Benin, we performed a hemagglutination inhibition (HI) assay against reference ferret postinfection serum (Appendix Table 2), as described elsewhere (12). We used HI results to build an antigenic map (Figure 2) using ACMACS software (https://acmacs-web.antigenic-cartography.org). The antigenic map revealed 2 slightly distinct antigenic profiles for Benin H5N1 viruses. A/poultry/Benin/21-A-09-031-O/2021 was antigenically similar to most of the World Health Organization candidate vaccine viruses used in the HI assay, especially to A/Sichuan/26221/2014-like (IDCDC-RG42A) and A/duck/Hyogo/1/2016 (NIID-001). In contrast, the other 4 Benin isolates that clustered together in the phylogenetic trees were 2–3 $\log_2$ away from the candidate viruses, suggesting a good but lower level of cross-reactivity. The most antigenically similar candidate virus to these 4 Benin isolates was A/Astrakhan/3212/2020-like (CBER-RG8A).
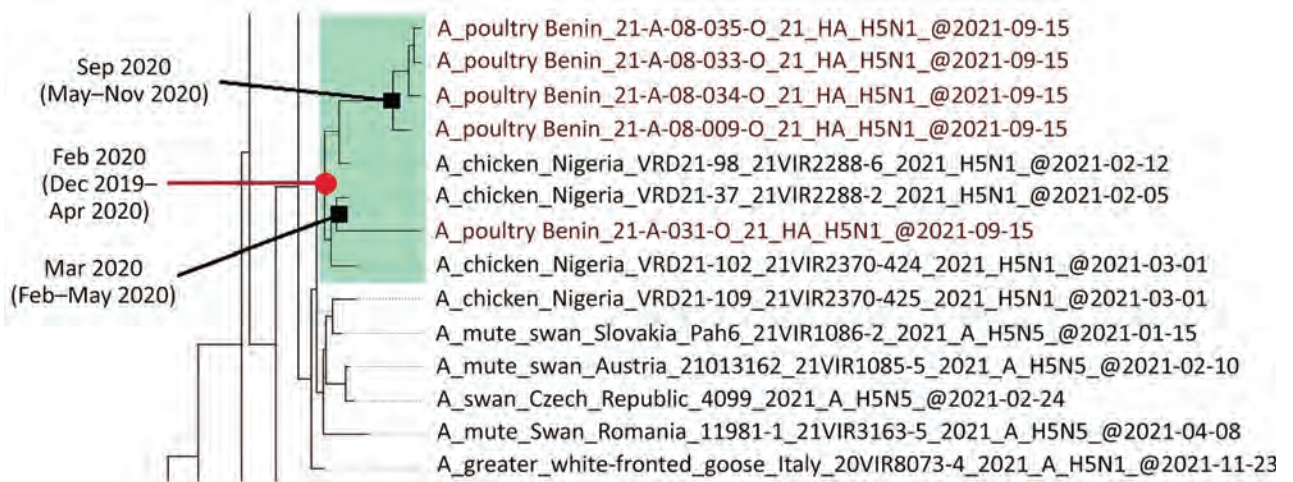

Figure 1. Maximum clade credibility tree of the hemagglutinin (HA) gene of highly pathogenic avian influenza A(H5N1) viruses from Benin (red) and reference viruses. Green box highlights viruses sharing the same common ancestor with the Benin isolates. The time to the most common ancestor and the 95% highest posterior density intervals are indicated for the relevant nodes.
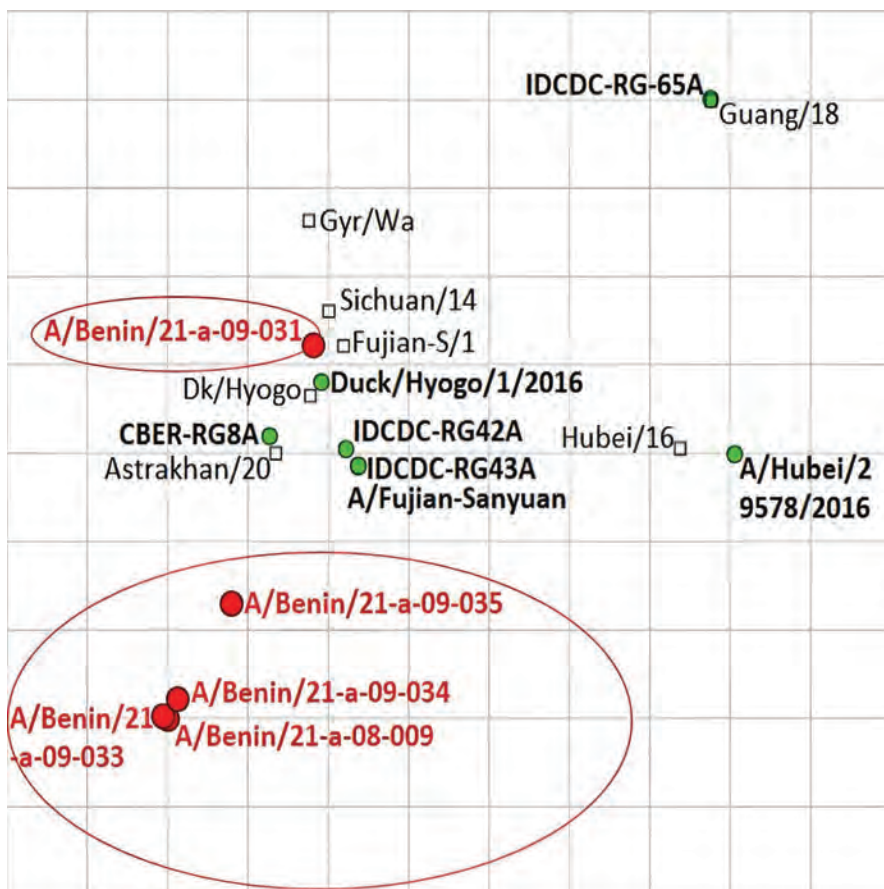
Figure 2. Antigenic map of highly pathogenic avian influenza A(H5N1) viruses from Benin based on hemagglutination inhibition data (Appendix Table, https://wwwnc.cdc.gov/EID/28/12/22-1020-App1.pdf). Circles indicate viruses and squares antiserum; red indicates viruses characterized in this study, and green dots indicate reference viruses. The spacing between grid lines is 1 unit of antigenic distance, corresponding to a 2-fold dilution of antiserum in the hemagglutination inhibition assay.

Amino acid sequence analysis showed that the H5N1 viruses from Benin had multiple basic amino acids motif (PLREKRRKR/GLF) at the HA cleavage site, characteristic of HPAI viruses. In addition, we detected a mammalian adaptation mutation in the polymerase basic 1 segment (113V) of the 5 Benin isolates, suggesting potential for these viruses to replicate more efficiently in mammalian cells (*13*).

Conclusions

Although several outbreaks occurred in the region, relatively little information was available on the genetic and antigenic diversity of HPAI H5N1 clade 2.3.4.4b viruses in poultry in West Africa. We characterized 5 HPAI H5N1 clade 2.3.4.4b viruses from Benin highly similar to viruses detected earlier in neighboring Nigeria. It is therefore likely that the Benin H5N1 viruses originated from the region because of the movement of infected poultry and poultry products across neighboring countries (*14*). The initial introduction of H5N1 viruses into the wider region might be related to the arrival of migratory birds. In fact, the tMRCA of Benin H5N1 viruses in 2021 corresponded to the period (January–March) when Eur-asian migratory birds are present in West Africa (*15*). Furthermore, the relationship between Benin H5N1 isolates and viruses detected earlier in Europe corroborates this hypothesis.

HPAI H5N1 clade 2.3.4.4b viruses represent a major concern for West Africa and have demonstrated the potential for spreading more widely in the region. Therefore, to monitor virus evolution and promptly identify viruses with increased zoonotic potential, the countries of West Africa require regional collaboration for long-term surveillance and whole-genome sequencing of HPAI viruses in both humans and animals.

About the author

Mr. Sanogo is an assistant lecturer at the University of Segou and a PhD student at the UMR Interactions Hôtes Agents pathogènes in Toulouse. His primary research interests include epidemiology and surveillance of animal influenza viruses.

References

1. Food and Agriculture Organization of the United Nations. Global AIV with zoonotic potential situation update: 2021 Oct 27 [cited 2022 Mar 15]. https://www.fao.org/animal-health/situation-updates/global-aiv-with-zoonotic-potential
2. Ducatez MF, Olinger CM, Owoade AA, Tarnagda Z, Tahita MC, Sow A, et al. Molecular and antigenic evolution and geographical spread of H5N1 highly pathogenic avian influenza viruses in western Africa. J Gen Virol. 2007;88:2297–306. https://doi.org/10.1099/vir.0.82939-0
3. Food and Agricultural Organization of the United Nations. Sub-Saharan Africa HPAI situation update: 2021 Oct 13 [cited 2022 Mar 15]. https://www.fao.org/animal-health/situation-updates/sub-saharan-africa-hpai
4. Nuñez IA, Ross TM. A review of H5Nx avian influenza viruses. Ther Adv Vaccines Immunother. 2019;7:2515135518821625. https://doi.org/10.1177/2515135518821625
5. Floyd T, Banyard AC, Lean FZX, Byrne AMP, Fullick E, Whittard E, et al. Encephalitis and death in wild mammals at a rehabilitation center after infection with highly pathogenic avian influenza A(H5N8) virus, United Kingdom. Emerg Infect Dis. 2021;27:2856–63. https://doi.org/10.3201/eid2711.211225
6. Oliver I, Roberts J, Brown CS, Byrne AMP, Mellon D, Hansen R, et al. A case of avian influenza A(H5N1) in England, January 2022. Euro Surveill. 2022;27. https://doi.org/10.2807/1560-7917.ES.2022.27.5.2200061
7. Barman S, Turner JCM, Hasan MK, Akhtar S, El-Shesheny R, Franks J, et al. Continuing evolution of highly pathogenic H5N1 viruses in Bangladeshi live poultry markets. Emerg Microbes Infect. 2019;8:650–61. https://doi.org/10.1080/22221751.2019.1605845
8. Minh BQ, Schmidt HA, Chernomor O, Schrempf D, Woodhams MD, von Haeseler A, et al. IQ-TREE 2: new models and efficient methods for phylogenetic inference in the genomic era. Mol Biol Evol. 2020;37:1530–4. https://doi.org/10.1093/molbev/msaa015
9. Smith GJD, Donis RO; World Health Organization/World Organisation for Animal Health/Food and Agriculture Organization (WHO/OIE/FAO) H5 Evolution Working Group. Nomenclature updates resulting from the evolution of avian influenza A(H5) virus clades 2.1.3.2a, 2.2.1, and 2.3.4 during 2013–2014. Influenza Other Respir Viruses. 2015;9:271–6. https://doi.org/10.1111/irv.12324
10. Suchard MA, Lemey P, Baele G, Ayres DL, Drummond AJ, Rambaut A. Bayesian phylogenetic and phylodynamic data integration using BEAST 1.10. Virus Evol. 2018;4:vey016. https://doi.org/10.1093/ve/vey016
11. Hill V, Baele G. Bayesian estimation of past population dynamics in BEAST 1.10 using the Skygrid coalescent model. Mol Biol Evol. 2019;36:2620–8. https://doi.org/10.1093/molbev/msz172
12. Kandeil A, Moatasim Y, El Taweel A, El Sayes M, Rubrum A, Jeevan T, et al. Genetic and antigenic characteristics of highly pathogenic avian influenza A(H5N8) viruses circulating in domestic poultry in Egypt, 2017–2021. Microorganisms. 2022;10:595. https://doi.org/10.3390/microorganisms10030595
13. Fusade-Boyer M. Circulation of avian influenza viruses in sub-Saharan Africa and crossing the species barrier [thesis; in French]. Toulouse, France: Université Fédérale Toulouse Midi-Pyrénées; 2021.
14. Monne I, Joannis TM, Fusaro A, De Benedictis P, Lombin LH, Ularamu H, et al. Reassortant avian influenza virus (H5N1) in poultry, Nigeria, 2007. Emerg Infect Dis. 2008;14:637–40. https://doi.org/10.3201/eid1404.071178
15. Cappelle J, Servan de Almeida R, Fofana B, Dakouo M, Balança G, Gil P, et al. Circulation of avian influenza viruses in wild birds in inner Niger delta, Mali. Influenza Other Respir Viruses. 2012;6:240–4. https://doi.org/10.1111/j.1750-2659.2011.00314.x

Address for correspondence: Mariette F. Ducatez, Interactions Hôtes-Agents Pathogènes (IHAP), UMR 1225, ENVT, INRAE, Université de Toulouse, 23 Chemin des Capelles, 31076, Toulouse, France; email: mariette.ducatez@envt.fr

Mass Mortality Caused by Highly Pathogenic Influenza A(H5N1) Virus in Sandwich Terns, the Netherlands, 2022

Jolianne M. Rijks,[1] Mardik F. Leopold,[1] Susanne Kühn, Ronald in 't Veld, Fred Schenk,
Allix Brenninkmeijer, Sander J. Lilipaly, Mónika Z. Ballmann, Leon Kelder, Job W. de Jong,
Wouter Courtens, Roy Slaterus, Erik Kleyheeg, Sandra Vreman, Marja J.L. Kik, Andrea Gröne,
Ron A.M. Fouchier, Marc Engelsma, Mart C.M. de Jong, Thijs Kuiken, Nancy Beerens

We collected data on mass mortality in Sandwich terns (*Thalasseus sandvicensis*) during the 2022 breeding season in the Netherlands. Mortality was associated with at least 2 variants of highly pathogenic avian influenza A(H5N1) virus clade 2.3.4.4b. We report on carcass removal efforts relative to survival in colonies. Mitigation strategies urgently require structured research.

The 2021–2022 epidemic of highly pathogenic avian influenza (HPAI) A(H5N1) virus clade 2.3.4.4b has been unprecedented in terms of numbers of dead wild birds, species affected, spatial extent, and incidence in spring 2022 (*1*). Across Europe, multiple colony-breeding seabirds experienced HPAI H5N1–associated mass mortalities during the breeding period, including the Sandwich tern (*Thalasseus sandvicensis*) (*1*,*2*). The Netherlands constitutes a major though vulnerable stronghold of the Sandwich tern in Europe; 15,000–20,000 breeding pairs have been documented across ≈10 colonies (https://stats.sovon.nl/stats/soort/6110). We sought to establish the scale of mortality occurring in Sandwich terns breeding in the Netherlands in 2022, characterize the associated HPAI H5N1 viruses and pathology, report on the carcass removal effort relative to survival, and investigate intracolony transmission dynamics.

The Study

We determined breeding colony locations and initial sizes in May 2022 through drone or ground counts (*3*). To establish breeding success and minimum estimates of mortality, we compiled data from late May through early July 2022 on numbers of live adults, chicks, fledglings, and late clutches in colonies, as well as on numbers of carcasses found in and around colonies, carcasses removed for destruction, and abandoned nests (Appendix 1 Table 1, https://wwwnc.cdc.gov/EID/article/28/12/22-1292-App1.xlsx). Sandwich terns lay 1–2 eggs and incubate for 21–29 days. Chicks fledge 25–30 days after hatching; annual fledging success is ≈0.5 per breeding pair (*4*–*6*). We used wild bird mortality databases to establish minimum estimates of adult mortality outside the colonies. Finally, we used data from the migration tracking website Trektellen (https://www.trektellen.nl) to compare the hourly averages of Sandwich tern passing rates at coastal observation points per week in 2022 to 2016–2021.

Author affiliations: Dutch Wildlife Health Centre, Utrecht University, Utrecht, the Netherlands (J.M. Rijks, M.J.L. Kik, A. Gröne); Wageningen Marine Research, Den Helder, the Netherlands (M.F. Leopold, S. Kühn); Staatsbosbeheer Zuid-Hollandse Delta, Numansdorp, the Netherlands (R. in 't Veld); Stichting Het Zeeuwse Landschap, Wilhelminadorp, the Netherlands (F. Schenk); Province of Groningen, Groningen, the Netherlands (A. Brenninkmeijer); Deltamilieu Projecten, Vlissingen, the Netherlands (S.J. Lilipaly, M.Z. Ballmann); Staatsbosbeheer Beheereenheid de Kop, Schoorl, the Netherlands (L. Kelder); Bureau Waardenburg, Culemborg, the Netherlands (J.W. de Jong); Research Institute for Nature and Forest, Brussels, Belgium (W. Courtens); Sovon Dutch Centre for Field Ornithology, Nijmegen, the Netherlands (E. Kleyheeg, R. Slaterus); Wageningen Bioveterinary Research, Lelystad, the Netherlands (S. Vreman, M. Engelsma,, N. Beerens); Department of Viroscience, Erasmus MC, Rotterdam, the Netherlands (R.A.M. Fouchier, T. Kuiken); Wageningen University and Research, Quantitative Veterinary Epidemiology group, Wageningen, the Netherlands (M.C.M. de Jong)

[1]These authors contributed equally to this article.

We observed clinical signs and tested 44 carcasses for avian influenza virus by using a quantitative PCR to detect the influenza A virus matrix gene; we then followed up with subtype-specific PCRs on cloacal and tracheal swab specimens (*7*). We performed necropsy with histopathology and immunohistochemistry on 6 of the carcasses to establish cause of death. To study the relationship between viruses detected in Sandwich terns and other bird species, we determined full-genome sequences directly on swab RNA from 20 birds and submitted them to the GISAID database (https://www.gisaid.org), then compared them to a sample of 57 other birds (Appendix 1 Table 2). We aligned sequences by using MAFFT version 7.475 (*8*), reconstructed phylogeny by using maximum-likelihood analysis with IQ-TREE software version 2.0.3 (*9*), and visualized the maximum-likelihood tree by using the R package ggtree (*10*).

To investigate HPAI H5N1 transmission dynamics within a breeding colony, we developed a susceptible-infectious-recovered model that included infection-fatality rate (IFR) and examined outcome as a function of IFR. IFR is the probability that a bird dies after infection, although in this study IFR also

Table. Mortality, fledgling success, carcass removal, and estimated fraction of Sandwich tern breeding population that died or disappeared in 10 breeding colonies, the Netherlands, 2022

Breeding colony no.	Date mortality first observed	Fledgling success (no. fledglings produced/no. initial breeding pairs)	Dead adults found	Dead chicks found	Abandoned eggs	Carcass removal	Estimated percentage of breeding population that died or disappeared from colony*
Colony 1	2022 May 30	1% (20/2,100)	342	425	Yes, all 700 late nests	Yes, with a 12-d delay, on 10 of next 18 d, adults and chicks	99%
Colony 2	2022 Jun 21	0% (0/150)	107	0	Yes, all 150 late nests	Once, with a 3-d delay, adults only	100%
Colony 3†	2022 Jun 4	0% (0/1,176)	170	Hundreds	Yes, many	Yes, with a 6-d delay, on 6 of next 18 d, adults only	100%
Colony 4†	2022 May 26	0.1% (5/3,374)	3,316	Thousands	Unknown	Twice, once 19 d after start, then 16 d later, adults only	99.8%
Colony 5	2022 May 29	0% (0/220)	400	0	Unknown	Once, 17 d after deaths started, adults only	100%
Colony 6	2022 May 31	Low (Few/3,016)‡	941	Thousands	Yes, all 245 late nests	Yes, without delay, on 15 of next 36 d, adults only	>92%
Colony 7	2022 May 31	11.1% (45/404)	115	Unknown	Yes, many of 40 late nests	Yes, without delay, on 14 of next 36 d, adults only	78%
Colony 8	2022 Jun 14	47.4% (65/137)	2	0	No (also no late nests)	No	5% or not applicable§
Colony 9	2022 Jun 6	9.5% (665/6,974)	2,368	3,122	No, there is activity above 400 late nests	Yes, with an 8-d delay, on 14 of next 27 d, adults and chicks	81%
Colony 10¶	2022 Jun 14	0% (0/600)	240	12	Unknown, 150 + 450 late nests	Yes, with a 7-d delay, on 3 of next 15 d, adults and chicks	100%
Overall		Low (Few/18,151 pairs)	8,001 (22% of breeding birds)	Thousands			

*Calculated by subtracting the ratio of fledgling success in 2022 over average fledgling success in previous years (0.5 fledgling per pair) from 100%.
†After colony 3 and colony 4 were decimated, a very late colony of 600 breeding pairs was established in July on Texel midway between these 2 colonies (53.022°N, 4.819°E), and this very late colony yielded 300 fledglings in September 2022.
‡Exact number not recorded.
§Because no carcass was examined, it is unclear if the 2 dead birds observed in this colony died from other causes or the cause of death was HPAI H5N1 but further infections in the colony were aborted.
¶In this colony, some very late birds did end up producing some fledglings (around 155) in August (Appendix 1 Table 1, https://wwwnc.cdc.gov/EID/article/28/12/22-1292-App1.xlsx).

includes birds leaving the colony. The model assumed a naive starting population, an infectious period of 5 days, and frequency-dependent transmission and considered only survivors of infection as recovered and total population size as not constant (Appendix 2, https://wwwnc.cdc.gov/EID/article/28/12/22-1292-App2.pdf).

Mass mortality was seen in 9 of the 10 Sandwich tern breeding colonies in 2022. In those colonies, out of a total of 18,151 breeding pairs, 8,001 adult Sandwich terns were found dead, and only a few chicks fledged (Video 1, https://wwwnc.cdc.gov/EID/article/28/12/22-1292-V1.htm; Video 2, https://wwwnc.cdc.gov/EID/article/28/12/22-1292-V2.htm). Only 1 small inland colony of 137 breeding pairs experienced no mass mortality and had a fledgling success rate (0.47 young/pair) consistent with previous years (0.50 young/pair) (Table; Figure 1, panel A). Outside of colonies, another 1,600 adult Sandwich

terns were reported dead between late May and end of June. The scale of mortality is reflected in the passage rate of Sandwich terns along the coast in May–June 2022 (Appendix 2 Figure 4).

Diseased birds were debilitated, unable to fly, and mostly lethargic, sometimes with wings spread out. At later stages, some displayed opisthotonos and occasionally flipped over backwards (Video 1, Video 3, https://wwwnc.cdc.gov/EID/article/28/12/22-1292-V3.htm; Appendix 2 Figures 5–10). We confirmed HPAI H5N1 virus infection in 23 of 24 dead Sandwich terns from colonies (the exception was a chick); infection was also confirmed in 20 of 20 birds outside of colonies (Appendix 2 Table 1). In the 4 necropsied PCR-confirmed adult birds, viral antigen expression was detected by immunohistochemistry in the pancreas (n = 3), duodenum (n = 4), or lung and nasal tissue (n = 1), colocalized with necrosis and inflammation (Appendix 2 Figure 18). Necropsy
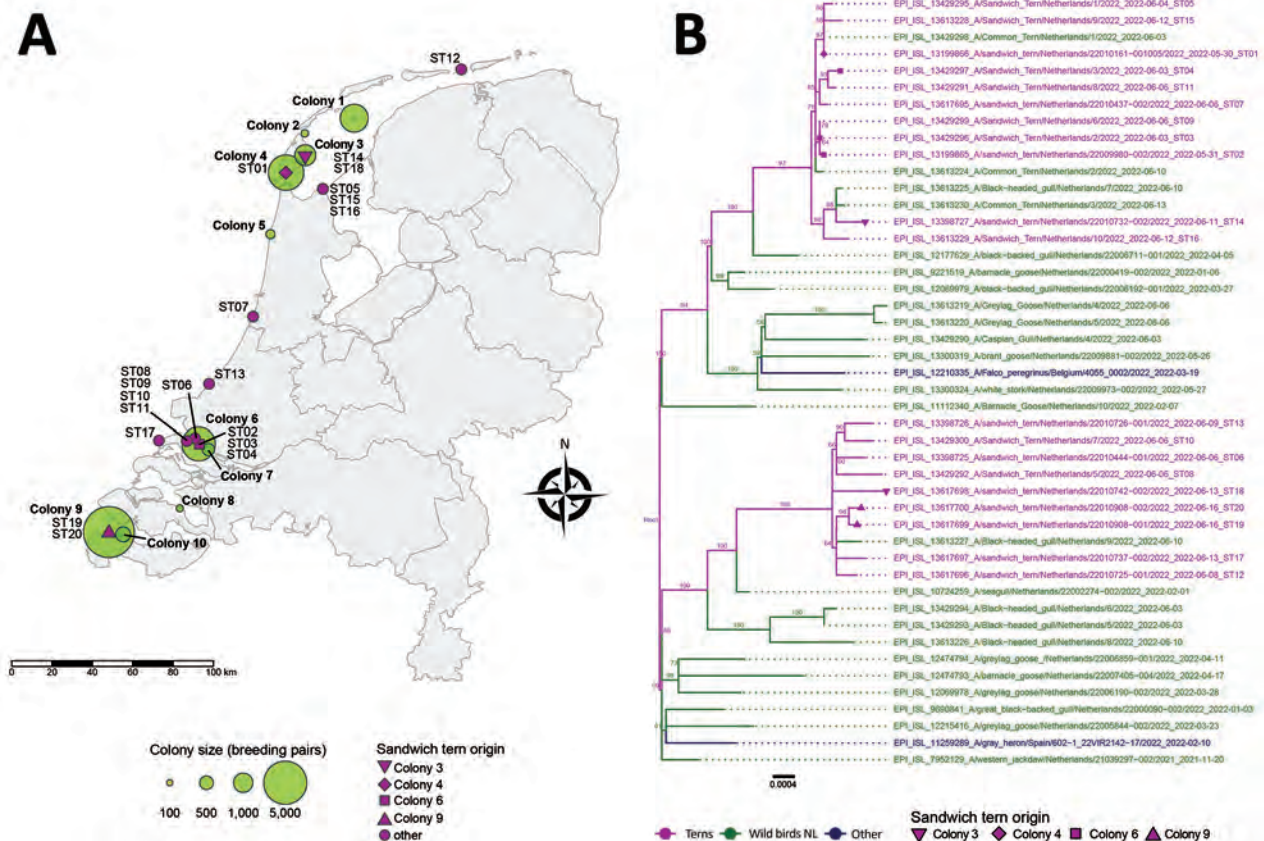

Figure 1. Location of Sandwich terns affected by locally acquired highly pathogenic avian influenza A(H5N1) clade 2.3.4.4b viruses and phylogeny of viral segments, the Netherlands. A) Location and size (number of breeding pairs) of the Sandwich tern breeding colonies and the origin (finding location) of the Sandwich terns from which virus sequences ST01–ST20 shown in the phylogenetic tree in panel B were obtained. B) Maximum-likelihood tree (1,000 bootstraps) of the concatenated viral segments showing the H5N1 viruses detected in Sandwich terns together with viruses from other wild birds. Bootstrap values >50 are indicated at the branches. Identification numbers and symbols of the Sandwich terns correspond to those in the map, and the date that the bird was found dead is indicated. The GISAID sequences used in the phylogenetic analysis are listed in Appendix 1 Table 2 (https://wwwnc.cdc.gov/EID/article/28/12/22-1292-App1xlsx).

findings and negative immunohistochemistry results in the 2 chicks we examined demonstrated that chick mortality was at least partly caused by starvation, likely after feeding was interrupted because of adult mortality (Appendix 2). This explanation was supported by field observations (Appendix 2 Figure 19).

Phylogenetic analysis demonstrated that the 20 fully sequenced viruses belonged to H5 clade 2.3.4.4b, and clustered with viruses detected in other wild bird species in the Netherlands, including in geese and gulls collected during January–April 2022 (Figure 1, panel B; Appendix 2). The Sandwich tern viruses clustered in 2 groups. Both variants were found in the northern and southern parts of the Netherlands and were even found within a single colony. These results suggest that at least 2 independent virus introductions into Sandwich terns occurred in the Netherlands, followed by transmission of both virus variants within and between breeding colonies.

Carcass removal effort was diverse (Table; Appendix 1, Table 1). In colonies with some survival, effort was overall more regular, frequent, and immediate or included chicks also, although survival might also have been affected by other undetermined factors.

In most colonies, a high proportion of the birds died or left (Table), indicating high IFR. The model shows that, even with a relatively low value of R_0 (R_0 = 2), at the higher end of the IFR range evidenced here, few of the birds remaining in the colony will have escaped infection at the end of the outbreak. Birds in the colony will have died or recovered and acquired immunity (Figure 2).

Conclusions

Our results substantiate that after Sandwich terns arrived in the Netherlands for breeding, HPAI H5N1 virus was introduced into their population at least twice. The virus then spread widely within and between breeding colonies, causing outbreaks that resulted in high adult and chick mortality in nearly all colonies. Infected birds probably died of systemic HPAI-associated disease, including acute pancreatic necrosis and duodenitis (11,12). Like other seabirds, Sandwich terns have low annual reproductive output but relatively long life-expectancy (2,4,6,13); therefore the effect of high adult mortality on population size could be seen for a long time. The Sandwich tern exemplifies how severely the continued circulation of HPAI H5N1 viruses in spring 2022 affected populations of colony-breeding birds without flock immunity in Europe (1).

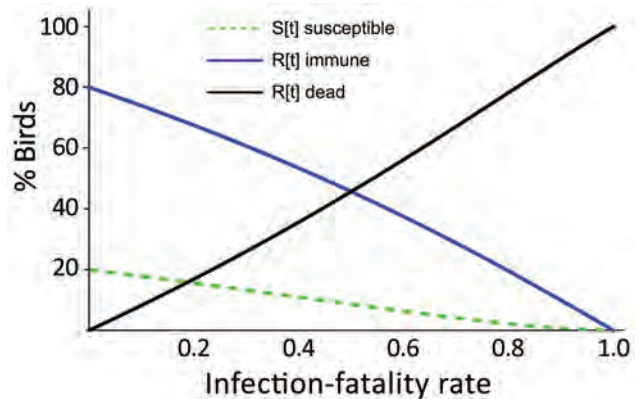Our study also demonstrates how outbreaks in breeding birds boosted virus propagation into the

Figure 2. Model result for the introduction of highly pathogenic avian influenza (HPAI) A(H5N1) clade 2.3.4.4b viruses into a local Sandwich tern breeding colony population, the Netherlands. Graph demonstrates the distribution at the end of the local HPAI H5N1 outbreak, for dead (or departed) birds, escaping susceptible birds, and immune birds as a function of the infection-fatality rate (IFR), for a Sandwich tern population that was naive for HPAI H5N1 at the start of the local outbreak, for R_0 = 2. The model output indicates that the fraction of birds infected with HPAI H5N1, and hence also the fraction that dies, will increase with infection-fatality rate and that at a rate above 90%, virtually no more susceptible birds remain, only immune or dead (or departed) birds.

summer of 2022. The future involvement of Sandwich terns in HPAI endemicity can be evaluated once future population size and flock immunity have been analyzed from count data and serosurveillance. On the basis of our model, colony survivors would be mostly immune to HPAI.

Confirming HPAI as a major mortality factor in breeding colonies of Sandwich terns and other seabird species (2,14,15) underlines the paradigm shift to HPAI as a mortality factor of concern to wild species, in addition to poultry and humans. It stresses the importance of close international cooperation and data exchange to better understand and mitigate the global effect of HPAI on nature. More structured research on appropriate strategies to reduce massive propagation is urgently required. Carcass removal takes away a source of infection but might simultaneously enhance spread of infection and thus requires controlled study.

About the Author

Dr. Rijks is a postdoctoral researcher at the Dutch Wildlife Health Centre in Utrecht, the Netherlands. Her primary research interests are wildlife diseases and epidemiology. Dr. Leopold is a senior seabird ecologist at Wageningen Marine Research. He has studied Sandwich terns on Texel since 2012.

References

1. European Food Safety Authority, European Centre for Disease Prevention and Control, European Reference Laboratory for Avian Influenza, Adlhoch C, Fusaro A, Gonzales JL, Kuiken T, Marangon S, Niqueux É, Staubach C, Terregino C, Aznar I, Muñoz Guajardo I and Baldinelli F. Scientific report: Avian influenza overview March–June 2022. EFSA J. 2022;20:e07415. https://doi.org/10.2903/j.efsa.2022.7415
2. Camphuysen CJ, Gear SC, Furness RW. Avian influenza leads to mass mortality of adult Great Skuas in Foula in summer 2022. Scottish Birds. 2022;4:312–23.
3. Vergeer JW, van Dijk AJ, Boele A, van Bruggen J, Hustings F. Sovon breeding bird research manual: breeding bird monitoring project and colony birds [in Dutch]. 2016 [cited 2022 Jul 19]. https://stats.sovon.nl/static/publicaties/Handleiding_Broedvogels_2016.pdf
4. Brenninkmeijer A, Stienen EWM. Ecological profile of the Sandwich tern (*Sterna sandvicensis*) [in Dutch]. Arnhem: DLO-Instituut voor Bos- en Natuuronderzoek; 1992.
5. Koffijberg K, de Boer P, Geelhoed SCV, Nienhuis J, Schekkerman H, Oosterbeek K, Postma J. Breeding success of coastal breeding birds in the Wadden Sea in 2019. WOt-technical report 209. Wageningen: Wettelijke Onderzoekstaken Natuur & Milieu; 2021. https://doi.org/10.18174/553633
6. Schekkerman H, Arts F, Buijs R-J, Courtens W, van Daele T, Fijn R, van Kleunen A, van der Jeugd H, Roodbergen M, Stienen E, de Vries L, Ens BJ. Population analysis of five coastal breeding bird in the SW Netherlands [in Dutch]. Nijmegen: Sovon Vogelonderzoek Nederland; 2021.
7. Beerens N, Heutink R, Bergervoet SA, Harders F, Bossers A, Koch G. Multiple reassorted viruses as cause of highly pathogenic avian influenza A(H5N8) virus epidemic, the Netherlands, Nijmegen. 2016. Emerg Infect Dis. 2017;23:1974–81. https://doi.org/10.3201/eid2312.171062
8. Katoh K, Standley DM. MAFFT multiple sequence alignment software version 7: improvements in performance and usability. Mol Biol Evol. 2013;30:772–80. https://doi.org/10.1093/molbev/mst010
9. Nguyen LT, Schmidt HA, von Haeseler A, Minh BQ. IQ-TREE: a fast and effective stochastic algorithm for estimating maximum-likelihood phylogenies. Mol Biol Evol. 2015;32:268–74. https://doi.org/10.1093/molbev/msu300
10. Yu G, Smith DK, Zhu H, Guan Y, Tsan-Yuk Lam T. ggtree: an r package for visualization and annotation of phylogenetic trees with their covariates and other associated data. Methods Ecol Evol. 2017;8:28–36 https://doi.org/10.1111/2041-210X.12628
11. Lean FZX, Vitores AG, Reid SM, Banyard AC, Brown IH, Núñez A, et al. Gross pathology of high pathogenicity avian influenza virus H5N1 2021–2022 epizootic in naturally infected birds in the United Kingdom. One Health. 2022;14:100392. https://doi.org/10.1016/j.onehlt.2022.100392
12. Garg PK, Singh VP. Organ failure due to systemic injury in acute pancreatitis. Gastroenterology. 2019;156:2008–23. https://doi.org/10.1053/j.gastro.2018.12.041
13. Hamer KC, Schreiber E, Burger J. Breeding biology, life histories, and life history-environment interactions in seabirds. In: Schreiber E, Burger J, editors. Biology of marine birds. London/New York: CRC Press; 2001. p. 217–262.
14. Banyard AC, Lean FZX, Robinson C, Howie F, Tyler G, Nisbet C, et al. Detection of highly pathogenic avian influenza virus H5N1 clade 2.3.4.4b in great skuas: a species of conservation concern in Great Britain. Viruses. 2022;14:212. 10.3390/v14020212 https://doi.org/10.3390/v14020212
15. Loeb J. Scottish seabirds hit by avian influenza. Vet Rec. 2022;190:488. 10.1002/vetr.1915 https://doi.org/10.1002/vetr.1915

Address for correspondence: Jolianne M. Rijks, Dutch Wildlife Health Centre, Utrecht University, Yalelaan 1, 3584CL, Utrecht, the Netherlands; email: j.m.rijks@uu.nl

Hepatitis E Virus Infections in Free-Ranging and Captive Cetaceans, Spain, 2011–2022

Javier Caballero-Gómez, Antonio Rivero-Juarez, Adrián Beato-Benítez,
Carolina Fernández-Maldonado, Mariano Domingo, Daniel García-Párraga,
Antonio Fernández, Eva Sierra, Rainer G. Ulrich, Eva Martínez-Nevado,
Cecilia Sierra-Arqueros, Rocío Canales-Merino, Antonio Rivero, Ignacio García-Bocanegra

Epidemiologic surveillance of hepatitis E virus in over 300 free-ranging and captive cetaceans in waters off Spain revealed extensive exposure to this pathogen. We suggest the persistent and widespread presence of hepatitis E in the marine environment off the coast of Spain may be driven by terrestrial sources of contamination.

Paslahepevirus balayani (previously known as hepatitis E virus [HEV]; family *Hepeviridae*) is the leading cause of acute viral hepatitis in humans (*1,2*). Although 8 different genotypes of HEV have been identified, HEV-3 is the genotype with the broadest geographic distribution, including Europe, where the number of hepatitis E cases has sharply increased in the past decade (*3*). The main reservoirs of this genotype are suids, but a wide range of other land mammals has been shown to be susceptible to this emerging genotype (*2*). Although echinoderms and several bivalve shellfish species from coastal waters have tested positive for HEV, the susceptibility of other marine animals, such as cetaceans, to HEV has been unknown, as has their possible role in the epidemiology of this family of viruses (*4*). We conducted a large-scale study to determine the seroprevalence and prevalence of HEV in cetacean populations, both free-ranging and captive, in Spain, and to assess the dynamics of seropositivity in marine animals sampled longitudinally during the study period.

The Study

We collected blood and liver samples from 304 cetaceans belonging to 13 different species in Spain during 2011–2022 (Table 1; Figure 1). We based our study on 240 free-ranging animals found stranded on the Atlantic and Mediterranean coasts of Spain and 64 cetaceans kept in captivity at 6 aquatic parks (deemed A–F) in Spain. We performed longitudinal surveillance on 30 of the 64 animals kept in aquatic parks during the study period.

We assessed the presence of HEV antibodies in serum or plasma using a commercial multispecies ELISA (MP Biomedicals, https://www.mpbio.com) and, whenever possible, further investigated seropositivity by Western blot analysis (Appendix, https://wwwnc.cdc.gov/EID/article/28/12/22-1188-App1.pdf). We determined the presence of HEV RNA by using 2 broad-spectrum reverse transcription PCR (RT-PCR) assays in parallel (Appendix) (*5,6*). We analyzed

Table 1. Distribution of hepatitis E virus seroprevalence in free-ranging and captive cetacean populations in Spain and results of bivariate analysis*

Variable	Categories	Free-ranging No. positive/no. analyzed (% positive)†	p value	Captive No. positive/no. analyzed (% positive)†	p value
Species‡	Atlantic spotted dolphin (*Stenella frontalis*)	1/1 (100.0)	0.191	NA	0.323
	Beluga (*Delphinapterus leucas*)	NA		0/2 (0.0)	
	Bottlenose dolphin (*Tursiops truncatus*)	0/2 (0.0)		21/55 (38.2)	
	Common dolphin (*Delphinus delphis*)	1/2 (50.0)		NA	
	Cuvier's beaked whale (*Ziphius cavirostris*)	1/1 (100.0)		NA	
	Killer whale (*Orcinus orca*)	NA		4/7 (57.1)	
	Risso's dolphin (*Grampus griseus*)	3/8 (37.5)		NA	
	Southern long-finned pilot whale (*Globicephala melas*)	0/1 (0.0)		NA	
	Striped dolphin (*Stenella coeruleoalba*)	38/57 (66.7)		NA	
Age§	Adult	33/45 (73.3)	0.006	20/47 (42.6)	0.406
	Young	11/27 (40.7)		4/12 (33.3)	
Sex	F	25/39 (64.1)	0.373	12/33 (36.4)	0.485
	M	19/33 (57.6)		12/30 (40.0)	

*Analyses by pearson's χ^2 or Fisher exact test. NA, not applicable.
†Animals with missing information excluded.
‡Samples from harbor porpoises (*Phocoena phocoena*), fin whales (*Balaenoptera physalus*), minke whales (*Balaenoptera acutorostrata*). and humpback whales (*Megaptera novaeangliae*) were also included in the study but were only tested by PCR.
§Age was classified using the mean reproductive age of each species.

associations between the presence of HEV antibodies and explanatory variables using Pearson χ^2 test or Fisher exact test and further included variables with p<0.05 in the bivariate analysis (except habitat status) in a generalized estimating equation model.

We identified 69 (50.7%, 95% CI 42.3%–59.1%) of 136 cetaceans as harboring anti-HEV antibodies (Table 1; Figures 1, 2; Appendix Table 1). We confirmed antibodies against HEV-3 in 5 of the 7 ELISA-positive animals analyzed by Western blot analysis: a free-ranging striped dolphin, a free-ranging Cuvier's beaked whale, a free-ranging Risso's dolphin, and 2 captive bottlenose dolphins. We found none (0.0%; 95% CI 0.0%–1.2%) of the 302 animals analyzed to be positive for HEV RNA (Figure 2).

We noted seroprevalence to be significantly higher in free-ranging animals (44/72; 61.1%; 95% CI 49.9%–72.4%) than in those kept in captivity (25/64; 39.1%; 95% CI 27.1%–51.0%) (relative risk = 2.5, 95% CI 1.2%–4.9%; p = 0.008). We found seropositivity in adult free-ranging cetaceans (33/45; 73.3%) to be

significantly higher than that in young animals (11/27; 40.7%; odds ratio 4.0, 95% CI 1.4–11.0; p = 0.006).

Our testing revealed seropositive animals in 5 of the 6 aquatic facilities sampled; within-zoo seroprevalence ranged from 27.8% in aquatic park D to 55.6% in aquatic park E (Table 2; Figure 2). Of the 30 longitudinally sampled animals, 21 remained seronegative, and 6 animals showed seropositivity at all samplings during the study period (Appendix Table 2). Two bottlenose dolphins seroconverted, 1 in 2013 and another in 2017. Seroreversions were detected in 2 animals (1 a dolphin that had shown seroconversion); 1 incident occurred 1 year after the first positive sampling, the other 5 years.

Conclusions

Our survey reveals high exposure to HEV in free-ranging and captive populations of cetaceans in Spain. The detection of HEV antibodies in Atlantic spotted, common, Risso's, and striped dolphins, as well as in Cuvier's beaked and killer whales, demonstrates
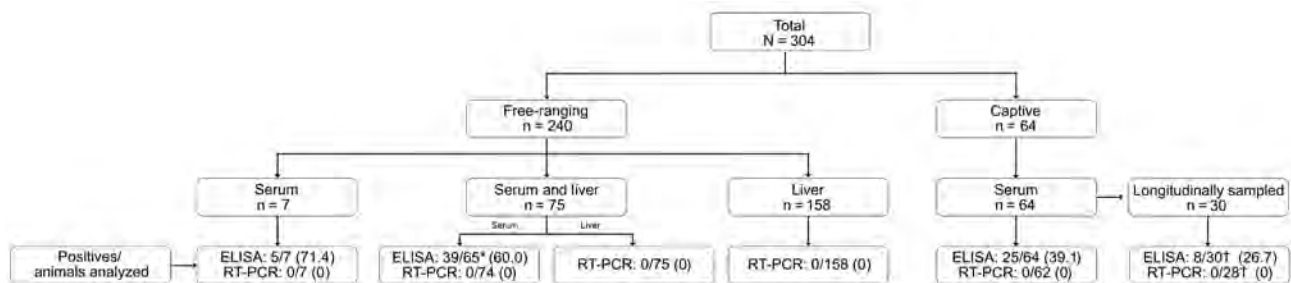
Figure 1. Flowchart of a survey of hepatitis E virus in 304 cetaceans belonging to 13 species in Spain during 2011–2022. Description of the study population, number of cetaceans, type of samples analyzed by ELISA and RT-PCR, and results obtained in each assay. *Ten of 75 serum samples were discarded for serologic analysis due to hemolysis. †Taking into account that 2–5 samples were collected per animal in longitudinally surveyed animals, 97 were analyzed by ELISA and 78 by RT-PCR. RT-PCR, reverse transcription PCR.

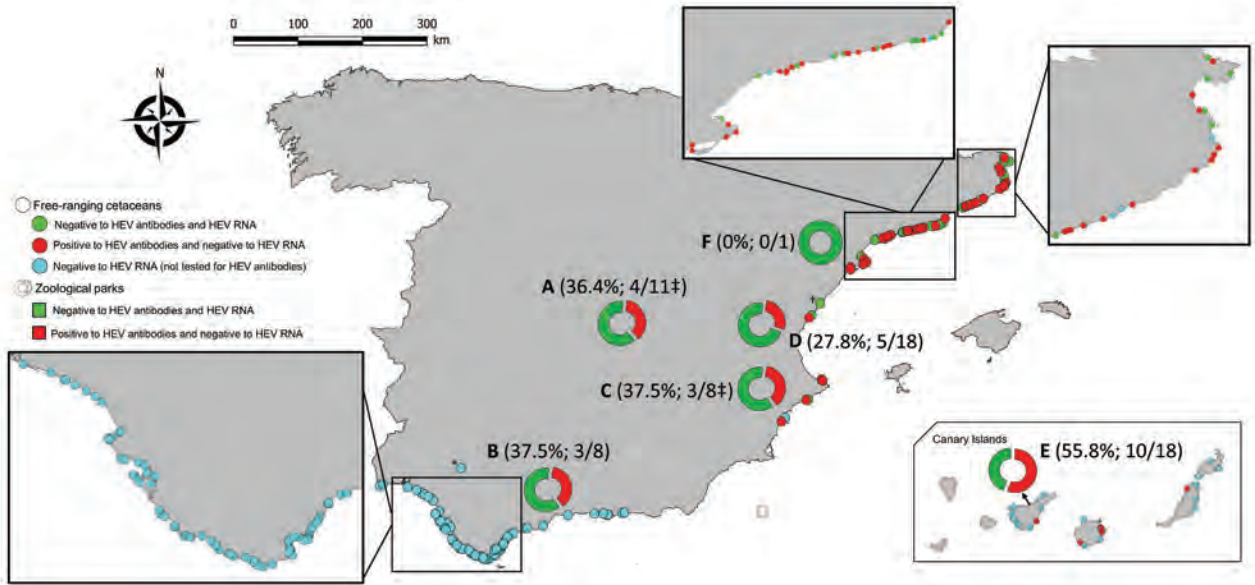**Figure 2.** Spatial distribution of cetaceans sampled in a survey of HEV in 304 cetaceans belonging to 13 species in Spain during n 2011–2022. The frequency of seropositivity and number of seropositive and total animals analyzed at each zoological park (A–F) is shown in parentheses. Callouts show detail of sampling along the Atlantic and Mediterranean coastlines. *Animal sampled in the Guadalquivir River. †This animal was not analyzed by reverse transcription PCR. ‡One of the sampled animals of this zoo park was not tested by reverse transcription PCR. HEV, hepatitis E virus.

an increase in the number of cetartiodactyls susceptible to this virus (2).

Ingestion of contaminated food is considered to be one of the main transmission routes of HEV in humans and has also been suggested for other mammal species, including dolphins (4). The seropositive species detected in our study feed on a wide variety of resources, including fish and cephalopods. The presence of HEV in these food resources has not yet been assessed, but the virus has been frequently detected in such other aquatic animals as sea urchins and bivalve shellfish in different areas of Europe (2,7), which provides evidence that HEV does abide in marine ecosystems. Of note, the virus is shed primarily in the feces of infected species, which can lead to viral contamination of the environment, and HEV has been shown to be highly resistant to even high concentrations of salt (8). Contaminated water has been considered a potential source of zoonotic HEV (9), because drinking tap water or water from private wells or nearby rivers has been suggested as a risk factor for acquiring HEV infection in humans (10). This hypothesis is supported by a study conducted in captive cetaceans all sharing the same tanks, which revealed the detection of seropositivity and active HEV infection (4).

The significantly higher seroprevalence we found in adult free-ranging animals compared with young animals likely reflects the increased cumulative exposure to HEV in these species. Our additional discovery of HEV antibodies in 4 free-ranging yearlings in 2011,

2019, and 2021 could suggest endemic circulation of HEV in cetaceans living in Spanish waters during the study period. Free-ranging cetaceans had a 2.5-times higher risk of being exposed to HEV than those kept in captivity, which might be explained by differences in diet or longer exposure to environmental contamination. Human- and swine-related HEV-3 strains have been detected in sewage and slurry in Spain (11) and in rivers and coastal waters in Italy (12). The high census of some susceptible domestic and wildlife species (13,14), combined with high coastal urbanization and insufficient control of urban sewage in some regions of our study area (15), might be contributing factors in the higher seropositivity we noted in free-ranging cetaceans. By contrast, cetaceans in zoological parks, including those analyzed in our study, live in large

Table 2. Distribution of hepatitis E virus seroprevalence in cetaceans in Spain, by sampling location, and results of bivariate analyses

Category	No. positive/no. analyzed (% positive)	p value
Free-ranging areas		
Atlantic Ocean	6/8 (75.0)	0.327
Mediterranean Sea	38/64 (59.4)	
Aquatic parks		
A	4/11 (36.4)	0.772
B	3/8 (37.5)	
C	3/8 (37.5)	
D	5/18 (27.8)	
E	10/18 (55.6)	
F	0/1 (0.0)	

water tanks that are frequently decontaminated with ozone, ultraviolet radiation, brine, or chlorine, some of which deactivates HEV (9). Nonetheless, the high seroprevalence we observed in the 5 zoos with seropositive animals indicates a wide circulation of the virus in these more controlled environments.

The 2 seroconversions we noted in captive bottlenose dolphins support the hypothesis of HEV circulation in zoos during our study period. However, 4 of the longitudinally surveyed cetaceans remained seropositive at all samplings. This finding might be due to the long-lived persistence of anti-HEV antibodies in cetaceans, which is supported by the significantly higher seroprevalence we detected in older, freeranging cetaceans. There is no known information about the long-term persistence of HEV antibodies in these species. Thus, possible loss of antibodies and reexposure in some of the persistently seropositive cetaceans during the study period cannot be ruled out, as evidenced by the seroreversions we observed in 2 bottlenose dolphins 1 and 5 years after the first seropositive sampling was detected.

In conclusion, the seropositivity noted in our study indicates widespread circulation of HEV in both free-ranging and captive cetacean populations in southwestern Europe. Additional molecular and serologic studies are warranted to determine the role of cetaceans in the epidemiology of HEV and to elucidate the sources of HEV infection, particularly in the free-ranging cetacean population.

This study did not involve the purposeful killing of animals. Samples from live cetaceans were collected from serum banks or animals in health programs or undergoing routine medical check-ups, and those from dead individuals were collected by veterinarians and animal keepers following routine procedures in compliance with Ethical Principles in Animal Research. Ethics approval by an Institutional Animal Care and Use Committee was not therefore deemed necessary.

About the Author

Dr. Javier Caballero-Gómez is a postdoctoral researcher at the Clinical Virology and Zoonoses Group at the Maimonides Biomedical Research Institute of Cordoba and the Animal Health and Zoonosis Research Group (GISAZ) at the University of Cordoba. His research interests are focused on the epidemiology of hepeviruses and other zoonotic emerging diseases.

References

1. Purdy MA, Drexler JF, Meng XJ, Norder H, Okamoto H, Van der Poel WHM, et al. ICTV virus taxonomy profile: *Hepeviridae* 2022. J Gen Virol. 2022;103. https://doi.org/10.1099/jgv.0.001778
2. Kenney SP. The current host range of hepatitis E viruses. Viruses. 2019;11:52. https://doi.org/10.3390/v11050452
3. Aspinall EJ, Couturier E, Faber M, Said B, Ijaz S, Tavoschi L, et al.; The Country Experts. Hepatitis E virus infection in Europe: surveillance and descriptive epidemiology of confirmed cases, 2005 to 2015. Euro Surveill. 2017;22:30561. https://doi.org/10.2807/1560-7917.ES.2017.22.26.30561
4. Montalvo Villalba MC, Cruz Martínez D, Ahmad I, Rodriguez Lay LA, Bello Corredor M, Guevara March C, et al. Hepatitis E virus in bottlenose dolphins *Tursiops truncatus*. Dis Aquat Organ. 2017;123:13–8. https://doi.org/10.3354/dao03085
5. Frías M, López-López P, Zafra I, Caballero-Gómez J, Machuca I, Camacho Á, et al. Development and clinical validation of a pangenotypic PCR-based assay for the detection and quantification of hepatitis E virus (*Orthohepevirus A* genus). J Clin Microbiol. 2021;59:e02075–20. https://doi.org/10.1128/JCM.02075-20
6. Johne R, Plenge-Bönig A, Hess M, Ulrich RG, Reetz J, Schielke A. Detection of a novel hepatitis E-like virus in faeces of wild rats using a nested broad-spectrum RT-PCR. J Gen Virol. 2010;91:750–8. https://doi.org/10.1099/vir.0.016584-0

7. Santos-Ferreira N, Mesquita JR, Rivadulla E, Inácio ÂS, Martins da Costa P, Romalde JL, et al. Hepatitis E virus genotype 3 in echinoderms: First report of sea urchin (*Paracentrotus lividus*) contamination. Food Microbiol. 2020;89:103415. https://doi.org/10.1016/j.fm.2020.103415

8. Wolff A, Günther T, Albert T, Johne R. Effect of sodium chloride, sodium nitrite and sodium nitrate on the infectivity of hepatitis E virus. Food Environ Virol. 2020;12:350–4. https://doi.org/10.1007/s12560-020-09440-2

9. Fenaux H, Chassaing M, Berger S, Gantzer C, Bertrand I, Schvoerer E. Transmission of hepatitis E virus by water: An issue still pending in industrialized countries. Water Res. 2019;151:144–57. https://doi.org/10.1016/j.watres.2018.12.014

10. Mansuy JM, Gallian P, Dimeglio C, Saune K, Arnaud C, Pelletier B, et al. A nationwide survey of hepatitis E viral infection in French blood donors. Hepatology. 2016;63:1145–54. https://doi.org/10.1002/hep.28436

11. Clemente-Casares P, Rodriguez-Manzano J, Girones R. Hepatitis E virus genotype 3 and sporadically also genotype 1 circulate in the population of Catalonia, Spain. J Water Health. 2009;7:664–73. https://doi.org/10.2166/wh.2009.120

12. La Rosa G, Proroga YTR, De Medici D, Capuano F, Iaconelli M, Della Libera S, et al. First detection of hepatitis E virus in shellfish and in seawater from production areas in Southern Italy. Food Environ Virol. 2018;10:127–31. https://doi.org/10.1007/s12560-017-9319-z

13. Bosch J, Peris S, Fonseca C, Martinez M, De la Torre A, Iglesias I, et al. Distribution, abundance and density of the wild boar on the Iberian Peninsula, based on the CORINE program and hunting statistics. Folia Zool (Brno). 2012;61:138–51. https://doi.org/10.25225/fozo.v61.i2.a7.2012

14. Ministerio de Agricultura, Pesca y alimentación. El sector de la carne de cerdo en cifras 2021. 2022 Spanish Report [cited 2022 Nov 15]. https://www.mapa.gob.es/es/agricultura/estadisticas/indicadoressectorporcino2021_tcm30-564427.pdf

15. European Commission. Urban waste water: The Commission decided today to refer SPAIN to the Court of Justice of the European Union for breach of the Urban Waste Water Treatment Directive [cited 2022 Apr 6]. https://ec.europa.eu/commission/presscorner/detail/es/ip_22_1923

Address for correspondence: Antonio Rivero-Juarez, Grupo de Virología Clínica y Zoonosis, Unidad de Enfermedades Infecciosas, Instituto Maimónides de Investigación Biomédica de Córdoba (IMIBIC), Hospital Universitario Reina Sofía, Universidad de Córdoba, 14004 Córdoba, Spain; email: arjvet@gmail.com

Sylvatic Transmission of Chikungunya Virus among Nonhuman Primates in Myanmar

Tierra Smiley Evans, Ohnmar Aung, Olivia Cords, Lark L. Coffey, Talia Wong, Christopher M. Weiss, Min Thein Maw, JoAnn Yee, Kodumudi Venkateswaran, Neeraja Venkateswaran, Peter Nham, Koen K.A. Van Rompay, Mary Kate Morris, Leo Oceguera, William Werthimer, Carl Hanson, Marc Valitutto, Kyaw Yan Naing Tun, Ye Tun Win, Wai Zin Thein, Susan Murray, Hlaing Myat Thu, Christine K. Johnson

Nonhuman primates living in proximity to humans increase risks for sylvatic arbovirus transmission. We collected serum samples from nonhuman primates in Hlawga National Park near Yangon, Myanmar, and detected antibodies against chikungunya (33%) and Japanese encephalitis (4%) viruses. Buffer zones between primate and human communities might reduce cross-species arbovirus transmission.

Several endemic and emerging arboviruses, such as chikungunya (CHIKV), Zika (ZIKV), and dengue (DENV) viruses, have evolutionary origins in nonhuman primates (NHPs) (*1,2*). These pathogens have adapted sylvatic to urban transmission cycles by using humans as amplifying hosts where NHPs are no longer required for virus maintenance. However, sylvatic arbovirus transmission cycles involving NHPs could act as sources of human infections, which would affect public health. NHPs could enable reemergence of arbovirus infections after immunity has waned following human–mosquito–human transmission. Sylvatic cycles can also provide selective environments where new viral strains can emerge.

CHIKV circulates in distinct enzootic, sylvatic transmission cycles in old world monkeys in the forests of sub-Saharan Africa (*2*). Limited data are available on sylvatic CHIKV transmission in Asia, but seroconversion has been detected in cynomolgus macaques (*Macaca fascicularis*), pig-tailed macaques (*M. nemistrina*), black-crested Sumatran langurs (*Presbytis melalophos*), and dusky leaf monkeys (*Presbytis obscura*) in Thailand (*3,4*), and virus has been isolated from long-tailed macaques in Malaysia (*5*). A sylvatic ZIKV lineage in Africa, infecting Cercopthecidae primate species, is known to circulate widely (*6*). The only positive ZIKV serology findings in primates in Asia have been in orangutans (*Pongo pygmaeus*) in Borneo, Malaysia, but those exposures were likely from an urban strain (*7*). Sylvatic DENV cycles occur in the forests of Malaysia in *Macaca* and *Presbytis* spp. monkeys (*8*) and also in West Africa; sylvatic DENV-2 circulates regularly between *Erythrocebus patas* monkeys and various *Aedes* spp. mosquitoes in Senegal (*8*). Seroprevalence of Japanese encephalitis virus (JEV) has been reported in cynomolgus monkeys, Japanese macaques (*M. fuscata*), green monkeys (*Chlorocebus sabaeus*), and pig-tailed macaques in several countries in Asia (*4,9,10*).

Myanmar is among the least studied but most heavily forested region in Asia, and CHIKV, ZIKV, DENV and JEV are highly endemic in humans. We investigated whether Myanmar peri-urban primates, living near the largest urban city of Yangon, are exposed to arboviruses of public health concern and could be sources of spillover or recipients of spillback of human pathogenic arboviral diseases.

The Study

We collected specimens from 107 rhesus monkeys (*Macaca mulata*) and 12 pig-tailed macaques within Hlawga National Park, an open zoo and wildlife sanctuary in Myanmar's Yangon region that covers 6.23 km² (Figure). NHPs are free ranging within this park and have frequent opportunities for human contact.

Author affiliations: University of California, Davis, California, USA (T. Smiley Evans, O. Aung, O. Cords, L.L. Coffey, T. Wong, C.M. Weiss, J. Yee, P. Nham, K.K.A. Van Rompay, C.K. Johnson); Livestock Breeding and Veterinary Department, Yangon, Myanmar (M.T. Maw, Y.T. Win, W.Z. Thein); Tetracore, Inc., Rockville, Maryland, USA (K. Venkateswaran, N. Venkateswaran); California Department of Public Health, Richmond, California, USA (M.K. Morris, L. Oceguera, W. Werthimer, C. Hanson); Smithsonian Institution, Washington, DC, USA (M. Valitutto, S. Murray); Department of Medical Research, Yangon (H.M. Thu)

Serum samples were collected during October 2016–August 2017, which spanned 2 dry/wet seasons. We used a Luminex xMAP multiplex bead-based assay (Luminex Corp., https://www.luminexcorp.com) to simultaneously measure total IgG, IgA, and IgM against CHIKV E1 envelope protein, ZIKV nonstructural protein 1 (NS1), ZIKV envelope protein, DENV-1–4 NS1, JEV NS1, West Nile virus NS1, yellow fever virus NS1, and tickborne encephalitis virus NS1 (Appendix Table, https://wwwnc.cdc.gov/EID/article/28/12/22-0893-App1.pdf). We confirmed positive serum samples by using the plaque reduction neutralization test (Appendix). Conventional reverse transcription PCR targeting conserved regions of *Flavivirus* and *Alphavirus* spp. was performed to detect arbovirus viremia (Appendix).

We identified virus-reactive antibodies among NHPs in Hlawga National Park, suggesting prior exposure to arboviruses, but we did not detect viruses by using PCR, suggesting absence of active infections. We found 33% (39/119) of NHPs were seropositive for CHIKV and 4% (5/119) were seropositive for JEV (Table); all serum samples were negative for ZIKV, West Nile virus, yellow fever virus, and tick-borne encephalitis virus. Using bivariate analysis, we showed specimens collected during the dry season were more likely to be seropositive for CHIKV (p = 0.05). Greater proportions of adult NHPs appeared to be seropositive for CHIKV; however, the difference was not statistically significant. We found no statistically significant associations between sex, age class, or species and specific arbovirus exposure. CHIKV and JEV in NHPs in Myanmar have not been reported, likely because of limited surveillance. Our findings extend the geographic range of potential sylvatic cycles for CHIKV to forests and peri-urban areas of Myanmar.

Our results indicate that NHPs were exposed to CHIKV during a period with no or limited human–mosquito–human transmission, suggesting that seropositive samples resulted from sylvatic exposures. IgG against CHIKV E2 protein can be detected up to 21 months postinfection (*11*). If similar kinetics occur in NHPs and extend to the E1 protein, NHP exposures to CHIKV could have occurred during 2013–2014 or earlier. However, in 2017, we detected CHIKV antibodies in NHPs that were <5 years of age, indicating exposure during an interepidemic period. Human cases of CHIKV were not reported by the Myanmar Ministry of Health during 2011–2018 (*12*), and CHIKV outbreaks are not commonly underreported because a large proportion of infected persons have indicative arthritic manifestations. In 2019, health officials reported widespread outbreaks of CHIKV in Mandalay, Nay Pyi
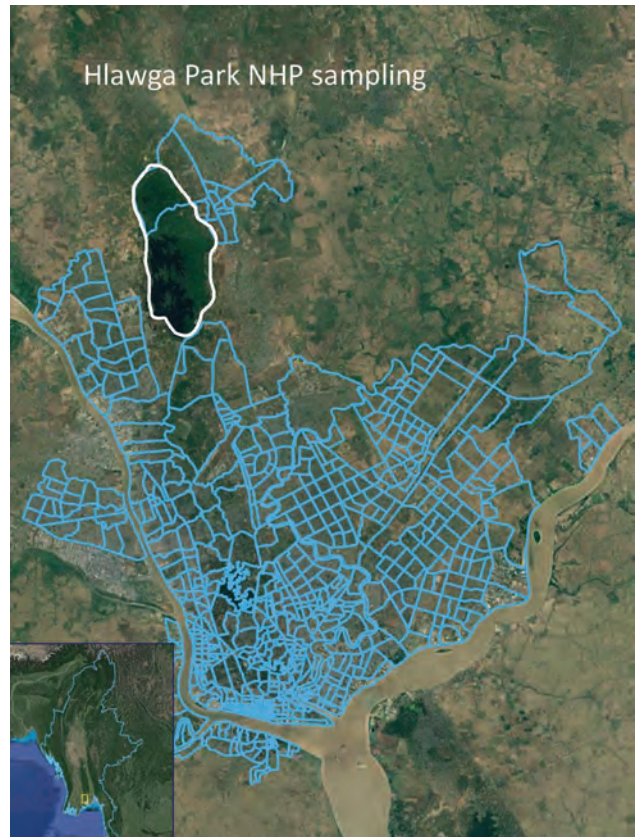
Figure. Hlawga National Park sampling site (white outline) in Yangon in study of sylvatic transmission of chikungunya virus among NHPs in Myanmar. Blue lines show the Yangon city wards south of the park. Inset shows location of Yangon in Myanmar (white box). NHP, nonhuman primate.

Taw, Kachin State, Tanintharyi, and Yangon regions of Myanmar, indicating reemergence of the virus (*12*).

We studied an NHP population that lived in a forested area outside of Yangon and could have played a role in the reemergence of CHIKV in humans. The large proportion of NHPs that were exposed indicated the virus was circulating among sylvatic mosquitos and primates in this park. The absence of reported human infections during the potential period of NHP infection suggested that spillover from humans to NHPs via mosquitoes was unlikely. *Aedes aegypti* and *A. albopictus* mosquitoes, the two primary urban vectors of CHIKV, are also known to feed almost exclusively on humans in the region, providing further evidence that NHP exposures to CHIKV in our study population were of sylvatic origin (*13*).

Our findings indicate that JEV is circulating at the periphery of Yangon, and NHPs can be occasional incidental hosts. JEV is endemic in Myanmar, particularly in the Yangon region (*14*). NHPs are not thought to be potential reservoirs, but are dead-end

Table. Chikungunya and Japanese encephalitis virus prevalence during October 2016–August 2017 in Hlawga National Park in study of sylvatic transmission of chikungunya virus among nonhuman primates in Myanmar*

Characteristic	Chikungunya virus			Japanese encephalitis virus		
	No. positive†	No. negative†	Period prevalence	No. positive†	No. negative†	Period prevalence
Species						
Macaca nemestrina (pig-tailed macaque)	8	4	67 (35–90)	1	11	8 (0–38)
Macaca mulatta (rhesus macaque)	31	76	29 (21–39)	4	103	4 (1–9)
Sex						
M	20	43	32 (21–45)	3	60	5 (0–13)
F	19	37	34 (22–48)	2	54	4 (0–12)
Age class						
Adult	23	35	40 (27–53)	1	57	2 (0–9)
Subadult	16	45	26 (16–39)	4	57	7 (2–16)
Season						
Wet	25	69	27 (18–37)	4	90	4 (1–11)
Dry	14	11	56 (35–76)	1	24	4 (0–20)
Overall	39	80	33 (24–42)	5	114	4 (1–10)

*Values are no. or % (95% binomial exact CI).
†No. positive or negative serum samples according to the total Ig detected by multiplex bead-based assay. Cutoff values were determined according to the lowest median fluorescence intensity value detected by a positive plaque reduction neutralization test.

hosts; they produce a low viremia that cannot subsequently infect mosquitoes (*1*). Low levels of viremia produced in experimental studies and sylvatic cycles involving waterfowl or pigs are well documented. Furthermore, JEV is transmitted to humans by infected *Culex* spp. mosquitoes (most commonly *Culex tritaeniorhynchus*), which feed on many mammals in the region (*15*), making it more plausible that NHPs could be incidental targets of this mosquito species.

We did not confirm NHP exposure to DENV or ZIKV. We identified positive samples by using the Luminex assay, but those samples tested negative when the plaque reduction neutralization assay was used for confirmation. DENV is endemic in humans in Myanmar, and our findings indicate that spillback of urban DENV strains to NHPs is not common in this region or was not detected in our sample size. Given the limited knowledge of the scope of human ZIKV circulation in Myanmar and lack of entomological data, further research is needed to examine potential sylvatic ZIKV cycles among NHPs in Asia.

Conclusions

Our study demonstrates the importance of conducting surveillance of peri-urban primates in regions of high arbovirus transmission and the need for less invasive methods that improve feasibility. Future research on molecular epidemiology of arboviruses in humans, NHPs, and mosquitoes is needed to confirm whether exposures result from potential sylvatic cycles of ongoing transmission or spillback events from urban strains. A heightened awareness of new CHIKV outbreak potential in humans living near NHPs in Hlawga National Park is warranted. Buffer zones between parks and human settlements might reduce future cross-species arbovirus transmission.

About the Author

Dr. Smiley Evans is a research epidemiologist at the One Health Institute, University of California, Davis, CA, USA. Her research focuses on disease transmission dynamics between humans and wildlife and the effects of biodiversity on disease emergence.

References

1. Weaver SC, Barrett ADT. Transmission cycles, host range, evolution and emergence of arboviral disease. Nat Rev Microbiol. 2004;2:789–801. https://doi.org/10.1038/nrmicro1006
2. Weaver SC, Winegar R, Manger ID, Forrester NL. Alphaviruses: population genetics and determinants of emergence. Antiviral Res. 2012;94:242–57. https://doi.org/10.1016/j.antiviral.2012.04.002

3. Marchette NJ, Rudnick A, Garcia R, MacVean DW. Alphaviruses in peninusular Malaysia: I. Virus isolations and animal serology. Southeast Asian J Trop Med Public Health. 1978;9:317–29.

4. Nakgoi K, Nitatpattana N, Wajjwalku W, Pongsopawijit P, Kaewchot S, Yoksan S, et al. Dengue, Japanese encephalitis and chikungunya virus antibody prevalence among captive monkey (*Macaca nemestrina*) colonies of northern Thailand. Am J Primatol. 2014;76:97–102. https://doi.org/10.1002/ajp.22213

5. Apandi Y, Nazni WA, Azleen ZAN, Vythilingham I, Noorazian MY, Azahari AH, et al. The first isolation of chikungunya virus from nonhuman primates in Malaysia. J Gen Mol Virol. 2009;1:035–9.

6. Faria NR, Azevedo RDSDS, Kraemer MUG, Souza R, Cunha MS, Hill SC, et al. Zika virus in the Americas: early epidemiological and genetic findings. Science. 2016;352:345–9. https://doi.org/10.1126/science.aaf5036

7. Wolfe ND, Kilbourn AM, Karesh WB, Rahman HA, Bosi EJ, Cropp BC, et al. Sylvatic transmission of arboviruses among Bornean orangutans. Am J Trop Med Hyg. 2001;64:310–6. https://doi.org/10.4269/ajtmh.2001.64.310

8. Vasilakis N, Cardosa J, Hanley KA, Holmes EC, Weaver SC. Fever from the forest: prospects for the continued emergence of sylvatic dengue virus and its impact on public health. Nat Rev Microbiol. 2011;9:532–41. https://doi.org/10.1038/nrmicro2595

9. Yuwono J, Suharyono W, Koiman I, Tsuchiya Y, Tagaya I. Seroepidemiological survey on dengue and Japanese encephalitis virus infections in Asian monkeys. Southeast Asian J Trop Med Public Health. 1984;15:194–200.

10. Inoue S, Morita K, Matias RR, Tuplano JV, Resuello RRG, Candelario JR, et al. Distribution of three arbovirus antibodies among monkeys (*Macaca fascicularis*) in the Philippines. J Med Primatol. 2003;32:89–94. https://doi.org/10.1034/j.1600-0684.2003.00015.x

11. Kam YW, Lee WWL, Simarmata D, Harjanto S, Teng TS, Tolou H, et al. Longitudinal analysis of the human antibody response to chikungunya virus infection: implications for serodiagnosis and vaccine development. J Virol. 2012;86:13005–15. https://doi.org/10.1128/JVI.01780-12

12. Luvai EAC, Kyaw AK, Sabin NS, Yu F, Hmone SW, Thant KZ, et al. Evidence of chikungunya virus seroprevalence in Myanmar among dengue-suspected patients and healthy volunteers in 2013, 2015, and 2018. PLoS Negl Trop Dis. 2021;15:e0009961. https://doi.org/10.1371/journal.pntd.0009961

13. Ponlawat A, Harrington LC. Blood feeding patterns of *Aedes aegypti* and *Aedes albopictus* in Thailand. J Med Entomol. 2005;42:844–9. https://doi.org/10.1093/jmedent/42.5.844

14. Thaung Y, Swaddiwudhipong W, Tin H, Thammawijaya P, Thitichai P, Tin TC. Epidemiological features of Japanese encephalitis among acute encephalitis syndrome cases in Myanmar, 2014–2016: implications to the vaccination program. OSIR. 2019;12:24–31. http://www.osirjournal.net/index.php/osir/article/view/137

15. Reuben R, Thenmozhi V, Samuel PP, Gajanana A, Mani TR. Mosquito blood feeding patterns as a factor in the epidemiology of Japanese encephalitis in southern India. Am J Trop Med Hyg. 1992;46:654–63. https://doi.org/10.4269/ajtmh.1992.46.654

Address for correspondence: Tierra Smiley Evans, One Health Institute, University of California, Davis, 1089 Veterinary Medicine Dr, Veterinary Medicine 3B, Davis, CA 95616, USA; tsmevans@ucdavis.edu

Pandemic or Panzootic— A Reflection on Terminology for SARS-CoV-2 Infection

Sara Agnelli,[1] Ilaria Capua[1]

As of October 2022, a total of 675 natural outbreaks of SARS-CoV-2 infection have occurred in animal species worldwide. Here, we provide a linguistic and etymologic critique of the term "pandemic" being used to describe the COVID-19 health crisis, as opposed to the term "panzootic," and discuss policy ramifications of more inclusive terminology.

As we approach the end of the third full year of the COVID-19 pandemic, the unfolding of COVID-19 continues to reveal many unexpected surprises. The most peculiar and most relevant to this paper is that we are being overwhelmed by the number of animal species which are susceptible to infection with SARS-CoV-2. As of October 2022, there have been 675 natural outbreaks in different species (*1*). A total of 58 animal species have been infected through natural and experimental infections, and these include human beings (*Homo sapiens*). Of these 58 animal species, 38 are reported in Meekins et al. (*2*) and the other 19 species are reported by other publications (*3–16*). Clearly, viral circulation and subsequent infection of susceptible hosts is not restricted to human beings but rather to a vast variety of animals (*1–13*; B. Pickering et al., unpub. data, https://doi.org/10.1101/2022.02.22.481551; S. Mahajan et al., unpub. data, https://doi.org/10.1101/2022.01.11.475327; L. Ulrich et al., unpub. data, https://doi.org/10.1101/2020.12.24.424203).

We argue that we could be at the very beginning of a macrocycle that may become the first real-time documented case of a true panzootic—that is, an infection that occurs in a vast number of animal species, which includes *Homo sapiens*. The situation is worrisome and monitored by international organizations such as the World Organization for Animal Health and a recent effort, SARS-ANI, is collecting relevant data on animal infections in a global open-access database (*17*).

COVID-19 is currently considered a pandemic. The English term "pandemic" (*18*) comes from the ancient Greek adjective *pàndemos*, which means "of" or "belonging to" the whole people, "public" (*pan*, "all," and *demos*, "people"). With this meaning of "public," the word *pàndemos* already appeared in the 8th century BCE, in a passage of the *Odyssey* (*19,* p. 200–1). Later, Plato (5th century BCE) used the term "pandemic" in the *Symposium* (*20*, p. 169–71) to describe the popular or "pandemic" love in contrast to heavenly love. Thus, the word "pandemic" with no link to any condition concerning health has been around for more than 2,800 years.

In the 2nd century CE, the Greek physician and philosopher Galen was the first to use the word pandemic in a medical treatise, although not as a medical term. *In De praesagitione ex pulsibus* 17(1).2, he refers to "the pandemic nature of famine" (*21*). Within the ancient Greek medical literature, the term "pandemic" and other terms linked to it (pandemía, pandemikós, etc.) were not associated with any specific medical condition but were used to generally describe an occurrence of variable origin and nature that was affecting "all the people."

At its first appearance in print in England in 1666 (*22*), the word "pandemic" was essentially used as a synonym for "endemic," which still means "a disease commonly occurring in a region or country." "Epidemic" became the most commonly used term for large-scale infectious disease outbreaks during the 19th century until the first documented international outbreak of influenza in 1889–1891 (*23*). In a world that had known endemic and epidemic diseases, the concept of a pandemic, i.e., of a disease which could affect all the population of the world, came into shape as the 1889 influenza pandemic appeared and spread

Author affiliation: One Health Center of Excellence for Research and Training, University of Florida, Gainesville, Florida, USA

[1]These authors contributed equally to this article.

worldwide. This first occurrence was followed by the 1917–1919 Spanish influenza outbreak, which solidified the concept of pandemic, which then became accepted by the public (*24*).

In recent times, the definitions of the term "pandemic" include concepts such as "extensively epidemic" (*25*), "an epidemic occurring worldwide or over a very wide area, crossing international boundaries, and usually affecting a large number of people" (*26,27*), and "distributed or occurring widely throughout a region, country, continent, or globally" (*28,29*), among others (*24*). Although there seems to be little disagreement that a pandemic is a large epidemic, the question arises whether pandemics do include infections of other animals as well. This is not merely a linguistic matter; it has significant emergency response and policy ramifications. Policy updates would include extensive surveillance events in animals from the very start of the event to understand transmission dynamics in potential animal reservoirs.

The concept behind the term "pandemic" has evolved over the centuries to describe philosophical, social, and medical issues which had 2 common characteristics: they affected human beings and were widespread phenomena. We can say that this is certainly true also for SARS-CoV-2 infection, but "pandemic" is perhaps insufficient to encompass and define the magnitude of what we are observing with multispecies infections caused by this virus (*2–17*).

We believe there is another term which would perhaps be more suitable to define the extent of what we are experiencing. The term "panzootic" which literally means "all" and "animals" has been only used rarely to describe extensive multispecies infections by a single pathogen (*30,31*). In addition, whether *Homo sapiens* is included or not in the "-zootic" part of the word remains to be established. To look at the history of a concept through the lexicon, and particularly to the ancient Greek word ζωον (zoon), from which the combining form -zoon comes, see Clackson (*32*). From a biological point of view, we are, of course, animals; this fact is reflected by the great number of zoonotic diseases that we are susceptible to as human beings. Some of these zoonotic events, such as HIV and swine influenza, have become pandemics.

The term "panzootic" entered veterinary and medical terminology approximately in the 19th century referring to a widespread outbreak of a disease affecting several kinds of animals. For instance, in the National Medical Dictionary (*33*), we find the entry "panzoötic," from the neo-Latin noun panzoötia, defined as an epizootic affecting many kinds of animals. In most Romance and Germanic languages, the spelling panzoötic with umlaut changed to panzootic at the beginning of the 20th century. In the New Sydenham Lexicon (*34*), the term "panzoötic" is referring to, or the same as, panzoötia (πας [pan], all; ζωον [zoon], an animal): a disease affecting a large number of animals inhabiting extensive areas of a country.

Throughout the 19th and the beginning of the 20th century, the word panzootic had a similar meaning in its different forms within the Romance (i.e., Spanish, Portuguese, Italian, and French) and Germanic (German, English, Dutch and Swedish) languages: that is, the term used to describe a disease affecting a high number of animals in large geographic areas. This definition could be linked to the massive outbreaks of deadly diseases among animals, which were caused by highly transmissible pathogens. For example, Rinderpest affected many species in many countries and caused famine and devastation in many of them (*35*).

Of particular interest for us is a study published in the Anales de la Academia de Ciencias Médicas, Físicas y Naturales de la Habana (*36*), in which tuberculosis, a significant disease for both humans and animals, is defined as a "panzootia universal." So, this case may be the first time panzootic was used to describe a disease which infected multiple animal species, including humans. The term panzootic was not particularly successful in gaining consensus and was virtually abandoned until a few decades ago. Since the 1980s, it has been used to describe Newcastle disease, a deadly disease of multiple species of birds which occasionally spills over to mammals, including humans, with minor consequences. Terminology is very important when defining a rare event; given the current and ever-growing evidence that SARS-CoV-2 originates from the animal reservoir and has the potential of infecting multiple mammalian species including *Homo sapiens*, it would seem reasonable to consider defining this event a potential panzootic.

We identified several reasons why defining SARS-CoV-2 as a potential panzootic rather than as a pandemic from the early phases of spread could have made a substantial difference. First, surveillance in animal populations could have started earlier, and thus active surveillance in animals would have unveiled positivity at earlier stages. Early identification of animal outbreaks could have allowed implementation of some targeted intervention strategies in advance, including developing vaccines for susceptible farm or pet animals, and prevention efforts to avoid widespread infection in wild animals. As an example, as of May 2022, SARS-CoV-2 has infected multiple white deer herds in 24 states of the United States. Infection in deer (*37,38*) was reported more than a year

after the World Health Organization declared a Public Health Emergency of International Concern on January 31, 2020. Joint research efforts between human and veterinary virologists would empower research addressing zoonoses in a coordinated manner to prevent uncontrolled spread in large animal populations that could eventually become permanent reservoirs of SARS-CoV-2 (L.C. Caserta et al., unpub. data, https://doi.org/10.1101/2022.09.02.506368). An additional reason that becomes more topical every day is that both scientists and the public need to keep in mind that this virus is capable of spreading to wild, domestic, and pet animal species, which can in turn become reservoirs of infection for other species, including humans.

Using the most appropriate word to describe an event with unknown characteristics is often more difficult than expected. In the case of SARS-CoV-2 we believe the word panzootic is a much better fit than the word pandemic for all the reasons we mention, but especially because this usage would frame a unique event in history. We will never know if this is truly a unique event or if centuries ago other pathogens have had similar multispecies transmission cycles. Now we have the tools to assess widespread transmission in humans and animals worldwide, sometimes in real time.

This catastrophic event with unique characteristics could mark a paradigm shift in the scientific terminology, which could be used to define future events properly. Not only recent infections like SARS-CoV-2 but also other infections such as highly pathogenic avian influenza, which is now infecting wild mammals such as foxes and bears, should be deemed as potentially panzootic pathogens. This paradigm shift would also be instrumental to delivering to the public concepts that must be understood and applied in everyday life for managing and preventing further multispecies spillovers and reverse-spillover events, such as those reported by Munnik et al. (*39*) and Yen et al. (*40*) from certain animals back to other animals, known as *Homo sapiens*.

Acknowledgments

About the Authors

Dr. Agnelli is the teaching program coordinator and interdisciplinary academic advisor at the University of Florida's One Health Center of Excellence, where she serves as a liaison between the One Health center and the humanities departments at the university and beyond.

Dr. Capua has spent most of her career as a veterinary virologist working on zoonotic viruses and emerging pathogens. She is a professor and directs the One Health Center of Excellence at the University of Florida.

References

1. World Organization for Animal Health. SARS-CoV-2 in animals—situation report 12; 2022 Apr. Report No 12 [cited 2022 Sep 19]. https://www.woah.org/app/uploads/2022/08/sars-cov-2-situation-report-12.pdf
2. Meekins DA, Gaudreault NN, Richt JA. Natural and experimental SARS-CoV-2 infection in domestic and wild animals. Viruses. 2021;13:1993. https://doi.org/10.3390/v13101993
3. US Department of Agriculture Animal and Plant Health Inspection Service (USDA APHIS). Confirmation of COVID-19 in a Canada lynx at a Pennsylvania zoo. 2021 Dec 21 [cited 2022 Sep 19]. https://www.aphis.usda.gov/aphis/newsroom/stakeholder-info/sa_by_date/sa-2021/sa-12/covid-lynx-pa
4. Banerjee A, Mossman K, Baker ML. Zooanthroponotic potential of SARS-CoV-2 and implications of reintroduction into human populations. Cell Host Microbe. 2021;29:160–4. https://doi.org/10.1016/j.chom.2021.01.004
5. Farzan Z. Chimpanzees & orangutans at Dehiwala zoo test COVID positive. 2021 Jul 18 [cited 2022 Sep 19]. https://www.newsfirst.lk/2021/07/18/chimpanzees-orangutans-at-dehiwala-zoo-test-covid-positive/
6. Giraldo-Ramirez S, Rendon-Marin S, Jaimes JA, Martinez-Gutierrez M, Ruiz-Saenz J. SARS-CoV-2 clinical outcome in domestic and wild cats: a systematic review. Animals (Basel). 2021;11:2056. https://doi.org/10.3390/ani11072056
7. Mallapaty S. The search for animals harbouring coronavirus—and why it matters. Nature. 2021;591:26–8. https://doi.org/10.1038/d41586-021-00531-z
8. Manes C, Gollakner R, Capua I. Could mustelids spur COVID-19 into a panzootic? Vet Ital. 2020;56:65–6. https://doi.org/10.12834/VetIt.2375.13627.1
9. Mastutik G, Rohman A, I'tishom R, Ruiz-Arrondo I, de Blas I. Experimental and natural infections of severe acute respiratory syndrome-related coronavirus 2 in pets and wild and farm animals. Vet World. 2022;15:565–89. https://doi.org/10.14202/vetworld.2022.565-589
10. McAloose D, Laverack M, Wang L, Killian ML, Caserta LC, Yuan F, et al. From people to *Panthera*: natural SARS-CoV-2 infection in tigers and lions at the Bronx Zoo. MBio. 2020;11:e02220–20. https://doi.org/10.1128/mBio.02220-20
11. Porter SM, Hartwig AE, Bielefeldt-Ohmann H, Bosco-Lauth AM, Root JJ. Susceptibility of wild canids to SARS-CoV-2. Emerg Infect Dis. 2022;28:1852–5. https://doi.org/10.3201/eid2809.220223
12. Sharun K, Dhama K, Pawde AM, Gortázar C, Tiwari R, Bonilla-Aldana DK, et al. SARS-CoV-2 in animals: potential for unknown reservoir hosts and public health implications. Vet Q. 2021;41:181–201. https://doi.org/10.1080/01652176.2021.1921311
13. Song TZ, Zheng HY, Han JB, Feng XL, Liu FL, Yang X, et al. Northern pig-tailed macaques (*Macaca leonina*) infected with SARS-CoV-2 show rapid viral clearance and persistent immune response. Zool Res. 2021;42:350–3. https://doi.org/10.24272/j.issn.2095-8137.2020.334
14. Wei C, Shan KJ, Wang W, Zhang S, Huan Q, Qian W. Evidence for a mouse origin of the SARS-CoV-2 Omicron

variant. J Genet Genomics. 2021;48:1111–21. https://doi.org/10.1016/j.jgg.2021.12.003

15. Xinhua. Mongolia confirms first animal deaths due to COVID-19. 2021 Sept 15 [cited 2022 Sep 19]. http://www.news.cn/english/2021-09/15/c_1310188921.htm

16. Gollakner R, Capua I. Is COVID-19 the first pandemic that evolves into a panzootic? Vet Ital. 2020;56:7–8. https://doi.org/10.12834/VetIt.2246.12523.1

17. Nerpel A, Yang L, Sorger J, Käsbohrer A, Walzer C, Desvars-Larrive A. SARS-ANI: a global open access dataset of reported SARS-CoV-2 events in animals. Sci Data. 2022;9:438. https://doi.org/10.1038/s41597-022-01543-8

18. Oxford English Dictionary Online. "pandemic, adj. and n." Oxford University Press. 2021 [cited 2022 Nov 3]. https://www.oed.com/view/Entry/136746

19. Homer, Dimock GE, Murray AT. Odyssey. New ed. Dimock GE, editor. Cambridge (MA): Harvard University Press; 2015.

20. Plato, Emlyn-Jones CJ, Preddy W. Lysis. Symposium. Phaedrus. Cambridge (MA): Harvard University Press; 2022.

21. Kühn CG, Claudii Galeni opera omnia, vol. 9. Leipzig: Knobloch; 1825 (repr. Hildesheim: Olms, 1965): 205–430.

22. Harvey G. On the original, contagion, and frequency of consumptions. Morbus Anglicus. London: Nathaniel Brook; 1666.

23. Byrne JP, Hays JN. Epidemics and pandemics: from ancient plagues to modern-day threats. Santa Barbara (CA): ABC-Clio, LLC; 2021.

24. Grennan D. What is a pandemic? JAMA. 2019;321:910. https://doi.org/10.1001/jama.2019.0700

25. Webster N. American dictionary of the English language. New York: S. Converse; 1828.

26. Clemow F. The recent pandemic of influenza: its place of origin and mode of spread. Lancet. 1894;143:139–43. https://doi.org/10.1016/S0140-6736(01)65971-3

27. Porta MS. A dictionary of epidemiology. 6th ed. Oxford: Oxford University Press; 2014.

28. Morens DM, Folkers GK, Fauci AS. What is a pandemic? J Infect Dis. 2009;200:1018–21. https://doi.org/10.1086/644537

29. University of Maryland Pathogenic Microbiology. Summary of host-parasite interactions [cited 2022 Sep 19]. https://science.umd.edu/classroom/bsci424/HostParasite Interactions/HostParasiteSummary.htm

30. Stedman TL. Stedman's medical dictionary. 28th ed. Philadelphia: Lippincott Williams & Wilkins; 2006.

31. Oxford English Dictionary Online. "panzootic, n. and adj." Oxford University Press. 2021 Dec [cited 2022 Sep 19]. www.oed.com/view/Entry/261369

32. Stray C, Clarke M, Katz JT. Liddell and Scott: the history, methodology, and languages of the world's leading lexicon of ancient Greek. Oxford: Oxford University Press; 2019.

33. Billings JS. The national medical dictionary: including English, French, German, Italian, and Latin technical terms used in medicine and the collateral sciences and a series of tables of useful data. Philadelphia: Lea Brothers & Co.; 1890.

34. New Sydenham Society. The New Sydenham Society's lexicon of medicine and the allied sciences. London: The Society; 1893.

35. Barrett T, Rossiter PB. Rinderpest: the disease and its impact on humans and animals. Adv Virus Res. 1999;53:89–110. https://doi.org/10.1016/S0065-3527(08)60344-9

36. Academia de Ciencias Médicas, Físicas y Naturales de La Habana. Anales De La Academia De Ciencias Médicas, Físicas Y Naturales De La Habana. 1895;32:305–342.

37. Palmer MV, Martins M, Falkenberg S, Buckley A, Caserta LC, Mitchell PK, et al. Susceptibility of white-tailed deer (Odocoileus virginianus) to SARS-CoV-2. J Virol. 2021;95:e00083–21. https://doi.org/10.1128/JVI.00083-21

38. Mallapaty S. COVID is spreading in deer. What does that mean for the pandemic? Nature. 2022;604:612–5. https://doi.org/10.1038/d41586-022-01112-4

39. Oude Munnink BB, Sikkema RS, Nieuwenhuijse DF, Molenaar RJ, Munger E, Molenkamp R, et al. Transmission of SARS-CoV-2 on mink farms between humans and mink and back to humans. Science. 2021;371:172–7. https://doi.org/10.1126/science.abe5901

40. Yen HL, Sit THC, Brackman CJ, Chuk SSY, Gu H, Tam KWS, et al. Transmission of SARS-CoV-2 delta variant (AY.127) from pet hamsters to humans, leading to onward human-to-human transmission: a case study. Lancet. 2022;399:1070–8. https://doi.org/10.1016/S0140-6736(22)00326-9

Address for correspondence: Ilaria Capua, One Health Center of Excellence, University of Florida, 1604 McCarty Dr, G047, Gainesville, FL 32611-0135, USA; email: icapua@ufl.edu

Hemotropic *Mycoplasma* spp. in Aquatic Mammals, Amazon Basin, Brazil

Aricia Duarte-Benvenuto, Carlos Sacristán,
Ana Carolina Ewbank, Irene Sacristán,
Roberta Zamana-Ramblas, Waleska Gravena,
Daniela M.D. Mello, Vera M. Ferreira da Silva,
Miriam Marmontel, Vitor L. Carvalho, Juliana Marigo,
José L. Catão-Dias

Author affiliations: University of São Paulo, São Paulo, Brazil
(A. Duarte-Benvenuto, C. Sacristán, A.C. Ewbank,
R. Zamana-Ramblas, J. Marigo, J.L. Catão-Dias); Centro de
Investigación en Sanidad Animal, INIA-CSIC, Madrid, Spain
(C. Sacristán, I. Sacristán); Universidade Federal do Amazonas,
Coari, Brazil (W. Gravena); Instituto Nacional de Pesquisas da
Amazônia, Manaus, Brazil (D.M.D. Mello, V.M. Ferreira da Silva);
Instituto de Desenvolvimento Sustentável Mamirauá, Tefé, Brazil
(M. Marmontel); Associação de Pesquisa e Preservação de
Ecossistemas Aquáticos, Caucaia, Brazil (V.L. Carvalho)

Hemotropic *Mycoplasma* spp. (hemoplasmas) are uncultivable bacteria that infect mammals, including humans. We detected a potentially novel hemoplasma species in blood samples from wild river dolphins in the Amazon River Basin, Brazil. Further investigation could determine pathogenicity and zoonotic potential of the detected hemoplasma.

Hemotropic *Mycoplasma* spp. (hemoplasmas) are uncultivable, cell-wall–deficient, pleomorphic bacteria that infect mammals, including humans (*1*). Although previously linked to anemia, starvation, and death, especially among immunosuppressed humans and animals (*2,3*), most hemoplasma species have subclinical manifestations (*1*). Hemoplasmas are thought to be host specific, but some reports suggest interspecies transmission and zoonotic potential (*3–5*). In aquatic mammals, hemoplasmas have only been reported in California sea lions (*Zalophus californianus*) (*6*).

Amazon river dolphins (*Inia geoffrensis*), Bolivian river dolphins (*I. boliviensis*), and Amazonian manatees (*Trichechus inunguis*) are endemic to the Amazon Basin. Both dolphin species have been classified as endangered, and *T. inunguis* manatees are classified as vulnerable (*7*). Infectious disease studies in these species are scarce. We used 16S rRNA PCR to detect and characterize hemoplasmas among aquatic mammals from the Amazon Basin Region, Brazil.

We analyzed blood samples of 50 wild river dolphins, including 32 *I. geoffrensis* and 18 *I. boliviensis*

dolphins live captured in scientific expeditions (*8*), during 2015 in the Guaporé and Negro Rivers; 2017 in the Tapajós River; and 2020 near Balbina hydroelectric dam (Table). We performed field hematology on wild dolphins and also analyzed blood samples collected during health assessments of 25 *T. inunguis* manatees under human care in Manaus in February 2022 (Appendix Tables 1, 2, https://wwwnc.cdc.gov/EID/article/28/12/22-0971-App1.pdf).

We extracted DNA by using the DNeasy Blood & Tissue Kit (QIAGEN, https://www.qiagen.com), following manufacturer instructions. We screened samples for *Mycoplasma* spp. by 16S rRNA PCR targeting a 384-bp fragment (*9*). We subjected positive samples to PCR targeting a 1,400-bp fragment of 16S rRNA (*10*) and confirmed amplicons by sequencing in both directions.

We used GraphPad Prism version 5 (GraphPad Software, https://www.graphpad.com) to compare prevalence among host species, sampling sites, sampling year, age, and sex, and hematological values in infected and noninfected animals; we considered $p \leq 0.05$ statistically significant. We used the median joining method in PopART software (University of Otagao, https://www.popart.otago.ac.nz) to generate a nucleotide sequence type network. We assessed phylogeographic structure among species and sampling sites by using pairwise fixation index tests (FSTs) in Arlequin (http://cmpg.unibe.ch/software/arlequin3), determining level of significance with 1,000 permutations, and using the nearest-neighbor statistic (S_{nn}) in DnaSP version 5 (Universitat de Barcelona, http://www.ub.edu/dnasp).

We detected *Mycoplasma* DNA in samples from 21 (65.6%, 95% CI 48.2%–83.0%) *I. geoffrensis* and 11 (61.1%, 95% CI 36.2%–86.1%) *I. boliviensis* dolphins. The percentage of *Inia* spp. dolphins testing hemoplasma-positive was higher than that reported for *Z. californianus* California sea lions (12.4%) (*6*). All manatees in our study tested PCR-negative for hemoplasma.

Mycoplasma nucleotide sequences from *Inia* spp. dolphins had <94.0% identity with the closest available sequence (GenBank accession no. CP003731), which was detected in alpacas (*Vicugna pacos*). We submitted 12 representative sequence types to GenBank (Table). Multilocus sequencing typing will be necessary to further characterize the *Mycoplasma* species we detected.

Among animals sampled, adult dolphins had significantly higher hemoplasma prevalence than did calves ($p = 0.0015$). We saw no statistically significant differences among remaining variables, including the hematologic parameters between hemoplasma-positive and hemoplasma-negative dolphins; however, our sample size was small.

Network analyses differentiated the obtained nucleotide sequence types into 3 distinct groups: 1 comprises sequences of all *I. geoffrensis* dolphins samples from Balbina and Tapajós; the other 2, harbor sequences of all *I. boliviensis* dolphins samples from Guaporé, which are greatly divergent (Figure). Our analysis showed statistically significant differences among populations (S_{nn} = 1.0, p = 0.0001; FST = 0.48, p = 0.003), confirming a geographic genetic structure. Haplotype diversity (Hd), average number of nucleotide differences (K), and nucleotide diversity (π) were higher among animals from Guaporé compared with the other 2 sites. For Guaporé, Hd was 0.82, K 43.6, and π 0.03; for Tapajós, Hd was 0.4, K 0.4, and π 0.0003; and for Balbina, Hd was 0.44, K 0.71, and π 0.0005. We also noted that *Mycoplasma* among host species shared genetic structure that differed between the 2 *Inia* species (Snn = 1.0, p = 0.0001; FST = 0.43, p = 0.000). The genetic structure difference between the species and sites likely

Table. Epidemiologic and molecular data of Hemotropic *Mycoplasma* spp. in aquatic mammals, Amazon Basin, Brazil*

Sample no.	Species	Age class/sex	Capture date	River	Hemoplasma detection	GenBank accession no.
1	*Inia geoffrensis*	Adult/F	2017 Oct 6	Tapajós	Y	ON711292
2	*I. geoffrensis*	Calf/M	2017 Oct 6	Tapajós	N	NA
3	*I. geoffrensis*	Adult/M	2017 Oct 7	Tapajós	N	NA
4	*I. geoffrensis*	Juvenile/M	2017 Oct 8	Tapajós	N	NA
5	*I. geoffrensis*	Juvenile/F	2017 Oct 10	Tapajós	Y	ON721292
6	*I. geoffrensis*	Adult/M	2017 Oct 10	Tapajós	Y	ON721292
7	*I. geoffrensis*	Adult/M	2017 Oct 10	Tapajós	Y	ON721292
8	*I. geoffrensis*	Adult/M	2017 Oct 11	Tapajós	Y	ON721300
9	*I. geoffrensis*	Adult/M	2017 Oct 11	Tapajós	Y	ON721302
10	*I. boliviensis*	Adult/M	2015 Feb 6	Guaporé	Y	ON721303
11	*I. boliviensis*	Calf/M	2015 Sept 22	Guaporé	Y	ON721296
12	*I. boliviensis*	Adult/M	2015 Sept 22	Guaporé	N	NA
13	*I. boliviensis*	Adult/F	2015 Sept 22	Guaporé	Y	ON721301
14	*I. boliviensis*	Juvenile/F	2015 Sept 22	Guaporé	N	NA
15	*I. boliviensis*	Juvenile/M	2015 Sept 22	Guaporé	N	NA
16	*I. boliviensis*	Adult/F	2015 Sept 23	Guaporé	N	NA
17	*I. boliviensis*	Calf/M	2015 Sept 23	Guaporé	N	NA
18	*I. boliviensis*	Adult/F	2015 Sept 23	Guaporé	Y	ON721296
19	*I. boliviensis*	Adult/M	2015 Sept 23	Guaporé	Y	ON721301
20	*I. boliviensis*	Adult/M	2015 Sept 24	Guaporé	Y	ON721297
21	*I. boliviensis*	Juvenile/M	2015 Sept 24	Guaporé	N	NA
22	*I. boliviensis*	Juvenile/M	2015 Sept 25	Guaporé	N	NA
23	*I. boliviensis*	Adult/M	2015 Sept 26	Guaporé	Y	ON121301
24	*I. boliviensis*	Adult/F	2015 Sept 27	Guaporé	Y	ON721296
25	*I. boliviensis*	Adult/M	2015 Sept 27	Guaporé	Y	ON121301
26	*I. boliviensis*	Adult/M	2015 Sept 27	Guaporé	Y	ON711298
27	*I. boliviensis*	Adult/M	2015 Sept 27	Guaporé	Y	ON721297
28	*I. geoffrensis*	Calf/M	2015	Negro	N	NA
29	*I. geoffrensis*	Adult/F	2020 Dec 2	Balbina	Y	ON721299
30	*I. geoffrensis*	Calf/F	2020 Dec 2	Balbina	N	NA
31	*I. geoffrensis*	Juvenile/M	2020 Dec 2	Balbina	N	NA
32	*I. geoffrensis*	Adult/M	2020 Dec 2	Balbina	Y	ON721299
33	*I. geoffrensis*	Adult/M	2020 Dec 2	Balbina	N	NA
34	*I. geoffrensis*	Juvenile/M	2020 Dec 3	Balbina	Y	ON721299
35	*I. geoffrensis*	Adult/M	2020 Dec 3	Balbina	N	NA
36	*I. geoffrensis*	Juvenile/M	2020 Dec 3	Balbina	Y	ON721299
37	*I. geoffrensis*	Juvenile/M	2020 Dec 4	Balbina	N	NA
38	*I. geoffrensis*	Juvenile/M	2020 Dec 4	Balbina	N	NA
39	*I. geoffrensis*	Juvenile/F	2020 Dec 4	Balbina	Y	ON721299
40	*I. geoffrensis*	Juvenile/M	2020 Dec 4	Balbina	Y	ON721299
41	*I. geoffrensis*	Adult/M	2020 Dec 4	Balbina	Y	ON721299
42	*I. geoffrensis*	Juvenile/M	2020 Dec 4	Balbina	Y	ON721295
43	*I. geoffrensis*	Juvenile/M	2020 Dec 5	Balbina	Y	ON721299
44	*I. geoffrensis*	Juvenile/M	2020 Dec 5	Balbina	Y	ON721299
45	*I. geoffrensis*	Adult/M	2020 Dec 5	Balbina	Y	ON721293
46	*I. geoffrensis*	Juvenile/M	2020 Dec 5	Balbina	Y	ON721293
47	*I. geoffrensis*	Juvenile/M	2020 Dec 5	Balbina	Y	ON721299
48	*I. geoffrensis*	Juvenile/M	2020 Dec 5	Balbina	Y	ON721299
49	*I. geoffrensis*	Adult/M	2020 Dec 6	Balbina	Y	ON721294
50	*I. geoffrensis*	Juvenile/M	2020 Dec 6	Balbina	N	NA

*Amazon river dolphins (*I. geoffrensis*) and Bolivian river dolphins (*I. boliviensis*) were live captured in scientific expeditions in Guaporé, Tapajós, and Negro rivers, and at the Balbina hydroelectric dam. NA, not applicable.
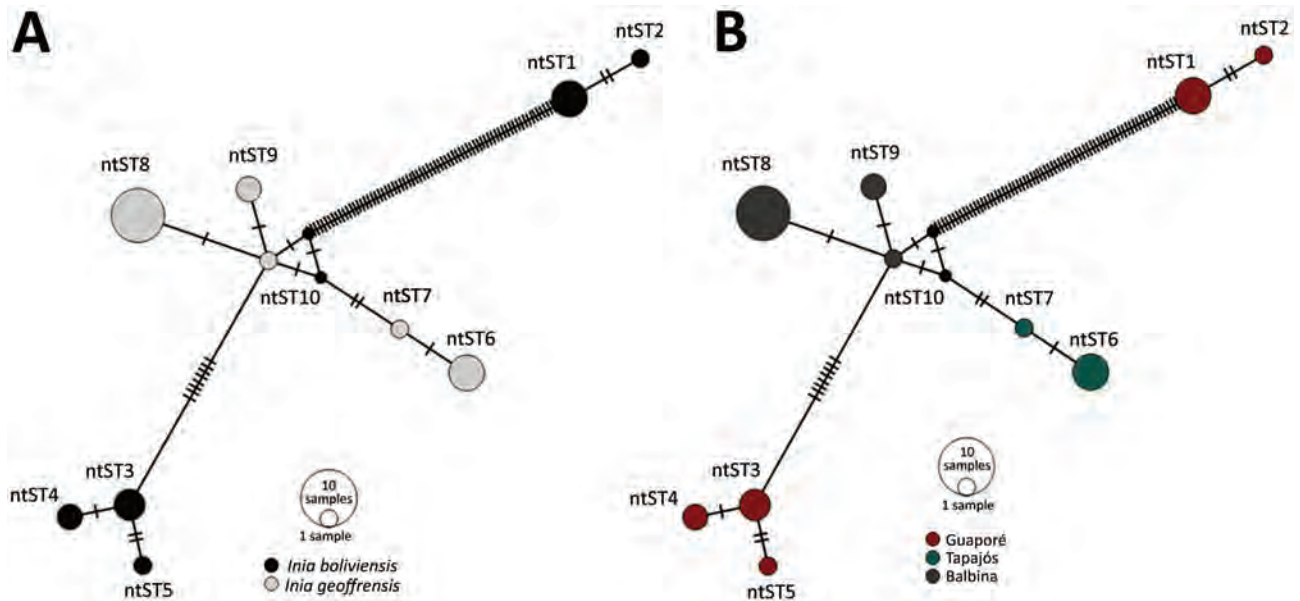
Figure. ntST network analyses of hemotropic *Mycoplasma* spp. (hemoplasmas) from aquatic mammals, Amazon Basin, Brazil. We noted hemoplasmas divergence between 2 dolphin species (A) and sampling sites (B). The analysis differentiated the retrieved hemoplasmas nucleotide sequence types in 3 distinct groups: 1 group comprised all sequences obtained from Amazon river dolphins (*Inia geoffrensis*) from the Balbina Dam and Tapajós River; the other 2 harbored all sequences from Bolivian river dolphins (*I. boliviensis*) from the Guaporé River. ntST, nucleotide sequence type.

reflects geographic separation of the studied populations (Appendix Figure 1). However, geographic separation does not explain the hemoplasma divergence between the 2 sequence types collected from *I. boliviensis* dolphins. All retrieved sequences clustered together and with other hemoplasma sequences of unknown pathogenicity (Appendix Figure 2).

Our findings indicate that aquatic mammals can be infected by hemoplasmas, but epidemiology remains unknown. In terrestrial mammals, hematophagous vectors are the main proposed transmission route (*1*). *T. inunguis* manatees in our study tested hemoplasma-negative despite being housed in tanks close to the forest without vector protection. This finding suggests food could be a transmission route among aquatic mammals because river dolphins are piscivorous and manatees are herbivorous. Also, 5 female dolphins captured with calves tested positive, but the calves tested negative, which might exclude vertical transmission. Endoparasitism or direct contact are other possible transmission routes.

In conclusion, we detected hemoplasmas in *I. geoffrensis* and *I. boliviensis* river dolphins. Pathogenicity and zoonotic potential require further investigation, but the high hemoplasma prevalence in adult mammals and detection among animals over several years suggest hemoplasma endemicity in these dolphin populations.

no. 1169/2019, ICMBio/MMA (authorization no. 13157), and SISGEN authorization no. AAF009C.

About the Author

Dr. Duarte-Benvenuto is a veterinarian and a doctorate student at the Laboratory of Wildlife Comparative Pathology in University of São Paulo, Brazil. Her primary research interest is wildlife disease and conservation, especially of aquatic mammals.

References

1. Millán J, Di Cataldo S, Volokhov DV, Becker DJ. Worldwide occurrence of haemoplasmas in wildlife: Insights into the patterns of infection, transmission, pathology and zoonotic potential. Transbound Emerg Dis. 2020;68:3236–56.
2. Sykes JE, Tasker S. Hemoplasma infections. In: Sykes JE, editor. Canine and feline infectious diseases. St. Louis: Saunders; 2013. p. 390–398.
3. Descloux, E., Mediannikov, O., Gourinat, A.C., Colot, J., Chauvet, M., Mermoud, I. et al. Flying fox hemolytic fever, description of a new zoonosis caused by *Candidatus* Mycoplasma haemohominis. Clin Infect Dis. 2021;73:e1445–52. https://doi.org/10.1093/cid/ciaa1648
4. Pires dos Santos A, Pires dos Santos R, Biondo AW, Dora JM, Goldani LZ, Tostes de Oliveira S, et al. Hemoplasma infection in HIV-positive patient, Brazil. Emerg Infect Dis. 2008;14:1922–4. https://doi.org/10.3201/eid1412.080964
5. Sacristán I, Acuña F, Aguilar E, García S, López MJ, Cevidanes A, et al. Assessing cross-species transmission of hemoplasmas at the wild-domestic felid interface in Chile using genetic and landscape variables analysis. Sci Rep. 2019;9:16816. https://doi.org/10.1038/s41598-019-53184-4
6. Volokhov DV, Norris T, Rios C, Davidson MK, Messick JB, Gulland FM, et al. Novel Hemotrophic mycoplasma identified in naturally infected California sea lions (*Zalophus californianus*). Vet Microbiol. 2011;149:262–8. https://doi.org/10.1016/j.vetmic.2010.10.026
7. International Union for Conservation of Nature and Natural Resources. The IUCN red list of threatened species [cited 2021 Jun 18]. https://www.iucnredlist.org
8. da Silva VMF, Martin AR. A study of the Boto, or Amazon River Dolphin (*Inia geoffrensis*), in the Mamirauá Reserve, Brazil: operation and techniques. Occas Pap IUCN Species Surviv Comm. 2001;23:121–30.
9. Cabello J, Altet L, Napolitano C, Sastre N, Hidalgo E, Dávila JA, et al. Survey of infectious agents in the endangered Darwin's fox (*Lycalopex fulvipes*): high prevalence and diversity of Hemotrophic mycoplasmas. Vet Microbiol. 2013;167:448–54. https://doi.org/10.1016/j.vetmic.2013.09.034
10. Harasawa R, Orusa R, Giangaspero M. Molecular evidence for Hemotropic mycoplasma infection in a Japanese badger (*Meles meles anakuma*) and a raccoon dog (*Nyctereutes procyonoides viverrinus*). J Wildl Dis. 2014;50:412–5. https://doi.org/10.7589/2013-09-229

Address for correspondence: Aricia Duarte-Benvenuto, Laboratório de Patologia Experimental e Comparada, 87 Prof. Dr. Orlando Marques de Paiva Ave, São Paulo 05508270, Brazil; email address: aricia.benvenuto@gmail.com

Human Thelaziosis Caused by *Thelazia callipaeda* Eyeworm, Hungary

Hajnalka Juhász, Géza Thury, Mária Szécsényi, Edit Tóth-Molnár, Katalin Burián, Zoltán Deim, Gabriella Terhes

Ocular infections with *Thelazia callipaeda* eyeworms in Europe have become more common. We report a case in Hungary caused by *T. callipaeda* eyeworms in a 45-year-old woman who had no travel history abroad.

Author affiliation: University of Szeged, Szeged, Hungary\

*T*helazia spp. (Spirurida, Thelaziidae) are vectorborne zoonotic nematodes that can parasitize conjunctiva and surrounding structures of wild and domestic animals as well as humans (*1*). Before 2022, a total of 16 species of *Thelazia* had been described; 3 species, *T. callipaeda*, *T. californiensis*, and *T. gulosa*, are known to infect humans. *T. callipaeda* nematodes, commonly known as eyeworms, cause autochthonous cases in Europe (*2*). The earliest reported endemic infection in Europe was detected in a dog in the Piedmont region of Italy in 1989. Since then, several animal and human cases have been documented throughout Europe (Appendix Table 1, https://wwwnc.cdc.gov/EID/article/28/12/22-0757-App1.pdf) (*1–4*). In Europe, under natural conditions, the only known vector and intermediate host of *T. callipaeda* eyeworms is the lachryphagous male *Phortica variegate* fly (*1,5*). The biologic activity of the fly is affected by temperature (20°C–25°C) and relative humidity (50%–75%) (*1,6*). The most common clinical manifestations of *T. callipaeda* infections are lacrimation, foreign body sensation, itchiness, conjunctivitis, and follicular hypertrophy of the conjunctiva; the affected eye may also show severe keratitis and corneal ulceration. Treatment of this infection in humans is primarily the mechanical removal of worms, which is more difficult in their immature stages (*7*).

In Hungary, *T. callipaeda* infection has been described in dogs (*3*). We report a case of conjunctivitis in a human caused by *T. callipaeda* eyeworms. Our goal is to draw the scientific community's attention to this spillover event.

A 45-year-old woman in Hungary was referred to an ophthalmologist in September 2020; she had a foreign-body sensation and redness in her left eye for a week. Slit-lamp examination revealed conjunctivitis. Empiric tobramycin and dexamethasone therapies were initiated. At the time of follow-up, 3 thin, creamy white live worms were removed from the conjunctival fornices of her left eye (Figure). Left eye examination revealed follicular conjunctival hypertrophy. The cornea was not affected, visual acuity was 20/20 on both eyes, and intraocular pressure was in the normal range. The patient's medical history was uneventful. Laboratory examination showed no elevated leukocytes, C-reactive protein, or erythrocyte sedimentation rate. The patient had no peripheral blood eosinophilia. Because of worsened conjunctivitis, 2% boric acid was applied for 5 days after removal of the worms. On the last follow-up visit, the patient had no symptoms.

Two worms were sent to the Department of Medical Microbiology, University of Szeged (Szeged, Hungary). We examined them under a light microscope (Leica DM 100; Leica Microsystems, https://www.leica-microsystems.com). Wet-mount preparation showed the presence of a characteristic vase-shaped buccal cavity (Figure, panel C) and serrated cuticula with transverse striations. The position of the vulva was anterior to the esophago-junction (8). The anterior half of the abdominal cavity contained first-stage larvae; the posterior part contained eggs. The nematodes were 15 mm and 14 mm long. We identified them as female *T. callipaeda* eyeworms on the basis of morphologic features. We isolated total DNA from one using QIAamp DNA mini kit (QIAGEN, https://www.qiagen.com) in accordance with tissue protocol; we then performed an in-house PCR targeting *cox*1 as described previously by Čabanová et al (9). Sequence analysis of the amplified PCR product (GenBank accession no. OP278871) showed 100% homology with *T. callipaeda* haplotype 1 strains in GenBank (Appendix Figure 1).

We describe an autochthonous case of a patient with *T. callipaeda* eyeworm ocular infection in Hungary. The patient had no travel history abroad. In July, she visited the Bükk National Park in northeastern Hungary, where she saw a lot of flies. This vector is widely distributed in southern and central Europe and exists in Hungary as well (1,10). Its lachryphagous activity depends mostly on temperature, so climatic changes affect the spread of infection toward the north, affecting new areas (1,6). Until December 2017, a total of 10 canine thelaziosis cases were identified by Farkas et al. in Hungary (3). Most of them visited the same park located in Borsod-Abaúj-Zemplén as our patient (3). That study also suggested that wild carnivores, mainly red foxes, had a role in spreading thelaziosis beyond the border (3). The emergence of human thelaziosis
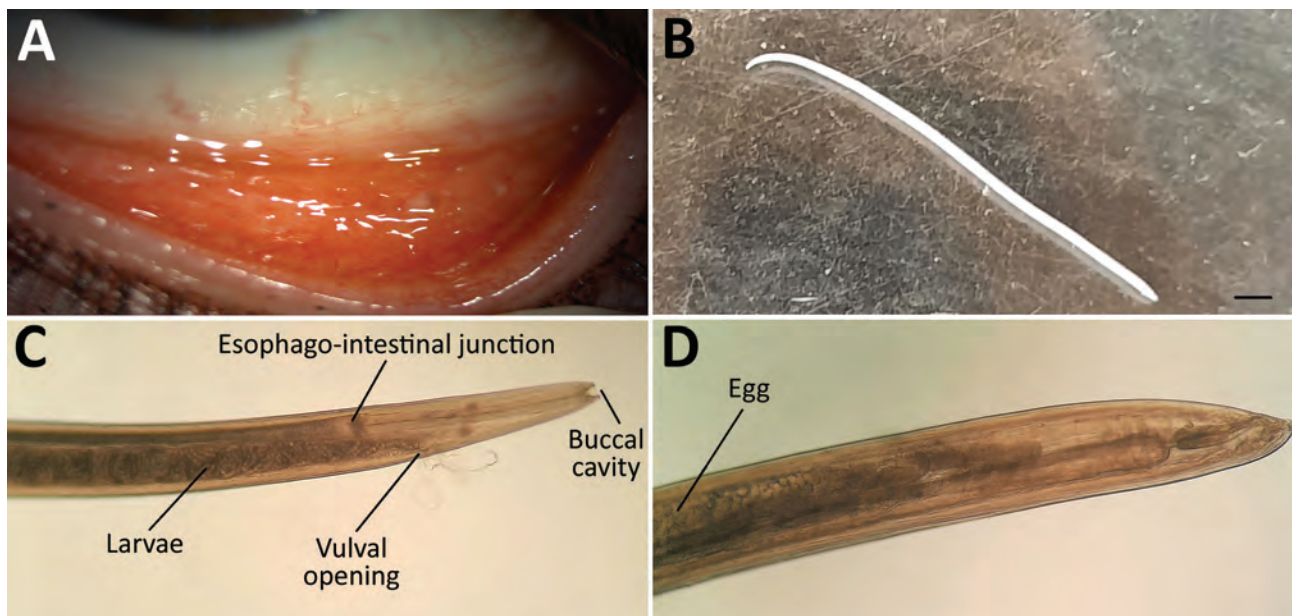
Figure. Imaging results for *Thelazia callipaeda* eyeworm infection in a woman in Hungary. A) Follicles in the inferior tarsal conjunctiva in the patient's left eye 5 days after removal of an adult female *T. callipaeda* worm. B) Female worm removed from the patient's left eye. Scale bar indicates 1 mm. C, D) Morphologic characteristics of the *T. callipaeda* worm from the patient (C) and eggs visible within the specimen (D). Original magnification ×100.

may be explained by the fact that the number of red foxes in Hungary has tripled during the past 50 years (Appendix Figure 2) (Appendix reference *11*). In human case-patients, the first-choice therapy is to remove the worms mechanically by flushing the conjunctival sac with sterile physiologic saline under local anesthesia (Appendix reference *12*).

From a therapeutic and epidemiologic standpoint, it is important to differentiate between infectious and allergic conjunctivitis. Furthermore, diagnosis can be difficult because immature larvae can hide in the excretory ducts of the lacrimal glands (*7*). Our findings indicate the need for education and raised awareness about this infection especially for ophthalmologists. Early and adequate diagnosis can help to prevent complications such as corneal ulceration.

About the Author

Ms. Juhász is a biologist specializing in clinical microbiology in the Department of Medical Microbiology, University of Szeged, Szeged, Hungary. Her primary research interests are human viral, bacterial, and parasitic infections, focusing on respiratory tract pathogens.

References

1. Palfreyman J, Graham-Brown J, Caminade C, Gilmore P, Otranto D, Williams DJL. Predicting the distribution of *Phortica variegata* and potential for *Thelazia callipaeda* transmission in Europe and the United Kingdom. Parasit Vectors. 2018;11:272. https://doi.org/10.1186/s13071-018-2842-4
2. do Vale B, Lopes AP, da Conceição Fontes M, Silvestre M, Cardoso L, Coelho AC. Systematic review on infection and disease caused by *Thelazia callipaeda* in Europe: 2001–2020. Parasite. 2020;27:52. https://doi.org/10.1051/parasite/2020048
3. Farkas R, Takács N, Gyurkovszky M, Henszelmann N, Kisgergely J, Balka G, et al. The first feline and new canine cases of *Thelazia callipaeda* (Spirurida: Thelaziidae) infection in Hungary. Parasit Vectors. 2018;11:338. https://doi.org/10.1186/s13071-018-2925-2
4. Morgado ACT, do Vale B, Ribeiro P, Coutinho T, Santos-Silva S, de Sousa Moreira A, et al. First report of human *Thelazia callipaeda* infection in Portugal. Acta Trop. 2022;231:106436. https://doi.org/10.1016/j.actatropica.2022.106436
5. Rolbiecki L, Izdebska JN, Franke M, Iliszko L, Fryderyk S. The vector-borne zoonotic nematode *Thelazia callipaeda* in the eastern part of Europe, with a clinical case report in a dog in Poland. Pathogens. 2021;10:55. https://doi.org/10.3390/pathogens10010055
6. Pombi M, Marino V, Jaenike J, Graham-Brown J, Bernardini I, Lia RP, et al. Temperature is a common climatic descriptor of lachryphagous activity period in *Phortica variegata* (Diptera: Drosophilidae) from multiple geographical locations. Parasit Vectors. 2020;13:89. https://doi.org/10.1186/s13071-020-3955-0
7. do Vale B, Lopes AP, da Conceição Fontes M, Silvestre M, Cardoso L, Coelho AC. Thelaziosis due to *Thelazia callipaeda* in Europe in the 21st century—a review. Vet Parasitol. 2019; 275:108957. https://doi.org/10.1016/j.vetpar.2019.108957
8. Otranto D, Lia RP, Buono V, Traversa D, Giangaspero A. Biology of *Thelazia callipaeda* (Spirurida, Thelaziidae) eyeworms in naturally infected definitive hosts. Parasitology. 2004;129:627–33. https://doi.org/10.1017/S0031182004006018
9. Čabanová V, Kocák P, Víchová B, Miterpáková M. First autochthonous cases of canine thelaziosis in Slovakia: a new affected area in Central Europe. Parasit Vectors. 2017;10:179. https://doi.org/10.1186/s13071-017-2128-2
10. Papp L. Dipterous guilds of small-sized feeding sources in forests of Hungary. Acta Zool Acad Sci Hung. 2002; 48:197–213.

Address for correspondence: Gabriella Terhes, Department of Medical Microbiology, University of Szeged, H-6725 Szeged, Semmelweis street 6, Szeged, Hungary; email: terhes.gabriella@med.u-szeged.hu

Severe Human Case of Zoonotic Infection with Swine-Origin Influenza A Virus, Denmark, 2021

Klara M. Andersen, Lasse S. Vestergaard, Jakob N. Nissen, Sophie J. George, Pia Ryt-Hansen, Charlotte K. Hjulsager, Jesper S. Krog, Marianne N. Skov, Søren Alexandersen, Lars E. Larsen, Ramona Trebbien

Author affiliations: Technical University of Denmark, Kongens Lyngby, Denmark (K.M. Andersen); Statens Serum Institut, Copenhagen, Denmark (K.M. Andersen, L.S. Vestergaard, J.N. Nissen, C.K. Hjulsager, J.S. Krog, S. Alexandersen, R. Trebbien); University of Copenhagen, Copenhagen (S.J. George, P. Ryt-Hansen, L.E. Larsen); Odense University

During routine surveillance at the National Influenza Center, Denmark, we detected a zoonotic swine influenza A virus in a patient who became severely ill. We describe the clinical picture and the genetic characterization of this variant virus, which is distinct from another variant found previously in Denmark.

Hospital, Odense, Denmark (M.N. Skov)

Human infections with swine influenza A viruses (IAVs) are sporadically reported (1–4). Increased surveillance has revealed substantial swine IAV circulation within pig herds and frequent reassortment with human seasonal IAVs (5). Despite no sustained human-to-human transmission of variant IAV cases since the 2009 influenza A(H1N1) pandemic, the zoonotic potential is of concern. We report a case of human infection with a swine-origin IAV that resulted in severe illness in a younger, otherwise healthy person employed at a swine slaughterhouse in Denmark. This case was detected 10 months after our previously reported case (4). The patient provided informed consent for publication of this case report.

On November 24, 2021, a person of ≈50 years of age was hospitalized after acute onset of illness characterized by dizziness on the night of November 23, 2021, followed by chest pain, pain radiating toward the left arm, diarrhea, and malaise that developed the next morning, but no fever. The patient called for emergency medical assistance, which arrived shortly. During ambulance transportation and at hospital arrival, the patient experienced repeated convulsions and was admitted to the intensive care unit and put on mechanical ventilation to manage seizures and associated reduced oxygen level. Extensive clinical examination, such as laboratory investigations (i.e., biochemical, microbiological, and immunological assays), multiorgan radiological ex-
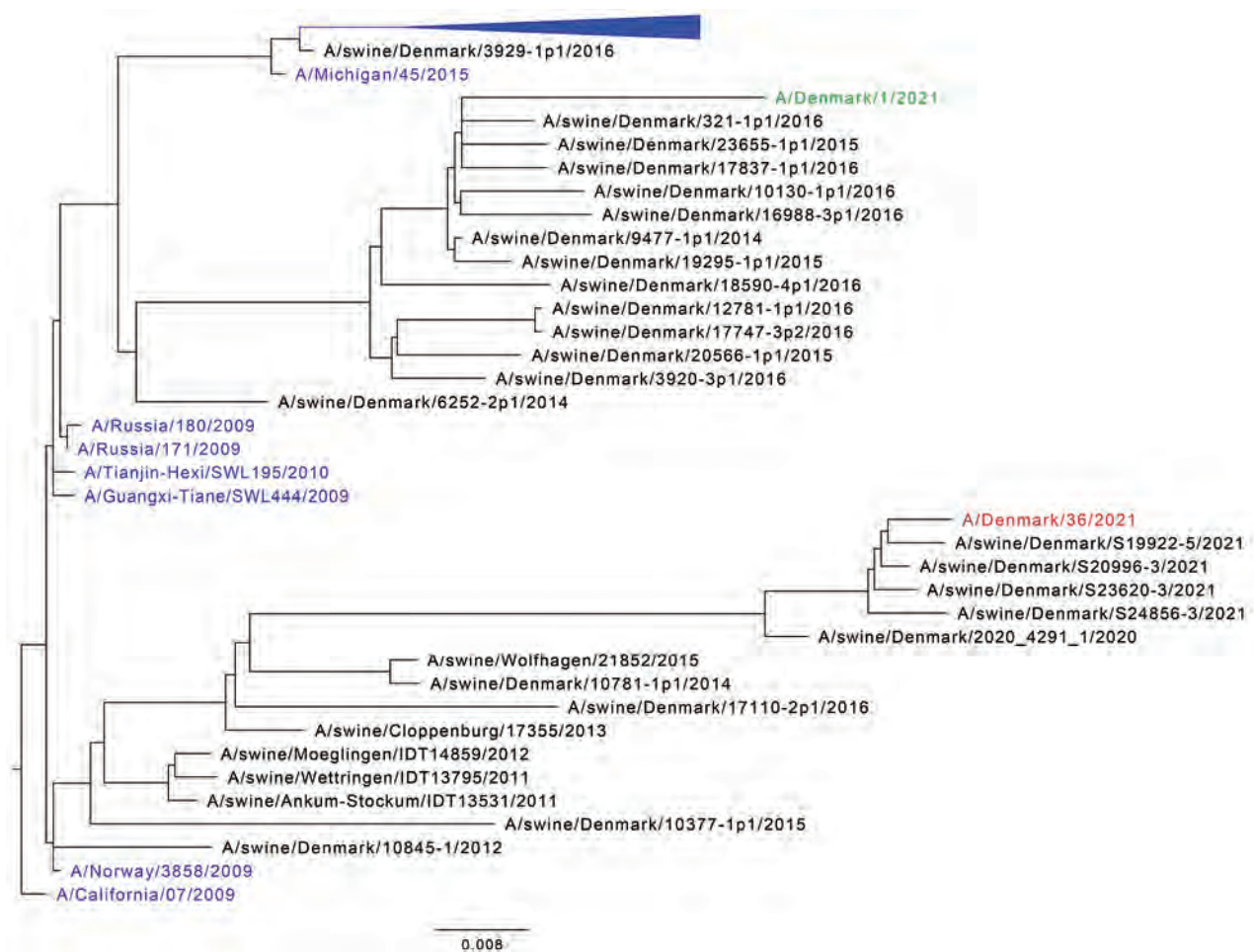
Figure. Maximum-likelihood phylogenetic tree of the hemagglutinin gene of influenza A virus from a patient in Denmark (A/Denmark/36/2021), the seasonal vaccine strain, and closely related strains. The tree includes the case variant virus A/Denmark/36/2021 (red), the 10 closest BLAST matches (https://blast.ncbi.nlm.nih.gov/Blast.cgi), the previously reported Denmark variant virus A/Denmark/1/2021 (green), human seasonal reference viruses with >85% nucleotide identity to A/Denmark/36/2021 (Appendix 2 Table, https://wwwnc.cdc.gov/EID/article/28/12/22-0935-App2.xlsx), and representative viruses from the passive surveillance program of influenza viruses in pigs from Denmark. The tree is rooted on A/California/07/2009. Human IAV sequences are shown in blue, and most seasonal reference viruses have been collapsed. Scale bar indicates nucleotide substitutions per site.

Table. Percentage nucleotide and amino acid identities between influenza A virus from a patient in Denmark (A/Denmark/36/2021), the seasonal vaccine strain, and closely related strains*

Gene	A/Victoria/2570/2019	A/swine/Denmark/S19 922-5/2021	A/swine/Denmark/24856 -3/2021	A/swine/Denmark/S222 82-5/2021	A/Denmark/1/202 1
Pairwise nucleotide identity to A/Denmark/36/2021, %					
PB2	94.8	99.4	98.9	99.4	96.1
PB1	94.7	99.5	98.9	99.3	93.6
PA	95.2	99.8	99.3	99.6	96.8
HA	90.7	99.0	98.7	72.6	89.9
NP	95.3	99.7	98.9	99.4	96.4
NA	86.9	99.3	98.7	n/a	87.0
MP	95.2	99.6	99.6	92.6	95.3
NS	79.7	99.9	99.1	99.6	92.8
Pairwise amino acid identity to A/Denmark/36/2021, %					
PB2	97.2	99.6	99.5	99.6	97.9
PB1	97.6	99.9	99.5	99.9	97.9
PA	97.6	99.9	99.3	99.4	98.3
PA-X	96.6	100	100	100	98.7
HA	90.3	98.8	98.6	75.8	88.5
NP	98.2	100	99.6	99.8	98.4
NA	85.1	98.9	97.4	n/a	86.1
M1	97.6	100	100	97.6	97.6
M2	94.9	100	100	90.7	93.8
NS1	72.4	99.6	98.3	99.1	91.7
NEP	85.1	100	100	100	95

*Seasonal vaccine strain, A/Victoria/2570/2019 (GISAID isolate no. EPI_ISL_517733; Appendix 2, https://wwwnc.cdc.gov/EID/article/28/12/22-0935-App2.xlsx); strains from passive surveillance Denmark: A/swine/Denmark/S19922–5/2021 (GenBank accession nos. ON716251–8), A/swine/Denmark/24856-3/2021 (accession nos. ON716275–82), A/swine/Denmark/S22282-5/2021 (accession nos. ON716267–74); and another recent variant case found in Denmark (A/Denmark/1/2021; GISAID isolate no. EPI_ISL_909652) (*4*). The A/swine/Denmark/S22282-5/2021 is of the H1N2 subtype and therefore no percentage similarity is reported to the neuraminidase gene segment and protein of this strain. HA, hemagglutinin; MP/M1/M2, matrix protein 1/2; NA, neuraminidase; n/a, not applicable; NEP, nuclear export protein; NP, nucleoprotein; NS/NS1, nonstructural protein; PA, polymerase acidic protein; PB1/2, polymerase basic protein 1/2.

aminations, and electroencephalography (Appendix 1, https://wwwnc.cdc.gov/EID/article/28/12/22-0935-App1.pdf), identified no cardiovascular, renal, neurologic, or other diseases that could explain the sudden severe illness. However, a tracheal sample collected and analyzed at the local microbiology laboratory was found positive for IAV (Appendix 1). No other microbiological agents were detected, including SARS-CoV-2 or other respiratory viruses, and the patient showed no signs of pneumonia. The patient received antiviral medication (oseltamivir) and various supportive treatments, and over the next 2 days the clinical condition improved; the patient was soon after discharged from the hospital.

The remaining sample material was submitted to the Danish National Influenza Center as part of routine influenza surveillance. The sample was confirmed positive for the pandemic H1N1 strain and was further analyzed by whole-genome sequencing (Appendix 1). Consensus sequences for the virus named A/Denmark/36/2021 were uploaded to GISAID (https://www.gisaid.org; isolate no. EPI_ISL_8786194). WGS confirmed the H1N1 subtype; however, the virus had closer similarity to swine IAVs (Figure) than to other human strains. BLAST (https://blast.ncbi.nlm.nih.gov/Blast.cgi) searches revealed no close matches to IAV sequences in GenBank or GISAID, but comparison to in-house

sequences from the passive surveillance of influenza viruses in pigs from Denmark revealed close similarity to 2021 swine IAVs (Table). Phylogenetic analyses showed that most gene segments were related to the pandemic H1N1 subtype (clade 1A3.3.2), whereas the neuraminidase and nonstructural segments belonged to the clade 1C Eurasian avian-like swine influenza A(H1N1) (Figure; Appendix 1 Figures 1–7). In contrast, another variant virus found recently in Denmark had a clade 1C nonstructural segment, whereas the 7 other gene segments were related to clade 1A3.3.2 pandemic H1N1 viruses (*4*).

In-depth interviews with the patient revealed occupational exposure to swine in a pig slaughterhouse in Denmark, which appears the most likely place of infection. The patient handled live pigs, carcasses, and meat during the slaughtering process while wearing protective equipment including gloves and gown but no face mask. The patient was previously healthy, had no underlying diseases or immune deficiencies, and had received the recommended quadrivalent seasonal influenza vaccine in October 2021.

No other cases of influenza had been reported at the patient's workplace or among close contacts. In the 2021–22 influenza season, 16,160 cases of influenza A virus occurred among 244,184 tested samples in Denmark; the H3N2 subtype was dominant. No other human cases of swine-origin

influenza virus were detected during this period. Genetic analyses and antigenic characterization of the virus (Appendix 1 Table 1, Figure 8) showed several genetic and antigenic differences and suggested poor reactivity to the contemporary human seasonal influenza vaccine.

This reported case is considered independent of the previously reported variant infection in Denmark (4), because the 2 viruses are genetically distinct (Table). The symptoms were also different; the earlier case was in an elderly patient with comorbidities who experienced classical influenza-like illness, but in this case, a previously healthy adult of younger age experienced unusual severe and sudden illness. Influenza-associated convulsions in adults are rare (6) and mostly accompanied by fever or encephalitis, which was not observed in this patient.

The identification of variant IAVs emphasizes the zoonotic potential of these strains and highlights the importance of continued monitoring of both human and swine IAVs. The reported case suggests a need for focusing on early registration of swine exposure for humans with influenza-like illness, as well as increased measures to reduce the swine IAV exposure risk for people with occupational contact with swine.

About the Author

Ms. Andersen is a PhD student at the Department of Health Technology, Technical University of Denmark and at the National Influenza Center, Statens Serum Institut, Denmark. Her research interests are the genetic evolution of influenza A viruses at the human/swine interface and using bioinformatics to identify genetic markers of zoonotic transmission.

References
1. Freidl GS, Meijer A, de Bruin E, de Nardi M, Munoz O, Capua I, et al.; FLURISK Consortium. Influenza at the animal-human interface: a review of the literature for virological evidence of human infection with swine or avian influenza viruses other than A(H5N1). Euro Surveill. 2014;19:20793. https://doi.org/10.2807/1560-7917.ES2014.19.18.20793
2. Parys A, Vandoorn E, King J, Graaf A, Pohlmann A, Beer M, et al. Human infection with Eurasian avian-like swine influenza A(H1N1) virus, the Netherlands, September 2019. Emerg Infect Dis. 2021;27:939–43. https://doi.org/10.3201/eid2703.201863
3. Dürrwald R, Wedde M, Biere B, Oh DY, Heßler-Klee M, Geidel C, et al. Zoonotic infection with swine A/H1$_{av}$N1 influenza virus in a child, Germany, June 2020. Euro Surveill. 2020;25:2001638. https://doi.org/10.2807/1560-7917.ES.2020.25.42.2001638
4. Nissen JN, George SJ, Hjulsager CK, Krog JS, Nielsen XC, Madsen TV, et al. Reassortant influenza A(H1N1)pdm09 virus in elderly woman, Denmark, January 2021. Emerg Infect Dis. 2021;27:3202–5. https://doi.org/10.3201/eid2712.211361
5. Ryt-Hansen P, Krog JS, Breum SØ, Hjulsager CK, Pedersen AG, Trebbien R, et al. Co-circulation of multiple influenza A reassortants in swine harboring genes from seasonal human and swine influenza viruses. eLife. 2021;10:10. https://doi.org/10.7554/eLife.60940
6. Ruisanchez-Nieva A, Martinez-Arroyo A, Gomez-Beldarrain M, Bocos Portillo J, Garcia-Monco JC. Influenza-associated seizures in healthy adults: Report of 3 cases. Epilepsy Behav Case Rep. 2017;8:12–3. https://doi.org/10.1016/j.ebcr.2017.01.003

Address for correspondence: Klara Marie Andersen, Statens Serum Institut, Artillerivej 5, 2300 Copenhagen S, Denmark; email: kman@ssi.dk

Autochthonous *Angiostrongylus cantonensis* Lungworms in Urban Rats, Valencia, Spain, 2021

María Teresa Galán-Puchades,[1] Mercedes Gómez-Samblás,[1] Antonio Osuna, Sandra Sáez-Durán, Rubén Bueno-Marí, Màrius V. Fuentes

Author affiliations: University of Valencia, Burjassot-Valencia, Spain (M.T. Galán-Puchades, S. Sáez-Durán, R. Bueno-Marí, M.V. Fuentes); University of Granada, Granada, Spain (M. Gómez-Samblás, A. Osuna); Laboratorios Lokímica,

[1]These first authors contributed equally to this article.

To determine the role of rats as potential reservoirs of zoonotic parasites, we examined rats trapped in urban sewers of Valencia, Spain, in 2021. Morphologic and molecular identification and sequencing identified autochthonous *Angiostrongylus cantonensis* nematodes, the most common cause of human eosinophilic meningitis, in pulmonary arteries of *Rattus norvegicus* and *R. rattus* rats.

Catarroja-Valencia, Spain (R. Bueno-Marí)

In Valencia, Spain, permanent rodent control campaigns are the responsibility of The Pest Control Section of the Health Service of Valencia City Council. As part of its tasks, the Section traps *Rattus norvegicus* and *R. rattus* rats in standard snap traps in the sewage system of Valencia. The trapped rodents were preserved in their entirety at −20°C and subsequently, to determine the potential reservoir role of zoonotic parasitic diseases, we defrosted the rats and analyzed the endoparasites.

In 2021, we collected 29 adult *A. cantonensis* nematodes (21 female and 8 male) from the organs of the first 27 trapped rats (25 *R. norvegicus* and 2 *R. rattus*) under a stereomicroscope once the rats had been dissected. The nematodes were detected in the pulmonary arteries of 2 *R. norvegicus* rats and 1 *R. rattus* rat; 7 young nematode adults were also found in the brain of the same *R. rattus* rat. Adult females showed the typical barber pole spiral of lungworms of the genus *Angiostrongylus* (Figure, panel A). After clarifying adult male worms with Amman's lactophenol and studying their morphology (Figure, panels B–D), we found that the measurements were consistent with rat

lungworm species of *A. cantonensis* (Table) (1,2).

The parasite morphology, its microhabitat, and the nature of the definitive hosts clearly suggested that the parasites were *A. cantonensis.* To confirm species identification, we isolated total genomic DNA by using the DNeasy Blood and Tissue kit (QIAGEN, https://www.qiagen.com) according to the manufacturer's instructions. We confirmed nematode species identity by PCR and sequencing of the cytochrome c oxidase subunit 1 (3); all sequences obtained were clustered with *A. cantonensis*. The phylogenetic tree grouped the *A. cantonensis* lungworms from Valencia close to the published sequences MK570629 and MN227185, corresponding to *A. cantonensis* lungworms isolated from Tenerife and Mallorca, respectively (Appendix Figure 1, https://wwwnc.cdc.gov/EID/article/28/12/22-0418-App1.pdf). We submitted the sequences we obtained to GenBank (accession no. ON819883 for the female specimen and ON819884 for the male). Likewise, when we sequenced the second internal transcribed spacer region, we found that our specimens formed a clade that differed from the other species of *Angiostrongylus* (Appendix Figure 2). We also submitted those sequences to GenBank (accession no. OM829831 for the male specimen and OM829832 for the female).

Male and female adult *A. cantonensis* lungworms live in the pulmonary arteries of *Rattus* rats, their preferred definitive hosts (4). Intermediate hosts are terrestrial or freshwater mollusks, such as snails and slugs. The female worms lay eggs, which give rise to L1 larvae that penetrate the alveolae and are swallowed by the rat and shed in the feces. After ingestion by an intermediate
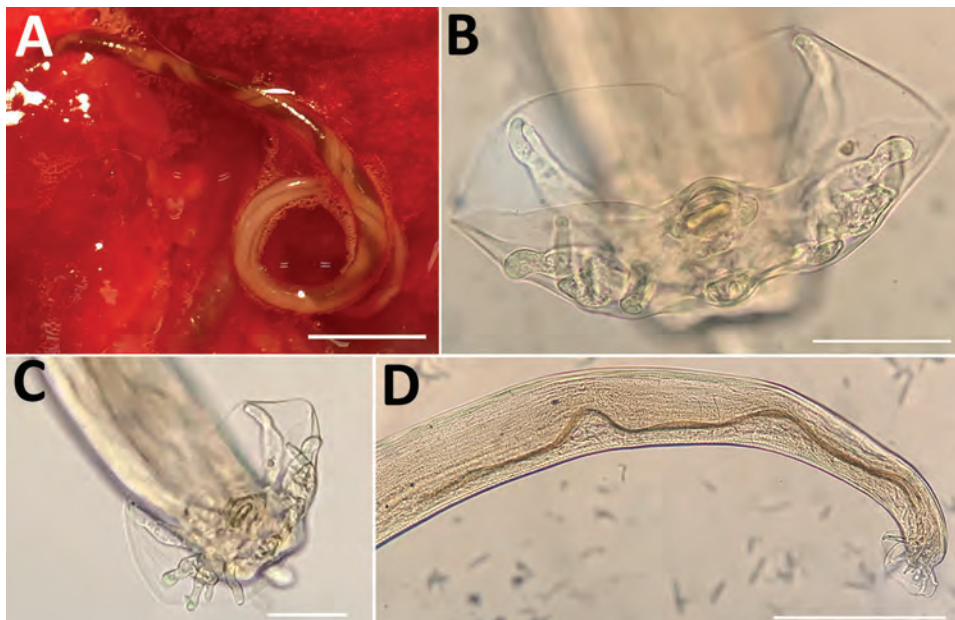

Figure. *Angiostrongylus cantonensis* lungworms from lungs of rats trapped in Valencia, Spain, 2021. A) Adult female with characteristic barber-pole appearance. Scale bar indicates 500 μm. B, C) Copulatory bursae of 2 male worms supported by bursal rays. Scale bars indicate 50 μm. D) Detail of the long spicula of a male worm. Scale bar indicates 300 μm.

Table. Measurements of 4 *Angiostrongylus cantonensis* male lungworms collected from rats trapped in Valencia, Spain, 2021*

Morphologic character	Range, mm	Mean, mm
Total length	14.08–21.08	17.21
Maximum width	0.25–0.38	0.28
Esophagus length	0.29–0.36	0.32
Esophagus maximum width	0.07–0.09	0.08
Distance from excretory pore to cephalic extremity	0.38–0.47	0.41
Spicules length	1.14–1.27	1.21
Gubernaculum length	0.10–0.13	0.11

*one from *Rattus norvegicus* and 3 from *R. rattus* rats.

host, L1 larvae molt into L3 larvae. When infected mollusks are ingested by a rat, the subsequent phase takes place in the rat brain, where L3 larvae turn into young adults (L5). After leaving the central nervous system, L5 young adult worms reach the pulmonary arteries, where they mature and reproduce. Paratenic hosts include crabs, shrimp, frogs, and lizards (*4*).

Angiostrongyliasis is a foodborne disease; therefore, human infection requires ingestion of raw/poorly cooked intermediate or paratenic hosts. Another source of infection is lettuce contaminated with infective larvae released by an intermediate host (*5*). Hence, when humans accidentally ingest L3 larvae, the larvae penetrate the intestinal wall and travel through the bloodstream to the brain, where they can cause acute eosinophilic meningitis (neuroangiostrongyliasis). Severe cases can result in radiculitis, cranial neuropathy, myelitis, encephalopathy, coma, and even death. Usually, the nematodes die in the central nervous system (*6*).

Neuroangiostrongyliasis is a global emerging disease with serious implications for animal and public health (*4*). Globalization has helped disperse, and probably continues to disperse, rat lungworms. Infected rats (and snails) travel by ship, thereby transferring the parasite between continents and countries (*7*). Infected rats have been found near the port of Valencia but also several kilometers from the coast, suggesting a wide distribution of the rat lungworm in the city (Appendix Figure 3).

A. cantonensis lungworms have been reported widely in Asia, Africa, and America. However, in Europe, they have thus far been reported exclusively at the insular level, specifically in *R. norvegicus* and *R. rattus* rats in Tenerife (Canary Islands) and in *Atelerix algirus* hedgehogs in Mallorca (Balearic Islands) (*2,8,9*). Although a possible autochthonous human case of *A. cantonensis* infection was (immunologically) diagnosed in France, the possibility of its being an imported case was not ruled out (*10*).

A. cantonensis lungworms, a dangerous invasive species, agents of a potentially fatal emerging infectious disease, are spreading into locations beyond their typical tropical/subtropical distribu-tion, probably favored not only by globalization but also by climate change. Epidemiologic surveys of rat populations in Europe, preferably in urban/peri-urban areas, with the involvement of government entities, pest control agencies, and experts in parasitic zoonoses, should help minimize future potential human infections.

About the Author

Prof. Galán-Puchades is director of the Research Group on Parasites and Health of the University of Valencia. Her research interests include neglected parasitic diseases.

References

1. Yousif F, Ibrahim A. The first record of *Angiostrongylus cantonensis* from Egypt. Z Parasitenkd. 1978;56:73–80. https://doi.org/10.1007/BF00925940
2. Foronda P, López-González M, Miquel J, Torres J, Segovia M, Abreu-Acosta N, et al. Finding of *Parastrongylus cantonensis* (Chen, 1935) in *Rattus rattus* in Tenerife, Canary Islands (Spain). Acta Trop. 2010;114:123–7. https://doi.org/10.1016/j.actatropica.2010.02.004
3. Rodpai R, Intapan PM, Thanchomnang T, Sanpool O, Sadaow L, Laymanivong S, et al. *Angiostrongylus cantonensis* and *A. malaysiensis* broadly overlap in Thailand, Lao PDR, Cambodia and Myanmar: a molecular survey of larvae in land snails. PLoS One. 2016;11:e0161128. https://doi.org/10.1371/journal.pone.0161128
4. Barratt J, Chan D, Sandaradura I, Malik R, Spielman D, Lee R, et al. *Angiostrongylus cantonensis*: a review of its distribution, molecular biology and clinical significance as a human pathogen. Parasitology. 2016;143:1087–118. https://doi.org/10.1017/S0031182016000652
5. Waugh CA, Shafir S, Wise M, Robinson RD, Eberhard ML, Lindo JF. Human *Angiostrongylus cantonensis*, Jamaica. Emerg Infect Dis. 2005;11:1977–8. https://doi.org/10.3201/eid1112.050217
6. Johnston DI, Dixon MC, Elm JL, Calimlim PS, Sciulli RH, Park SY. Review of cases of angiostrongyliasis in Hawaii, 2007-2017. Am J Trop Med Hyg. 2019;101:608–16. https://doi.org/10.4269/ajtmh.19-0280
7. Hochberg NS, Blackburn BG, Park SY, Sejvar JJ, Effler PV, Herwaldt BL. Eosinophilic meningitis attributable to *Angiostrongylus cantonensis* infection in Hawaii: clinical characteristics and potential exposures. Am J Trop Med Hyg.

2011;85:685–90. https://doi.org/10.4269/ajtmh.2011.11-0322.

8. Martín-Carrillo N, Feliu C, Abreu-Acosta N, Izquierdo-Rodriguez E, Dorta-Guerra R, Miquel J, et al. A peculiar distribution of the emerging nematode *Angiostrongylus cantonensis* in the Canary Islands (Spain): recent introduction or isolation effect? Animals (Basel). 2021;11:1267. https://doi.org/10.3390/ani11051267

9. Paredes-Esquivel C, Sola J, Delgado-Serra S, Puig Riera M, Negre N, Miranda MA, et al. *Angiostrongylus cantonensis* in North African hedgehogs as vertebrate hosts, Mallorca, Spain, October 2018. Euro Surveill. 2019;24:1900489. https://doi.org/10.2807/1560-7917.ES.2019.24.33.1900489

10 Nguyen Y, Rossi B, Argy N, Baker C, Nickel B, Marti H, et al. Autochthonous case of eosinophilic meningitis caused by *Angiostrongylus cantonensis*, France, 2016. Emerg Infect Dis. 2017;23:1045–6. https://doi.org/10.3201/eid2306.161999

Laboratory Features of Trichinellosis and Eosinophilia Threshold for Testing, Nunavik, Quebec, Canada, 2009–2019

Luke B. Harrison, Michael D. Libman, Chelsea Caya, Momar Ndao, Cedric P. Yansouni

Author affiliations: McGill University Health Centre, Montreal, Quebec, Canada (L.B. Harrison, M.D. Libman, C. Caya, C.P. Yansouni); National Reference Centre for Parasitology, Montreal

Prolonged eosinophilia is characteristic of trichinellosis. To determine the optimal eosinophil threshold for reflex *Trichinella* testing, we examined all 43 cases in Nunavik, Quebec, Canada, during 2009–2019. Using receiver operating characteristic analysis, we determined that eosinophil counts $\geq 0.8 \times 10^9$ cells/L should prompt consideration of trichinellosis and testing to rapidly identify potential outbreaks.

(M. Ndao)

Trichinella nativa infection is associated with ingestion of parasitized sylvatic animals and periodic outbreaks among residents of northern Canada (*1–3*). In the Arctic region of Nunavik in Quebec, outbreaks associated with polar bear and walrus consumption have prompted public health interventions, including a highly successful community-led active surveillance system that examines hunted meat for evidence of *Trichinella* encystment (*4,5*). We report a 10-year case series of *Trichinella* infection in Nunavik and describe the laboratory features. Eosinophilia is a well-characterized feature of infection that is readily available for most cases. We performed receiver operating characteristic (ROC) analysis to define an optimal threshold of eosinophilia to prompt reflex *Trichinella* antibody testing and rapid reporting to public health authorities for timely outbreak investigation (*1–3*).

In a retrospective test-negative case–control study, we reviewed laboratory and public health records to identify cases of trichinellosis in Nunavik that occurred from 2009 through 2019. Our study was approved by the Research Institute of the McGill University Health Centre Research and Ethics Board (REB #2020-5312).

We first reviewed all requests for *Trichinella* serologic testing sent from Quebec to the National Reference Centre for Parasitology, the only testing site for Quebec, during 2009–2019 (Appendix, https://wwwnc.cdc.gov/EID/article/28/12/22-1144-App1.pdf). To define an initial set of cases (with positive *Trichinella* serologic results), we selected specimens originating from Nunavik. One author (L.B.H.) reviewed the charts and confirmed cases if the clinical evolution was compatible with the positive serologic results. Because trichinellosis is notifiable by provincial law, we cross-referenced cases with the public health database to identify other cases determined epidemiologically and reviewed those charts. We defined a set of region-matched controls as those with negative *Trichinella* serologic results. Those controls are therefore persons from the general population, from the same region who had clinical manifestations that prompted testing for trichinellosis. Although serologic results early in the disease course could be negative, chart review of controls did not yield additional suspected cases on the basis of clinical evolution. We extracted available clinical and laboratory data by chart review at the McGill University Health Centre and at regional health centers in Nunavik. We calculated summary statistics and tests (*t*-test and χ^2), comparing cases and controls by using R (*6*), and generated ROC curves by using the pROC R package (*7*).

We identified 43 cases of trichinellosis and a set of 31 region-matched controls (Table). We excluded 4

Table. Characteristics of patients and controls in study of *Trichinella* infections in Nunavik, Quebec, Canada, 2009–2019*

Characteristic	Case-patients, n = 43	Controls, n = 31	Test statistic (95% CI)	p value
Demographics				
Mean age, y (range, SD)	39.1 (5–75, 16.1)	45.8 (0–80, 22.4)	t = –1.48 (–15.59 to 2.32)	0.144
Female, no. (%)	30 (69.8)	16 (51.6)	χ^2 = 3.77	0.052
Male, no. (%)	13 (30.2)	15 (48.4)		
Level of care received, no. with available information/total no. (%)				
Outpatient	18/27 (67)	15/24 (63)	NA	NA
Inpatient	9/27 (33)	9/24 (38)	NA	NA
Critical care	0/27	0/24	NA	NA
Evacuated to southern Quebec	7/27 (26)	8/24 (33)	NA	NA
Unknown	16/43 (37)	7/31 (23)	NA	NA
Positive *Trichinella* serologic result (OD ≥0.3), no. (%)	39 (91)‡	NA	NA	NA
Biochemical features during illness, mean, (range, SD†)				
Eosinophils, × 10⁹ cells/L	5.35 (0.80–17.40, 3.81)	0.80 (0–4.5, 1.00)	t = 6.47 (3.14, 5.95)	<0.001
Thrombocytes, × 10⁹/L	545 (294–977, 169)	479 (208–1009, 210)	t = 1.45 (-24.43, 154.90)	0.151
Creatinine kinase, U/L	1562 (103–8081, 1511)	956 (28–6470, 1730)	t = 1.42 (-245.92, 1458.90)	0.160
C-reactive protein, mg/L	66.5 (8–191.7, 42.1)	66.6 (0.5–253.0, 82.9)	t = -0.03 (-38.05, 36.83)	0.974
Alanine aminotransferase, U/L	140.2 (21.0–541.0, 128.1)	85.1 (16.0–334.0, 75.6)	t = 1.82 (-5.56, 115.91)	0.074

*NA, not applicable; OD, optical density; t, Student t statistic.
†Maximum value recorded.
‡4 cases were determined epidemiologically, and initially negative serologic testing was not repeated.

possible case-patients with weakly positive serologic results but ambiguous clinical manifestations consistent with past infection. Information on signs and symptoms was available for only 19/43 case-patients, but demographic, laboratory, and clinical outcomes were well documented.

Case-patients had a median age of 40 years and were mostly female (30/43, 69.8%), which may result from chance (p = 0.052), differential exposure to parasitized meat, food sharing, food preparation practices, or selection bias (*8*). When available, clinical features were similar to those previously described for trichinellosis (i.e., fever, rash and myalgia) (*9*). No patients died, and 9/27 (33%) patients with documented illness required hospitalization. Epidemiologic investigations revealed sporadic cases and 2 suspected point-source outbreaks (*8*). In 1 outbreak, seals were suspected as the source of infection, which could represent a change in epidemiology from previous outbreaks associated with polar bear and walrus meat and might reflect the surveillance program targeting game meat from the latter animals but not seals.

Laboratory information was available for 41/43 case-patients, a larger series of findings in *Trichinella* infection in Nunavik than previously reported. Features of *Trichinella* infection in Nunavik, presumptively caused by *T. nativa*, are similar to those reported for *T. spiralis* infection (*9*), including elevated creatinine kinase and eosinophilia (Table). The variable that differed most between cases and controls was peak absolute eosinophilia (5.35 vs. 0.80 × 10⁹ cells/L; p<0.001). Among case-patients, peak eosinophilia was noted early and declined over months; among
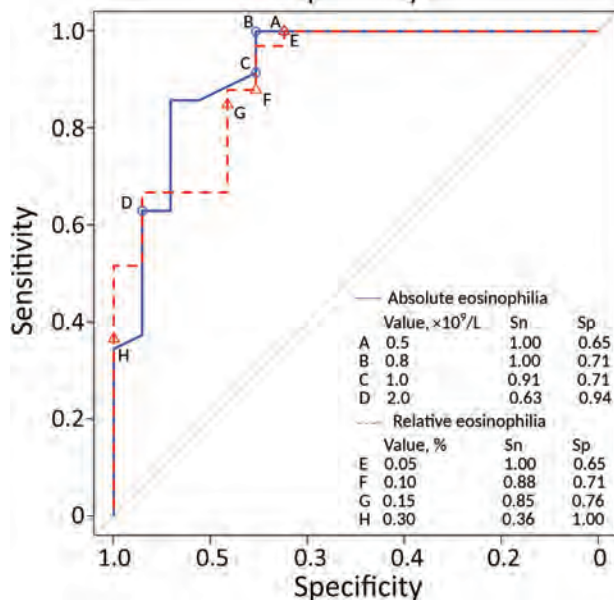
Figure. Receiver operating characteristic curve comparing performance of thresholds of absolute and relative eosinophilia to trigger automatic reporting of possible trichinellosis. Sn and Sp for the thresholds of absolute eosinophilia examined were 0.5 × 10⁹ (Sn = 1.0, Sp = 0.65), 0.8 × 10⁹ (Sn = 1.0, Sp = 0.71), 1.0 × 10⁹ (Sn = 0.91, Sp = 0.71), 2.0 × 10⁹ (Sn = 0.63, Sp = 0.94) and for relative eosinophilia were 5% (Sn = 1.0, Sp = 0.65), 10% (Sn = 0.88, Sp = 0.71), 15% (Sn = 0.85, Sp = 0.76), and 30% (Sn = 0.36, Sp = 1.0).

controls, counts were frequently elevated but stable over time (Appendix Figure). Using ROC analysis, we identified an absolute eosinophilia threshold of $\geq 0.8 \times 10^9$ cells/L, which identified all cases in this series with a specificity of 71% (Figure). We assessed the potential effect on resource use of this threshold by examining the region's whole-population distribution of absolute eosinophil counts. Among 8,562 persons who submitted a specimen for complete blood count for any reason from January 2019 through April 2022, a total of 287 had eosinophil counts that exceeded our threshold (86 [1.2%] specimens/year).

Automated flags and reflex testing in Nunavik now incorporate the threshold identified in our analysis. In the absence of a defined alternative diagnosis, eosinophil counts of $\geq 0.80 \times 10^9$ cells/L should prompt clinical consideration of trichinellosis and further investigation. Early identification of outbreaks is critical in this region—where hunted meat is shared widely within and among communities—to limit exposures and enable delivery of postexposure prophylactic anthelmintic therapy, which has evidence of effectiveness in this serious illness (1,4,10). The cost–benefit ratio of this threshold will require ongoing assessment.

Acknowledgments

About the Author

Dr. Harrison is chief resident in Infectious Diseases and Medical Microbiology at the McGill University Health Centre. His research interests include evolutionary biology.

References

1. Schellenberg RS, Tan BJK, Irvine JD, Stockdale DR, Gajadhar AA, Serhir B, et al. An outbreak of trichinellosis due to consumption of bear meat infected with *Trichinella nativa*, in 2 northern Saskatchewan communities. J Infect Dis. 2003;188:835–43. https://doi.org/10.1086/378094
2. Dalcin D, Zarlenga DS, Larter NC, Hoberg E, Boucher DA, Merrifield S, et al. *Trichinella nativa* outbreak with rare thrombotic complications associated with meat from a black bear hunted in northern Ontario. Clin Infect Dis. 2017;64:1367–73. https://doi.org/10.1093/cid/cix165
3. MacLean JD, Viallet J, Law C, Staudt M. Trichinosis in the Canadian Arctic: report of five outbreaks and a new clinical syndrome. J Infect Dis. 1989;160:513–20. https://doi.org/10.1093/infdis/160.3.513
4. Proulx JF, MacLean JD, Gyorkos TW, Leclair D, Richter AK, Serhir B, et al. Novel prevention program for trichinellosis in Inuit communities. Clin Infect Dis. 2002;34:1508–14. https://doi.org/10.1086/340342
5. Larrat S, Simard M, Lair S, Bélanger D, Proulx J-F. From science to action and from action to science: the Nunavik Trichinellosis Prevention Program. Int J Circumpolar Health. 2012;71:18595. https://doi.org/10.3402/ijch.v71i0.18595
6. R Core Team. R: a language and environment for statistical computing. Version 4.1.3 [cited 2022 Apr 1]. https://www.R-project.org
7. Robin X, Turck N, Hainard A, Tiberti N, Lisacek F, Sanchez J-C, et al. pROC: an open-source package for R and S+ to analyze and compare ROC curves. BMC Bioinformatics. 2011;12:77. https://doi.org/10.1186/1471-2105-12-77
8. Ducrocq J, Proulx J-F, Simard M, Lévesque B, Iqaluk M, Elijassiapik L, et al. The unique contribution of a local response group in the field investigation and management of a trichinellosis outbreak in Nunavik (Québec, Canada). Can J Public Heal_th. 2020;111:31–9. https://doi.org/10.17269/s41997-019-00255-8
9. Gottstein B, Pozio E, Nöckler K. Epidemiology, diagnosis, treatment, and control of trichinellosis. Clin Microbiol Rev. 2009;22:127–45. https://doi.org/10.1128/CMR.00026-08
10. Faber M, Schink S, Mayer-Scholl S, Ziesch S, Schönfelder R, Wichmann-Schauer H, et al. Outbreak of trichinellosis due to wild boar meat and evaluation of the effectiveness of post exposure prophylaxis, Germany, 2013. Clin Infect Dis. 2015;60:e98-104.

Address for correspondence: Luke B. Harrison, McGill University Health Centre, Rm E5.1815, 1001 Blvd Decarie, Montreal, QC H4A 3J1, Canada; email: luke.harrison@mail.mcgill.ca

Dirofilaria repens Testicular Infection in Child, Italy

Sara Ugolini, Mario Lima, Michela Maffi, Francesco Pierangeli, Marzia Vastano, Tommaso Gargano, Stefania Varani, Andrea Gustinelli, Monica Caffara, Maria L. Fioravanti

Author affiliations: Wythenshawe Hospital, Manchester, UK (S. Ugolini); University of Manchester NHS Foundation Trust, Manchester (S. Ugolini); IRCCS Azienda Ospedaliero–Universitaria di Bologna, Bologna, Italy (M. Lima, M. Maffi, M. Vastano, T. Gargano, S. Varani); Ospedali Riuniti di Ancona, Ancona, Italy (F. Pierangeli); Alma Mater Studiorum–University of

Testicular *Dirofilaria repens* infection was identified and confirmed by sequence analysis in a child in northeastern Italy. Because human dirofilariasis is emerging in southern and eastern Europe, this parasitic infection should be considered in the differential diagnosis of scrotal swelling in disease-endemic countries to avoid unnecessary interventions, such as orchiectomy.

Bologna, Bologna (M. Lima, T. Gargano, S. Varani, A. Gustinelli, M. Caffara, M.L. Fioravanti)

Dirofilariasis is a zoonotic nematode infection that typically affects canines and other carnivores and can be transmitted to humans by Culicidae mosquitos. Dirofilariasis incidence has increased worldwide; new cases have been reported in previously nonendemic regions (1,2). This changing trend is likely related to global warming and subsequent increases in vector density and activity during the year. Canine dirofilariasis is endemic in Mediterranean countries of Europe and has 2 main etiologic agents: *Dirofilaria repens*, the main agent of subcutaneous infections, and *D. immitis*, the agent largely responsible for cardiopulmonary infections (1–3). Humans are usually dead-end hosts, and infection is mainly caused by a single immature worm (2). A clinical manifestation of human dirofilarial infection is pulmonary dirofilariasis, which has

been predominantly detected within the Americas, although recent cases have been reported in Europe. In addition, *D. repens* nematodes cause human subcutaneous dirofilariasis (HSD), which is typical of the Old World (1–3); subcutaneous or ocular infection and infections in male genitalia, female mammary glands, lungs, liver, and mesentery have been described.

We report a case of dirofilariasis that occurred in September 2017 in a boy 13 years of age living in Bologna (northeastern Italy) who was born in Taormina (Sicily, Italy). The patient had a 5-month history of swelling in the left testicle. During initial assessment, the left testicle had a tender nodule upon palpation without associated scrotal hyperemia or inguinal lymphadenopathy. Ultrasonography showed a 1-cm, well-defined cyst containing a coiled structure with parallel echogenic walls and movement within the cyst (Figure, panel A). Subsequent magnetic resonance imaging showed the cyst was located on the testis without signs of infiltration and contained fluid mixed with tubular structures and moving artifacts (Figure, panel B). The patient was scheduled for surgical excision and histologic diagnosis. Routine preoperative laboratory tests showed normal blood cell counts: erythrocytes, 5.07×10^{12} cells/L; leukocytes, 5.30×10^9 cells/L; and eosinophils, 0.10×10^9 cells/L. Intraoperative exploration revealed a well-circumscribed, encapsulated tense nodule in the left side of the scrotum (Figure, panel C). To collect samples for
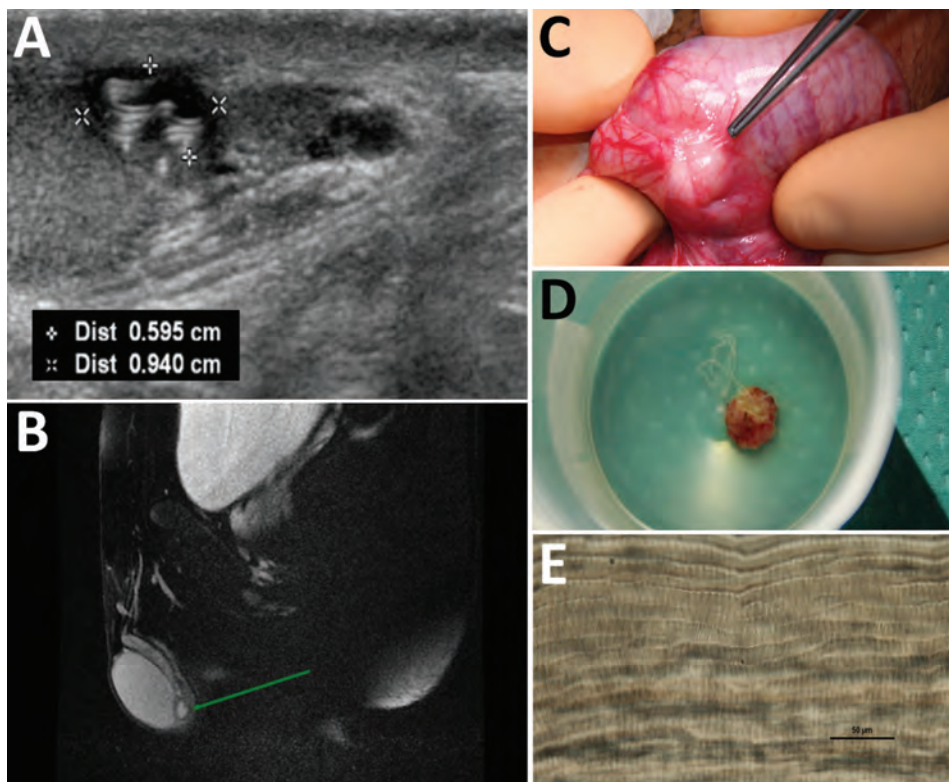
Figure. Diagnostic evaluation of *Dirofilaria repens* testicular infection in a child from Italy, a boy 13 years of age who had a 5-month history of swelling in the left testicle. A) Ultrasound scan showed a 0.5 × 0.9 cm hypoechoic cyst with moving artifacts and thread-like hyperechoic structures. B) Magnetic resonance imaging showed the cyst was located on the testis without signs of infiltration and contained fluid mixed with tubular structures and moving artifacts. C) Exploration of the scrotum before cyst excision showed a well-circumscribed, encapsulated tense nodule on the left side. D) The cyst was excised and a coiled roundworm was found in the opened capsule. E) We identified the nematode as a female *D. repens* nematode by microscopically observing typical longitudinal ridges on the body surface. Scale bar indicates 50 μm. Dist, distance.

histology and microbiology, we opened the cyst and found a coiled, thread-like roundworm (Figure, panel D). Further macroscopic examination indicated the worm was potentially a dirofilarial nematode. Because both ends of the worm were not visible, we identified the worm by microscopic observations and molecular sequence analysis of the remaining portions after fixing in 70% ethanol. The parasite was 423–588 µm wide with a cuticular layer 13–15 µm thick; the external surface was characterized by longitudinal ridges spaced 6–9 µm apart (Figure, panel E). We identified the nematode as a female *D. repens* by the longitudinal ridges, which we confirmed by molecular identification (*4*). We performed phylogenetic analysis of the 12S rRNA and cytochrome c oxidase subunit 1 mitochondrial genes; our specimen clustered with and was identical to *D. repens* sequences obtained from humans and dogs in Italy (Appendix Figure, https://wwwnc.cdc.gov/EID/article/28/12/22-0424-App1.pdf). The patient had an uneventful postoperative course, and no further therapy was administered. At 20-month follow-up, the patient had no residual symptoms, and ultrasonography showed no testicular abnormalities.

HSD localization in male genitalia (testis, scrotum, verga, spermatic cord, and epididymis) has been previously described (*5–9*) and might be related to a *D. repens* tropism in response to sex hormones (*1*). Our case highlights that testicular dirofilariasis might mimic a testicular tumor and lead to unnecessary orchiectomy because of misdiagnosis. A helminthic infection should be considered in this differential diagnosis for gradual-onset testicular swelling with or without signs of inflammation, especially in endemic areas. Serologic tests for helminthic infections are performed only in specialized laboratories and are not routinely available. In addition, the accuracy and usefulness of those tests have been debated (*10*). Ultrasonography and magnetic resonance imaging can help identify features of dirofilariasis, such as dirofilarial nodules with suspicious inner hypoechoic/T1-hypointense findings, or might demonstrate moving worms (*10*). Imaging results should be consistent with a thick-walled lesion, semiliquid content with a central signal caused by the worm, and a macroscopic thread-like structure. The definitive diagnosis of HSD can only be achieved by postoperative identification of the worm by using morphologic, histologic, or molecular analysis. When malignancy cannot be excluded, an excisional biopsy is indicated for histologic diagnosis. The complete extraction of the worm is usually curative, and no specific antihelminth therapy is indicated in the absence of secondary lesions (*8,9*).

In conclusion, diagnoses of human dirofilaria-sis have increased in countries in Europe, and clinical awareness of this parasitic infection should be strengthened through education and interdisciplinary collaboration among clinicians, surgeons, and parasitologists. Clinicians should consider HSD in the differential diagnosis of subcutaneous or superficial tissue nodules of the testicles. Excisional biopsies should be performed for parasitologic, molecular, and histologic analyses to avoid invasive surgical procedures that might cause permanent reduction in quality of life, such as orchiectomy.

About the Author

Dr. Ugolini is a senior clinical fellow in cardiothoracic surgery at Manchester University NHS Foundation Trust, UK. She qualified as a pediatric surgeon in 2021 in Italy, and this case occurred while she was in training.

References

1. Pampiglione S, Rivasi F. Human dirofilariasis due to *Dirofilaria* (Nochtiella) *repens*: an update of world literature from 1995 to 2000. Parassitologia. 2000;42:231–54.
2. Simón F, Diosdado A, Siles-Lucas M, Kartashev V, González-Miguel J. Human dirofilariosis in the 21st century: a scoping review of clinical cases reported in the literature. Transbound Emerg Dis. 2021 Jul 1 [Epub ahead of print]. https://doi.org/10.1111/tbed.14210
3. Miterpáková M, Antolová D, Rampalová J, Undesser M, Krajčovič T, Víchová B. *Dirofilaria immitis* pulmonary dirofilariasis, Slovakia. Emerg Infect Dis. 2022;28:482–5. https://doi.org/10.3201/eid2802.211963
4. Suzuki J, Kobayashi S, Okata U, Matsuzaki H, Mori M, Chen KR, et al. Molecular analysis of *Dirofilaria repens* removed from a subcutaneous nodule in a Japanese woman after a tour to Europe. Parasite. 2015;22:2. https://doi.org/10.1051/parasite/2015002
5. Fleck R, Kurz W, Quade B, Geginat G, Hof H. Human dirofilariasis due to *Dirofilaria repens* mimicking a scrotal tumor. Urology. 2009;73:209.e1–3. https://doi.org/10.1016/j.urology.2008.02.015
6. Tripi F, Scarlata F, Verde V, Voti G, Chiaramonte C. Human dirofilariasis presenting as scrotal mass. J Urol Nephrol Open Access. 2016;3:1–4. https://doi.org/10.15226/2473-6430/3/1/00120
7. Leccia N, Patouraux S, Carpentier X, Boissy C, Del Giudice P, Parks S, et al. Pseudo-tumor of the scrotum, a rare clinical presentation of dirofilariasis: a report of two autochtonous cases due to *Dirofilaria repens*. Pathog Glob Health. 2012;106:370–2. https://doi.org/10.1179/2047773212Y.0000000029
8. D'Amuri A, Senatore SA, Carlà TG, Floccari F, Villani E,

Leocata P, et al. Cutaneous dirofilariasis resulting in orchiectomy. J Cutan Pathol. 2012;39:304–5. https://doi.org/10.1111/j.1600-0560.2011.01828.x

9. Kallampallil J, Wood SJ, O'Dempsey T, Craigie RJ. Nematode infection mimicking paratesticular malignancy. BMJ Case Rep. 2013;2013:bcr2013200775. https://doi.org/10.1136/bcr-2013-200775

10. European Society of Dirofilariosis and Angiostrongylosis. Guidelines for clinical management of human Dirofilaria infections. 2017 [cited 2022 Aug 8]. https://www.esda.vet/media/attachments/2021/08/19/human-dirofilaria-infections.pdf

Address for correspondence: Sara Ugolini, Department of Cardiothoracic Surgery, Wythenshawe Hospital, University of Manchester NHS Foundation Trust, Southmoor Rd, Wythenshawe, Manchester M23 9LT, UK; email: sara.ugolini@mft.nhs.uk

Severe Fever with Thrombocytopenia Syndrome Virus Infection, Thailand, 2019–2020

Patthaya Rattanakomol, Sarawut Khongwichit, Piyada Linsuwanon, Keun Hwa Lee, Sompong Vongpunsawad, Yong Poovorawan

Author affiliations: Chulalongkorn University, Bangkok, Thailand (P. Rattanakomol, S. Khongwichit, S. Vongpunsawad, Y. Poovorawan); US Army Medical Directorate–Armed Forces Research Institute of Medical Sciences, Bangkok, Thailand (P. Linsuwanon); Hanyang University, Seoul, South Korea (K.H. Lee)

Infection with severe fever with thrombocytopenia syndrome (SFTS) virus, which can cause hemorrhagic febrile illness, is often transmitted by ticks. We identified 3 patients with SFTS in or near Bangkok, Thailand. Our results underscore a need for heightened awareness by clinicians of possible SFTS virus, even in urban centers.

Severe fever with thrombocytopenia syndrome (SFTS) is a tickborne viral disease associated with acute fever, possibly accompanied by vomiting, diarrhea, fatigue, myalgia, and leukocytopenia (1). Most reports of infection have come from studies in South Korea, Japan, and China, although Taiwan, Vietnam, and Myanmar have had confirmed cases in recent years (2). Severe infections can cause hemorrhagic fever and multiple organ failure leading to death. SFTS results from infection by the SFTS virus (SFTSV, newly renamed *Dabie bandavirus*), an RNA virus in the family Phenuiviridae, genus *Bandavirus* (3). More frequent arbovirus infections in Thailand, primarily dengue and chikungunya, often confound diagnosis of febrile illness caused by other viruses such as SFTSV because most clinicians lack awareness.

Testing during an upsurge in chikungunya virus infection in Thailand at the end of 2018 found that >70% of acute febrile illnesses were laboratory-confirmed chikungunya (4). As the proportion of chikungunya virus–positive samples eventually decreased, we began to screen for other common viral etiologies of acute fever, including dengue and Zika viruses (Appendix Figure, https://wwwnc.cdc.gov/EID/article/28/12/22-1183-App1.pdf). Because SFTSV had been reported in 2 patients in Vietnam (5) at the time, when the samples from Thailand tested negative for all 3 more common viruses, we began examining for possible SFTSV infection. The Institutional Review Board of Chulalongkorn University Faculty of Medicine approved this study (IRB number 0453/65).

We subjected de-identified archived RNA samples from 712 patients from Bangkok and surrounding areas, hospitalized during October 2018–March 2021, to reverse transcription PCR to detect the nucleoprotein gene region of the small (S) segment of SFTSV (6). Three samples tested positive, so we used 3 primer sets described elsewhere (7) to determine full-length S-segment nucleotide sequences. We deposited sequences in the GenBank database (accession numbers ON840548–50) and constructed the SFTSV S-segment phylogenetic tree using MEGA11 (https://www.megasoftware.net).

Phylogenetic analysis suggested that the 3 SFTSV strains from Thailand shared ≈99.7% nucleotide sequence identities and were genetically closest to the SFTSV strains from China identified in 2012–2017 (99.3%–99.6% nucleotide identity) (Figure; Appendix Table). On the basis of available clinical records, all 3 patients reported myalgia with lower than normal leukocyte (<3,000 cells/μL) and platelet (<110,000 cells/μL) counts (Table). Two patients experienced elevated alanine and aspartate aminotransferase levels (>60 U/L). Although patient 1 did not demonstrate substantially altered leukocyte count or blood chemistry, he experienced gastrointestinal symptoms (abdominal pain, nausea, vomiting, and diarrhea).

ON840548_Thailand_2019

ON840550_Thailand_2020

ON840549_Thailand_2020

99 KU664012_China_2012

86 MK524357_China_2017

KR230805_China_2014

MT683685_South Korea_2017

AB985544_Japan_2013

AB985559_Japan_2014

99 MF094816_South Korea_2015

KP663742_South Korea_2014

98 LC462231_Japan_2018

98 MN830173_Taiwan_2019

62 KP663733_South Korea_2014

OM425208920_China_2020

MZ773046_China_2020

HQ141603_China_2010

90 NC043452_China_2014

MK524369_China_2017

KF358693_South Korea_2012

91 OM452026_China_2018

NC_024496_Heartland virus] Outgroup

0.50

Figure. Phylogenetic analysis of the S segment sequence (1,674 bp) of 3 SFTSV strains from Thailand (bold) compared with reference sequences. The tree was generated using the maximum-likelihood method based on the Kimura 2-parameter model with 1,000 bootstrap replicates. Strains are noted with GenBank accession numbers, country, and year of isolation. Bootstrap values >70% are indicated at the branch nodes. Scale bar indicates the number of substitutions per site.

Table. Characteristics and detection of severe fever with thrombocytopenia syndrome virus in 3 patients in Thailand, 2019–2020.

Category	Patient 1	Patient 2	Patient 3
Age, y/sex	60/M	16/M	52/F
Location	Bangkok	Chachoengsao	Bangkok
Collection date	2019 Nov 14	2020 May 10	2020 Oct 19
Clinical manifestations			
Temperature	37.2°C	40.6°C	38.1°C
Clinical signs and symptoms	Myalgia, arthralgia, cough, nausea, vomiting, abdominal pain, diarrhea	Myalgia	Myalgia, arthralgia
Laboratory findings (reference range)			
Leukocytes, cells/µL (4,100–10,900)	1,790	900	2,770
Neutrophils, % (40–72)	45	31	62
Lymphocytes, % (18–49)	42	59	34
Platelets, cells/µL (140,000–400,000)	107,000	45,000	121,000
Aspartate aminotransferase, U/L (<40)	Not done	102	1,758
Alanine aminotransferase, U/L (<41)	24	63	973
Pathogens tested for but not detected	*Rickettsia/Orientia* spp., influenza A/B	*Rickettsia/Orientia* spp., influenza A/B, Epstein-Barr, hepatitis B/C, SARS-CoV-2, malaria, *Leptospira*, *Burkholderia pseudomallei*	*Rickettsia/Orientia* spp., hepatitis A/B

Patients reported no history of travel within 3 weeks before symptom onset. Patients 1 and 3 lived in Bangkok, whereas patient 2 lived in Chachoengsao Province, ≈40 km east of Bangkok. Because international travel was severely limited during the global coronavirus pandemic beginning in 2020, transboundary transmission of SFTSV was unlikely.

A study in South Korea found that roughly one quarter of SFTSV infections accompanied scrub typhus caused by *Orientia tsutsugamushi* infection (8) and suggested the possibility of the chigger mite as a potential vector of the virus. To further investigate potential co-infection with tickborne and chiggerborne bacteria, we performed multiplexed quantitative PCR to detect *Orientia* and *Rickettsiae* spp. None of our 3 patients tested positive for these bacteria.

Our study identified SFTSV by analyzing febrile illnesses among patients who previously tested negative for arboviruses typically suspected of causing acute fever in Thailand. We found that <0.5% of these samples tested positive for SFTSV, which represented only 0.1% prevalence when all febrile illnesses were considered. However, this percentage might be higher in patients residing in rural areas or who engage in agriculture. A strength of this study was confirmation of SFTSV from full-length S-segment nucleotide sequences from 3 symptomatic patients residing in urban areas during November 2019–October 2020.

We do not know how the patients in our study contracted SFTSV, particularly the identities of any likely reservoir hosts and arthropod vectors, because of limited available clinical information regarding viral exposure. To date, 4 tick species are known vectors for SFTSV: *Haemaphysalis longicornis*, *Amblyomma testudinarium*, *Rhipicephalus microplus*, and *Ixodes nipponensis*, the last of which is not present in Thailand (9,10). *R. microplus* is often found in livestock animals in countries in Southeast Asia, but all 3 patients in our study were urban dwellers. Our study was limited by using data from retrospective evaluation of clinical records, which could have been more comprehensive had physicians initially suspected SFTS. Also, the fact that patients did not travel internationally could not rule out domestic rural exposure to SFTSV. Another limitation was that insufficient S-segment sequences from SFTSV strains previously identified in countries in Southeast Asia, such as Myanmar and Vietnam, were available in the public database, preventing direct genetic comparison with the strains from Thailand identified in this study. Nevertheless, our finding of detailed molecular evidence of SFTSV infection in Thailand, although in very few patients to date, should increase awareness of SFTS and warrants further exploration into possible transmission cycles in tropical urban settings.

About the Author

Dr. Rattanakomol is a postdoctoral fellow in the Center of Excellence in Clinical Virology of Chulalongkorn University. Her research interests include emerging and reemerging respiratory and arthropod-borne viral infections.

References

1. .Seo JW, Kim D, Yun N, Kim DM. Clinical update of severe fever with thrombocytopenia syndrome. Viruses. 2021;13:1213. https://doi.org/10.3390/v13071213
2. Casel MA, Park SJ, Choi YK. Severe fever with thrombocytopenia syndrome virus: emerging novel phlebovirus and their control strategy. Exp Mol Med. 2021;53:713–22. https://doi.org/10.1038/s12276-021-00610-1
3. International Committee on Taxonomy of Viruses. Taxon details: severe fever with thrombocytopenia syndrome virus [cited 2022 Jun 19]. https://ictv.global/taxonomy/taxondetails?taxnode_id=202100166
4. Khongwichit S, Chansaenroj J, Thongmee T, Benjamanukul S, Wanlapakorn N, Chirathaworn C, et al. Large-scale outbreak of Chikungunya virus infection in Thailand, 2018-2019. PLoS One. 2021;16:e0247314. https://doi.org/10.1371/journal.pone.0247314
5. Tran XC, Yun Y, Van An L, Kim SH, Thao NTP, Man PKC, et al. Endemic severe fever with thrombocytopenia syndrome, Vietnam. Emerg Infect Dis. 2019;25:1029–31. https://doi.org/10.3201/eid2505.181463
6. Zhang YZ, He YW, Dai YA, Xiong Y, Zheng H, Zhou DJ, et al. Hemorrhagic fever caused by a novel Bunyavirus in China: pathogenesis and correlates of fatal outcome. Clin Infect Dis. 2012;54:527–33. https://doi.org/10.1093/cid/cir804
7. Han XH, Ma Y, Liu HY, Li D, Wang Y, Jiang FH, et al. Identification of severe fever with thrombocytopenia syndrome virus genotypes in patients and ticks in Liaoning Province, China. Parasit Vectors. 2022;15:120. https://doi.org/10.1186/s13071-022-05237-3
8. Wi YM, Woo HI, Park D, Lee KH, Kang CI, Chung DR, et al. Severe fever with thrombocytopenia syndrome in patients suspected of having scrub typhus. Emerg Infect Dis. 2016;22:1992–5. https://doi.org/10.3201/eid2211.160597
9. Takhampunya R, Sakolvaree J, Chanarat N, Youngdech N, Phonjatturas K, Promsathaporn S, et al. The bacterial community in questing ticks from Khao Yai national park in Thailand. Front Vet Sci. 2021;8:764763. https://doi.org/10.3389/fvets.2021.764763
10. Zhang X, Zhao C, Cheng C, Zhang G, Yu T, Lawrence K, et al. Rapid spread of severe fever with thrombocytopenia syndrome virus by parthenogenetic Asian longhorned ticks. Emerg Infect Dis. 2022;28:363–72. https://doi.org/10.3201/eid2802.211532

Address for correspondence: Yong Poovorawan, Center of Excellence in Clinical Virology, Faculty of Medicine, Chulalongkorn University, 1873 Rama 4 Rd, Pathumwan, Bangkok 10330, Thailand; email: yong.p@chula.ac.th

Omicron BA.5 Neutralization among Vaccine-Boosted Persons with Prior Omicron BA.1/BA.2 Infections

Rune M. Pedersen, Line L. Bang, Ditte S. Tornby, Lone W. Madsen, Dorte K. Holm, Thomas V. Sydenham, Isik S. Johansen, Thøger G. Jensen, Ulrik S. Justesen, Thomas E. Andersen

Author affiliation: University of Southern Denmark, Odense, Denmark

Worldwide, millions of persons have received multiple COVID-19 vaccinations and subsequently recovered from SARS-CoV-2 Omicron breakthrough infections. In 2 small, matched cohorts (n = 12, n = 24) in Denmark, we found Omicron BA.1/BA.2 breakthrough infection after 3-dose BNT162b2 vaccination provided improved Omicron BA.5 neutralization over 3-dose vaccination alone.

The SARS-CoV-2 Omicron variant has dominated the COVID-19 pandemic since late 2021, bringing ≥3 waves of increasingly immunity-evasive Omicron subvariants. An early wave of the Omicron subvariant BA.1 was rapidly replaced by a subvariant BA.2 wave during spring 2022. BA.2 was recently replaced by the even more transmissible BA.5, which is now globally dominant, accounting for 75%–95% of cases in most countries by August 2022 (1).

Because a large percentage of the worldwide population was infected by Omicron during early 2022, discussions have centered around whether convalescent patients acquired natural immunity that might later protect against BA.4/BA.5 subvariants (2). Serum neutralization studies have indicated that neither vaccination nor previous infection during the early Omicron waves offer effective protection against BA.5 (3–6). However, a recent large-scale epidemiologic study found that very few BA.5-infected persons had prior Omicron infection, indicating that previous Omicron infection might confer protection against BA.5 (7). To assess whether Omicron BA.1/BA.2 infection provides additional BA.5-specific neutralization capacity than vaccines alone, we compared authentic virus neutralization capacity among persons receiving 3-dose BNT162b2 vaccine (Pfizer-BioNTech, https://www.pfizer.com) regimens only and vaccinated persons who subsequently were infected with BA.1/BA.2.

We recruited healthy participants from among Odense University Hospital staff and the public in Odense, Denmark; all participants signed informed consent. We collected serum from the 24 participants in the vaccinated cohort during November 18, 2021–February 4, 2022, four weeks after they received the third BNT162b2 vaccination (Table). We collected serum from the 12 participants in the convalescent cohort during January 26–April 19, 2022, four weeks after Omicron BA.1/BA.2 breakthrough infection (Table). We performed plaque reduction neutralization tests (PRNTs) against authentic SARS-CoV-2 clinical isolates of Delta and Omicron BA.1, BA.2, and BA.5 variants, as previously described (8). We recorded $PRNT_{90}$ titers, the highest dilution of a serum sample yielding >90% plaque reduction. We identified lineages by nanopore whole-genome sequencing using a MinION sequencing instrument (Oxford Nanopore Technologies, https://nanoporetech.com) and uploaded sequences to GenBank (accession no. ON055856 for Delta, ON055874 for BA.1, ON055857 for BA.2, and OP225643 for BA.5). We analyzed all serum samples for spike-specific antibodies by using the Liaison TrimericS IgG Quantitative Immunoassay (DiaSorin, https://www.diasorin.com). To verify SARS-CoV-2–naive status among the vaccinated cohort, we analyzed serum for nucleocapsid-specific antibodies by using Alinity SARS-CoV-2 IgG

Table. Characteristics of persons with and without Omicron BA.1/BA.2 breakthrough infection who received COVID-19 vaccines and booster doses, Denmark*

Characteristics	Vaccines and booster	Vaccines, booster, and Omicron breakthrough
Total no. persons	24	12
Sex, no. (%)		
F	17 (70.8)	8 (66.6)
M	7 (29.2)	4 (33.4)
Median age, y (IQR)	41 (32–51)	47 (40–50)
Median no. days (IQR) between vaccination, infection, and sampling		
Between first and second dose	29 (27–36)	28 (26–34)
Between second and third dose	152 (42–199)	200 (159–228)
Between third dose and sampling	29 (23–34)	90 (77–143)
Between third dose and infection	NA	55 (31–109)
Between infection and sampling	NA	33 (24–38)

*Participants received 3 doses of BNT162b2 (Pfizer-BioNTech, https://www.pfizer.com), 2 initial vaccines and a booster dose. IQR, interquartile range; NA, not applicable
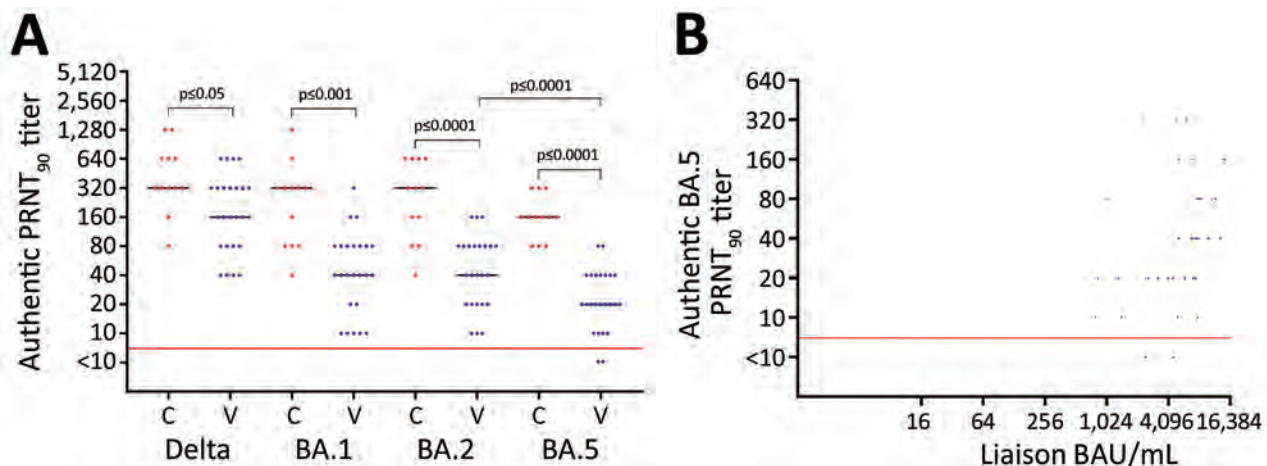
Figure. Neutralization of SARS-CoV-2 variants among vaccine-boosted persons with and without prior Omicron BA.1/BA.2 infections, Denmark. A) PRNT$_{90}$ titers against SARS-CoV-2 Delta variant and Omicron variants BA.1, BA.2, and BA.5. B) Correlation between the levels of spike antibodies and PRNT$_{90}$ titers. Participants received 3 doses of BNT162b2 (Pfizer-BioNTech, https://www.pfizer.com), 2 initial vaccines and a booster dose. We analyzed titers for 24 vaccinated participants (blue dots) who received 3 BNT162b2 doses only and 12 convalescent participants (red dots) who received 3 vaccine doses and had Omicron BA.1/BA.2 infection. For statistical analysis, a Kruskal-Wallis test was applied initially to account for the multiple comparisons problem. Subsequently, unpaired PRNT$_{90}$ titers were compared with the Wilcoxon rank-sum test, whereas paired PRNT$_{90}$ titers were compared with the Wilcoxon sign rank test. Red horizontal lines indicate neutralization threshold; horizontal bars indicate median neutralization titer for each SARS-CoV-2 strain. BAU, binding antibody units; C, convalescent participant; PRNT$_{90}$, plaque reduction neutralization tests with plaque reduction $\geq$90%; V, vaccinated participant.

assay (Abbott Diagnostics, https://www.abbott.com). This study was approved by the Regional Committees on Health Research Ethics for Southern Denmark (approval no. S 20210007C). Experiments involving live SARS-CoV-2 virus were conducted in Biosafety Level 3 facilities (license no. 20200016905/5).

We found serum from the vaccinated cohort neutralized BA.5 with a median PRNT$_{90}$ titer of 20 (IQR 10–40), whereas serum from the convalescent cohort neutralized BA.5 with a median PRNT$_{90}$ titer of 160 (IQR 160–160). Wilcoxon rank-sum test demonstrated this 8-fold increase in neutralization after Omicron infection was statistically significant (p<0.0001). Also, the convalescent cohort neutralized SARS-CoV-2 Delta and Omicron BA.1/BA.2 strains at statistically significantly higher levels than did the vaccinated cohort (Figure 1, panel A). In vaccinated and convalescent cohorts, BA.5 was neutralized at median titers of 2–8 times lower than for the other virus strains (Figure 1, panel A). The median levels of SARS-CoV-2 spike-specific antibodies differed between cohorts; the level in the vaccinated cohort was 5,535 (IQR 1,440–8,090) binding antibody units/mL and in the convalescent cohort was 5,675 (IQR 4,970–7,730) binding antibody units/mL, but this difference was not statistically significant by Wilcoxon rank-sum test (p = 0.6505). Moreover, we noted a clear correlation between the levels of spike antibodies and PRNT$_{90}$ titers in the vaccinated cohort (Spearman r$_s$ = 0.6624; p = 0.0004) but not in the convalescent cohort (Spearman r$_s$ = −0.2048, p = 0.5531) (Figure 1, panel B).

Results from published in vitro neutralization studies indicate previous BA.1/BA.2 infection does not confer noticeable humoral protection against BA.5 (3–6,9). We analyzed 2 small but highly matched cohorts that were similar in demography, blood sampling time points, and antibody levels. Our results showed that infection during the spring Omicron BA.1/BA.2 wave greatly strengthened BA.5 neutralization capacity among persons receiving 3-dose vaccine regimens. This result agrees with another recent epidemiologic study that showed prior Omicron infection was highly protective against BA.5 (7). As in that study, we collected blood samples from citizens of Denmark during January–April 2022. During that timeframe, BA.2 accounted for 86% of SARS-CoV-2–positive tests in Denmark (https://www.covid19genomics.dk/statistics). BA.5 is closely related to BA.2 (5); thus, the BA.5 protection that we and others observe might be because BA.2 was predominant among convalescent patient cohorts, contrary to previous studies that analyzed BA.1 convalescent serum samples (3–5,9).

In this study, Omicron BA.1/BA.2 infection appeared to reduce susceptibility to newer Omicron subvariants such as BA.5 among persons who receive 3-dose BNT162b2 vaccine regimens. Together with the recently reported slower waning of Omicron infection-induced immunity (10), this finding suggests that previous Omicron infection confers an appreciable additional degree of humoral protection.

About the Author

Dr. Pedersen is a clinical microbiologist at Odense University Hospital, Denmark. His research interests include viral infections, gastrointestinal infections, and vaccine studies.

References

1. Ritchie H, Mathieu E, Rodés-Guirao L, Appel C, Giattino C, Ortiz-Ospina E, et al. Coronavirus pandemic (COVID-19). OurWorldInData.org [cited 2022 Aug 6]. https://ourworldindata.org/coronavirus
2. Suryawanshi R, Ott M. SARS-CoV-2 hybrid immunity: silver bullet or silver lining? Nat Rev Immunol. 2022;22:591–2. https://doi.org/10.1038/s41577-022-00771-8
3. Qu P, Faraone J, Evans JP, Zou X, Zheng YM, Carlin C, et al. Neutralization of the SARS-CoV-2 Omicron BA.4/5 and BA.2.12.1 Subvariants. N Engl J Med. 2022;386:2526–8. https://doi.org/10.1056/NEJMc2206725
4. Cao Y, Yisimayi A, Jian F, Song W, Xiao T, Wang L, et al. BA.2.12.1, BA.4 and BA.5 escape antibodies elicited by Omicron infection. Nature. 2022;608:593–602. https://doi.org/10.1038/s41586-022-04980-y
5. Tuekprakhon A, Nutalai R, Dijokaite-Guraliuc A, Zhou D, Ginn HM, Selvaraj M, et al.; OPTIC Consortium; ISARIC4C Consortium. Antibody escape of SARS-CoV-2 Omicron BA.4 and BA.5 from vaccine and BA.1 serum. Cell. 2022;185:2422–2433.e13. https://doi.org/10.1016/j.cell.2022.06.005
6. Wang Q, Guo Y, Iketani S, Nair MS, Li Z, Mohri H, et al. Antibody evasion by SARS-CoV-2 Omicron subvariants BA.2.12.1, BA.4 and BA.5. Nature. 2022;608:603–8. https://doi.org/10.1038/s41586-022-05053-w
7. Hansen CH, Friis NU, Bager P, Stegger M, Fonager J, Fomsgaard A, et al. Risk of reinfection, vaccine protection, and severity of infection with the BA.5 omicron subvariant: a nation-wide population-based study in Denmark. Lancet Infect Dis. 2022 Oct 18 [Epub ahead of print]. https://doi.org/10.1016/S1473-3099(22)00595-3
8. Pedersen RM, Bang LL, Madsen LW, Sydenham TV, Johansen IS, Jensen TG, et al. Serum neutralization of SARS-CoV-2 Omicron BA.1 and BA.2 after BNT162b2 booster vaccination. Emerg Infect Dis. 2022;28:1274–5. https://doi.org/10.3201/eid2806.220503
9. Kliker L, Zuckerman N, Atari N, Barda N, Gilboa M, Nemet I, et al. COVID-19 vaccination and BA.1 breakthrough infection induce neutralising antibodies which are less efficient against BA.4 and BA.5 Omicron variants, Israel, March to June 2022. Euro Surveill. 2022;27:2200559. https://doi.org/10.2807/1560-7917.ES.2022.27.30.2200559
10. Planas D, Staropoli I, Porot F, Guivel-Benhassine F, Handala L, Prot M, et al. Duration of BA.5 neutralization in sera and nasal swabs from SARS-CoV-2 vaccinated individuals, with or without Omicron breakthrough infection. Med (NY). 2022 Oct 5 [Epub ahead of print]. https://doi.org/10.1016/j.medj.2022.09.010

Address for correspondence: Thomas Emil Andersen, Department of Clinical Microbiology, Odense University Hospital, University of Southern Denmark, J. B. Winsløws Vej 21, 2nd Fl, Odense 5000, Denmark; email: thandersen@health.sdu.dk

Serologic Surveillance for SARS-CoV-2 Infection among Wild Rodents, Europe

Vincent Bourret, Lara Dutra, Hussein Alburkat, Sanna Mäki, Ella Lintunen, Marine Wasniewski, Ravi Kant, Maciej Grzybek, Vinaya Venkat, Hayder Asad, Julien Pradel, Marie Bouilloud, Herwig Leirs, Valeria Carolina Colombo, Vincent Sluydts, Peter Stuart, Andrew McManus, Jana A. Eccard, Jasmin Firozpoor, Christian Imholt, Joanna Nowicka, Aleksander Goll, Nathan Ranc, Guillaume Castel, Nathalie Charbonnel, Tarja Sironen

Author affiliations: University of Helsinki Medicum and Veterinary Medicine, Helsinki, Finland (V. Bourret, L. Dutra, H. Alburkat, S. Mäki, E. Lintunen, R. Kant, V. Venkat, H. Asad, T. Sironen); Université de Toulouse, Institut national de recherche pour l'agriculture, l'alimentation et l'environnement (INRAE), UR 0035 Comportement et écologie de la faune sauvage, Castanet-Tolosan, France (V. Bourret, N. Ranc); ANSES-Nancy, Laboratoire de la rage et de la faune sauvage, Malzéville, France (M. Wasniewski); Medical University of Gdansk Department of Tropical Parasitology, Gdynia, Poland (M. Grzybek, J. Nowicka, A. Goll); Université de Montpellier, INRAE, Montferrier-sur-Lez, France (J. Pradel, M. Bouilloud, G. Castel, N. Charbonnel); University of Antwerp Evolutionary Ecology Group, Wilrijk, Belgium (H. Leirs, V.C. Colombo, V. Sluydts); Consejo Nacional de Investigaciones Científicas y Técnicas, Buenos Aires, Argentina (V.C. Colombo); Munster Technological University Department of Biological and Pharmaceutical Sciences, Tralee, Ireland (P. Stuart, A. McManus); University of Potsdam Institute of Biochemistry and Biology, Potsdam, Germany (J.A. Eccard, J. Firozpoor); Julius Kühn Institute, Münster, Germany (C. Imholt)

We report results from serologic surveillance for exposure to SARS-CoV-2 among 1,237 wild rodents and small mammals across Europe. All samples were negative, with the possible exception of 1. Despite suspected potential for human-to-rodent spillover, no evidence of widespread SARS-CoV-2 circulation in rodent populations has been reported to date.

Esitämme tulokset serologisesta tutkimuksesta, jossaseulottiin SARS-CoV-2 tartuntojen varalta 1,237 luonnonvaraista jyrsijää ja piennisäkästä eri puolilta Eurooppaa. Kaikki näytteet olivat negatiivisia, yhtä näytettä lukuun ottamatta. SARS-CoV-2:n läikkymisen ihmisistä jyrsijöihin on arveltu olevan mahdollista, mutta todisteet viruksen laajamittaisesta leviämisestä jyrsijäpopulaatioissa puuttuvat.

Reverse transmission of diverse zoonotic pathogens (bacteria, viruses, eukaryotic parasites, fungi) from humans to animals has been recognized and documented as a global concern for years (*1*). On July 6, 2022, the World Organisation for Animal Health (OIE) stated, "While occasional occurrences of COVID-19 in domestic or zoo animals show little long-term consequence, infections at wildlife population levels indicate the possibility of further evolution of the virus in animals, and a future reintroduction of the virus into humans at a later date" (*2*). From a One Health perspective, "There is an urgent need to develop frameworks to assess the risk of SARS-CoV-2 becoming established in wild mammal populations"

(*3*). In particular, wild rodents are suspected of being among the species more susceptible to SARS-CoV-2 infection, and susceptibility to experimental infection has been confirmed among various rodent species (*4*–*6*). Specific courses of infection may differ among rodent host species, but infection usually results in little or no detectable disease, although infectious virus may shed for 4–7 days after infection and disease may be transmitted to naive rodents (*4*–*6*). These characteristics suggest the potential for reverse transmission, broad circulation, and possible long-term establishment of SARS-CoV-2 in rodent populations. Such an event would be of concern: hamsters, for example, have transmitted SARS-CoV-2 to humans,
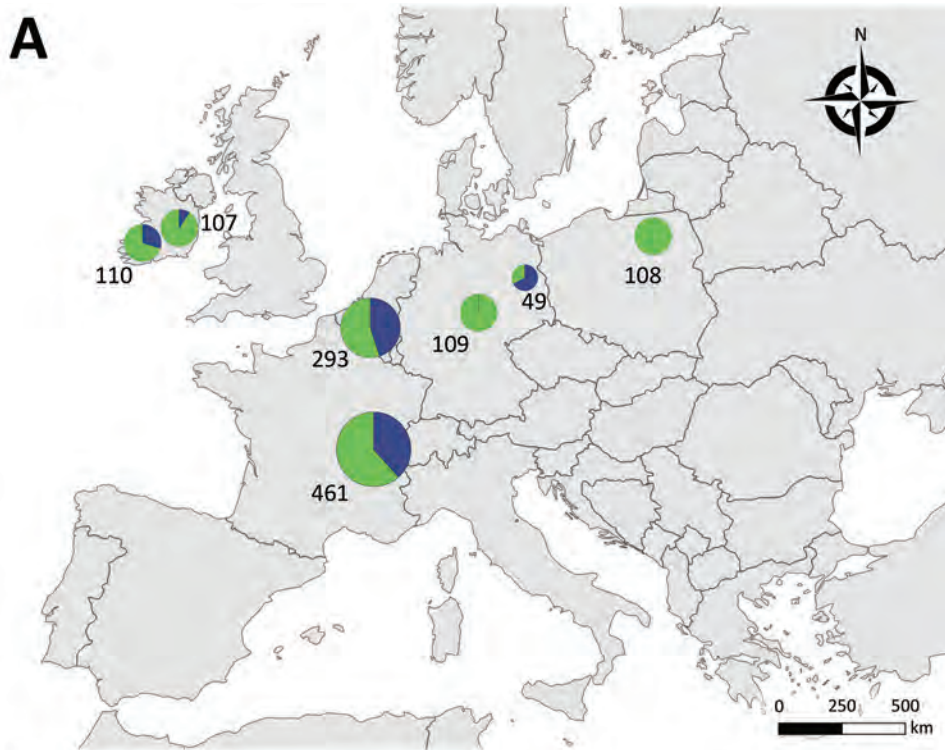
Figure. Sampling of various areas in Europe to detect SARS-CoV-2 antibody response in wild rodents. A) Location of sampling areas. Colors indicate the proportion of samples taken in the 2 habitat types (green: forests; blue: urban parks) and symbol size and numbers indicate sample size. Samples were taken from up to 8 different sites in each country (Appendix Figure 1, https://wwwnc.cdc.gov/EID/article/28/12/22-1235-App1.pdf). B) Number of individuals sampled, by date and taxonomy. Details of sampling periods, habitats, and rodent species are provided in Appendix 2 (https://wwwnc.cdc.gov/EID/article/28/12/22-1235-App2.xlsx).
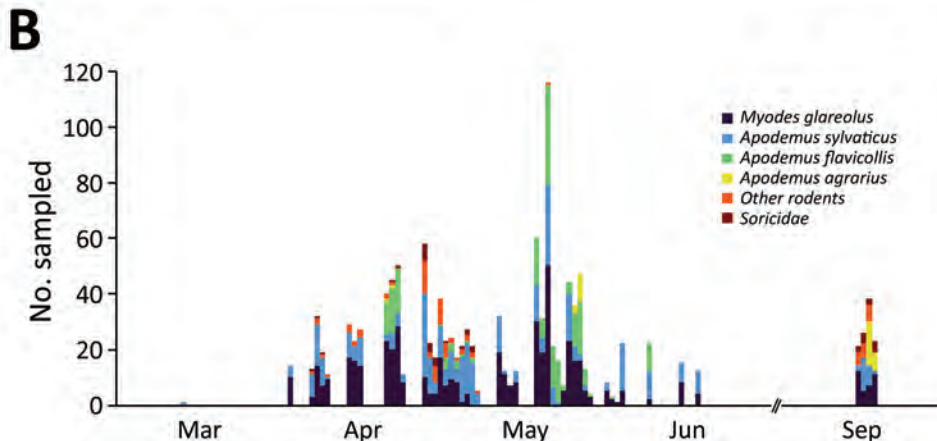
followed by subsequent person-to-person transmission (7). Consequently, on December 6, 2021, the joint United Nations Food and Agriculture Organization and OIE (FAO-OIE) Advisory Group on SARS-CoV-2 Evolution in Animals indicated that a large surveillance study of rodent populations exposed to human contact was needed to close a major gap in SARS-CoV-2 research.

Animal experiments have shown that antibodies can be detected consistently for several weeks or longer after rodent infection with SARS-CoV-2, although detectable virus shedding lasts only a few days (4–6). When field prevalence is low or unknown among the target population, serologic testing is the preferred method to maximize chances of detecting circulation of viruses such as SARS-CoV-2 that cause brief infection but maintain longer-lasting serologic response. A recent survey in Hong Kong found a Norway rat (*Rattus norvegicus*) to be potentially seropositive for SARS-CoV-2 (8). Considering the high biodiversity and ubiquity of rodents, this finding called for broader surveillance studies in other continents, habitats, and noncommensal rodent species. To investigate its possible reverse zoonotic transmission and establishment in wild rodents in different settings, we conducted a large-scale serologic survey of SARS-CoV-2 in multiple rodent species across Europe.

We sampled animals in urban parks and zoos, which offer ample opportunity for transmission between humans and rodents, and forests, because other wild forest mammals such as deer have become naturally infected with SARS-CoV-2 (9). During 2021, we sampled 1,202 rodents and 35 Soricidae shrews (genera *Sorex* and *Crocidura*) from 23 forests sites and 8 urban parks in 5 countries in Europe (Ireland, Belgium, France, Germany, and Poland) (Figure 1; Appendix 1 Figure 1, https://wwwnc.cdc.gov/EID/article/28/12/22-1235-App1.pdf; Appendix 2, https://wwwnc.cdc.gov/EID/article/28/12/22-1235-App2.xlsx). We then assessed each rodent's SARS-CoV-2 serologic status using an infected cell-based immunofluorescent assay (IFA; Appendix 1) (10). We chose the IFA instead of a neutralization assay as the initial screening test because it is scalable to a large number of samples and can be effective in detecting both neutralizing and nonneutralizing antibodies.

All but one of the rodents sampled were IFA negative for SARS-CoV-2. The one IFA-positive rodent (assayed twice on different days to rule out any handling error) was a wood mouse (*Apodemus sylvaticus*) sampled in an urban park near the city of Antwerp, Belgium, on April 6, 2021. We then tested this IFA-positive sample using a seroneutralization assay (Appendix 1), and results were negative, suggesting that the sample had no detectable neutralizing antibodies against the virus strain used in the seroneutralization assay. The sample was also negative by microsphere immunoassay (Appendix 1). The overall serologic status of this wood mouse was therefore unconfirmed. To further investigate possible virus circulation in the area, we used the Luna SARS-CoV-2 RT-qPCR Multiplex Assay Kit (New England BioLabs, https://www.neb.com) to test samples from all 59 rodents captured in the same location as the wood mouse (Appendix 1). PCRs were all negative (including for the IFA-positive wood mouse), which could be expected given the short virus-shedding period described in rodents (4–6).

Our main conclusion on the basis of this survey is that there is no evidence of a major SARS-CoV-2 spread among wild rodents in northern Europe as of April–September 2021. A similar conclusion had been reached in the study from Hong Kong (8), an area with a denser human population and large populations of pest rodents. In that study, serum from 1 urban brown rat was positive in some but not all serologic tests used, and all SARS-CoV-2 PCR tests were negative (8) Taken together, these results indicate no evidence of widespread SARS-CoV-2 circulation in rodent populations to date.

Programme 2021–2030. The National Science Centre, Poland, supported M.G., J.N., and A.G. under the BiodivERsA3 program (2019/31/Z/NZ8/04028). Sampling from Thuringia (Germany) was funded by the DFG Priority Program 1374.

Trapping data from this study will be available in Germany in the Biodiversity Exploratories Information System (https://doi.org/10.17616/R32P9Q).

About the Author

Dr. Bourret is a DVM with a PhD in virology from University of Cambridge, UK. He is a researcher at INRAE, France, and works on wildlife disease ecology and One Health topics.

References

1. Messenger AM, Barnes AN, Gray GC. Reverse zoonotic disease transmission (zooanthroponosis): a systematic review of seldom-documented human biological threats to animals. PLoS One. 2014;9:e89055. https://doi.org/10.1371/journal.pone.0089055
2. World Organisation for Animal Health. Crossing the species barrier: COVID-19, an example of reverse zoonosis [cited 2022 Jul 7]. https://www.woah.org/en/crossing-the-species-barriers-covid-19-an-example-of-reverse-zoonosis
3. Delahay RJ, de la Fuente J, Smith GC, Sharun K, Snary EL, Flores Girón L, et al. Assessing the risks of SARS-CoV-2 in wildlife. One Health Outlook. 2021;3:7. https://doi.org/10.1186/s42522-021-00039-6
4. Bosco-Lauth AM, Root JJ, Porter SM, Walker AE, Guilbert L, Hawvermale D, et al. Peridomestic mammal susceptibility to severe acute respiratory syndrome coronavirus 2 infection. Emerg Infect Dis. 2021;27:2073–80. https://doi.org/10.3201/eid2708.210180
5. Griffin BD, Chan M, Tailor N, Mendoza EJ, Leung A, Warner BM, et al. SARS-CoV-2 infection and transmission in the North American deer mouse. Nat Commun. 2021;12:3612. https://doi.org/10.1038/s41467-021-23848-9
6. Chan JFW, Zhang AJ, Yuan S, Poon VKM, Chan CCS, Lee ACY, et al. Simulation of the clinical and pathological manifestations of coronavirus disease 2019 (COVID-19) in a golden Syrian hamster model: implications for disease pathogenesis and transmissibility. Clin Infect Dis. 2020;71:2428–46. https://doi.org/10.1093/cid/ciaa644
7. Yen HL, Sit THC, Brackman CJ, Chuk SSY, Gu H, Tam KWS, et al.; HKU-SPH study team. Transmission of SARS-CoV-2 delta variant (AY.127) from pet hamsters to humans, leading to onward human-to-human transmission: a case study. Lancet. 2022;399:1070–8. https://doi.org/10.1016/S0140-6736(22)00326-9
8. Miot EF, Worthington BM, Ng KH, de Lataillade LG, Pierce MP, Liao Y, et al. Surveillance of rodent pests for SARS-CoV-2 and other coronaviruses, Hong Kong. Emerg Infect Dis. 2022;28:467–70. https://doi.org/10.3201/eid2802.211586
9. Kuchipudi SV, Surendran-Nair M, Ruden RM, Yon M, Nissly RH, Vandegrift KJ, et al. Multiple spillovers from humans and onward transmission of SARS-CoV-2 in white-tailed deer. Proc Natl Acad Sci U S A. 2022;119:e2121644119. https://doi.org/10.1073/pnas.2121644119
10. Haveri A, Smura T, Kuivanen S, Österlund P, Hepojoki J, Ikonen N, et al. Serological and molecular findings during SARS-CoV-2 infection: the first case study in Finland, January to February 2020. Euro Surveill. 2020;25:2000266. https://doi.org/10.2807/1560-7917.ES.2020.25.11.2000266

Address for correspondence: Vincent Bourret, UR 0035 CEFS, INRAE, 24 chemin de Borde-Rouge, Auzeville CS 52627, 31326 Castanet Tolosan CEDEX, France; email: vincent.bourret@inrae.fr

Delayed Diagnosis of Acute Q Fever, China

Dan Li, Hui Liu, Ming Liu, Caiyun Chang, Xiaodong Zhao, Hao Yu, Lina Yan, Huiju Han, Xue-jie Yu

Author affiliations: State Key Laboratory of Virology, School of Public Health, Wuhan University, Wuhan, China (D. Li, L. Yan, H. Han, X.-j. Yu); Jinan Center for Disease Control and Prevention, Jinan, China (H. Liu, M. Liu, C. Chang, X. Zhao); University of Texas MD Anderson Cancer Center, Houston, Texas, USA (H. Yu)

We report a patient in China with fever of unknown origin who visited 3 hospitals in 3 weeks and was finally given a diagnosis of acute Q fever, determined by metagenomics next-generation sequencing. Our results indicate that physicians are unfamiliar with Q fever and the disease is neglected in China.

Q fever is an important worldwide zoonosis with nonspecific symptoms, making diagnosis challenging (1–3). Humans become infected mainly by inhalation of *Coxiella burnetii*–contaminated aerosols from animal waste or contaminated soil (4). *C. burnetii* is listed as a biologic weapon in the United States, and Q fever is a nationally notifiable disease in the United States, Australia, Netherlands, and Japan, but it is not a notifiable disease in China (2,5–7). Serologic epidemiology indicates that *C. burnetii* is widely distributed in China, but Q fever is rarely reported and might be neglected (2,7). We report a case of Q fever in a man in Shandong Province, China. The need for ethics approval and informed consent was waived,
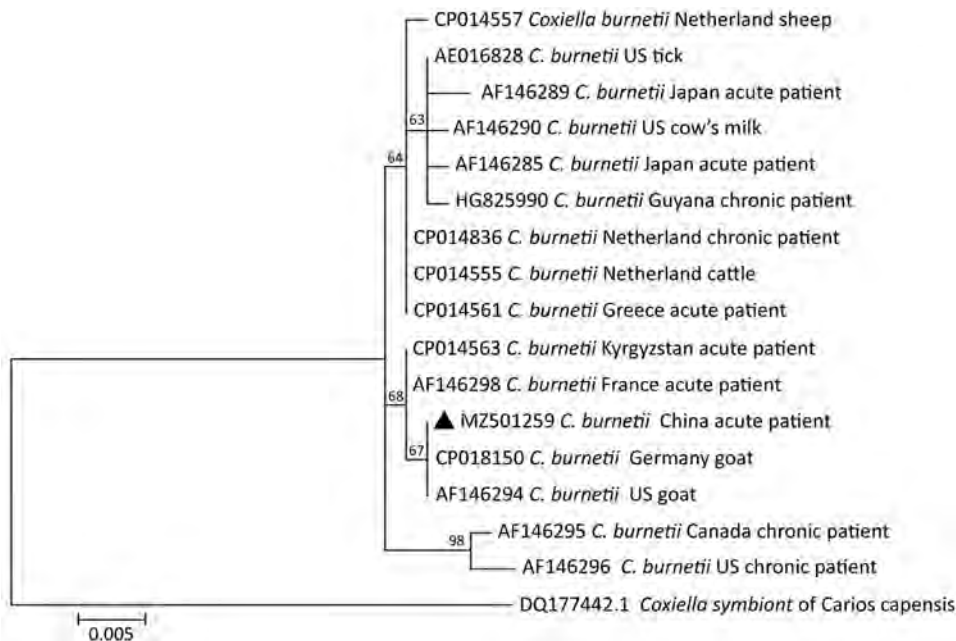
Figure 2. Phylogenetic tree of *Coxiella burnetii* from a patient with Q fever in Shandong Province, China, 2019. Triangle indicates the strain detected in this study. The phylogenetic tree was constructed using the complete isocitrate dehydrogenase gene sequence (1,300-bp) with the maximum-likelihood method using MEGA 7.0 (https://www.megasoftware. net). Bootstrap values >50% from 1,000 replicates (shown on the nodes). Scale bar indicates substitutions per site.

granted by the National Health Commission of China as part of outbreak investigation of infectious disease.

A 55-year-old man in a rural area of Jinan, Shandong Province, China, had fever (38.3 °C), headache, fatigue, loss of appetite, and myalgia develop on August 24, 2019 (Figure 1, https://wwwnc.cdc.gov/EID/article/28/12/22-1118-F1.htm). He visited a local town hospital and was treated with acetaminophen and chlorpheniramine. When his symptoms persisted, he visited a county hospital on the 9th day after illness onset with a body temperature of 38.5°C and was treated with oral cefprozil and levofloxacin. On the 14th day of illness, with no improvement of his symptoms, he was transferred to a local municipal hospital. At admission, his body temperature was 39.0°C. Blood tests revealed elevation in neutrophil count and ratio, C-reactive protein, serum procalcitonin, and liver enzymes (Table). Bacterial culture showed no growth of microorganisms in either aerobic or anaerobic cultures (BD BACTEC FX 200 blood culture instrument, https://www.bd.com). We used PCR or immunologic test kits to test for viruses (influenza virus, severe fever with thrombocytopenia syndrome virus, Hantan virus, hepatitis B, hepatitis C, Epstein-Barr, and cytomegalovirus) and bacteria (*Brucella*, *Mycobacterium tuberculosis*, typhoid, and paratyphoid). We observed no positive results.

We sent samples to the CapitalBio MedLab in Beijing, China, where metagenomics next-generation sequencing (mNGS) was performed to determine the etiologic agent (Ion Proton Sequencer, https://www.thermofisher.com). A blood sample obtained from the patient provided DNA for that analysis (QIAamp MinElute ccfDNA Mini Kit; https://www.qiagen.com). On the 19th day after illness onset, the mNGS result revealed *C. burnetii* sequences in the patient's blood sample; no other pathogens were observed. The sequence coverage rate of the *C. burnetii* genome was 97.66% (2,078,829 bp) with 137,272 reads (average length 141 bp, average quality 23), 1,105 contigs (range 262–16,242 bp), and an estimated 1.80×10^4 copies/mL of *C. burnetii* in the sequencing sample. The mNGS result clearly indicated that the patient was infected with *C. burnetii*. Phylogenetic analysis revealed that the isocitrate dehydrogenase sequence from the patient formed a monophyletic group with sequences of *C. burnetii* from goats and from humans diagnosed with acute Q fever from GenBank (Figure). The isocitrate dehydrogenase sequence homology between the patient and those sequences were 99.85%–99.92%.

Table. Blood and biochemical indicators for a patient with Q fever, Shandong Province, China, 2019

Category	Value	Reference range
Neutrophil count, × 10⁹ cells/L	8.30	2.00–7.00
Neutrophils, %	86.20	50.00–70.00
Leukocyte, × 10⁹ cells/L	9.64	4–10
Leukomonocyte, × 10⁹ cells/L	0.79	0.80–4.0
Platelet, × 10⁹/L	210	100–300
Erythrocytes, × 10¹² cells/L	4.13	4.0–5.5
C-reactive protein, mg/L	21.96	0.068–8.20
Serum procalcitonin, ng/mL	2.50	0–0.05
Alanine aminotransferase, U/L	99	0–40
Alkaline phosphatase, U/L	208	40–150
Aspartate transaminase, U/L	51	0–40
Gamma-glutamyl transpeptidase, U/L	333	12–64

We performed cardiac ultrasound of the patient, which showed normal cardiopulmonary function and ruled out Q fever endocarditis. We treated the patient with oral doxycycline (100 mg 2×/d). His symptoms disappeared in 1 week, and he was discharged and continued on oral doxycycline (100 mg 2×/d) for 1 more week. We followed the patient for 1 year, noting no recurrence of Q fever.

This patient worked as a woodworker in a village without nearby abattoirs. He did not raise animals, but there were goats in his village, and mice were often observed around his living and working places. He denied any contact with domesticated or wild animals, ingestion of unpasteurized dairy products or uncooked meat, tick bite, exposure to similar patients, or any travel history to other places in China or abroad in the months before his illness.

Multiple factors likely delayed diagnosis of this patient with Q fever. Although nonspecific symptoms contributed, the greatest obstacles to diagnosis, we believe, were unawareness of the existence of Q fever by physicians and lack of conventional diagnostic reagents of Q fever, such as serologic and *C. burnetii*–specific PCR reagents, in the medical institutions our patient visited (*8,9*).

In conclusion, we report a patient with febrile illness from Shandong Province, China, without etiologic diagnosis and appropriate treatment for 3 weeks, until mNGS revealed *C. burnetii* genomic sequences in the patient's blood. Our study suggests that physicians need to be more aware that Q fever is widespread in China and should be considered when diagnosing patients with persistent fever of unknown origin, even without clear exposure history. In addition, conventional diagnostic reagents of Q fever should be stored in local medical institutions in China. mNGS is a method to randomly sequence all nucleic acids and identify organisms by bioinformatics analysis in a sample, which is useful in identifying unknown pathogens. Our case supports previous studies that demonstrated that mNGS can be used to diagnose Q fever and other pathogens in humans (*10*).

Contigs of *C. burnetii* from this patient are available upon request from the authors.

Acknowledgments

About the Author
Dan Li is a PhD candidate at the School of Public Health, Wuhan University, Wuhan, Hubei, China. Her research interest is epidemiology of emerging infectious diseases.

References

1. Derrick EH. "Q" fever, a new fever entity: clinical features, diagnosis and laboratory investigation. Rev Infect Dis. 1983;5:790–800. https://doi.org/10.1093/clinids/5.4.790
2. El-Mahallawy HS, Lu G, Kelly P, Xu D, Li Y, Fan W, et al. Q fever in China: a systematic review, 1989-2013. Epidemiol Infect. 2015;143:673–81. https://doi.org/10.1017/S0950268814002593
3. Karageorgou I, Kogerakis N, Labropoulou S, Hatzianastasiou S, Mentis A, Stavridis G, et al. Q fever endocarditis and a new genotype of *Coxiella burnetii*, Greece. Emerg Infect Dis. 2020;26:2527–9. https://doi.org/10.3201/eid2610.191616
4. Parker NR, Barralet JH, Bell AM. Q fever. Lancet. 2006;367:679–88. https://doi.org/10.1016/S0140-6736(06)68266-4
5. Madariaga MG, Rezai K, Trenholme GM, Weinstein RA. Q fever: a biological weapon in your backyard. Lancet Infect Dis. 2003;3:709–21. https://doi.org/10.1016/S1473-3099(03)00804-1
6. Devaux CA, Osman IO, Million M, Raoult D. *Coxiella burnetii* in dromedary camels (*Camelus dromedarius*): a possible threat for humans and livestock in North Africa and the Near and Middle East? Front Vet Sci. 2020;7:558481. https://doi.org/10.3389/fvets.2020.558481
7. Huang M, Ma J, Jiao J, Li C, Chen L, Zhu Z, et al. The epidemic of Q fever in 2018 to 2019 in Zhuhai city of China determined by metagenomic next-generation sequencing. PLoS Negl Trop Dis. 2021;15:e0009520. https://doi.org/10.1371/journal.pntd.0009520
8. Stein A, Raoult D. Detection of *Coxiella burnetti* by DNA amplification using polymerase chain reaction. J Clin Microbiol. 1992;30:2462–6. https://doi.org/10.1128/jcm.30.9.2462-2466.1992
9. Anderson A, Bijlmer H, Fournier PE, Graves S, Hartzell J, Kersh GJ, et al. Diagnosis and management of Q fever—United States, 2013: recommendations from CDC and the Q Fever Working Group. MMWR Recomm Rep. 2013;62 (RR-03):1–30.
10. Simner PJ, Miller S, Carroll KC. Understanding the promises and hurdles of metagenomic next-generation sequencing as a diagnostic tool for infectious diseases. Clin Infect Dis. 2018;66:778–88. https://doi.org/10.1093/cid/cix881

Address for correspondence: Xue-jie Yu, School of Public Health, Wuhan University, Doghulu 115, Wuhan City, Hubei Province 430071, China; email: yuxuejie@whu.edu.cn; Hui Liu, Jinan Center for Disease Control and Prevention, Weiliulu 2, Jinan City, Shandong Province 250021, China; email: jncdclh@jn.shandong.cn

Bombali Ebolavirus in *Mops condylurus* Bats (Molossidae), Mozambique

Camille Lebarbenchon, Steven M. Goodman,
Axel O.G. Hoarau, Gildas Le Minter,
Andréa Dos Santos, M. Corrie Schoeman,
Christophe Léculier, Hervé Raoul,
Eduardo S. Gudo, Patrick Mavingui

Author affiliations: Processus Infectieux en Milieu Insulaire
Tropical, University of Reunion, Inserm, CNRS, IRD, Saint-Denis,
Reunion Island, France (C. Lebarbenchon, A.O.G. Hoarau,
G. Le Minter, P. Mavingui); Field Museum of Natural History,
Chicago, USA S.M. Goodman); Association Vahatra,
Antananarivo, Madagascar (S.M. Goodman); Eduardo Mondlane
University, Maputo, Mozambique (A. Dos Santos); University of
Kwa-Zulu Natal, Kwa-Zulu Natal, South Africa (M.C. Schoeman);
Jean Mérieux Inserm P4 Laboratory, Lyon, France (C. Léculier,
H. Raoul); National Institute of Health, Maputo, Mozambique
(E.S. Gudo)

We detected Bombali ebolavirus RNA in 3 free-tailed
bats (*Mops condylurus*, Molossidae) in Mozambique.
Sequencing of the large protein gene revealed 98%
identity with viruses previously detected in Sierra Leone,
Kenya, and Guinea. Our findings further support the
suspected role of *Mops condylurus* bats in maintaining
Bombali ebolavirus.

Six viruses of the genus *Ebolavirus* have been documented to date (Zaire, Sudan, Bundibugyo, Taï Forest, Reston, and Bombali), and some have caused outbreaks in Africa, resulting in high human fatality rates. Bombali virus (BOMV) was first identified in free-tailed bats of the family Molossidae, specifically the species *Mops condylurus* and *Chaerephon pumilus*, in 2016 in the Bombali District in Sierra Leone (*1*). This virus was later detected in *M. condylurus* bats in Kenya (*2,3*) in 2018 and in Guinea (*4*) in 2019 (Figure, panel A). Human infections have not been documented, including in patients with febrile illness symptoms in areas where BOMV has been found in bats (*2*).

We detected BOMV RNA in 3 *M. condylurus* bats (all female) captured in Mozambique in the southeastern portion of this species' geographic range (Figure, panel A). In May 2015, we obtained samples from 54 *M. condylurus* bats residing in buildings in the Inhassoro District of southeastern Mozambique and from 211 other bats (representing 10 species), mostly from caves (Appendix, https://wwwnc.cdc.gov/EID/article/28/12/22-0853-App1.pdf). We screened all samples for viruses belonging to the families *Astroviridae* (*5*), *Coronaviridae* (*6*), and *Paramyxoviridae* (*7*). We performed RNA extraction with the QIAamp Viral RNA Mini Kit (QIAGEN, https://www.qiagen.com) and reverse transcription with the ProtoScript II Reverse Transcriptase and Random Primer 6 (New England BioLabs, https://www.neb.com). We screened complementary DNA with 3 assays targeting the large (L) protein gene of Filoviriridae (Appendix) and submitted PCR products of the expected size for direct Sanger sequencing (GenoScreen, https://www.genoscreen.fr). We did not attempt virus isolation in this study. We processed samples in a Biosafety Level 3 laboratory at the University of Reunion (Saint-Denis, Reunion Island, France) and transferred original samples to the Biosafety Level 4 laboratory at Inserm Jean Mérieux (Lyon, France).

To date, BOMV is the only ebolavirus that has been recurrently detected by PCR, across multiple years (2015–2019), and in bat populations located >5,000 km apart (*1–4*). Our study provides support for BOMV in the southern range of where *M. condylurus* bats are known to reside (Figure, panel A). Partial sequencing of the L protein gene revealed that the BOMV sequences detected in bats from Mozambique were closely related to those sequences reported in bats from Sierra Leone, Kenya, and Guinea (Figure, panel B). Although our findings are based on short sequences (587 bp), this finding could suggest a strong association between BOMV and *M. condylurus* bats across their geographic range.

BOMV epidemiology in *M. condylurus* bats is unknown. Seasonal variation of environmental conditions and population structure are important drivers for the transmission dynamics of infectious agents in natural systems (*8*). For instance, pulses of Marburg virus, paramyxovirus, and coronavirus shedding have been shown to coincide with a seasonal increase of juveniles in bat populations (*9,10*). Although our study was based on a limited sampling, we detected BOMV only in female bats (χ^2 = 4.6; df = 1; p<0.05; no. tested females/males: 26/28) and did not find differences between adults and subadults (χ^2 = 0.5; df = 1; p = 0.46; no. tested adults/subadults: 29/25). Previous reports likewise reported BOMV more frequently in female bats (Figure, panel A) (*1–3*). All prior studies reported BOMV-positive bats during the month of May (Figure, panel A) (*1–4*). Whether these observations reflect a biologic phenomenon remains to be tested. Across their geographic range, female *M. condylurus* bats usually have 2 birthing periods that occur between September and early May, and some variation in virus shedding can be anticipated with
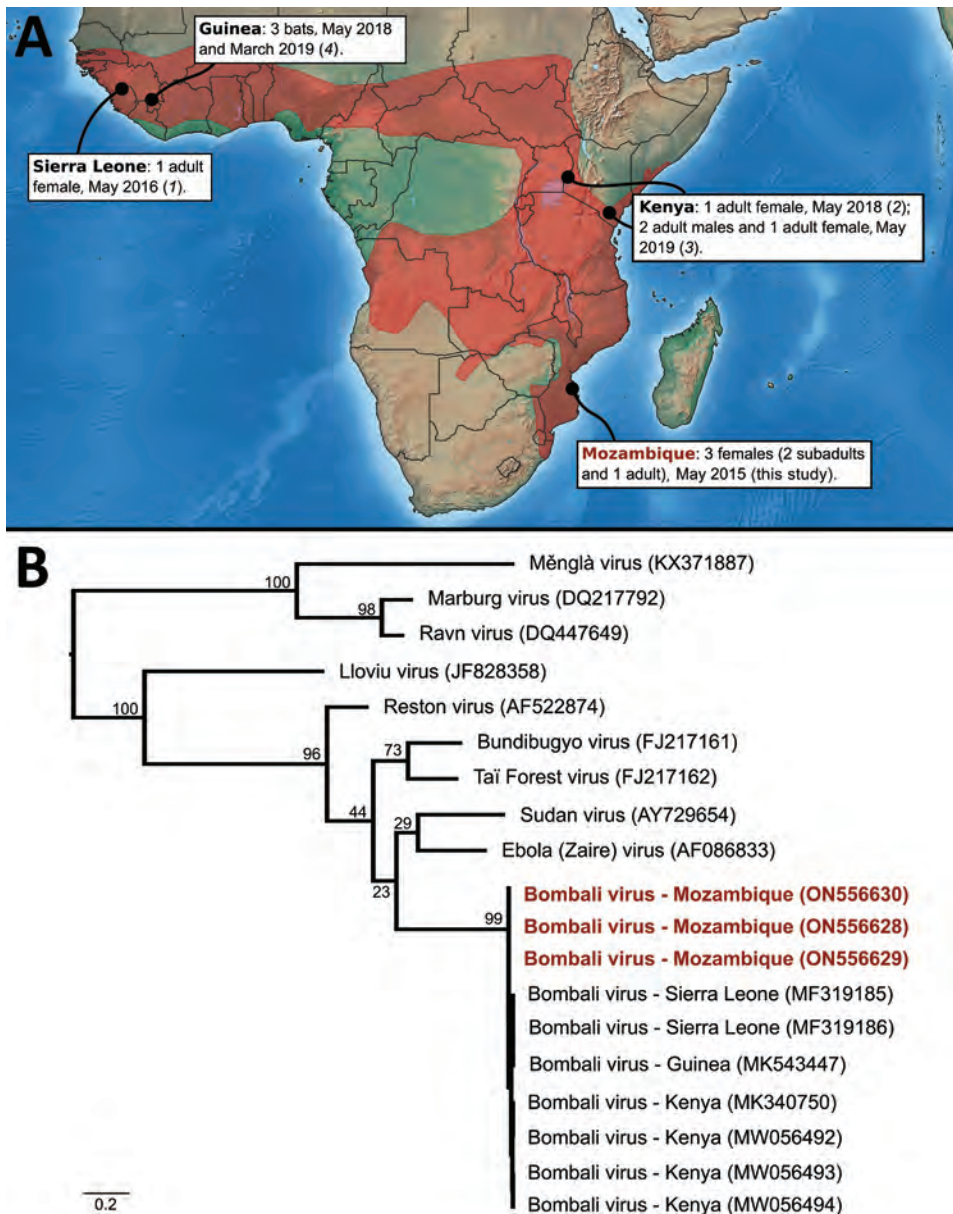
Figure. Bombali virus detection in Angolan free-tailed bats (*Mops condylurus*). A) Geographic range highlighted in red. Information regarding the sex of positive *M. condylurus* bats in Guinea is not available (*4*). The map was generated with data available from Natural Earth (https://www.naturalearthdata.com) and the International Union for Conservation of Nature Red List Web site (https://www.iucnredlist.org). B) Maximum-likelihood tree based on partial nucleotide sequences (587 bp) of the large protein gene of selected filoviruses. Red indicates sequences generated in this study. The phylogenetic analysis was conducted with the transversion plus gamma evolutionary model (α = 0.32) and 1,000 bootstraps (Appendix, https://wwwnc.cdc.gov/EID/article/28/12/22-0853-App1.pdf). All but 1 of the Bombali virus were detected in *Mops condylurus* bats, with the exception of MF319186, which collected from a *Chaerephon pumilus* bat (*1*).

each reproductive cycle, as documented for other bat–virus systems. Longitudinal studies are needed to investigate biologic and ecologic factors involved in the transmission dynamics of BOMV in *M. condylurus* bats but also to fully assess virus spillover risk to other hosts, including humans.

In Mozambique, neither BOMV nor other species of ebolavirus have been detected in humans, highlighting that our findings should not be considered evidence of a major threat to local communities, but should be instead considered a catalyst for further investigation and surveillance. Additional studies should focus on other Molossidae bats, because BOMV was initially reported in another member of the family, *Chaerephon pumilus* (*1*), and these bats commonly roost in synanthropic settings and therefore generate opportunities for spillover. Indeed, most BOMV-positive bats were captured in day-roost sites in buildings occupied by humans or livestock (*1,3,4*). Assessing livestock exposure to BOMV also would be prudent, given their key role as intermediate hosts in the emergence of zoonotic viruses.

The discovery of ebolavirus in wild animals raises questions regarding virus spillover and epidemic potential. In addition to the identification of molecular factors involved in the ability of the virus to replicate in human cells, risk assessment should include environmental factors across the local, social,

and habitat landscape. Employing a One Health approach (i.e., collaborative, multisectoral, and transdisciplinary) might prevent future outbreaks, promote sustainable development of human communities, and offer protection for bats that play a key functional role in ecosystems.

About the Author

Dr. Lebarbenchon is an associate professor at the University of La Réunion–National Institute of Health and Medical Research. His research focuses on the ecology and evolution of emerging viruses in bats and wild birds on tropical islands.

References

1. Goldstein T, Anthony SJ, Gbakima A, Bird BH, Bangura J, Tremeau-Bravard A, et al. The discovery of Bombali virus adds further support for bats as hosts of ebolaviruses. Nat Microbiol. 2018;3:1084–9. https://doi.org/10.1038/s41564-018-0227-2
2. Forbes KM, Webala PW, Jääskeläinen AJ, Abdurahman S, Ogola J, Masika MM, et al. Bombali Virus in *Mops condylurus* bat, Kenya. Emerg Infect Dis. 2019;25:955–7. https://doi.org/10.3201/eid2505.181666
3. Kareinen L, Ogola J, Kivistö I, Smura T, Aaltonen K, Jääskeläinen AJ, et al. Range expansion of Bombali virus in *Mops condylurus* bats, Kenya, 2019. Emerg Infect Dis. 2020;26:3007–10. https://doi.org/10.3201/eid2612.202925
4. Karan LS, Makenov MT, Korneev MG, Sacko N, Boumbaly S, Yakovlev SA, et al. Bombali virus in *Mops condylurus* bats, Guinea. Emerg Infect Dis. 2019;25:1774–5. https://doi.org/10.3201/eid2509.190581
5. Hoarau F, Le Minter G, Joffrin L, Schoeman MC, Lagadec E, Ramasindrazana B, et al. Bat astrovirus in Mozambique. Virol J. 2018;15:104. https://doi.org/10.1186/s12985-018-1011-x
6. Joffrin L, Goodman SM, Wilkinson DA, Ramasindrazana B, Lagadec E, Gomard Y, et al. Bat coronavirus phylogeography in the Western Indian Ocean. Sci Rep. 2020;10:6873. https://doi.org/10.1038/s41598-020-63799-7
7. Hoarau AOG, Goodman SM, Al Halabi D, Ramasindrazana B, Lagadec E, Le Minter G, et al. Investigation of astrovirus, coronavirus and paramyxovirus co-infections in bats in the western Indian Ocean. Virol J. 2021;18:205. https://doi.org/10.1186/s12985-021-01673-2
8. Altizer S, Dobson A, Hosseini P, Hudson P, Pascual M, Rohani P. Seasonality and the dynamics of infectious diseases. Ecol Lett. 2006;9:467–84. https://doi.org/10.1111/j.1461-0248.2005.00879.x
9. Amman BR, Carroll SA, Reed ZD, Sealy TK, Balinandi S, Swanepoel R, et al. Seasonal pulses of Marburg virus circulation in juvenile *Rousettus aegyptiacus* bats coincide with periods of increased risk of human infection. PLoS Pathog. 2012;8:e1002877. https://doi.org/10.1371/journal.ppat.1002877
10. Joffrin L, Hoarau AOG, Lagadec E, Torrontegi O, Köster M, Le Minter G, et al. Seasonality of coronavirus shedding in tropical bats. R Soc Open Sci. 2022;9:211600. https://doi.org/10.1098/rsos.211600

Address for correspondence: Camille Lebarbenchon or Patrick Mavingui, UMR Processus Infectieux en Milieu Insulaire Tropical (PIMIT; Université de La Réunion, CNRS, Inserm, IRD), GIP CYROI, 2 Rue Maxime Rivière, 97400 Saint-Denis, La Réunion, France; emails: camille.lebarbenchon@univ-reunion.fr or patrick.mavingui@cnrs.fr

Hand, Foot, and Mouth Disease as Differential Diagnosis of Monkeypox, Germany, August 2022

Anahita Fathi, Stefan Schmiedel

Author affiliations: University Medical Center Hamburg-Eppendorf, Hamburg, Germany (A. Fathi, S. Schmiedel); Bernhard Nocht Institute for Tropical Medicine, Hamburg (A. Fathi); German Center for Infection Research, Partner Site Hamburg-Lübeck-Borstel-Riems, Hamburg (A. Fathi, S. Schmiedel)

To the Editor: Lewis et al. recommend considering hand, foot, and mouth disease (HFMD) as a differential diagnosis for monkeypox on the basis of a series of 9 patients from Argentina and Bolivia with suspicion of monkeypox, of which 3/9 patients had laboratory-confirmed monkeypox and 4/9 patients had HFMD (1). HFMD is common in young children worldwide. Symptoms are usually mild and transient and consist of influenza-like illness, oral sores or pustules, and a palmar and plantar rash (2). However, reports about atypical HFMD, which is characterized by severe symptoms, unusual localization of the rash, and occurrence in immunocompetent adults, have recently increased.

Like HFMD, monkeypox often clinically manifests with influenza-like symptoms and a pustular rash (3). As of September 2022, >3,500 cases have been reported in Germany (4), and differential diagnosis and testing has become increasingly necessary.

We report a case of a 20-year-old man who sought evaluation for monkeypox at University Medical Center Hamburg-Eppendorf (Germany). Two days before, he began experiencing myalgias and fever, followed by a generalized rash with painful pustular lesions on the arms, hands, feet, mouth, scalp, and anus. He was taking HIV preexposure prophylaxis but had no concurrent conditions. He reported sexual contact with 2 male partners in the 14 days before symptom onset and had regularly visited his family in the previous 29 days, during which time multiple family members experienced influenza-like symptoms and a rash. The patient had called an urgent care provider the day before our evaluation and had been placed under quarantine for suspicion of monkeypox because of his clinical manifestations and medical history.

We swabbed anal, oral, and skin lesions and assessed the specimens for orthopoxvirus and enterovirus nucleic acids by PCR, which was positive for enterovirus but negative for orthopoxvirus, confirming HFMD. In conclusion, we support the suggestion to consider atypical HFMD as a differential diagnosis of monkeypox.

References

1. Lewis A, Josiowicz A, Hirmas Riade SM, Tous M, Palacios G, Cisterna DM. Introduction and differential diagnosis of monkeypox in Argentina, 2022. Emerg Infect Dis. 2022;28:2123–5. https://doi.org/10.3201/eid2810.221075
2. Centers for Disease Control and Prevention. Symptoms and diagnosis of hand, foot, and mouth disease. 2022 [cited 20 Sep 2022]. https://www.cdc.gov/hand-foot-mouth/about/signs-symptoms.html
3. Thornhill JP, Barkati S, Walmsley S, Rockstroh J, Antinori A, Harrison LB, et al.; SHARE-net Clinical Group. Monkeypox virus infection in humans across 16 countries—April–June 2022. N Engl J Med. 2022;387:679–91. https://doi.org/10.1056/NEJMoa2207323
4. Robert Koch Institut. International monkeypox outbreak: number of cases and assessment of the situation in Germany [in German]. 2022 [cited 20 Sep 2022]. https://www.rki.de/DE/Content/InfAZ/A/Affenpocken/Ausbruch-2022-Situation-Deutschland.html

Address for correspondence: Anahita Fathi, University Medical Center Hamburg-Eppendorf, 1st Medical Department, Division of Infectious Diseases, Martinistr. 52, 20246 Hamburg, Germany; email: a.fathi@uke.de
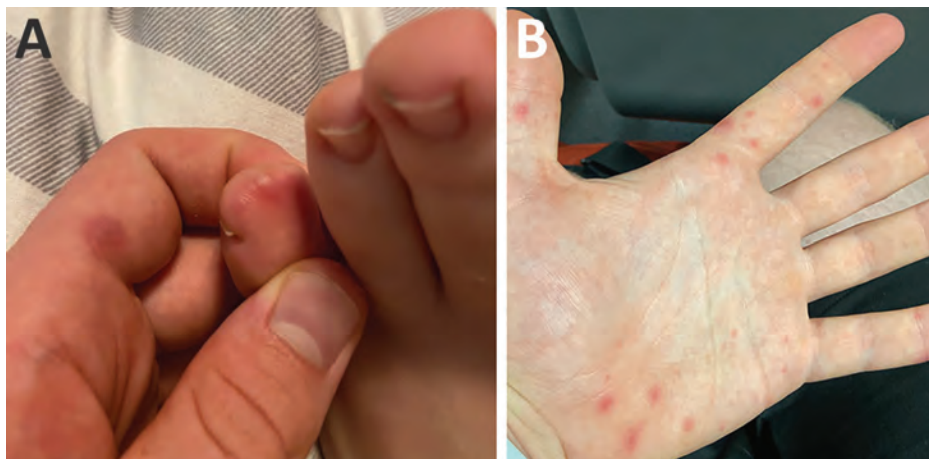
Figure. Painful pustular lesions on left foot (A) and hand (B) of a 20-year-old man 1 day after onset of influenza-like symptoms, Germany. PCR results were positive for enterovirus but negative for orthopoxvirus, confirming hand, foot, and mouth disease rather than monkeypox.

Global Health Security: A Blueprint for the Future

Lawrence O. Gostin

Global Health Security: A Blueprint for the Future Harvard University Press, Cambridge, Massachusetts, USA, 2021; ISBN: 9780674976610 (cloth); Pages: 352; Price: $45

Lawrence Gostin's Global Health Security: A Blueprint for the Future comes along at an opportune time, as a pandemic reminds humankind of the importance of public health response to our wellbeing and security. The book addresses the types of infectious disease outbreaks and actions needed to prepare and respond, emphasizing the roles of multinational agreements and international cooperation. For readers knowledgeable about global health security, the content might serve as a refresher, for persons unfamiliar with the subject, as an introduction. Gostin, director of Georgetown Law School's O'Neill Institute for National and Global Health Law, shaped by experiences as a lawyer and interactions with the World Health Organization, examines scientific and policy approaches. He discusses COVID-19 throughout the book and emphasizes health equity, drawing attention towards disadvantaged populations in low- and middle-income countries

The book is separated into 2 sections: "Growing Threats" encompasses topics as diverse as mosquitoborne diseases, climate change, and biosafety and biosecurity. "From Risk to Action" focuses on global health security governance, pathogen sharing, universal health coverage, and developing and using medical countermeasures. The chapter aptly titled "Humanity's Biggest Killer" outlines the history, epidemiology, and clinical manifestations of mosquitoborne diseases. Gostin discusses interventions such as genetically engineered mosquitoes, long-lasting insecticidal bed nets, and vaccination, but cautions "optimism should be tempered…by the limits of traditional strategies, hurdles still to overcome for newer possibilities (from scientific challenges to special publics), and the weaknesses of the health systems." In another chapter he discusses how behavior such as prophylactic use of antimicrobials in livestock and their overprescription by clinicians contributes to antimicrobial resistance and how lack of economic incentives for private sector investment inhibits development of antimicrobials. Gostin drives home potential dangers from complacency: "Imagine if we lived in a world where once fully treatable infections became life-threatening and routine surgeries posed lethal risks."

The final chapter, "Global Medical War Chest," focuses on regulatory considerations, market incentives, and clinical trial design for medical countermeasure development. Gostin argues that "financing, law, and ethics must be in place—not just when an outbreak strikes, but more importantly during periods of calm…Collectively, policies and processes that support all the building blocks of research and development can save millions of lives."

Gostin might have highlighted certain topics in greater detail, such as misinformation and disinformation and transformative technologies. Additional information about cultural influences on health would have been beneficial, as would perspective on the history of combatting outbreaks, such as through use of face masks. On the other hand, given that global coordination is critical because infectious disease spread does not recognize geographic borders, information about multinational policies and governance is particularly insightful. The author's use of first-person perspective and storytelling helps keep readers emotionally invested, and the tabletop exercise outbreak scenarios, list of health entity abbreviations, and headings used to guide the reader are valuable additions.

Global Health Security could be beneficial for policymakers reflecting on lessons learned from the COVID-19 pandemic and considering strategies to combat future outbreaks. Gostin's perspective provides an important lesson: "When the world fully funds and thoroughly prepares for dangerous outbreaks, it is highly likely that dangerous pathogens can be rapidly brought under control. If we neglect the threat, wait until it is too large to stop, and then panic, many lives, and dollars, will be lost. Most of the human and economic suffering is preventable."

Katherine M. Bianchi

Author affiliation: Biomedical Advanced Research & Development Authority, Office of the Assistant Secretary for Preparedness and Response, US Department of Health and Human Services, Washington, DC, USA

Address for correspondence: Katherine Bianchi, United States Department of Health and Human Services, Administration for Strategic Preparedness and Response, Biomedical Advanced Research and Development Authority, 200 Independence Ave, Washington, DC 20201, USA; email: katherine.bianchi@hhs.gov

Rafael Barradas (1890–1929), *Urban Landscape (Paisaje urbano),* **1919** (detail). Oil on cardboard, 23 1/2 in × 27 1/2 in / 59.7cm × 69.9 cm. The Museum of Fine Arts, Houston. Museum purchase funded by the 2017 Latin American Experience Gala and Auction, 2018.229. Photograph © The Museum of Fine Arts, Houston, Texas, USA; Will Michels.

A Multiplicity of Perspectives

Byron Breedlove

Finding a point of reference within the jumble of images that comprise the frenzied street scene sprawled across *Urban Landscape (Paisaje urbano),* this month's cover image, may initially prove challenging. A kaleidoscopic assortment of wedges, semicircles, rectangles, and other shapes seems to vibrate, morph, and blur. Swaths and streaks of color compete for attention. Pedestrians in the foreground jostle and nudge one another. To the left, a woman grasps a shopping basket. On the right, several uniformed soldiers pass among the crowd. Between them, indistinct images suggest a bustling scrum of people engaged in their daily routines. A stream of equestrians and yellow horse-drawn carriages, perhaps taxis, flows across the middle of the image. The few trees, green blots perched on a hill, and some patches of pale blue sky are the only nods to the natural world.

It is not improbable that some viewers might also imagine the sounds and smells from this teeming thoroughfare or experience a tinge of claustrophobia from the crush of the crowd. If so, then its creator, Uruguayan artist Rafael Barradas, would have been pleased.

Born in 1890 to Spanish parents in Montevideo, Uruguay, Barradas did not receive formal academic training or study art. His biography from the National Museum of Visual Arts, Uruguay, notes that Barradas learned his craft more informally, participating in gatherings with intellectuals and collaborating as an illustrator in newspapers and magazines published in Montevideo and Buenos Aires.

In 1913, Barradas traveled to Europe and settled in Barcelona, Spain, where he met a number of artists and poets, including a kindred spirit, the painter Joaquín Torres-García, also from Uruguay. They "were among the preeminent Uruguayan artists to establish a vital connection with Europe's prewar vanguards," according to the Museum of Fine Arts, Houston, Texas, USA. The allure of futurism, cubism,

and synchromism in art led Barradas and Torres-García "to propose 'vibrationism' — essentially an art reflecting a unity of the senses — as a unique contribution to Modernist theory."

Within the European avant-garde art community of that time, art historian M. Lluïsa Faxedas Brujats explains that vibration referred to the "physical phenomenology of light and to the assumed vibration of colours," the comparison between light and sound that lead to "all kinds of research into synaesthesia," and a connection "between the individual and his or her environment." Gabriel Peluffo Linari, who researches Latin American art, describes vibrationism as having a "syncretic language with a wide range of colors" that "presented a multiplicity of perspectives" and "combined elements of cubism and Italian futurism."

During this somewhat short phase of his career (by 1924 Barradas had moved on from vibrationism and was mostly painting landscapes), the artist was striving to appeal to as many senses as possible in his colorful, complex, abstract paintings. The Museum of Fine Arts, Houston, uses musical terminology to describe the syncretic elements of this work, noting, "*Urban Landscape* reflects the clamorous city streets of Madrid, where Barradas had settled in 1919, with sound and motion distilled in a colorful fugue."

When *Urban Landscape* was painted more than a century ago, according to United Nations' data, only 20% of the world's population lived in cities; in less developed countries, that percentage was around 5%. In October 2022, the World Bank estimates that "some 56% of the world's population—4.4 billion inhabitants—live in cities." The United Nations recently projected that by 2050, 68% of people will live in urban areas. Urbanization and the accompanying loss of natural habitat for animals have amplified the spillover of zoonoses—infections that are naturally transmissible from animals to humans—since Barradas' lifetime. As urban populations increase, so does human contact with synanthropic wildlife, migrating birds, domestic and wild animals sold in markets, and house pets, which in turn contributes to the spread of zoonotic infections. Plus, the overcrowding of people within megacities further propagates human-to-human spread of infections that have zoonotic origins but can now spread directly among people.

Infectious disease specialist Carl-Johan Neiderud writes that "Urbanization leads to many challenges for global health and the epidemiology of infectious diseases. New megacities can be incubators for new epidemics, and zoonotic diseases can spread in a more rapid manner and become worldwide threats." Integral to the global response to zoonotic infections is the concept of One Health, which CDC describes as "a collaborative, multisectoral, and transdisciplinary approach—working at the local, regional, national, and global levels—with the goal of achieving optimal health outcomes recognizing the interconnection between people, animals, plants, and their shared environment." Such "a multiplicity of perspectives" from experts working in multiple disciplines and sectors can bolster public health preparedness and response for the next zoonotic pandemic.

Bibliography

1. Brujats ML. Barradas' vibrationism and its Catalan context [cited 2022 Nov 8]. https://journals.ub.uni-heidelberg.de/index.php/rihajournal/article/view/70202/71095
2. Centers for Disease Control and Prevention. One Health basics [cited 2022 Oct 27] https://www.cdc.gov/onehealth/basics/index.html
3. Ellwanger JH, Byrne LB, Chies JA. Examining the paradox of urban disease ecology by linking the perspectives of urban One Health and ecology with cities. Urban Ecosyst. 2022;1–11. https://doi.org/10.1007/s11252-022-01260-5
4. Hassell JM, Begon M, Ward MJ, Fèvre EM. Urbanization and disease emergence: dynamics at the wildlife-livestock-human interface. Trends Ecol Evol. 2017;32:55–67. https://doi.org/10.1016/j.tree.2016.09.012
5. Linari GP. Composición vibracionista [cited 2022 Oct 31]. https://www-bellasartes-gob-ar.translate.goog/coleccion/obra/10668/?_x_tr_sl=es&_x_tr_tl=en&_x_tr_hl=en&_x_tr_pto=sc
6. Museum of Fine Arts, Houston. Rafael Barradas, *Paisaje urbano* [cited 2022 Oct 20]. https://emuseum.mfah.org/objects/139860/paisaje-urbano
7. National Museum of Visual Arts. Rafael Barradas (1890−1929) [cited 2022 Oct 20]. https://mnav.gub.uy/cms.php?a=2
8. Neiderud CJ. How urbanization affects the epidemiology of emerging infectious diseases. Infect Ecol Epidemiol. 2015;5:27060. https://doi.org/10.3402/iee.v5.27060
9. Oybin M. The first anthological exhibition of the Uruguayan artist Rafael Barradas [in Spanish] [cited 2022 Oct 31]. https://www.pagina12.com.ar/371287-la-primera-exposicion-antologica-del-artista-uruguayo-rafael
10. United Nations. World urbanization prospects: the 2014 revision [cited 2022 Oct 24]. https://population.un.org/wup/publications/files/wup2014-report.pdf
11. United Nations Environment Programme and International Livestock Research Institute. Preventing the next pandemic: zoonotic diseases and how to break the chain of transmission. Nairobi, Kenya, 2020 [cited 2022 Nov 8]. https://www.unep.org/resources/report/preventing-future-zoonotic-disease-outbreaks-protecting-environment-animals-and
12. World Bank. Urban development. Overview [cited 2022 Oct 24]. https://www.worldbank.org/en/topic/urbandevelopment/overview

Address for correspondence: Byron Breedlove, EID Journal, Centers for Disease Control and Prevention, 1600 Clifton Rd NE, Mailstop H16-2, Atlanta, GA 30329-4027, USA; email: wbb1@cdc.gov

EMERGING INFECTIOUS DISEASES®

Emerging Infectious Diseases thanks the following reviewers for their support through thoughtful, thorough, and timely reviews in 2022. Please contact us if your name is missing from this list.

Joseph Abrams
Laith Abu-Raddad
Bahaa Abu-Raya
Anna Acosta
Douglas Adamoski
Laura Adams
Blythe Adamson
Simon Adebola
Bishwa Adhikari
Cornelia Adlhoch
Rakesh Aggarwal
Maria Aguero-Rosenfeld
Hector Aguillar-Carreno
Ayman Ahmed
Takaaki Akaike
Andrei R. Akhmetzhanov
Munirul Alam
Abdullah Alanazi
Cesar G. Albariño
M. John Albert
Ivailo Alexiev
Afsar Ali
Sheikh Ali
Denise Allen
Samantha E. Allen
Gregório G. Almeida
Karen Alroy
Jaffar A. Al-Tawfiq
Christian L. Althaus
Carmen Amaro
Donne Ameme
Brian R. Amman
Aranzuzu Amor
Thomas Emil Andersen
Evan J. Anderson
Kathryn (Katie)
   B. Anderson
Larry Anderson
Robert Anderson
David R. Andes
Jason R. Andrews
Charlotte Anraad
Vernon Ansdell
Gregory Anstead
Joshua J. Anzinger
Charles Apperson
Abdel-Satar Arafa

Bob Arbeit
Matthew J. Arduino
Alexandre Arenales
Philip M. Armstrong
Bailey L. Arruda
Ann Arvin
Garret Asay
Peter Auguste
Andrew Auld
Kari Auranen
John Austin
Abdu F. Azad
Marwan Azar
Andrew S. Azman
Tara M. Babu
Laura Bachmann
Edgar Badell
Yuan Bai
J. Kevin Baird
Nicolle Baird
Andreina Baj
Julia M. Baker
Marissa Baker
Michelle L. Baker
Pablo C. Baldi
Davit Baliashvili
April Baller
Valerie D. Bampoe
Arinjay Banerjee
Carlo Alberto Barcella
Brianne Barker
Bridget Barker
Sophie Baron
Ian G. Barr
Joel Barratt
Lisa Barrios
Vanessa Barrs
Albert Barskey
Casey Barton Behravesh
Sridhar Basavaraju
Elizabeth M. Batty
Fernando Bauermann
Bernard Beall
Jeremy Bechelli
Robert A. Bednarczyk
Martin Beer
Amy Beeson

Robin Behn
Marcel A. Behr
Melissa Bell
Fernando
   Bellissimo-Rodrigues
Anna Beltrame
John Beltrami
Ronen Ben-Ami
Jeff Bender
Chris Van Beneden
Kaitlin Benedict
John E. Bennett
Stephen R. Benoit
William Bentley
Tomas Bergström
Yohannes Berhane
Frank Berkowitz
Stephen Bertke
Ian Beveridge
Sangeeta Bhatia
Kyle Bibby
Brad J. Biggerstaff
Zeno Bisoffi
Aaron Bivins
Allison Black
Carina Blackmore
David Blair
David D. Blaney
Joel Blankson
Lucas S. Blanton
Martin J. Blaser
Bradley J. Blitvich
Evan M. Bloch
Tegan K. Boehmer
Debrah Boeras
Petra Bogovic
Nadia Boisen
Sameh W. Boktor
Benjamin M. Bolker
Marc Bonten
Carl Boodman
Ray Borrow
Angela Bosco-Lauth
Paolo Bosetti
Valerie Bouchez
Asha Bowen
Michael D. Bowen

William A. Bower
Andrew Bowman
Richard S. Bradbury
Andreas Brave
Romulus Breban
Byron Breedlove
Edward Breitschwerdt
David Brett-Major
Ryan Brewster
Sylvain Brisse
Seth C. Britch
Amadea Britton
John T. Brooks
Tim Brooks
Yolanda Brooks
Tal Brosh-Nissimov
Allison C. Brown
Catherine Brown
Corrie Brown
Justin Brown
Rebecca Brown
Alfredo Bruno
Scott Brunt
Udo Buchholz
Alexandra Buckley
Dora Buonfrate
Brandy Burgess
Nathan D.
   Burkett-Cadena
Felicity J. Burt
Michael P. Busch
Corey Butler
Jay Butler
Adeel A. Butt
Rachel L. Byrne
Renee M. Calanan
Charles H. Calisher
Sébastien
   Calvignac-Spencer
Bernard Camins
Angela P. Campbell
Eric Cardinale
Luís Cardoso
Laura Carroll
Irene Casas
Cynthia H. Cassell
Francois Castonguay

Alessandro Catenazzi
Godfred Cato
Simon Cauchemez
Alyson Cavanaugh
Eleonora Cella
Joon-Seok Chae
Jong-Yil Chai
Serafeim C. Chaintoutis
Justin Chan
Paul K.S. Chan
Yoke-Fun Chan
Jagdish Chander
Kelly Charniga
Rémi N. Charrel
Armando
    Chaure-Pardos
Nora Chea
Liang Chen
Mark I. Chen
Yang Chen
Chi Ngai Cheung
Peter Pak Hang Cheung
Sylvia Chiang
Young June Choe
Hongjo Choi
Mary Joung Choi
B.B. Chomel
Terence Chorba
Eric J. Chow
Nancy Chow
Anuradha Chowdhary
Gerardo Chowell
Rebecca C. Christofferson
Paul R. Cieslak
Alexander T. Ciota
Jesse Clark
Patrick Clay
Mario Coccia
Gaia Codolo
Lark L. Coffey
Adam L. Cohen
Regev Cohen
Vito Colella
Philippe Colson
Richard Condit
Constantin Constantinoiu
Jennifer Cope
Mary Corcoran
Anne Cori
Victor Max Corman
Stephane Corvec
Caitlin Cossaboom
Varea Costello

Matthew Cotten
Robert H. Cowie
Benjamin Cowling
Pascal Crépey
Julio Croda
Colin J. Crooks
Nicolas Crossland
Trevor A. Crowell
John A. Crump
Andrea T. Cruz
Fuqiang Cui
Jie Cui
Jing Cui
Walter H. Curioso
Dustin W. Currie
Daniel R. Curtis
Christopher Czaja
Dora Dadzie
Ron Dagan
Daniel Dalcin
Charles Daley
David Dance
Côme Daniau
M. Carolina
    Danovaro-Holliday
Sanchita Das
Akbar Dastjerdi
Miles P. Davenport
Michael David
Charles T. Davis
Bernard Davoust
Marcos de Almeida
Miranda de Graaf
Priscila M. de Macedo
Marie de Perio
Gil C. De Santis
Daniela de Souza Rajao
Mark J. Delorey
Walter Demczuk
Angel N. Desai
Jay Desai
Christina Deschermeier
David Deshazer
Michael E. DeWitt
Vijaykrishna
    Dhanasekaran
Georges Diatta
James Diaz
Richard C. Dicker
Jennifer Dien Bard
Elizabeth Dietrich
Rhoel R. Dinglasan
Gerhard Dobler

Anna Dolgova
Vajeera Dorabawila
Florence C.
    Doucet-Populaire
Scott Dowell
John M. Drake
Michel Drancourt
Jan Felix Drexler
Michele Drigo
Mignon du Plessis
Mariette Ducatez
Christian Ducrot
Nisha K. Duggal
Igor Dumic
John Stephen Dumler
Kevin H. Dunn
Jake Dunning
Alan Dupuis
Alexandre Duvignaud
Clare A. Dykewicz
Zoe A. Dyson
Rebecca Earnest
Gregory Ebel
Mark Eberhard
Paul H. Edelstein
Chris Edens
Tobias Eisenberg
Marwa Elgendy
Katherine D. Ellingson
Ivo Elliott
Akira Endo
David M. Engelthaler
Jonathan H. Epstein
Lauren H. Epstein
Dean D. Erdman
Marina Eremeeva
Koray Ergunay
Christian Erikstrup
Álvaro A.
    Faccini-Martínez
Alzhraa Fahmy
Joseph O. Falkinham
Ibrahim-Soce Fall
Mehdi Fatahi-Bafghi
Joseph R. Fauver
Michelle Felicella
Mariet C.W. Feltkamp
Shuo Feng
Florence Fenollar
Stefan Fernandez
Antonio Fernández

María del Pilar
    Fernández
Olivier Ferraris
Marcelo Ferreira
Tiago Ferreira
Ezio Ferroglio
Cindy Feuer
Patricia I. Fields
Helen Fifer
Anthony Fiore
Kerstin Fischer
Robert J. Fischer
Dan Fishbein
Katherine E.
    Fleming-Dutra
Jennifer Flood
Jannik Fonager
Kristian Forbes
Andrea Forde
Pierre-Edouard Fournier
Ashley L. Fowlkes
Brian D. Foy
Louise K.
    Francois Watkins
John Frean
David O. Freedman
Caroine Frey
Rachel Friedman
Matthieu Fritz
Jonathan Frye
Hans-Peter Fuehrer
Isaac Chun-Hai Fung
Nathan Woo Furukawa
Yuki Furuse
Alice Fusaro
Carine Gachen
Kenneth Gage
Sebastien Gagneux
John Galgiani
Manoj Gambhir
Dionicia Gamboa
Feng Gao
Adolfo García-Sastre
Richard S. Garfein
Mutien-Marie Garigliany
Aura R. Garrison
Michelle L. Gatton
Philippe Gautret
Yang Ge
Jay E. Gee
Cyril R. Geismar
Kathleen Gensheimer
Jemma L. Geoghegan

Dale N. Gerding
Peter Gerner-Smidt
Giovanni Ghielmetti
Rory Gibb
Katherine Gibney
David I. Gibson
Michael Giladi
Marta Giovanetti
Aharona
  Glatman-Freedman
Jacques Godfroid
Wil H.F. Goessens
Jeremy A.W. Gold
Noreen Goldman
Jonathan Golub
Gabriel Gonzalez
Catherine Gordon
Richard Gorman
Carolyn Gould
Nelesh P. Govender
Solène Grayo
Monica H. Green
Richard Greene
Sharon K. Greene
Justin Greenlee
Nichar Gregory
Jonathan Grein
Megan Greischar
Charles Grose
Nathan Grubaugh
Haogao Gu
Lidia Gual Gonzalez
Jeannette Guarner
Jonathan B. Gubbay
Alice Guh
Emilande Guichet
Adi V. Gundlapalli
Maryam B. Haddad
Andrew D. Haddow
Stephen C. Hadler
Ferry Hagen
Natasha Halasa
Nicholas Haley
Aron J. Hall
Carina M. Hall
John Halperin
Eric S. Halsey
Scott B. Halstead
Sarah A. Hamer
Axel Hamprecht
David Hampson
Andrew R. Hansen
Jennifer Harcourt

Timm Harder
Jim Harnisch
Rafael Harpaz
Tasnim Hasan
Takehiro Hashimoto
Henrik Hasman
Claire Hastie
Ben M. Hause
Anthony Hawksworth
Qiushui He
Craig Hedberg
Adriana Heguy
Fabian Heinrich
Amy Heinzerling
Meghan E. Hermance
Daniel Herrera-Esposito
Lara Herrero
David L. Heymann
Edward M. Hill
Nichola J. Hill
Susan L. Hills
Markus Hilty
William S. Hlavacek
Martin Hoenigl
Bernard Hoet
Nicole Hoff
Catherine A. Hogan
Mike Holbrook
F. Blaine Hollinger
NaTasha D. Hollis
Edward C. Holmes
Ki Ho Hong
Grace Hood
Sarah A. Hook
Katherine C. Horton
Margaret Hosie
Paul Hoskisson
Linda Houhamdi
Jennifer A. House
Rebecca Howie
Casey R.J. Hubert
Vit Hubka
Stéphane Hué
Karsten Hueffer
Gareth J. Hughes
Sun Huh
Ralph Huits
James Hull
Muhammad Jami Husain
Christina Hutson
Jahun Ibrahim
Tim J.J. Inglis
Hon Sang Ip

Shareen Iqbal
Seema Irfan
Masahiro Ishikane
John Iskander
Anne J. Jääskeläinen
Brendan R. Jackson
Jesse T. Jacob
Jan Jacobs
Chris Janssen
Claire M. Jardine
Stephane Jaureguiberry
Barbara Javor
Martyn Jeggo
Claire Jenkins
Emily Jenkins
Kwang Cheol Jeong
John Jereb
Jose-Luis Jimenez
Magnus Johansson
Jefferson M. Jones
T. Stephen Jones
Lisa Jones-Engel
Stephen Jordan
M. Patricia Joyce
Kathleen G. Julian
Angelo Kaggwa
Edwin Kamau
Suchit Kamble
Abraar Karan
André Karch
Erik A. Karlsson
Nadira D. Karunaweera
Hideki Katagiri
Haru Kato
Alan R. Katz
Mark A. Katz
Julia Kawagoe
Yoshihiro Kawaoka
Ghazi Kayali
Aubrey R.D. Kehoe
Eben Kenah
Steven Kerr
Jennifer Kertes
Alexander C. Keyel
Sakirul Khan
David Khoury
Yury Khudyakov
James C. Kile
Marie Killerby
Mary L. Killian
Peter Kilmarx
Eun-Jin Kim
Hee-Jin Kim

Ju Sang Kim
Linda G. Kimsey
Thomas Kingsley
Amy E. Kirby
Martyn D. Kirk
Hannah L. Kirking
Irina Kislaya
Aaron Kite-Powell
Moses C. Kiti
Sabra L. Klein
Boris Klempa
John Klena
Jackie Kleynhans
Jacqueline Knee
Marian Knight
Miwako Kobayashi
Guus Koch
Marleen Kock
Richard A. Kock
Anson Van Arsdale
  Koehler
Aaron Kofman
Haruki Koike
Nicholas Komar
Irina Kontsevaya
Shireen Kotay
Colleen S. Kraft
Peter J. Krause
Cécile Kremer
Mirjam Kretzschmar
Amanda Kreuder
Bala Krishnamurthy
Erna G. Kroon
Andi Krumbholz
Matthew J. Kuehnert
Amy J. Kuenzi
Thijs Kuiken
Ashutosh Kumar
Amber Kunkel
Satoshi Kutsuna
Kin On Kwok
Marcelo B. Labruna
Kristine A. Lacek
Marcus Vinicius
  G. Lacerda
Raskit Lachmann
Po-Ying Lai
Tsan Yuk Lam
Amy J. Lambert
Frederic Lamoth
Fan-Yun Lan
Ruiting Lan
Claudio F. Lanata

Robert S. Lane
Andrew S. Lang
Adam J. Langer
Tatiana Lanzieri
Kayla Laserson
Brent Lasker
E.H.Y. Lau
Rachel Lau
Catharine Laube
Ana Lauer
James V. Lawler
Tan Le Van
Sixto M. Leal
Fabian Z.X. Lean
Phillip Lederer
Edith R. Lederman
Christine Lee
Dong-Hun Lee
Gwenyth Lee
Rogan Lee
Sarah Lee
Vernon J. Lee
Vincent Legros
Andrew Leidner
Juliana D. Leite
Natasha Lelijveld
Audrey Lenhart
David A. Leon
S.R. Leon
Eyal Leshem
Fernanda Lessa
Andrew Letizia
Michael Letko
Char Leung
Kathy Leung
Vivian Leung
Min Z. Levine
Karen Levy
Eric Lewitus
Feng Li
You Li
Shu-Chen Liao
Michael Libman
Michael Lin
Sally Lin
Nicole Lindsey
William G. Lindsley
Natalie M. Linton
Marc Lipsitch
Anastasia P. Litvintseva
Carol Y. Liu
Dakai Liu
Spencer Lloyd

Shawn R. Lockhart
Latania K. Logan
Caroline Loiez
Virgil Lokossou
Maureen Long
S. Wesley Long
Jeffrey M. Lorch
Elsa Lorthe
Ron Louie
Naomi W. Lucchi
Joseph D. Lutgring
Samantha Lycett
Meghan M. Lyman
Frederik Lyngse
Kevin Ma
David Mabey
Duncan MacCannell
John Mackenzie
Ryan A. Maddox
Zachary J. Madewell
Susan
    Madison-Antenucci
Alexandra Mailles
Arshpreet Kaur Mallhi
Svenn-Erik Mamelund
Nina Marano
Gabriele Margos
Robert Markewitz
Wanda Markotter
Suzanne M. Marks
Chandapiwa
    Marobela-Raborokgwe
Linsey Marr
Theodore K. Marras
Tom Marrie
Zachary Marsh
Barbara J. Marston
Emily T. Martin
Constanza
    Martinez-Valdebenito
Haruhiko Maruyama
Grace Marx
Santiago Mas-Coma
Brian Maskery
Alberto Mateo Urdiales
Blaine A. Mathison
Yasufumi Matsumura
Keita Matsuno
Luke J. Matthews
Max Maurin
Carla Mavian
Alfredo Mayor
Denise McAloose

J. Trenton McClure
David McCormick
L. Clifford McDonald
Anita K. McElroy
Lesley McGee
Peter B. McIntyre
Debbie McKenzie
Sandra McLellan
Martina McMenamin
Lucy McNamara
John McQuiston
Thembi Mdluli
Dana Meaney-Delman
Oleg Mediannikov
Adam Meijer
Julianne Meisner
Asuncion Mejias
Cléa Melenotte
Martin I. Meltzer
Leonel Mendoza
João Mesquita
Kevin Messacar
Abhishek Mewara
Sylvain Meylan
Claire M. Midgley
Sofie Midgley
Nkuchia M. M'ikanatha
Maureen Miller
Michele Miller
Mathieu Million
Donald K. Milton
Imran Mirza
Nischay Mishra
Fuminari Miura
Atsushi Miyawaki
Igor Mokrousov
Noelle-Angelique
    M. Molinari
Susana Monge-Corella
Susan P. Montgomery
Patrick K. Moonan
Cynthia Moore
Penny Moore
Rachel A. Moore
Jacob Moran-Gilad
Gonzalo Moratorio
David Morens
Clint N. Morgan
Leah F. Moriarty
Konosuke Morimoto
Tomoaki Morioka
Masatomo Morita
Stephen S. Morse

Eric Mossel
Eric Mucker
Barbara Mühlemann
Rudzani Muloiwa
Erik Munson
Vincent Munster
Yannick Munyeku
    Bazitama
David R. Murdoch
Kristy O. Murray
Daniel Musher
Scott A. Nabity
Irving Nachamkin
Koo Nagasawa
Tomaka Nakamura
Allyn K. Nakashima
Ho Namkoong
Jai P. Narain
Masa Narita
Hema Narra
James Nataro
Kathleen Navarro
Shevanthi Nayagam
Maria Negron
Christina A. Nelson
Martha Nelson
Nicole Nemeth
Louis Nevejan
Paul Newton
Terry Fei Fan Ng
Minh-Hong Nguyen
Brooke E. Nichols
Nathalie Nicolay
Lise Nigrovic
Eric J. Nilles
Melissa S. Nolan
Romolo Nonno
Peter Norberg
Robert Norton
Shannon Novosad
Ignacio Novo-Veleiro
Norbert Nowotny
Tommy Nyberg
Sylvia Ofori
Agbaya S. Oga
Tsuyoshi Ogata
Elizabeth Ohlsen
Tochi Okwor
Kevin J. Olival
Cristina Oliveira
Fabiano Oliveira
Margaret A. Olsen
Victoria A. Olson

Pascale Ondoa
Seth E. O'Neal
Lulla Opatowski
Oddvar Oppegaard
Tanja Opriessnig
Walter A. Orenstein
Carlos Orsorio
Stephen Ostroff
José A. Oteo
Domenico Otranto
Subhendu K. Otta
Janet Ousley
Egon A. Ozer
Samuel Packard
Tasleem Padamsee
Christopher D. Paddock
Clinton R. Paden
John Paget
Gustavo Palacios
Ana M. Palomar
Claire Panosian
Jesse Papenburg
John R. Papp
Peter G. Pappas
Miguel Paredes
Bharat Parekh
Sunil Parikh
Saverio G. Parisi
Ina Park
Gabriel I. Parra
Colin Parrish
Julie Parsonnet
W. Clyde Partin
Prabasaj Paul
Gabriela Paz-Bailey
Malik J.S. Peiris
Andrew Pekosz
Stephanie Perniciaro
Nita Perumal
Patricia Pesavento
Trevor Peter
Esklid Petersen
Maria Skaalum Petersen
Josh Petrie
Mary Petrone
Silviu O. Petrovan
Brad Pickering
David M. Pigott
Jamison Pike
Tamara Pilishvili
Andrea Pilotto
Ville N. Pimenoff
Benjamin A. Pinsky

Johann D.D. Pitout
Nottasorn Plipat
Raina K. Plowright
Mateusz Plucinski
Laurent Poirel
Philip M. Polgreen
Wendy Pons
Leo L.M. Poon
Yong Poovorawan
Ann M. Powers
N. Pradeep Kumar
Ranjan Premaratna
John F. Prescott
D Rebecca Prevots
Erin P. Price
Bobbi Pritt
Marifi Pulido
Mirja Puolakkainen
Michael A. Purdy
Lawrence J. Purpura
Muriel Rabone
Justin Radolf
Jayna Raghwani
Gabriel Rainisch
Andrew Ramey
Mario Ramirez
Madhura Rane
Stéphane Ranque
Agam Rao
Didier Raoult
Mohammed Rasheed
Angela Rasmussen
Hugo R. Razuri
Gemma Recio Comí
Linzhu Ren
Marc Rendell
Susan Resnick
Mary G. Reynolds
Chanu Rhee
Daniel Rhoads
Guilherme S. Ribeiro
Marcio Ribeiro
Allen L. Richards
Hans L. Rieder
Thomas V. Riley
Irene Rivero Calle
David Robertson
Ashley Robinson
Joan L. Robinson
Ian Christopher
  N. Rocha
Barry Rockx
Jesús Rodríguez-Baño

Natalia
  Rodriguez-Valero
Elena Roel
Dawn Roellig
Elizabeth
  Rogawski-McQuade
Eric Rogier
Pierre E. Rollin
Thomas Romig
Shannon E. Ronca
Kathleen M. Ross
John Rossow
Paul Rota
Chad Roy
Pavitra Roychoudhury
Joseph Rubin
Jose M. Rubio
Amy Rubis
Jeanne Ruff
Thomas A. Russo
Daniel Ruzek
Sukhyun Ryu
Antonio Saad
Jamal Saad
Chiara Sacco
Karampreet Sachathep
Lisa Saiman
Jien Saito
Yoshihiro Sakoda
Henrik Salje
Johanna S. Salzer
Mark Salzman
Matthew Samore
Ana L. Sanchez
Liliana Sanchez-Gonzalez
Maria Paz Sanchez-Seco
Anna-Lena Sander
Sarah G.H. Sapp
R. Tedjo Sasmono
P.S. Satheshkumar
Kei Sato
Sharon Saydah
H.S. Schaaf
Elissa Schechter-Perkins
Manuel Schibler
Patricia Schlagenhauf
Sarah Schmedes
Randal J. Schoepp
Gabriele Schönian
Gunther Schonrich
Tony Schountz
Amy J. Schuh
Jonathan Schultz

Julian Schulze zur Wiesch
Tom G. Schwan
Ilan S. Schwartz
Tatjana Schwarz
Carlos Seas
Arlene Seid
Stephanie N. Seifert
James J. Sejvar
Zuzana Sekeyova
Tara Kirk Sell
Rangaraj Selvarangan
Omoleke Semeeh
Vera A. Semenova
Jan C. Semenza
Pinar Sen
Denis Sereno
Joe Sexton
Sean V. Shadomy
Sharaf A. Shah
Shokoofeh Shamsi
Andi L. Shane
Aditya Sharma
Tyler M. Sharp
Frederic E. Shaw
Harsha Sheorey
Wun-Ju Shieh
Tom Shimabukuro
Yusuke Shimakawa
Kayoko Shioda
George Shirreff
Kirsty Short
Adrienne Showler
Susan A. Shriner
Pei-Yun Shu
Bhavarth Shukla
Salvatore Siciliano
Benjamin J. Silk
Eric Simões
Colin R. Simpson
Les Sims
Andreas Sing
Burton Singer
Pushpendra Singh
Nikolaos V. Sipsas
Geetha Sivasubramanian
Beth Skaggs
Pavel Skums
Rachel B. Slayton
Dallas Smith
Kimothy Smith
Robert P. Smith
Georges Snounou
Rodrigo Martins Soares

Jeremy Sobel
Kimia Sobhani
Rami Sommerstein
Klara Sondén
Gail Sondermeyer
   Cooksey
Frank J. Sorvillo
Paul M. Southern
Erica Spackman
Erica Spatz
Anne C. Spaulding
Hillary Spencer
John Spencer
Adel Spotin
Siddharth Sridhar
Kirsten St. George
David Stallknecht
Allen C. Steere
Paola Stefanelli
Eike Steinmann
Benjamin Stoff
Mars Stone
Gregory A. Storch
Susan Stramer
Marc A. Strassburg
Jeffrey Strich
James E. Strong
Matthew Stuckey
David Sue
Jonathan Sugimoto
Sheena Sullivan
Kaiyuan Sun
Rebecca Sunenshine
Heungsup Sung
Colin Sutherland
Melissa Sutton
Yasunori Suzuki
Christine Szablewski
Matias Pablo Juan Szabó
Muhamed-Kheir Taha
Michal Tal
Sandra Tallent
Amish Talwar
Kathrine R. Tan
Kelvin Tan
Ippei Tanaka
Julian Wei-Tze Tang
Patrick Tang
Amna Tariq
Jacqueline Tate
Terrie E. Taylor

Sarah A. Teatero
Sam Telford
Stefano Tempia
Mark Tenforde
Chong G. Teo
Richard Teran
Karen Terio
Anders Ternhag
Eyasu H. Teshale
Brenda Tesini
Urusa Thaenhkam
Nicolas Theopold
Joe Theu
Caroline Theunissen
Karine Thivierge
Janelle Thompson
Rachel Thomson
Natalie Thornburg
Guo-Bao Tian
Rebekah Tiller
Sharon Tirosh-Levy
Boghuma Titanji
Mitsuru Toda
Kentaro Tohma
Kouki Tomari
Krzysztof Tomasiewicz
Stephen M. Tompkins
Noel Tordo
Paul Torgerson
Gabriela Torrea
Fernando Torres-Velez
Jonathan S. Towner
Denise Traicoff
Cuc Hong Tran
Quan Tran
Antoni Trilla
Giliane de Souza
   Trindade
Bhupendra Tripathi
Damien Tully
Ho-Jui Tung
Claire E. Turner
Felix Twum
Gérald Umhang
Elizabeth R. Unger
Tamara Ursini
Boniface Ushie
Timothy Uyeki
Ronald O. Valdiserri
Snigdha Vallabhaneni
Chris Van Beneden

Saskia van der Kam
Mark van der Linden
Kristien Van Reeth
Hanna Vauhkonen
Gonzalo M.
   Vazquez-Prokopec
Aldo Venuti
Guilherme G. Verocai
Pauline Vetter
Nicolas Vignier
Jan Vinjé
Leo G. Visser
Mathew Vogt
Lara Vojnov
Asisa Volz
Christian Johannes von
Wintersdorff
Neil M. Vora
Duc J. Vugia
Janna Vuopio
Supaporn
   Wacharapluesadee
Jesse J. Waggoner
Heather D.
   Stockdale Walden
Ronald Waldman
David H. Walker
Ryan MacLaren Wallace
Julia Walochnik
Michelle Waltenburg
Henry (Xiufeng) Wan
Steve Wassilak
Richard J. Webby
J. Todd Weber
Manuel Weber
Scott Weese
David Weetman
Michael R. Weigand
Francois-Xavier Weill
Robert A. Weinstein
Paul Weiss
Thomas Weitzel
Rory Welsh
Silvano Wendel
Bruce G. Weniger
Guido Werner
Nick Wheelhouse
Doug Whiteside
Hilary Whitham
Cyndy Whitney

Nathan Wiederhold
Joost Wiersinga
Pushpa Ranjan
   Wijesinghe
Caran R. Wilbanks
Melisa Willby
Angela Willemsen
Margaret M. Williams
Samantha Williams
Amy Wilson
Dean L. Winslow
Carla A. Winston
Carl Heinz
   Wirsing von Konig
Cameron R. Wolfe
Darren Wong
Frank Wong
Michelle Wong
Gwen Wood
Kate R. Woodworth
Kimberly A. Workowski
Gary Wormser
Henry Wu
Rebecca M. Wurtz
Anne L. Wyllie
Hui Xie
Guang Xu
Hayley Yaglom
Dafna Yahav
Bingyi Yang
Patrick Yang
Claude Kwe Yinda
Sungsu Youk
Alexander Tin Han Yu
Chun-Hsien Yu
Lili Yu
Xue-Jie Yu
Seong-Su Yuk
Chee Fu Yung
Hans L. Zaaijer
Bianca Zecchin
Xinjian Zhang
Huachen Zhu
Stephan Zientara
Annetta Zintl
Casey M. Zipfel
Sarah Zohdy
Armineh Zohrabian
Jason Zucker

EMERGING INFECTIOUS DISEASES®

Upcoming Issue • January 2023 • Vectorborne Infections

- Comprehensive Review of Emergence and Virology of Tickborne Bourbon Virus in the United States

- Multicenter Case-Control Study of COVID-19–Associated Mucormycosis Outbreak, India

- *Akkermansia muciniphila* Associated with Improved Linear Growth among Young Children, Democratic Republic of the Congo

- Seroepidemiology and Carriage of Diphtheria in Epidemic-Prone Area and Implications for Vaccination Policy, Vietnam

- Risk for Severe Illness and Death among Pediatric Patients with Down syndrome Hospitalized for COVID-19, Brazil

- COVID-19 Booster Dose Vaccination Coverage and Factors associated with Booster Vaccination among Adults, United States, March 2022

- Risk for Severe COVID-19 Outcomes among Persons with Intellectual Disabilities, the Netherlands

- Molecular Tools for Early Detection of Invasive Malaria Vector *Anopheles stephensi* Mosquito

- Clinical Forms of Japanese Spotted Fever from Case-Series Study, Zigui County, Hubei Province, China, 2021

- Genomic Confirmation of *Borrelia garinii*, United States

- Pathologic and Immunohistochemical Evidence of Possible *Francisellaceae* among Aborted Ovine Fetuses, Uruguay

- Efficient Inactivation of Monkeypox Virus by World Health Organization–Recommended Hand Rub Formulations and Alcohols

- Catheter-Related Bloodstream Infection Caused by *Mycolicibacterium iranicum*

- SARS-CoV-2 Omicron (BA.5) Infections in Vaccinated Persons, Rural Uganda

- Increased Seroprevalence of Typhus Group Rickettsiosis, Galveston County, Texas, USA

- Monkeypox Virus Infection in 18-Year-Old Woman after Sexual Intercourse, France, September 2022

- Monkeypox Virus Infection in 22-Year-Old Woman after Sexual Intercourse, New York, USA

- Rapid Seroprevalence Survey of SARS-CoV-2 in Central and Western Divisions of Fiji, 2021

- Genomic Epidemiology Linking Nonendemic Coccidioidomycosis to Travel

- *Photobacterium damselae* subsp. *damselae* Pneumonia in Dead, Stranded Bottlenose Dolphin, Eastern Mediterranean Sea

**Complete list of articles in the January issue at
https://wwwnc.cdc.gov/eid/#issue-295**

Earning CME Credit

To obtain credit, you should first read the journal article. After reading the article, you should be able to answer the following, related, multiple-choice questions. To complete the questions (with a minimum 75% passing score) and earn continuing medical education (CME) credit, please go to http://www.medscape.org/journal/eid. Credit cannot be obtained for tests completed on paper, although you may use the worksheet below to keep a record of your answers.

You must be a registered user on http://www.medscape.org. If you are not registered on http://www.medscape.org, please click on the "Register" link on the right hand side of the website.

Only one answer is correct for each question. Once you successfully answer all post-test questions, you will be able to view and/or print your certificate. For questions regarding this activity, contact the accredited provider, CME@medscape.net. For technical assistance, contact CME@medscape.net. American Medical Association's Physician's Recognition Award (AMA PRA) credits are accepted in the US as evidence of participation in CME activities. For further information on this award, please go to https://www.ama-assn.org. The AMA has determined that physicians not licensed in the US who participate in this CME activity are eligible for AMA PRA Category 1 Credits™. Through agreements that the AMA has made with agencies in some countries, AMA PRA credit may be acceptable as evidence of participation in CME activities. If you are not licensed in the US, please complete the questions online, print the AMA PRA CME credit certificate, and present it to your national medical association for review.

Article Title

Clinical and Epidemiologic Characteristics and Therapeutic Management of Patients with *Vibrio* Infections, Bay of Biscay, France, 2001–2019

CME Questions

1. Which one of the following statements regarding the epidemiology of patients with *Vibrio* spp. infections in the current study by Hoefler and colleagues is most accurate?

A. The cohort was split evenly between women and men
B. The average age of patients was 24 years
C. Most infections occurred after eating or handling raw seafood
D. More than 80% of infections occurred between June and September

2. Which of the following expressions of *Vibrio* infection were most common in the current study??

A. Digestive disorders and cellulitis
B. Digestive disorders and pneumonia
C. Osteitis and sepsis
D. Soft tissue infection and otitis

3. Which of the following *Vibrio* species were most commonly isolated in the current study?

A. *V. cholerae* and *V. vulnificus*
B. *V. cholerae* and *V. parahaemolyticus*
C. V. alginolyticus and *V. parahaemolyticu*s
D. *V. vulnificus* and *V. alginolyticus*

4. Which one of the following statements regarding treatment and outcomes of *Vibrio* infection in the current study is most accurate?

A. Only half of patients received antibiotics
B. 8% of patients underwent surgery
C. Cure was achieved in 70% of patients with chronic infection
D. The mortality rate associated with acute infection was 14%

Earning CME Credit

To obtain credit, you should first read the journal article. After reading the article, you should be able to answer the following, related, multiple-choice questions. To complete the questions (with a minimum 75% passing score) and earn continuing medical education (CME) credit, please go to http://www.medscape.org/journal/eid. Credit cannot be obtained for tests completed on paper, although you may use the worksheet below to keep a record of your answers.

You must be a registered user on http://www.medscape.org. If you are not registered on http://www.medscape.org, please click on the "Register" link on the right hand side of the website.

Only one answer is correct for each question. Once you successfully answer all post-test questions, you will be able to view and/or print your certificate. For questions regarding this activity, contact the accredited provider, CME@medscape.net. For technical assistance, contact CME@medscape.net. American Medical Association's Physician's Recognition Award (AMA PRA) credits are accepted in the US as evidence of participation in CME activities. For further information on this award, please go to https://www.ama-assn.org. The AMA has determined that physicians not licensed in the US who participate in this CME activity are eligible for AMA PRA Category 1 Credits™. Through agreements that the AMA has made with agencies in some countries, AMA PRA credit may be acceptable as evidence of participation in CME activities. If you are not licensed in the US, please complete the questions online, print the AMA PRA CME credit certificate, and present it to your national medical association for review.

Article Title

Acinetobacter baumannii among Patients Receiving Glucocorticoid Aerosol Therapy during Invasive Mechanical Ventilation, China

CME Questions

1. What was the rate of isolation of *Acinetobacter baumannii* (AB) from patients with invasive mechanical ventilation (IMV) in the current study by Zhang and colleagues?

A. 4%
B. 9%
C. 32%
D. 54%

2. Which of the following statements regarding the role of aerosol inhalation in the isolation of AB in the current study is most accurate?

A. Any aerosol inhalation during IMV was associated with a higher risk for AB
B. Only aerosol inhalation with corticosteroids during IMV was associated with a higher risk for AB
C. Aerosol inhalation during IMV did not significantly affect the risk for AB
D. Aerosol inhalation with corticosteroids during IMV was associated with a lower risk for AB

3. Which of the following was the LEAST significant risk factor for AB in the current study?

A. Aerosol inhalation with glucocorticoids (AIG)
B. Being a current or former smoker
C. IMV for ≥ 5 days
D. Use of a broad-spectrum antibiotic for ≥ 7 days

4. Which of the following statements regarding risk factors for 30-day mortality in the current study is most accurate?

A. Any inhalation therapy was associated with a higher risk for mortality
B. Only inhalation therapy with corticosteroids was associated with a higher risk for mortality
C. Inhalation therapy with or without corticosteroids was not associated with a higher risk for mortality
D. AB was not associated with a higher risk for mortality